This Page is Inserted by IFW Indexing and Scanning Operations and is not part of the Official Record

BEST AVAILABLE IMAGES

Defective images within this document are accurate representations of the original documents submitted by the applicant.

Defects in the images include but are not limited to the items checked:

- ☐ BLACK BORDERS
- ☐ IMAGE CUT OFF AT TOP, BOTTOM OR SIDES
- ☐ FADED TEXT OR DRAWING
- ☐ BLURRED OR ILLEGIBLE TEXT OR DRAWING
- ☐ SKEWED/SLANTED IMAGES
- ☐ COLOR OR BLACK AND WHITE PHOTOGRAPHS
- ☐ GRAY SCALE DOCUMENTS
- ☐ LINES OR MARKS ON ORIGINAL DOCUMENT
- ☐ REFERENCE(S) OR EXHIBIT(S) SUBMITTED ARE POOR QUALITY
- ☐ OTHER: _____

IMAGES ARE BEST AVAILABLE COPY.
As rescanning these documents will not correct the image problems checked, please do not report these problems to the IFW Image Problem Mailbox.

Journal of Antimicrobial Chemotherapy (1989) **24**, 533–537

Antifungal activity of saperconazole (R 66 905) *in vitro*

F. C. Odds

Department of Microbiology, University of Leicester, PO Box 138, Medical Sciences Building, University Road, Leicester LE1 9HN, UK

Saperconazole, a novel orally active triazole antifungal, inhibited *Candida* spp., *Aspergillus* spp. and dermatophyte fungi *in vitro*. Its minimal inhibitory concentrations for *Candida* spp. and dermatophytes were relatively high, like those of comparable triazole antifungals, but all of the *Aspergillus* isolates tested were inhibited by less than 0·1 mg/l. Relative inhibition factors of saperconazole were in the range 31–76% for *Candida* isolates, 6–18% for *Aspergillus* isolates and 5–10% for dermatophytes. These figures predict a good inhibitory activity of saperconazole for all the fungi tested, with particularly strong activity against *Aspergillus* spp. and dermatophytes. Saperconazole inhibited hyphal branch formation in *C. albicans* at concentrations as low as 10^{8} M.

Introduction

Saperconazole (Figure 1) is a novel, fluorinated triazole derivative with potential as a clinical antifungal agent given by oral administration (Van Cutsem & Janssen, 1988). This study evaluated the antifungal activity of saperconazole *in vitro* in tests for minimal inhibitory concentrations (MICs) and relative inhibition factors (RIFs) against *Candida* species and other fungal pathogens. Ketoconazole was used throughout as a reference compound.

Materials and methods

The fungal isolates tested were all originally obtained from clinical material: they were maintained on Sabouraud's glucose agar (Oxoid) at 37°C (*Candida* and *Aspergillus* isolates) or 30°C (dermatophytes). The isolates of *C. albicans* included three known to be resistant to azole antifungals, and the isolates of other *Candida* species included *C. kefyr* Holt, known to be exquisitely sensitive to azoles. *C. glabrata, C. guilliermondii, C. krusei, C. parapsilosis* and *C. tropicalis* were all included among the *Candida* species tested. The *Aspergillus* isolates consisted of two strains of *A. flavus* and six strains of *A. fumigatus*, and the dermatophytes comprised three strains of *Trichophyton mentagrophytes*, two strains of *T. rubrum* and a single strain of *Microsporum canis*. All the *Aspergillus* and dermatophyte isolates were the same as were used in previous studies (Odds & Abbott, 1984; Odds, Webster & Abbott, 1984).

For MIC tests, isolates were suspended in water at a concentration of 10^{5} cells or conidia per ml and inoculated on phosphate-buffered yeast nitrogen base/1% glucose medium, pH 7·0 (Shadomy & Espinel-Ingroff, 1980) and on Eagle's minimal essential

0305–7453/89/100533+05 $02.00/0 © 1989 The British Society for Antimicrobial Chemotherapy

UM00012055
NOVARTIS EXHIBIT 1517
Novartis v. Regents, IPR2023-01347
Page 801 of 4460

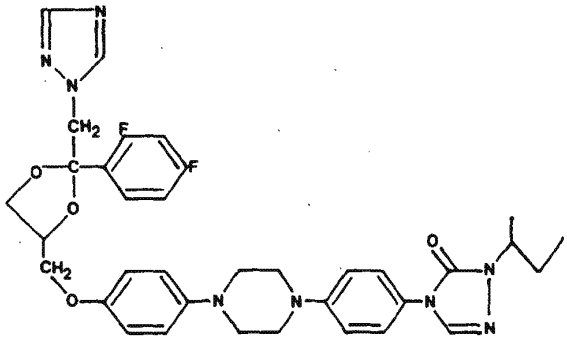


Figure 1. Saperconazole (R 66 905): molecular weight = 673 Da.

medium without glutamine (Gibco), buffered at pH 7·2 with 0·02 M HEPES and gelled with agar (16 g/l). Saperconazole was prepared as a 100 × concentrated stock solution in dimethyl sulphoxide (DMSO), and stock dilutions in DMSO were added to molten agar media at 56°C to give final drug concentrations over the range 0·1 to 100 mg/l. The final concentration of DMSO was therefore 1% (v:v), at which level no inhibitory effects of the solvent were noted: DMSO was routinely included in drug-free control media at this concentration. Ketoconazole was used as the reference compound in the same way as saperconazole.

Relative inhibition factors (RIFs) were determined as previously described (Odds & Abbott, 1984) with ketoconazole again used as the reference compound. The RIF tests were performed in duplicate. Effects of saperconazole on hyphal branching in *C. albicans* were determined with strain 73/055 as previously described (Odds *et al.*, 1985; Odds, Cheesman & Abbott, 1986). No reference compound was tested in these experiments.

Results

MICs of saperconazole and ketoconazole for a selection of fungal pathogens are summarized in Table I. Saperconazole was less active than ketoconazole against *C. albicans* on both the test media, although the MICs of both compounds were similar for other *Candida* species. Against *Aspergillus* species, saperconazole possessed impressive inhibitory activity, with MICs for all isolates below the minimum concentration of compound tested. The MICs of saperconazole for dermatophytes were generally higher than those of ketoconazole.

RIFs for saperconazole and ketoconazole against the panel of test fungi are summarized in Table II. In terms of RIF, the two compounds possessed broadly similar activity against all the *Candida* species tested, but saperconazole was notably superior to ketoconazole against *Aspergillus* and dermatophyte isolates. The data for saperconazole suggest an even greater anti-aspergillus activity for saperconazole than for itraconazole, which was previously found to have a mean RIF of 25% against the same *Aspergillus* isolates.

The inhibitory effects of saperconazole against hyphal branching in *C. albicans* revealed behaviour characteristic of the more recent azole compounds (Table III). It showed less activity than ketoconazole at 10^{-9} M, less activity than itraconazole at

UM00012056
NOVARTIS EXHIBIT 1517
Novartis v. Regents, IPR2023-01347
Page 802 of 4460

Table I. Minimal inhibitory concentrations (MICs) of saperconazole and ketoconazole against pathogenic fungi *in vitro*. Tests were done on yeast nitrogen base/glucose (YNBG) agar, pH 7·0 and on Eagle's minimal essential medium (EMEM) agar, 7·2

Fungal species	Medium	no.	Ketoconazole MICs (mg/l) range	gmean[a]	MIC_{50}[b]	MIC_{90}[a]	Saperconazole MICs (mg/l) range	gmean[a]	MIC_{50}[b]	MIC_{90}[a]
C. albicans	YNBG	20	6·3–50	14·0	12·5	25·0	6·3–>100	>100	>100	>100
	EMEM	20	0·4–50	15·0	25·0	50·0	0·1–>100	33·0	100·0	>100
Candida spp.	YNBG	12	0·1–25	0·7	0·4	25·0	0·1–>100	0·7	0·2	>100
	EMEM	9[b]	0·1–6·3	0·3	0·2	6·3	0·1–50	0·2	0·1	50·0
Aspergillus spp.	YNBG	8	0·4–6·3	2·1	3·2	6·3	<0·1	<0·1	<0·1	<0·1
	EMEM	8	3·2–12·5	8·9	12·5	12·5	<0·1	<0·1	<0·1	<0·1
Dermatophytes	EMEM	6	0·8–6·3	2·3	3·2	6·3	3·2–25	11·0	12·5	25·0

[a]Geometric mean; [b]three isolates of *C. glabrata* did not grow on EMEM.

UM00012057

NOVARTIS EXHIBIT 1517
Novartis v. Regents, IPR2023-01347
Page 803 of 4460

Table II. Relative inhibition factors (RIFs) of ketoconazole and saperconazole against pathogenic fungi *in vitro*

Fungal species	No.	Ketoconazole RIFs (%) range	Ketoconazole RIFs (%) mean ± S.E.M.	Saperconazole RIFs (%) range	Saperconazole RIFs (%) mean ± S.E.M.
C. albicans	16	33–76	51 ± 3	33–76	51 ± 4
Candida spp.	12	39–74	57 ± 3	31–68	47 ± 4
Aspergillus spp.	8	42–75	61 ± 4	6–18	14 ± 1
Dermatophytes	6	7–28	17 ± 3	5–10	7 ± 1

Table III. Effects of saperconazole on hyphal branching in *C. albicans* strain 73/055. Hyphae were grown for 7·5 h at 37°C in EMEM pH 7·3 containing various concentrations of saperconazole, then numbers of hyphal branches per mycelium were counted for determination of % inhibition of branching. Figures for other antifungals are historical data from Odds *et al.* (1985, 1986)

Antifungal	% reduction in branches/mycelium at: 10^{-9} M	10^{-8} M	10^{-7} M	10^{-6} M	10^{-5} M
Saperconazole	15	23	88	86	94
Fluconazole	NT[a]	2	15	94	98
Ketoconazole	74	98	94	96	98
Itraconazole	25	95	88	94	97

[a]Not tested.

10^{-8} M and more activity than fluconazole at 10^{-7} M. Comparison with historical data on hyphal branching was considered reliable since the effects of ketoconazole on hyphal branching in *C. albicans* 73/055 have been found consistently reproducible over a period of four years.

Discussion

Saperconazole behaves in a broadly similar manner to itraconazole, to which it is closely related chemically, in terms of its antifungal activity *in vitro*. Its activity *in vitro* against *Aspergillus* species, however, is clearly superior to that of itraconazole, the RIFs of which ranged from 19 to 30% in studies from this laboratory (Odds *et al.*, 1984). This compound seems to have the potential to be a useful addition to the range of azole antifungals available for oral treatment of mycoses.

References

Odds, F. C. & Abbott, A. B. (1984). Relative inhibition factors—a novel approach to the assessment of antifungal antibiotics *in vitro*. *Journal of Antimicrobial Chemotherapy* **13,** 31–43.

Odds, F. C., Cheesman, S. L. & Abbott, A. B. (1986). Antifungal effects of fluconazole (UK 49858), a new triazole antifungal, *in vitro*. *Journal of Antimicrobial Chemotherapy* **18,** 473–8.

Odds, F. C., Cockayne, A., Hayward, J. & Abbot, A. B. (1985). Effects of imidazole- and triazole-derivative antifungal compounds on the growth and morphological development of *Candida albicans* hyphae. *Journal of General Microbiology* **131,** 2581–9.

UM00012058
NOVARTIS EXHIBIT 1517
Novartis v. Regents, IPR2023-01347
Page 804 of 4460

Odds, F. C., Webster, C. E. & Abbott, A. B. (1984). Antifungal relative inhibition factors: BAY-1–9139, bifonazole, butoconazole, isoconazole, itraconazole (R 51211), oxiconazole, Ro 14–4767/002, sulconazole, terconazole and vibunazole (BAY n–7133) compared *in vitro* with nine established antifungal agents. *Journal of Antimicrobial Chemotherapy* **14**, 105–14.

Shadomy, S. & Espinel-Ingroff, A. (1980). Susceptibility testing with antifungal drugs. In *Manual of Clinical Microbiology*, 3rd edn. (Lennette, E. H., Balows, A., Hausler, W. J. & Truant, J. P., Eds), pp. 647–653. American Society for Microbiology, Washington, DC.

Van Cutsem, J. & Janssen, P. A. J. (1988). Oral and parenteral treatment of invasive aspergillosis in non-predisposed and in immunocompromised guinea pigs with saperconazole (R66905) and parenteral treatment with amphotericin B. In *Program and Abstracts of the Twenty-Eighth Interscience Conference on Antimicrobial Agents and Chemotherapy, Los Angeles, 1988*. Abstract 176, p. 141. American Society for Microbiology, Washington, DC.

(*Received 10 April 1989; accepted 18 May 1989*)

UM00012059

NOVARTIS EXHIBIT 1517
Novartis v. Regents, IPR2023-01347
Page 805 of 4460

This Page is Inserted by IFW Indexing and Scanning Operations and is not part of the Official Record

BEST AVAILABLE IMAGES

Defective images within this document are accurate representations of the original documents submitted by the applicant.

Defects in the images include but are not limited to the items checked:

- ☐ BLACK BORDERS
- ☐ IMAGE CUT OFF AT TOP, BOTTOM OR SIDES
- ☐ FADED TEXT OR DRAWING
- ☐ BLURRED OR ILLEGIBLE TEXT OR DRAWING
- ☐ SKEWED/SLANTED IMAGES
- ☐ COLOR OR BLACK AND WHITE PHOTOGRAPHS
- ☐ GRAY SCALE DOCUMENTS
- ☐ LINES OR MARKS ON ORIGINAL DOCUMENT
- ☐ REFERENCE(S) OR EXHIBIT(S) SUBMITTED ARE POOR QUALITY
- ☐ OTHER: _____

IMAGES ARE BEST AVAILABLE COPY.
As rescanning these documents will not correct the image problems checked, please do not report these problems to the IFW Image Problem Mailbox.

PA/4524/28456

J|A|C|S COMMUNICATIONS

Published on Web 06/21/2003

Crystal Engineering of Novel Cocrystals of a Triazole Drug with 1,4-Dicarboxylic Acids

Julius F. Remenar,*,† Sherry L. Morissette,† Matthew L. Peterson,† Brian Moulton,‡ J. Michael MacPhee,† Héctor R. Guzmán,† and Örn Almarsson†

Transform Pharmaceuticals, Inc., 29 Hartwell Avenue, Lexington, Massachusetts 02421-3102, and Department of Chemistry, University of South Florida, Tampa, Florida 33620-5205

Received April 24, 2003; E-mail: jremenar@transformpharma.com

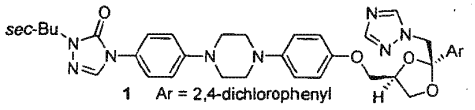
Crystal engineering of pharmaceutical solids represents a fertile, emerging area of research.[1,2] The impetus for discovery of diverse crystal forms of drugs stems from the critical need to balance stability, bioavailability, and other performance characteristics, and also to provide valuable intellectual property protection. In the case of poorly water-soluble drugs, the dissolution rate and oral absorption of the compound can be strongly influenced by the physical state of the drug.[3] Current strategies to deal with inadequate solubility, dissolution rate, and absorption of neutral crystal forms include salt formation,[4] physical stabilization of amorphous solids,[5] complexation,[6-8] or encapsulation of organic solutions.[9] The use of a crystalline solid is nearly always the best approach for limiting physical and chemical instability of a marketed drug.[5] In addition to stability and bioavailability, crystal form characteristics such as morphology and moisture sorption can impact pharmaceutical development. The challenges of pharmaceutical research and development provide a unique opportunity to showcase the power and utility of crystal engineering to solve real-world problems.[10]

Itraconazole (**1**) is an example of an extremely water-insoluble antifungal drug that is marketed in the amorphous form (Sporanox capsule) to achieve the required oral bioavailability (Table 1).[11] Co-administration of acidic beverages with Sporanox capsules is required to achieve maximum absorption of the weak base.[12] Although the use of an acid addition salt would seem to be a logical strategy for improving the absorption properties of **1**, a survey of the patent literature failed to reveal specific reports of crystalline salts of **1**. Solution chemistry suggests that a pK_a difference of two units between acid and base is needed to form a salt that is stable in water.[13] Given the pK_a value of 3.7 for the piperazine of **1**, conventional wisdom would limit a salt screen to those strong acids having dissociation constants below 1.7. However, recent examples[1,2] illustrate that crystalline phases can be engineered by combining molecules[14] selected to match hydrogen-bond donors with acceptors and by considering structural complementarities. In short, it is becoming clear that supramolecular synthesis[15] can be applied to active pharmaceutical ingredients in the same way that it has been applied in model compounds.[16] These systems, referred to as cocrystals, could be extended to include organic acid and base combinations with pK_a differences that are inconsistent with salt formation in water. On the basis of these premises, a high-throughput (HT) crystallization screen was conducted to search for salts and cocrystals of **1** with a large number of pharmaceutically acceptable acids, which were chosen to provide a wide range of dissociation constants, shapes, sizes, and heterosynthons.

We report here the discovery of stable cocrystals consisting of hydrogen-bonded trimers of two molecules of **1** and one molecule of a 1,4-dicarboxylic acid resulting from a HT crystallization screen

† Transform Pharmaceuticals, Inc.
‡ University of South Florida.

Table 1. Cocrystal Forms of *cis*-Itraconazole (**1**)



1 Ar = 2,4-dichlorophenyl

$[\mathbf{1}]_2$X	X	$[\mathbf{1}]_2$X	X
2a	fumaric acid	**2d**	L-tartaric acid
2b	succinic acid	**2e**	D-tartaric acid
2c	L-malic acid	**2f**	DL-tartaric acid

for **1**. The crystal structure of one congener (Figure 1) reveals an unanticipated and specific interaction between the triazole of **1** and the diacid in the solid state, which suggests a new heterosynthon for cocrystallizing triazole-containing compounds into binary (and potentially higher order) phases.[17]

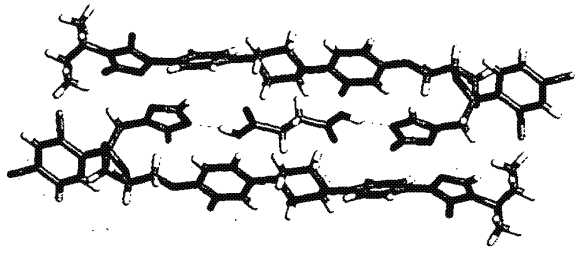


Figure 1. Trimer unit of **2b** from the single-crystal X-ray structure.

Multicomponent crystals of **1** formed from polar aprotic solvents or solvent mixtures of hydrocarbons with polar aprotic solvents and required the presence of dicarboxylic acids. Polar protic solvents, including water and C_{1-3} alcohols, yielded only crystalline free base of **1**, suggesting that H-bond donating solvents interfere with cocrystal formation. Likewise, no salts or cocrystal forms of **1** were found with monoprotic carboxylic acids, such as acetic and benzoic acid. The ratio of **1** to diacid in the binary phases of **1** with fumaric acid (**2a**) and DL-tartaric acid (**2f**) was shown to be 2:1 by solution ^{1}H NMR of dissolved crystal samples. Thus, it appeared that 1 equiv of a dicarboxylic acid was tethering two drug molecules. Additional diacid−**1** combinations, selected on the basis of their similarity to fumaric and tartaric acid, containing 0.5 equiv of diacid relative to **1** yielded crystalline compounds **2b**−**2e** from THF. Compound **2b** is perhaps the most surprising of these, because succinic acid has pK_a values of 4.2 and 5.6, both of which exceed the pK_a of the conjugate acid of **1**. Maleic acid, with *Z* regiochemistry around the C=C bond, is the only 1,4-dicarboxylic acid tested that has not produced cocrystals with **1**, despite being the strongest acid (pK_{a1} of 1.9). Cocrystals could not be made with **1** and malonic, glutaric, or adipic acid. The results indicate that

10.1021/ja035776p CCC: $25.00 © 2003 American Chemical Society

UM00012061

NOVARTIS EXHIBIT 1517
Novartis v. Regents, IPR2023-01347
Page 807 of 4460

geometric fit may be more important than acid−base chemistry in directing crystallization of **1** with 1,4-dicarboxylic acids.

Hexagonal platelike crystals of **2b** were grown for single-crystal X-ray structure determination from a solution in 10/2/1 1,2-dichloroethane/ethyl acetate/1,4-dioxane. Figure 1 shows the trimeric building block from the single-crystal structure. The two molecules of **1** are oriented in antiparallel fashion to form a pocket with a triazole at either end. The extended succinic acid molecule fills the pocket, bridging the triazole groups.[18] Interestingly, interaction between the 1,4-diacid and the strongest base on **1** (piperazine) is absent in the structure of **2b**, but we cannot rule out an interaction of the α hydroxyl groups on tartaric or malic acid with the piperazine nitrogens.[19] There are no current examples of a 1,2,4-triazole-1,4-dicarboxylic acid cocrystal structure in the Cambridge Structural Database (CSD).[20] It should be noted that the crystal structure contains only two of the four stereoisomers of **1**; studies probing enantiomeric enrichment are ongoing.

Identification of multiple crystal forms of the same drug with acceptable solubility, dissolution, and stability allows for selection of the optimal form for dosage form development. To demonstrate this feature, the dissolution of the cocrystals in aqueous medium was studied to assess their potential impact on bioavailability of the drug from a solid dosage form. Figure 2 compares the dissolution profiles of **2b**−**d** into 0.1 N HCl to those of crystalline **1** (95% of all crystalline particles < 10 μm) and commercial Sporanox beads (amorphous **1**). Crystal form **2c** rivals the dissolution of the commercial product containing amorphous **1**. In general, the cocrystals behave more similarly to Sporanox than to crystalline **1**. The cocrystal forms achieve and sustain from 4- to 20-fold higher concentrations than that achieved from crystalline **1**. The practical implication is significant, because the ability to form a supersaturated solution, even transiently, can have a dramatic impact on absorption and bioavailability.[21]

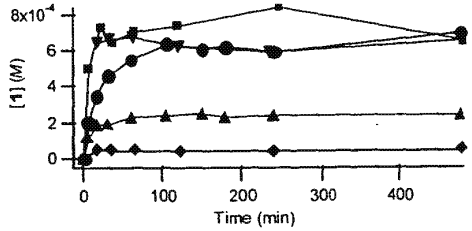


Figure 2. Dissolution profiles into 0.1 N HCl at 25 °C for Sporanox beads (■), **2c** (▼), **2d** (●), **2b** (▲), and **1** (◆).

Crystal morphology and particle size are important for handling of a drug substance and for reliable manufacture of dosage forms with uniform drug content. The morphology of the cocrystals of **1** ranges from fine needles for **2a** and **2d**−**f**, to needles or rectangular plates for **2c**, and hexagonal plates for **2b**. Form **2b** is particularly easy to filter and dry to a free-flowing powder.

In conclusion, cocrystals of **1** possessing diverse physical properties have been engineered on the basis of structures identified from HT crystallization. The solubility and dissolution properties of cocrystals can be similar to those of the amorphous compound and superior to the crystalline pure phase, thus presenting opportunities to increase bioavailability even in cases where stable, crystalline salt forms cannot be found. It is clear that satisfying the geometric constraints is a criterion of cocrystal formation and must be considered when attempting to tailor crystal forms. The observation that the acid moieties in **2b** do not associate with the strongest base in **1** is inconsistent with the principle of strongest-to-strongest interactions dominating self-assembly.[22] Differences in pK_a in water may not reliably predict interactions in the solid state or the capacity for a drug and salt-former to form cocrystals. Thus, studies limited to systems that follow the generally accepted rules of matching pK_a values to ensure a strong salt pair in water are likely to overlook real opportunities for producing optimal medicines with minimal process and formulation issues.

Acknowledgment. The authors wish to thank Profs. Joel Bernstein, Leslie Leiserowitz, and Roger Davey for helpful discussions.

Supporting Information Available: Micrographs and powder X-ray diffraction patterns for **2a**−**2f** (PDF); crystallographic data from **2b** (CIF). This material is available free of charge via the Internet at http://pubs.acs.org.

References

(1) Walsh, B. R. D.; Bradner, M. W.; Fleischman, S.; Morales, L. A.; Moulton, B.; Rodríguez-Hornedo, N.; Zaworotko, M. J. *Chem. Commun.* **2003**, 186−187.
(2) Oswald, I. D. H.; Allan, D. R.; McGregor, P. A.; Motherwell, W. D. S.; Parson, S.; Pulham, C. R. *Acta Crystallogr., Sect. B: Struct. Crystallogr. Cryst. Chem.* **2002**, *B58*, 1057−1066.
(3) Hörter, D.; Dressman, J. B. *Adv. Drug Delivery Rev.* **1997**, *25*, 3−14.
(4) *Handbook of Pharmaceutical Salts*; Stahl, P. H., Wermuth, C. G., Eds.; Verlag Helvetica Chimica Acta; Zürich and Wiley-VCH: Weinheim, 2002; Chapter 6.
(5) Byrn, S. R.; Pfeiffer, R. R.; Stowell, J. G. *Solid-State Chemistry of Drugs*; SSCI Inc.: West Lafayete, IN, 1999; p 250.
(6) Kataoka, K.; Harada, A.; Nagasaki, Y. *Adv. Drug Delivery Rev.* **2001**, *47*, 113−131.
(7) Loftsson, T.; Brewster, M. E. *J. Pharm. Sci.* **1996**, *85*, 1017−1025.
(8) Uekama, K.; Otagiri, M. *Crit. Rev. Ther. Drug Carrier Syst.* **1987**, *3*, 1−40.
(9) Walker, S. E.; Ganley, J. A.; Bedford, K.; Eaves, T. *J. Pharm. Pharmacol.* **1980**, *32*, 389−393.
(10) Seddon, K. R.; Zaworotko, M. *Crystal Engineering: The Design and Application of Functional Solids*; NATO-ASI Series; Kluwer: Norwell, MA, 1999; Vol. 539.
(11) Sporanox capules (made by Janssen Pharmaceutica) contain amorphous itraconazole coated on 0.4−0.5 mm diameter sucrose spheres. Other inactive ingredients include hydroxypropyl methylcellulose, poly(ethylene glycol) (PEG) 20 000, and starch.
(12) Only about 30% bioavailability of **1** is achieved from commercial Sporanox capsules under optimal conditions, while up to 55% can be absorbed from the marketed solution formulation in acidified HP-β-cyclodextrin (Physician's Desk Reference, Electronic Library, Thomson MicroMedex Inc., 2003).
(13) Serajuddin, A. T. M.; Pudipeddi, M. In *Handbook of Pharmaceutical Salts*; Stahl, P. H., Wermuth, C. G., Eds.; Verlag Helvetica Chimica Acta: Zürich and Wiley-VCH: Weinheim, 2002; p 138.
(14) Aakeröy, C. B.; Beatty, A. M.; Helfrich, B. A. *Angew. Chem., Int. Ed.* **2001**, *40*, 3240−3242.
(15) Desiraju, G. R. *Angew. Chem., Int. Ed. Engl.* **1995**, *34*, 2311−2327.
(16) Moulton, B.; Zaworotko, M. J. *Chem. Rev.* **2001**, *101*, 1629−1658.
(17) $2(C_{35}H_{38}Cl_2N_8O_4)\cdot C_4H_6O_4$; $P2_1/c$; a = 30.145(4) Å, b = 5.7435(7) Å, c = 21.580(3) Å, β = 105.133(2)°; Z = 4; T = 100(2) K; GOF = 1.010; R^2 = 0.0925; wR^2 = 0.2153.
(18) The bond distances (N···O = 2.755 Å and (C=O)O−H = 0.925 Å) and the N···H−O bond angle (170.4°) are consistent with a hydrogen-bonding interaction between the 4-nitrogen of each 1,2,4-triazole and a carboxylic acid moiety. The carboxylic acid bond distances (C1B···O1B = 1.205(5) Å and C1B···O2B = 1.326(4) Å) indicate that the acid proton has not been transferred to the triazole. Furthermore, a peak consistent with intensity normally observed for protons was located from the difference map at 0.961(2) Å from O2B along the O2B···N3 vector.
(19) In the crystal structure of Figure 1, the α carbon pro-S hydrogen of succinic acid that is closest to a piperazine nitrogen is 2.65 Å, and the angle is 131°.
(20) A search of the CSD using ConQuest v. 1.5 revealed one example of intermolecular hydrogen bonding between a triazole and a carboxylic acid (REFCODE KOPSOX) and seven examples where a triazole is protonated by a carboxylic acid. There are many examples of hydrogen-bonding interactions between carboxylic acids and heterocyclic nitrogen in the CSD.
(21) Kwei, G. Y.; Novak, L. B.; Hettrick, L. A.; Reiss, E. R.; Ostovic, D.; Loper, A. E.; Lui, C. Y.; Higgins, R. J.; Chen, I. W.; Lin, J. H. *Pharm. Res.* **1995**, *12*, 884−888.
(22) Etter, M. C. *Acc. Chem. Res.* **1990**, *23*, 120−126.

JA035776P

UM00012062
NOVARTIS EXHIBIT 1517
Novartis v. Regents, IPR2023-01347
Page 808 of 4460

14

Advances in the Chemistry of Novel Broad-Spectrum Orally Active Azole Antifungals: Recent Studies Leading to the Discovery of SCH 56592

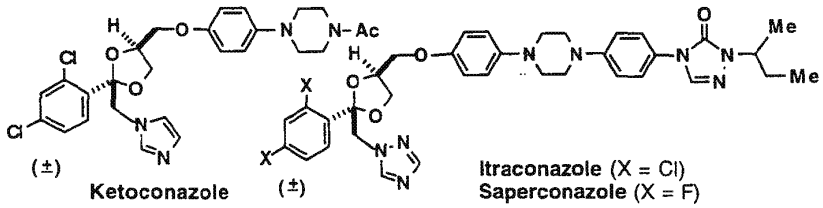
A. K. Saksena,* V. M. Girijavallabhan, R. G. Lovey, R. E. Pike, H. Wang, Y. T. Liu, P. Pinto, F. Bennett, E. Jao, N. Patel, J. A. Desai, D. F. Rane, A. B. Cooper and A. K. Ganguly

SCHERING-PLOUGH RESEARCH INSTITUTE, KENILWORTH, NJ 07033, USA

INTRODUCTION

Therapeutic breakthroughs in certain areas of medicine (e.g. diabetes mellitus, cancer chemotherapy, extensive surgery and organ transplantation) have created a sharp increase in the number of immunocompromised hosts highly susceptible to systemic fungal infections. Widespread incidence of life threatening *Candidiasis, Cryptococcosis* and *Aspergillosis* in patients with AIDS has underscored the need for safe and efficacious antifungal agents.

In marked contrast to other antiinfectives, the pace of discovery of newer antifungals for systemic infections has been rather slow. Thus for over forty years, Amphotericin B (AMB) remains the only broad-spectrum drug for the management of most systemic infections. However, severe toxicity of amphotericin B continues to be a major problem not easily dealt with even today.[1]



The Azole Antifungals: Two decades of early research in the azole area led to only topically active agents until ketoconazole (KTZ, Janssen) the first orally effective agent was introduced into clinical practice. However, some of the side effects associated with prolonged therapy with KTZ (e.g., hepatotoxicity and testosterone biosynthesis inhibition) result from marked inhibition of mammalian cytochrome P-450-dependent enzymes. Due to the very nature of fungal growth inhibition by azoles, specific binding to fungal rather than mammalian cytochrome P-450 is imperative. Itraconazole (ITZ, Janssen), a relatively selective inhibitor of fungal cytochrome P-450, now in clinical use, offers certain advantages over ketoconazole in terms of oral efficacy, broader spectrum and fewer side effects.

UM00012063
NOVARTIS EXHIBIT 1517
Novartis v. Regents, IPR2023-01347
Page 809 of 4460

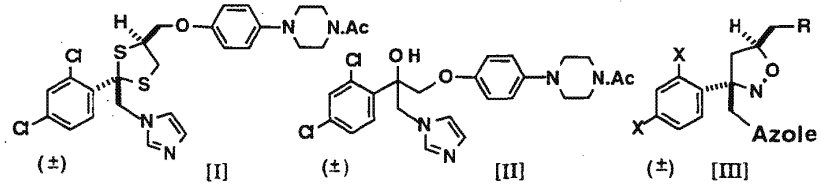
ITZ is the most effective azole for the treatment of *Aspergillosis*.[2] Fluconazole (FLZ, Pfizer), the most recently introduced azole is a relatively narrow spectrum agent used extensively against *Candida* and *Cryptococcus* infections.[3] However it lacks efficacy against *Aspergillus* infections. There have been increasing reports of FLZ resistance in AIDS patients with oropharyngeal and/or esophageal *Candidiasis;* resistance to FLZ in *Cryptococcus neoformans* has also been reported.[4a,b]

OBJECTIVES:

At Schering-Plough we sought to develop a novel antifungal agent with broad-spectrum activity against the key pathogens *Candida, Histoplasma, Cryptococcus, Blastomyces* and *Aspergillus* with reduced host toxicity. The new agent should not be a P-450 enzyme inducer, should have superior activity against *Aspergillus* versus ITZ and comparable activity against *Candida* versus FLZ and ITZ. In view of reported emergence of intrinsically FLZ resistant strains of *C. glabrata* and *C. krusei,*[4a,b] activity against these pathogenic strains would also be a very desirable attribute in a new azole antifungal. Further, where oral administration is impractical such as in critically ill AIDS and cancer patients, a water soluble version of the new clinical entity would be of definite advantage.

THE NATURE OF THE PROBLEM

The major features common to the three Janssen azoles viz KTZ, ITZ and SPZ include a trisubstituted 1,3-dioxolane having a defined *cis*-relationship between a azolyl methyl group and a lipophilic phenylpiperazinyl moiety. Early work on new analogs based on Janssen leads in several laboratories centered on a combination of azolylmethyl and phenylpiperizinyl group either in a dithiolane ring [I] or in conformationally mobile acyclic systems [II]. These analogs as well as several hundred isoxazolidines [III] incorporating elements of Janssen azoles did not provide a single analog worthy of preclinical evaluation.[3]



(±) [I] (±) [II] (±) [III]

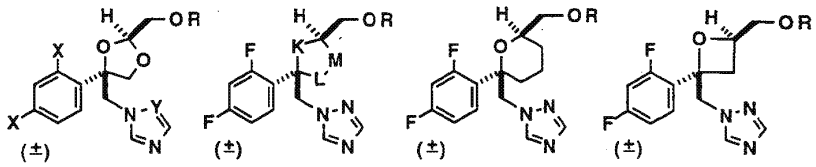
WORKING HYPOTHESIS:

The ketal functionality present in Janssen azoles has the potential to get at least partially inactivated in the stomach by acid hydrolysis. Any modification that would inhibit such inactivation but retain other physicochemical properties, may provide agents with improved absorption and efficacy.

Early Explorations: [5] In meeting the above criteria, it was of interest to explore whether novel analogs of the type **A**, but especially types **B** to **F** would have certain desirable attributes in terms of oral potency, antifungal spectrum,

UM00012064
NOVARTIS EXHIBIT 1517
Novartis v. Regents, IPR2023-01347
Page 810 of 4460

pharmacokinetics and lack of toxicity. Oxygen containing heterocycles being relatively flexible, it was not apparent at the outset in what manner the subtle conformational differences between these analogs would be reflected in their *in-vivo* (PO) antifungal profile.



A: X = F; Cl
Y = N; CH

B: K=O; L=M=CH_2
C: L=O; K=M=CH_2
D: M=O; K=L=CH_2

E

F

Chemistry involved in the stereoselective construction of these ring systems having a defined *cis* relationship between the triazolylmethyl and the nonligating lipophilic groups (OR") was not well documented. A logical understanding of structure-activity relationship also placed an important constraint that we bring about only one change at a time; in the present context the nature of the central ring.

In early studies we had shown that the acetal analogs of the type **A** were equiactive to KTZ *in-vitro* and *in-vivo* (topical; *Candida*). Although at least two analogs from this series had oral activity comparable to KTZ and ITZ, their level of activity at 100 mpk did not offer ample prospects for any further improvement.

Based on our original premise, the tetrahydrofurans of the types **B-D** were likely to be even more stable in a hydrolytic/metabolic sense. We were encouraged to find that these compounds were clearly more active than the type **A** analogs in mouse *Candida* as well as *Aspergillus* models. Of further interest is the fact that analogs of the types **B** and **C** were more active than KTZ and ITZ at a dose of 10 mpk; the type **C** being the most active. *This interesting result could not have been predicted at the outset.*

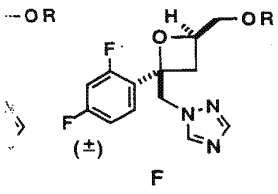
We may draw attention to the fact that Janssen azoles did not provide adequate protection at doses below 100 mpk in the same mouse *Candida* infection model. In contrast even our least active type **D** analogs had excellent protection at 50 mpk.[5c]

Importance of the Central Ring Size: While the above modifications were in progress, we showed that increasing or decreasing the central ring size by one carbon (viz 6 and 4-membered analogs) had a profoundly adverse effect on oral activity.[5, 6] Thus, the importance of a central 5-membered ring was amply demonstrated by the lack of *in-vivo* oral activity of analogs of the types **E** and **F**.

Role of Side Chains: For rapid identification of novel side chains, we had in hand a highly stereoselective route to 2,2,5-trisubstituted tetrahydrofurans via aqueous Diels-Alder reactions of electron deficient 2-aryl furans **1**. Use of an aqueous version of the Diels-Alder reaction made possible isolation of previously inaccessible adducts **2** which were successfully elaborated (via **3**) in a general stereocontrolled route to type **B** analogs.[7] As we did not have an efficient

UM00012065
NOVARTIS EXHIBIT 1517
Novartis v. Regents, IPR2023-01347
Page 811 of 4460

ntaining heterocycles being
in what manner the subtle
uld be reflected in their *in-*



F

uction of these ring systems
lmethyl and the nonligating
A logical understanding of
ant constraint that we bring
ext the nature of the central

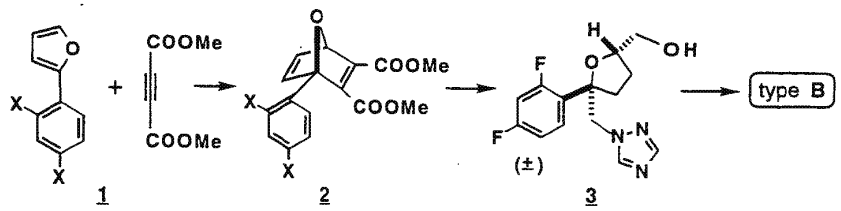
analogs of the type **A** were
lida). Although at least two
o KTZ and ITZ, their level of
ny further improvement.
furans of the types **B-D** were
etabolic sense. We were
more active than the type **A**
els. Of further interest is the
ctive than KTZ and ITZ at a
his interesting result could not

ssen azoles did not provide
ame mouse *Candida* infection
gs had excellent protection at

bove modifications were in
the central ring size by one
undly adverse effect on oral
membered ring was amply
alogs of the types **E** and **F**.

el side chains, we had in hand
etrahydrofurans via aqueous
furans **1**. Use of an aqueous
ble isolation of previously
borated (via **3**) in a general
e did not have an efficient

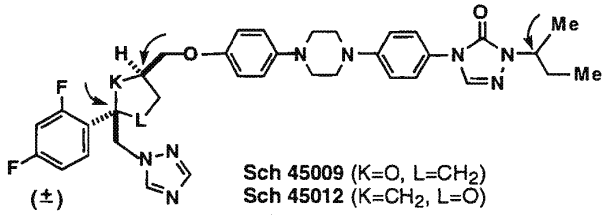
stereoselective route to the more active type **C** compounds at the time, we used type **B** template to introduce a host of side chains. This interim strategy proved invaluable later.



Thus, using type **B** analogs as examples, considerable oral activity was maintained with analogs having diverse side chains. The importance of an aromatic spacer group for oral activity also became clear from these studies. It was also shown that analogs having triazolyl functionality were more active (PO) than those containing imidazolyl group.[5, 7]

INITIAL LEAD: SCH 45012

Following modifications of types **B** and **C** analogs, Sch 45009 and Sch 45012 were synthesized and their activity compared with ITZ and saperconazole (SPZ) in systemic *Candida* and pulmonary *Aspergillus* infection models.[5a, c] Both Sch 45009 and Sch 45012 had comparable broad-spectrum activity *in-vitro*. However, in animal models, Sch 45012 was shown to be more active than Sch 45009, ITZ and SPZ.[5, 8b]

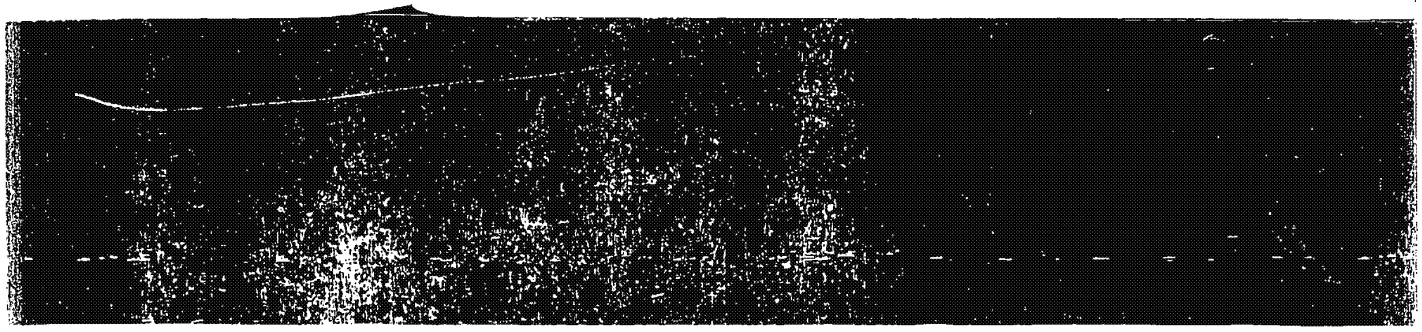


Sch 45009 (K=O, L=CH_2)
Sch 45012 (K=CH_2, L=O)

With its three chiral centers, two in a defined *cis*-stereochemical relationship (arrows), Sch 45012 is a mixture of four optical isomers. Having met our primary objectives, we sought all four stereoisomers of Sch 45012 for detailed biological evaluation and enzyme induction studies.

Chiral Epoxide Route to Sch 45012 Isomers:

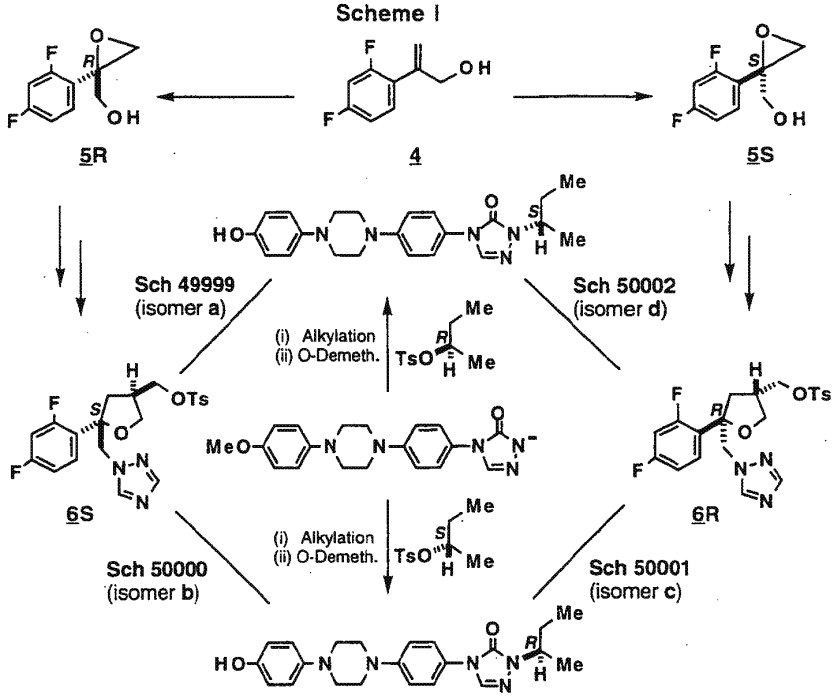
Based on our synthesis of the racemic type **C** analogs, the Sharpless-Katsuki asymmetric epoxidation offered a promising approach. Indeed the readily available allyl alcohol **4** could be converted to both **5R** and **5S** epoxy alcohols which acted as key intermediates to provide respectively the **6S** and **6R** *cis*-tosylates from which all four stereoisomers of (±) Sch 45012 were derived.[8a]



UM00012066
NOVARTIS EXHIBIT 1517
Novartis v. Regents, IPR2023-01347
Page 812 of 4460

Predictable course of the Sharpless-Katsuki asymmetric epoxidation and origin of the chiral side chains from the known (R) and (S)-2-butanols, enabled us to assign relative and absolute stereochemistry to each stereoisomer. Later, the structure of Sch 50002 was also verified by X-ray crystallography.[8d] (Scheme I)

Scheme I



Initial supplies of all four isomers of (±) Sch 45012 provided sufficient material for preliminary *in vitro* and *in vivo* biological evaluation. Results indicated the two (5S)-(+) isomers, Sch 49999 and Sch 50000 to be virtually inactive "dystomers" and the two (5R)-(-) isomers, Sch 50001 and Sch 50002 identified as the two "eutomers" of (±) Sch 45012.[8a, c]

Although we had made significant progress, we were far from a situation to provide sufficiently large quantities of Sch 50001 and Sch 50002 for detailed biological evaluation and enzyme induction studies. *Nonethless, at this point we had discovered an important absolute stereochemistry requirement for optimal oral activity in a given series*.

A Rapid Synthesis of Sch 45012 Isomers via (±) *cis*-Tosylate: The racemic *cis*-tosylate **6**, available in large amounts at the time, when coupled with the phenylpiperazinyl side chains derived from (R) and (S)-2-butanols produced a pair of mixtures. These two-component sets were composed of in each case, the so-called isomers **a/d** (Sch 49999/Sch 50002) and **b/c** (Sch 50000/Sch 50001) respectively. Unlike the original four-component mixture of Sch 45012 isomers,

UM00012067
NOVARTIS EXHIBIT 1517
Novartis v. Regents, IPR2023-01347
Page 813 of 4460

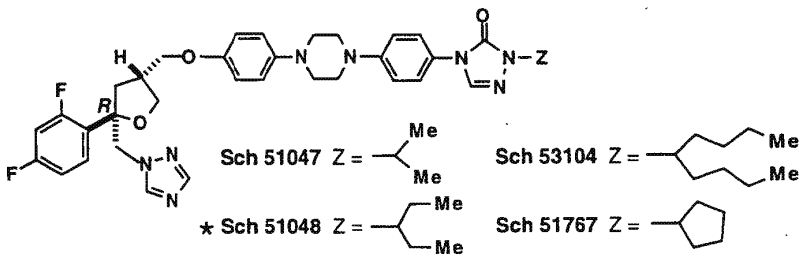
preparative separation of these two pairs on a Chiralcel® OD column proved relatively trivial. In this manner adequate quantities of all four isomers were quickly made available for detailed biology.

SCH 50001 vs SCH 50002

In terms of *in-vitro* activity both Sch 50001 and Sch 50002 were equiactive. Both compounds were devoid of liver P-450 enzyme inducing capability. *In-vivo* however, Sch 50002 was more efficacious (PO) than Sch 50001 in *Candida* as well as *Aspergillus* infection models, both compounds being clearly more efficacious than ITZ and SPZ.[8]

ACHIRAL SIDE CHAIN SUBSTITUTION:

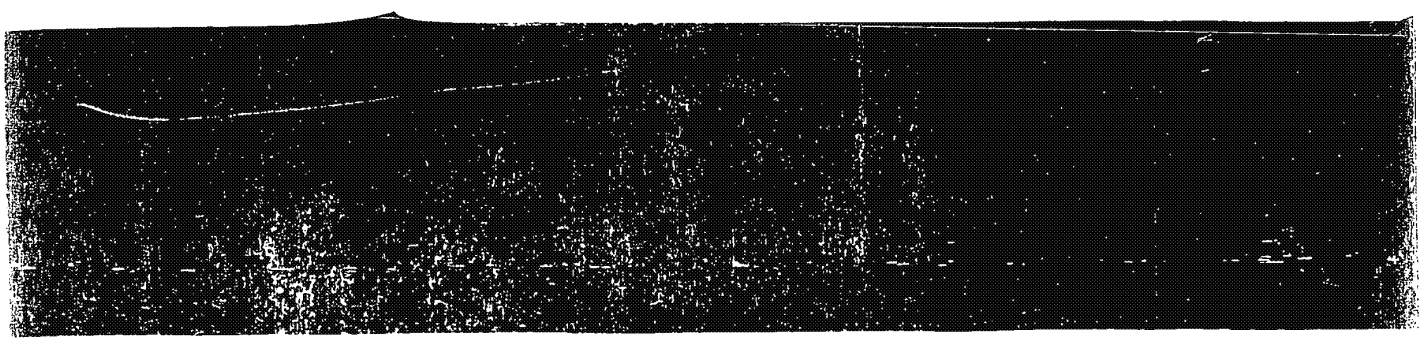
With the identification of Sch 50002 as an excellent lead structure, concerted efforts were devoted to introduction of a variety of side chains. A number of saturated, unsaturated and polar side chains were shown to have excellent *in vitro* activity. In general, branched alkyl chains appeared to have a desirable effect on *in vivo* activity. The presence of either relatively basic or acidic side chains also resulted in profound loss in activity.[9]



SCH 51048, A BROAD-SPECTRUM ANTIFUNGAL:

In a most productive study aimed at elimination of chirality of the side chain of Sch 50002, two analogs, Sch 51047 and Sch 51048 were prepared. Interestingly the 3-pentyl analog, Sch 51048 was found to have greatly improved therapeutic potential over Sch 50002 and other existing drugs against a variety of systemic fungal infections in normal and immunocompromised infection models; the isopropyl analog, Sch 51047 was the least active compound in this comparison. Sch 51767, a conformationally rigid cyclopentyl side-chain analog, was also shown to have reduced albeit significant percent survival compared to ITZ. The lack of activity of Sch 53104 a 9-carbon branched chain analog highlighted the importance of optimal carbon chain length.

Biology of Sch 51048 and other analogs has been discussed in some detail elsewhere.[9] In view of this new development, further efforts on Sch 50002 were curtailed in support of this promising new azole. With one chiral center eliminated from its side chain, Sch 51048 would also be a relatively less expensive compound to synthesize.



UM00012068
NOVARTIS EXHIBIT 1517
Novartis v. Regents, IPR2023-01347
Page 814 of 4460

NEW SYNTHETIC ROUTES TO SCH 51048 AND ANALOGS:

Synthetic problems associated with our original route to the *cis*-tosylate **6R** were mainly associated with our inability to take advantage of the chirality induced at the benzylic carbon via the Sharpless-Katsuki epoxidation, an excellent step by itself. In the meantime a few kg of Sch 51048 was made available for preclinical toxicity by this first route in its original tedious version.

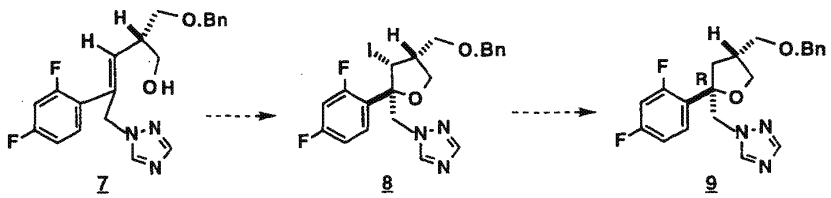
Attempts to overcome these problems required extensive exploratory chemistry culminating in at least three practical enantioselective routes to Sch 51048 and its analogs.

ACYCLIC STEREOSELECTION *VIA* HALOCYCLIZATION :

A conceptually different approach not involving chiral epoxide intermediate was next considered. Halocyclization is an effective way to construct the tetrahydrofuran ring system although stereoselectivity is often difficult to predict or rationalize. The major activity and success in this regard has been in the formation of 2,5-substituted tetrahydrofurans in which the chiral centers in the product bears a 1,3-relationship.[10a] These cyclizations not unexpectedly lead to the thermodyanamically more stable *trans*-products. In contrast Rychnovsky and Bartlett have shown that cyclization of appropriate benzyl ether derivatives can give thermodyanamically less stable *cis*-2,5-substituted tetrahydrofurans with high diastereoselectivity.[10b]

A careful search in the literature led us to conclude that no examples existed of stereoselective halocyclizations leading to the uncommon *2,2,4-cis-trisubstituted tetrahydrofurans* needed in our present studies. In any case we speculated that the bulky 2,4-difluorophenyl substituent on the electrophilic olefinic end may enforce a directive influence in favor of the desired 2,2,4-trisubstituted tetrahydrofurans. Two approaches were investigated which are now described.

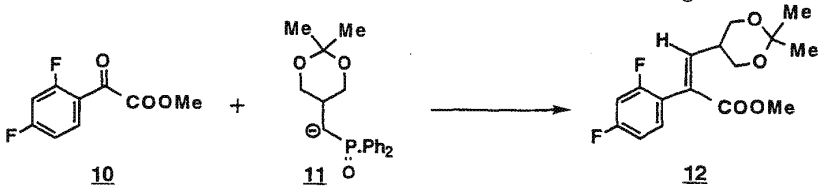
(i) 5-Endo-trig-cyclization Approach: Our original idea was to take advantage of halocyclization of a chiral olefin such as 7. Specific conditions to obtain either 2,5-*cis* or *trans* substituted tetrahydrofurans via 5-endo halo- (and seleno) cyclizations of β-hydroxyalkenes have been described. Interestingly depending on the nature of electrophile, either E or Z olefins could be used in these cases as long as their geometrical homogeniety was ensured.[10c] It appeared *2,2,4-cis-trisubstituted* tetrahydrofurans could also be obtained by application of this methodology.



7 8 9

UM00012069
NOVARTIS EXHIBIT 1517
Novartis v. Regents, IPR2023-01347
Page 815 of 4460

Due to lack of energetic barriers, geometrically homogeneous trisubstituted olefins are all the more difficult to prepare. We succeeded in devising a specific methodology to prepare exclusively the Z olefin **12** by Horner-Wittig reaction of the 2,4-difluorophenyl pyruvate ester **10** with the phosphine oxide **11**.[11] Conversion of **12** to the desired olefin **7** could be foreseen as a straightforward



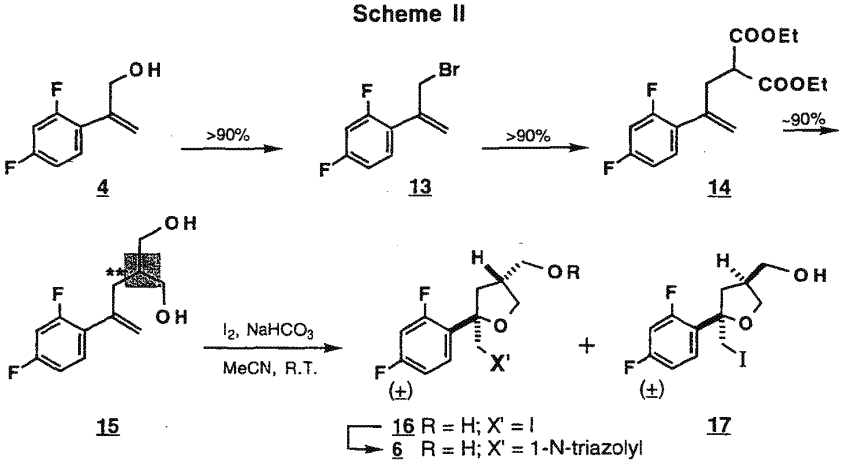
10 11 12

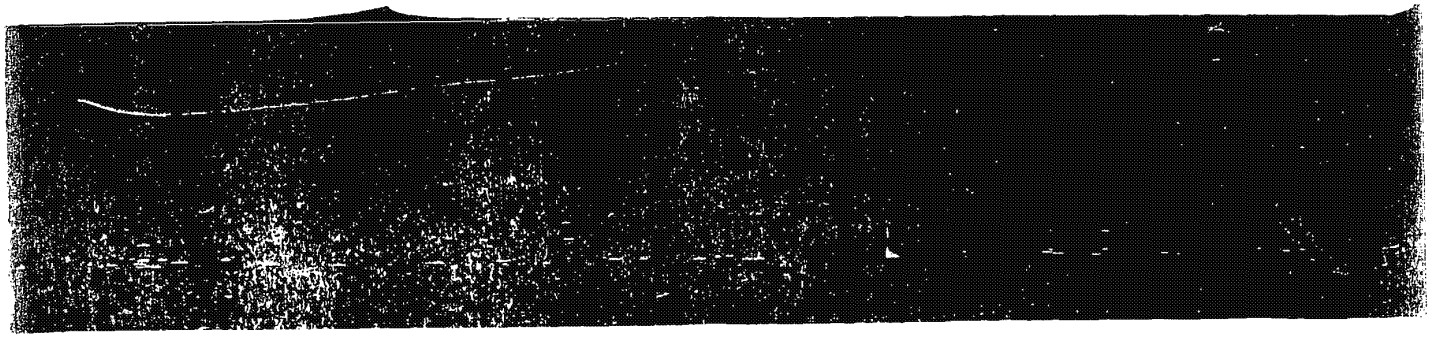
transformation. But we did not pursue this route, as a more promising approach involving a novel 5-exo type halocyclizations emerged.

(ii) 5-Exo-cyclization Approach: While the above studies were in progress, we discovered a unprecedented yet remarkably simple 2,4-diastereoselective 5-exo halocyclization of 2,2-disubstituted olefins.[12] Synthesis of the key olefinic homochiral diol **15** was accomplished quite simply and in high yields from the allyl alcohol **4**. (Scheme II)

In the very first iodocyclization attempt at room temperature, the *cis:trans* ratio of the iodoalcohols **16** and **17** was an impressive 88:12. This stereoselectivity improved at lower temperatures (0°—>5°C) to better than 90:10 in favor of the desired *cis*-diastereomer **16**. An attractive feature of this 5-exo-cyclization approach is that the resulting iodomethyl functionality presents itself as an electrophile for the direct introduction of the azolyl moiety. The scope and limitations of this 2,4-diastereoselective 5-exo-halocyclization process have been discussed elsewhere. The presence of a 2-aryl substituent on the olefinic end appears to dictate the observed 2,4-diastereoselectivity.[12]

Scheme II





UM00012070

NOVARTIS EXHIBIT 1517
Novartis v. Regents, IPR2023-01347
Page 816 of 4460

Displacement of iodine in a neopentyl-like system by the highly nucleophilic triazolyl anion posed no problems. In preliminary experiments, protection of the alcohol functionality during triazole anion displacement was considered necessary only as a precaution to prevent intramolecular oxy-anion displacement of iodine. As we will show later this was found quite unnecessary thus saving two steps. In this manner we accomplished the shortest and most efficient synthesis of the racemic *cis*-tosylate **6**.

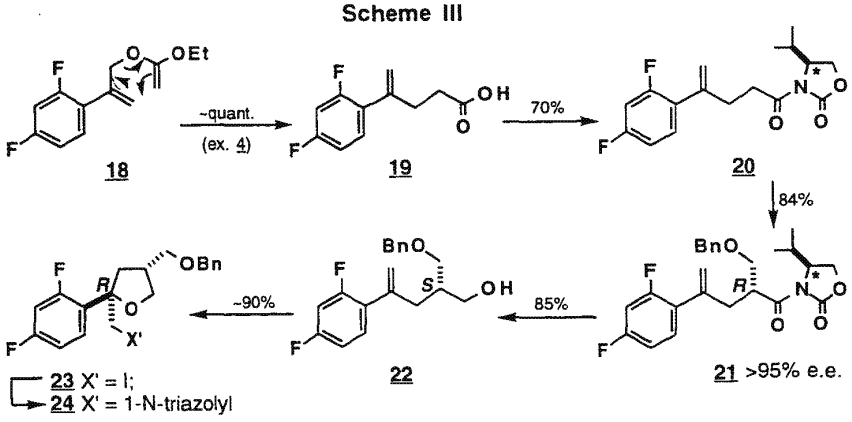
From this success it appeared that we were close to a breakthrough if only we could devise an efficient synthesis of a desymmetrized derivative of the diol **15**. An elegant enzymatic desymmetrization of **15** will be described later. In this conceptually distinct approach, the chiral induction on the benzylic carbon would follow by the very nature of the iodocyclization process.

ASYMMETRIC SYNTHESIS *VIA* CHIRAL IMIDE-ENOLATES:

Enantioselective chemical routes to **6R** (and **6S**) were viewed as being directly accessible via the chiral imide technology developed independently by the Evans[13a] and Oppolzer[13b] groups. A wide choice of electrophiles, excellent diastereoface selective alkylations, and aldol condensations led us to choose Evans' methodology. However it was not clear at the outset in what manner the 2,2-disubstituted olefin functionality placed β to the site of an enolate would influence overall efficiency of electrophilic substitutions; to the best of our knowledge these type of substrates have not been studied earlier.[14]

(a) From Valinol Derived Chiral Auxilliary: In a one-pot sequence, the readily available allyl alcohol **4** was subjected to Claisen-Johnson orthoester rearrangement (via **18**) providing the olefinic acid **19** in virtually quantitative yield. Our first experiments were conducted with lithium enolates of **20** using benzyloxymethyl bromide as the electrophilic reagent. Although high diastereoselectivity of the desired benzyl ether **21** was observed, the chemical yields were unacceptably low (~30%).

Scheme III



UM00012071
NOVARTIS EXHIBIT 1517
Novartis v. Regents, IPR2023-01347
Page 817 of 4460

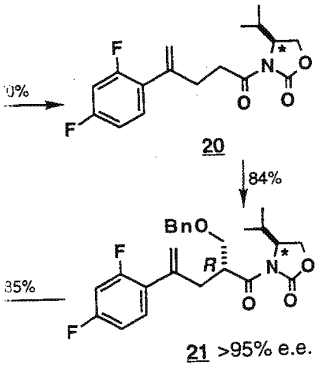
e system by the highly
preliminary experiments,
e anion displacement was
intramolecular oxy-anion
as found quite unnecessary
shed the shortest and most

e to a breakthrough if only
rized derivative of the diol
ll be described later. In this
the benzylic carbon would
is.

IDE-ENOLATES:

re viewed as being directly
ped independently by the
of electrophiles, excellent
ensations led us to choose
e outset in what manner the
e site of an enolate would
tutions; to the best of our
lied earlier.[14]

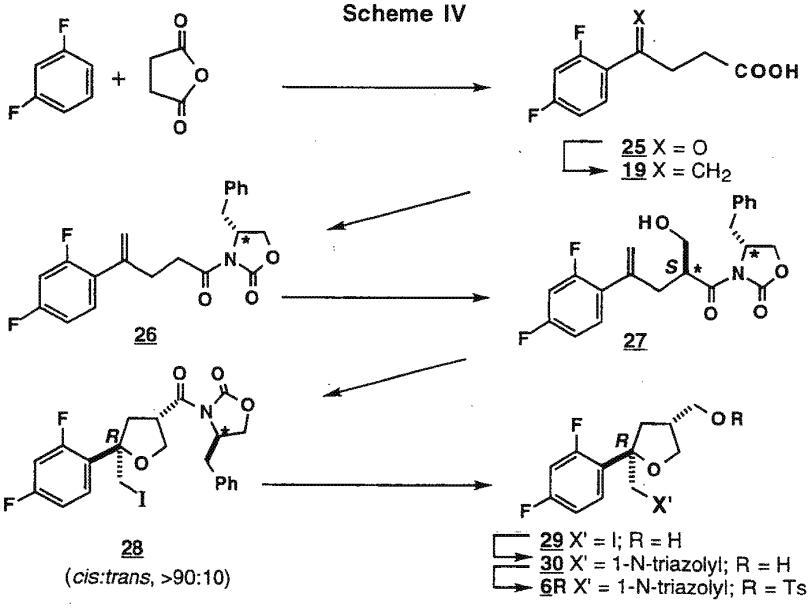
ne-pot sequence, the readily
laisen-Johnson orthoester
19 in virtually quantitative
lithium enolates of 20 using
reagent. Although high
was observed, the chemical



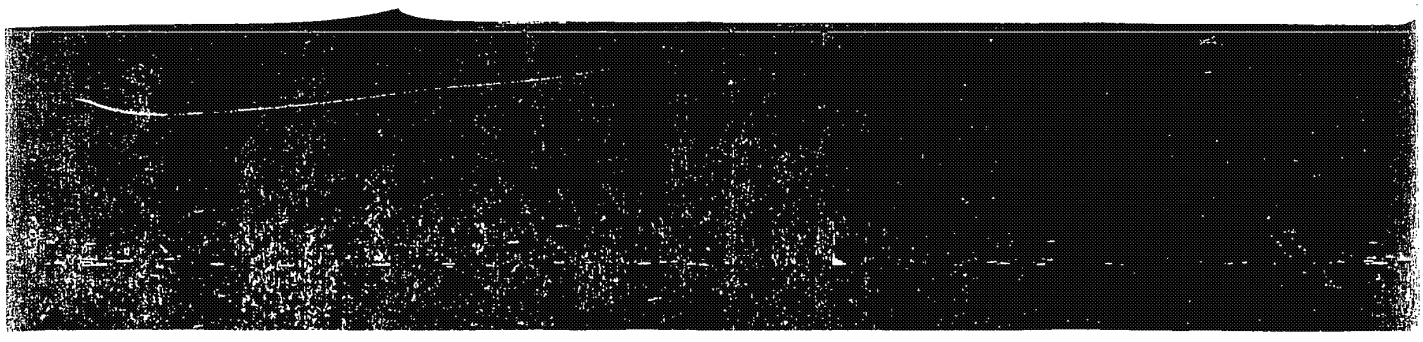
In a marked improvement, alkylation of **20** with benzyloxymethyl chloride via Evans' titanium enolate protocol[13c] gave **21** in excellent yields. Most importantly no isomerization of the 2,2-disubstituted olefin was detected during either lithium or titanium enolate formation, a requirement crucial to success in this chiral imide route to **6R**. Reduction of **21** with LAH in tetrahydrofuran gave the desired (S)-diol monobenzyl ether **22** (85% yield) with the oxazolidinone auxilliary recovered in 70% yield by chromatography. The remaining steps from the iodocyclization onwards proceeded as expected according to Scheme II. Thus the desired (-)-(2R)-*cis*-tosylate **6R** was obtained in excellent yields and over 99% optical purity. (Scheme III)

(b) From Phenylalinol Derived Chiral Auxiliary: The following alternative approach was undertaken as we were keen to avoid yield limiting protection-deprotection operations. The allyl alcohol **4** we had been using so far was prepared in 4-steps from 2,4-difluorobenzene. Thus synthesis of the olefinic acid **19** used above required a total of 6-steps. We were able to obtain **19** in two simple steps by Friedel-Craft reaction of 2,4-difluorobenzene with succinic anhydride to provide the keto acid **25**. Wittig reaction of **25** with 2 equivalents of methylene triphenyl phosphorane then gave **19** in ~60% yield over 2 steps.

Scheme IV



Diastereoface hydroxymethylation of **26** was best carried out with symtrioxane using Evans' titanium enolate protocol to give **27**. The direct iodocyclization of **27** at room temperature with a high degree of diastereoselectivity in favor of the desired *cis*-iodo imide **28** is noteworthy. Lithium borohydride reduction of **28** provided the iodoalcohol **29** which was

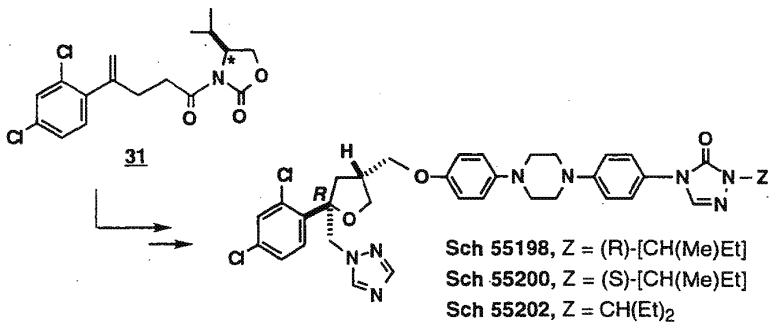


UM00012072
NOVARTIS EXHIBIT 1517
Novartis v. Regents, IPR2023-01347
Page 818 of 4460

displaced directly with sodium-triazole followed by tosylation; the **6R** *cis*-tosylate so obtained was identical in all respects to the authentic material. (Scheme IV)

Notably, as we had hoped, no protecting groups were required throughout this entire sequence. This "protecting group free" new route to **6R** offers excellent opportunity for large scale operations.[14]

Dichloro Analogs: No problems arose in the successful application of the above 2,4-diastereoselective 5-exo iodocyclizations combined with Evans' chiral imide enolate chemistry to prepare the dichloro analogs of Sch 50001, Sch 50002 and Sch 51048. As reported earlier,[12] presence of the bulkier ortho-chlorine substituent considerably slowed down the rate of iodocyclization but the *cis:trans* selectivity was still a respectable 78:28. These dichloro analogs had excellent broad-spectrum antifungal activity *in vitro* but they were found to be less active in animal infection models than the corresponding difluoro analogs.



HYDROXYLATED ANALOGS OF SCH 51048:

In an effort to further improve oral absorption properties of Sch 51048, sythesis of analogs having polar side chains was undertaken. An added incentive behind this investigation was to see if we could prepare water soluble salts and/or derivatives from these polar side chains for possible parenteral use.

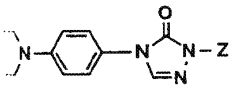
Key Triazolone: A synthesis of the triazolone **35** via a linear sequence was reported earlier.[9] In a more direct approach to this key intermediate, the side chain triazolone **32** was first demethylated, then partially N-SEM protected to provide a suitable fragment **33** which was used to alkylate the *cis*-tosylate **6R**. The resulting N-SEM protected intermediate **34** from this convenient source was used to introduce a variety of side chains. (Scheme V)

Sacrificing methodology development and efficiency for speed, the two isomeric olefins **36** and **37** and the allylic alcohol **38** were converted to the mesylates **39**, **40** and **41** which could be coupled to the triazolone core **35** in the presence of sodium hydride. This effort took barely three weeks to give the resulting three pairs, Sch 55801, Sch 55803 and Sch 55805, in amounts sufficient for MICs. Biological evaluation of these diastereomeric pairs provided unexpectedly promising results. *Thus while introduction of relatively basic or acidic side chains*

UM00012073
NOVARTIS EXHIBIT 1517
Novartis v. Regents, IPR2023-01347
Page 819 of 4460

sylation; the **6R** *cis*-tosylate
c material. (Scheme IV)
s were required throughout
route to **6R** offers excellent

ful application of the above
ed with Evans' chiral imide
ch 50001, Sch 50002 and Sch
r ortho-chlorine substituent
but the *cis:trans* selectivity
ad excellent broad-spectrum
ess active in animal infection



, Z = (R)-[CH(Me)Et]
, Z = (S)-[CH(Me)Et]
, Z = $CH(Et)_2$

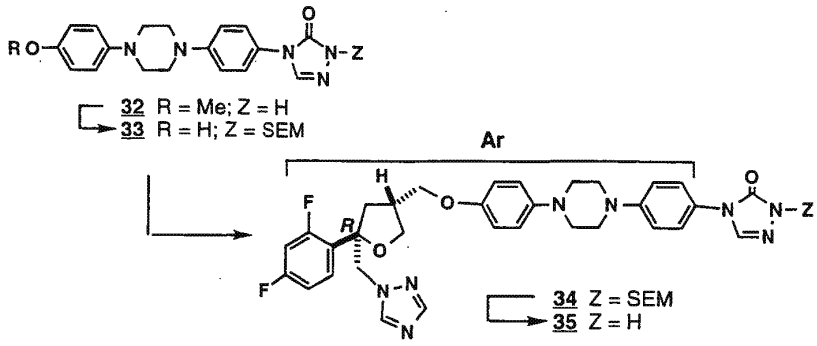
ion properties of Sch 51048,
ertaken. An added incentive
re water soluble salts and/or
parenteral use.

via a linear sequence was
is key intermediate, the side
partially N-SEM protected to
ylate the *cis*-tosylate **6R**. The
convenient source was used

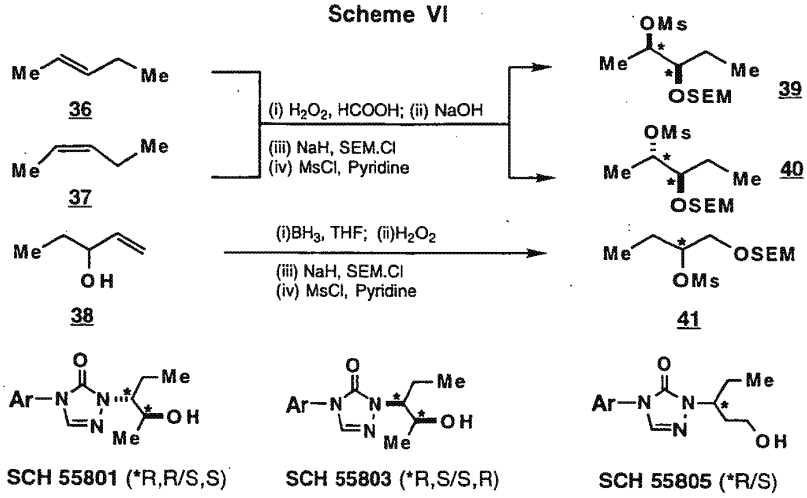
fficiency for speed, the two
38 were converted to the
the triazolone core **35** in the
ely three weeks to give the
805, in amounts sufficient for
pairs provided unexpectedly
ely basic or acidic side chains

resulted in reduced activity, incorporation of hydroxyl groups led to greatly improved in-vivo activity. (Scheme VI)

Scheme V

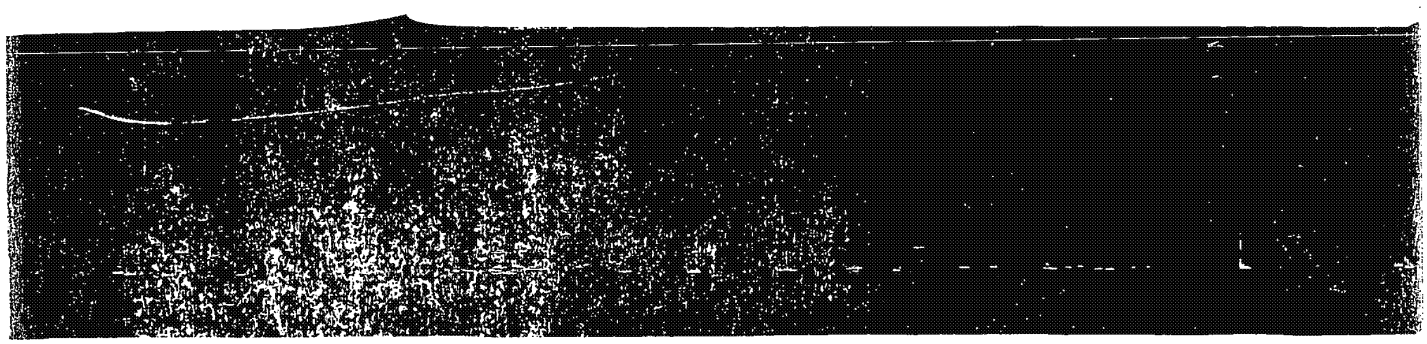


Scheme VI



Coupling Step: Compared to the methanesulfonate used above, the bromophenylsulfonate group proved to be a better choice leading to nearly complete reactions and higher isolated yields of N-alkylated products. Analysis of comparative kinetic data for substitution and elimination reactions of various leaving groups led us to surmise that a spatially more bulky group would actually be more desirable here and one with higher acidity of its conjugate acid. At the same time, *use of cesium carbonate*[15] as base in place of sodium hydride or hydroxide significantly improved N-alkylation yields in reactions virtually free of by-products.

With the new procedure to synthesize the triazolone segment **35** and efficient methodology to attach hydroxylated side chains in place, we now describe synthesis of all six hydroxylated analogs of Sch 51048.



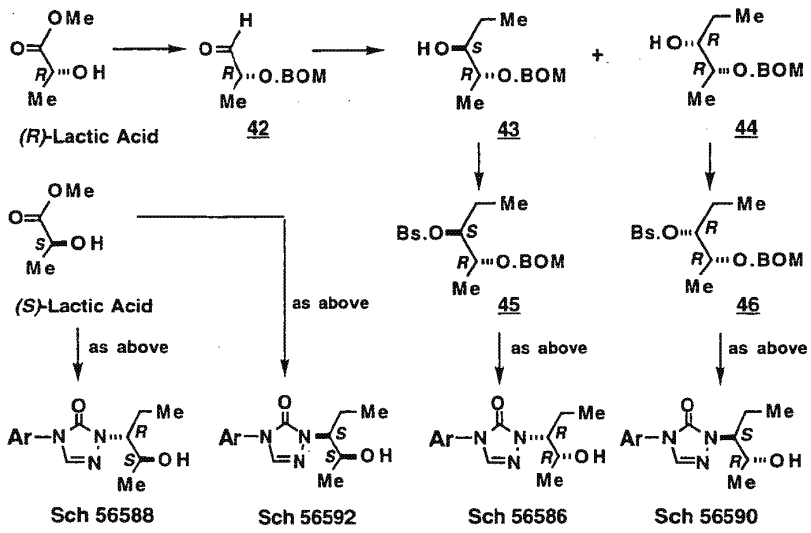
UM00012074
NOVARTIS EXHIBIT 1517
Novartis v. Regents, IPR2023-01347
Page 820 of 4460

(i) Secondary Hydroxy Analogs:

Among the various approaches that we considered, use of (R) and (S)-lactic acids appeared most appropriate as chiral sources to prepare the four secondary hydroxy analogs of Sch 51048. This may be exemplified in the synthesis of Sch 56586 and Sch 56590, the (R),(R) and (R),(S) isomers respectively.

Protection of (R)-methyl lactate as a benzyloxymethyl (BOM) ether followed by DIBAL reduction provided the aldehyde **42**. Grignard reaction of **42** with EtMgBr in tetrahydrofuran gave the (S),(R) and (R),(R) monoprotected diols **43** and **44** (~50:50) which were separated by chromatography. Paradoxically, this lack of stereoselectivity in the presence of tetrahydrofuran by design, proved extremely useful especially since we needed initially both **43** and **44**. The brosylates **45** and **46** derived from these alcohols were then used to N-alkylate the triazolone **35** according to conditions described above. Acid catalysed deprotection of the BOM ether finally gave the targeted Sch 56586 (R),(R) and Sch 56590 (S),(R) analogs.

Scheme VII



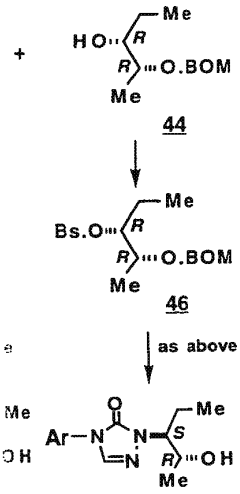
Following the above set of reactions using (S)-methyl lactate, the remaining secondary hydroxy analogs, Sch 56588 (R),(S) and Sch 56592 (S),(S) were synthesised.

(ii) Primary Hydroxy Analogs:

The commercially available methyl (R)-3-hydroxyvalerate acted as a common source for the two remaining optical isomers of hydroxylated Sch 51048. LAH reduction of (R)-3-hydroxyvalerate gave the diol, which was selectively protected as the mono SEM ether **47**. A portion of this monoprotected (R)-diol was used to provide the monoprotected (S)-alcohol **49**. Now both (S) and (R)-

UM00012075
NOVARTIS EXHIBIT 1517
Novartis v. Regents, IPR2023-01347
Page 821 of 4460

l, use of (R) and (S)-lactic
epare the four secondary
d in the synthesis of Sch
ctively.
oxymethyl (BOM) ether
. Grignard reaction of **42**
(R) monoprotected diols
aphy. Paradoxically, this
furan by design, proved
y both **43** and **44**. The
en used to N-alkylate the
id catalysed deprotection
(R) and Sch 56590 (S),(R)



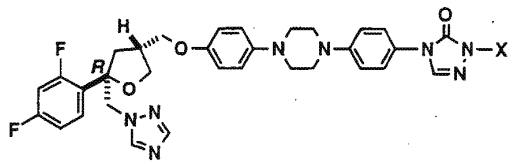
Sch 56590

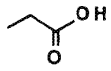
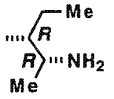
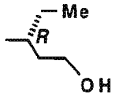
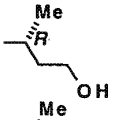
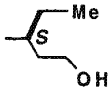
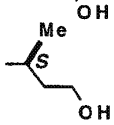
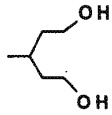
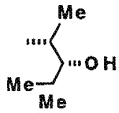
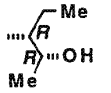
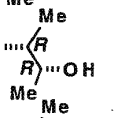
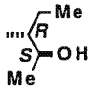
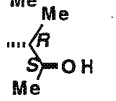
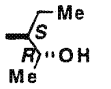
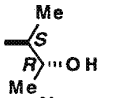
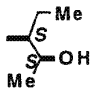
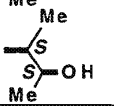
thyl lactate, the remaining
Sch 56592 (S),(S) were

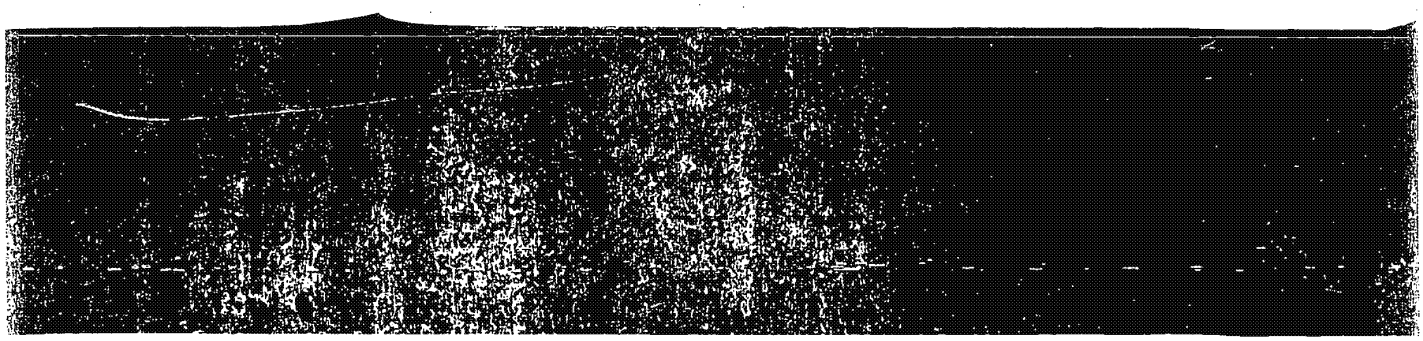
troxyvalerate acted as a
f hydroxylated Sch 51048.
ol, which was selectively
is monoprotected (R)-diol
. Now both (S) and (R)-

MICs of Polar Side Chain Analogs:

(mcg/ml)



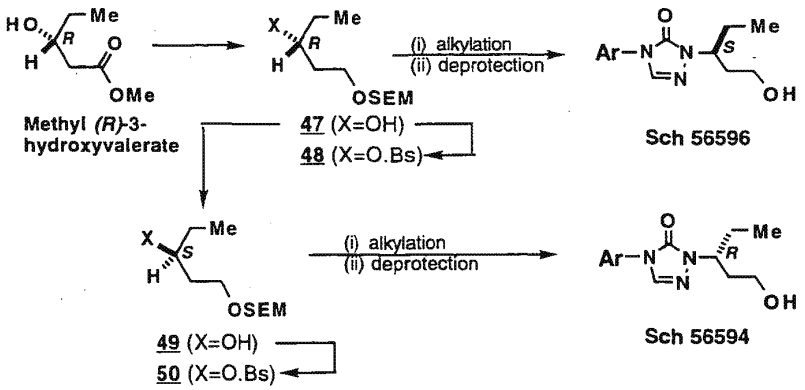
Sch No.	X	*Ca. alb.* N=31	*Asp.* N=37	Sch No.	X	*Ca. alb.* N=31	*Asp.* N=37
54160		0.790	40.30	57138		0.010	2.370
56594		0.021	0.088	56998		0.012	0.060
56596		0.025	0.077	56996		0.009	0.060
57033		0.198	0.810	56810 (Syn-mix.)		0.006	0.090
56586		0.014	0.077	56986		0.006	0.090
56588		0.005	0.130	57276		0.030	0.080
56590		0.019	0.086	56984		0.007	0.050
56592		0.018	0.048	57270		0.020	0.060



UM00012076
NOVARTIS EXHIBIT 1517
Novartis v. Regents, IPR2023-01347
Page 822 of 4460

alcohols were converted to the brosylates **48** and **50** respectively. Finally, N-alkylation of the triazolone **35** with these brosylates under the above established conditions followed by deprotection, completed synthesis of Sch 56594 and Sch 56596, the two primary hydroxy isomers.

Scheme VIII



This successfully completed synthesis of *all six* optical isomers of hydroxylated Sch 51048 for *in vivo* evaluation. Although presented in only its essential details, the entire effort was a major undertaking on our part involving considerable methodology development.

(iii) Synthesis of Additional Hydroxy Analogs:

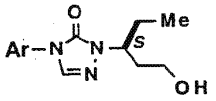
Synthetic methodology devised in the course of preparing the above six hydroxy analogs was successfully applied to synthesis of a variety of rational hydroxylated analogs of Sch 51048 within a short period of time. For example all eight hydroxylated analogs of Sch 50001/Sch 50002 were synthesized. In all, over 50 hydroxylated analogs were synthesized for biological evaluation. Without going into a detailed discussion of synthetic operations, we are giving MICs of some of the more significant analogs. One purpose of this investigation was to look for more accessible hydroxy side chains which may show at least comparable antifungal activity *in vivo* to the original six hydroxylated analogs of Sch 51048.[18]

SELECTED COMPOUND: SCH 56592

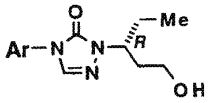
Preliminary biological evaluation (*in vitro*) showed most hydroxylated analogs of Sch 51048 as having excellent broad-spectrum antifungal activity against *Candida albicans* (31 strains) and *Aspergillus* (38 strains). The *in vitro* activity of a selected number of analogs was compared with ITZ, FLZ and AMB against 285 strains of yeasts and filamentous fungi, comprising 19 different genera and 37 different species, including FLZ resistant strains.[19] In order to select one compound with the best overall biological profile for further preclinical evaluation Sch 56588, Sch 56592 and Sch 56984 were subjected to detailed *in vivo* evaluation in several

UM00012077
NOVARTIS EXHIBIT 1517
Novartis v. Regents, IPR2023-01347
Page 823 of 4460

) respectively. Finally, N-
nder the above established
hesis of Sch 56594 and Sch



Sch 56596

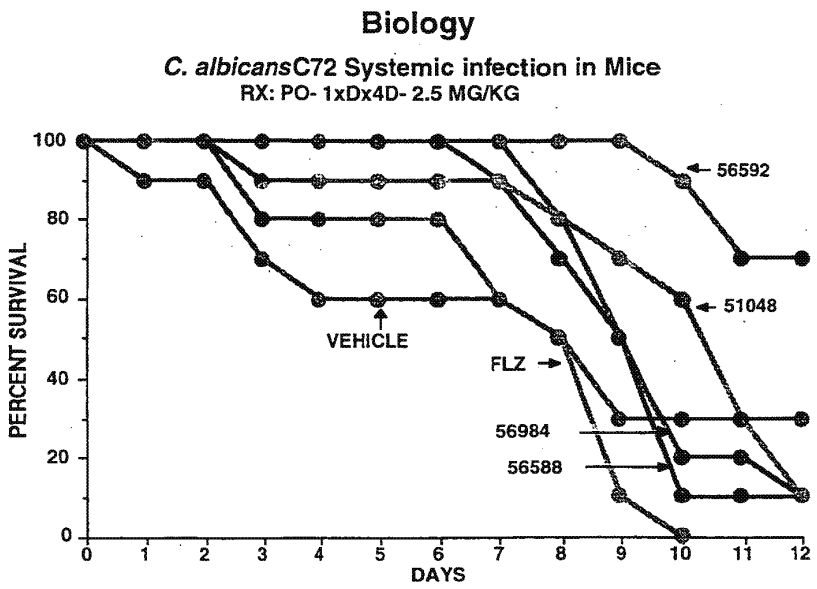


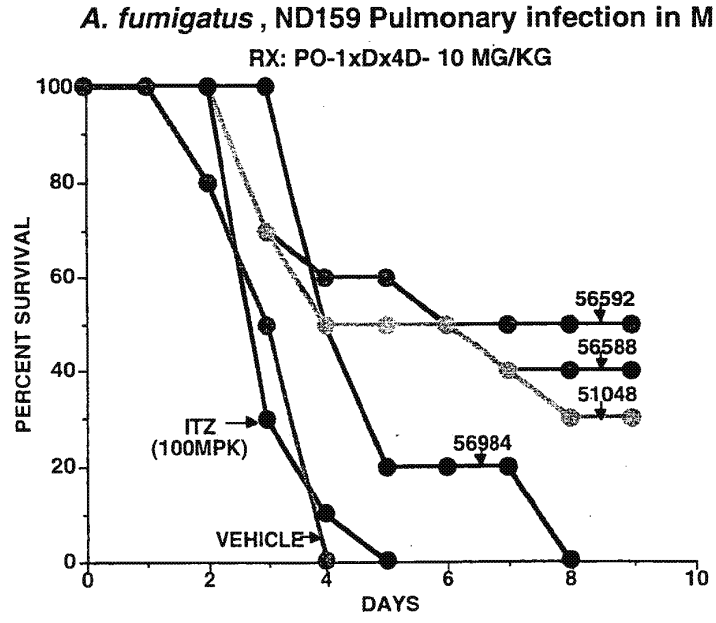
Sch 56594

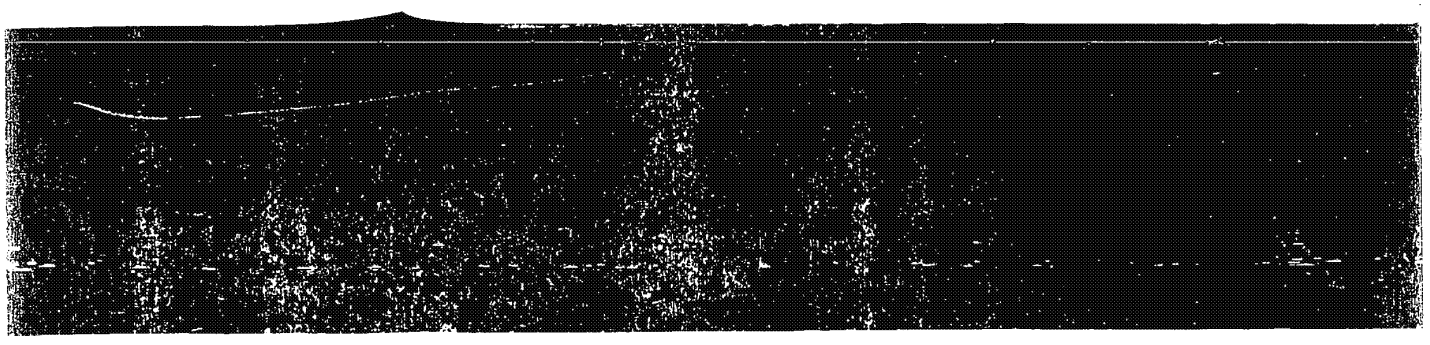
all six optical isomers of
ough presented in only its
aking on our part involving

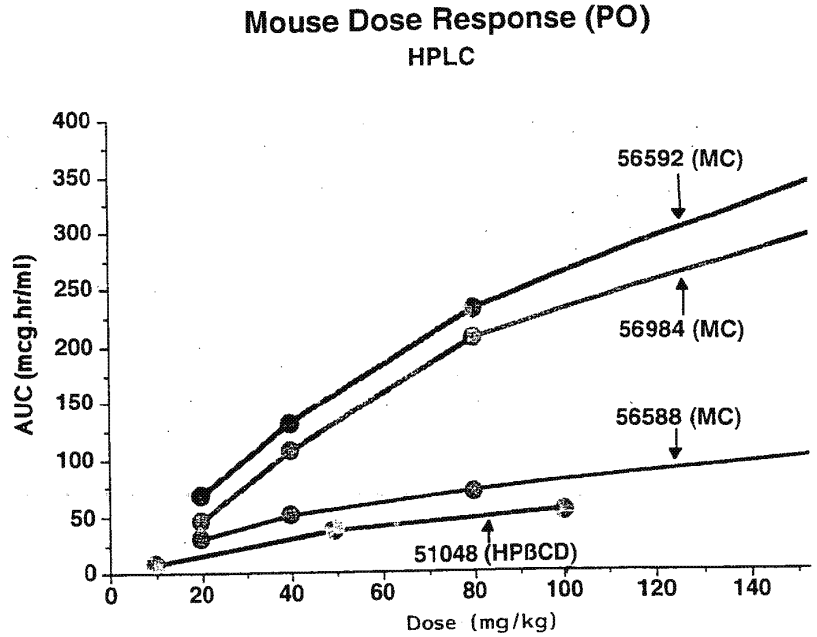
of preparing the above six
esis of a variety of rational
iod of time. For example all
ere synthesized. In all, over
gical evaluation. Without
ions, we are giving MICs of
of this investigation was to
ay show at least comparable
ted analogs of Sch 51048.[18]

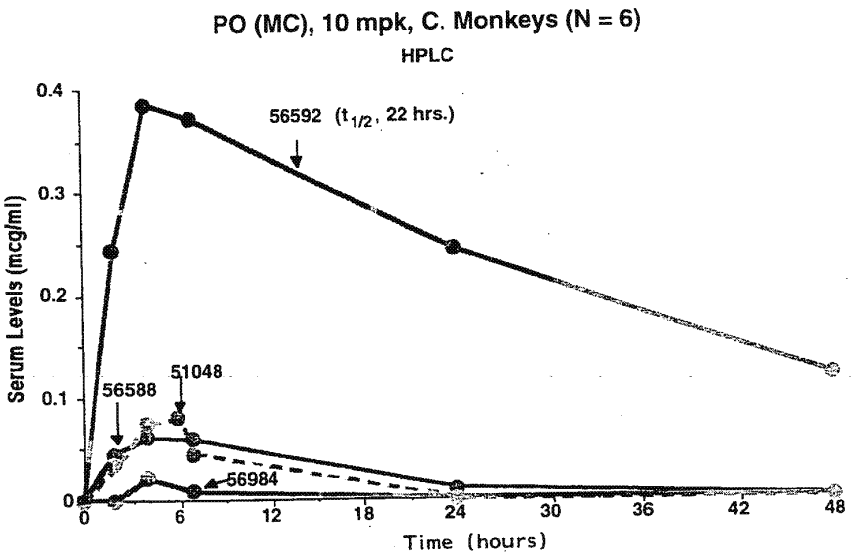
ost hydroxylated analogs of
ngal activity against *Candida*
in vitro activity of a selected
d AMB against 285 strains of
ent genera and 37 different
to select one compound with
cal evaluation Sch 56588, Sch
n vivo evaluation in several



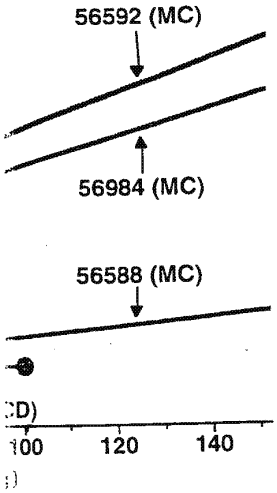





Mouse Dose Response (PO)
HPLC
AUC (mcg.hr/ml)
400
350
300
250
200
150
100
50
0
0
20
40
60
80
100
120
140
Dose (mg/kg)
56592 (MC)
56984 (MC)
56588 (MC)
51048 (HPβCD)


PO (MC), 10 mpk, C. Monkeys (N = 6)
HPLC
Serum Levels (mcg/ml)
0.4
0.3
0.2
0.1
0
0
6
12
18
24
30
36
42
48
Time (hours)
56592 (t1/2, 22 hrs.)
51048
56588
56984

se (PO)

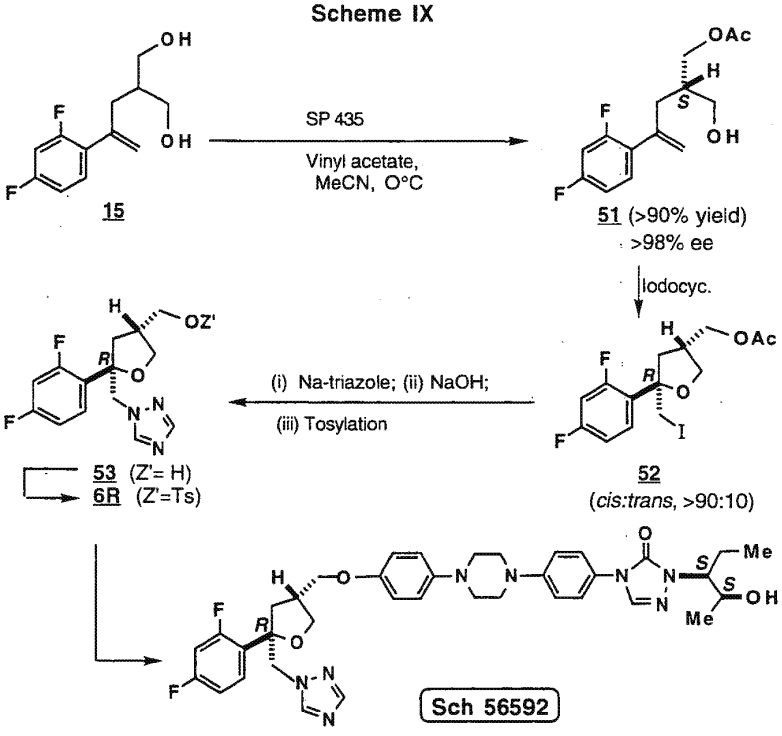


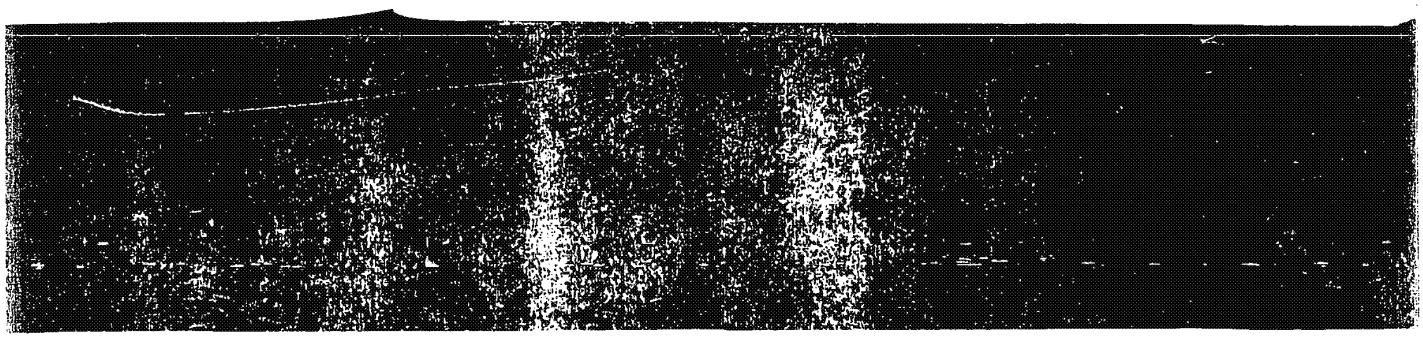
normal and immunocompromised infection models (*Candida* and *Aspergillus*).[5c] A comparision of *in vivo* efficacy and pharmacokinetic profile of these three compounds is shown. Based on the overall efficacy and bioavailability in 5 animal species, Sch 56592 was recommended for further development.

PRACTICAL SYNTHESIS OF SCH 56592:

Enzymatic desymmetrization[17] of the homochiral diol **15** was considered an attractive possibility from the outset. Successful model reactions in the presence of PPL convinced us that the optical purity of a desymmetrized (R)-monoester of **15** carried all the way to the 6S *cis*-tosylate. But it took a systematic screening of 169 hydrolases to make it a practical proposition. Out of these hydrolases only 6 displayed desirable reactivity and selectivity and only Novo SP 435 showed enhanced pro-(S) selectivity under the conditions of the screen. Complete consumption of the diol **15** was imperative to ensure optical integrity of the final product. Thus, under the optimised conditions <10% diester of **15** was also formed; this did not interfere with iodocyclization and subsequent triazolyl anion displacement reaction. The most practical route to Sch 56592 now conducted on over 30 kg batches was accomplished as follows.[12, 18]

Scheme IX





CONCLUSION:

We have described here a significant effort leading to the discovery of Sch 56592 a potent antifungal agent now undergoing phase I clinical trials. Its excellent broad-spectrum activity (P.O.) and superiority over most existing antifungal agents has been confirmed by outside investigators. Detailed biology of Sch 56592 has been discussed elsewhere.[19,20]

Systematic studies directed at understanding of stereo and regiochemical requirements for optimal oral activity led to the discovery of tetrahydrofurans with specific placement of the ring oxygen (cf. type C). *This significant result could not have been predicted at the outset.*

Efficient stereo and enantioselective synthesis of *2,4-cis-trisubstituted* tetrahydrofurans was critical to our success in the rapid synthesis of analogs. In the course of these studies we discovered a unprecedented *2,4-cis-selective* halocyclization of 2,2-disubstituted olefins, which provided a powerful methodology utilized in three most practical routes to Sch 56592 and its analogs.

ACKNOWLEDGEMENTS:

We would like to cordially thank Dr. George Miller's group for carrying out all the biology referred to in this presentation; and our colleagues in the Chemical Development and Preparatory Groups for providing many bulk intermediates critical to our need. Indeed our profound appreciation to Drs. Birendra Pramanik and Mohindar Puar for their invaluable analytical support.

REFERENCES AND NOTES:

1. Reviews: J. A. Cuomo, W. E. Dismukes, *The New England Journal of Medicine*, **1994**, 330, p. 263; R. J. Hay, "Recent Advances in Chemistry of Antiinfective Agents", *Royal Society of Chemistry, Special Publication No. 119*, **1993**, p. 163.
2. K. De Beule, *International J. of Antimic. Agents*, **1996**, 6, p.175.
3. K. Richardson, "Recent Advances in Chemistry of Antiinfective Agents", *Royal Society of Chemistry, Special Publication No. 119*, **1993**, p. 182.
4. Minireviews: (a) J. H. Rex, M. G. Rinaldi and M. A. Pfaller, *Antimicrob. Agents Chemother.* , **1995**, 39, p. 1; (b) N. H. Georgopapadakou and T. J. Walsh, *Antimicrob. Agents Chemother.* , **1996**, 40, p. 279. DeVries, J. G. and Kellog, R. M. *J. Am. Chem. Soc.*, **1979**, 101, 2759.
5. (a) A. K. Saksena, , V. M. Girijavallabhan, D. F. Rane, R. E. Pike, J. A. Desai, A. B. Cooper, E. Jao, A. K. Ganguly, D. Loebenberg, R. S. Hare and R. Parmegiani, *9th International Symposium on Future Trends in Chemotherapy, Geneva, Switzerland*, 26-28, March **1990**, Abstract No. 128; (b) V. M. Girijavallabhan, A. K. Ganguly, A. K. Saksena, A. B. Cooper, R. Lovey, D. F. Rane, R. E. Pike, J. A. Desai and E. Jao, "Recent Advances in Chemistry of Antiinfective Agents", *Royal Society of Chemistry, Special Publication No. 119*, **1993**, p. 191; (c) For a detailed description of these infection models, see: D. Loebenberg, A. Cacciapuoti, R. Parmegiani, E. L. Moss, F. Menzel, B. Antonacci, C. Norris, T. Yarosh-Tomaine, R. S. Hare, and G. H. Miller, *Antimicrob.Agents Chemother.*, **1992**, 36, p. 64.
6. D. F. Rane, V. M. Girijavallabhan, M. S. Puar, A. K. Saksena, D. Loebenberg and R. M. Parmegiani, *Bioorg. Med. Chem. Lett.*, **1994**, 4, p. 1313.

UM00012081
NOVARTIS EXHIBIT 1517
Novartis v. Regents, IPR2023-01347
Page 827 of 4460

he discovery of Sch 56592 a
l trials. Its excellent broad-
sting antifungal agents has
logy of Sch 56592 has been

f stereo and regiochemical
overy of tetrahydrofurans
This significant result could

sis of *2,4-cis-trisubstituted*
id synthesis of analogs. In
ecedented *2,4-cis-selective*
ch provided a powerful
ch 56592 and its analogs.

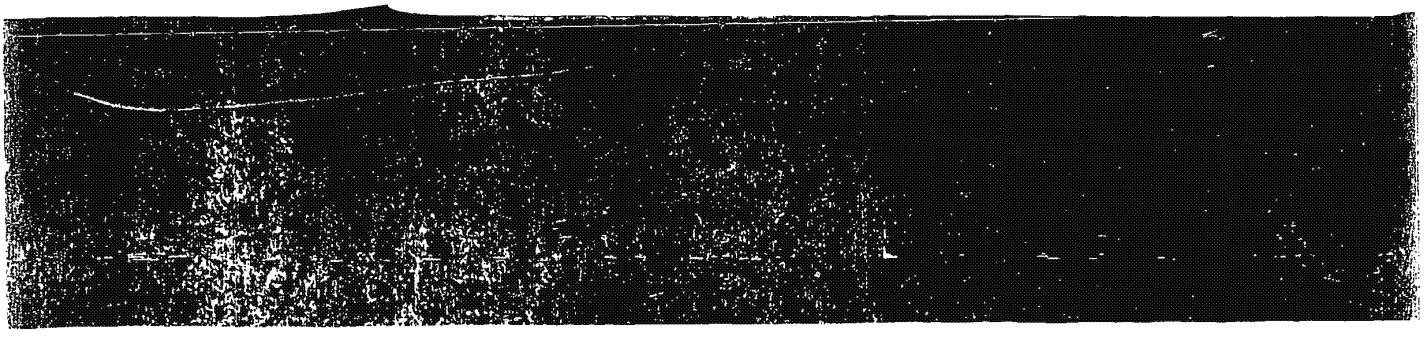
roup for carrying out all the
lleagues in the Chemical
many bulk intermediates
to Drs. Birendra Pramanik
ort.

England Journal of Medicine,
Chemistry of Antiinfective
ion No. 119, **1993**, p. 163.
5, 6, p.175.
of Antiinfective Agents",
9, **1993**, p. 182.
. Pfaller, *Antimicrob. Agents*
padakou and T. J. Walsh,
DeVries, J. G. and Kellog, R.

ne, R. E. Pike, J. A. Desai, A.
nberg, R. S. Hare and R.
ure Trends in Chemotherapy,
ract No. 128; (b) V. M.
B. Cooper, R. Lovey, D. F.
Advances in Chemistry of
Special Publication No. 119,
se infection models, see: D.
L. Moss, F. Menzel, B.
Hare, and G. H. Miller,

K. Saksena, D. Loebenberg
94, 4, p. 1313.

7. A. K. Saksena, V. M. Girijavallabhan, D. F. Rane, R. E. Pike, J. A. Desai, Y-T. Chen, E. Jao, A. K. Ganguly, *Heterocycles*, **1993**, 35, p. 129; Aqueous Diels-Alder: R. Breslow and D. C. Rideout, *J. Am. Chem. Soc.*, **1980**, 102, p. 7816
8. (a) A. K. Saksena, V. M. Girijavallabhan, R. G. Lovey, R. E. Pike, J. A. Desai, A. K. Ganguly, R. S. Hare, D. Loebenberg, A. Cacciapuoti and R. M. Parmegiani, *Bioorg. Med. Chem. Lett.*, **1994**, 4, p. 2023; (b) SPZ is Janssen's investigational azole reported to have better activity compared to ITZ against a wide range of *Aspergillus* strains *in vitro* and *in vivo*; (c) The terms "eutomer" and "dystomer" were coined by Prof. E. J. Ariens (University of Nijmegen, The Netherlands), to denote the active and the "other" enantiomer respectively; (d) X-ray crystallography of Sch 50002 was performed by Prof. Andrew T. McPhail (Duke University).
9. A. K. Saksena, V. M. Girijavallabhan, R. G. Lovey, R. E. Pike, J. A. Desai, A. K. Ganguly, R. S. Hare, D. Loebenberg, A. Cacciapuoti and R. M. Parmegiani, *Bioorg. Med. Chem. Lett.*, **1995**, 5, p. 127; R. A. Fromtling and J. Castaner, *Drugs of the Future*, 1995, 20 (3), p. 241.
10. (a) Reviews: P. A. Bartlett in " Asymmetric Synthesis", Vol. 3, Academic Press, Inc. **1984**, 411; G. Cardillo and M. Orena, *Tetrahedran*, **1990**, 46, p. 3321; (b) S. D. Rychnovsky and P. A. Bartlett, *J. Am. Chem. Soc.*, **1981**, 103, p. 3963; (c) B. H. Lipshutz and J. C. Barton, *J. Am. Chem. Soc.*, **1992**, 114, p. 1084.
11. A. K. Saksena and R. E. Pike, unpublished.
12. A. K. Saksena, V. M. Girijavallabhan, R. G. Lovey, R. E. Pike, H. Wang, and A. K. Ganguly, *Tetrahedron Lett.*, **1995**, 36, p. 1787.
13. (a) Review: D. A. Evans, *Aldrichimica Acta*, 15, 23 (1982); (b) W. Oppolzer, J. Blagg, I. Rodrigues, and E. Walther, *J. Am. Chem. Soc.*, **1990**, 112, p. 2767; (c) D. A. Evans, F. Urpi, T. C. Somers, J. S. Clark, and M. T. Bilodeau, *J. Am. Chem.* Soc., **1990**, 112, p. 8215.
14. A. K. Saksena, V. M. Girijavallabhan, H. Wang, Y-T. Liu, R. E. Pike and A. K. Ganguly, *Tetrahedron Lett.*, **1996**; accepted for publication.
15. J. G. DeVries and R. M. Kellog, *J. Am. Chem. Soc.*, **1979**, 101, p. 2759.
16. O. Mitsunobu, *Synthesis*, **1981**, p. 1; S. F. Martin and J. A. Dodge, *TetrahedronLett.*, **1991**, 32, p. 3017.
17. P. G. Hultin, F.-J. Muesseler, J. B. Jones, *J. Org. Chem.*, **1991**, 56, p. 5375; and cited references.
18. A. K. Saksena, V. M. Girijavallabhan, R. G. Lovey, F. Bennett, R. E. Pike, H. Wang, P. Pinto, Y.T. Liu, N. Patel and A. K. Ganguly, *35th Interscience Conference on Antimicrobial Agents and Chemotherapy (ICAAC), San Francisco,* 17-20 September 1995 (abstract nos. F 61 and F 83); we shall describe a very practical methodology to introduce Sch 56592 side chain at a future date.
19. *35th Interscience Conference on Antimicrobial Agents and Chemotherapy (ICAAC), San Francisco,* 17-20 September 1995: (a) D. Loebenberg, A. Cacciapuoti, R. Parmegiani, E. L. Moss, F. Menzel, B. Antonacci, C. Norris, T. Yarosh-Tomaine, R. S. Hare, G. H. Miller, (abst. nos. F 62, F 66 and F 67); (b) A. Nomeir, P. Kumari, M. J. Hilbert, D. Loebenberg, A. Cacciapuoti, F. Menzel, E. L. Moss, F. Menzel, R. S. Hare, G. H. Miller, M. N. Cayen and C. C. Lin (abs. no. F 68); (c) J. N. Galgiani, M. L. Lewis and T. Peng (abs. no. F 63); (d) J. R. Perfect and W. A. Schell (abs. no. F 64); (e) A. M. Sugar and X-P Liu (abs. no. F 65).
20. A. M. Sugar and X-P Liu, *Antimicrob.Agents Chemother.*, **1996**, 40, p. 1314.



UM00012082

NOVARTIS EXHIBIT 1517
Novartis v. Regents, IPR2023-01347
Page 828 of 4460

This Page is Inserted by IFW Indexing and Scanning Operations and is not part of the Official Record

BEST AVAILABLE IMAGES

Defective images within this document are accurate representations of the original documents submitted by the applicant.

Defects in the images include but are not limited to the items checked:

- ☐ BLACK BORDERS
- ☐ IMAGE CUT OFF AT TOP, BOTTOM OR SIDES
- ☐ FADED TEXT OR DRAWING
- ☐ BLURRED OR ILLEGIBLE TEXT OR DRAWING
- ☐ SKEWED/SLANTED IMAGES
- ☐ COLOR OR BLACK AND WHITE PHOTOGRAPHS
- ☐ GRAY SCALE DOCUMENTS
- ☐ LINES OR MARKS ON ORIGINAL DOCUMENT
- ☐ REFERENCE(S) OR EXHIBIT(S) SUBMITTED ARE POOR QUALITY
- ☐ OTHER: _____

IMAGES ARE BEST AVAILABLE COPY.
As rescanning these documents will not correct the image problems checked, please do not report these problems to the IFW Image Problem Mailbox.

Pergamon

Tetrahedron Letters, Vol. 37, No. 32, pp. 5657-5660, 1996
Copyright © 1996 Elsevier Science Ltd
Printed in Great Britain. All rights reserved
0040-4039/96 $15.00 + 0.00

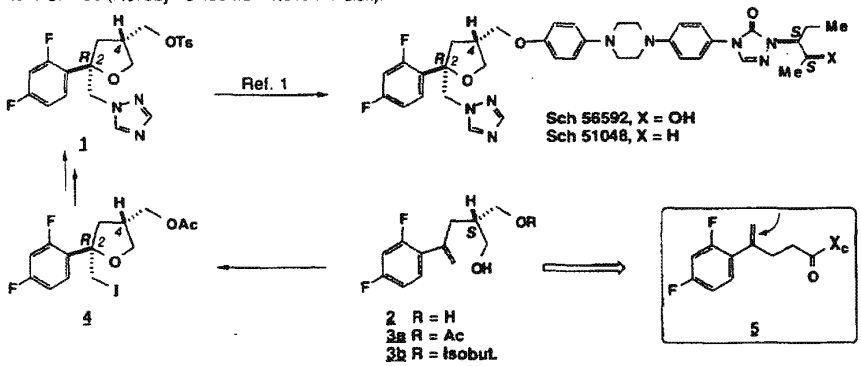
PII: S0040-4039(96)01203-8

CONCISE ASYMMETRIC ROUTES TO 2,2,4-TRISUBSTITUTED TETRAHYDROFURANS VIA CHIRAL TITANIUM IMIDE ENOLATES: KEY INTERMEDIATES TOWARDS SYNTHESIS OF HIGHLY ACTIVE AZOLE ANTIFUNGALS SCH 51048 AND SCH 56592

Anil K. Saksena,* Viyyoor M. Girijavallabhan, Haiyan Wang, Yi-Tsung Liu,* Russell E. Pike and Ashit K. Ganguly.
Schering-Plough Research Institute, 2015 Galloping Hill Road, Kenilworth, New Jersey 07033, U.S.A.

Abstract: Two complimentary approaches to the key (-)-(2R)-*cis*-tosylate **1** and its (+)-(2S)-enantiomer **15** via generation of chiral imide enolates having a 2,2-disubstituted olefin functionality in the β-position, are described. In a "protecting group free" sequence, reaction of the titanium enolate generated from (4R)-benzyl-2-oxazolidinone derived imide **5b** with s-trioxane provided a convenient intermediate **19** which could be directly subjected to 2,4-diastereoselective iodocyclization. Copyright © 1996 Elsevier Science Ltd

As part of an extensive search for orally effective antifungal agents we recently described a practical synthesis of **Sch 56592** which posesses improved therapeutic potential over **Sch 51048** and other clinically useful agents against a variety of systemic fungal infections in normal and immunocompromised infection models.[1,2] Both compounds belong to an uncommon 2,2,4-trisubstituted *cis*-tetrahydrofuran family of orally active broad-spectrum antifungals. In our earlier chemoenzymatic route to these compounds, the key (-)-(2R)-*cis*-tosylate **1** was secured *via* an unprecedented and remarkably efficient 2,4-diastereoselective 5-exo-halocyclization process. The (4S)-diol monoester synthons **3a** and **3b** of high optical purity (~99% ee) were obtained in this case by organic-phase enzymatic acylation of **2** in the presence of Novo SP 435 (Novozyme 435 from Novo Nordisk).[2]

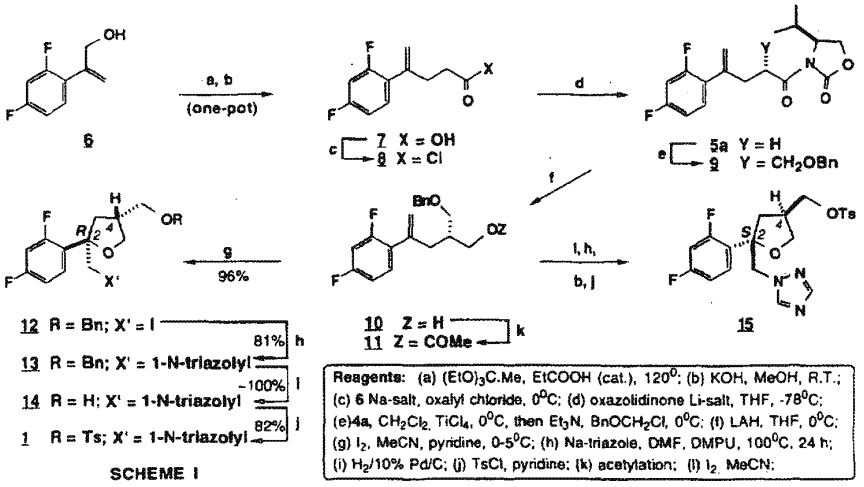


Enantioselective chemical routes to **1** and its corresponding (+)-(2S)-enantiomer **15** were viewed as being directly accessible *via* the chiral imide enolate technology developed independently by the Evans[3] and Oppolzer[4] groups. At the outset it was not clear in what manner the unsaturation (arrow) β to the site of enolate derived from **5** would influence the efficiency of electrophilic substitutions; to the best of our knowledge these type of substrates have not been studied earlier. The wide choice of electrophiles, excellent diastereoselectivities for both alkylations and aldol condensations, and easy access to chiral auxiliaries led us to choose the Evans methodology.[5] We now describe two complimentary routes to **1** using chiral oxazolidinones derived from (S)-valinol and (R)-phenylalaninol respectively.

Synthesis of the desired olefinic acid **7** was accomplished quite simply and in high yields from the allyl alcohol **6** available in bulk from our original chiral epoxide route to **1**.[6] In a one-pot sequence **6** was subjected to Claisen-Johnson orthoester rearrangement[7] with triethyl orthoacetate followed by basic hydrolysis of the resulting ethyl ester to provide **7**

UM00012084
NOVARTIS EXHIBIT 1517
Novartis v. Regents, IPR2023-01347
Page 830 of 4460

as a crystalline solid, m.p. 65° C in 86% yield.[8] Treatment of the acid chloride **8** with the lithium salt of (4S)-(-)-4-isopropyl-2-oxazolidinone according to standard conditions[5] readily provided the chiral imide **5a** in over 80% yield.[8,9] Our first experiments to introduce the benzyloxmethyl funtionality were conducted with the lithium enolate of **5a** using benzyloxymethyl bromide as the alkylating reagent. Although excellent diastereofacial selectivity for the desired benzyl



SCHEME I

Reagents: (a) $(EtO)_3C.Me$, EtCOOH (cat.), 120°; (b) KOH, MeOH, R.T.; (c) **6** Na-salt, oxalyl chloride, 0°C; (d) oxazolidinone Li-salt, THF, -78°C; (e)**4a**, CH_2Cl_2, $TiCl_4$, 0°C, then Et_3N, $BnOCH_2Cl$, 0°C; (f) LAH, THF, 0°C; (g) I_2, MeCN, pyridine, 0-5°C; (h) Na-triazole, DMF, DMPU, 100°C, 24 h; (i) H_2/10% Pd/C; (j) TsCl, pyridine; (k) acetylation; (l) I_2, MeCN;

ether **9** [10] (over 98:2) was realized, the chemical yields were unacceptably low (~30%). Under these conditions ~40% unchanged **5a** was recovered, plus intractable products. Under the same conditions, saturated substrates have been reported to provide the corresponding benzyl ethers in over 70% yields.[5]

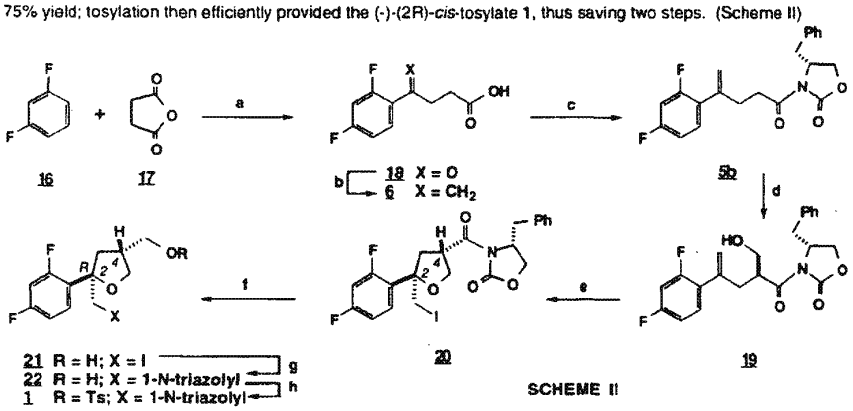
Titanium enolates of N-acyloxazolidinones have been utilized with greatly improved results over Li-enolates in terms of operational simplicity and high diastereofacial selectivity.[11,12] Thus in a marked improvement, alkylation of **5a** with benzyloxymethyl chloride via Evans' titanium enolate protocol[12] gave the benzyl ether **9** in 84% yields (>98% de). No isomerization of the 2,2-disubstituted olefin was detected during either lithium or titanium enolate formation, a requirement crucial to success in this chiral imide route to **1**. Reduction of **9** with LAH in tetrahydrofuran gave the desired (-)-(2S)-diol monobenzyl ether **10**[13] (85% yield) with ~80% recovery of the chiral auxiliary. The remaining steps from iodocyclization onwards proceeded as expected[2] to provide *cis*-1-N-triazolyl benzyl ether **13** and the corresponding *trans*-isomer **13a** (*cis:trans*; >90:10).[14] The undesired **13a** was readily separated from **13** by chromatography. Hydrogenolytic debenzylation of **13** followed by tosylation of the resulting alcohol **14** provided the desired (-)-(2R)-*cis*-tosylate **1**[6] in overall 90% yield and excellent optical purity (>99% e.e.). (Scheme I)

In principle, synthesis of the enantiomeric (+)-(2S)-*cis*-tosylate **15** could be easily carried out by following the above sequence using an appropriate chiral auxiliary such as (4R)-(+)-4-isopropyl-2-oxazolidinone. This was found quite unnecessary as iodocyclization of **11** under the equilibrating conditions according to Rychnovsky and Bartlett[15] provided the iodoacetate of opposite configuration. As we have reported earlier,[2] under these conditions the *'cis:trans'* diastereoselectivity was relatively poor (70:30). However following established conditions, the (+)-(2S)-*cis*-tosylate **15** could be prepared from the major iodocyclization product after chromatographic separation from the minor *trans*-isomer.

The following alternative approach to **1** was undertaken as we were keen to avoid yield limiting protection-deprotection operations. The allyl alcohol **6** we had been using so far was prepared in 4-steps from 1,3-

difluorobenzene.[6] In this manner synthesis of the olefinic acid **7** used above required a total of 6-steps. We were able to synthesize **7** in two simple steps by Friedel-Crafts reaction of m-difluorobenzene with succinic anhydride to provide the crystalline keto acid **18**, m.p. 110°C in over 90% yield. Wittig reaction of **18** in tetrahydrofuran with two equivalents of methylene triphenyl phosphorane then gave the olefinic acid **7** in ~60% yield over 2 steps.

The (R)-phenylalaninol derived chiral imide **5b** was produced in 90% yield by activation of **7** with pivaloyl chloride followed by in-situ reaction of the resulting anhydride with the Li-salt of (4R)-(+)-4-benzyl-2-oxazolidinone.[5] Diastereofacially selective hydroxymethylation of **5b** was best carried out with sym-trioxane using titanium enolate chemistry[12] to provide the aldol product **19** in ~60% yield.[16] The direct iodocyclization of **19** at room temperature with a high degree of diastereoselectivity in favor of the desired *cis*-iodo imide **20** (*cis:trans*, >90:10; 90% yield) is noteworthy.[17] In contrast iodocyclization of **3a** or **10** type substrates required lower temperatures (0-5°C) to achieve the same degree of diastereoselectivity. Lithium borohydride reduction of **20** under controlled conditions followed by chromatography provided the *cis*-iodoalcohol **21**[18] and recovered (4R)-benzyl-2-oxazolidinone in ~90% and 71% yields respectively. As we have noted earlier, displacement of iodine in a neopentyl-like system by the highly nucleophilic triazolyl anion posed no problems.[2] Hydroxyl protection used in our earlier study, proved unnecessary. Indeed direct displacement of iodine in **21** with sodium-triazole according to conditions described earlier,[2] provided the alcohol **22** in 75% yield; tosylation then efficiently provided the (-)-(2R)-*cis*-tosylate **1**, thus saving two steps. (Scheme II)



SCHEME II

Reagents: (a) Friedel-Craft; (b) $Ph_3P{=}CH_2$ (2 equiv.), THF; (c) pivaloyl chloride activation of **6**, oxazolidinone Li-salt, THF, -78°C; (d) **18**, CH_2Cl_2, $TiCl_4$, 0°C, then s-Trioxane, 0°C; (e) I_2, MeCN, pyridine, 0-5°C; (f) $LiBH_4$, THF, -78°C to R.T., 2h; (g) Na-triazole, DMF, DMPU, 100°C, 24 h; (h) TsCl, pyridine.

Notably, no protecting groups were required throughout this entire sequence. This concise new route to **1** offers excellent opportunity for large scale operations. These examples further enhance the scope of Evans' imide enolates as well as the unprecedented 2,4-diastereoselective halocyclizations[2] reported recently.

Based on its superior efficacy and pharmacokinetic profile, **Sch 56592** is in Phase I clinical trials at the present time.[1, 19] We shall report on additional examples of diastereoselective bond constructions with chiral imides of the type **5a** and **5b** in future communications. Further chemistry relating to **Sch 56592** and structure-activity relationships in this series of novel orally active broad-spectrum antifungals will also be reported elsewhere.

Acknowledgements: We would like to cordially thank Professor Ronald Breslow and Sir Derek Barton, FRS for stimulating discussions. We also wish to thank Dr. Birendra Pramanik for mass spectral data and Dr. Mohinder S. Puar for high resolution nmr experiments.

References and Notes:

1. (a) A. K. Saksena, V. M. Girijavallabhan, R. G. Lovey, F. Bennett, R. E. Pike, H. Wang, P. Pinto, Y.T. Liu, N. Patel and A. K. Ganguly, *35th Interscience Conference on Antimicrobial Agents and Chemotherapy (ICAAC), San Francisco, 17-20 September 1995* (abstract nos. F 61 and F 83); (b) A. K. Saksena, V. M. Girijavallabhan, R. G. Lovey, R. E. Pike, J. A. Desai, A. K. Ganguly, R. S. Hare, D. Loebenberg, A. Cacciapouti and R. M. Parmegiani, *Bioorg. Med. Chem. Lett.*, **1995**, 5, 2023; **Sch 56592**: (-)-4- [4- [4- [[(R-*cis*)-5- (2,4-difluorophenyl)-tetrahydro-5- (1H-1,2,4-triazol-1-ylmethyl)-3-furanyl] methoxy]phenyl]-1-piperazinyl] phenyl]-2,4-dihydro-2- [(S)-1- ethyl-2(S)-hydroxypropyl]-3H- 1,2,4-triazol-3-one.
2. A. K. Saksena, V. M. Girijavallabhan, R. G. Lovey, R. E. Pike, H. Wang, A. K. Ganguly, B. Morgan, A. Zaks and M.S. Puar, *Tetrahedron Lett.* **1995**, 36, 1787.
3. Review: D. A. Evans, *Aldrichimica Acta*, **1994**, 15, 23; and cited references.
4. W. Oppolzer, J. Blagg, I. Rodrigues and E. Walther, *J. Am. Chem. Soc.* **1990**, 112, 2767; and cited references.
5. D. A. Evans, M.D. Ennis and D.J. Mathre, *J. Am. Chem. Soc.* **1982**, 104, 1737.
6. A. K. Saksena, V. M. Girijavallabhan, R. G. Lovey, R. E. Pike, J. A. Desai, A. K. Ganguly, R. S. Hare, D. Loebenberg, A. Cacciapouti and R. M. Parmegiani, *Bioorg. Med. Chem. Lett.*, **1994**, 4, 2023.
7. W. S. Johnson, L. Werthmann, W. R. Bartlett, T. T. Brocksom, Tsung-tee Li, D. J. Faulkner, M. R. Peterson, *J. Am. Chem. Soc.* **1990**, 112, 8215.
8. Yields refer to isolated products and have not been optimised. All new compounds were characterised by PMR, CMR and high resolution mass spectra. When necessary diff NOE, COSY and NOESY spectra were obtained. *Cis:trans* ratios of iodocyclization products were determined by NMR as fully described in ref. 2. Where applicable, optical purity of key intermediates was determined by chiral shift NMR spectroscopy. Chiralcel® OD Analytical Columns (Chiral Technologies Inc.) were also used to determine optical purity of a number of final compounds. Selected spectral data is given here.
9. **7**: MS = 213 $(M+H)^+$; ^{1}HNMR [$CDCl_3$] δ 2.48 (t , J = 6.0 Hz , 2H), 2.80 (t , J = 6.0 Hz , 2H), 5.19 (s , 1H), 5.28 (s,1H),6.78 - 6.90 (m , 2H), 7.18 - 7.30 (m , 1H). **5a**: MS = 324 $(M+H)^+$. ^{1}HNMR [$CDCl_3$] δ 0.90 (dd, J = 6.7 Hz,18.0 Hz, 6H), 2.30 - 2.43 (m, 1H), 2.74 - 2.90 (m, 2H), 2.95 - 3.20 (m, 2H), 4.15 - 4.30 (m, 2H), 4.40 - 4.47 (m, 1H), 5.20 (s, 1H), 5.30 (s,1H), 6.77 - 6 92 (m, 2H), 7.20 - 7.30 (m, 1H).
10. **9**: MS = 444 $(M + H)^+$. ^{1}HNMR [$CDCl_3$] δ 0.75 (dd, J = 5.3 Hz, 33.8 Hz, 6H), 2.19 - 2.30 (m, 1H), 2.62 (dd, J = 6.0 Hz, 15.0 Hz, 1H), 2.91 (dd, J = 7.5 Hz, 12.8 Hz, 1H), 3.60 (dd, J = 6.0 Hz, 10.5 Hz, 1H), 3.66 (t, J = 7.5 Hz, 1H), 4.12 (m, 2H), 4.31 (m, 2H); 4.43 (dd, J = 12.0 Hz, 18.8 Hz, 2 H), 5.10 (s, 1H); 5.23 (s, 1H), 6.70 - 6.85 (m, 2H), 7.09 - 7.34 (m, 6H).
11. M. Nerz-Stormes and E.R. Thornton, *Tetrahedron Lett.* **1986**, 27, 897; *J. Org. Chem.* **1991**, 56, 2489.
12. D.A. Evans, F. Urpi, T.C. Somers, J.S. Clark, M.T. Bilodeau, *J. Am. Chem. Soc.* **1990**, 112, 8215.
13. **10**: $[\alpha]_D^{25}$ -28.4° (c = 1.18, $CHCl_3$). MS = 341 $(M+Na)^+$. ^{1}HNMR [$CDCl_3$] δ 1.77 - 1.91 (m, 1H), 2:42 (t, J = 4.5 Hz, 1H, exchangeable with D_2O), 2.50 (d, J = 7.5 Hz, 2H), 3.45 (dd, J = 6.8 Hz, 9.0 Hz, 1H), 3.52 - 3.75 (m, 3H), 4.46 (dd, J = 7.5 Hz, 13.5 Hz, 2H); 5.17 (s, 1H), 5.23 (s, 1H), 6.73 - 6.86 (m, 2H), 7.12 - 7.38 (m, 6H).
14. **13** (*cis*-isomer): $[\alpha]_D^{25}$ = - 42.1° (c = 1.17, $CHCl_3$), MS = 386 $(M+H)^+$. ^{1}HNMR [$CDCl_3$] δ 1.90 (m, 1H), 2.42 (m, 2H), 3.17 (dd, J = 6.8 Hz, 9.0 Hz, 1H), 3.28 (dd, J = 6.8 Hz, 9.0 Hz, 1H), 3.66 (dd, J = 7.5 Hz, 9.0 Hz, 1H); 4.04 (t, J = 7.5 Hz, 1H); 4.41 (s, 2H); 4.52 (q, J = 12.8 Hz, 2H), 6.72 - 6.86 (m, 2H), 7.21 - 7.37 (m, 6H), 7.76 (s, 1H), 8.06 (s, 1H).

13a (*trans*-isomer): $[\alpha]_D^{25}$ = +10.6° (c = 1.12, $CHCl_3$), MS = 386 $(M+H)^+$. ^{1}HNMR [$CDCl_3$] δ 1.89 - 2.0 (m, 1H); 2.06 - 2.21 (m, 1H); 2.55 - 2.68 (m, 1H); 3.12 (dd, J = 7.5 Hz, 8.2 Hz, 1H); 3.22 (dd, J = 7.5 Hz, 8.2 Hz, 1H); 3.59 (t, J = 7.9 Hz, 1H); 4.06 (dd, J = 7.5 Hz, 8.2 Hz, 1H); 4.34 (s, 2H); 4.50 (d, J = 15.0 Hz, 2H); 6.70 - 6.85 (m, 2H); 7.13 - 7.40 (m, 6H); 7.80 (s, 1H); 8.05 (s, 1H). **1**: $[\alpha]_D^{25}$ = -39.4° (c = 1.16, $CHCl_3$).[2] **15**: $[\alpha]_D^{25}$ = +37.4° = 1.12, $CHCl_3$)..
15. S. D. Rychnovsky and P. A. Bartlett, *J. Am. Chem. Soc.* **1981**, 103, 3963.
16. **Procedure**: A stirred and cooled (0°C) solution of the chiral imide **5b** (2.18 g, 5.88 mmol) in CH_2Cl_2 (25 ml) was treated with 1M $TiCl_4$ (6.5 ml) in CH_2Cl_2. After 5 minutes Hunig's base (1.12 ml) was added and the solution stirred for an additional 30 minutes. A solution of 1,3,5-trioxane (0.67 g, 7.44 mmol) in CH_2Cl_2 (5 ml) was added followed by another 6.5 ml 1M $TiCl_4$ in CH_2Cl_2. The reaction mixture was stirred for 2.5 h at 0°-3°C. Addition of saturated NH_4Cl and extractive work-up gave the crude product. Chromatography on silica gel using 15-25% EtOAc in n-hexane as eluent provided pure **19** (1.33 g).

5b: $[\alpha]_D^{25}$ = -44.4° (c = 1.67, $CHCl_3$): MS = 371 $(M+H)^+$. ^{1}HNMR [$CDCl_3$] δ 2.74 (dd, J = 9.6 Hz, 13.3 Hz, 1H), 2.82 - 3.12 (m, 4H), 3.28 (dd, J = 3.4 Hz, 13.3 Hz, 1H), 4.13 - 4.19 (m, 2H), 4.58 - 4.71 (m, 1H), 5.20 (s, 1H), 5.31 (m, 1H), 6.74 - 7.34 (m, 8H).

19: $[\alpha]_D$ = -62.9° (c = 1.7, $CHCl_3$); MS = 402 $(M+H)^+$. ^{1}HNMR [$CDCl_3$] δ 2.64 - 3.01 (m, 3H), 3.24 (dd, J = 3.4 Hz, 13.5 Hz, 1H), 3.77 - 3.91 (bs, 2H), 4.0 - 4.18 (m, 3H), 4.49 - 4.61 (m, 1H), 5.19 (s, 1H), 5.33 (s, 1H); 6.73 - 7.4 (m, 8H).
17. **Procedure**: A stirred solution of **19** (1 g, 2.5 mmol) in CH_3CN (20 ml) was treated with pyridine (0.45 ml). After cooling to 0°C iodine (1.78 g) was added allowing the reaction mixture to warm to room temperature. After ~20 h the reaction was quenched with dilute aq. sod sullite and extracted with Et_2O (2 x 20 ml); the ether extract was dried over $MgSO_4$ and concentrated to dryness in vacuo to provide a residue. Chromatography over silica gel using 50-75% EtOAc in hexane as eluent gave pure iodo-imide **20** (1.2 g). MS = 528 $(M+H)^+$. ^{1}HNMR [$CDCl_3$] δ 2.61 - 2.95 (m, 3H), 3.28 (dd, J = 3.4 Hz, 13.3 Hz, 1H), 3.79 (AB quartet, J = 16.7 Hz, 2H), 4.05 - 4.33 (m, 5H), 4.65 - 4.76 (m, 1H). 6.75 - 7.61 (m, 8H).
18. **Procedure**: The iodo-imide **20** (0.9 g) from above was dissolved in THF and the solution cooled to -78°C. A 2M $LiBH_4$ solution in THF (0.85 ml) was then added with stirring while warming to room temperature. After stirring at room temperature for 2 h, the reaction mixture was cooled to -10°C and quenched with saturated NH_4Cl. Evaporation of THF *in vacuo* followed by extractive isolation with CH_2Cl_2 gave the iodo alcohol **21** (0.45 g). Its acetate was identical to the authentic material.[2]
19. *35th Interscience Conference on Antimicrobial Agents and Chemotherapy (ICAAC), San Francisco, 17-20 September1995* (abstract nos. F 61, F 62, F63, F 64, F 65, F 66, F 67, F 68, and F 83)

(*Received in USA* 24 *April* 1996; *revised* 11 *June* 1996; *accepted* 12 *June* 1996)

UM00012087
NOVARTIS EXHIBIT 1517
Novartis v. Regents, IPR2023-01347
Page 833 of 4460

Pergamon

Tetrahedron Letters 43 (2002) 3359–3363

TETRAHEDRON LETTERS

Mono *N*-arylation of piperazine(III): metal-catalyzed *N*-arylation and its application to the novel preparations of the antifungal posaconazole and its advanced intermediate

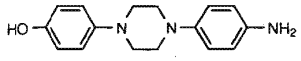
Michael Hepperle, Jeffrey Eckert, Dinesh Gala,* Lan Shen, C. Anderson Evans and Andrew Goodman

Schering-Plough Research Institute, 2015 Galloping Hill Road, Kenilworth, NJ 07033, USA

Received 25 January 2002; revised 7 March 2002; accepted 12 March 2002

Abstract—A novel application of Pd^0-catalyzed arylation to mono *N*-arylated piperazines, its mechanism, and its application towards the novel syntheses of the key differentially *N*,*N*′-diarylated piperazine antifungal intermediate *N*-(4-hydroxyphenyl)-*N*′-(4-aminophenyl)piperazine **5** as well as posaconazole **1** are described. © 2002 Elsevier Science Ltd. All rights reserved.

Mono and diarylated piperazines are key moieties of a variety of biologically active compounds such as Neuropeptide Y antagonists, G-Protein-coupled receptor ligands, cholesterol ester transfer protein inhibitors, $5\text{-}HT_{1D}$ receptor agonists GPIIb/IIIa antagonist, serotonin-3 antagonists, and orally active broad-spectrum triazole antifungals (**1–4**), the compounds of interest for the current manuscript.[1–7] These triazole antifungals such as Sch 51048, Sch 56592, itraconazole, and hydroxyitraconazole[3] utilize an unsymmetrically *N*,*N*′-diarylated piperazine moiety **5**.



5: Common antifungal intermediate

Typical synthetic routes[1–6] to these differentially *N*,*N*′-diaryl substituted piperazines encompass the reaction of anilines to the mono *N*-aryl piperazines (via carcinogenic intermediates under high pressure and/or temperature and specialized catalyst conditions) which are then reacted with appropriate arylhalides. Alternately these differentially substituted piperazines are made by reacting electron withdrawing groups containing arylhalides either with a large excess of piperazine under harsh reaction conditions or with mono-*N* protected piperazine, usually as a carbamate, to avoid a mixture of mono-, di-, and unsubstituted piperazines which require chromatographic purifications.[7,8] Our interest has been in seeking a mild, selective method for mono-*N*-arylation of piperazine which could be utilized for preparation of **5**.

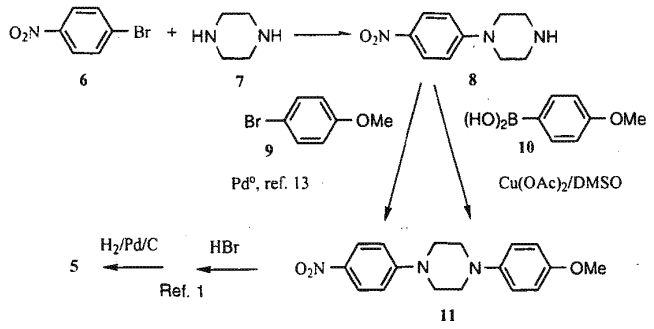
In previous publications[1,2] we described a direct sequential *N*-arylation of piperazine nitrogens for the preparation of the common antifungal intermediate **5**. There it was shown that the reaction of equimolar amounts of electron deficient arylhalides with piperazine, without the use of catalyst, led to the mono *N*-arylated piperazines which were then converted to the differentially *N*,*N*′-diaryl substituted piperazines. Electron rich aromatic halides do not react with piperazine under these conditions. Thus, towards the synthesis of antifungal intermediate **5** we reported that the reaction of piperazine **7** with *p*-chloro or bromonitrobenzene **6** led to the mono arylated piperazine **8** (Scheme 1), which reacted with boronic acid derivative **10** to generate **11**.

Interestingly, under standard Pd^0 coupling conditions[9,10] **8** reacted very slowly with *p*-bromoanisole **9** as after 3 days it led to 58% isolated yield of **11**. Compound **11** produced via either of the above reactions were indistinguishable from the one obtained via alternate synthesis and could be converted to the desired compound **5** as shown in Scheme 1. For a large scale preparation of **5**, the use of **9** is more desirable compared to the use of **10**.[11] The slow arylation of piperazine **9** with **8** was intriguing. Very little information is available in the literature pertaining to Pd^0-catalyzed *N*-arylation of piperazine.[12] In view of novel and useful results obtained in our laboratory on piperazine

* Corresponding author.

0040-4039/02/$ - see front matter © 2002 Elsevier Science Ltd. All rights reserved.
PII: S0040-4039(02)00556-7

UM00012088
NOVARTIS EXHIBIT 1517
Novartis v. Regents, IPR2023-01347
Page 834 of 4460



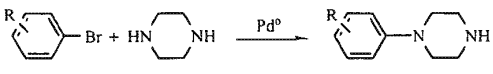
Scheme 1. Reactivity of *N*-*p*-nitrophenyl piperazine.

N-arylation with electron deficient aromatic halides,[1,2] we decided to investigate Pd^0-catalyzed piperazine *N*-arylation with non electron deficient aromatic halides in general. This work has led us to the discovery that almost equimolar amounts of non-electron deficient arylhalides and piperazine react in the presence of a Pd^0 catalyst to produce only mono *N*-arylated piperazines. This finding has been applied to the preparation of the common antifungal intermediate **5** as well as to posaconazole, **1**, and are described in this manuscript.

The results of piperazine mono *N*-arylation with Pd^0 catalysis (experimental conditions derived from Ref. 9 are described in Ref. 13) are shown in Table 1. In general the stronger the electron donating group on the arylhalide, the higher the piperazine *N*-arylation yield. A steric hindrance played a role (entries 4 and 5) in lowering yields. Most importantly for our work, compound **9** and **15** reacted with piperazine to produce intermediates that were suitable for the preparation of **5**.

Preliminary laboratory work undertaken to understand factors that govern Pd^0-catalyzed piperazine mono *N*-arylation is detailed below. The use of racemic Binap in place of chiral one during the formation of **18** did not alter the outcome of the reaction ruling out any facial selectivity imparted by the catalyst. Solubility of **9**, **11–15** and mono *N*-aryl piperazines **16–21** in toluene, the use of several lots of reagents, ligands, as well as catalyst eliminated the possibility that the selectivity

Table 1. Pd^0-catalyzed piperazine mono *N*-arylation



9, 11-15 7 16-21

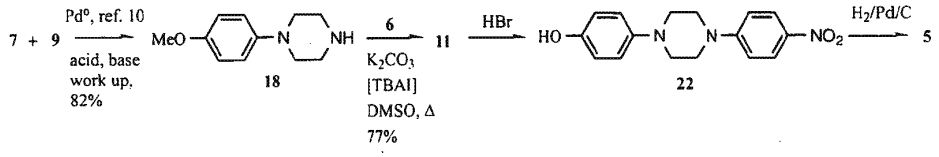
#	R	Product/% yield	Reaction time (h)
1	H (**11**)	**16**[4]/42	24
2	4-CH_3 (**12**)	**17**/69	48
3	4-OCH_3 (**9**)	**18**/82	24
4	2-CH_3 (**13**)	**19**/35	48
5	2-OCH_3 (**14**)	**20**/10	96
6	4-OCH_2Ph (**15**)	**21**/80	3[14]

was imparted by insolubility or specific set of reagents. Isolated **18** subjected to the reaction conditions with fresh reagents and the catalyst essentially resulted in a recovery of **18**. While this mechanism remained under investigation, we applied the above finding to the syntheses of **5** as detailed below.

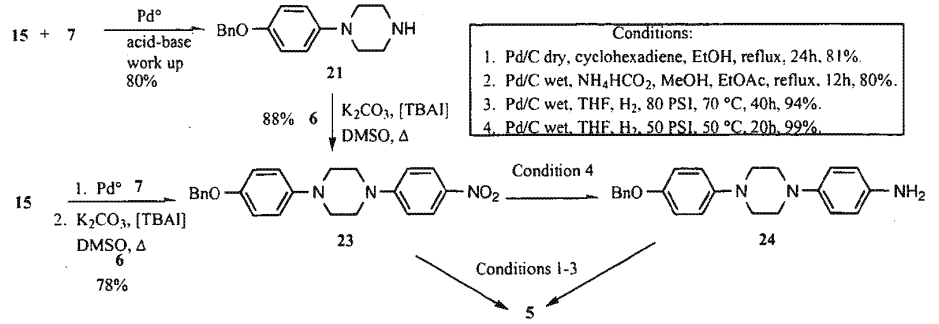
As shown in Scheme 2, arylhalide **6** was reacted with **18** using conditions described previously for *N*-arylation of piperazine with electron deficient aryl halides[1] to obtain compound **11** indistinguishable from the one made via alternate routes shown in Scheme 1. Note that the one-pot, two-step conversion, i.e. Pd^0 coupling to crude **18** followed by its reaction with **6**, without acid base work up, can be carried out in one pot to obtain 75% isolated yield of **11**. The residual reagents and byproducts form Pd^0 coupling reaction did not interfere with the conversion of **18** to **11** and the removal of one acid–base work up minimized the loss of mass resulting in an improved yield. Compound **11** was then converted to the desired antifungal intermediate **5** via demethylation followed by hydrogenation. All yields reported in this manuscript are upoptimized. In this preparation of **5**, demethylation requires an excess of refluxing aqueous HBr for a prolonged period (24+ h) of time. The isolation of nitrophenol **22** from HBr requires a pH control, it is labor intensive, and moderate yielding (75–80%).

Changing the reaction order, i.e. hydrogenation prior to demethylation encountered difficulties as well. Although insolubility of **11** in many solvents slowed down the reduction, the main problems resided in the fact that the resultant aniline intermediate formed a HBr salt with aq. HBr. Thus, yet larger excess of HBr and much longer (2+ days) refluxing time was needed for the demethylation reaction. These difficulties were overcome by the use of benzyloxy group in place of methoxy group (Scheme 3). Benzyloxy derivative **23** is more soluble compared to **11**, and its deprotection does not require harsh HBr treatment. The reaction of piperazine with **15** in the presence of Pd^0 catalyst resulted in mono *N*-arylated piperazine **21**. The use of larger amount of the catalyst allowed for improved yield of **21** with short reaction time. Compound **21** readily reacted with the arylhalide **6** under the conditions described previously[1] to form **23**. Compound **23** was then con-

UM00012089
NOVARTIS EXHIBIT 1517
Novartis v. Regents, IPR2023-01347
Page 835 of 4460



Scheme 2. Preparation of **5** via Pd^0-catalyzed mono-*N*-arylation of piperazine.



Scheme 3. A short, convenient synthesis of antifungal intermediate **5**.

verted to **5** via one of the several conditions depicted in the scheme. Further work towards streamlining the preparation of **5** showed that the isolation of **21** was unnecessary towards the preparation of **23** as **21**, prepared in situ, readily reacted with **6** to form **23**. Improved yield for one-pot preparation reflects the loss of **21** during the acid base workup. This two-pot synthesis (**15** to **23** to **5**) via the transfer hydrogenation (eliminating pressure reactor) is the most large scale amenable preparation of **5** reported to date. Note that the aniline **24** could be isolated, if needed, by using the milder hydrogenation conditions. Compound **24**, upon further hydrogenation as shown in conditions 1–3 could be converted to **5**.

Next we investigated the application of the above methods to the preparation of the azole antifungal posaconazole **1**. The known[3–6] disconnections for the synthesis of the above azole antifungals are shown in Fig. 1. In the case of Sch 51048 and Sch 56592 the chiral tetrahydrofuran moiety was appended to the di-arylated piperazine containing the *N,N'*-substituted urea entity. This was then cyclized to the hydroxy protected triazolone, i.e. *O*-benzyl **1**.[4,6] For itraconazole, the original synthesis consisted of reacting the preformed triazolone containing piperazine to the dichlorophenyl dioxolane azole. This was then subjected to triazolone-*N*-alkylation to the desired product.[3] Sepracor has recently used Pd^0 catalysis to append the preformed haloaryl triazolone to the mono-*N*-substituted piperazine as shown in Fig. 1.[5] We recognized that the piperazine mono-*N*-arylation findings offered an alternate, novel convergent approach (Fig. 2) for the preparation of **1** similar to the one used above for the preparation of differentially-*N,N'*-diarylated piperazine **5**. Furthermore, this chemistry may be applicable to the preparation of a variety of bioactive classes of *N,N'*-substituted piperazines and to important piperazines for combinatorial library work.[1–7]

Initial work towards the preparation of antifungal **1** (Scheme 4) led to the following findings. The preparation of the arylhalide **27** from sulfonate **25** (available to us[6]) progressed well. Next, the Pd^0-catalyzed reaction between arylhalide **27** and **7** under above described conditions resulted in only the mono-*N*-aryl piperazine **28** albeit in small amount (~5% yield with 0.5 mol% catalyst). On the other the reaction of triazolone **29**[15] with **7** under previously described reaction conditions[1] led to degradation of **29** instead of the formation of **30**.

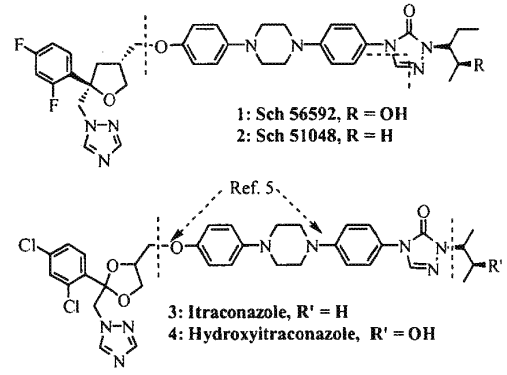


Figure 1. The antifungals and their synthetic disconnections.

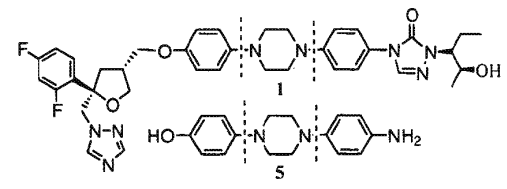
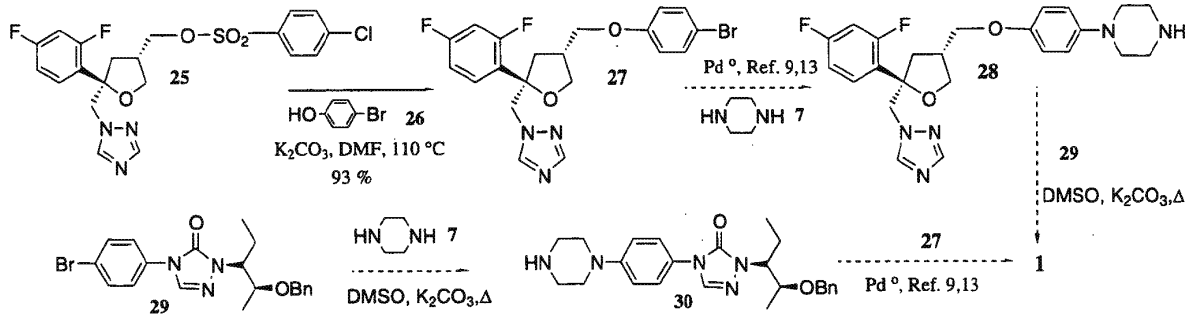


Figure 2. New disconnection for the synthesis of **1**, and **5**.

UM00012090
NOVARTIS EXHIBIT 1517
Novartis v. Regents, IPR2023-01347
Page 836 of 4460



Scheme 4. Synthesis of antifungal **1** via piperazine mono-*N*-arylations methods.

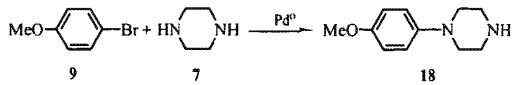
Thus, the outcomes of the initial efforts for both the Pd^0-catalyzed as the non-catalyzed piperazine mono *N*-arylation towards the preparation of **1** were discouraging.

In view of the above mono-*N*-arylation of piperazine with non-electron deficient aromatic halide, and in view of Pd^0-catalyzed amination of arylhalides in general,[12] the low yield for the reaction between **7** and **27** was intriguing. Good solubility of **7** and **27** in toluene, the use of several lots of reagents, ligands, as well as the catalyst eliminated the possibility that the low yield was imparted by specific set of reagents. Increasing the catalyst amount to 2 mol% led to ~20% solution yield of **9** suggesting a catalyst poisoning in this reaction.

This prompted us to further investigate Pd^0-catalyzed arylation of piperazine. Due to simplicity of the substrates the reaction between **9** and **7** to form **18** (Scheme 5) was chosen as a model reaction to study the above mechanism with NMR. In one set of experiments the mixture of **18** and the catalyst (prepared as described previously)[9–13] was first subjected to the reaction conditions (80°C, toluene). The use of this pretreated catalyst for reaction between fresh **7** and **9** led to no additional product **18**. This suggested a catalyst deactivation during pretreatment with **18**. This deactivation can be either due to chelation of the catalyst with **18** or due to catalyst poisoning by non-specific binding. ^1H and ^{31}P NMR probing of this reaction showed that the formation of the catalyst progressed as reported previously.[16] When this catalyst was treated with **18** and warmed, ^{31}P NMR signals for the catalytic species significantly decreased and ^{31}P NMR signals for the BINAP increased correspondingly. The catalyst by itself did not generate BIINAP ^{31}P NMR signals upon heating. Thus, under the reaction conditions, mono *N*-arylpiperazine **18** appears to compete with BINAP for $Pd_2(dba)_3$ or displace BINAP from the catalytic spices interfering with the catalytic cycle.[9,16] This NMR study suggests that mono *N*-aryl piperazines displace BINAP from the catalytic species there by preventing its diarylation. Finally comparative rate/extent of catalyst deactivation by product compared to the rate of piperazine *N*-arylation govern the extent of mono *N*-arylation reaction. Although additional studies are needed to fully understand this mechanism, the above study generated sufficient information for us to complete the novel synthesis of **1**.

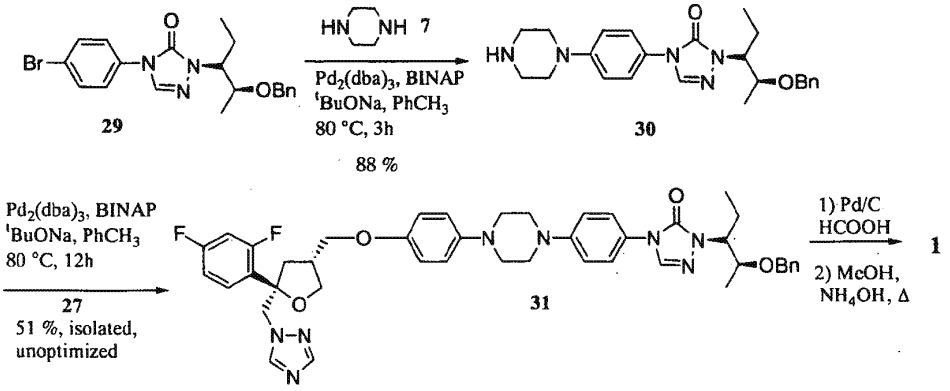
Based on the above observations, the strategy for the synthesis of **1** was revised (Scheme 6). First triazolone **29** was reacted with **7** under Pd^0-catalyzed conditions to produce compound **30** in 88% isolated yield.[17] This may be due to the possibility that product **30** of this reaction forms faster than the catalyst deactivation. Coupling of **30**, with **27** to form **31** was then accomplished also via Pd^0 catalysis. This reaction was slower compared to the preparation of **30**.[18] Alternately, a one-pot coupling of piperazine with **29** followed by the reaction of **30** with **27** can be achieved in a reasonable time (1 day) with a fresh does of catalyst added to the reaction mixture after the formation of **30**. The product profile was less clean in the latter case. Compound **31** was debenzylated via the known transfer hydrogenation procedure[6] to obtain posaconazole **1**, identical to the one obtained via the previous route.[6]

In summary, a Pd^0-catalyzed method for the mono *N*-arylation of piperazine from commercially available inexpensive raw materials without the use of protecting groups, high pressure/temperature equipment, or chromatographic purification has been discovered. This method has been applied to a short, convenient preparation of the key differentially *N,N'*-diaryl substituted piperazine antifungal intermediate. After a limited mechanistic investigation, this mono-*N*-arylation finding has been used to develop a novel synthesis of the antifungal posaconazole. The Pd^0 catalysis method complements our recently published direct, mono *N*-arylation of piperazine with arylhalides containing electron withdrawing groups.



Scheme 5. Model reaction for mechanism study via NMR.

UM00012091
NOVARTIS EXHIBIT 1517
Novartis v. Regents, IPR2023-01347
Page 837 of 4460



Scheme 6. Novel synthesis of **1** via Pd^0-catalyzed piperazine mono-*N*-arylation.

Acknowledgements

We thank Dr. George Wu for many discussions on the mechanism aspect of this project.

References

1. Hepperle, M.; Eckert, J.; Gala, D. *Tetrahedron Lett.* **1999**, *40*, 5655.
2. Eckert, J.; Chan, T.-M.; Osterman, R. M.; Lambert, J. B.; Gala, D. *Tetrahedron Lett.* **1999**, *40*, 5661.
3. Heeres, J.; Backx, L. J. J.; VanCutsem, J. *J. Med. Chem.* **1984**, *27*, 894.
4. Saksena, A. K.; Girijvallabhan, V. M.; Wang, H.; Liu, Y. T.; Pike, R. E.; Ganguly, A. K. *Tetrahedron Lett.* **1996**, *37*, 5657.
5. Tanoury, G. J.; Senanayake, C. H.; Hett, R.; Kuhn, A. M.; Kessler, D. W.; Wald, S. A. *Tetrahedron Lett.* **1998**, *39*, 6845.
6. Andrews, D. R.; Gala, D.; Gosteli, J.; Gunter, F.; Mergelsberg, I.; Sudhakar, A. US Patent 5,625,064: April 29, 1997.
7. For recent literature on *N*-phenylpiperazine useful for (a) Neuropeptide Y antagonist: Wood, P. L. *Drug Discov. Develop.* **1998**, *1*, 34; (b) G-Protein-coupled receptor ligands: Kubinyi, H. *Drug Discov. Develop.* **1998**, *1*, 4.
8. Coop, A.; Rice, K. C. *Tetrahedron Lett.* **1998**, *39*, 8925.
9. Wolfe, J. P.; Wagaw, S.; Buchwald, S. L. *J. Am. Chem. Soc.* **1996**, *118*, 7215.
10. Louie, J.; Driver, M. S.; Hamann, B. C.; Hartwig, J. F. *J. Org. Chem.* **1997**, *62*, 1268.
11. Typically, the aromatic halides (Ar-X) are converted to Grignard reagents (Ar-Mg-X) which up on reaction with trimethylborate ($B(OMe)_3$) followed by hydrolysis lead to arylborates ($Ar\text{-}B(OH)_2$).
12. For reviews on Pd^0-catalyzed amination of aromatic halides, please see: (a) Wolfe, J. P.; Wagaw, S.; Marcoux, J.-F.; Buchwald, S. L. *Acc. Chem. Res.* **1998**, *31*, 805; (b) Hartwig, J. F. *Synlett* **1997**, 329; (c) Frost, C. G.; Mendonça, P. *J. Chem. Soc., Perkin Trans. 1* **1998**, 2615.
13. Typical experimental procedure (unless noted otherwise): To a solution of piperazine (5.5 mmol) in toluene was added $Pd_2(dba)_3$ (0.025 mmol) and (+), (−), or (±)-BINAP (0.075 mmol). Arylhalide (5 mmol) was added dropwise, followed by NaO'Bu (7.5 mmol) as a suspension in THF. The resulting mixture was heated to 80–90°C for prescribed amount of time. The reaction was cooled to ambient temperature and diluted with EtOAc and water. After separation of the layers, the organic phase was washed once with water. The combined aqueous layers were back extracted with EtOAc. The resulting combined organic layers were extracted with 1N HCl. The combined acidic layers were treated with NaOH to pH 12. The mixture was then extracted with CH_2Cl_2, dried over Na_2SO_4, filtered, and concentrated under reduced pressure to afford the product. $CsCO_3$, NaHMDS, or KHMDS as bases offered no advantage over NaO'Bu.
14. Twice the amount of the catalyst/ligands added to shorten the reaction time.
15. A gift of this compound from Dr. Anantha Sudhakar is appreciated.
16. Amatore, C.; Broeker, G.; Jutand, A.; Khalil, F. *J. Am. Chem. Soc.* **1997**, *119*, 5176.
17. Laboratory work had indicated that under the Pd^0 catalysis condition, electron withdrawing group containing **29** first monoarylates piperazine to form **30**. When **30** was allowed to react with fresh catalyst and more **29**, the bis arylation set in. The bis arylation was slow (required ~3 days for ~80% yield of the symmetrically *N,N'*-bis-substituted piperazine).
18. Presumably due to the steric bulk associated with the reacting species.

UM00012092
NOVARTIS EXHIBIT 1517
Novartis v. Regents, IPR2023-01347
Page 838 of 4460

ANTIMICROBIAL AGENTS AND CHEMOTHERAPY, Dec. 1989, p. 2063–2068
0066-4804/89/122063-06$02.00/0
Copyright © 1989, American Society for Microbiology
Vol. 33, No. 12

Oral and Parenteral Therapy with Saperconazole (R 66905) of Invasive Aspergillosis in Normal and Immunocompromised Animals

JAN VAN CUTSEM,* FRANS VAN GERVEN, AND PAUL A. J. JANSSEN
Janssen Research Foundation, B-2340 Beerse, Belgium

Received 14 March 1989/Accepted 17 August 1989

Saperconazole (R 66905) is a broad-spectrum antifungal triazole with potent in vitro activity against *Aspergillus* spp. A total of 279 strains were tested in brain heart infusion broth. Development of the *Aspergillus* spp. was completely inhibited at 0.1 and 1 μg of saperconazole per ml for 80.3 and 99.6% of the strains, respectively. Normal and immunocompromised guinea pigs were infected intravenously with *Aspergillus fumigatus* and treated orally, intravenously, or intraperitoneally with saperconazole or intraperitoneally with amphotericin B. Leukopenia, neutropenia, lymphocytosis, and monocytosis were obtained with mechlorethamine hydrochloride; leukopenia, neutrophilia, and lymphopenia were obtained with cyclophosphamide. Saperconazole was dissolved for oral treatment in polyethylene glycol and for parenteral treatment in cyclodextrins. Amphotericin B was given parenterally as Fungizone (E. R. Squibb & Sons). Treatment was given once daily for 14 days. An early starting treatment was efficacious, but the activity of saperconazole was maintained even when the onset of the treatment was delayed to the moribund state. The activity of saperconazole was not altered in immunocompromised animals. Saperconazole was clearly superior to amphotericin B and free of side effects. The oral and parenteral formulations of saperconazole were equipotent. The systemic activity of saperconazole in guinea pigs was confirmed in invasive aspergillosis in pigeons.

Infections with various *Aspergillus* spp. become more and more common, especially in predisposed and exposed humans and animals. Fungi of this genus are widespread in the environment. *Aspergillus fumigatus* is considered to be the most important pathogenic species and is responsible for various invasive and chronic diseases (19).

The introduction of the broad-spectrum triazole itraconazole, the first antifungal agent orally and parenterally active in aspergillosis, constituted a marked progress in the therapeutic armament (5, 18). Itraconazole can be favorably compared with parenteral amphotericin B (10, 11, 15, 16). In this paper we report the in vitro and in vivo activity of the new broad-spectrum triazole saperconazole.

(Portions of these results have been published previously [J. Van Cutsem and P. A. J. Janssen, 10th Congr. I.S.H.A.M., Rev. Ibér. Micol. 5:S1, O2, 11, 1988; J. Van Cutsem and P. A. J. Janssen, Program Abstr. 28th Intersci. Conf. Antimicrob. Agents Chemother., abstr. no. 65, 1988].)

MATERIALS AND METHODS

Chemistry. Saperconazole is a lipophilic fluorinated triazole that is poorly soluble in water (J. Heeres, L. J. J. Backx, L. J. E. Van der Veken, and J. Van Cutsem, submitted for publication). The chemical structure of R 66905 (saperconazole) is given in Fig. 1. Its formula is as follows: $C_{35}H_{38}F_2N_8O_4$ or *cis*-[4-[4-[4-[4-[(2,4-difluorophenyl)-2-(1*H*-1,2,4-triazol-1-ylmethyl)-1,3-dioxolan-4-yl]methoxy]phenyl]-1-piperazinyl]phenyl]-2,4-dihydro-2-(1-methylpropyl)-3*H*-1,2,4-triazol-3-one. Its molecular weight is 673.

In vitro experiments. A total of 279 *Aspergillus* isolates were tested in vitro; 221 of these were *A. fumigatus*. All isolates were identified by conventional methods. The large majority of these fungi were fresh isolates from a wide variety of pathologies in humans and animals as follows: for *A. fumigatus*, 95 from humans and 104 from animals; for *A. niger*, 4 from humans and 7 from animals; for *A. flavus*, 3 from humans and 8 from animals; for *A. terreus*, 2 from humans; for *A. flavipes*, 2 from humans. All others were laboratory strains or isolated from the environment or not specified. Saperconazole was dissolved in dimethyl sulfoxide (DMSO) and diluted by serial decimal amounts ranging from 100 to 0.001 μg/ml in brain heart infusion broth. The inoculum consisted of a standardized 4-mm^2 culture block containing hyphae and spores for tubes with 5 ml of medium supplemented with drug solution or with solvent. Cultures were incubated at 25°C for 2 weeks: initial readings took place after 1 week, and final scoring was done after 2 weeks. The fungal development was graded from 0 to 4 as follows: 0, no visible growth; 4, growth equivalent to that of the controls; 1, 2, and 3, 25, 50 and 75% of control growth, respectively. In Table 1, only the decimal concentration that completely inhibited fungal growth for 14 days is reported.

In vivo experiments. (i) Guinea pigs. Male immunocompetent (normal) or immunocompromised Albino guinea pigs weighing 500 g (±50 g) (Pirbright strain) were infected intravenously (i.v.) with 25,000 CFU of *A. fumigatus* B19119 per g of body weight. This strain, isolated from lung aspergillosis of a pigeon, needed 1 μg of saperconazole per ml for complete in vitro growth inhibition. All guinea pigs were maintained in individual cages and received water and

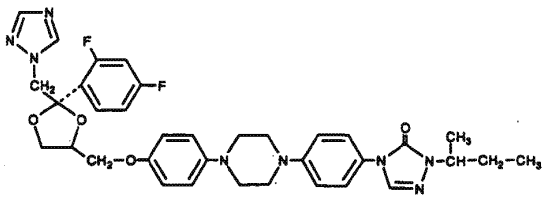


FIG. 1. Chemical structure of R 66905 (saperconazole).

* Corresponding author.

UM00012093
NOVARTIS EXHIBIT 1517
Novartis v. Regents, IPR2023-01347
Page 839 of 4460

TABLE 1. Antifungal activity in vitro[a] of saperconazole against *Aspergillus* spp.

Fungal species (no. of strains)	No. of strains completely inhibited at the following concn (μg/ml):			
	0.01	0.1	1	10
A. fumigatus (221)		187	34	
A. niger (19)		5	13	1
A. nidulans (8)	1	7		
A. flavus (15)		10	5	
A. versicolor (1)		1		
A. amstelodami (2)		1	1	
A. restrictus (1)		1		
A. penicilloides (1)		1		
A. candidus (1)		1		
A. terreus (3)		2	1	
A. flavipes (2)		2		
Other *Aspergillus* species (5)		5		

[a] Complete absence of fungal development after 14 days of incubation at 25°C in brain heart infusion broth.

nonmedicated feed ad libitum. Intraperitoneal (i.p.) administration of 0.25 mg of mechlorethamine hydrochloride per kg on days 5 and 4 before infection resulted in leukopenia, neutropenia, lymphocytosis, and monocytosis, persisting for the whole experimental period (28 days) (13; J. Van Cutsem and P. A. J. Janssen, Proc. VIth Mediterr. Congr. Chemother., 1988, in press). To induce more pronounced immunodepression, a series of guinea pigs received six doses of mechlorethamine hydrochloride. Four doses of 10 or 20 mg of cyclophosphamide per kg were administered to other groups of guinea pigs; in these animals pronounced leukopenia, neutrophilia, and lymphopenia were obtained (13).

The animals were treated orally with saperconazole, ketoconazole, or fluconazole dissolved in polyethylene glycol 200 (PEG 200). The treatment was given once daily for 14 consecutive days, starting on the day of infection or on day 1, 2, 3, or 4 after infection. Saperconazole, dissolved in dimethyl-β-cyclodextrin and in hydroxypropyl-β-cyclodextrin was also administered i.p. and i.v. As a reference drug, amphotericin B was administered i.p. as the pharmaceutical preparation for clinical use (Fungizone; Squibb). The highest dosage of amphotericin B that could be used in guinea pigs without mortality was 5 mg/kg of body weight. In all experiments the drugs were administered on the basis of milligrams per kilogram of body weight.

The activity evaluation was based on behavior, weight loss or gain, survival, lesions at necropsy, histology, and cultures of nine organs of all animals. The selected organs for culture investigations were lungs, liver, left kidney, spleen, brain, left eye, skin of the back, peritoneum, and

TABLE 2. Treatment of systemic aspergillosis in normal guinea pigs, starting on the day of infection[a]

Antifungal agent (mg/kg)	Route	Animals		Mean survival in days	% of negative organs	*P*[b]	
		Total no.	% Survivors			Survivors	Negative organs
Untreated	Oral	40	0	5.5	1.4		
Excipient (PEG 200)	Oral	138	0	5.4	1.3		
Ketoconazole							
10	Oral	18	0	5.9	6.5		
20	Oral	24	29	12.4	20.2		
40	Oral	24	42	16.3	22.5		
42.9[c]					172.8		
Fluconazole							
10	Oral	12	0	6.9	1.2		
20	Oral	12	0	7.2	3		
40	Oral	12	25	13.9	17		
45.6[c]					96.5		
Saperconazole							
0.31	Oral	20	0	7.3	5.6		
0.63	Oral	46	33	14.4	25.8	≤0.001	≤0.001
1.25	Oral	74	80	24.6	86.7	≤0.001	≤0.001
2.5	Oral	28	96	27.8	96.8	≤0.001	≤0.001
5	Oral	12	100	>28[d]	100	NS	≤0.001
10	Oral	4	100	>28	100		
0.82[c]					0.79		
Excipient (saline)	i.p.	30	0	5.7	1.2		
Amphotericin B							
0.63	i.p.	12	0	6.6	2.5		
1.25	i.p.	18	17	10.4	11.4		
2.5	i.p.	36	39	15.8	29.8		
5	i.p.	24	67	21	68.5		
3.28[c]					3.58		

[a] Once-daily treatment for 14 consecutive days.
[b] Statistics: chi-square test (two-tailed probability), saperconazole versus amphotericin B on the basis of milligrams per kilogram. NS, Not significant.
[c] ED_{50}.
[d] Surviving animals were sacrificed on day 28.

UM00012094
NOVARTIS EXHIBIT 1517
Novartis v. Regents, IPR2023-01347
Page 840 of 4460

TABLE 3. Therapeutic treatment of systemic aspergillosis in normal guinea pigs, starting 1 day after infection[a]

Antifungal agent (mg/kg)	Route	Animals		Mean survival in days	% of negative organs	P[b]	
		Total no.	% Survivors			Survivors	Negative organs
PEG 200							
Excipient	Oral	78	0	5.5	2.1		
Saperconazole							
0.63	Oral	24	54.2	17.8	36.6	NS	NS
1.25	Oral	36	72	22.6	63.6	≤0.05	≤0.001
2.5	Oral	36	100	>28[c]	91.4	≤0.001	≤0.001
5	Oral	30	100	>28	96.7	≤0.001	≤0.001
10	Oral	4	100	>28	100		
0.67[d]					0.87		
Dimethyl-β-cyclodextrin							
Excipient	i.p.	12	0	5.1	1.9		
Saperconazole							
1.25	i.p.	12	58	20.5	55.2	NS	≤0.001
5	i.p.	12	92	26.8	93.8	≤0.05	≤0.001
Excipient	i.v.	12	0	5	1.1		
Saperconazole							
1.25	i.v.	12	67	21.3	61.5	NS	≤0.001
5	i.v.	12	100	>28	99	≤0.05	≤0.001
Hydroxypropyl-β-cyclodextrin							
Excipient	i.p.	12	0	5.9	1.9		
Saperconazole							
0.31	i.p.	6	50	17.7	46.3		
0.63	i.p.	6	50	19.5	66.7	NS	≤0.001
1.25	i.p.	12	83	24.3	74.8	≤0.05	≤0.001
2.5	i.p.	6	100	>28	92.6	≤0.05	≤0.001
5	i.p.	6	100	>28	96.3	NS	≤0.001
0.42[c]					0.37		
Excipient (saline)	i.p.	12	0	5.6	1.7		
Amphotericin B							
0.63	i.p.	12	25	11.7	25.6		
1.25	i.p.	12	33	12.9	28.7		
2.5	i.p.	24	33	13.9	25.4		
5	i.p.	18	50	18.5	61		
6.82[c]					5.04		

[a] Once-daily treatment for 14 consecutive days.
[b] Statistics: chi-square test (two-tailed probability), various saperconazole treatment schedules versus amphotericin B on the basis of milligrams per kilogram. NS, Not significant.
[c] Surviving animals were sacrificed on day 28.
[d] ED_{50}.

thigh muscle. All survivors were sacrificed 28 days after infection, and cultures were made from the same organs.

(ii) Pigeons. Pigeons (*Columba livia*) with a mean weight of 400 g (±30 g) were infected i.v. in a wing vein with 7,800 CFU of *A. fumigatus* B19119 per g of body weight. Saperconazole dissolved in PEG 200 was administered by gavage at 0, 2.5, 5, or 10 mg/kg starting on the day of infection and continued once daily for 14 consecutive days. For the activity evaluation, the same parameters as for infection in guinea pigs were used, except for cultures; five organs were studied (lungs, air sacs, liver, spleen, left kidney). The total duration of the experiment was 28 days.

Statistics. The mean effective doses (ED_{50s}) were calculated for the amount of drug needed for survival and for negativation of organs by probit analysis of ED_{50} by the method of Finney. The efficacy was analyzed by the chi-square test (two-tailed probability).

RESULTS

In vitro results. The in vitro antifungal activity of saperconazole against *Aspergillus* spp. is given in Table 1. The antifungal activity of saperconazole was complete at 1 μg/ml for all but one strain of *A. niger*. Eighty percent of all strains showed complete absence of growth at 0.1 μg/ml (85% for *A. fumigatus*), and this result persisted during the 14 days of the test.

In vivo results. (i) Guinea pigs. All infected, untreated, or excipient-treated normal or immunocompromised guinea pigs died in the various experiments within a mean of 4.7 to 5.9 days (range, 4 to 8 days), with invasion of 94 to 100% of all investigated organs. Animals became sick from day 3 on, and the majority were moribund 4 days after infection. Weight loss in the infected untreated and excipient-treated animals varied between 30 and 45% of the initial weight. Macroscopic necrotic foci were present in various organs, e.g., kidneys, spleen, liver, and lungs. Histological examination demonstrated severe invasion by the fungus, especially in the kidney, spleen, liver, lung, thigh muscle, peritoneum, and brain. A large number of fungal elements were also present in the eye and the skin samples. Normal guinea pigs treated orally or parenterally from the day of infection on (Table 2) responded partially (longer survival in days;

UM00012095
NOVARTIS EXHIBIT 1517
Novartis v. Regents, IPR2023-01347
Page 841 of 4460

TABLE 4. Oral therapeutic treatment of systemic aspergillosis with saperconazole in normal guinea pigs starting 2 days after infection[a]

Saperconazole (mg/kg) in PEG 200	Animals		Mean survival in days	% of negative organs	P[b]	
	Total no.	% Survivors			Survivors	Negative organs
Excipient	12	0	4.8	0		
1.25	12	25	12.8	31.5	NS	≤0.001
2.5	12	100	>28[c]	97.2	≤0.001	≤0.001
5	6	100	>28	90.2	≤0.001	≤0.001
10	6	100	>28	98.1	≤0.001	≤0.001
1.38[d]				1.44		

[a] Oral treatment once daily for 14 consecutive days.
[b] Statistics: chi-square test (two-tailed-probability), saperconazole versus excipient on the basis of milligrams per kilogram. NS, Not significant.
[c] Surviving animals were sacrificed on day 28.
[d] ED_{50}.

some animals survived) at doses of 20 mg of ketoconazole, 40 mg of fluconazole, 1.25 mg of amphotericin B, and 0.63 mg of saperconazole per kg. An oral dose of 1.25 mg of saperconazole per kg resulted in higher cure rates than 2.5 or 5 mg of amphotericin B per kg. When the onset of the treatment was delayed for 24 h (Table 3), the therapeutic results obtained with orally administered saperconazole or i.p. amphotericin B were not different from those obtained with a treatment starting on the day of infection. Excellent results were also obtained with saperconazole administered i.p. or i.v., dissolved in dimethyl-β-cyclodextrin; results were not different from those after oral treatment. Oral therapeutic treatment with saperconazole of immunocompetent guinea pigs infected with *A. fumigatus* starting 2 or 3 days after infection (Tables 4 and 5) was also highly efficacious. In guinea pigs immunocompromised with mechlorethamine hydrochloride (Table 6), the oral treatment starting the day of infection or 1, 2, 3, or 4 days after infection, when the guinea pigs were very sick and 67% were moribund, was successful. Repeated predisposing treatment with six doses of mechlorethamine hydrochloride was unable to alter the antiaspergillar activity of saperconazole. Parenteral treatment of aspergillosis in immunocompromised guinea pigs by saperconazole dissolved in dimethyl-β-cyclodextrin or in hydroxypropyl-β-cyclodextrin was highly efficacious, and the results were largely superior to those obtained with amphotericin B (Table 7). Guinea pigs infected with *Aspergillus* spp. and receiving four doses of cyclophosphamide administered at 10 or 20 mg/kg (Table 8) responded as well as

TABLE 5. Oral therapeutic treatment of systemic aspergillosis with saperconazole in normal guinea pigs starting 3 days after infection[a]

Saperconazole (mg/kg) in PEG 200	Animals		Mean survival in days	% of negative organs	P[b]	
	Total no.	% Survivors			Survivors	Negative organs
Excipient	12	0	5.1	0		
2.5	6	0	9.8	24.1	NS	≤0.001
5	12	83	24.0	74.1	≤0.001	≤0.001
10	18	83	24.4	77.8	≤0.001	≤0.001
4.2[c]				3.6		

[a] Oral treatment, once daily for 14 consecutive days.
[b] Statistics: chi-square test (two-tailed probability), saperconazole versus excipient on the basis of milligrams per kilogram. NS, Not significant.
[c] ED_{50}.

TABLE 6. Oral treatment[a] of systemic aspergillosis with saperconazole in immunocompromised guinea pigs with mechlorethamine hydrochloride

Saperconazole (mg/kg) in PEG 200	No. of injections of MCE-HCl[b]	Start of treatment on day:	Animals		Mean survival in days	% of negative organs
			Total no.	% Survivors		
Excipient	2	0	18	0	5.8	2
0.63	2	0	24	46	16	39
1.25	2	0	12	100	>28[c]	96.3
2.5	2	0	12	100	>28	96.6
0.64[d]						0.7
Excipient	6	0	18	0	5.6	3.1
1.25	6	0	18	94	27.2	90.1
2.5	6	0	12	92	27.3	97.2
Excipient	2	1	18	0	5.9	2.9
0.63	2	1	18	78	24.5	66.3
1.25	2	1	18	100	>28	90.4
2.5	2	1	18	100	>28	99.4
5	2	1	6	100	>28	94.6
0.54[d]						0.39
Excipient	2	2	12	0	5.2	1.9
0.63	2	2	18	50	18.7	45
1.25	2	2	24	87	25.4	82.2
2.5	2	2	12	92	26.4	88.8
5	2	2	6	100	>28	94.4
0.58[d]						0.62
Excipient	2	3	12	0	5.7	0
1.25	2	3	12	67	21	64
2.5	2	3	18	61	20.7	50.4
5	2	3	12	92	26.3	93.2
0.88[d]						1.22
Excipient	2	4	6	0	5.6	1.8
2.5	2	4	6	33	14	33
5	2	4	6	67	20.7	60

[a] Oral treatment, once daily for 14 consecutive days.
[b] Mechlorethamine hydrochloride (0.25 mg/kg) induced leukopenia, neutropenia, lymphocytosis, and monocytosis.
[c] Surviving animals were sacrificed on day 28.
[d] ED_{50}.

immunocompetent animals. Saperconazole was not only life saving; all or almost all organs of surviving guinea pigs were free of *Aspergillus* spp. When some organs still remained positive at the end of the experiment, only small amounts of fungal elements were present, mainly in the kidney or in the spleen. In the various experiments, saperconazole administered orally, i.p., or i.v. was free of side effects. The side effects observed with amphotericin B administered at 2.5 and 5 mg/kg were mainly emaciation and erect dull, greyish hairs.

(ii) Pigeons. All control animals infected with *A. fumigatus* died within 2 to 5 days (mean, 3.3 days) (Table 9). They had necrotic foci in the lungs, air sacs, liver, spleen, and kidneys. These organs were highly positive by histology and on cultures. Saperconazole administered at 2.5 mg/kg was not active, but when it was given at 5 or 10 mg/kg, 92 or 100%, respectively, survived and organ cultures were negative. No drug-related side effects were observed in the pigeons.

DISCUSSION

The evaluation of the new lipophilic, broad-spectrum triazole saperconazole demonstrated a high antiaspergillar

UM00012096
NOVARTIS EXHIBIT 1517
Novartis v. Regents, IPR2023-01347
Page 842 of 4460

TABLE 7. Therapeutic parenteral treatment[a] of systemic aspergillosis with saperconazole in immunocompromised guinea pigs with mechlorethamine hydrochloride, starting 1 day after infection

Saperconazole (mg/kg) in PEG 200	Animals		Mean survival in days	% of negative organs	Statistics P^b	
	Total no.	% Survivors			Survivors	Negative organs
Excipient (HP-β-CD)[c]	12	0	5.8	3.7		
Saperconazole						
0.63	12	33	15.6	57.4	NS	≤0.01
1.25	12	67	23.7	73	NS	≤0.01
2.5	12	100	>28[d]	90.7	NS	≤0.001
5	12	100	>28	96.3	≤0.05	≤0.001
0.86[e]				0.52		
Excipient (saline)	12	0	5.9	6		
Amphotericin B						
0.63	12	33	15.3	37.8		
1.25	12	50	16.5	53.7		
2.5	12	67	18.9	64.8		
5	12	58	21	62		
1.51[e]				1.20		

[a] i.p. treatment, once daily for 14 consecutive days.
[b] Statistics: chi-square test (two-tailed probability), saperconazole versus amphotericin B on the basis of milligrams per kilogram. NS, Not significant.
[c] HP-β-CD, Hydroxypropyl-β-cyclodextrin.
[d] Surviving animals were sacrificed on day 28.
[e] ED_{50}.

TABLE 8. Oral treatment[a] of systemic aspergillosis with saperconazole in immunocompromised guinea pigs with cyclophosphamide

Saperconazole (mg/kg) in PEG 200	CPP[b] (mg/kg)	Start of treatment on day:	Animals		Mean survival in days	% of negative organs
			Total no.	% Survivors		
Excipient	10	0	6	0	5.9	4
0.63	10	0	6	17	11.3	32
1.25	10	0	6	67	24.8	88.3
2.5	10	0	6	100	>28[c]	92.6
0.99[d]						0.77
Excipient	10	1	6	0	5.8	2
0.63	10	1	6	33	14.2	39.4
1.25	10	1	6	83	24.5	79.6
2.5	10	1	6	100	>28	94.5
0.78[d]						0.75
Excipient	20	0	6	0	4.7	1.9
0.63	20	0	6	33	13.8	33.4
1.25	20	0	6	83	27.5	90.7
2.5	20	0	6	100	>28	96.3
0.78[d]						0.75
Excipient	20	1	6	0	5.4	5.6
0.63	20	1	6	17	10.8	24
1.25	20	1	6	67	20.3	68.5
2.5	20	1	6	100	>28	89.8
0.99[d]						0.98

[a] Oral treatment, once daily for 14 consecutive days.
[b] Cyclophosphamide (4 injections) induced leukopenia, neutrocytosis, and lymphopenia.
[c] Surviving animals were sacrificed on day 28.
[d] ED_{50}.

activity in vitro and in vivo. The in vitro activity of azoles depends on a large variety of factors (7) and was clearly demonstrated for itraconazole (3, 14). The temperature for the assay is not physiologic. However, for another azole (enilconazole), the influence of the temperature was evaluated on its fungistatic and fungicidal activity: 4, 18, 25, 37, and 45°C were used for five strains of *A. fumigatus* (14). It appeared clear that there was no major difference between the results at 25°C and those obtained at the physiologic temperature, especially due to the duration of the assay as carried out in this study. As for itraconazole, the higher pH of brain heart infusion broth and the slower onset of growth may favorably influence the activity of saperconazole. The higher pH of this medium may also allow a higher concentration of active nonprotonated drug (18). The activity of saperconazole against a large series of *Aspergillus* strains tested in vitro gave a clear image of the potency of the compound. For in vivo studies in guinea pigs and pigeons, a highly pathogenic strain of *A. fumigatus*, with profuse sporulation and capable of inducing a homogeneous systemic and disseminated disease, was selected. Moreover, the selection of the strain of *A. fumigatus* for in vivo experiments was also based on the fact that it belonged to the 15% of strains that needed 1 μg/ml for complete growth inhibition during the 14-day test period. There is a real need for active drugs in aspergillar infections. Up to now, only amphotericin B, enilconazole, and itraconazole may be considered as really active compounds in aspergillosis. The therapeutic use of amphotericin B is restricted by side effects, severe toxicity problems (1, 7), and by the exclusive use of the parenteral route (4, 8). Enilconazole is not active by the oral or parenteral route and can be used only as a fungicidal compound for disinfection, prophylaxis, and topical treatment by fumigation or by spray (9, 17). Itraconazole is a potent antiaspergillar triazole that can be administered orally and parenterally (10, 11, 13). Ketoconazole and fluconazole appeared to be only marginally active, whereas terbinafine is not active (12).

Guinea pigs and pigeons were preferred for their high susceptibility to *Aspergillus* infections. More uniform and large invasion of various organs, especially the lungs, in general the portal of entry of *Aspergillus* under natural conditions, is an interesting aspect in favor of these species. Important also is the higher persistent immunodepression in guinea pigs compared with that in mice, which regain immunity if the dosage of the immunodepressing agent is not lethal.

In our animal experiments in rats we obtained a pronounced neutropenia after treatment with cyclophospha-

TABLE 9. Oral treatment[a] of systemic aspergillosis with saperconazole in pigeons starting on the day of infection

Saperconazole (mg/kg) in PEG 200	Pigeons		Mean survival in days	% of negative organs
	Total no.	% Survivors		
Excipient	12	0	3.3	0
2.5	6	0	4.7	0
5	12	92	26.2	91.7
10	12	100	>28[b]	100
4.2[c]				4.2

[a] Oral treatment, once daily for 14 consecutive days.
[b] Surviving animals were sacrificed on day 28.
[c] ED_{50}.

UM00012097
NOVARTIS EXHIBIT 1517
Novartis v. Regents, IPR2023-01347
Page 843 of 4460

mide (unpublished data). In the guinea pigs however, the administration of 4 × 10 or 4 × 20 mg of cyclophosphamide per kg resulted in an increase of the percentage of neutrophils by 72% (group of 18 guinea pigs) and 76% (group of 17 guinea pigs), respectively (13). The effects of cyclophosphamide in guinea pigs on the neutrophils were comparable to those obtained with hydrocortisone acetate (increase of 97%) and with prednisolone acetate (increase of 152%), but after administration of 2 × 0.25 mg of mechlorethamine hydrochloride per kg only 62% of neutrophils were counted (161 guinea pigs). All of these data were statistically significant by the Mann-Whitney U test (two-tailed probability) P at $\leqq 0.001$ (13).

Systemic disseminated aspergillosis in the guinea pig is a reliable model that allows good extrapolation from the experimental infection to the natural disease in humans and animals (2, 11). An inoculum of 25,000 spores of *A. fumigatus* per g of body weight of guinea pigs infected i.v. resulted in a standardized model with repeatable survival and organ positivity. The response to oral and parenteral treatment with saperconazole was comparable for immunocompetent guinea pigs and mechlorethamine hydrochloride- or cyclophosphamide-immunocompromised guinea pigs. Delayed start of treatment with saperconazole had no influence on the results. Even when treatment with saperconazole started in moribund animals (day 4), the majority of the animals were cured. The results obtained with saperconazole were largely superior to those with amphotericin B. The activity of saperconazole in the pigeon model supports the value of this new triazole in another animal species. The activities of saperconazole given orally, i.p., and i.v. were comparable and will open new therapeutic possibilities in both patients who can take oral therapy and patients with a poor absorption profile, where a safe parenteral drug is needed. Saperconazole was given to human volunteers. The half-life of saperconazole after a single dose of 200 mg was 20 h (V. Van de Velde, P. Van Rooy, A. Van Peer, R. Woestenborghs, J. Mesens, J. Heykants, and G. Cauwenbergh, Clin. Res. Rep. R 66905/5, November 1988).

With the increasing need for new therapeutic agents with anti-*Aspergillus* activity and because of its highly curative value in models that mimic natural dissemination in various organs, saperconazole is a candidate for clinical trials. This is supported not only by its activity (P. Van Rooy, K. De Beule, J. De Crée, and G. Cauwenbergh, Clin. Res. Rep. R 66905/6, January 1989; V. Van de Velde, P. Van Rooy, A. Van Peer, K. De Beule, R. Woestenborghs, J. Heykants, and G. Cauwenbergh, Clin. Res. Rep. R 66905/9, March 1989; P. Van Rooy, K. De Beule, J. De Crée and G. Cauwenbergh, Clin. Res. Rep. R 66905/10, April 1989) but also by potential oral and parenteral treatment.

ACKNOWLEDGMENTS

We are grateful to S. Sas for secretarial work and to P. Lenaerts for statistical analysis.

LITERATURE CITED

1. **Aisner, J., J. Murillo, S. C. Schimpff, and A. C. Steere.** 1979. Invasive aspergillosis in acute leukemia: correlation with nose cultures and antibiotic use. Ann. Intern. Med. **90**:4–9.
2. **Cauwenbergh, G., and J. Van Cutsem.** 1988. Role of animal and human pharmacology in antifungal drug design. Ann. N.Y. Acad. Sci. **544**:264–269.
3. **Espinel-Ingroff, A., S. Shadomy, and R. J. Gebhart.** 1984. *In-vitro* studies with R 51211 (itraconazole). Antimicrob. Agents Chemother. **26**:5–9.
4. **Graybill, J. R., and J. Ahrens.** 1985. Itraconazole treatment of murine aspergillosis. Sabouraudia, J. Med. Vet. Mycol. **23**: 219–223.
5. **Heeres, J., L. J. J. Backx, and J. Van Cutsem.** 1984. Antimycotic azoles: synthesis and antifungal properties of a series of novel triazol-3-ones. J. Med. Chem. **27**:894–900.
6. **Odds, F. D., C. E. Webster, and A. B. Abbott.** 1984. Antifungal relative inhibition factors. J. Antimicrob. Chemother. **14**:105–114.
7. **Pennington, J. E.** 1977. Aspergillus pneumonia in hematologic malignancy: improvements in diagnosis and therapy. Arch. Intern. Med. **137**:769–771.
8. **Saag, M. S., and W. E. Dismukes.** 1988. Azole antifungal agents: emphasis on new triazoles. Antimicrob. Agents Chemother. **32**:1–8.
9. **Van Cutsem, J.** 1983. Antifungal activity of enilconazole on experimental aspergillosis in chickens. Avian Dis. **27**:36–42.
10. **Van Cutsem, J., and P. A. J. Janssen.** 1987. Etude de l'activité antifongique par le modèle animal préclinique. Méd. Mal. Infect. **8/9**:428–435.
11. **Van Cutsem, J., and P. A. J. Janssen.** 1988. *In-vitro* and *in-vivo* models to study the activity of antifungals against *Aspergillus*, p. 215–227. *In* H. Vanden Bossche, D. W. R. Mackenzie, and G. Cauwenbergh (ed.), *Aspergillus* and aspergillosis. Plenum Publishing Corp., New York.
12. **Van Cutsem, J., and P. A. J. Janssen.** 1989. Le traitement de l'aspergillose expérimentale par l'énilconazole et par l'itraconazole. Bull. Soc. Fr. Mycol. Méd. **18**:55–59.
13. **Van Cutsem, J., F. Van Gerven, J. Fransen, and P. A. J. Janssen.** 1988. Modèles animaux d'immunodépression dans l'étude des mycoses et des antifongiques. Bull. Soc. Fr. Mycol. Méd. **17**:9–24.
14. **Van Cutsem, J., F. Van Gerven, and P. A. J. Janssen.** 1986. The *in-vitro* evaluation of azoles, p. 51–64. *In* K. Iwata and H. Vanden Bossche (eds.), *In-vitro* and *in-vivo* evaluation of antifungal agents. Elsevier Science Publishers, Amsterdam.
15. **Van Cutsem, J., F. Van Gerven, and P. A. J. Janssen.** 1987. Activity of orally, topically and parenterally administered itraconazole in the treatment of superficial and deep mycoses: animal models. Rev. Infect. Dis. **9**:S15–S32.
16. **Van Cutsem, J., F. Van Gerven, and P. A. J. Janssen.** 1987. The *in-vitro* and *in-vivo* antifungal activity of itraconazole, p. 177–192. *In* R. A. Fromtling (ed.), Recent trends in the discovery, development and evaluation of antifungal agents. J. R. Prous, Barcelona.
17. **Van Cutsem, J., F. Van Gerven, and P. A. J. Janssen.** 1988. *In-vitro* activity of enilconazole against *Aspergillus spp.* and its fungicidal efficacy in a smoke generator against *Aspergillus fumigatus*. Mycoses **31**:143–147.
18. **Van Cutsem, J., F. Van Gerven, M. A. Van de Ven, M. Borgers, and P. A. J. Janssen.** 1984. Itraconazole, a new triazole that is orally active in aspergillosis. Antimicrob. Agents Chemother. **26**:527–534.
19. **Young, R. C., J. E. Bennett, C. L. Vogel, P. P. Carbone, and V. T. De Vita.** 1970. Aspergillosis. The spectrum of the disease in 98 patients. Medicine **49**:147–173.

UM00012098
NOVARTIS EXHIBIT 1517
Novartis v. Regents, IPR2023-01347
Page 844 of 4460

Rev. Inst. Med. trop. S. Paulo
42(4): 231-234, July-August, 2000.

CENTRAL NERVOUS SYSTEM PARACOCCIDIOIDOMYCOSIS. REPORT OF A CASE SUCCESSFULLY TREATED WITH ITRACONAZOL

Luis A. VILLA(1), Angela TOBÓN(2), Antonio RESTREPO(3), Daniel CALLE(4), David S. ROSERO(4), Beatriz L. GÓMEZ(2) & Angela RESTREPO(2)

SUMMARY

Paracoccidioidomycosis (PCM) is a primary pulmonary infection that often disseminates to other organs and systems. Involvement of the central nervous system (CNS) is rare and due to the fact that both clinical alertness and establishment of the diagnosis are delayed, the disease progresses causing serious problems. We report here a case of neuroparacoccidioidomycosis (NPCM), observed in a 55 year-old male, who consulted due to neurological symptoms (left hemiparesis, paresthesias, right palpebral ptosis, headache, vomiting and tonic clonic seizures) of a month duration. Upon physical examination, an ulcerated granulomatous lesion was observed in the abdomen. To confirm the diagnosis a stereotactic biopsy was taken; additionally, mycological tests from the ulcerated lesion and a bronchoalveolar lavage were performed. In the latter specimens, *P. brasiliensis* yeast cells were visualized and later on, the brain biopsy revealed the presence of the fungus. Treatment with itraconazole (ITZ) was initiated but clinical improvement was unremarkable; due to the fact that the patient was taking sodium valproate for seizure control, drug interactions were suspected and confirmed by absence of ITZ plasma levels. The latter medication was changed to clonazepam and after several weeks, clinical improvement began to be noticed and was accompanied by diminishing *P. brasiliensis* antigen and antibody titers. In the PCM endemic areas, CNS involvement should be considered more often and the efficacy of itraconazole therapy should also be taken into consideration.

KEYWORDS: Paracoccidioidomycosis; Central nervous system; Itraconazole

INTRODUCTION

Paracoccidioidomycosis (PCM), a mycosis caused by the dimorphic fungus *Paracoccidioides brasiliensis*, is a systemic disease that afflicts predominantly rural adult males living in the endemic countries of South and Central America. The primary lesion occurs in the lungs[13] but often disseminates to other organ and systems, notably the oral mucosa, the adrenal glands, the reticulo-endothelial system, the skin, and less frequently to other organs such as the central nervous system (CNS). According to AJELLO[1], the latter manifestation was initially described by Pereira and Jacobs in 1919.

In neuroparacoccidioidomycosis (NPCM), as well as in other more common forms of the mycosis, patients are predominantly males, age 30-50 years. The CNS manifestations may become apparent in the meninges or in the cerebral parenchyma where they give rise to the corresponding clinical manifestations, including those of a pseudotumoral lesion[9,10,14-16,18-20].

The diagnosis of NPCM is difficult to establish. Neuroimaging studies such as Computerized Tomography (CT) and Magnetic Resonance Imaging (MRI) are helpful in suggesting the disease but they do not furnish a definitive diagnosis[8,17]. The latter is obtained only when the fungus is observed microscopically or isolated from biopsies or from the cerebrospinal fluid (CSF)[6,14]. However, the latter sample, is not too effective as repeated specimens, large quantities of and prolonged incubation of the cultures are required[16]. Consequently, invasive procedures are often needed to obtain representative samples for diagnosis.

Detection of *P. brasiliensis* may be improved by immunologic testing for antibodies, such as the agar gel immunodiffusion and the complement fixation[6,11,14], and more recently, also by antigen detection procedures[11].

Amphotericin B, administered either by the intravenous or the intrathecal routes, has been used in the treatment of NPCM. When the dose has been completed, treatment is followed with sulfonamides for chronic supportive therapy[2,9,10,14,20]. Certain sulfonamide-trimethoprim combinations, such as cotrimoxazol and cotrimazine, have also been used due to the high drug levels attained in the CSF[2]. Surgery is reserved for patients in whom granulomas are accessible and the symptoms have failed to improve with specific therapy[14]. We present here the record of a Colombian patient with NPCM whose symptoms and neurological signs improved or resolved during therapy with itraconazole.

(1) Departamento de Neurología, Facultad de Medicina, Universidad de Antioquia y Hospital Universitario San Vicente de Paúl.
(2) Unidad de Micología Médica, Corporación para Investigaciones Biológicas (CIB), Medellín, Colombia.
(3) Departamento de Medicina Interna, Instituto de los Seguros Sociales (ISS).
(4) Facultad de Medicina, Universidad Pontificia Bolivariana, Medellín, Colombia.
Correspondence to: Angela Restrepo M., Ph.D., Corporación para Investigaciones Biológicas (CIB), Carrera 72A # 78B-141, Medellín, Colombia. Fax (057) 441 5514, email: angelares@epm.net.co

UM00012099
NOVARTIS EXHIBIT 1517
Novartis v. Regents, IPR2023-01347
Page 845 of 4460

CASE REPORT

The patient was a 55 year-old male patient, car driver in the city of Medellín but who in his younger years, was a farmer in a rural region. He ingested alcohol regularly and has been a heavy cigarette smoker (35 packets/year). He attended the Social Security Hospital because for the last month, he had been experiencing a progressive problem characterized by left hemiplegia, accompanied by paresthesias and right palpebral ptosis. For the last three days, he has also experienced tonic-clonic seizures of the left extremities with secondary generalization, global headache and persistent vomiting.

Physical signs showed that the patient was alert and cooperative. Additionally, his vital signs were within normal limits. A non-painful cutaneous ulceration, 3X2 centimeters, was observed in the abdomen in the periumbilical zone; it had raised borders and a granulomatous appearance. This lesion was first noticed a year ago but the patient disregarded it, as it caused no major discomfort.

Neurological examination disclosed that the patient was conscious, had a highly preserved cortical function and his memory was also normal.



Fig. 1 - CT brain scan at diagnosis showing a ring-enhancing lesion in the right mesencephalon with mass effect and peri-lesional edema.

There were no signs of meningeal irritation; the ocular funduscopic examination revealed that there was venous congestion with papilledema. The pupillae were isochoric and normoreactive; common ocular motor nerve palsy was noticed. There was central right facial paresia and left hypoesthesia and hemiparesis (in a scale of 0-5, the muscle strength was 4/4 in all segments of the left hemibody). Pathological reflexes (Hoffman, Babinski) were absent. Simple and contrasted CNS CT scans, thoracic X-rays as well as laboratory tests were ordered.

At the level of the right thalamus, CT scans revealed a ring-enhancing lesion accompanied by a large area of peri-lesional edema (Fig. 1). A representative biopsy was then taken and the new CT indicated that the lesion involved not only the right thalamus but also the mesencephalon; it measured 18X16 mm and had a necrotic center. The thoracic X-rays showed bilateral interstitial infiltrates in both basal fields. Diagnostic impressions comprised toxoplasmosis, lymphoma, tuberculosis and astrocytoma. A stereotaxic biopsy was carried out with the aid of a CT scan and reported, later on, as compatible with cryptococcosis, a diagnosis that prompted fluconazole treatment.

The blood biochemical parameters and the hematological tests were normal with the exception of leukocytosis (22,900/mm^3) and neutrophilia (19,150/mm^3). Sedimentation rate was 35 mm and the C reactive protein was 1.44 mg/dL. Tests for HIV and toxoplasmosis (IgM) were negative. Repeated searching for AFB in sputum (3 samples) also gave negative results.

Three weeks later and due to lack of response, the initial diagnosis was questioned and mycological studies such as direct KOH examination and cultures were ordered. These included specimens from the abdominal ulcer as well as a brochoalveolar lavage (BAL). Serum and CSF were also subjected to immunological testing for antibody (agar gel immunodiffusion and complement fixation) and antigen detection (inhibition ELISA). Additionally, authorization to revise the brain biopsy slides was solicited.

Direct examination of both clinical specimens revealed the presence of *P. brasiliensis* multiple budding yeast cells. The latter were also observed in the H&E-stained brain tissue; a few days later, the immunological tests revealed the presence of antibodies against the fungus, as well high levels of circulating antigen. Consequently, the diagnosis of PCM became firmly established.

Treatment with itraconazole (ITZ), 400 mg/day, was initiated. The patient had been receiving sodium valproate (400 mg/day in the morning and 200 mg/day in the evening) to avoid seizures. One month after antifungal therapy, clinical response was minimal; consequently, ITZ plasma levels were determined and found that they were undetectable. At this time, sodium valproate was suspended and replaced by clonazepam, 1mg/day; ITZ continued to be administered at the same dose (Table 1).

Fifteen days later, ITZ plasma levels have attained acceptable levels (4.60 µg/mL), and as a consequence, the ITZ dose was lowered to 300 mg/day. During the first two months at this dose, the abdominal ulceration and the common ocular motor nerve palsy healed; the headache diminished and disappeared on prolonged therapy (7 months). The hemiparesis became less noticeable but persisted as sequelae.

UM00012100
NOVARTIS EXHIBIT 1517
Novartis v. Regents, IPR2023-01347
Page 846 of 4460

After 5 months of therapy, ITZ levels were sufficiently high (9.76 µg/mL) to allow a decrease in the dose (200 mg/day); the latter was maintained until completing a year of therapy (Table 1). Laboratory tests failed to reveal drug toxicity. Periodically, control tests to determine the presence of both antibodies and circulating antigens, were done. Antigen titers diminished after correction for the anti-seizure medication and became undetectable 5 months after suspending the ITZ-sodium valproate combination.

At time of this report, the patient has been followed for 2 years without experiencing clinical or mycological relapses. A CT scan taken six months after the end of treatment, revealed substantial improvement, as shown in Fig. 2.

DISCUSSION

In countries where PCM is endemic, the neurological manifestations of this disorder should be taken into consideration in undiagnosed patients with signs and symptoms of chronic meningoencephalitis or expansive CNS processes. According to autopsy studies, NPCM occurs more often than suspected by the physician and consequently, treatment is delayed and death may ensue[15,19].

CNS involvement represents dissemination from the primary pulmonary focus which is often a silent process; when other extra-pulmonary lesions are present in the patient, diagnosis becomes simpler as samples for laboratory examination are easier to obtain. PLÁ *et al.*[16] revised 22 NPCM cases and found that most patients had lesions outside the brain, mostly in the lungs (13/17 cases with X-rays films), the teguments (8 cases) and the lymph nodes (1 case). These results reveal the disseminated pattern of this mycosis[6,10,14,16].

In the patient reported here, there were indications of previous lung involvement and also, presence of a cutaneous lesion that should have led to suspect a multisystemic disorder. Nonetheless, this important lesion was disregarded.

The clinical manifestations of the CNS in PCM are those of a chronic meningitis or of an expansive tumor-like lesion (paracoccidioidoma)[9,10,14]. Histologically, the latter is characterized by granulomas that may be localized anywhere within the CNS, especially in areas with adequate blood supply, such as the cerebral hemispheres, the cerebellum and more rarely, the thalamus, the medulla and the spinal cord[15,19]. Involvement of the thalamus such as was observed in our patient, was recorded in only two of the 22 cases revised by PLÁ *et al.*[16].

Treatment of NPCM has relied on amphotericin B, an effective medication known to be nephrotoxic and capable of producing systemic effects[4]. Several authors consider that sulfonamides by their capacity to penetrate into the brain, are the drugs of choice. Nonetheless, prolonged periods of continuous treatment (3-5 years) are required before adequate results can be obtained[3,10,14,20]. The azole derivatives ketoconazole, fluconazole and itraconazole have all been used for the treatment of non-meningeal forms of PCM. Itraconazol is considered by our group as the choice medication in other forms of PCM[12,13] and although it does not attain adequate CNS levels, this drug concentrates in the tissues[14]. Nonetheless, the adequacy of its use in CNS disease has not been definitively demonstrated.

Table 1
Itraconazole plasma levels and laboratory findings: influence of concomitant sodium valproate treatment

Month	Itraconazol levels * (µg/mL)	Complement fixation	*P. brasiliensis* antigen titers (µg/mL)	Concommitant therapy Itraconazol/ Valproato/ Clonazepam (mg/day)
1	Not detectable	1:64	11	400/500/0
2	4.60	1:64	19	400/0/1
5	9.76	1:16	15	300/0/1
7	4.60	1:8	0	200/0/1

* Therapeutic failures are associated with levels <2µg/mL

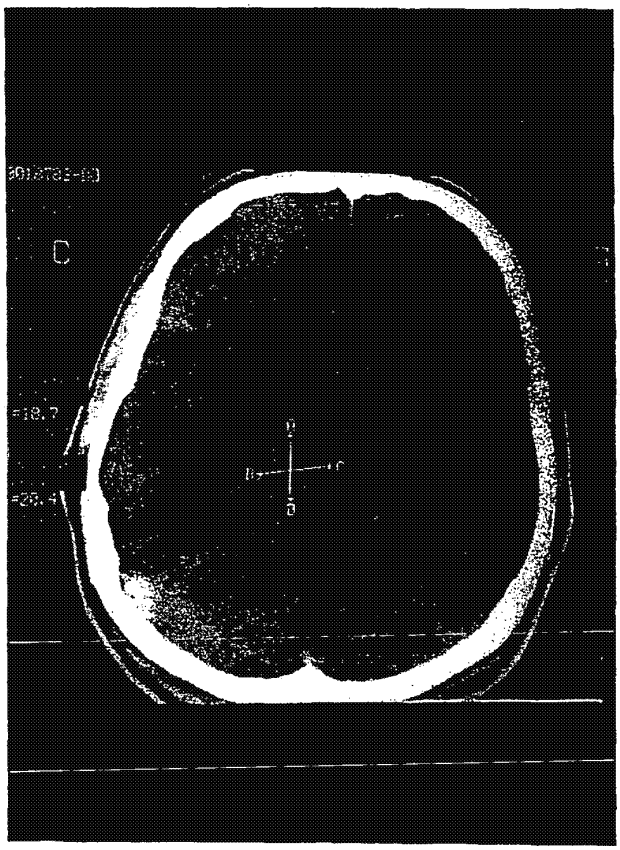


Fig. 2 - CT brain scan at the end of ITZ therapy. The edema has subsided, uptake of the contrast media is less intense although the lesion's size remains unaltered.

UM00012101
NOVARTIS EXHIBIT 1517
Novartis v. Regents, IPR2023-01347
Page 847 of 4460

The efficacy of ITZ in PCM, even in severe juvenile cases[12], as well as the known toxicity of amphotericin B[4], led us to use ITZ at a dose twice the one generally employed (200 mg/day). However, we initially disregarded the possible interaction with sodium valproate that resulted in lowered ITZ plasma levels due to their metabolism through the cytochrome P450 system[5]. Upon interruption of the latter drug and replacement by another anti-seizure medication, clinical response was achieved, and was accompanied by an important elevation of ITZ plasma levels and significant decreases in the titers of both circulating antigen and serum antibody.

Clinical response was noticed after two months with healing of the abdominal ulceration; intracraneal hypertension took a longer time (7 months) to resolve but improvement was gradual and marked. Although at the end of therapy hemiparesis was still present, the degree of impairment was minor. Previous reports do not mention the duration of the neurological sequelae and only one author[18] refers to their persistence.

To the best of our knowledge, this is the first NPCM case that has been treated and responded to ITZ therapy. It is recommended that CNS involvement be considered in all patients with PCM in order to promptly establish both the diagnosis and the specific treatment, thus avoiding permanent brain damage and death of the patient.

RESUMO

Paracoccidioidomicose do sistema nervoso central. Apresentação de um caso tratado com êxito com itraconazole

A paracoccidioidomicose (PCM) é infecção pulmonar primária que algumas vezes pode se disseminar a outros órgãos e sistemas. O envolvimento do sistema nervoso central (SNC) é raro e devido ao fato que a alerta clínica e o estabelecimento do diagnóstico são tardios, a doença progride e o paciente piora. Aquí apresentamos caso de neuroparacoccidioidomicose (NPCM) observada em homem de 55 anos de idade que referia sintomas neurológicos (hemiparalisia esquerda, parestesias, ptose pálpebral direita, dor de cabeça, vômito e convulsões) de um mes de duração. Ao exame físico, foi achada lesão ulcerada e granulomatosa no abdômen. Como o diagnóstico era duvidoso, foi indicada biopsia estereotáxica; além disso provas micológicas a partir da lesão ulcerada e um lavado broncoalveolar foram realizados. Nas últimas amostras *P. brasiliensis* foi observado e depois a biopsia do cérebro revelou a presença do fungo. O tratamento com itraconazol foi iniciado mas a melhoria clínica não foi detectável; devido ao fato que o paciente estava tomando valproato de sódio para o controle das convulsões, foi suspeita interação entre os dois medicamentos, que foi confirmada pela ausência do nível plasmático do antimicótico. Este último medicamento foi trocado por clonazepam e depois de algumas semanas a melhoria clínica foi percebida e acompanhada pela diminuição dos títulos de antígenos e anticorpos do *P. brasiliensis*. Em áreas endêmicas, o envolvimento do SNC deve ser considerado em doentes com PCM e a eficácia do itraconazole deve ser considerada.

ACKNOWLEDGEMENTS

The authors sincerely express their appreciation to Dr. Luz Elena Cano for providing assistance with the manuscript and to Dr. Myrtha Arango for her kind cooperation with the mycological analysis.

REFERENCES

1. AJELLO, L. - Paracoccidioidomycosis: a historical review. In: PAN AMERICAN SYMPOSIUM OF PARACOCCIDIOIDOMYCOSIS, 1., Washington, Pan American Health Organization, 1972. **Proceedings**. p. 3-10. (Sci. Publ. 254).

2. BARBOSA, W. & VASCONCELOS, W.M.P. - Ação da sulfametoxazol associada ao trimetoprim na terapêutica da blastomicose sul-americana. **Rev. Pat. trop.**, 2: 329-339, 1973.

3. BARRAVIERA, B.; MENDES, R.P.; MACHADO, J.M. *et al.* - Evaluation of treatment of paracoccidioidomycosis with cotrimazine (combination of sulfadiazine and trimetoprim). Preliminary report. **Rev. Inst. Med. trop. S. Paulo**, 31: 53-55, 1989.

4. BENNETT, J.E. - Antifungal agents. In: MANDELL, G.L.; BENNETT, J.E. & DOLIN, R. **Principles and practice of infectious diseases**. 4. ed. New York, Churchill Livingstone, 1995. p. 2678-2682.

5. BRODEL, T.T. & ELEWSIKI, B.E. - Clinical pearl: systemic antifungal drugs and interactions. **J. Amer. Acad. Derm.**, 33: 259-260, 1995.

6. BRUMMER, E.; CASTAÑEDA, E. & RESTREPO, A. - Paracoccidioidomycosis: an update. **Clin. Microbiol. Rev.**, 6: 89-117, 1993.

7. COMO, J.A. & DISMUKES, W.E. - Oral azole drugs as systemic antifungal therapy. **New Engl. J. Med.**, 330: 263-272, 1994.

8. DE CASTRO, C.C.; YAMAGA, L.Y.I.; BERNARD, G.; SHIKANAI-YASUDA, M.A. & CERRI, G.G. - MRI of central nervous system (CNS) paracoccidioidomycosis (PCM). In: ENCONTRO INTERNACIONAL SOBRE PARACOCCIDIOIDOMICOSE, 7. Campos do Jordão, 1999. **Proceedings**. p. 116.

9. DEL NEGRO, G.; MELO E ALBUQUERQUE, F.J. & PIMENTA DE CAMPOS, E. - Localização nervosa da blastomicose sul-americana. **Rev. Hosp. Clin. Fac. Med. S. Paulo**, 9: 64-80, 1954.

10. DUARTE, A.L.W.P.; BARUFFA, G.; TERRA, H.B.G. *et al.* - Paracoccidioidomicose sistêmica com envolvimento do sistema nervoso central. **Rev. Soc. bras. Med. trop.**, 32: 439-442, 1999.

11. GOMEZ, B.L.; FIGUEROA, J.I.; HAMILTON, A.J. *et al.* - Antigenemia in patients with paracoccidioidomycosis: detection of the 87-kilodalton determinant during and after antifungal therapy. **J. clin. Microbiol.**, 36: 3309-3316, 1998.

12. NARANJO, M.S; TRUJILLO, M.; MUNERA, M.I. *et al.* - Treatment of paracoccidioidomycosis with itraconazol. **J. med. vet. Mycol.**, 28: 71-90, 1990.

13. NEGRONI, R. - Paracoccidioidomycosis (South American Blastomycosis, Lutz Mycosis). **Int. J. Derm.**, 32: 847-859, 1993.

14. NOBREGA, J.P.S. & SPINA-FRANÇA NETTO, A. - Neuroparacoccidioidomycosis. In: FRANCO, M.; LACAZ, C.S.; RESTREPO, A. & DEL NEGRO, G. **Paracoccidioidomycosis**. Boca Ratón, CRC Press, 1994. p. 321-330.

15. PEREIRA, W.C.; RAPHAEL, A. & SALLUM, J. - Lesões neurológicas na blastomicose sul-americana. Estudo anátomo-patológico de 14 casos. **Arq. Neuropsiquiatr.**, 23: 95-112, 1965.

16. PLA, M.P.; HARTUNG, C.; MENDOZA, P.; STUKANOFF, A. & MORENO, M.J. - Neuroparacoccidioidomycosis: case reports and review. **Mycopathologia** (Den Haag), 127: 139-144, 1994.

17. RODACKI, M.A.; DE TONI, G.; BORBA, L.A. & OLIVEIRA, G.G. -Paracoccidioidomycosis of the central nervous system: CT findings. **Neuroradiology**, 37: 636-641, 1995.

18. SKACEL, M.; CARREGAL, E.; COSTA, R.L.B.; BORDY, F.B. & VALLE, A.C.F. - Comportamento do sistema nervoso central na paracoccidioidomicose. In: ENCONTRO INTERNACIONAL SOBRE PARACOCCIDIOIDOMICOSE, 7, Campos do Jordão, 1999. **Proceedings**. p. 110.

19. TORO, G. - Paracoccidioidomycosis. In: VINKEN, P.J.; BRUYN, G. & KLAWANS, H.L. **Handbook of clinical neurology**. Amsterdam, Elsevier, 1988. p. 455-465.

20. VALLE, A.C.F.; SKACEL, M.; COSTA, R.L.B. *et al.* - A case report of intraspinal paracoccidioidomycosis. **Rev. Inst. Med. trop. S Paulo**, 40: 203-207, 1998.

Received: 19 January 2000
Accepted: 10 April 2000

UM00012102
NOVARTIS EXHIBIT 1517
Novartis v. Regents, IPR2023-01347
Page 848 of 4460

This Page is Inserted by IFW Indexing and Scanning Operations and is not part of the Official Record

BEST AVAILABLE IMAGES

Defective images within this document are accurate representations of the original documents submitted by the applicant.

Defects in the images include but are not limited to the items checked:

- ☐ BLACK BORDERS
- ☐ IMAGE CUT OFF AT TOP, BOTTOM OR SIDES
- ☐ FADED TEXT OR DRAWING
- ☐ BLURRED OR ILLEGIBLE TEXT OR DRAWING
- ☐ SKEWED/SLANTED IMAGES
- ☐ COLOR OR BLACK AND WHITE PHOTOGRAPHS
- ☐ GRAY SCALE DOCUMENTS
- ☐ LINES OR MARKS ON ORIGINAL DOCUMENT
- ☐ REFERENCE(S) OR EXHIBIT(S) SUBMITTED ARE POOR QUALITY
- ☐ OTHER: _____

IMAGES ARE BEST AVAILABLE COPY.
As rescanning these documents will not correct the image problems checked, please do not report these problems to the IFW Image Problem Mailbox.

Call No.
Title, Author, Edition, ©, ISBN, *etc.*: Ordered for: SL

West, Anthony R.
Solid state chemistry and its applications

Publisher, Address: Wiley, New York

Price: No. Copies: Vendor:
P.O. No.
Date Ordered: Rec'd: Cat'd: Comp:
Remarks: Gift 3/3/88

FORM PTO-1456 (3-81) ORDER CARD U.S. DEPARTMENT OF COMMERCE PAT. AND TM OFFICE

ANTHONY R. WEST,

Department of Chemistry
University of Aberdeen

SCIENTIFIC LIBRARY
Mar 3 1988
PAT. & T.M. OFFICE

JOHN WILEY & SONS
Chichester · New York · Brisbane · Toronto · Singapore

UM00012104

NOVARTIS EXHIBIT 1517
Novartis v. Regents, IPR2023-01347
Page 850 of 4460

Chapter 10

Solid Solutions

10.1 *Substitutional solid solutions* 358
10.2 *Interstitial solid solutions* 361
10.3 *More complex solid solution mechanisms* 361
10.3.1 *Creating cation vacancies* 362
10.3.2 *Creating interstitial anions* 362
10.3.3 *Creating anion vacancies* 363
10.3.4 *Creating interstitial cations* 363
10.3.5 *Double substitution* 364
10.4 *General comments on the requirements for solid solution formation* 365
10.5 *Experimental methods for studying solid solutions* 366
10.5.1 *X-ray powder diffraction* 366
10.5.2 *Density measurements* 370
10.5.3 *Changes in other properties—thermal activity and DTA* 372
Questions 372
References 373

Solid solutions are very common in crystalline materials. A solid solution is basically a crystalline phase that can have variable composition. Often, certain properties of materials, e.g. conductivity, ferromagnetism, are modified by changing the composition in such a way that a solid solution forms and great use may be made of this in designing new materials that have specific properties.

Simple solid solution series are one of two types: in *substitutional* solid solutions, the atom or ion that is being introduced directly replaces an atom or ion of the same charge in the parent structure; in *interstitial* solid solutions, the introduced species occupies a site that is normally empty in the crystal structure and no ions or atoms are left out. Starting with these two basic types, a considerable variety of more complex solid solution mechanisms may be derived, by having both substitution and interstitial formation occurring together and/or by introducing ions of different charge to those in the host structure.

10.1 Substitutional solid solutions

An example of a substitutional solid solution is the series of oxides formed on reacting together Al_2O_3 and Cr_2O_3 at high temperatures. Both of these end-member phases have the corundum crystal structure (approximately hexagonal

close packed oxide ions
available octahedral sit
$(Al_{2-x}Cr_x)O_3$: $0 \leq x \leq 2$
distributed at random ov
Al_2O_3. Thus, while any pa
the probability that it is or
structure is considered as
out, it is useful to think of
properties, atomic numbe
Cr^{3+}.

If a range of simple sul
minimum requirements t
must have the same cha
created) and be fairly simi
alloy formation, it has bee
the metal atoms that are r
substantial range of solid
systems, the limiting diff
larger than 15 per cent, al
this is because it is difficul
Let us use the Pauling c
example, i.e. Li^+ 0.60, N
Rb^+ and Rb^+, Cs^+ pair
common to get solid solu
However, Na^+ and K^+ sa
(e.g. KCl and NaCl at hig
than the Na^+ ion. Some
ranges of compositions a
in size of Li^+ and K^+ ap
solution to form, howeve
based on $r_{O^{2-}} = 1.26$ Å (F
in size of the alkali catio

In systems that exhibit
two end-member phases
however, and just becau
they form solid solutions
salt structure but they a
together to form solid so

While complete range
example, with Al_2O_3–Cr_2
only partial or limited ra
the end-member phases
mineral forsterite, Mg_2
Zn_2SiO_4 and vice versa.
crystal structures of olivi

UM00012105
NOVARTIS EXHIBIT 1517
Novartis v. Regents, IPR2023-01347
Page 851 of 4460

by partial replacement of Si^{4+} by Al^{3+}
enter normally empty interstitial holes

ıula, $Li_x(Si_{1-x}Al_x)O_2$ for $0 < x \lesssim 0.5$
O_2 (Fig. 10.4), shows that wide ranges
hat special compositions exist at $x =$
.33 (i.e. $LiAlSi_2O_6$, spodumene). β-
a very small, perhaps even slightly
ceramics containing β-spodumene as
ınally stable and resistant to thermal
rature applications (Chapter 18). The
e too small to accommodate cations
have lower densities than quartz with
fed tridymite and cristobalite solid
lid solutions, form but in these the
K^+.

mechanisms occur, two of which are

ace simultaneously. For example, in
ıy Fe^{2+} at the same time as Si^{4+} is
$(Mg_{2-x}Fe_x)(Si_{1-y}Ge_y)O_4$. Silver
ete range of solid solutions in which
$Ag_{1-x}Na_x)(Br_{1-y}Cl_y)$: $0 < x, y < 1$.
ıt charge, providing that overall
clase feldspars a complete range of
$_2Si_2O_8$, and albite, $NaAlSi_3O_8$.
$Al_{2-x}Si_{2+x})O_8$: $0 < x < 1$, and the
it occur simultaneously and to the
n is given later in Fig. 11.12.
ialons, which are solid solutions in
e Si_3N_4 parent structure. β-Silicon
ıeir corners to form a 3-D network.
d forms the corner of three SiN_4
ıs partly replaced by Al^{3+} and N^{3-}
balance is retained. The structural
tetrahedra and the solid solution
$_xO_x$). Silicon nitride is potentially,
ıpter 20). The recent discovery of
ers at Newcastle has opened up a
possible applications of nitrogen-

10.4 General comments on the requirements for solid solution formation

The factors that govern whether or not solid solutions, especially the more complex ones, form are understood only qualitatively. For a given system, it is not usually possible to predict whether solid solutions will form or, if they do form, what is their compositional extent. Instead, this has to be determined experimentally. If we are restricted to solid solutions that exist under equilibrium conditions (Fig. 9.1) and are represented on the appropriate phase diagram, then solid solutions form only if they have lower free energy than any other phase or assemblage of phases with the same overall composition. Under non-equilibrium conditions, however, and by using 'chemie douce' or other preparative techniques (Chapter 2), it is often possible to prepare solid solutions that are much more extensive than those existing, if at all, under equilibrium conditions. A simple example is provided by the β-aluminas, $Na_2O \sim 8\,Al_2O_3$. Part or all of the Na^+ ions may be ion exchanged for a variety of other monovalent ions, including Li^+, K^+, Ag^+ and Cs^+, even though most of these ion exchanged materials are not thermodynamically stable (Chapter 13).

The limitations on the relative sizes of ions that either substitute directly for each other or enter interstitial sites have been referred to above. In the more complex solid solution mechanisms, the charges of the ions that take part are often different to each other. Clearly charge balance must be preserved overall, but within this limitation and provided the size requirements are met, there is often much scope for introducing ions of different charge. A rather extreme example of this is Li_2TiO_3. This has, at high temperatures, a rock salt structure in which Li^+, Ti^{4+} ions are disordered over the octahedral sites in a cubic close packed oxide ion array. It can form two series of solid solutions with either excess Li_2O or excess TiO_2 and of respective formulae

$$\text{(a)}\quad Li_{2+4x}Ti_{1-x}O_3: \quad 0 < x \lesssim 0.08$$
$$\text{(b)}\quad Li_{2-4x}Ti_{1+x}O_3: \quad 0 < x \lesssim 0.19.$$

Both of these involve the interchange of mono- and tetravalent ions with the creation of either interstitial Li^+ ions (a) or Li^+ vacancies (b) to maintain electroneutrality. The large difference in charge of Li^+ and Ti^{4+} obviously does not prevent solid solution formation. Part of the reason why solid solutions form appears to be that both Li^+ and Ti^{4+} are able to occupy similar-sized octahedral sites with metal–oxygen distances in the range 1.9 to 2.2 Å.

There are many other examples in which ions of similar size but very different charge can replace each other in solid solution formation. The ilmenite-like phase $LiNbO_3$ forms a limited range of solid solution by $5Li^+ \rightleftharpoons Nb^{5+}$ substitution on octahedral sites (Fig. 3.10a). The Zr^{4+} ion can be replaced by Ca^{2+}, Y^{3+} ions in the eight coordinate sites of the cubic stabilized zirconia structure, e.g. $Zr_{1-x}Ca_xO_{2+x}$. Na^+ is also of a similar size to Zr^{4+} and these ions replace each other in the solid solution series, $Na_{5-4x}Zr_{1+x}P_3O_{12}$: $0 < x < 0.15$.

UM00012106
NOVARTIS EXHIBIT 1517
Novartis v. Regents, IPR2023-01347
Page 852 of 4460

This Page is Inserted by IFW Indexing and Scanning Operations and is not part of the Official Record

BEST AVAILABLE IMAGES

Defective images within this document are accurate representations of the original documents submitted by the applicant.

Defects in the images include but are not limited to the items checked:

- ❑ BLACK BORDERS
- ❑ IMAGE CUT OFF AT TOP, BOTTOM OR SIDES
- ❑ FADED TEXT OR DRAWING
- ❑ BLURRED OR ILLEGIBLE TEXT OR DRAWING
- ❑ SKEWED/SLANTED IMAGES
- ❑ COLOR OR BLACK AND WHITE PHOTOGRAPHS
- ❑ GRAY SCALE DOCUMENTS
- ❑ LINES OR MARKS ON ORIGINAL DOCUMENT
- ❑ REFERENCE(S) OR EXHIBIT(S) SUBMITTED ARE POOR QUALITY
- ❑ OTHER: _____

IMAGES ARE BEST AVAILABLE COPY.
As rescanning these documents will not correct the image problems checked, please do not report these problems to the IFW Image Problem Mailbox.

Crystalline forms of pharmaceuticals and characterization thereof

Judith Aronhime
Global solid-state characterization group, API R&D

Steve Lee
Kenyon&Kenyon

UM00012108
NOVARTIS EXHIBIT 1517
Novartis v. Regents, IPR2023-01347
Page 854 of 4460

Summary:

1. Powder X-ray Diffraction (PXRD) is the Gold Standard for Identifying Solid Powder Forms.

2. PXRD and Single Crystal X-Ray Analysis are complementary techniques, and can be directly compared.

3. To compare solid form claims to the prior art, PXRD data are invaluable.

4. Other characteristics of solid forms cannot be directly compared.

UM00012109
NOVARTIS EXHIBIT 1517
Novartis v. Regents, IPR2023-01347
Page 855 of 4460

Polymorphism

Polymorphs are different solid forms of the same compound.

Polymorphs may have different physical or chemical properties (like hygroscopicity, solubility, and chemical stability).

Polymorphism presents both a challenge to pharmaceutical companies and opportunities.

UM00012110
NOVARTIS EXHIBIT 1517
Novartis v. Regents, IPR2023-01347
Page 856 of 4460

Unpredictability of Polymorphs

There are infinite ways to generate polymorphs.

We cannot predict:

The existence of polymorphs

Their properties

How to make them

Theoretical calculations to predict polymorphs are not reliable: they predict many more polymorphs than can be isolated.

UM00012111
NOVARTIS EXHIBIT 1517
Novartis v. Regents, IPR2023-01347
Page 857 of 4460

This Page is Inserted by IFW Indexing and Scanning Operations and is not part of the Official Record

BEST AVAILABLE IMAGES

Defective images within this document are accurate representations of the original documents submitted by the applicant.

Defects in the images include but are not limited to the items checked:

- ☐ BLACK BORDERS
- ☐ IMAGE CUT OFF AT TOP, BOTTOM OR SIDES
- ☐ FADED TEXT OR DRAWING
- ☐ BLURRED OR ILLEGIBLE TEXT OR DRAWING
- ☐ SKEWED/SLANTED IMAGES
- ☐ COLOR OR BLACK AND WHITE PHOTOGRAPHS
- ☐ GRAY SCALE DOCUMENTS
- ☐ LINES OR MARKS ON ORIGINAL DOCUMENT
- ☐ REFERENCE(S) OR EXHIBIT(S) SUBMITTED ARE POOR QUALITY
- ☐ OTHER: _____

IMAGES ARE BEST AVAILABLE COPY.
As rescanning these documents will not correct the image problems checked, please do not report these problems to the IFW Image Problem Mailbox.

Chemistry beyond the molecule

Gautam R. Desiraju

Supramolecular chemistry has grown in importance because it goes beyond the molecule — the focus of classical chemistry. It also offers a fresh interface with biological and materials science.

For a long time chemists tried to understand nature at a level that was purely molecular — they considered only structures and functions involving strong covalent bonds. But some of the most important biological phenomena do not involve making and breaking covalent bonds — the linkages that connect atoms to form molecules. Instead, biological structures are usually made from loose aggregates that are held together by weak, non-covalent interactions. Because of their dynamic nature, these interactions are responsible for most of the processes occurring in living systems. Chemists have been slow to recognize the enormous variety — in terms of structure, properties and functions — offered by this more relaxed approach to making chemical compounds.

The slow shift towards this new approach began in 1894, when Emil Fischer proposed that an enzyme interacts with its substrate as a key does with its lock[1]. This elegant mechanism contains the two main tenets of what would become a new subject, supramolecular chemistry[2,3]. These two principles are molecular recognition and supramolecular function.

Molecular recognition is implicit in the lock-and-key model — provided both the geometry and the non-covalent interactions are compatible between the interacting partners, you get recognition. Such highly specific interactions also lead to useful supramolecular functions. For example, it is important that an enzyme works only on the appropriate substrate. A key without its own lock or a lock without its own key is quite useless.

The initial motivation behind supramolecular chemistry was to design chemical systems that mimic biological processes. The rise of the supramolecular approach was aided by observations of stable compounds that did not involve covalent bonds. Early examples of these 'addition products' include donor–acceptor complexes and clathrate compounds (Fig. 1). Some donor–acceptor complexes do not involve normal covalent bonding. Instead, they are held together by one molecule donating electrons, or perhaps sharing a hydrogen atom, with another.

A classic example of a donor–acceptor complex is formed by silver ions (Ag^+) and ethene ($CH_2=CH_2$), in which the ethene donates some electrons from its double bond to Ag^+ (Fig. 1a). The interaction is not so strong that it leads to a covalent bond, but it is strong enough to form a stable complex.

Back in 1948, H. M. Powell[4] described a series of what he called clathrates — derived from the Latin *clathratus*, meaning 'enclosed by the bars of a grating'. These inclusion compounds are formed when small molecules, such as methanol, hydrogen sulphide or sulphur dioxide, are completely enclosed in cavities formed by a host compound, such as the β-quinol network (Fig. 1b). Here we have addition products with little or no direct attachment — and no covalent bonds — between the 'host' and the 'guest'. Powell's work was the beginning of what would eventually become a major part of supramolecular chemistry — the design of host cages that allow the selective inclusion and expulsion of guest molecules. One of the oldest uses of clathrates is in crude oil refining, in which undesirable paraffins are removed from gasoline by trapping in clathrate lattices.

The early clathrates were discovered by chance, but rational design has led to enhanced properties. For example, a host matrix made from a copper-based polymer material absorbs and releases methane. This organic–inorganic hybrid competes with porous zeolites in its absorptive capacity, and could offer new applications for clathrates, such as the purification of drugs and trapping and storage of toxic materials[5].

Chemists could not understand these inclusion compounds in terms of normal covalent bonding, and they were often relegated to the fringes of chemistry. But with the discovery of useful properties, chemists had to take these compounds seriously — the citadel of the isolated molecule was vulnerable after all.

Intermolecular interactions

The term supramolecular chemistry was coined in 1969 by Jean-Marie Lehn in his study of inclusion compounds and cryptands (Fig. 1c)[2]. The award of the 1987 Nobel Prize in Chemistry to Charles Pedersen, Donald Cram and Lehn signified the formal arrival of the subject on the chemical scene. Lehn defined supramolecular

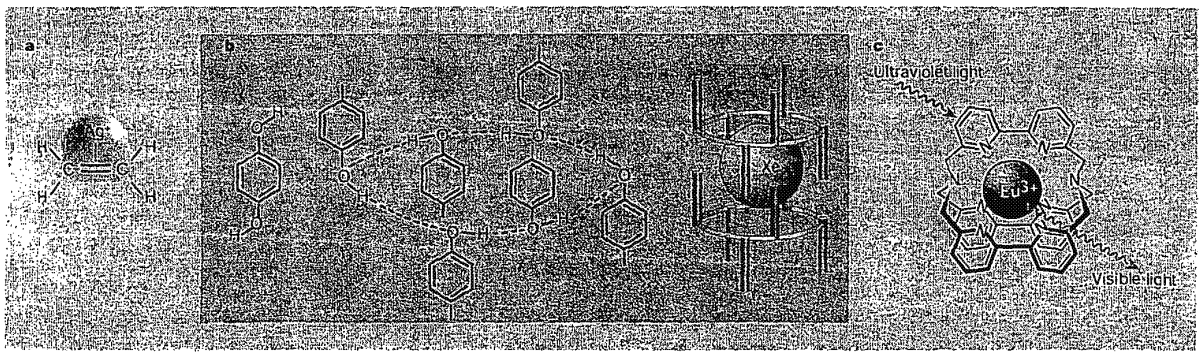


Figure 1 Supramolecular structures formed by intermolecular interactions. a, A donor–acceptor complex involving silver and ethene. b, Hydroquinone molecules assemble into a clathrate using hydrogen bonds. This means they can form solid-state host–guest complexes in which the hydroquinone network is the host and the guest is a small molecule, such as the xenon atom shown. c, A cryptand contains a spherical internal cavity studded with donor sites, suitable for enclosing a metal ion. Ultraviolet light absorbed by the cryptand shown here excites the metal ion, Eu(III), which then emits radiation at longer (visible) wavelengths.

© 2001 Macmillan Magazines Ltd

UM00012113
NOVARTIS EXHIBIT 1517
Novartis v. Regents, IPR2023-01347
Page 859 of 4460

SCOTT CHILDS

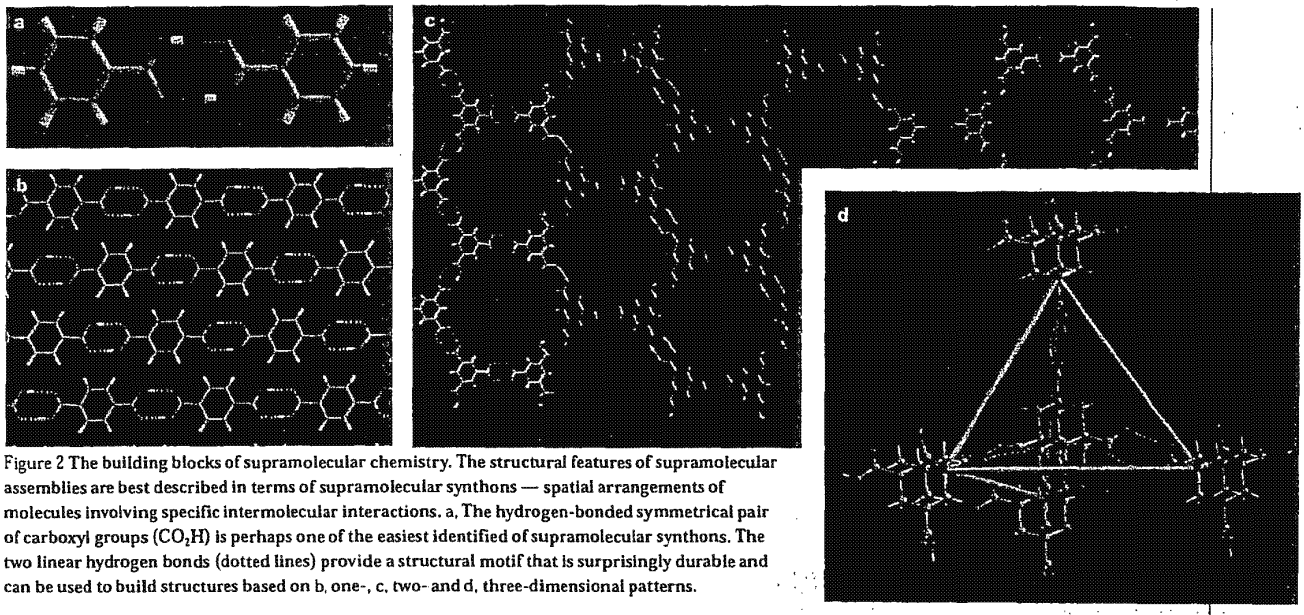


Figure 2 The building blocks of supramolecular chemistry. The structural features of supramolecular assemblies are best described in terms of supramolecular synthons — spatial arrangements of molecules involving specific intermolecular interactions. a, The hydrogen-bonded symmetrical pair of carboxyl groups (CO_2H) is perhaps one of the easiest identified of supramolecular synthons. The two linear hydrogen bonds (dotted lines) provide a structural motif that is surprisingly durable and can be used to build structures based on b, one-, c, two- and d, three-dimensional patterns.

chemistry as "the chemistry of the intermolecular bond". Just as molecules are built by connecting atoms with covalent bonds, supramolecular compounds are built by linking molecules with intermolecular interactions.

Supramolecular structures are the result of not only additive but also cooperative interactions, and their properties generally follow from their supramolecular character (Boxes 1, 2). So even with the clathrates, their whole is more than the sum of their parts. These properties are important in both materials science (magnetism, conductivity, sensors, nonlinear optics) and biology (receptor–protein binding, drug design, protein folding).

In any supramolecular assembly, a large number of intermolecular interactions is possible — but only a few are actually observed. The weakness of these interactions makes it difficult to predict supramolecular structures and means that, in solution, supramolecular structures are not always stable over time. But this flexibility also means that they are frequently favoured in important mechanisms, notably in biological reactions and in crystallization processes, where the ability to form short-lived transition states and to perform trial-and-error correction easily is essential.

Intermolecular interactions are divided into two classes: isotropic, medium-range forces and anisotropic, long-range forces. Isotropic forces define the shape of the individual molecules, as well as size and close packing of molecules, whereas anisotropic forces determine intermolecular orientations and functions. For example, the three-dimensional shapes of biomolecules, such as proteins and enzymes, are the result of medium-range intermolecular interactions. At a simple level, all molecular recognition can be said to arise from isotropic interactions, in other words by the fitting together of bumps and hollows among the components of the supramolecular structure. But most directional effects — and function is related to these effects — depend on the anisotropic interactions. Generally, the anisotropic interactions

Box 1 Hard applications

Supramolecular chemistry has always been associated with new materials and applications. Chemistry is driven by the desire for new functions, with the study of structure as a necessary first step towards the achievement of that goal. Ideally, useful materials would be designed by taking a single molecule and 'sticking it' to others of its kind to form three-dimensional assemblies. Implied in such a strategy is the ability to fine-tune function without necessarily disturbing structure. Accordingly, the total synthesis of a useful material can be dissected into molecular and supramolecular components. Traditional organic chemistry already provides all the necessary technology for the synthesis of the molecular building blocks. Supramolecular synthesis, which requires manipulation of intermolecular interactions, is still evolving.

Most solid-state devices, such as electronics, require a degree of order that is only possible with crystalline materials. Unlike porous materials, crystals have densely packed molecules and any chemical change is likely to destroy the crystal and its properties. But organoplatinum molecules have successfully been engineered to make a crystalline material that reversibly binds sulphur dioxide (SO_2) gas[18]. When the colourless organoplatinum crystals are bathed in SO_2 they turn bright orange and their total volume increases by about a quarter, but the crystals remain perfectly ordered. The SO_2 can be absorbed and expelled many times without loss of crystallinity. Part of the reason for this remarkable behaviour is that the crystalline framework is held together by supramolecular interactions — a string of hydrogen bonds — which can more easily tolerate such deformation. These organoplatinum crystals might find use as a gas-storage device, a sensor or even as an optical switch.

Nanocrystalline materials with ultrafine grains are potentially useful in molecular-scale electronics as magnetic[19], semiconducting, dielectric and ferroelectric materials. Part of the problem chemists have with molecule-based systems is connecting them to the macroscopic world. One approach is to modify a nanocrystalline surface with supramolecular components. For example, a ruthenium complex bound to nanocrystalline titanium dioxide gives a supramolecular structure that undergoes photochemically driven electron- and energy-transfer processes. This makes them attractive materials for use in solar cells[20]. Supramolecular aggregates of organic molecules have also been used to make molecular switches, whose conductivity is controlled by the chemical state of the molecule. Chemical sensors based on such switches could in theory be used to detect individual molecules of a pollutant. G.R.D.

© 2001 Macmillan Magazines Ltd

UM00012114
NOVARTIS EXHIBIT 1517
Novartis v. Regents, IPR2023-01347
Page 860 of 4460

involve partially charged atoms, such as nitrogen, oxygen, chlorine, phosphorus and sulphur.

Isotropic interactions include van der Waals forces, which act between all atoms and molecules. These can be repulsive or attractive depending on the distance between the interacting non-bonded atoms, and are responsible for gross supramolecular arrangements. Although these forces are individually weak — they have bond energies of 8 kJ mol^{-1} compared with the 400 kJ mol^{-1} of covalent bonds — they become significant when considered in numbers. This is the essence of supramolecular thinking. The remarkable ability of the house lizard to stick to a ceiling is a result of millions of van der Waals interactions formed by the spatulae at the ends of fine hairs that cover the soles of its feet[6].

Although at a simple level molecular recognition can be said to hinge on isotropic interactions, at a higher level it is an anisotropic interaction that is the master key: the hydrogen bond[7]. In any hydrogen bond, X–H···A, a hydrogen atom acts as a bridge between two atoms X and A. These atoms always tend to be negatively charged (electronegative), which gives the hydrogen bond an electrostatic character, as the electropositive hydrogen atom holds the negative atoms in thrall.

If X and A are both quite electronegative, for example in N–H···O, the hydrogen bond is 'strong' or 'conventional' (20–40 kJ mol^{-1}). But if either or both X and A are of moderate to weak electronegativity, such as in C–H···O, the hydrogen bond is 'weak' or 'non-conventional' (2–20 kJ mol^{-1})[8]. In some systems, such as those involving the HF_2^- ion, the strength of the hydrogen bonds can reach quasi-covalent levels (170 kJ mol^{-1}). Hydrogen bonds can also form between more than two atoms. The importance of hydrogen bonds that are formed with double and triple bonds, such as C=C and C≡C, is increasingly being recognized. For example, hydrogen bonds formed by groups such as OH, NH and CH with the double bonds in aromatic rings are recognized as being key in the stabilization of biomolecular structures[9].

In general, the hydrogen bond is a composite interaction, which can have pronounced covalent, electrostatic or van der Waals components and consequently spans a wide energy range. The strength of interaction dictates the length and orientation of the hydrogen bond: short, linear bonds are almost always the strongest. But even weak bonds can be significant. Weak interactions tend to be hydrophobic, so they can persist in ionic solvents better than stronger hydrogen bonds.

Predicting supramolecular structures is hard, not only because of the sheer numbers of possible interactions involved, but also because in energetic terms there is not much to choose between these various interactions. If one interaction is not much more energetically favourable than the others, then there is no clear winner to predict. The challenge for the supramolecular chemist attempting to synthesize these structures is to ensure that the molecules involved are oriented in such a way that maximizes the strength of the desired interactions. Two examples of instances where intermolecular interactions are crucial are crystal engineering and crystallization.

Crystal engineering

Organic crystals are supramolecular entities in that they are built from molecules. In crystal engineering, the supramolecular chemist aims to design and control packing arrangements to design crystals with specific properties. But this is not routinely possible from knowledge of the molecular structure alone. The best chemists can do is to find recurring packing patterns adopted by certain functional groups and rely on the robustness of such motifs to create new solid-state structures. These small repetitive units are called supramolecular synthons[10]. They economically but fully define the essence of a structure, and embody specific intermolecular interactions (Fig. 2). Repetition is what qualifies a structural motif to be considered a synthon and it is repetition that is the key to successful crystal engineering.

Even after identifying an important intermolecular interaction, failure to predict a crystal structure can arise because the same interaction can be used to make many different synthons. For example, the carboxyl group (CO_2H) usually assembles in crystals via pairs of O–H···O hydrogen bonds[11]. But in cubane acids, the carboxyls form a synthon containing both O–H···O and C–H···O interactions (Fig. 3, overleaf).

Crystal engineering is shifting its focus from devising structures to designing properties. Property design can only follow from structure and our understanding of the principles by which molecules assemble into crystals is still rudimentary. Chemists are trying various computational and experimental approaches towards crystal design. And the synthon concept tries to simplify what is essentially a very difficult problem. But even with apparently straightforward synthons, things can go wrong.

In coordination polymers, for example, the relatively strong coordinate bonds (a type of covalent bond) between organic molecules and metal atoms are used to generate a solid network. This approach offers greater structural repetition because the coordinate bonds have both strength and explicit geometries. The first metal–organic networks were developed to mimic zeolites — microporous materials used for catalysis and separation processes. But even these seemingly reliable synthons failed when the packing density was low — more often than not the porous structure was unstable to collapse. The latest generation of open networks, which use a dicarboxylate linker to help stabilize the structure, can survive the loss or exchange of guest molecules[12].

Crystallization of molecules in solution is also a supramolecular process. Like other chemical reactions, it is governed by thermodynamic and kinetic factors. In molecular chemistry, pure energy considerations — enthalpy — are usually the decisive factor, so chemists only have to worry about identifying the strongest and weakest bonds, because they usually want to make the strongest

Box 2 Soft solutions

On the softer, non-crystalline side of supramolecular chemistry, desirable properties include solubility and chirality (molecular asymmetry). For example, a water-soluble polyfullerene has been synthesized using supramolecular methodology[21]. The reactants are prearranged in the cavity of a cyclodextrin, a container molecule, and then the polymerization is carried out. Potential biomedical applications of this supramolecular polymer follow from the fact that it scavenges the natural 'free radical', 1,1-diphenyl-2-picrylhydrazyl, more strongly than C_{60} itself, and that it cleaves DNA oligonucleotides in the presence of light.

Hydrogen-bonded systems often display chirality at the supramolecular level. Chemists want to control chirality so that supramolecular products are purely left- or right-handed isomers, and not a mixture of both. Supramolecular structures can now be designed to form sufficiently stable hydrogen bonds that pure-handed isomeric assemblies can be isolated[22]. The efficacy of drugs that are administered in crystalline form as fine powders can depend strongly on whether they have the correct isomeric structure and also the correct polymorphic structure.

Polymorphism is when a given molecule can exist in different crystalline forms, which are stable under different conditions. Polymorphs can therefore be thought of as supramolecular isomers, species in which the relative positioning of the same molecules is different. Polymorphs of a drug can have quite different properties. Their solubilities can be different, as well as their biological activity. In some cases, the less stable form will crystallize first, and then slowly transform, over time, into the more stable crystal. This can be a problem if the active form of a drug is the less stable polymorph, and turns into the more stable — but less active and perhaps even harmful — form during storage. In this context, can one design a molecule that is guaranteed to crystallize in a particular polymorphic form under physiological conditions? This is now a supramolecular challenge for the pharmaceutical industry. **G.R.D.**

© 2001 Macmillan Magazines Ltd

UM00012115
NOVARTIS EXHIBIT 1517
Novartis v. Regents, IPR2023-01347
Page 861 of 4460

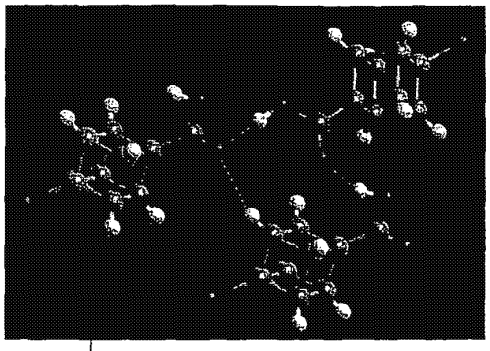


Figure 3 **In many cubane acids, the carboxyl groups (CO_2H) form a synthon based on extended O–H···O and C–H···O bonds. In 4-bromocubanecarboxylic acid, for example, the C–H···O hydrogen bond provides the overall synthon with additional support[11]. It is thought that without this interaction, the exotic topology could not be realized.**

bonds and break the weakest. But in supramolecular chemistry, there are so many possible interactions that you have to consider both the enthalpy and entropy (disorder) inherent in every interaction. It is surprising, then, that although putative crystal structures can be similar in terms of energy, many organic molecules yield only one crystal structure under given conditions. Molecules seem to know how to crystallize into the correct structure, even if chemists cannot predict it.

Crystallization is a complex but highly efficient process in which a number of molecular groups compete with each other to be sites for intermolecular interactions that might lead to a stable crystal structure. Before the earliest stage of crystallization — known as nucleation — all molecular groups present in the solution try out different possible routes to alternative intermolecular interactions. But only a few of these interactions will be thermodynamically, kinetically or statistically sustained. The stable interactions lead to robust synthons and alternative possibilities are quickly and efficiently excluded. In this respect, there are similarities between the crystallization of a small organic molecule and the folding of a protein. Both proceed through intermediate, structure-determining clusters, resulting in a considerable increase in crystallization or folding efficiency.

A fascinating example of such a mechanism is provided by molybdenum chemistry. Molybdenum can form giant molecular clusters or rings with nanometre-sized cavities. Addition of two Mo_{36} 'hub-caps' to the wheel-like Mo_{176} cluster results in a Mo_{248} cluster[13]. The hub-caps are not stable in solution, showing that crystallization can proceed in steps, with complex structures forming from more simple ones that are not necessarily stable on their own.

Similarly, solvation — roughly the opposite to crystallization — is a phenomenon in which the enthalpic advantage of retaining solvent in a crystal outweighs the entropic advantage of expelling it into the bulk solvent[14]. An understanding of crystallization is important for the development of supramolecular chemistry and crystal engineering; both experimental and computational approaches (molecular dynamics) are currently being used to tackle this exciting problem.

A study of the protein apoferritin recently provided the first ever observations of protein nucleation[15]. By using atomic force microscopy, tiny clusters of apoferritin can be watched as they slowly grow or dissolve. Protein crystallization is more an art than a science, yet it is vital for determining protein structure.

A quiet revolution

Almost unobtrusively, chemistry is changing from a subject to a language that is needed to communicate core issues in biological and materials science. This change will surely lead to striking and unexpected practical applications, and supramolecular chemistry is at the vanguard (Boxes 1 and 2). Stephen Lippard recently made a 'wish list' for chemistry that represents this change[16]. Beyond what I have already discussed here, new goals for supramolecular chemistry include building porous structures — clathrates or coordination compounds — that have internal sites for catalysis, and designing solid-state reactions that are environmentally friendly because they are solvent free.

So far, the success stories include one published on page 452 of this issue[17]. The authors of this paper have created supramolecular nanotubes that have important biological activity *in vivo* (Fig. 4). By synthesizing cyclic peptides consisting of alternating D- and L-amino acids, a synthon that self-assembles into a nanotube is created. The resulting nanotubes have selective antibacterial activity in mice by increasing the permeability of bacterial membranes. They are highly effective against drug-resistant bacteria, highlighting the advantages of a non-biological treatments over conventional ones.

Friedrich Wöhler's synthesis of urea in 1828, the first laboratory synthesis of a naturally occurring compound, symbolized the end of the vitalistic approach to chemistry — the idea that living organisms differ from non-living substances because they possess a 'vital force'. But with the arrival of Emil Fischer and supramolecular chemistry, chemists are now more than ever concerned with the transition from chemistry to biology. How do life processes work? The fantastic levels of specificity achieved by biological machines may be reduced to weak interactions, to chemical recognition and function, and inexorably down to physics itself. Yet, a reductionist approach is simplistic beyond the extreme. A scientifically more acceptable view of vitalism is that living and non-living matter differ not in content but rather in organizational complexity — and our understanding of this theme may well turn out to be the biggest breakthrough in supramolecular science. ■

Gautam R. Desiraju is at the School of Chemistry, University of Hyderabad, Hyderabad 500 046, India.
e-mail: desiraju@uohyd.ernet.in

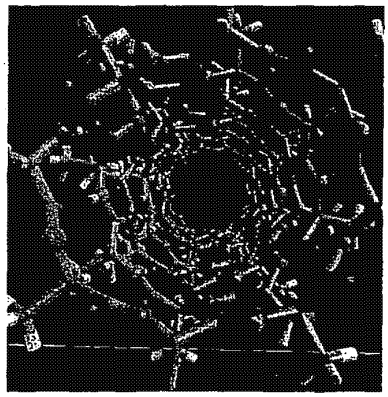


Figure 4 **Supramolecular approach to a biological problem. Cyclic peptides with alternating D- and L-amino acids create a flat, ring-shaped synthon. When several cyclic peptides are stacked together they can self-assemble into a stable nanotube. The walls of the tube are β-pleated sheets. In mice, these nanotubes have selective antibacterial activity by increasing the permeability of bacterial membranes[17]. (The structure shown here features different side groups from those used by Fernandez-Lopez *et al.* in ref. 17.)**

SCOTT CHILDS

1. Fischer, E. *Ber. Dt. Chem. Ges.* 27, 2985–2993 (1894).
2. Lehn, J.-M. *Supramolecular Chemistry: Concepts and Perspectives* (VCH, Weinheim, 1995).
3. Desiraju, G. R. *Nature* 408, 407 (2000).
4. Powell, H. M. *J. Chem. Soc.* 61–73 (1973).
5. Noro, S., Kitagawa, S., Kondo, M. & Seki, K. *Angew. Chem. Int. Ed. Engl.* 39, 2081–2084 (2000).
6. Autumn, K. *et al. Nature* 405, 681–685 (2000).
7. Jeffrey, G. A. *An Introduction to Hydrogen Bonding* (Oxford Univ. Press, New York, 1997).
8. Desiraju, G. R. & Steiner, T. *The Weak Hydrogen Bond in Structural Chemistry and Biology* (Oxford Univ. Press, Oxford, 1999).
9. Steiner, T. & Koellner, G. *J. Mol. Biol.* 305, 535–557 (2001).
10. Desiraju, G. R. *Angew. Chem. Int. Ed. Engl.* 34, 2311–2327 (1995).
11. Kuduva, S. S., Craig, D. C., Nangia, A. & Desiraju, G. R. *J. Am. Chem. Soc.* 121, 1936–1944 (1999).
12. Li, H., Eddaoudi, M., O'Keefe, M. & Yaghi, O. M. *Nature* 402, 276–279 (1999).
13. Müller, A., Shah, S. Q. N., Bögge, H. & Schmidtmann, M. *Nature* 397, 48–50 (1999).
14. Nangia, A. & Desiraju, G. R. *Chem. Commun.* 605–606 (1999).
15. Yau, S.-T. & Vekilov, P. G. *Nature* 406, 494–497 (2000).
16. Lippard, S. J. *Chem. Eng. News* 7 August 64–65 (2000).
17. Fernandez-Lopez, S. *et al. Nature* 412, 452–455 (2001).
18. Albrecht, M., Lutz, M., Spek, A. L. & van Koten, G. *Nature* 406, 970–974 (2000).
19. Kahn, O. *Acc. Chem. Res.* 33, 647–657 (2000).
20. Freemantle, M. *Chem. Eng. News* 19 June, 48–58 (2000).
21. Samal, S., Choi, B.-J. & Geckeler, K. E. *Chem. Commun.* 1373–1374 (2000).
22. Prins, L. J., De Jong, F., Timmerman, P. & Reinhoudt, D. N. *Nature* 408, 181–184 (2000).

© 2001 Macmillan Magazines Ltd

UM00012116
NOVARTIS EXHIBIT 1517
Novartis v. Regents, IPR2023-01347
Page 862 of 4460

This Page is Inserted by IFW Indexing and Scanning Operations and is not part of the Official Record

BEST AVAILABLE IMAGES

Defective images within this document are accurate representations of the original documents submitted by the applicant.

Defects in the images include but are not limited to the items checked:

- ☐ BLACK BORDERS
- ☐ IMAGE CUT OFF AT TOP, BOTTOM OR SIDES
- ☐ FADED TEXT OR DRAWING
- ☐ BLURRED OR ILLEGIBLE TEXT OR DRAWING
- ☐ SKEWED/SLANTED IMAGES
- ☐ COLOR OR BLACK AND WHITE PHOTOGRAPHS
- ☐ GRAY SCALE DOCUMENTS
- ☐ LINES OR MARKS ON ORIGINAL DOCUMENT
- ☐ REFERENCE(S) OR EXHIBIT(S) SUBMITTED ARE POOR QUALITY
- ☐ OTHER: _____

IMAGES ARE BEST AVAILABLE COPY.
As rescanning these documents will not correct the image problems checked, please do not report these problems to the IFW Image Problem Mailbox.

Are Crystal Structures Predictable?

ANGELO GAVEZZOTTI*

Dipartimento di Chimica Fisica ed Elettrochimica, Università di Milano, Milano, Italy

Received May 16, 1994

"No": by just writing down this concise statement, in what would be the first one-word paper in the chemical literature, one could safely summarize the present state of affairs, earn an honorarium from the American Chemical Society, and do a reasonably good service to his or her own reputation. In the mainstream of academic tradition, one could then concede a "maybe", or even a conditional "yes", thus making a good point for discussion; and then, in the mainstream of publication policy tradition, proceed eventually to have his or her papers rejected by referees taking the opposite stand.

Fortunately, there is a rhetorical way out of this predicament, known to medieval philosophers as *amplificatio*: in plain words it means, when you cannot provide an answer, just rephrase and expand the statement of the question. To this very old trick we will resort in this paper. In fact, the title question is a bit too straightforward and simple-minded; such broad terms as "crystal structure" and "prediction" need be defined in more detail. There are several levels of desirable *a priori* information on a solid; they will be described by posing a number of typical, more restricted questions, in order of increasing complexity. Organic substances only will be considered.

It is assumed that it need not be explained to the reader why control or prediction of the structure of a solid, at a molecular level, is desirable; there are several self-evident justifications, on both theoretical and practical grounds, for striving to understand the basic factors that dictate the arrangement of molecules in space when they recognize each other at a short distance and eventually coagulate in a rigid configuration. While the present knowledge of intramolecular valence can be considered satisfactory, that of intermolecular "valence" is rudimentary; and the perspective of being able to design molecular solids with predetermined physical properties, which depend on structure, is appealing (an understatement) to applied chemists in the fields of pigments,[1] pharmaceuticals,[2] magnets,[3] conductors,[4] and photosensitive[5] or optoelectronic[6] materials. So one has here a big theoretical challenge going hand in hand with big business.

In the early days of X-ray crystallography, guessing at the crystal structure by minimizing intermolecular repulsions was considered a viable method of solving the phase problem, when cell dimensions and diffraction intensities were available. From such a perspective, knowledge of the cell volume implied that intermolecular attractions had been satisfied, and that only mutual avoidance between rigid objects had to be accomplished, either by rough (but surprisingly efficient) mechanical devices[7a] or by computer sieving.[7b] These procedures were suddenly made obsolete, and dismissed, by the advent of direct methods. Crystal structure prediction resurfaced only in very recent times, and with a much more ambitious connotation; the new problem is to consider an organic compound for which a structural formula has been written on paper, but whose synthesis (presumably expensive in terms of materials or human resources) has not yet been accomplished. In keeping with the rhetorical profile of this paper, typical questions on its future as a solid will now be posed.

1. *Will this compound crystallize at all?* Thermodynamics holds that any substance must crystallize, provided it is pure and the temperature is low (or pressure is high) enough. But organic chemistry thrives in mild temperature–pressure regimes, prone to the much more elusive dictates of kinetics. Dissolution always works in the proper solvent while crystal growth from solution is problematic; melting nearly always occurs at higher temperatures than freezing; a crystal is more readily destroyed than built. The organic solid state ranges from waxes or glasses to disordered, strained, or twinned crystals, to powders, and eventually, to well-shaped single crystals. Chemists often come to grips with tough problems in the control of solidification, crystal growth, and crystal morphology, mainly due to the perverse kinetic control of nucleation; and this is a well-developed research field of its own.[8]

For example, sexithienyl, a compound of great importance in nonlinear optics, has a high melting point, yet no single crystals of this substance could be grown, in spite of considerable effort. A reasonable and stable crystal structure has been predicted[9] by calculations based on empirical potentials. Recently, a Rietveld analysis of powder specimens (the best that

Angelo Gavezzotti (born in 1944) studied chemistry at the University of Milano and graduated in 1968 with a thesis in X-ray crystallography. He has worked in the fields of theoretical and structural chemistry with supervision and friendly advice from M. Simonetta. He spent research terms in Orsay, France (1973), and in Ann Arbor, MI (1977–1978), with L. S. Bartell. He is presently professor of physical chemistry at the University of Milano, and his research interests focus on the structural chemistry of organic crystals. He served a three-year term as Coeditor of *Acta Crystallographica*.

* New address: Dipartimento di Chimica Strutturale e Stereochimica Inorganica, Università di Milano, Milano, Italy.

(1) Klebe, G.; Graser, F.; Hädicke, E.; Berndt, J. *Acta Crystallogr.* **1989**, *B45*, 69–77.
(2) Haleblian, J.; McCrone, W. *J. Pharm. Sci.* **1969**, *58*, 911–929.
(3) Miller, J. S.; Epstein, A. J.; Reiff, W. M. *Acc. Chem. Res.* **1988**, *21*, 114–120.
(4) Hunig, S.; Erk, P. *Adv. Mater.* **1991**, *3*, 225–236.
(5) For the structural problems connected with epitaxy and photoconductivity of small molecules on polymers, see: Scaringe, R. P.; Perez, S. *J. Phys. Chem.* **1987**, *91*, 2394–2403 and references therein.
(6) Chemla, D. S.; Zyss, J. *Nonlinear Optical Properties of Organic Molecules and Crystals*; Academic Press: Orlando, 1987.
(7) (a) Kitaigorodski, A. I. *Organic Chemical Crystallography*; Consultants Bureau: New York, 1961 (the structure-seeking apparatus). For a review of Kitaigorodski's work, see also: Struchkov, Y. T.; Fedin, E. I. *Acta Chem. Hung.* **1993**, *130*, 159–172. (b) Rabinovich, D.; Schmidt, G. M. J. *Nature (London)* **1966**, *211*, 1391–1393.
(8) Hulliger, J. *Angew. Chem., Int. Ed. Engl.* **1994**, *33*, 143–162.
(9) Gavezzotti, A.; Filippini, G. *Synth. Met.* **1991**, *40*, 257–266.

0001-4842/94/0127-0309$04.50/0 © 1994 American Chemical Society

UM00012118
NOVARTIS EXHIBIT 1517
Novartis v. Regents, IPR2023-01347
Page 864 of 4460

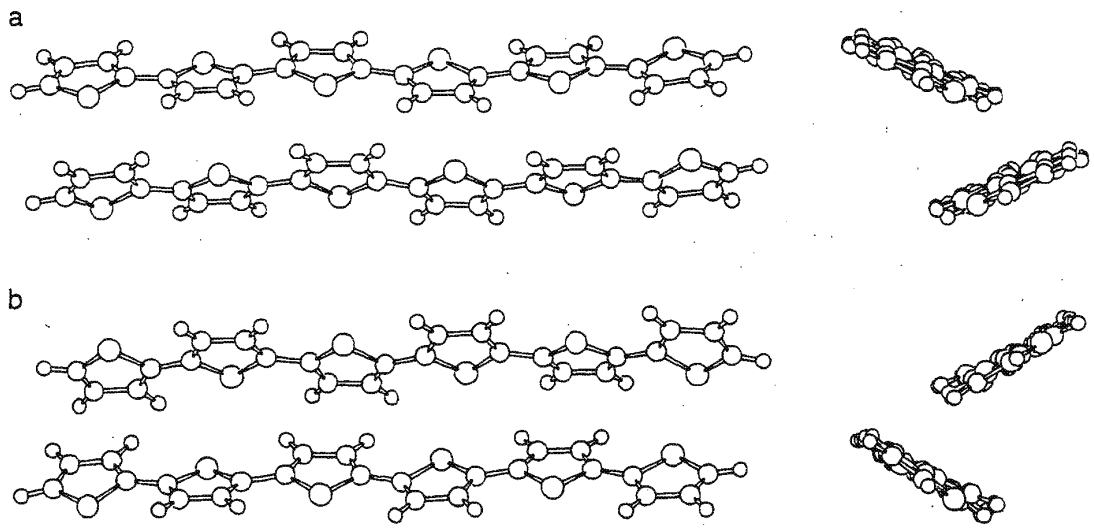


Figure 1. (a) The main motif in the predicted crystal structure of sexithienyl (ref 9; $P2_1/a$, $Z = 2$). (b) The same for the structure from a Rietveld refinement of powder data (ref 10; $P2_1/c$, $Z = 4$). The two structures differ mainly in the interplanar angle between neighbor molecules (49° vs 67°), better shown in the side views on the right.

could be obtained) has been published.[10] While the agreement between the main features of the predicted and experimental crystal structures is pleasing (Figure 1), the riddle of the lack of sexithienyl single crystals is still unanswered.

2. *Is this crystal high-melting*? The melting temperature (T_m) is high for high melting enthalpy or for low melting entropy. The entropic factor implies that disordered crystals, or crystals whose liquids are heavily associated (*e.g.*, by hydrogen bonding), have higher T_m's. Correlations between T_m and crystal cohesion should therefore be taken with caution.

A very old rule of thumb states that more symmetric molecules form higher-melting crystals;[11] this idea has been analyzed[12] using ortho-, meta-, and para-disubstituted benzenes (XC_6H_4Y, X and Y being any substituents). A survey of their T_m's shows that para isomers are the highest-melting ones, with very few exceptions; for only 18 out of 238 para–meta and para–ortho couples, the para isomer melts at a lower temperature. However, the definition of molecular symmetry in this context is really elusive and merges uncomfortably with that of molecular shape. The rule of thumb stays such, and cannot be given a sound theoretical or structural foundation. T_m is still one of the most difficult crystal properties to predict.

3. *What is the lattice energy (heat of sublimation)*? Extensive statistical studies have been conducted on relationships between molecular and crystal properties for non-hydrogen-bonding compounds containing C, H, N, O, S, and Cl atoms,[13-16] as well as for the most common families of hydrogen-bonding compounds[17] (acids, alcohols, and amides). Correlations were found which allow an estimate of sublimation enthalpies from molecular parameters like the number of valence electrons (Z) or the van der Waals surface (S). For example, in non-hydrogen-bonded oxohydrocarbons,

$$\Delta H_s = 0.201Z + 9.4 \text{ kcal/mol}$$

$$\Delta H_s = 0.077S(\text{Å}^2) + 8.9 \text{ kcal/mol}$$

Standard deviations of these linear regressions are comparable to experimental uncertainties of measurements;[18] at least in this respect, truly predictive correlations between molecular and crystal properties can be established. In some cases, errors in experimental ΔH_s's have been detected by redeterminations prompted by large deviations from the correlation.[14] Needless to say, the total lattice energy as such carries no information on the geometrical structure of the crystal.

4. *Will the crystal structure be non-centrosymmetric*? This is a simple but vital requirement for some practical applications of crystal chemistry.[19] Crystal centrosymmetry is often a matter of debate, and it is sometimes one of the refinable parameters in X-ray crystal structure analysis, rather than a stringent *a priori* condition.[20] One sees here a wide gap between the high (sometimes too high) resolution of diffraction experiments, where a single non-centrosymmetrically arranged atom in a large molecule would make a total difference, and the coarse view of the applied chemist. No one, except a neutron diffractionist, would consider non-centrosymmetric a hypothetical $P2_1$ crystal structure of monodeuteriobenzene.

(10) Porzio, W.; Destri, S.; Mascherpa, M.; Bruckner, S. *Acta Polym.* **1993**, *44*, 266–272.
(11) An early statement is by Hückel: Hückel, W. *Theoretische Grundlage der Organischen Chemie*; Akademische Verlagsgesellschaft: Leipzig, 1931; Vol. II, pp 185–186.
(12) Gavezzotti, A. To be published.
(13) Gavezzotti, A. *J. Am. Chem. Soc.* **1989**, *111*, 1835–1843.
(14) Gavezzotti, A. *J. Phys. Chem.* **1991**, *95*, 8948–8955.
(15) Gavezzotti, A.; Filippini, G. *Acta Crystallogr.* **1992**, *B48*, 537–545.
(16) Gavezzotti, A.; Filippini, G. *Acta Chim. Hung.* **1993**, *130*, 205–220.
(17) Gavezzotti, A.; Filippini, G. *J. Phys. Chem.* **1994**, *98*, 4831–4837.
(18) For a review of available sublimation enthalpies of organic compounds, see: Chickos, J. S. In *Molecular Structure and Energetics*; Liebman, J. F., Greenberg, A., Eds.; VCH: New York, 1987; Vol. 2.
(19) Paul, I. C.; Curtin, D. Y. *Chem. Rev.* **1981**, *81*, 525–541.
(20) For a $P1$ reassigned as $P\bar{1}$, see: Marsh, R. E. *Acta Crystallogr.* **1990**, *C46*, 1356–1357. See also: Marsh, R. E. *Acta Crystallogr.* **1994**, *A50*, 450, 455. The author is so assiduous in this kind of exercise that papers so reconsidered are commonly said to have been "marshed".

UM00012119
NOVARTIS EXHIBIT 1517
Novartis v. Regents, IPR2023-01347
Page 865 of 4460

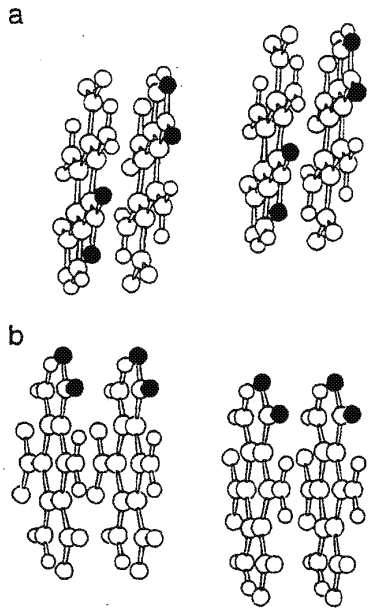


Figure 2. Arrangement of molecules in (a) the X-ray crystal structure of 1,3,5-triamino-2,4,6-trinitrobenzene (ref 24; $P\bar{1}$, $Z = 2$) and (b) the simulated crystal structure (ref 26; $P1$, $Z = 2$). Oxygen atoms in one nitro group are filled in.

The opinion that molecules with a high dipole moment tend to crystallize in a head-to-tail centrosymmetric fashion is untenable, as has been demonstrated by a detailed analysis:[21] the dipole representation of a charge distribution applies at large distances from it, while neighbor molecules in crystals see each other at distances comparable to molecular dimensions. On the other hand, the carboxylic acid group nearly always forces crystal centrosymmetry by forming cyclic dimers.[17,22] As is often the case, we only know how to produce the effect we do not want.

A crystal grown out of a solution containing only one enantiomer will perforce be non-centrosymmetric, but nothing can be said *a priori* on the spontaneous resolution of racemic solutions by crystallization. The relative stability of resolved and racemic crystals has been analyzed,[23] but there are at present no really predictive concepts on this fascinating subject, which may be related to the chirality of the chemistry of life.

Quite often, non-centrosymmetric molecular layers are readily formed, but they cannot be prevented from assuming an apparently very favorable centrosymmetric arrangement in the crystal. For example, the crystal structure of 1,3,5-triamino-2,4,6-trinitrobenzene has been assigned to a centrosymmetric space group ($P\bar{1}$) by X-ray analysis,[24] while the material displays a second harmonic generation propensity,[25] a property of non-centrosymmetric structures. Plausible non-centrosymmetric structures, with lattice energies quite comparable to that of the X-ray one, have been generated (Figure 2); the discussion of the results[26] has a lot of academic ifs and buts, perhaps contributing to confusion more than to the advancement of knowledge. The formation of non-centrosymmetric domains seems, however, the most likely explanation of the unusual properties of this crystal.

5. *Will some parts of the molecule take up a predictable orientation in the crystal?* Use of the information contained in the Cambridge Structural Database[27] has led to a number of statistical studies on the geometry of hydrogen bonding, of halogen–halogen interactions, and of other preferred approach paths between chemically recognizable molecular moieties. The reader is referred to an excellent review[28] on the subject.

Much work (and speculation) has been devoted[29] to the so-called π–π interactions between aromatic rings, driving to stacking, against the "electrostatic" attractions between rim hydrogen atoms and core carbon atoms, driving to T-shaped arrangements; preference for the latter is often assumed, quoting as a key example the benzene crystal, which in fact does contain also almost stacked neighbor molecules. A paper[30] in which the distribution of phenyl group orientations in hydrocarbon crystals has been examined, with peaks for both parallel and T-shaped arrangements, and a non-negligible population in between, has not been considered too seriously. Rules for the prediction of the appearance of herringbone *versus* stacked motifs in condensed aromatics have, apparently, been derived.[31]

In crystals of *monofunctional* carboxylic acids and amides, virtually no exceptions to the formation of cyclic dimers for the former and of single N–H–O=C hydrogen bonds in the latter were found.[17] Hydrogen bond formation has undoubtedly a very high priority in the construction of a crystal structure, but molecules with several acceptor and/or donor groups quite often crystallize in different polymorphic forms with different hydrogen-bonding networks.[32]

To conclude this section, one could say that some broad trends in the dependence of crystal packing from the presence of certain substituents or fragments have been identified; but this "substituent effect" in crystal chemistry stands on a shaky pedestal, since interactions in crystals of complex molecules are diverse and diffuse, and relying on local effects is always dangerous.

6. *What can be the space group and the number of molecules in the asymmetric unit?* The very concept of "space group" needs a little revision for crystal chemistry purposes. The presence or absence of a center of symmetry may be questionable;[20] the same applies to every symmetry element. To the eyes of an X-ray crystallographer, a glide plane is or is not present according to an extinction pattern, but the borderline between extinct and very weak reflections can sometimes be a matter of subjective judgement (parasitic diffraction phenomena also contribute). Minor molecular displacements may destroy some

(21) Whitesell, J. K.; Davis, R. E.; Saunders, L. L.; Wilson, R. J.; Feagins, J. P. *J. Am. Chem. Soc.* **1991**, *113*, 3267–3270.
(22) Leiserowitz, L. *Acta Crystallogr.* **1976**, *B32*, 775–802.
(23) Brock, C. P.; Schweizer, W. B.; Dunitz, J. D. *J. Am. Chem. Soc.* **1991**, *113*, 9811–9820.
(24) Cady, H. H.; Larson, A. C. *Acta Crystallogr.* **1965**, *18*, 485–496.
(25) Ledoux, I.; Zyss, J.; Siegel, J. S.; Brienne, J.; Lehn, J. M. *Chem. Phys. Lett.* **1990**, *172*, 440–444.
(26) Filippini, G.; Gavezzotti, A. Submitted.
(27) Allen, F. H.; Kennard, O.; Taylor, R. *Acc. Chem. Res.* **1983**, *16*, 146–153.
(28) Desiraju, G. R. *Crystal Engineering*; Elsevier: Amsterdam, 1989.
(29) See, *e.g.*: Dahl, T. *Acta Chem. Scand.* **1994**, *48*, 95–106 and references therein.
(30) Gavezzotti, A. *Chem. Phys. Lett.* **1989**, *161*, 67–72.
(31) Desiraju, G. R.; Gavezzotti, A. *Acta Crystallogr.* **1989**, *B45*, 473–482.
(32) Sulfa drugs provide striking examples: see, *e.g.*: Bar, I.; Bernstein, J. *J. Pharm. Sci.* **1985**, *74*, 255–263.

UM00012120
NOVARTIS EXHIBIT 1517
Novartis v. Regents, IPR2023-01347
Page 866 of 4460

symmetry element and bring about a change in space group (to the overdetailed eyes of the X-ray analyst), without really affecting the properties of the solid. For the crystal chemist, the prediction of the space group may be a whimsical exercise, if what counts is just a broad understanding of how molecules arrange themselves in space. Besides, in a molecular crystal (here meaning one in which distinguishable chemical entities appear, for which forces within the entity are considerably stronger than forces between entities) a distinction must be made between intramolecular, or point-group, symmetry and the true "intermolecular" symmetry, when the asymmetric unit is less than one molecule.[33]

Overall, crystal symmetry has two facets. On one side, in a milestone *mathematical* development, it was demonstrated that the combinations of symmetry elements give rise to no fewer and no more than 230 independent three-dimensional space groups. On the other side, crystal symmetry has to do with the mutual recognition of molecules to form a stable solid, a fascinating and essentially *chemical* problem that requires an evaluation of intermolecular forces. It should be clear that no necessary relationship holds between these two views; 230 space groups exist, but molecules cannot freely choose among them. Far from it, there are rather strict conditions that can be met only by a limited number of combinations of very few symmetry elements; for organic compounds, these are the inversion center, the 2-fold screw axis, and the glide plane, plus the ubiquitous translation (sometimes disguised as centering), itself a respectable, if often forgotten, symmetry operator. Thus, the choice of the space group for organic crystals is usually restricted to those including the above combinations: $P1$, $P\bar{1}$, $P2_1$, $P2_1/c$, $C2/c$, $P2_12_12_1$, $Pbca$. The well-known statistics on space group populations[34] for organic compounds confirms this, as Kitaigorodski pointed out decades ago.[35]

Some crystals reach a stable (or at least a lasting metastable) state with more than one molecule in the asymmetric unit. Statistics on the Cambridge Database have these occurrences at 8.3%,[36] but this is presumably an underestimation, since the Database is socially biased: structures with several molecules in the asymmetric unit pose a small supplementary technical problem in final space group assignment and structure refinement and were often in the past (and probably still are) put aside by busy crystallographers as unsavory members of their waiting lists. Once again, the reader is reminded of the discussion on the presence or absence of a symmetry operator, in this case the one that could provide a relationship between the partners of the plurimolecular asymmetric unit.

Some basic rules that preside over the formation of intra- and intermolecular hydrogen bonding have been identified.[37] In addition, it turns out that molecules which form very stable clusters in the liquid by hydrogen bonding are more likely to form plurimolecular asymmetric units, since these clusters are carried over intact into the crystal, and perfect symmetry within them is energetically irrelevant, or even slightly unfavorable: 40% of the alcohol crystals in the Cambridge Database have more than one molecule in the asymmetric unit.[17] For non-hydrogen-bonded crystals a similar explanation may be proposed, although no simple rules based on chemical reasoning can be put forward for preaggregation in the liquid state.

7. *What are the cell parameters?* The cell volume per molecule is rather easily estimated from molecular volume, after the Kitaigorodski idea of a constant packing coefficient;[35] hence, the crystal density too can be roughly estimated (see refs 15 and 17 for average packing coefficients of different chemical classes). If space is to be efficiently used in a condensed phase, there must be broad correlations between molecular dimensions and cell edges: for example, if D_s is the shortest molecular dimension, C_s the shortest cell edge, D_h the longest molecular dimension, and C_h the longest cell edge, the following restrictions apply[38] (Å):

$$D_s - 2 < C_s < D_s + 5$$

$$C_h > D_h - 3$$

Cell dimensions are indeed a bad identifier of a crystal structure, since their choice is not always unique. Distances between molecular centers of mass may be more useful; of course, some of these coincide with the length of screw or glide translations and, hence, are equal to one-half the cell parameters along unique crystallographic axes. These distances are the main quantitative descriptors of crystal geometry and are dictated solely by the strength and directionality of intermolecular forces. At this level, therefore, not much can be predicted with decent accuracy unless quantitative intermolecular potentials are available.

The systematic calibration of a set of potential energy parameters for organic crystals containing H, C, N, O, S, and Cl atoms, with[17] or without[39] hydrogen bonds, has been (painstakingly) accomplished. The reader will be spared the details of, and the endless disputes on, the methods employed in such work; space forbids also a quotation of the many alternative force fields available in the literature.[40] Suffice it to say that these parameters are as few as possible, and that with them one can safely calculate lattice energies (since experimental heats of sublimation[18] are reproduced), trusting that lattice dynamics is not grossly misrepresented (since reasonable lattice vibration frequencies are calculated[41] for observed crystal structures). The functional form includes one exponential and one inverse sixth power term in interatomic distances, so that computing times are not inflated by slowly-converging summations. These potentials (Table 1) have been tailored for the explicit task of performing large scale searches of crystal potential surfaces, or, in fewer words, for crystal structure prediction.

8. *Are crystal structures predictable?* Of course, the final question is whether it is possible to predict *ab initio* the complete structure of any organic crystal,

(33) See the discussion in the following: Scaringe, R. P. In *Electron Crystallography of Organic Molecules*; Fryer, J. R., Dorset, D. L., Eds.; Kluwer: Dordrecht, 1991, especially pp 92–94.
(34) Baur, W. H.; Kassner, D. *Acta Crystallogr.* **1992**, *B48*, 356–369.
(35) See ref 7a, introductory chapters.
(36) Padmaja, N.; Ramakumar, S.; Viswamitra, M. A. *Acta Crystallogr.* **1990**, *A46*, 725–730.
(37) Etter, M. C. *Acc. Chem. Res.* **1990**, *23*, 120–126.
(38) Gavezzotti, A. *J. Am. Chem. Soc.* **1991**, *113*, 4622–4629.
(39) Filippini, G.; Gavezzotti, A. *Acta Crystallogr.* **1993**, *B49*, 868–880.
(40) See refs 17 and 39 for perspective and discussion; see also: Pertsin, A. J.; Kitaigorodski, A. I. *The Atom–Atom Potential Method*; Springer-Verlag: Berlin, 1987.
(41) The lattice-dynamical procedure is described in the following: Filippini, G.; Gramaccioli, C. M. *Acta Crystallogr.* **1986**, *B42*, 605–609.

UM00012121
NOVARTIS EXHIBIT 1517
Novartis v. Regents, IPR2023-01347
Page 867 of 4460

Table 1. Atom–Atom Potential Parameters: $E = A \exp(-BR_{ij}) - CR_{ij}^{-6}$

interaction	A^a	B^b	C^c	ϵ^d	R^e
H–H	5774	4.01	26.1	0.010	3.36
H–C	28 870	4.10	113	0.049	3.29
H–N	54 560	4.52	120	0.094	2.99
H–O	70 610	4.82	105	0.121	2.80
H–S	64 190	4.03	279	0.110	3.35
H–Cl	70 020	4.09	279	0.120	3.30
C–C	54 050	3.47	578	0.093	3.89
C–N	117 470	3.86	667	0.201	3.50
C–O	93 950	3.74	641	0.161	3.61
C–S	126 460	3.41	1504	0.217	3.96
C–Cl	93 370	3.52	923	0.160	3.83
N–N	87 300	3.65	691	0.150	3.70
N–O	64 190	3.86	364	0.110	3.50
O–O	46 680	3.74	319	0.080	3.61
O–S	110 160	3.63	906	0.189	3.72
O–Cl	80 855	3.63	665	0.139	3.72
S–S	259 960	3.52	2571	0.445	3.83
Cl–Cl	140 050	3.52	1385	0.240	3.83
HB–O (amides)	3 607 810	7.78	238	4.0	1.80
HB–O (acids)	6 313 670	8.75	205	7.0	1.60
HB–O (alcohols)	4 509 750	7.78	298	5.0	1.80
HB–N (=N–H–N)	7 215 600	7.78	476	8.0	1.80
HB–N ($-NH_2$–N)	1 803 920	7.37	165	2.0	1.90

[a] Kcal/mol. [b] $Å^{-1}$. [c] Kcal/(mol·$Å^{-6}$). [d] Potential well depth (kcal/mol). [e] Distance at the minimum (Å). From refs 17 and 39.

space group, cell parameters, and atomic positions, much in the same style as in X-ray single-crystal structure analysis. The answer here is definitely "no".

Undoubtedly, no true prediction in the above sense can be accomplished without calculating the crystal potential energy, but one fundamental point is the choice of the best coordinates for the energy space. Intramolecular structure can be described by just a few (mostly torsional) conformational parameters, full relaxation of intramolecular vibrational degrees of freedom being pointless, since coupling with intermolecular vibrations is negligible. The location of molecules in the cell is described by three translational and three rotational rigid-body coordinates (restrictions apply for some point-group symmetries). Rather than using space groups and cell parameters, it is more convenient[38] to start from the constituents of spacial symmetry, that is, the four basic symmetry operators (inversion center, screw, glide, and translation); molecular clusters are built under their action, and their energies are calculated by empirical potentials. In this procedure, molecular conformation must be assumed as fixed, and the fact that polymorphs may exist with different molecular conformations is one addition to an already uncomfortably long list of difficulties. Anyway, a number of promising clusters are selected and are translated in space or coupled with other operators until a full three-dimensionally periodic crystal structure is reached.[42] One advantage of this procedure is that, say, a two-molecular cluster over a center of symmetry can be used to try both $P\bar{1}$ and $P2_1/c$. The most questionable feature is that there is no guarantee that a stable cluster will actually appear in the crystal, whose stability is determined by the overall features of its three-dimensional structure.

(42) Gevezzotti, A. *PROMET: A Program for the Generation of Possible Crystal Structures from the Molecular Structure of Organic Compounds*, and *Space Group Symmetry: A Primer*, University of Milano, 1993 (available from the author upon request). Using this program is an excellent way of learning the basics of space group symmetry.

Methods[38,43] which involve an examination of a great many possible crystal structures, using strategical shortcuts and sequential sieves, may be called "static". Their success in full prediction has been modest, but encouraging; they should be helpful when auxiliary information—from spectroscopy, powder or partial single-crystal diffraction, or structural correlation to similar compounds—is available. The construction of stable aggregates is made much easier when the consideration of predominant hydrogen-bonding schemes is possible.[44]

A "dynamic" approach uses Monte Carlo or molecular dynamics calculations.[45–47] The starting point is a collection of molecules in random orientations, and the predicted equilibrium state is the result of averaging over a large configurational space, or of evolution in time after solution of the classical equations of motion. In both cases, molecular interactions must be calculated by empirical potentials, which retain their pivotal role in the whole procedure. Computing times increase steeply with the number of molecules in the statistical sample and put a severe strain even on present-day machines. Ideally, this approach allows the simulation of the complete phase behavior of the substance, as a function of temperature and pressure. Although its scope and promise are certainly wider than those of the static approach, only the reproduction of the crystal structure of benzene[48] and a few other organic molecules[46] has been achieved so far, and a definite proof that such methods can give an unequivocal solution to the problem of crystal structure prediction has not been produced. The author of the present paper would be more than happy if this statement could be falsified in the near future. The computer software described and used in ref 46 (presumably the best available at the moment) is now being commercialized by a profit company (module "Polymorph" of the CERIUS package, by Molecular Simulations).

Polymorphism

Does the blame for the present, hardly satisfactory situation lie with technicalities? Is it just a matter of better path-finding algorithms and faster computers, or are there other basic obstacles to crystal structure prediction by calculations? There are. All computations and experiments demonstrate that many crystal structures for the same compound have quite similar lattice energies, or heats of sublimation. The ΔH_s of a medium-size organic molecule is 20–50 kcal/mol; heats of melting (ΔH_m) are typically $^1/_3$ of ΔH_s; enthalpy differences between crystalline phases[49] must be, in all evidence, just a fraction of ΔH_m, or something like 1–5 kcal/mole: just the range of experimental uncertainties of ΔH_s's on which empirical potentials are calibrated. Besides, crystalline

(43) Holden, J. R.; Du, Z.; Ammon, H. L. *J. Comput. Chem.* **1993**, *14*, 422–437.
(44) See, for example: Zerkowski, J. A.; Whitesides, G. M. *J. Am. Chem. Soc.* **1994**, *116*, 4298–4304.
(45) Linert, W.; Renz, F. *J. Chem. Inf. Comput. Sci.* **1993**, *33*, 776–781.
(46) Karfunkel, H. R.; Gdanitz, J. R. *J. Comput. Chem.* **1992**, *13*, 1171–1183.
(47) Perlstein, J. *J. Am. Chem. Soc.* **1994**, *116*, 455–470.
(48) Gdanitz, R. J. *Chem. Phys. Lett.* **1992**, *190*, 391–396.
(49) A vast literature deals with differences in solution enthalpies and phase transformation enthalpies of polymorphic pharmaceuticals; typical results are from a few down to fractions of a kcal/mol. For one example, see: Kojima, H.; Kiwada, H.; Kato, Y. *Chem. Pharm. Bull.* **1982**, *30*, 1824–1830. See also ref 32 and references therein.

UM00012122
NOVARTIS EXHIBIT 1517
Novartis v. Regents, IPR2023-01347
Page 868 of 4460

Table 2. Organization and Tools of an Ideal Department of Organic Solid State Chemistry

experimental	theoretical
synthetic chemistry commercially available compounds	Cambridge Structural Database First-principles calculations on sample systems
(re)crystallization studies of nucleation studies of morphology systematic search for polymorphs	empirical methods crystal potentials
standardized studies of dissolution	lattice dynamics
X-ray crystallography single crystal powder and Rietveld	search of crystal potential hypersurfaces Monte Carlo methods
thermochemistry differential scanning calorimetry thermogravimetry vapor pressure measurements	molecular dynamics
solid-state NMR	
ultramicroscopy (SEM/TEM, AFM)[a]	

[a] The acronyms refer to surface visualization techniques: scanning and tunneling electron microscopy; atomic force microscopy.

phases with higher enthalpy are usually less dense and, hence, will tend to have a higher vibrational entropy; thus, free energy differences are likely to be even smaller than enthalpy differences. And, above all, thermodynamic laws are systematically violated by organic crystals; witness the frequent observation of coexisting and (even more outrageously) separately melting polymorphs. Kinetic aspects are crucial here.

Even a casual consideration of the literature on polymorphism[50] provides convincing evidence that this phenomenon is pervasive. Therefore, the problem should not be formulated as prediction of *the* crystal structure of an organic compound, but as (1) generation of a set of polymorphs, (2) unequivocal detection of the most stable one at a given temperature, and (3) modeling of the nucleation kinetics to determine which phase will actually appear under given conditions. Empirical potentials may be intrinsically too crude to handle the thermodynamic aspects of the problem, unless it is proved (as we are presently trying to do,[51] with reasonably good chances of success) that the approximations do not affect *comparisons* of lattice energies and vibrational entropies of polymorphs.[52] There is no sound and well-accepted method for treating the kinetic aspects of crystal nucleation and of phase transformations at a molecular level, although pioneering contributions, again using molecular dynamics methods, have appeared.[53]

(50) See the extensive production of Kuhnert-Brandstaetter and coworkers; an entry point to this literature is the following: Kuhnert-Brandstaetter, M.; Solliger, H. W. *Mikrochim. Acta (Wien)* **1990**, *III*, 247–258.

(51) Filippini, G.; Gavezzotti, A. Work in progress.

(52) When the use of empirical methods is questionable, one should go back to first principles; but crystal structure prediction for an organic compound by quantum chemical calculations is at present, and most likely will be in the not-so-near future, impossible, since calculations without electron correlation are useless, and calculations including it are unfeasible. Carefully designed calculations on small key systems are, however, vital for a better understanding of intermolecular forces. Even a cursory mention of the vast literature in the field would be beyond the scope of this Account.

(53) (a) Bartell, L. S. *J. Phys. Chem.* **1990**, *94*, 5102–5109. (b) Chen, J.; Bartell, L. S. *J. Phys. Chem.* **1993**, *97*, 10645–10648.

(54) Such a laboratory could be set up in an academic environment with an initial investment of about 2 million dollars, and work with a yearly budget of half a million—peanuts in comparison with, say, money allocations for fancy high-energy physics machinery whose applicative spinoffs, if any, are much more problematic.

Concluding Remarks

Organic solid state chemistry is still a sporadic discipline. Organic solid state problems are approached from different points of view, with different methods and for different purposes: vapor pressures of solids are measured for pesticides; densities for explosives; heats of fusion and solubilities for pharmaceuticals. Crystallographers just consider solids as stiff containers for the molecular systems they want to study. Prior to solution of the structure prediction problem, the principles of organic solid state chemistry should be worked out by a deliberate and coordinated effort. The ideal laboratory for this task might be organized as in Table 2: its specific purpose should be a systematic study of large classes of organic solids for the establishment of the thermodynamic, kinetic, and structural principles of the organization of matter in solids at a molecular level.[54]

In the absence of such a chimeric entity, the state of the art in organic crystal structure prediction can be summarized by saying that we are still at the stage of exploration and data collection, with a reasonable amount of data organization. The problem is, at least, being seriously considered, methods are being developed and tested, and pieces of the puzzle are slowly falling into place. A cooperation between statistical studies on available crystal structures, energetic studies based on crystal thermodynamics and kinetics, and static or dynamic computational techniques will presumably guide theoretical chemists to real predictions of crystal structure without their having to synthesize the molecule. Whether this will be for the next years or the next decades remains to be seen. The ideas and the work summarized in this Account will (hopefully) be acknowledged as preliminary but useful, and indispensable in paving the way.

Massimo Simonetta founded in the 1960s an X-ray and structural chemistry laboratory in Milano; incentives to the study of crystal packing came originally from the author's collaboration with him and other members of that group and were later corroborated by suggestions from the discussions with J. D. Dunitz. In recent times, the valuable cooperation of Giuseppe Filippini is gratefully acknowledged. This paper is dedicated to the memory of my wife, Alessandra Gara.

UM00012123
NOVARTIS EXHIBIT 1517
Novartis v. Regents, IPR2023-01347
Page 869 of 4460

Risperdal®—Cont.

Respiratory System Disorders: *Infrequent:* hyperventilation, bronchospasm, pneumonia, stridor. *Rare:* asthma, increased sputum, aspiration.

Skin and Appendage Disorders: *Frequent:* increased pigmentation*, photosensitivity*. *Infrequent:* increased sweating, acne, decreased sweating, alopecia, hyperkeratosis, pruritus, skin exfoliation. *Rare:* bullous eruption, skin ulceration, aggravated psoriasis, furunculosis, verruca, dermatitis lichenoid, hypertrichosis, genital pruritus, urticaria.

Cardiovascular Disorders: *Infrequent:* palpitation, hypertension, hypotension, AV block, myocardial infarction. *Rare:* ventricular tachycardia, angina pectoris, premature atrial contractions, T wave inversions, ventricular extrasystoles, ST depression, myocarditis.

Vision Disorders: *Infrequent:* abnormal accommodation, xerophthalmia. *Rare:* diplopia, eye pain, blepharitis, photopsia, photophobia, abnormal lacrimation.

Metabolic and Nutritional Disorders: *Infrequent:* hyponatremia, weight increase, creatine phosphokinase increase, thirst, weight decrease, diabetes mellitus. *Rare:* decreased serum iron, cachexia, dehydration, hypokalemia, hypoproteinemia, hyperphosphatemia, hypertriglyceridemia, hyperuricemia, hypoglycemia.

Urinary System Disorders: *Frequent:* polyuria/polydipsia*. *Infrequent:* urinary incontinence, hematuria, dysuria. *Rare:* urinary retention, cystitis, renal insufficiency.

Musculo-skeletal System Disorders: *Infrequent:* myalgia. *Rare:* arthrosis, synostosis, bursitis, arthritis, skeletal pain.

Reproductive Disorders, Female: *Frequent:* menorrhagia*, orgastic dysfunction*, dry vagina*. *Infrequent:* nonpuerperal lactation, amenorrhea, female breast pain, leukorrhea, mastitis, dysmenorrhea, female perineal pain, intermenstrual bleeding, vaginal hemorrhage.

Liver and Biliary System Disorders: *Infrequent:* increased SGOT, increased SGPT. *Rare:* hepatic failure, cholestatic hepatitis, cholecystitis, cholelithiasis, hepatitis, hepatocellular damage.

Platelet, Bleeding and Clotting Disorders: *Infrequent:* epistaxis, purpura. *Rare:* hemorrhage, superficial phlebitis, thrombophlebitis, thrombocytopenia.

Hearing and Vestibular Disorders: *Rare:* tinnitus, hyperacusis, decreased hearing.

Red Blood Cell Disorders: *Infrequent:* anemia, hypochromic anemia. *Rare:* normocytic anemia.

Reproductive Disorders, Male: *Frequent:* erectile dysfunction*. *Infrequent:* ejaculation failure.

White Cell and Resistance Disorders: *Rare:* leukocytosis, lymphadenopathy, leucopenia, Pelger-Huet anomaly.

Endocrine Disorders: *Rare:* gynecomastia, male breast pain, antidiuretic hormone disorder.

Special Senses: *Rare:* bitter taste.

* Incidence based on elicited reports.

Post Introduction Reports: Adverse events reported since market introduction which were temporally (but not necessarily causally) related to RISPERDAL® therapy, include the following: anaphylactic reaction, angioedema, apnea, atrial fibrillation, cerebrovascular disorder, diabetes mellitus aggravated, including diabetic ketoacidosis, intestinal obstruction, jaundice, mania, pancreatitis, Parkinson's disease aggravated, pulmonary embolism. There have been rare reports of sudden death and/or cardiopulmonary arrest in patients receiving RISPERDAL®. A causal relationship with RISPERDAL® has not been established. It is important to note that sudden and unexpected death may occur in psychotic patients whether they remain untreated or whether they are treated with other antipsychotic drugs.

DRUG ABUSE AND DEPENDENCE

Controlled Substance Class: RISPERDAL® (risperidone) is not a controlled substance.

Physical and Psychologic Dependence: RISPERDAL® has not been systematically studied in animals or humans for its potential for abuse, tolerance or physical dependence. While the clinical trials did not reveal any tendency for any drug-seeking behavior, these observations were not systematic and it is not possible to predict on the basis of this limited experience the extent to which a CNS-active drug will be misused, diverted and/or abused once marketed. Consequently, patients should be evaluated carefully for a history of drug abuse, and such patients should be observed closely for signs of RISPERDAL® misuse or abuse (e.g., development of tolerance, increases in dose, drug-seeking behavior).

OVERDOSAGE

Human Experience: Premarketing experience included eight reports of acute RISPERDAL® overdosage with estimated doses ranging from 20 to 300 mg and no fatalities. In general, reported signs and symptoms were those resulting from an exaggeration of the drug's known pharmacological effects, i.e., drowsiness and sedation, tachycardia and hypotension, and extrapyramidal symptoms. One case, involving an estimated overdose of 240 mg, was associated with hyponatremia, hypokalemia, prolonged QT, and widened QRS. Another case, involving an estimated overdose of 36 mg, was associated with a seizure. Postmarketing experience includes reports of acute RISPERDAL® overdosage, with estimated doses of up to 360 mg. In general, the most frequently reported signs and symptoms are those resulting from an exaggeration of the drug's known pharmacological effects, i.e., drowsiness, sedation, tachycardia and hypotension. Other adverse events reported since market introduction which were temporally, (but not necessarily causally) related to RISPERDAL® overdose, include prolonged QT interval, convulsions, cardiopulmonary arrest, and rare fatality associated with multiple drug overdose.

Management of Overdosage: In case of acute overdosage, establish and maintain an airway and ensure adequate oxygenation and ventilation. Gastric lavage (after intubation, if patient is unconscious) and administration of activated charcoal together with a laxative should be considered. The possibility of obtundation, seizures or dystonic reaction of the head and neck following overdose may create a risk of aspiration with induced emesis. Cardiovascular monitoring should commence immediately and should include continuous electrocardiographic monitoring to detect possible arrhythmias. If antiarrhythmic therapy is administered, disopyramide, procainamide and quinidine carry a theoretical hazard of QT-prolonging effects that might be additive to those of risperidone. Similarly, it is reasonable to expect that the alpha-blocking properties of bretylium might be additive to those of risperidone, resulting in problematic hypotension.

There is no specific antidote to RISPERDAL®. Therefore appropriate supportive measures should be instituted. The possibility of multiple drug involvement should be considered. Hypotension and circulatory collapse should be treated with appropriate measures such as intravenous fluids and/or sympathomimetic agents (epinephrine and dopamine should not be used, since beta stimulation may worsen hypotension in the setting of risperidone-induced alpha blockade). In cases of severe extrapyramidal symptoms, anticholinergic medication should be administered. Close medical supervision and monitoring should continue until the patient recovers.

DOSAGE AND ADMINISTRATION

Usual Initial Dose: RISPERDAL® (risperidone) can be administered on either a BID or a QD schedule. In early clinical trials, RISPERDAL® was generally administered at 1 mg BID initially, with increases in increments of 1 mg BID on the second and third day, as tolerated, to a target dose of 3 mg BID by the third day. Subsequent controlled trials have indicated that total daily risperidone doses of up to 8 mg on a QD regimen are also safe and effective. However, regardless of which regimen is employed, in some patients a slower titration may be medically appropriate. Further dosage adjustments, if indicated, should generally occur at intervals of not less than 1 week, since steady state for the active metabolite would not be achieved for approximately 1 week in the typical patient. When dosage adjustments are necessary, small increments/decrements of 1–2 mg are recommended.

Antipsychotic efficacy was demonstrated in a dose range of 4 to 16 mg/day in the clinical trials supporting effectiveness of RISPERDAL®, however, maximal effect was generally seen in a range of 4 to 8 mg/day. Doses above 6 mg/day for BID dosing were not demonstrated to be more efficacious than lower doses, were associated with more extrapyramidal symptoms and other adverse effects, and are not generally recommended. In a single study supporting QD dosing, the efficacy results were generally stronger for 8 mg than for 4 mg. The safety of doses above 16 mg/day has not been evaluated in clinical trials.

Pediatric Use: Safety and effectiveness in pediatric patients have not been established.

Dosage in Special Populations: The recommended initial dose is 0.5 mg BID in patients who are elderly or debilitated, patients with severe renal or hepatic impairment, and patients either predisposed to hypotension or for whom hypotension would pose a risk. Dosage increases in these patients should be in increments of no more than 0.5 mg BID. Increases to dosages above 1.5 mg BID should generally occur at intervals of at least 1 week. In some patients, slower titration may be medically appropriate.

Elderly or debilitated patients, and patients with renal impairment, may have less ability to eliminate RISPERDAL® than normal adults. Patients with impaired hepatic function may have increases in the free fraction of the risperidone, possibly resulting in an enhanced effect (See CLINICAL PHARMACOLOGY). Patients with a predisposition to hypotensive reactions or for whom such reactions would pose a particular risk likewise need to be titrated cautiously and carefully monitored (See PRECAUTIONS). If a once-a-day dosing regimen in the elderly or debilitated patient is being considered, it is recommended that the patient be titrated on a twice-a-day regimen for 2–3 days at the target dose. Subsequent switches to a once-a-day dosing regimen can be done thereafter.

Maintenance Therapy: While there is no body of evidence available to answer the question of how long the patient treated with RISPERDAL® should remain on it, the effectiveness of maintenance treatment is well established for many other antipsychotic drugs. It is recommended that responding patients be continued on RISPERDAL®, but at the lowest dose needed to maintain remission. Patients should be periodically reassessed to determine the need for maintenance treatment.

Reinitiation of Treatment in Patients Previously Discontinued: Although there are no data to specifically address reinitiation of treatment, it is recommended that when restarting patients who have had an interval off RISPERDAL®, the initial titration schedule should be followed.

Switching from Other Antipsychotics: There are no systematically collected data to specifically address switching from other antipsychotics to RISPERDAL®, or concerning concomitant administration with other antipsychotics. While immediate discontinuation of the previous antipsychotic treatment may be acceptable for some patients, gradual discontinuation may be most appropriate for others. In all cases, the period of overlapping antipsychotic administration should be minimized. When transferring patients from depot antipsychotics, if medically appropriate, initiate RISPERDAL® therapy in place of the next scheduled injection. The need for continuing existing medication should be reevaluated periodically.

HOW SUPPLIED

RISPERDAL® (risperidone) tablets are imprinted "JANSSEN", and either "Ris" and the strength "1", "2" "3", or "4" or "R" and the strength "1", "2" "3", or "4":

0.25 mg dark-yellow tablet: bottles of 60 NDC 50458-301-60, bottles of 500 NDC 50458-301-50.

0.5 mg red-brown tablet: bottles of 60 NDC 50458-302-60, bottles of 500 NDC 50458-302-50.

1 mg white tablet: bottles of 60 NDC 50458-300-60, pack of 100 NDC 50458-300-01, bottles of 500 NDC 50458-300-50.

2 mg orange tablet: bottles of 60 NDC 50458-320-60, pack of 100 NDC 50458-320-01, bottles of 500 NDC 50458-320-50.

3 mg yellow tablet: bottles of 60 NDC 50458-330-60, pack of 100 NDC 50458-330-01, bottles of 500 NDC 50458-330-50.

4 mg green tablet: bottles of 60 NDC 50458-340-60, pack of 100 NDC 50458-350-01.

RISPERDAL® (risperidone) 1 mg/mL oral solution (NDC 50458-305-03) is supplied in 30mL bottles with a calibrated (in milligrams and milliliters) pipette. The maximum calibrated volume is 0.25 mL, while the minimum calibrated volume is 3 mL.

Tests indicate that RISPERDAL® (risperidone) oral solution is compatible in the following beverages: water, coffee, orange juice and low-fat milk; it is NOT compatible with cola or tea; however.

STORAGE AND HANDLING RISPERDAL® tablets should be stored at controlled room temperature 15°–25°C (59°–77°F). Protect from light and moisture. Keep out of reach of children.

RISPERDAL® 1 mg/mL oral solution should be stored at controlled room temperature 15°–25°C (59°–77°F). Protect from light and freezing keep out of reach of children.

US Patent 4,804,663

May 1999, December 2000

JANSSEN PHARMACEUTICA
Titusville, NJ 08560

Shown in Product Identification Guide, page 11b

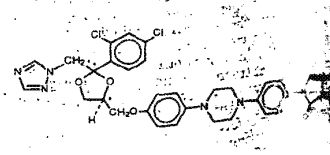
SPORANOX®
[*spôr'ah-nāks'*]
(itraconazole)
100 mg capsules

Congestive Heart Failure
SPORANOX® (itraconazole) Capsules should not be administered for the treatment of onychomycosis in patients with evidence of ventricular dysfunction such as congestive heart failure (CHF) or a history of CHF. Evidence of signs or symptoms of congestive heart failure were observed during administration of SPORANOX® Capsules. Discontinue administration. When itraconazole was administered intravenously to dogs and healthy volunteers, negative inotropic effects were observed. See CLINICAL PHARMACOLOGY: Special Populations, CONTRAINDICATIONS, WARNINGS, PRECAUTIONS: Drug Interactions and ADVERSE REACTIONS: Post-marketing Experience for information.)

Drug Interactions: Coadministration of cisapride, pimozide, quinidine, or dofetilide with SPORANOX® (itraconazole) Capsules, Injection or Oral Solution is contraindicated. SPORANOX®, a potent inhibitor of cytochrome P450 3A4 isoenzyme system (CYP3A4), can significantly increase plasma concentrations of drugs metabolized through this pathway. Serious cardiovascular events, including QT prolongation, torsades de pointes, ventricular tachycardia, cardiac arrest, and/or sudden death have occurred in patients using cisapride, pimozide, quinidine, or dofetilide concomitantly with SPORANOX®, a potent inhibitor of CYP3A4 inhibitors. See CONTRAINDICATIONS, WARNINGS, and PRECAUTIONS: Drug Interactions for more information.

DESCRIPTION

SPORANOX® is the brand name for itraconazole, a synthetic triazole antifungal agent. Itraconazole is a racemic mixture of four diastereomers (two pairs of enantiomers); each possessing three chiral centers. It is represented by the following structural formula and molecular structure:



UM00012124
NOVARTIS EXHIBIT 1517
Novartis v. Regents, IPR2023-01347
Page 870 of 4460

...INFORMATION

...sec-butyl]-4-[p-[4-[p-[[(2R*,4S*)-2-(2,4-dichlo-
...-[(2R*,4S*)-2-(2,4-dichlorophenyl)-2-(1H-1,2,4-triazol-1-ylmethyl)-1,3-dioxolan-4-
...-[4-[4-[4-[(2R,4S)-2-(2,4-dichlorophenyl)-2-(1H-1,2,4-triazol-1-ylmethyl)-1,3-dioxolan-4-yl]methoxy]phenyl]-1-piperazinyl]phenyl]-1-piperazinyl]phenyl]-Δ²-1,2,4-triazo-
...mixture with (±)-1-[(R*)-sec-butyl]-4-[p-[4-[p-[4-[(2R,4S)-2-(2,4-dichlorophenyl)-2-(1H-1,2,4-triazol-1-yl-
...-[(2R,4S)-2-(2,4-dichlorophenyl)-2-(1H-1,2,4-triazol-1-yl-
...dioxolan-4-yl]methoxy]phenyl]-1-piperazinyl]
...2,4-triazolin-5-one

or

...[2S]-sec-butyl]-4-[p-[4-[p-[[(2R,4S)-2-(2,4-dichlorophe-
...-[(2R,4S)-2-(2,4-dichlorophenyl)-2-(1H-1,2,4-triazol-1-ylmethyl)-1,3-dioxolan-4-yl]meth-
...-[4-[4-[4-[(2R,4S)-2-(2,4-dichlorophenyl)-2-(1H-1,2,4-triazol-1-ylmethyl)-1,3-dioxolan-4-yl]methoxy]phenyl]-1-piperazinyl]phenyl]-Δ²-1,2,4-triazolin-5-one

...-1-piperazinyl]-phenyl]-Δ²-1,2,4-triazolin-5-one has a molecular formula of $C_{35}H_{38}Cl_2N_8O_4$ and ...has a molecular formula of $C_{35}H_{38}Cl_2N_8O_4$ and ...weight of 705.64. It is a white to slightly yel-...It is insoluble in water, very slightly soluble ...and freely soluble in dichloromethane. It has a ...(based on extrapolation of values obtained from ...solutions) and a log (n-octanol/water) partition ...5.66 at pH 8.1.

...ANOX® Capsules contain 100 mg of itraconazole ...sugar spheres. Inactive ingredients are gelatin, ...ylmethylcellulose, polyethylene glycol (PEG) ...sucrose, titanium dioxide, FD&C Blue No. 1, ...No. 2, D&C Red No. 22 and D&C Red No. 28.

CLINICAL PHARMACOLOGY

...kinetics and Metabolism: NOTE: The plasma ...reported below were measured by high-per-...liquid chromatography (HPLC) specific for ...When itraconazole in plasma is measured by a ...values reported are approximately 3.3 times ...those obtained by HPLC due to the presence of ...metabolite, hydroxyitraconazole. (See MICRO-...OGY.)

...pharmacokinetics of itraconazole after intravenous ad-...and its absolute oral bioavailability from an ...were studied in a randomized crossover study ...male volunteers. The observed absolute oral ...bility of itraconazole was 55%.

...bioavailability of itraconazole is maximal when ...ANOX® (itraconazole) Capsules are taken with a full ...the pharmacokinetics of itraconazole were studied in ...male volunteers who received, in a crossover de-...100-mg doses of itraconazole as a polyethylene ...mule, with or without a full meal. The same 6 vol-...also received 50 mg or 200 mg with a full meal in a ...design. In this study, only itraconazole plasma ...trations were measured. The respective pharmacoki-...meters for itraconazole are presented in the table

...table at top of page]

...the SPORANOX® dose results in approximately a ...increase in the itraconazole plasma concentra-...

...given in the table below represent data from a cross-...pharmacokinetics study in which 27 healthy male vol-...each took a single 200-mg dose of SPORANOX® ...with or without a full meal:

...table at right]

...of itraconazole under fasted conditions in indi-...with relative or absolute achlorhydria, such as pa-...with AIDS or volunteers taking gastric acid secretion ...(e.g., H_2 receptor antagonists), was increased ...SPORANOX® Capsules were administered with a ...beverage. Eighteen men with AIDS received single ...doses of SPORANOX® Capsules under fasted con-...with 8 ounces of water or 8 ounces of a cola beverage ...crossover design. The absorption of itraconazole was in-...when SPORANOX® Capsules were coadministered ...cola beverage, with AUC_{0-24} and C_{max} increasing ...121% and 95% ± 128%, respectively.

...healthy men received single 200-mg doses of ...ANOX® Capsules under fasted conditions either 1) ...2) with water, after ranitidine 150 mg b.i.d. for ...or 3) with cola, after ranitidine 150 mg b.i.d. for 3 ...SPORANOX® Capsules were administered af-...ranitidine pretreatment, itraconazole was absorbed to a ...extent than when SPORANOX® Capsules were ad-...ministered alone, with decreases in AUC_{0-24} and C_{max} of ...37% and 42% ± 39%, respectively. When ...ANOX® Capsules were administered with cola after ...ranitidine pretreatment, itraconazole absorption was com-...parable to that observed when SPORANOX® Capsules were ...administered alone. (See PRECAUTIONS: Drug Interac-...

...concentrations were reached within 15 days ...oral doses of 50 mg to 400 mg daily. Values given ...table below are data at steady-state from a pharma-...study in which 27 healthy male volunteers took ...SPORANOX® Capsules b.i.d. (with a full meal) for ...

...table at right]

...protein binding of itraconazole is 99.8% and ...hydroxyitraconazole is 99.5%. Following intravenous ...administration, the volume of distribution of itraconazole ...was 796 ± 185 liters.

...itraconazole is metabolized predominately by the cyto-...chrome P450 3A4 isoenzyme system (CYP3A4), resulting in ...the formation of several metabolites, including hydroxyitra-...conazole, the major metabolite. Results of a pharmacokinet-...ic study suggest that itraconazole may undergo saturable ...metabolism with multiple dosing. Fecal excretion of the par-...ent drug accounts between 3–18% of the dose. Renal excretion ...of unchanged drug is less than 0.03% of the dose. About 40% ...of the dose is excreted as inactive metabolites in the urine.

	50 mg (fed)	100 mg (fed)	100 mg (fasted)	200 mg (fed)
C_{max} (ng/mL)	45 ± 16*	132 ± 67	38 ± 20	289 ± 100
T_{max} (hours)	3.2 ± 1.3	4.0 ± 1.1	3.3 ± 1.0	4.7 ± 1.4
$AUC_{0-\infty}$ (ng•h/mL)	567 ± 264	1899 ± 838	722 ± 289	5211 ± 2116

*mean ± standard deviation

	Itraconazole		Hydroxyitraconazole	
	Fed	Fasted	Fed	Fasted
C_{max} (ng/mL)	239 ± 85*	140 ± 65	397 ± 103	286 ± 101
T_{max} (hours)	4.5 ± 1.1	3.9 ± 1.0	5.1 ± 1.6	4.5 ± 1.1
$AUC_{0-\infty}$ (ng•h/mL)	3423 ± 1154	2094 ± 905	7978 ± 2648	5191 ± 2489
$t_{1/2}$ (hours)	21 ± 5	21 ± 7	12 ± 3	12 ± 3

*mean ± standard deviation

	Itraconazole	Hydroxyitraconazole
C_{max} (ng/mL)	2282 ± 514*	3488 ± 742
C_{min} (ng/mL)	1855 ± 535	3349 ± 761
T_{max} (hours)	4.6 ± 1.8	3.4 ± 3.4
AUC_{0-12h} (ng•h/mL)	22569 ± 5375	38572 ± 8450
$t_{1/2}$ (hours)	64 ± 32	56 ± 24

*mean ± standard deviation

No single excreted metabolite represents more than 5% of a dose. Itraconazole total plasma clearance averaged 381 ± 95 mL/minute following intravenous administration. (See CONTRAINDICATIONS and PRECAUTIONS: Drug Interactions for more information.)

Special Populations:

Renal Insufficiency: A pharmacokinetic study using a single 200-mg dose of itraconazole (four 50-mg capsules) was conducted in three groups of patients with renal impairment (uremia: n=7; hemodialysis: n=7; and continuous ambulatory peritoneal dialysis: n=5). In uremic subjects with a mean creatinine clearance of 13 mL/min. × 1.73 m^2, the bioavailability was slightly reduced compared with normal population parameters. This study did not demonstrate any significant effect of hemodialysis or continuous ambulatory peritoneal dialysis on the pharmacokinetics of itraconazole (T_{max}, C_{max}, and AUC_{0-8}). Plasma concentration-versus-time profiles showed wide intersubject variation in all three groups.

Hepatic Insufficiency: A pharmacokinetic study using a single 100-mg dose of itraconazole (one 100-mg capsule) was conducted in 6 healthy and 12 cirrhotic subjects. No statistically significant differences in AUC were seen between these two groups. A statistically significant reduction in mean C_{max} (47%) and a twofold increase in the elimination half-life (37 ± 17 hours) of itraconazole were noted in cirrhotic subjects compared with healthy subjects. Patients with impaired hepatic function should be carefully monitored when taking itraconazole. The prolonged elimination half-life of itraconazole observed in cirrhotic patients should be considered when deciding to initiate therapy with other medications metabolized by CYP3A4. (See BOX WARNING, CONTRAINDICATIONS, and PRECAUTIONS: Drug Interactions.)

Decreased Cardiac Contractility: When itraconazole was administered intravenously to anesthetized dogs, a dose-related negative inotropic effect was documented. In a healthy volunteer study of SPORANOX® Injection (intravenous infusion), transient, asymptomatic decreases in left ventricular ejection fraction were observed using gated SPECT imaging; these resolved before the next infusion, 12 hours later. If signs or symptoms of congestive heart failure appear during administration of SPORANOX® Capsules, SPORANOX® should be discontinued. (See CONTRAINDICATIONS, WARNINGS, PRECAUTIONS: Drug Interactions and ADVERSE REACTIONS: Post-marketing Experience for more information.)

MICROBIOLOGY

Mechanism of Action: In vitro studies have demonstrated that itraconazole inhibits the cytochrome P450-dependent synthesis of ergosterol, which is a vital component of fungal cell membranes.

Activity In Vitro and In Vivo: Itraconazole exhibits in vitro activity against *Blastomyces dermatitidis, Histoplasma capsulatum, Histoplasma duboisii, Aspergillus flavus, Aspergillus fumigatus, Candida albicans,* and *Cryptococcus neoformans.* Itraconazole also exhibits varying in vitro activity against *Sporothrix schenckii, Trichophyton* species, *Candida krusei,* and other *Candida* species. The bioactive metabolite, hydroxyitraconazole, has not been evaluated against *Histoplasma capsulatum* and *Blastomyces dermatitidis.* Correlation between minimum inhibitory concentration (MIC) results in vitro and clinical outcome has yet to be established for azole antifungal agents.

Itraconazole administered orally was active in a variety of animal models of fungal infection using standard laboratory strains of fungi. Fungistatic activity has been demonstrated against disseminated fungal infections caused by *Blastomyces dermatitidis, Histoplasma duboisii, Aspergillus fumigatus, Coccidioides immitis, Cryptococcus neoformans, Paracoccidioides brasiliensis, Sporothrix schenckii, Trichophyton rubrum,* and *Trichophyton mentagrophytes.*

Itraconazole administered at 2.5 mg/kg and 5 mg/kg via the oral and parenteral routes increased survival rates and sterilized organ systems in normal and immunosuppressed guinea pigs with disseminated *Aspergillus fumigatus* infections. Oral itraconazole administered daily at 40 mg/kg and 80 mg/kg increased survival rates in normal rabbits with disseminated disease and in immunosuppressed rats with pulmonary *Aspergillus fumigatus* infection, respectively. Itraconazole has demonstrated antifungal activity in a variety of animal models infected with *Candida albicans* and other *Candida* species.

Resistance: Isolates from several fungal species with decreased susceptibility to itraconazole have been isolated in vitro and from patients receiving prolonged therapy.

Several in vitro studies have reported that some fungal clinical isolates, including *Candida* species, with reduced susceptibility to one azole antifungal agent may also be less susceptible to other azole derivatives. The finding of cross-resistance is dependent on a number of factors, including the species evaluated, its clinical history, the particular azole compounds compared, and the type of susceptibility test that is performed. The relevance of these in vitro susceptibility data to clinical outcome remains to be elucidated. Studies (both in vitro and in vivo) suggest that the activity of amphotericin B may be suppressed by prior azole antifungal therapy. As with other azoles, itraconazole inhibits the ^{14}C-demethylation step in the synthesis of ergosterol, a cell wall component of fungi. Ergosterol is the active site for amphotericin B. In one study the antifungal activity of amphotericin B against *Aspergillus fumigatus* infections in mice was inhibited by ketoconazole therapy. The clinical significance of test results obtained in this study is unknown.

INDICATIONS AND USAGE

SPORANOX® (itraconazole) Capsules are indicated for the treatment of the following fungal infections in immunocompromised and non-immunocompromised patients:

1. Blastomycosis, pulmonary and extrapulmonary
2. Histoplasmosis, including chronic cavitary pulmonary disease and disseminated, non-meningeal histoplasmosis, and
3. Aspergillosis, pulmonary and extrapulmonary, in patients who are intolerant of or who are refractory to amphotericin B therapy.

Specimens for fungal cultures and other relevant laboratory studies (wet mount, histopathology, serology) should be obtained before therapy to isolate and identify causative organisms. Therapy may be instituted before the results of the cultures and other laboratory studies are known; however, once these results become available, antiinfective therapy should be adjusted accordingly.

SPORANOX® Capsules are also indicated for the treatment of the following fungal infections in non-immunocompromised patients:

1. Onychomycosis of the toenail, with or without fingernail involvement, due to dermatophytes (tinea unguium), and
2. Onychomycosis of the fingernail due to dermatophytes (tinea unguium).

Continued on next page

UM00012125

NOVARTIS EXHIBIT 1517
Novartis v. Regents, IPR2023-01347
Page 871 of 4460

Sporanox Caps—Cont.

Prior to initiating treatment, appropriate nail specimens for laboratory testing (KOH preparation, fungal culture, or nail biopsy) should be obtained to confirm the diagnosis of onychomycosis.

(See CLINICAL PHARMACOLOGY: Special Populations, CONTRAINDICATIONS, WARNINGS, and ADVERSE REACTIONS: Post-marketing Experience for more information.)

Description of Clinical Studies:

Blastomycosis: Analyses were conducted on data from two open-label, non-concurrently controlled studies (N=73 combined) in patients with normal or abnormal immune status. The median dose was 200 mg/day. A response for most signs and symptoms was observed within the first 2 weeks, and all signs and symptoms cleared between 3 and 6 months. Results of these two studies demonstrated substantial evidence of the effectiveness of itraconazole for the treatment of blastomycosis compared with the natural history of untreated cases.

Histoplasmosis: Analyses were conducted on data from two open-label, non-concurrently controlled studies (N=34 combined) in patients with normal or abnormal immune status (not including HIV-infected patients). The median dose was 200 mg/day. A response for most signs and symptoms was observed within the first 2 weeks, and all signs and symptoms cleared between 3 and 12 months. Results of these two studies demonstrated substantial evidence of the effectiveness of itraconazole for the treatment of histoplasmosis, compared with the natural history of untreated cases.

Histoplasmosis in HIV-infected patients: Data from a small number of HIV-infected patients suggested that the response rate of histoplasmosis in HIV-infected patients is similar to that of non-HIV-infected patients. The clinical course of histoplasmosis in HIV-infected patients is more severe and usually requires maintenance therapy to prevent relapse.

Aspergillosis: Analyses were conducted on data from an open-label, "single-patient-use" protocol designed to make itraconazole available in the U.S. for patients who either failed or were intolerant of amphotericin B therapy (N=190). The findings were corroborated by two smaller open-label studies (N=31 combined) in the same patient population. Most adult patients were treated with a daily dose of 200 to 400 mg, with a median duration of 3 months. Results of these studies demonstrated substantial evidence of effectiveness of itraconazole as a second-line therapy for the treatment of aspergillosis compared with the natural history of the disease in patients who either failed or were intolerant of amphotericin B therapy.

Onychomycosis of the toenail: Analyses were conducted on data from three double-blind, placebo-controlled studies (N=214 total; 110 given SPORANOX® Capsules) in which patients with onychomycosis of the toenails received 200 mg of SPORANOX® Capsules once daily for 12 consecutive weeks. Results of these studies demonstrated mycologic cure, defined as simultaneous occurrence of negative KOH plus negative culture, in 54% of patients. Thirty-five percent (35%) of patients were considered an overall success (mycologic cure plus clear or minimal nail involvement with significantly decreased signs) and 14% of patients demonstrated mycologic cure plus clinical cure (clearance of all signs, with or without residual nail deformity). The mean time to overall success was approximately 10 months. Twenty-one percent (21%) of the overall success group had a relapse (worsening of the global score or conversion of KOH or culture from negative to positive).

Onychomycosis of the fingernail: Analyses were conducted on data from a double-blind, placebo-controlled study (N=73 total; 37 given SPORANOX® Capsules) in which patients with onychomycosis of the fingernails received a 1-week course (pulse) of 200 mg of SPORANOX® Capsules b.i.d., followed by a 3-week period without SPORANOX®, which was followed by a second 1-week pulse of 200 mg of SPORANOX® Capsules b.i.d. Results demonstrated mycologic cure in 61% of patients. Fifty-six percent (56%) of patients were considered an overall success and 47% of patients demonstrated mycologic cure plus clinical cure. The mean time to overall success was approximately 5 months. None of the patients who achieved overall success relapsed.

CONTRAINDICATIONS

Congestive Heart Failure: SPORANOX® (itraconazole) Capsules should not be administered for the treatment of onychomycosis in patients with evidence of ventricular dysfunction such as congestive heart failure (CHF) or a history of CHF. (See CLINICAL PHARMACOLOGY: Special Populations, WARNINGS, PRECAUTIONS: Drug Interactions-Calcium Channel Blockers, and ADVERSE REACTIONS: Post-marketing Experience.)

Drug Interactions: Concomitant administration of SPORANOX® (itraconazole) Capsules, Injection, or Oral Solution and certain drugs metabolized by the cytochrome P450 3A4 isoenzyme system (CYP3A4) may result in increased plasma concentrations of those drugs, leading to potentially serious and/or life-threatening adverse events. Cisapride, oral midazolam, pimozide, quinidine, dofetilide, and triazolam are contraindicated with SPORANOX®. HMG CoA-reductase inhibitors metabolized by CYP3A4, such as lovastatin and simvastatin, are also contraindicated with SPORANOX®. (See BOX WARNING, and PRECAUTIONS: Drug Interactions.)

SPORANOX® should not be administered for the treatment of onychomycosis to pregnant patients or to women contemplating pregnancy.

SPORANOX® is contraindicated for patients who have shown hypersensitivity to itraconazole or its excipients. There is no information regarding cross-hypersensitivity between itraconazole and other azole antifungal agents. Caution should be used when prescribing SPORANOX® to patients with hypersensitivity to other azoles.

WARNINGS

SPORANOX® (itraconazole) Capsules and SPORANOX® Oral Solution should not be used interchangeably. This is because drug exposure is greater with the Oral Solution than with the Capsules when the same dose of drug is given. In addition, the topical effects of mucosal exposure may be different between the two formulations. Only the Oral Solution has been demonstrated effective for oral and/or esophageal candidiasis.

Hepatic Effects: SPORANOX® has been associated with rare cases of serious hepatotoxicity, including liver failure and death. Some of these cases had neither pre-existing liver disease nor a serious underlying medical condition. If clinical signs or symptoms develop that are consistent with liver disease, the risks and benefits of continued SPORANOX® use should be reassessed. (See PRECAUTIONS: Information for Patients and ADVERSE REACTIONS.)

Cardiac Dysrhythmias: Life-threatening cardiac dysrhythmias and/or sudden death have occurred in patients using cisapride, pimozide, or quinidine concomitantly with SPORANOX® and/or other CYP3A4 inhibitors. Concomitant administration of these drugs with SPORANOX® is contraindicated. (See BOX WARNING, CONTRAINDICATIONS, and PRECAUTIONS: Drug Interactions.)

Cardiac Disease: SPORANOX® Capsules should not be administered for the treatment of onychomycosis in patients with evidence of ventricular dysfunction such as congestive heart failure (CHF), or a history of CHF. SPORANOX® Capsules should not be used for other indications in patients with evidence of ventricular dysfunction unless the benefit clearly outweighs the risk.

For patients with risk factors for congestive heart failure; physicians should carefully review the risks and benefits of SPORANOX® therapy. These risk factors include cardiac disease such as ischemic and valvular disease; significant pulmonary disease such as chronic obstructive pulmonary disease; and renal failure and other edematous disorders. Such patients should be informed of the signs and symptoms of CHF, should be treated with caution, and should be monitored for signs and symptoms of CHF during treatment. If signs or symptoms of CHF appear during administration of SPORANOX® Capsules, discontinue administration.

When itraconazole was administered intravenously to anesthetized dogs, a dose-related negative inotropic effect was documented. In a healthy volunteer study of SPORANOX® Injection (intravenous infusion), transient, asymptomatic decreases in left ventricular ejection fraction were observed using gated SPECT imaging; these resolved before the next infusion, 12 hours later.

Cases of CHF, peripheral edema, and pulmonary edema have been reported in the post-marketing period among patients being treated for onychomycosis and/or systemic fungal infections. (See CLINICAL PHARMACOLOGY: Special Populations; CONTRAINDICATIONS; PRECAUTIONS: Drug Interactions, and ADVERSE REACTIONS: Post-marketing Experience for more information.)

PRECAUTIONS

General: Hepatic enzyme test values should be monitored in patients with pre-existing hepatic function abnormalities or those who have experienced liver toxicity with other medications. Hepatic enzyme test values should be monitored periodically in all patients receiving continuous treatment for more than 1 month, or at any time a patient develops signs or symptoms suggestive of liver dysfunction.

SPORANOX® (itraconazole) Capsules should be administered after a full meal. (See CLINICAL PHARMACOLOGY: Pharmacokinetics and Metabolism.)

Under fasted conditions, itraconazole absorption was decreased in the presence of decreased gastric acidity. The absorption of itraconazole may be decreased with the concomitant administration of antacids or gastric acid secretion suppressors. Studies conducted under fasted conditions demonstrated that administration with 8 ounces of a cola beverage resulted in increased absorption of itraconazole in AIDS patients with relative or absolute achlorhydria. This increase relative to the effects of a full meal is unknown. (See CLINICAL PHARMACOLOGY: Pharmacokinetics and Metabolism.)

Information for Patients:

- The topical effects of mucosal exposure may be different between the SPORANOX® Capsules and Oral Solution. Only the Oral Solution has been demonstrated effective for oral and/or esophageal candidiasis. SPORANOX® Capsules should not be used interchangeably with SPORANOX® Oral Solution.
- Instruct patients to take SPORANOX® Capsules with a full meal.
- Instruct patients about the signs and symptoms of congestive heart failure, and if these signs or symptoms occur during SPORANOX® administration, they should discontinue SPORANOX® and contact their healthcare provider immediately.
- Instruct patients to report any signs and symptoms that may suggest liver dysfunction so that the appropriate laboratory testing can be done. Such signs and symptoms may include unusual fatigue, anorexia, nausea, vomiting, jaundice, dark urine, or pale stools.
- Instruct patients to contact their physician before taking any concomitant medications with itraconazole to ensure there are no potential drug interactions.

Drug Interactions: Itraconazole and its major metabolite, hydroxyitraconazole, are inhibitors of CYP3A4. The potential for the following drug interactions may occur (See Table below and the following drug class subheadings for more detail):

1. SPORANOX® may decrease the elimination of drugs that are metabolized by CYP3A4, resulting in increased plasma concentrations of these drugs when they are administered with SPORANOX®. These elevated plasma concentrations may increase or prolong both therapeutic and adverse effects of these drugs. Whenever possible, plasma concentrations of these drugs should be monitored, and dosage adjustments made, after concomitant SPORANOX® therapy is initiated. When appropriate, clinical monitoring for signs or symptoms of increased or prolonged pharmacologic effects is advised. Upon discontinuation, depending on the dose and duration of treatment, itraconazole plasma concentrations decline gradually (especially in patients with hepatic cirrhosis or those receiving CYP3A4 inhibitors). This is particularly important when initiating therapy with drugs whose metabolism is affected by itraconazole.
2. Inducers of CYP3A4 may decrease the plasma concentrations of itraconazole, SPORANOX® may not be effective in patients concomitantly taking SPORANOX® and any of these drugs. Therefore, administration of these drugs with SPORANOX® is not recommended.
3. Other inhibitors of CYP3A4 may increase the plasma concentrations of itraconazole. Patients who must take SPORANOX® concomitantly with one of these drugs should be monitored closely for signs or symptoms of increased or prolonged pharmacologic effects of SPORANOX®.

[See table at bottom of next page]

Antiarrhythmics: The class IA antiarrhythmic quinidine and class III antiarrhythmic dofetilide are known to prolong the QT interval. Coadministration of quinidine or dofetilide with SPORANOX® may increase plasma concentrations of quinidine or dofetilide which could result in serious cardiovascular events. Therefore, concomitant administration of SPORANOX® and quinidine or dofetilide is contraindicated. (See BOX WARNING, CONTRAINDICATIONS, and WARNINGS.)

Concomitant administration of digoxin and SPORANOX® has led to increased plasma concentrations of digoxin.

Anticonvulsants: Reduced plasma concentrations of itraconazole were reported when SPORANOX® was administered concomitantly with phenytoin. Carbamazepine, phenobarbital, and phenytoin are all inducers of CYP3A4. Although interactions with carbamazepine and phenobarbital have not been studied, concomitant administration of SPORANOX® and these drugs would be expected to result in decreased plasma concentrations of itraconazole. In addition, in vivo studies have demonstrated an increase in plasma carbamazepine concentrations in subjects concomitantly receiving ketoconazole. Although there are no data regarding the effect of itraconazole on carbamazepine metabolism, because of the similarities between ketoconazole and itraconazole, concomitant administration of SPORANOX® and carbamazepine may inhibit the metabolism of carbamazepine.

Antimycobacterials: Drug interaction studies have demonstrated that plasma concentrations of azole antifungal agents and their metabolites, including itraconazole and hydroxyitraconazole, were significantly decreased when these agents were given concomitantly with rifabutin or rifampin. In vivo data suggest that rifabutin is metabolized by CYP3A4. SPORANOX® may inhibit the metabolism of rifabutin. Although no formal study data are available for isoniazid, similar effects should be anticipated. Therefore, the efficacy of SPORANOX® could be substantially reduced if given concomitantly with one of these agents. Coadministration is not recommended.

Antineoplastics: SPORANOX® may inhibit the metabolism of busulfan, docetaxel, and vinca alkaloids.

Antipsychotics: Pimozide is known to prolong the QT interval and is partially metabolized by CYP3A4. Coadministration of pimozide with SPORANOX® could result in serious cardiovascular events. Therefore, concomitant administration of SPORANOX® and pimozide is contraindicated. (See BOX WARNING, CONTRAINDICATIONS, and WARNINGS.)

Benzodiazepines: Concomitant administration of SPORANOX® and alprazolam, diazepam, oral midazolam, or triazolam could lead to increased plasma concentrations of these benzodiazepines. Increased plasma concentrations could potentiate and prolong hypnotic and sedative effects. Concomitant administration of SPORANOX® and oral midazolam or triazolam is contraindicated. (See CONTRAINDICATIONS and WARNINGS.) If midazolam is administered parenterally, special precaution and patient management is required since the sedative effect may be potentiated.

Calcium Channel Blockers: Edema has been reported in patients concomitantly receiving SPORANOX® and

UM00012126
NOVARTIS EXHIBIT 1517
Novartis v. Regents, IPR2023-01347
Page 872 of 4460

calcium channel blockers. Appropriate dosage may be necessary.
channel blockers can have a negative inotropic effect may be additive to those of itraconazole; can inhibit the metabolism of calcium channel such as dihydropyridines (e.g., nifedipine and felodipine) and verapamil. Therefore, caution should be used administering itraconazole and calcium channel (See CLINICAL PHARMACOLOGY: Special Populations, CONTRAINDICATIONS, WARNINGS, and ADVERSE REACTIONS: Post-marketing Experience for more information).

Acid Suppressors/Neutralizers: Reduced plasma concentrations of itraconazole were reported when SPORANOX® Capsules were administered concomitantly with H2-receptor antagonists. Studies have shown that absorption of itraconazole is impaired when gastric acid production is decreased. Therefore, SPORANOX® should be administered with a cola beverage if the patient has achlorhydria or is taking H_2-receptor antagonists or other gastric acid suppressors. Antacids should be administered at least 1 hour before or 2 hours after administration of SPORANOX® Capsules. In a clinical study, when SPORANOX® Capsules were administered with omeprazole (a proton pump inhibitor), the bioavailability of itraconazole was significantly reduced.

Gastrointestinal Motility Agents: Coadministration of SPORANOX® with cisapride can elevate plasma cisapride concentrations which could result in serious cardiovascular events. Therefore, concomitant administration of SPORANOX® with cisapride is contraindicated. (See BOXED WARNING, CONTRAINDICATIONS, and WARNINGS.)

HMG-CoA Reductase Inhibitors: Human pharmacokinetic data suggest that SPORANOX® inhibits the metabolism of atorvastatin, cerivastatin, lovastatin, and simvastatin, which may increase the risk of skeletal muscle toxicity, including rhabdomyolysis. Concomitant administration of SPORANOX® with HMG CoA-reductase inhibitors, such as lovastatin and simvastatin, is contraindicated. (See CONTRAINDICATIONS and WARNINGS.)

Immunosuppressants: Concomitant administration of SPORANOX® and cyclosporine or tacrolimus has led to increased plasma concentrations of these immunosuppressants. Concomitant administration of SPORANOX® and sirolimus could increase plasma concentrations of sirolimus.

Macrolide Antibiotics: Erythromycin and clarithromycin are inhibitors of CYP3A4 (See Table 1) and may increase plasma concentrations of itraconazole. In a small pharmacokinetic study involving HIV infected patients, erythromycin was shown to increase plasma concentrations of itraconazole. Similarly, following administration of 200 mg of erythromycin ethyl succinate and 200 mg itraconazole single doses, the mean C_{max} and $AUC_{0-\infty}$ of itraconazole increased by 44% (90% CI: 119-175%) and 36% (90% CI: 108-171%), respectively.

Non-nucleoside Reverse Transcriptase Inhibitors: Nevirapine is an inducer of CYP3A4. In vivo studies have shown that nevirapine induces the metabolism of ketoconazole, significantly reducing the bioavailability of ketoconazole. Studies involving nevirapine and itraconazole have not been conducted. However, because of the similarities between ketoconazole and itraconazole, concomitant administration of SPORANOX® and nevirapine is not recommended.

In a clinical study, when 8 HIV-infected subjects were treated concomitantly with SPORANOX® Capsules 100 mg twice daily and the nucleoside reverse transcriptase inhibitor zidovudine 8 ± 0.4 mg/kg/day, the pharmacokinetics of zidovudine were not affected. Other nucleoside reverse transcriptase inhibitors have not been studied.

Oral Hypoglycemic Agents: Severe hypoglycemia has been reported in patients concomitantly receiving azole antifungal agents and oral hypoglycemic agents. Blood glucose concentrations should be carefully monitored when SPORANOX® and oral hypoglycemic agents are coadministered.

Polyenes: Prior treatment with itraconazole, like other azoles, may reduce or inhibit the activity of polyenes such as amphotericin B. However, the clinical significance of this drug effect has not been clearly defined.

Protease Inhibitors: Concomitant administration of SPORANOX® and protease inhibitors metabolized by CYP3A4, such as indinavir, ritonavir, and saquinavir, may increase plasma concentrations of these protease inhibitors. In addition, concomitant administration of SPORANOX® and indinavir and ritonavir (but not saquinavir) may increase plasma concentrations of itraconazole. Caution is advised when SPORANOX® and protease inhibitors must be given concomitantly.

Other:

- In vitro data suggest that alfentanil is metabolized by CYP3A4. Administration with SPORANOX® may increase plasma concentrations of alfentanil.
- Human pharmacokinetic data suggest that concomitant administration of SPORANOX® and buspirone results in significant increases in plasma concentrations of buspirone.
- SPORANOX® may inhibit the metabolism of methylprednisolone.
- In vitro data suggest that trimetrexate is extensively metabolized by CYP3A4. In vitro animal models have demonstrated that ketoconazole potently inhibits the metabolism of trimetrexate. Although there are no data regarding the effect of itraconazole on trimetrexate metabolism, because of the similarities between ketoconazole and itraconazole, concomitant administration of SPORANOX® and trimetrexate may inhibit the metabolism of trimetrexate.
- SPORANOX® enhances the anticoagulant effect of coumarin-like drugs, such as warfarin.

Table 1. Selected Drugs that are predicted to alter the plasma concentration of itraconazole or have their plasma concentration altered by SPORANOX®[1]

Drug plasma concentration increased by itraconazole	
Antiarrhythmics	digoxin, dofetilide,[2] quinidine[2]
Anticonvulsants	carbamazepine
Antimycobacterials	rifabutin
Antineoplastics	busulfan, docetaxel, vinca alkaloids
Antihistamines	pimozide[2]
Benzodiazepines	alprazolam, diazepam, midazolam,[2,3] triazolam[2]
Calcium Channel Blockers	dihydropyridines, verapamil
Gastrointestinal Motility Agents	cisapride[2]
HMG-CoA Reductase Inhibitors	atorvastatin, cerivastatin, lovastatin,[2] simvastatin[2]
Immunosuppressants	cyclosporine, tacrolimus, sirolimus
Oral Hypoglycemics	oral hypoglycemics
Protease Inhibitors	indinavir, ritonavir, saquinavir
Other	alfentanil, buspirone, methylprednisolone, trimetrexate, warfarin
Decrease plasma concentration of itraconazole	
Anticonvulsants	carbamazepine, phenobarbital, phenytoin
Antimycobacterials	isoniazid, rifabutin, rifampin
Acid Suppressors/Neutralizers	antacids, H_2-receptor antagonists, proton pump inhibitors
Non-nucleoside Reverse Transcriptase Inhibitors	nevirapine
Increase plasma concentration of itraconazole	
Macrolides	clarithromycin, erythromycin
Protease Inhibitors	indinavir, ritonavir

[1] This list is not all-inclusive.
[2] Caution with SPORANOX® based on clinical and/or pharmacokinetics studies. (See WARNINGS and below.)
[3] For parenterally administered midazolam, see the Benzodiazepine paragraph below.

Carcinogenesis, Mutagenesis, and Impairment of Fertility: Itraconazole showed no evidence of carcinogenicity potential in mice treated orally for 23 months at dosage levels up to 80 mg/kg/day (approximately 10× the maximum recommended human dose [MRHD]). Male rats treated with 25 mg/kg/day (3.1× MRHD) had a slightly increased incidence of soft tissue sarcoma. These sarcomas may have been a consequence of hypercholesterolemia, which is a response of rats, but not dogs or humans, to chronic itraconazole administration. Female rats treated with 50 mg/kg/day (6.25× MRHD) had an increased incidence of squamous cell carcinoma of the lung (2/50) as compared to the untreated group. Although the occurrence of squamous cell carcinoma in the lung is extremely uncommon in untreated rats, the increase in this study was not statistically significant.

Itraconazole produced no mutagenic effects when assayed in DNA repair test (unscheduled DNA synthesis) in primary rat hepatocytes, in Ames tests with *Salmonella typhimurium* (6 strains) and *Escherichia coli*, in the mouse lymphoma gene mutation tests, in a sex-linked recessive lethal mutation (*Drosophila melanogaster*) test, in chromosome aberration tests in human lymphocytes, in a cell transformation test with C3H/10T½ C18 mouse embryo fibroblasts cells, in a dominant lethal mutation test in male and female mice, and in micronucleus tests in mice and rats.

Itraconazole did not affect the fertility of male or female rats treated orally with dosage levels of up to 40 mg/kg/day (5× MRHD), even though parental toxicity was present at this dosage level. More severe signs of parental toxicity, including death, were present in the next higher dosage level, 160 mg/kg/day (20× MRHD).

Pregnancy: Teratogenic effects. Pregnancy Category C: Itraconazole was found to cause a dose-related increase in maternal toxicity, embryotoxicity, and teratogenicity in rats at dosage levels of approximately 40–160 mg/kg/day (5–20× MRHD), and in mice at dosage levels of approximately 80 mg/kg/day (10× MRHD). In rats, the teratogenicity consisted of major skeletal defects; in mice, it consisted of encephaloceles and/or macroglossia.

There are no studies in pregnant women. SPORANOX® should be used for the treatment of systemic fungal infections in pregnancy only if the benefit outweighs the potential risk. SPORANOX® should not be administered for the treatment of onychomycosis to pregnant patients or to women contemplating pregnancy. SPORANOX® should not be administered to women of childbearing potential for the treatment of onychomycosis unless they are using effective measures to prevent pregnancy and they begin therapy on the second or third day following the onset of menses. Effective contraception should be continued throughout SPORANOX® therapy and for 2 months following the end of treatment.

Nursing Mothers: Itraconazole is excreted in human milk; therefore, the expected benefits of SPORANOX® therapy for the mother should be weighed against the potential risk from exposure of itraconazole to the infant. The U.S. Public Health Service Centers for Disease Control and Prevention advises HIV-infected women not to breast-feed to avoid potential transmission of HIV to uninfected infants.

Pediatric Use: The efficacy and safety of SPORANOX® have not been established in pediatric patients. No pharmacokinetic data on SPORANOX® Capsules are available in children. A small number of patients ages 3 to 16 years have been treated with 100 mg/day of itraconazole capsules for systemic fungal infections, and no serious unexpected adverse effects have been reported. SPORANOX® Oral Solution (5 mg/kg/day) has been administered to pediatric patients (N=26; ages 6 months to 12 years) for 2 weeks and no serious unexpected adverse events were reported.

The long-term effects of itraconazole on bone growth in children are unknown. In three toxicology studies using rats, itraconazole induced bone defects at dosage levels as low as 20 mg/kg/day (2.5× MRHD). The induced defects included reduced bone plate activity, thinning of the zona compacta of the large bones, and increased bone fragility. At a dosage level of 80 mg/kg/day (10× MRHD) over 1 year or 160 mg/kg/day (20× MRHD) for 6 months, itraconazole induced small tooth pulp with hypocellular appearance in some rats. No such bone toxicity has been reported in adult patients.

HIV-Infected Patients: Because hypochlorhydria has been reported in HIV-infected individuals, the absorption of itraconazole in these patients may be decreased.

ADVERSE REACTIONS

SPORANOX® has been associated with rare cases of serious hepatotoxicity, including liver failure and death. Some of these cases had neither pre-existing liver disease nor a serious underlying medical condition. If clinical signs or symptoms develop that are consistent with liver disease, the risks and benefits of continued SPORANOX® use should be reassessed. (See WARNINGS: Hepatic Effects and PRECAUTIONS: Information for Patients.)

Adverse Events in the Treatment of Systemic Fungal Infections

Adverse event data were derived from 602 patients treated for systemic fungal disease in U.S. clinical trials who were

Continued on next page

LIM00012127
NOVARTIS EXHIBIT 1517
Novartis v. Regents, IPR2023-01347
Page 873 of 4460

Sporanox Caps—Cont.

immunocompromised or receiving multiple concomitant medications. Treatment was discontinued in 10.5% of patients due to adverse events. The median duration before discontinuation of therapy was 81 days (range: 2 to 776 days). The table lists adverse events reported by at least 1% of patients.

Treatment of Systemic Fungal Infections: Adverse Events Occurring with an Incidence of Greater than or Equal to 1%

Body System/Adverse Event	Incidence (%) (N=602)
Gastrointestinal	
Nausea	11
Vomiting	5
Diarrhea	3
Abdominal Pain	2
Anorexia	1
Body as Whole	
Edema	4
Fatigue	3
Fever	3
Malaise	1
Skin and Appendages	
Rash*	9
Pruritus	3
Central/Peripheral Nervous System	
Headache	4
Dizziness	2
Psychiatric	
Libido Decreased	1
Somnolence	1
Cardiovascular	
Hypertension	3
Metabolic/Nutritional	
Hypokalemia	2
Urinary System	
Albuminuria	1
Liver and Biliary System	
Hepatic Function Abnormal	3
Reproductive System, Male	
Impotence	1

*Rash tends to occur more frequently in immunocompromised patients receiving immunosuppressive medications.

Adverse events infrequently reported in all studies included constipation, gastritis, depression, insomnia, tinnitus, menstrual disorder, adrenal insufficiency, gynecomastia, and male breast pain.

Adverse Events Reported in Toenail Onychomycosis Clinical Trials

Patients in these trials were on a continuous dosing regimen of 200 mg once daily for 12 consecutive weeks.

The following adverse events led to temporary or permanent discontinuation of therapy.

Clinical Trials of Onychomycosis of the Toenail: Adverse Events Leading to Temporary or Permanent Discontinuation of Therapy

Adverse Event	Incidence (%) Itraconazole (N=112)
Elevated Liver Enzymes (greater than twice the upper limit of normal)	4
Gastrointestinal Disorders	4
Rash	3
Hypertension	2
Orthostatic Hypotension	1
Headache	1
Malaise	1
Myalgia	1
Vasculitis	1
Vertigo	1

The following adverse events occurred with an incidence of greater than or equal to 1% (N=112): headache: 10%; rhinitis: 9%; upper respiratory tract infection: 8%; sinusitis, injury: 7%; diarrhea, dyspepsia, flatulence, abdominal pain, dizziness, rash: 4%; cystitis, urinary tract infection, liver function abnormality, myalgia, nausea: 3%; appetite increased, constipation, gastritis, gastroenteritis, pharyngitis, asthenia, fever, pain, tremor, herpes zoster, abnormal dreaming: 2%.

Adverse Events Reported in Fingernail Onychomycosis Clinical Trials

Patients in these trials were on a pulse regimen consisting of two 1-week treatment periods of 200 mg twice daily, separated by a 3-week period without drug.

The following adverse events led to temporary or permanent discontinuation of therapy.

Clinical Trials of Onychomycosis of the Fingernail: Adverse Events Leading to Temporary or Permanent Discontinuation of Therapy

Adverse Event	Incidence (%) Itraconazole (N=37)
Rash/Pruritus	3
Hypertriglyceridemia	3

The following adverse events occurred with an incidence of greater than or equal to 1% (N=37): headache: 8%; pruritus, nausea, rhinitis: 5%; rash, bursitis, anxiety, depression, constipation, abdominal pain, dyspepsia, ulcerative stomatitis, gingivitis, hypertriglyceridemia, sinusitis, fatigue, malaise, pain, injury: 3%.

Post-marketing Experience

In worldwide post-marketing experience with SPORANOX® Capsules in treatment of onychomycosis and/or systemic fungal infections, peripheral edema, allergic reactions, including rash, pruritus, urticaria, angioedema, and, in rare instances, anaphylaxis and Stevens-Johnson syndrome, have been reported. Post-marketing experiences have also included reports of elevated liver enzymes and rarely liver failure. Rare cases of congestive heart failure and pulmonary edema have been reported. Rare cases of alopecia, hypertriglyceridemia, menstrual disorders, and neutropenia, and isolated cases of neuropathy have also been reported, although the causal association with SPORANOX® is uncertain. (See CLINICAL PHARMACOLOGY: Special Populations, CONTRAINDICATIONS, WARNINGS, and PRECAUTIONS: Drug Interactions for more information).

OVERDOSAGE

Itraconazole is not removed by dialysis. In the event of accidental overdosage, supportive measures, including gastric lavage with sodium bicarbonate, should be employed.

Limited data exist on the outcomes of patients ingesting high doses of itraconazole. In patients taking either 1000 mg of SPORANOX® (itraconazole) Oral Solution or up to 3000 mg of SPORANOX® (itraconazole) Capsules, the adverse event profile was similar to that observed at recommended doses.

DOSAGE AND ADMINISTRATION

SPORANOX (itraconazole) Capsules should be taken with a full meal to ensure maximal absorption.

SPORANOX Capsules is a different preparation than SPORANOX Oral Solution and should not be used interchangeably.

Treatment of Blastomycosis and Histoplasmosis: The recommended dose is 200 mg once daily (2 capsules). If there is no obvious improvement, or there is evidence of progressive fungal disease, the dose should be increased in 100-mg increments to a maximum of 400 mg daily. Doses above 200 mg/day should be given in two divided doses.

Treatment of Aspergillosis: A daily dose of 200 to 400 mg is recommended.

Treatment in Life-Threatening Situations: In life-threatening situations, a loading dose should be used whether given as oral capsules or intravenously.

- IV Injection: the recommended intravenous dose is 200 mg b.i.d. for four consecutive doses, followed by 200 mg once daily thereafter. Each intravenous dose should be infused over 1 hour. The safety and efficacy of SPORANOX® Injection administered for greater than 14 days is not known. See complete prescribing information for SPORANOX® (itraconazole) Injection.
- Capsules: although clinical studies did not provide for a loading dose, it is recommended, based on pharmacokinetic data, that a loading dose of 200 mg (2 capsules) three times daily (600 mg/day) be given for the first 3 days of treatment.

Treatment should be continued for a minimum of three months and until clinical parameters and laboratory tests indicate that the active fungal infection has subsided. An inadequate period of treatment may lead to recurrence of active infection.

SPORANOX® Capsules and SPORANOX® Oral Solution should not be used interchangeably. Only the oral solution has been demonstrated effective for oral and/or esophageal candidiasis.

Treatment of Onychomycosis: Toenails with or without fingernail involvement: The recommended dose is 200 mg (2 capsules) once daily for 12 consecutive weeks.

Treatment of Onychomycosis: Fingernails only: The recommended dosing regimen is 2 treatment pulses, each consisting of 200 mg (2 capsules) b.i.d. (400 mg/day) for 1 week. The pulses are separated by a 3-week period without SPORANOX.®

HOW SUPPLIED

SPORANOX® (itraconazole) Capsules are [illegible] taining 100 mg of itraconazole, with a blue [illegible] pink transparent body, imprinted with "JAN[illegible] "SPORANOX 100." The capsules are supplied in blister packs of 3 × 10 capsules (NDC [illegible] bottles of 30 capsules (NDC 50458-290-04) PulsePak® containing 7 blister packs × [illegible] (NDC 50458-290-28).

Store at controlled room temperature 15°-25°C [illegible]

Protect from light and moisture.

Keep out of reach of children.

© Janssen 2001

U.S. Patent Nos. 4,267,179; 5,633,015

Distributed by:

JANSSEN PHARMACEUTICA PRODUCTS, LP

Titusville, New Jersey 08560, USA

Capsule contents manufactured by:

41544

JANSSEN PHARMACEUTICA N.V.

Beerse, Belgium

Shown in Product Identification Guide, page [illegible]

SPORANOX®

[spōr-a-nŏx]

(ITRACONAZOLE)

INJECTION

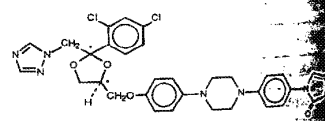
Congestive Heart Failure: When itraconazole [illegible] ministered intravenously to dogs and healthy volunteers, negative inotropic effects were seen [illegible] or symptoms of congestive heart failure occur during administration of SPORANOX® (itraconazole) [illegible] continued SPORANOX® use should be reassessed. CLINICAL PHARMACOLOGY: Special Populations, CONTRAINDICATIONS, WARNINGS, PRECAUTIONS: Drug Interactions and ADVERSE REACTIONS: Post-marketing Experience for information.)

Drug Interactions: Coadministration of cisapride, pimozide, quinidine, or dofetilide with SPORANOX® (itraconazole) Capsules, Injection or Oral Solution contraindicated. SPORANOX®, a potent cytochrome P450 3A4 isoenzyme system (CYP3A4) inhibitor, can increase plasma concentrations of drugs metabolized by this pathway. Serious cardiovascular events including QT prolongation, torsades de pointes, ventricular tachycardia, cardiac arrest, and/or sudden death have occurred in patients using cisapride, pimozide, quinidine, concomitantly with SPORANOX® and other CYP3A4 inhibitors. (See CONTRAINDICATIONS, WARNINGS, and PRECAUTIONS: Drug Interactions for more information.)

DESCRIPTION

For intravenous infusion (NOT FOR IV BOLUS INJECTION)

SPORANOX® is the brand name for itraconazole, a synthetic triazole antifungal agent. Itraconazole is a [illegible] chemic mixture of four diastereomers (two enantiomeric pairs), each possessing three chiral centers. It is represented by the following structural formula and nature:



(±)-1-[(R*)-sec-butyl]-4-[p-[4-[p-[[(2R*,4S*)-2-(2,4-dichlorophenyl)-2-(1H-1,2,4-triazol-1-ylmethyl)-1,3-dioxolan-4-yl]methoxy]phenyl]-Δ²-1,2,4-triazolin-5-one. [illegible] one mixture with (±)-1-[(R*)-sec-butyl]-4-[p-[4-[4-[4R*)-2-(2,4-dichlorophenyl)-2-(1H-1,2,4-triazol-1-ylmethyl)-1,3-dioxolan-4-yl]methoxy] phenyl]-1-piperazinyl]phenyl]-Δ²-1,2,4-triazolin-5-one.

or

(±)-1-[(RS)-sec-butyl]-4-[p-[4-[p-[[(2R,4S)-2-(2,4-dichlorophenyl)-2-(1H-1,2,4-triazol-1-ylmethyl)-1,3-dioxolan-4-yl]methoxy]phenyl]-1-piperazinyl]phenyl]-Δ²-1,2,4-triazolin-5-one.

Itraconazole has a molecular formula of $C_{35}H_{38}Cl_2N_8O_4$, a molecular weight of 705.64. It is a white to slightly yellowish powder. It is insoluble in water, very slightly soluble in alcohols, and freely soluble in dichloromethane. It has a pKa of 3.70 (based on extrapolation of values obtained in methanolic solutions) and a log (n-octanol/water) partition coefficient of 5.66 at pH 8.1.

SPORANOX® (itraconazole) Injection is a [illegible] free clear, colorless to slightly yellow solution for intravenous infusion. Each mL contains 10 mg of itraconazole solubilized by hydroxypropyl-β-cyclodextrin (400 mg) as molecular inclusion complex, with 3.8 µL hydrochloric acid, 20 µL propylene glycol, and sodium hydroxide for pH adjustment to 4.5, in water for injection. [illegible] Injection is packaged in 25 mL colorless glass vials containing 250 mg of itraconazole, contents of which

UM00012128
NOVARTIS EXHIBIT 1517
Novartis v. Regents, IPR2023-01347
Page 874 of 4460

This Page is Inserted by IFW Indexing and Scanning Operations and is not part of the Official Record

BEST AVAILABLE IMAGES

Defective images within this document are accurate representations of the original documents submitted by the applicant.

Defects in the images include but are not limited to the items checked:

- ☐ BLACK BORDERS
- ☐ IMAGE CUT OFF AT TOP, BOTTOM OR SIDES
- ☐ FADED TEXT OR DRAWING
- ☐ BLURRED OR ILLEGIBLE TEXT OR DRAWING
- ☐ SKEWED/SLANTED IMAGES
- ☐ COLOR OR BLACK AND WHITE PHOTOGRAPHS
- ☐ GRAY SCALE DOCUMENTS
- ☐ LINES OR MARKS ON ORIGINAL DOCUMENT
- ☐ REFERENCE(S) OR EXHIBIT(S) SUBMITTED ARE POOR QUALITY
- ☐ OTHER: _____

IMAGES ARE BEST AVAILABLE COPY.
As rescanning these documents will not correct the image problems checked, please do not report these problems to the IFW Image Problem Mailbox.

ELSEVIER

Journal of Chromatography B, 738 (2000) 93–98

JOURNAL OF CHROMATOGRAPHY B

www.elsevier.com/locate/chromb

High-performance liquid chromatographic analysis of the anti-fungal agent SCH 56592 in dog serum

Hong Kim[a,*], Paul Likhari[b], Pramila Kumari[a], Chin-Chung Lin[a], Amin A. Nomeir[a]

[a]*Department of Drug Metabolism and Pharmacokinetics, Schering-Plough Research Institute, 2015 Galloping Hill Road, Kenilworth, NJ 07033, USA*

[b]*Bioassay Laboratory, Houston, TX 77099, USA*

Received 15 June 1999; received in revised form 5 October 1999; accepted 27 October 1999

Abstract

SCH 56592 is a novel triazole antifungal agent that is active both orally and intravenously. This compound is in phase II–III clinical trials for the treatment of systemic fungal infections. A high-performance liquid chromatographic (HPLC) method was developed for the analysis of SCH 56592 in serum of dogs, a species used for safety evaluation. The HPLC analysis involved protein precipitation with methanol followed by separation on a C_{18} column and quantitation by UV absorbance at 262 nm. The method was sensitive with a limit of quantification of 0.05 μg/ml in dog serum. The linearity was satisfactory as indicated by correlations of >0.996, in addition to visual examination of the calibration curves. The precision and accuracy were satisfactory as indicated by coefficients of variation (C.V.) ranging from 2.0 to 3.8%, and bias values ranging from −6.5 to 10%. Moreover, SCH 56592 was stable in dog serum after being subjected to three freeze–thaw cycles. The assay was shown to be sensitive, specific, accurate, precise, and reliable for use in pharmacokinetic or toxicokinetic studies. © 2000 Elsevier Science B.V. All rights reserved.

Keywords: SCH 56592; Antifungal agent

1. Introduction

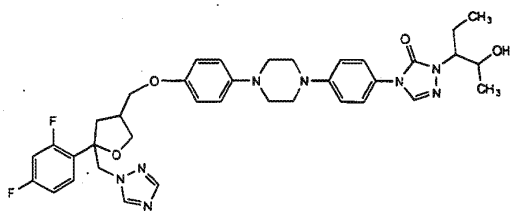
Fungal infections have substantially increased over the past two decades, and invasive forms are now an important cause of morbidity and mortality [1]. The rise in frequency of fungal infection has been due to an increasing number of immunosuppressed patients, for example individuals with hematological malignancies, organ and bone marrow transplants, and AIDS patients advancing to late-stage AIDS. Although amphotericin B is still used to treat these infections, a number of new systemic antifungal agents have been discovered during the past two decades. The azole antifungal agents are far less toxic than amphotericin B [1], and can usually be given by more than one route of administration.

SCH 56592, 4-[4-[4-[4-[[5-(2,4-difluorophenyl)-tetrahydro-5-(1H-1,2,4-triazol-1-ylmethyl)-3-furanyl]methoxy]phenyl-1-piperazinyl]phenyl]-2-(1-ethyl-2-hydroxypropyl]-2,4-dihydro-3H-1,2,4-triazol-3-one (Fig. 1), is a novel triazole antifungal agent that is active both orally and intravenously [2,3]. The in vitro and in vivo profiles of SCH 56592 in animal models showed significant advantages over existing agents in terms of potency and spectrum [3–5]. SCH 56592 was more active than itraconazole

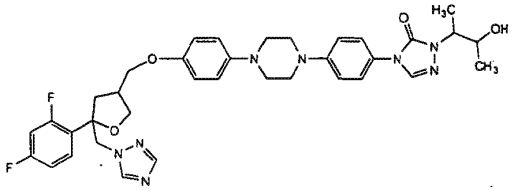
*Corresponding author.

0378-4347/00/$ – see front matter © 2000 Elsevier Science B.V. All rights reserved.
PII: S0378-4347(99)00489-2

UM00012130
NOVARTIS EXHIBIT 1517
Novartis v. Regents, IPR2023-01347
Page 876 of 4460



SCH 56592



SCH 56984 (Internal standard)

Fig. 1. Chemical structures of SCH 56592 and SCH 56984 (internal standard).

(ITZ) and fluconazole (FLZ) against all 283 strains tested and more active than amphotericin B (AMB) against 95% of these strains [3]. SCH 56592 was fungicidal against all strains of *C. krusei* that are resistant to FLZ [3]. SCH 56592 also was very active against other species including FLZ-resistant strains of *C. albicans*, *C. tropicalis*, some strains of *C. glabrata*, dermatophytes and many opportunistic fungi [5,6].

Results from several infection animal models have shown that SCH 56592 appears to be more potent (lower minimal inhibitory concentrations and minimal fungicidal concentrations) than FLZ and ITZ against *Candida albicans*, *Aspergillus flavus* and *A. fumigatus* [7,8]. SCH 56592 was also very active against vaginal infections in hamsters when given orally or topically, and against *T. mentagrophytes* infections in guinea pigs when given orally or topically [9].

SCH 56592 is a hydroxylated derivative of SCH 51048, the previous lead compound in this series [10]. In an effort to further improve the oral absorption properties of SCH 51048, synthesis of its novel analogs having polar side chains was undertaken. While introduction of relatively basic or acidic side chains resulted in loss of activity, incorporation of hydroxyl groups led to greatly improved in vivo activity [11]. SCH 56592 was the lead compound that emerged from these efforts.

HPLC methods with ultraviolet detection have been widely used to determine the plasma and serum concentrations of azole antifungal agents such as FLZ [12], ITZ [13], and miconazole [14]. We report here on the development and validation of sensitive, precise and accurate HPLC method for the analysis of SCH 56592 in dog serum. The method was used to evaluate the pharmacokinetics of this drug candidate in dogs

2. Experimental

2.1. Reagents

Methanol, acetonitrile, methylene chloride, diethyl amine and ammonium phosphate monobasic were purchased from Fisher Scientific (Fair Lawn, NJ, USA). SCH 56592 and SCH 56984 (internal standard) were provided by the Chemical Research Division, Schering-Plough Research Institute (Kenilworth, NJ, USA).

2.2. Calibration standard and sample preparation

A stock solution of SCH 56592 was prepared in methanol at 200 μg/ml; the internal standard was prepared in methanol at 0.4 μg/ml. The stock solutions were stored at −20°C. Eight calibration standards (at 0.05, 0.1, 0.5, 1, 2, 4, 8, and 20 μg/ml) were prepared in triplicate on each of the three validation days. Three sets of quality control samples (QC samples) at concentrations of 0.1 (low), 1.5 (medium) and 15 μg/ml (high) were prepared in bulk from separate weighings, aliquoted and stored at −20°C for use during the entire validation and sample analysis. A 0.6-ml volume of the internal standard solution in methanol was added to 0.2 ml of dog serum, vortexed for 30 s at high speed and centrifuged at 4500 *g* at room temperature for 5 min. A 0.05-ml sample of the supernatant was injected onto the HPLC column for SCH 56592 analysis.

2.3. Chromatographic conditions

The HPLC system consisted of a Shimadzu LC-9A pump and a Waters 486 absorbance detector set

UM00012131
NOVARTIS EXHIBIT 1517
Novartis v. Regents, IPR2023-01347
Page 877 of 4460

at 262 nm. The separation was accomplished on a 5-μm Ultrasphere ODS, 150×4.6 mm column which was preceded by an on-line filter. The Millennium 2020 Chromatography Manager Software System was used for data handling. The mobile phase consisted of 0.09 *M* ammonium phosphate monobasic acetonitrile–triethylamine (530:470:0.5, v/v/v), and was delivered at 1 ml/min.

2.4. Administration of SCH 56592

Six male beagle dogs were dosed orally with a 200-mg experimental tablet of SCH 56592 (approximately 15 mg/kg) for pharmacokinetic evaluation. Blood samples were collected at intervals after dosing, centrifuged and serum stored at −20°C pending analysis.

2.5. Pharmacokinetic analysis

Serum concentrations equal to or above the lower limit of quantitation (LOQ, 0.05 μg/ml) were used for pharmacokinetic analysis using model-independent methods [15]. The maximum serum concentration (C_{max}) and time of maximum serum concentration (T_{max}) were the observed values. The area under the serum concentration–time curve from time zero to the time of the final measurable sample [AUC(tf)] was calculated using the linear trapezoidal method.

3. Results and discussion

Initially, the UV spectrum of SCH 56592 was determined which showed a maximum absorbance (λ_{max}) at 262 nm. Therefore, the analysis were carried out at 262 nm. The HPLC analysis by UV absorbance showed that the limit of quantitation (LOQ) was 0.05 μg/ml of serum, which provided adequate sensitivity to conduct pharmacokinetic studies in animals. Typical chromatograms of drug-free dog serum and serum spiked with SCH 56592 and the internal standard (SCH 56984) are illustrated in Fig. 2. The retention times of the internal standard and SCH 56592 were approximately 6.7 and 8.7 min, respectively. There were no endogenous peaks in serum of six undosed dogs that coeluted with SCH

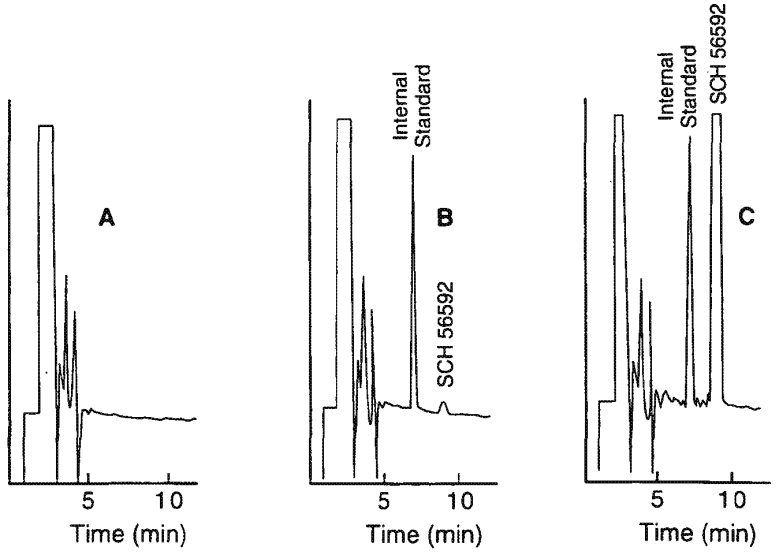


Fig. 2. Typical chromatograms of blank dog serum (A) and blank dog serum spiked with both SCH 56592 at the LOQ (B) or at 20 μg/ml (C) and the internal standard.

UM00012132
NOVARTIS EXHIBIT 1517
Novartis v. Regents, IPR2023-01347
Page 878 of 4460

56592 or the internal standard, indicating that the method was selective. The linearity was evaluated over a concentration range of 0.05–20 μg/ml. Linear regression parameters of the peak height ratios versus concentrations along with back-calculated concentrations of nine calibration curves are presented in Table 1. The results showed highly reproducible calibration curves with correlation coefficients of >0.99, indicating that the response was linear over the concentration range studied. Intra-day precision and accuracy were evaluated at SCH 56592 concentrations of 0.1, 1.5 and 15 μg/ml. Five samples were analyzed at each concentration on the same day. The results showed satisfactory intra-day precision and accuracy as indicated by coefficients of variation (C.V.) of ≤4.0% and bias of ≤6.3% (Table 2). Inter-day precision and accuracy were evaluated at the same concentrations as above and the samples were analyzed on three separate days. The results demonstrated satisfactory inter-day precision and accuracy as shown by C.V. and bias values of ≤5.0% and ≤5.3%, respectively (Table 3). The LOQ, defined as the lowest concentration in the calibration curve that could be determined with acceptable precision and accuracy, was 0.05 μg/ml. At this concentration, the precision and accuracy from back-calculated concentrations were satisfactory (C.V.= 2.1%, bias=6.0%; Table 1). The recovery was consistent over a concentration range of 0.1–15 μg/ml (>73%; Table 4). The recovery of the internal

Table 2
Intra-day precision and accuracy for the analysis of SCH 56592 in dog serum

Nominal concentration (μg/ml)	Concentration found (mean) (μg/ml)[a]	Precision (% C.V.)	Accuracy (% bias)
0.1	0.10	4.0	0.0
1.5	1.48	2.0	−1.3
15.0	14.1	1.7	−6.3

[a] $n=5$.

Table 3
Inter-day and accuracy for the analysis of SCH 56592 in dog serum

Nominal concentration (μg/ml)	Concentration found (mean) (μg/ml)[a]	Precision (% C.V.)	Accuracy (% bias)
0.1	0.10	5.0	0.0
1.5	1.47	2.5	−2.0
15.0	14.2	3.7	−5.3

[a] $n=5$.

Table 1
Back-calculated concentrations and calibration curve parameters for the analysis of SCH 56592 in dog serum

	Nominal concentration								Slope	Intercept	Correlation coefficient (r)
	0.05	0.1	0.5	1	2	4	8	20			
	Concentration found (μg/ml)										
Day 1	0.046	0.11	0.55	1.04	2.10	3.89	7.61	18.30	0.745371	0.011543	0.9967
	0.046	0.11	0.55	1.07	2.02	4.03	7.50	18.30	0.745297	0.014585	0.9969
	0.046	0.11	0.55	1.04	2.05	4.11	7.54	18.00	0.743520	0.015915	0.9964
Day 2	0.048	0.11	0.52	0.95	1.98	4.27	7.97	19.30	0.710598	0.010672	0.9989
	0.048	0.10	0.54	0.96	2.00	4.02	7.81	19.50	0.708858	0.009744	0.9991
	0.048	0.11	0.52	1.01	1.98	4.15	7.83	18.90	0.718699	0.008615	0.999
Day 3	0.048	0.11	0.54	1.02	1.97	4.13	7.78	18.70	0.776689	0.009909	0.9985
	0.048	0.11	0.54	1.00	2.00	4.15	7.80	18.50	0.757875	0.012770	0.9984
	0.047	0.11	0.56	1.00	1.99	4.16	7.72	18.40	0.745573	0.012760	0.9977
Mean	0.047	0.11	0.54	1.01	2.01	4.10	7.73	18.70	0.739164	0.011835	0.998
Precision (%C.V.)	2.1	2.7	2.6	3.8	2.1	2.6	2.0	2.6	–[a]	–	–
Accuracy (% bias)	−6.0	10.0	8.0	1.0	0.5	2.5	−3.4	−6.5	–	–	–

[a] Not appropriate to calculate these parameters.

UM00012133
NOVARTIS EXHIBIT 1517
Novartis v. Regents, IPR2023-01347
Page 879 of 4460

Table 4
Recovery of SCH 56592 and internal standard from dog serum

Concentration (μg/ml)	Mean % recovery[a]
0.1	76.6
1.5	74.5
15.0	73.2
Internal standard, 0.4 μg/ml	73.3

[a] $n=3$.

standard at the concentration used (0.4 μg/ml) was 73.3%.

In the method development phase, we have attempted to use acetonitrile to precipitate serum protein. The chromatogram showed that the SCH 56592 peak was asymmetric (tailing). Also, the assay was developed using 0.2 ml serum, three volumes of methanol were added to give a total volume of the extracted supernatant of approximately 0.7 ml, of which only 0.05 ml was injected. Therefore, the sample volume may be reduced to 0.05 ml serum which would result in approximately 0.15 ml volume of the supernatant, sufficient for two injections in HPLC. Consequently, if the sample volume is a limitation, the analysis can be performed with only 0.05 ml without any loss of sensitivity. However, we used 0.2 ml volume for convenience.

The stability of SCH 56592 in serum was evaluated through three freeze–thaw cycles at concentrations of 0.1, 1.5 and 15 μg/ml. The samples were thawed in a water bath at room temperature and frozen within 5 min of thawing in each cycle. After three cycles, the changes from nominal concentrations were −10.0, −1.3 and −6.0% for the 0.1, 1.5 and 15 μg/ml, respectively, demonstrating that SCH 56592 was stable in serum through three freeze–thaw cycles (Table 5). Long-term stability was determined following 348 days of storage at −20°C at the concentrations above. The changes from the nominal concentrations ranged from 6 to 12% indicating that SCH 56592 was stable in serum for at least 348 days (Table 6). In-process stability was performed for up to 48 h after sample processing. Three sets of processed serum samples at the above SCH 56592 concentrations were analyzed after storage at room temperature for 48 h. The changes from nominal concentrations were 0.0, 0.0 and −2.7% for the 0.1, 1.5 and 15 μg/ml concentrations, respectively, demonstrating that SCH 56592 was stable under the conditions evaluated.

Table 5
Three-cycle freeze–thaw stability of SCH 56592 in dog serum

Freeze–thaw cycle	Parameter	Observed concentration (μg/ml)[a]		
		0.1[b]	1.5[b]	15[b]
First	Mean	0.11	1.56	14.8
	% C.V.	6	4	1
	% Change	10	4	−1.3
Second	Mean	0.11	1.57	15.3
	% C.V.	11	4	4
	% Change	10	4.7	2
Third	Mean	0.09	1.48	14.1
	% C.V.	16	5	3
	% Change	−10	−1.3	−6

[a] $n=3$.
[b] Nominal concentration.

The analytical method was used to characterize the pharmacokinetic profile of SCH 56592 in the dog following oral administration of a 200-mg experimental tablet of SCH 56592. SCH 56592 was quantifiable in serum between 2 and 72 h after oral administration (Fig. 3). The mean C_{max} of SCH 56592 was 1.5 μg/ml which was attained at a mean T_{max} of 24 h. The area under the serum concentration–time curve ($AUC_{0-72\ h}$) was 60.4 μg.h/ml (Table 7).

In conclusion, an HPLC assay for the determination of SCH 56592 in dog serum was developed and was shown to be accurate and reliable over a concentration range of 0.05–20 μg/ml with an average C.V. of 2.6% and an average bias of 4.7%. The method was used to determine serum concen-

Table 6
Stability of SCH 56592 in dog serum following storage at −20°C for 348 days

Nominal concentration (μg/ml)	Observed concentration (μg/ml)[a]		
	Mean	% C.V.	% Change
0.1	0.11	11.0	10.0
1.5	1.41	3.0	−6.0
15.0	13.2	0.5	−12.0

[a] $n=6$ for each concentration.

UM00012134
NOVARTIS EXHIBIT 1517
Novartis v. Regents, IPR2023-01347
Page 880 of 4460

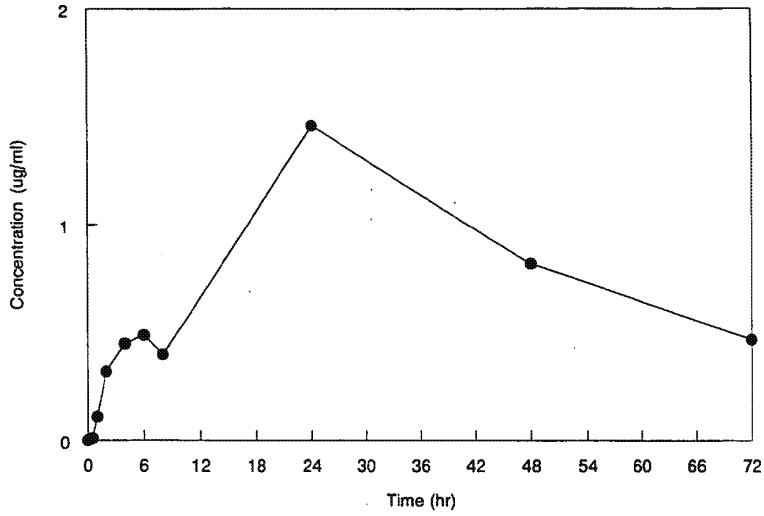


Fig. 3. Mean (n=6) serum concentration–time profile of SCH 56592 in dogs after 200-mg oral dose.

Table 7
Mean pharmacokinetic parameter of SCH 56592 in beagle dogs following oral administration of a 200-mg tablet

Parameter (unit)	Mean (n=6)	% C.V.
C_{max} (μg/ml)	1.5	48
T_{max} (h)	24	0
AUC (0–72 h) (μg/h/ml)	60.4	49

trations of SCH 56592 in the dog following oral administration of a 200-mg tablet.

References

[1] D. Armstrong, Rev. Inf. Dis. 11 (1989) 1591–1609.
[2] A.M. Sugar, X.P. Liu, Antimicrob. Agents Chemother. 20 (1996) 1314–1316.
[3] M.A. Pfaller, S. Messer, R.N. Jones, Antimicrob. Agents Chemother. 41 (1997) 233–235.
[4] J.R. Graybill, R. Bocanegra, L.K. Najvar, D. Lobenberg, M.F. Luther, Antimicrob. Agents Chemother. 42 (1998) 2467–2473.
[5] J.N. Galgiani, M.L. Lewis, Antimicrob. Agents Chemother. 41 (1997) 180–183.
[6] R. Parmegiani, A. Cacciapuoti, D. Loebenberg, B. Antonacci, C. Norris, T. Yorsh-Tomaine, M. Michalski, R.S. Hare, G. Miller, Program abstract of the 35th Interscience Conference on Antimicrobial Agents, Chermother. Abstr. F62 (1995) 123.
[7] J.R. Graybill, L.K. Najvar, R. Bocanegra, M.F. Luther, Program abstract of the 36th Interscience Conference on Antimicrobial Agents, Chermother. Abstr. F99 (1996) 116.
[8] A. Cacciapuoti, R. Parmegiani, D. Loebenberg, B. Antonacci, E.L. Moss, F. Menzel, C. Norris, R.S. Hare, G. Miller, Program abstract of the 35th Interscience Conference on Antimicrobial Agents, Chermother. Abstr. F66 (1995) 124.
[9] R. Parmegiani, A. Cacciapuoti, D. Loebenberg, B. Antonacci, C. Norris, T. Yorsh-Tomaine, M. Michalski, R.S. Hare, G. Miller, Program abstract of the 35th Interscience Conference on Antimicrobial Agents, Chermother. Abstr. F67 (1995) 124.
[10] A.M. Sugar, M. Picard, Antimicrob. Agents Chemother. 39 (1995) 996–997.
[11] A.K. Saksena, V.M. Girijavallabhan, R.G. Lovey et al., Program abstract of the 35th Interscience Conference on Antimicrobial Agents, Chermother. Abstr. F83 (1995) 127.
[12] M. Cociglio, S. Brandissou, R. Alric, F. Bressolle, J. Chromatogr. B 686 (1996) 11–17.
[13] D. Compas, D.J. Touw, P.N.F.C. de Goede, J. Chromatogr. B 687 (1996) 453–456.
[14] M. Kobylinska, K. Kobylinska, B. Sobik, J. Chromatogr. B 685 (1996) 191–195.
[15] M. Gilbaldi, D. Perrier, in: Pharmacokinetics, 2nd Edition, Marcel Dekker, New York, 1982, pp. 409–417.

UM00012135
NOVARTIS EXHIBIT 1517
Novartis v. Regents, IPR2023-01347
Page 881 of 4460

ELSEVIER

Advanced Drug Delivery Reviews 48 (2001) 3–26

Advanced DRUG DELIVERY Reviews

www.elsevier.com/locate/drugdeliv

Crystalline solids

Sudha R. Vippagunta[a], Harry G. Brittain[b], David J.W. Grant[a,*]

[a]*Department of Pharmaceutics, College of Pharmacy, University of Minnesota, Weaver–Densford Hall, 308 Harvard Street S.E., Minneapolis, MN 55455, USA*

[b]*Center for Pharmaceutical Physics, 10 Charles Road, Milford, NJ 08848, USA*

Received 18 October 2000; accepted 21 December 2000

Abstract

Many drugs exist in the crystalline solid state due to reasons of stability and ease of handling during the various stages of drug development. Crystalline solids can exist in the form of polymorphs, solvates or hydrates. Phase transitions such as polymorph interconversion, desolvation of solvate, formation of hydrate and conversion of crystalline to amorphous form may occur during various pharmaceutical processes, which may alter the dissolution rate and transport characteristics of the drug. Hence it is desirable to choose the most suitable and stable form of the drug in the initial stages of drug development. The current focus of research in the solid-state area is to understand the origins of polymorphism at the molecular level, and to predict and prepare the most stable polymorph of a drug. The recent advances in computational tools allow the prediction of possible polymorphs of the drug from its molecular structure. Sensitive analytical methods are being developed to understand the nature of polymorphism and to characterize the various crystalline forms of a drug in its dosage form. The aim of this review is to emphasize the recent advances made in the area of prediction and characterization of polymorphs and solvates, to address the current challenges faced by pharmaceutical scientists and to anticipate future developments.
© 2001 Elsevier Science B.V. All rights reserved.

Keywords: Crystallinity; Polymorphs; Hydrates; Solvates; Formulation; Drug substance; Phase transformation; Characterization

Contents

1. Introduction 4
2. Recent advances in the identification, prediction and characterization of polymorphs 6
   2.1. Types of polymorphism 6
   2.2. Packing polymorphism 7
   2.3. Conformational polymorphism 8
   2.4. Phase transformations in the solid state 9
   2.5. Prediction of polymorphs 11
   2.6. Directing the crystallization of specific polymorphs 12
   2.7. Characterization of polymorphs using a combination of analytical techniques 13
3. Recent advances in the identification and characterization of hydrates and solvates 15
   3.1. Introduction to solvates and hydrates 15
   3.2. Structural aspects 15

*Corresponding author. Tel.: + 1-612-6243-956; fax: + 1-612-6250-609.
E-mail address: grant001@tc.umn.edu (D.J.W. Grant).

0169-409X/01/$ – see front matter © 2001 Elsevier Science B.V. All rights reserved.
PII: S0169-409X(01)00097-7

3.3. Phase transformation of hydrates and solvates 17
3.4. Prediction of the formation of hydrates and solvates 18
3.5. Characterization of hydrates and solvates 18
4. Current challenges and future directions 18
4.1. Origins of the challenges 18
4.2. Phase transformations during processing 19
4.3. Degree of crystallinity 21
4.4. Characterization of mixtures of polymorphs 21
5. Conclusions 23
References 24

1. Introduction

Most organic and inorganic compounds of pharmaceutical relevance can exist in one or more crystalline forms. When applied to solids, the adjective, *crystalline,* implies an ideal crystal in which the structural units, termed *unit cells,* are repeated regularly and indefinitely in three dimensions in space. The unit cell has a definite orientation and shape defined by the translational vectors, a, b, and c, and hence has a definite volume, V, that contains the atoms and molecules necessary for generating the crystal. Each crystal can be classified as a member of one of seven possible crystal systems or crystal classes that are defined by the relationships between the individual dimensions, a, b, and c, of the unit cell and between the individual angles, α, β, and γ of the unit cell [1,2]. The structure of a given crystal may be assigned to one of the seven crystal systems, to one of the 14 Bravais lattices, and to one of the 230 space groups [1]. All the 230 possible space groups, their symmetries, and the symmetries of their diffraction patterns are compiled in the International Tables for Crystallography [3].

The common crystalline forms found for a given drug substance are polymorphs and solvates. Crystalline polymorphs have the same chemical composition but different internal crystal structures and, therefore, possess different physico–chemical properties. The different crystal structures in polymorphs arise when the drug substance crystallizes in different crystal packing arrangements and/or different conformations. The occurrence of polymorphism is quite common among organic molecules, and a large number of polymorphic drug compounds have been noted and catalogued [4–7].

Solvates, also known as pseudopolymorphs, are crystalline solid adducts containing solvent molecules within the crystal structure, in either stoichiometric or nonstoichiometric proportions, giving rise to unique differences in the physical and pharmaceutical properties of the drug. If the incorporated solvent is water, a solvate is termed a hydrate. Adducts frequently crystallize more easily because two molecules often can pack together with less difficulty than single molecules. While no definite explanations can be given, possible reasons include adduct symmetry, adduct-induced conformation changes, and the ability to form hydrogen bonds through the solvent molecules [2,8,9]. Desolvated solvates are produced when a solvate is desolvated and the crystal retains the structure of the solvate [10]. Desolvated solvates are less ordered than their crystalline counterparts and are difficult to characterize, because analytical studies indicate that they are unsolvated materials (or anhydrous crystal forms) when, in fact, they have the structure of the solvated crystal form from which they were derived [11].

Because different crystalline polymorphs and solvates differ in crystal packing, and/or molecular conformation as well as in lattice energy and entropy, there are usually significant differences in their physical properties, such as density, hardness, tabletability, refractive index, melting point, enthalpy of fusion, vapor pressure, solubility, dissolution rate, other thermodynamic and kinetic properties and even color [12]. Differences in physical properties of various solid forms have an important effect on the processing of drug substances into drug products [13], while differences in solubility may have implications on the absorption of the active drug from its dosage form [14], by affecting the dissolution rate and possibly the mass transport of the molecules. These concerns have led to an increased regulatory

UM00012137
NOVARTIS EXHIBIT 1517
Novartis v. Regents, IPR2023-01347
Page 883 of 4460

interest in understanding the solid-state properties and behavior of drug substances. For approval of a new drug, the drug substance guideline of the US Food and Drug Administration (FDA) states that "appropriate" analytical procedures need to be used to detect polymorphs, hydrates and amorphous forms of the drug substance and also stresses the importance of controlling the crystal form of the drug substance during the various stages of product development [11]. It is very important to control the crystal form of the drug during the various stages of drug development, because any phase change due to polymorph interconversions, desolvation of solvates, formation of hydrates and change in the degree of crystallinity can alter the bioavailability of the drug. When going through a phase transition, a solid drug may undergo a change in its thermodynamic properties, with consequent changes in its dissolution and transport characteristics [15].

Various pharmaceutical processes during drug development significantly influence the final crystalline form of the drug in the dosage form. The various effects of pharmaceutical processing on drug polymorphs, solvates and phase transitions have been described in detail by Brittain and Fiese [16] and will be discussed in later chapters. Briefly, processes such as lyophilization and spray drying may lead to the formation of the amorphous form of drug, which tends to be less stable and more hygroscopic than the crystalline product. Also, processing stresses, such as drying, grinding, milling, wet granulation, oven drying and compaction, are reported to accelerate the phase transitions in pharmaceutical solids. The degree of polymorphic conversion will depend on the relative stability of the phases in question, and on the type and degree of mechanical processing applied. Keeping these factors in mind, it is desirable and usual to choose the most stable polymorphic form of the drug in the beginning and to control the crystal form and the distributions in size and shape of the drug crystals during the entire process of development. The presence of a metastable form during processing or in the final dosage form often leads to instability of drug release as a result of phase transformation [17].

Crystallization plays a critical role in controlling the crystalline form and the distribution in size and shape of the drug. The significance of crystallization mechanisms and kinetics in directing crystallization pathways of pharmaceutical solids and the factors affecting the formation of crystals have been reviewed in detail by various researchers [12,18,19]. A crystalline phase is created as a consequence of molecular aggregation processes in solution that lead to the formation of nuclei, which achieve a certain size during the nucleation phase to enable growth into macroscopic crystals to take place during the growth phase. The factors affecting the rate and mechanisms by which crystals are formed are: solubility, supersaturation, rate at which supersaturation and desupersaturation occur, diffusivity, temperature, and the reactivity of surfaces towards nucleation. The various forces responsible for holding the organic crystalline solids together, such as nonbonded interactions and hydrogen bonding, have been discussed in detail by Byrn et al. [2] and Etter [20].

Various analytical methods are being currently used to characterize the crystalline form of the drug during the various steps of processing and development. These methods have been reviewed recently in detail by many authors [7,10,21–25]. The single most valuable piece of information about the crystalline solid, including the existence of polymorphs and solvates, is the molecular and crystalline structure, which is determined by single-crystal X-ray diffractometry [2]. Powder X-ray diffractometry provides a "fingerprint" of the solid phase and may sometimes be used to determine crystal structure. Once the existence of polymorphism (or solvate formation) is definitely established by single-crystal and powder X-ray diffractometry, spectral methods, such as Fourier transform infrared absorption (FTIR) spectroscopy, Fourier transform Raman scattering (FT Raman) spectroscopy, solid-state nuclear magnetic resonance (SSNMR) spectroscopy, ultraviolet and visible (UV–Vis) and/or fluorescence spectroscopy [23] may be employed for further characterization. Of special significance are thermal methods, such as differential scanning calorimetry (DSC), thermogravimetric analysis (TGA) and optical microscopy using a hot stage [24]. These methods are almost always employed for further characterization. Modulated (temperature) differential scanning calorimetry (MDSC) in combination with DSC and optical microscopy are able to identify the glass

UM00012138
NOVARTIS EXHIBIT 1517
Novartis v. Regents, IPR2023-01347
Page 884 of 4460

transition of amorphous forms with much greater clarity and allow unique insights into the glass transitional and polymorphic behavior of drug substances [26].

Because solid-state NMR spectroscopy can be used to study crystalline solids, as well as pharmaceutical dosage forms, this powerful method is finding increasing application in deducing the nature of polymorphic variations [27], such as variations in hydrogen bonding network and molecular conformations among polymorphs [28,29] and for the determination of molecular conformations and mobility of drugs in mixtures and dosage forms [2]. Solid-state ^{13}C-NMR in conjunction with the techniques, known as high power proton decoupling, cross polarization (CP), and magic-angle spinning (MAS) offers information not obtained readily by other techniques. Recently, two-dimensional ^{13}C-solid-state NMR spectroscopy has been used to study the three conformational polymorphs of 5-methyl-2-[(2-nitrophenyl)amino]-3-thiophenecarbonitrile [30]. Use of two-dimensional NMR and total suppression of spinning side bands (TOSS) pulse sequences allowed the separation of isotropic and anisotropic chemical shifts for the three forms. This is a very powerful method for analyzing differences in the chemical environment and is finding increased application in the study of conformational polymorphism.

With advances in analytical methods, the current focus of research in the solid-state area is to understand polymorphism and pseudopolymorphism at the molecular level. Knowledge of the crystal packing arrangements and the various intermolecular forces involved in the different packing arrangements will help in the prediction and preparation of the most stable polymorphs of a given compound well in advance, to avoid surprises during product development. A current emphasis is on the development of software to predict crystal structures of polymorphs from molecular structures. A thorough understanding of the physicochemical properties of polymorphs and solvates (hydrates) is of primary importance to the selection of a suitable crystalline form and development of a successful pharmaceutical product. Bray et al. [31] have shown that, by thorough characterization of four different crystalline forms of L-738,167, a fibrinogen receptor antagonist by various analytical techniques, it was possible to determine the suitability of one or two forms for the development of pharmaceutical oral dosage forms.

The present review aims to emphasize the recent advances made in the area of prediction and characterization of polymorphs and solvates, attempts to address the current challenges and problems faced by pharmaceutical scientists and intends to anticipate future development. This review does not attempt to provide solutions to the problems but attempts to review comprehensively the advances made in recent years to help address these problems.

2. Recent advances in the identification, prediction and characterization of polymorphs

2.1. Types of polymorphism

Based on differences in the thermodynamic properties, polymorphs are classified as either enantiotropes or monotropes, depending upon whether one form can transform reversibly to another or not. In an enantiotropic system, a reversible transition between polymorphs is possible at a definite transition temperature below the melting point. In a monotropic system, no reversible transition is observed between the polymorphs below the melting point. Four useful rules have been developed by Burger and Ramburger [32,33] to determine qualitatively the enantiotropic or monotropic nature of the relationship between polymorphs. These rules are the heat of transition rule, heat of fusion rule, infrared rule and density rule.

If, by use of the above rules, it is established that the polymorphs of a particular drug are enantiotropic or monotropic, then the next goal is to define the thermodynamically stable (or metastable) domain of each crystalline phase of a substance as a function of temperature. The plot of the Gibbs free energy difference, ΔG, against the absolute temperature, T, gives the most complete and quantitative information on the stability relationship of polymorphs [22], with the most stable polymorph having the lowest Gibbs free energy. The ΔG between the polymorphs may be obtained using several techniques operating at

UM00012139
NOVARTIS EXHIBIT 1517
Novartis v. Regents, IPR2023-01347
Page 885 of 4460

different temperatures, such as solubility [34] and intrinsic dissolution rate. Yu [35] has derived thermodynamic equations to calculate ΔG between two polymorphs and its temperature slope from the melting data. This method is essentially an extension of the heat of fusion rule, which is based on statistical mechanics. Extrapolating ΔG to zero gives an estimate of the transition temperature, from which the existence of monotropy or enantiotropy is inferred. The integration of different types of data provides the ΔG vs. T curve over a wide temperature range and allows the consistency between techniques to be checked [22]. Another approach to establish the order of stability among various polymorphs has been studied using pressure versus temperature plots, e.g., for sulfanilamide and piracetam [36]. This approach is based upon Ostwald's principle of least vapor pressure, according to which the stable polymorph exhibits the lowest vapor pressure. The accuracy of this approach to establish the stability hierarchy among the polymorphs has been shown to be very much dependent on the accuracy of the experimental data.

In recent years, the main focus of research has been the characterization of polymorphs arising from structural differences in the crystal lattice. It has been established for some time that organic molecules are capable of forming different crystal lattices through two different mechanisms. One of the mechanisms is termed *packing polymorphism*, and represents instances where conformationally relatively rigid molecules can be assembled into different three-dimensional structures through the invocation of different intermolecular mechanisms. The other mechanism is termed *conformational polymorphism* and arises when a nonconformationally rigid molecule can be folded into different arrangements, which subsequently can be packed into alternative crystal structures. The distinction between *packing polymorphism* and *conformational polymorphism* is somewhat artificial because different packing arrangements impose different conformations on the molecules, however slight, and different conformations will inevitably pack differently. The structural aspects associated with polymorphs have been reviewed recently [2], as have the analogous features of solvate and hydrate systems [9]. In the next section, the results of some more recent investigations are discussed.

2.2. Packing polymorphism

An investigation into the structures and charge densities of two polymorphs of *p*-nitrophenol has been performed with the aim of deducing the different modes of inter-molecular hydrogen bonding that lead to the formation of the two structures shown in Fig. 1a and b [37]. A detailed analysis of the charge density of the two forms indicates charge migration from the benzene ring region to the nitro and hydroxyl groups that accompanies the transformation of one form into the other. In addition, polarization of the oxygen lone-pair electrons was found to be substantially larger in the crystal forms than in the free molecule, resulting in considerably larger dipole moments in the solid state.

During the study of a new crystal form (form I) of

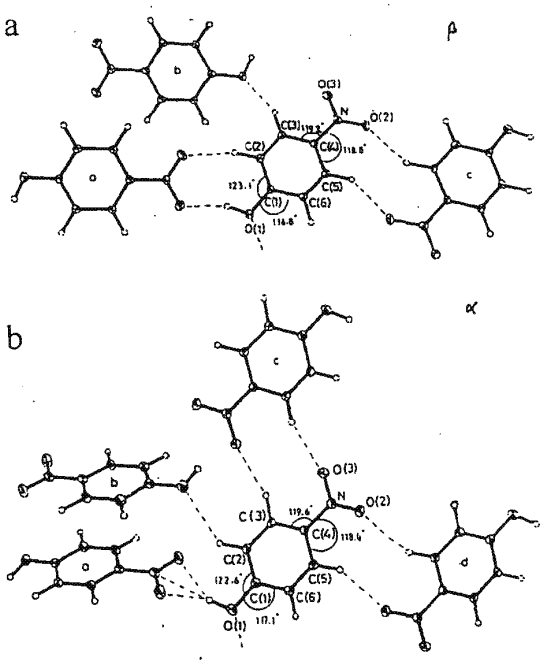


Fig. 1. Molecular packing diagrams of the (a) β polymorph of *p*-nitrophenol, (b) α polymorph of *p*-nitrophenol, showing 50% probability displacement ellipsoids ([37], reproduced with the permission of the American Chemical Society).

UM00012140
NOVARTIS EXHIBIT 1517
Novartis v. Regents, IPR2023-01347
Page 886 of 4460

chlordiazepoxide, it was found that the heat of transition between the two forms (forms I and II) is rather modest, and kinetic factors permit the existence of the metastable phase [38]. Both structures contain four crystallographically independent molecules linked in dimers through hydrogen bonding, but the dimers are packed differently to yield the two crystal forms. Because the dimers in the fundamental units are spaced differently in the two forms, it was proposed that the solid-state enantiotropic transformation entailed rearrangement of the dimer units.

A different approach has been taken during an evaluation of the different structures formed by sulfathiazole [39]. Using a graph set approach to classify the known structural differences and similarities among the various forms, it became possible to identify packing motifs common to three of the four crystal structures. Fig. 2 shows the unit cells of the polymorphs I, II, III and IV, where molecules are paired as hydrogen-bonded dimers. At the end of the process, the authors were able to deduce possible links between the observed patterns of hydrogen bonding, processes of nucleation, and the crystal growth observed from a number of solvent systems. Interestingly, the analysis did not indicate a relationship between the appearance of a particular polymorph from solution and the growth of its fastest growing surface. Rather, it appeared as if the different solvents affected the process of polymorph formation through their effects on nucleation of the various forms.

2.3. Conformational polymorphism

The conformational polymorphism of the two forms of piroxicam pivalate has been studied in detail [40]. This compound is distinctive in that the high-melting form (polymorph 1) contains an unanticipated array of associated molecules bound as centrosymmetric dimers through hydrogen bonding, with the amido nitrogen atom acting as the donor and the pyridine nitrogen as the acceptor (Scheme 1, structure I). The low-melting form (polymorph 2) contains molecules of two distinct conformational states coexisting in the same crystal (Fig. 3), but linked through different hydrogen bonding arrangements. This latter finding represents another unusual aspect of the crystallography of the substance.

The inclusion of different solvent molecules in a crystal lattice can lead to the existence of different packing patterns, and has also been found to influence the molecular conformation of paroxetine hydrochloride in two solvate forms [41]. One form

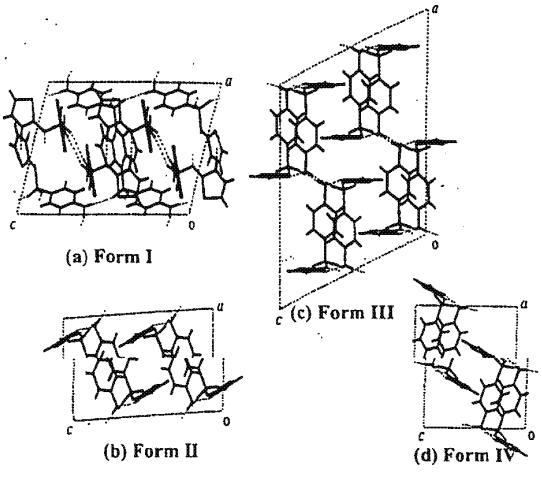
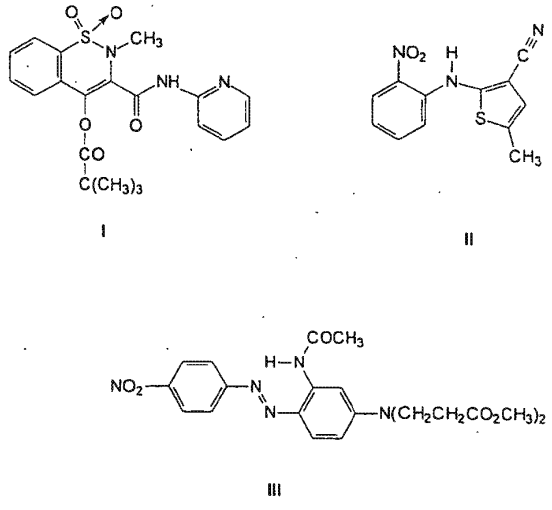


Fig. 2. Unit cells of four polymorphs (I, II, III and IV) of sulfathiazole showing hydrogen bonds, with the dimer structure clearly discernible ([39], reproduced with the permission of the Royal Society of Chemistry).



Scheme 1. Molecular structure of piroxicam pivalate (I) [40], 5-methyl-2-[2-(nitrophenyl)amino]-3-thiophenecarbonitrile (II) [30], 2′-acetamido-4′-[*N*,*N*-bis(2-methylcarbonylethyl)amino]-4-nitroazobenzene (III) [48].

UM00012141
NOVARTIS EXHIBIT 1517
Novartis v. Regents, IPR2023-01347
Page 887 of 4460

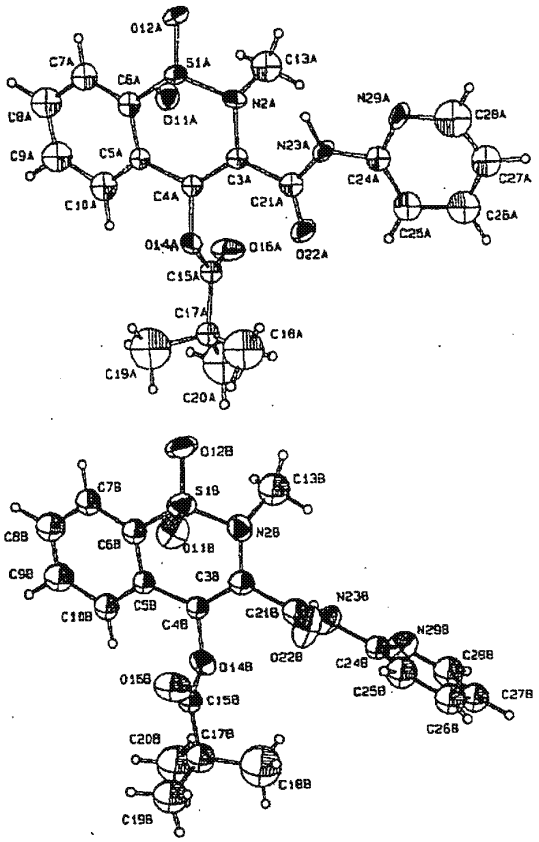


Fig. 3. Conformations of the two independent molecules of piroxicam pivalate (I) in polymorph 2. Thermal ellipsoids are drawn at the 40% probability level, and H atoms are shown as spheres of arbitrary size ([40], reproduced with the permission of the American Pharmaceutical Association).

was obtained as a hemihydrate, and the other as the solvate of isopropanol (2-propanol). In the unit cell of the hemihydrate, one finds two protonated paroxetine and two chloride ions together with one water molecule. Interestingly, the two paroxetine molecules are conformationally nonequivalent, and exhibit a number of different bond angles and torsion angles. In the other form, the unit cell contains one protonated paroxetine molecule, one chloride ion, and one isopropanol molecule disordered along a molecular channel. Furthermore, the conformation of the paroxetine molecule in the isopropanol solvate is different from either molecular conformation observed in the hemihydrate phase. Crystals of the isopropanol solvate decomposes in the open air at room temperature, because the isopropanol molecules are released easily through the channel. The hemihydrate is relatively stable.

In an impressive fundamental study, the polymorphism of 5-methyl-2-[2-(nitrophenyl)amino]-3-thiophenecarbonitrile (Scheme 1, structure II) has been catalogued [42,43] and discussed in detail [2]. This compound was crystallized as six solvent-free polymorphs, each of which differed in the mode of packing and in molecular conformation. The different conformers yielded sufficient perturbations on the respective molecular orbital so that a variety of crystal colors (red, orange, and yellow) were observed. To obtain a more detailed evaluation of the relative stability, the authors considered a partitioning of polymorphic energy differences into lattice and conformational contributions, and were able to deduce general trends that appeared valid in the absence of hydrogen bonding. The act of crystallization was found to feature an interplay of opposing forces, with perpendicular molecular conformations being favored in fluid solutions, while a preference for planar/high dipole conformers existed in most crystal forms, as shown in Fig. 4 [42]. The unusual polymorphism displayed by this system may result from one or more of the following factors: the preference for perpendicular conformations in solutions, the preference for planar/high dipole conformers in crystals, the formation of inter- and intramolecular hydrogen bonds, and the thermodynamic tendency towards low energy and high entropy.

2.4. Phase transformations in the solid state

Studies of phase transformations in the solid state are important, because the sudden appearance or disappearance of a crystalline form can threaten process development, and can lead to serious pharmaceutical consequences if the transformation occurs in the dosage forms. Hence, an understanding of the kinetics and mechanism of phase transformations is of practical importance. The rearrangement of molecules into a new structure during phase transformation may or may not involve a solvent or vapor phase. To explain the mechanism of solid–solid

UM00012142
NOVARTIS EXHIBIT 1517
Novartis v. Regents, IPR2023-01347
Page 888 of 4460

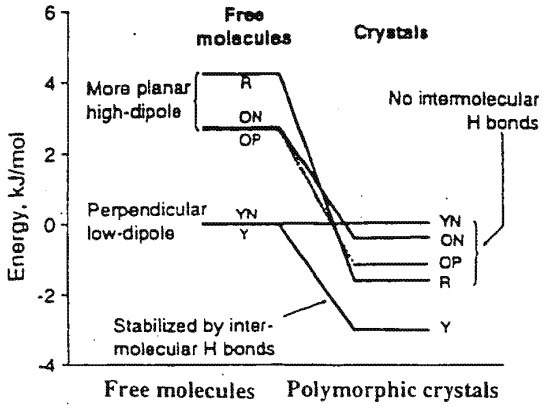


Fig. 4. Comparison of conformational energies and crystal energies of the various polymorphs of 5-methyl-2-[2-(nitrophenyl)amino]-3-thiophenecarbonitrile (II). Form R (red prisms, m.p. 106.2°C), form Y (yellow prisms, m.p. 109.8°C), form OP (orange plates, m.p. 112.7°C), form ON (orange needles, m.p. 114.8°C), form YN (yellow needles, m.p. not measurable) ([42], reproduced with the permission of the American Chemical Society).

physical transition, four steps have been proposed: (a) molecular loosening in the initial phase; (b) formation of an intermediate solid solution; (c) nucleation of the new solid phase and (d) growth of the new phase [2]. In an interesting study, Skwierczynski [44] has proposed a two-environment model to describe the decomposition reaction kinetics of a crystalline solid, aspartame. The decomposition reaction of aspartame is a simple unimolecular thermally-induced aminolysis and the reaction proceeds under anhydrous conditions, i.e., water is not a reactant [45]. This model links the chemistry of the solid-state reaction with the molecular mobility of the reactant as the reaction proceeds. The advantage of this model is that it can be used to determine the shelf life of a product from kinetic data gathered at elevated temperatures. Apart from solid–solid physical transformations, solution-mediated physical transformations among polymorphs are also known to occur in processes, such as wet granulation and during dissolution testing.

While the majority of studies have probed the equilibrium properties of polymorphic and solid-state solvated systems, relatively few have been concerned with the dynamics of phase transformation. Byrn et al. [2] have reviewed briefly the aspect of polymorphic interconversions and the factors affecting the transformations. In one study, the contribution of hydrogen bonding to the $\alpha \rightarrow \beta$ phase change of resorcinol has been detailed [46]. The α form is more stable than the β form at room temperature, but is less dense than the β form. The transition of $\alpha \rightarrow \beta$ at an estimated transition temperature of 337 ± 1 K is accompanied by an increase in crystal density, with the structure shifting from an open array of molecules (linked through hydrogen bonding) to a denser structure resembling molecular crystals. Through the use of a simple potential model, it was concluded that, during the phase transformation, the energy of the hydrogen bonds decreases along with the extent of such bonding. The energy liberated by this process is almost offset by the enhanced Van der Waals energies associated with the increase in crystal density, and consequently the transition enthalpy is rather small. Accompanying the shifts in hydrogen bonding is a number of effective proton transfers, altering the covalent and ionic portions of the crystal. It was also learned that the increase in entropy produced from the redistribution of protons was of the same order of magnitude as the entropy of the phase transition.

A number of spectroscopic techniques have been used to study the processes associated with a polymorphic transition of 2-(2,4-dinitrobenzyl)-3-methylpyridine [47]. The two interconverting structures coexisted over a temperature range of at least 8–9°C. The phase change was associated with a molecular tautomerization that translated through the collective changes of a large number of molecules, yielding domains having definite short-range order. The slowly evolving spectroscopy that took place above the transition temperature was interpreted as the annealing of domains into a long-range ordered system. The process of phase transformation appeared to consist of an initial fast redistribution of the mole ratio of the coexisting phases, followed by a much slower process involving a macroscopic relaxation of the system. Although local thermodynamic equilibrium was thought to exist in individual domains, the magnitude noted for the temperature range of the phase transition was proposed to arise from nonequilibrium conditions existing among the various types of domain.

UM00012143
NOVARTIS EXHIBIT 1517
Novartis v. Regents, IPR2023-01347
Page 889 of 4460

A combination of solid-state ^{15}N-NMR spectroscopy and X-ray crystallography was used to study polymorphic transitions in an azobenzene dyestuff, 2′-acetamido-4′-[*N*,*N*-bis(2-methylcarbonylethyl)amino]-4-nitroazobenzene (Scheme 1, structure III) [48]. This work established that the structure of one polymorph was disordered, and that the process of phase transformation entailed a crankshaft-type motion of the azo linkage. The ORTEP plots of the two molecular conformations for the X-ray structure determination of structure III at 293 K are shown in Fig. 5. Selective polarization inversion and band shape-fitting experiments were used to deduce the thermodynamic parameters of the exchange process.

Raman spectroscopy was used to study the effect of pressure on the phase transitions in hexamethylbenzene and hexa(methyl-d_3)benzene [49]. The form II → form III transition of the partially deuterated substance was found to take place at a lower pressure relative to that of the analogous hexamethylbenzene compound, which was attributed to differences in the energies of the intramolecular methyl torsional vibration in the two crystal forms. In another study performed by the same group, the effects of both temperature and pressure on the phase transitions of tetrafluoro-1,4-benzoquinone were considered [50]. In this system, the changes in environmental conditions were found to influence a number of intermolecular and intramolecular vibrational modes, yielding conformational changes that in turn produced the observed phase transitions.

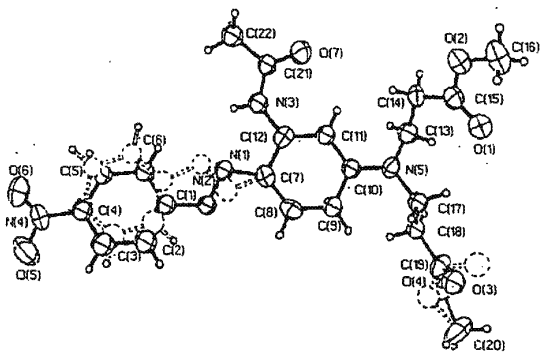


Fig. 5. ORTEP plots of the two molecular conformations (1 and 2) for the X-ray structure determination of 2′-acetamido-4′-[*N*,*N*-bis(2-methoxycarbonylethyl)amino]-4-nitroazobenzene (Scheme I Structure) at 293 K. Thermal ellipsoids are shown at 30% for clarity, with conformer 2 being represented by the solid lines and Conformer 1 by the dotted lines ([48], reproduced with the permission of the American Chemical Society).

2.5. Prediction of polymorphs

The main challenge in managing the phenomenon of multiple solid forms of a drug is the inability to predict the number of forms that can be expected in a given case. This prediction would involve quantification of the myriad intermolecular forces within any proposed crystal structure as well as the ability to postulate the likely packing modes for a given molecule in all its configurations [10]. Accurate theoretical prediction of polymorphs from studies of molecular dynamics and crystal structure generation would be of outstanding importance in drug research [36].

More research is now being directed towards developing computational tools to understand the nature of polymorphism and to predict polymorphic forms at an early stage in the drug development process. The recent developments in computational chemistry allow the prediction of possible polymorphic forms based only on the molecular structure of the drug. The Polymorph Predictor, from Molecular Simulations, is currently the only commercial software package that can predict the possible polymorphs of an organic compound from its molecular structure [51]. The package developed by Karfunkel and co-workers [52–54] uses a Monte Carlo simulated annealing approach to generate thousands of possible crystal packing alternatives for a given molecule. Each of the unique crystal structures is then subjected to a lattice energy minimization to obtain the relative stability ranking of the various packing possibilities and the resulting lowest-energy structures are the potential polymorphs. This method has been successfully employed to generate known polymorphs of primidone (Fig. 6A and B) and progesterone, starting from the molecular structures alone [55]. It has also been used to predict polymorphs for a range of small molecules and to predict unknown polymorphic structures of 4-amidinoindanone guanylhydrazone, a selective inhibitor of *S*-adenosylmethionine decarboxylase [56], and of aspirin [57].

UM00012144
NOVARTIS EXHIBIT 1517
Novartis v. Regents, IPR2023-01347
Page 890 of 4460

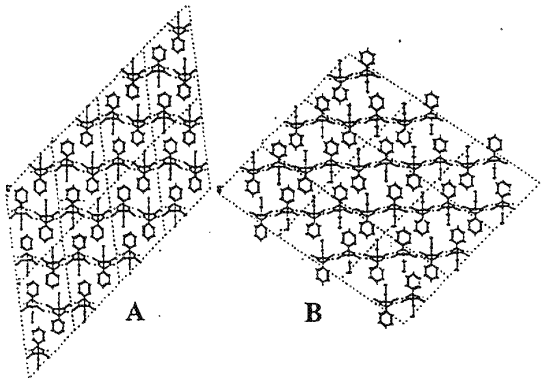


Fig. 6. Comparison of the crystal structure of primidone A (A) versus the most likely packing arrangement, frame 7 (B) ([55], reproduced with the permission of Elsevier Science).

The theoretical predictions of lattice energies, entropies, morphologies and polymorphs should stimulate experimental activities and vice versa. The current crystal-modeling efforts have the potential of producing more quantitative tools for bridging structures and properties, which could help in creating solid forms with desired properties [22]. There are many limitations in using computational methods for predicting polymorphs theoretically. The first limitation is that the ab initio screening is useful only for nonionic rigid molecules. For more complex systems, the method is very useful for generating plausible crystal structures, but it is not accurate enough to determine which of these possible structures can actually be crystallized [58]. In addition, the limitations in computer power can restrict the use of this method for predicting polymorphs of complex molecules. An issue of concern is that the existing methods only predict the lattice energies, which relate to internal energies or enthalpies of the crystals. However, the relative thermodynamic stability of polymorphs is determined by the Gibbs free energy, which is a linear function of both enthalpy and entropy. Predictions of the relative stability of polymorphs will be more accurate when the entropies, as well as lattice energies, are considered. Application of molecular dynamics may enable the entropies to be calculated. Hence, no general method is currently available for the prediction or interpretation of the properties of complicated polymorphic or pseudopolymorphic systems.

2.6. Directing the crystallization of specific polymorphs

Complementing the different computational methods for predicting the stable polymorphs of a given compound, various experimental methods are also being employed extensively to control the type of polymorph formed during the crystallization process. Many studies have reported the role of additives in controlling the outcome of the crystallization process. Some of the preselected additives are capable of inhibiting the nucleation and/or growth of the unwanted polymorphs. For the first time, the role of reaction by-products in controlling polymorph appearance of a drug has been reported [59]. This drug is sulfathiazole that is known to exist as polymorphs, forms I, II, III and IV, that differ in the hydrogen-bond network. Form I was found to be different from the other three forms as a result of a different hydrogen bonding at the aniline moiety of the molecule. From studies of the hydrogen-bonding pattern, it was predicted that the ethamido derivative of sulfathiazole could selectively control the formation of form I over other forms by entering the growing face of form I without disrupting the structure (Fig. 7a). Because a similar effect was not possible with the other forms, incorporation of the ethamido derivative in the other forms should inhibit their growth (Fig. 7b). Experimentally, it was shown that the ethamido by-product stabilized form I over the other polymorphs. This study clearly shows that the combination of crystal morphology and the hydrogen-bond network analysis of the different polymorphs offer a new and powerful approach to understanding and controlling polymorph appearance and stability in the presence of additives.

A similar approach was also applied to stabilize a metastable α conformational polymorph of L-glutamic acid using additives [60]. Methods such as DREIDING and TRIPOS force fields were used to select appropriate additives which could mimic the α and β conformations. Four additives were chosen for this study of which two were present exclusively in the β conformation and theoretically should selectively inhibit the crystallization of the β phase and thus stabilize the metastable α phase. Experimentally, it was proven that the additives, by virtue of their conformation, were able to selectively inhibit the

UM00012145
NOVARTIS EXHIBIT 1517
Novartis v. Regents, IPR2023-01347
Page 891 of 4460

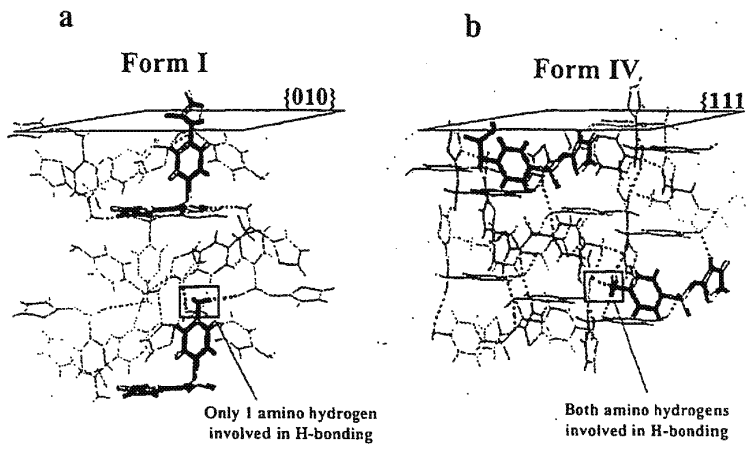


Fig. 7. Possible binding interaction of ethamidosulfamide in the fastest growing faces of (a) form I and (b) form IV of sulfathiazole ([59], reproduced with the permission of Elsevier Science).

appearance of the stable β polymorph of L-glutamic acid by interfering with either the nucleation rates or the growth rates and thus stabilize the metastable form. These studies demonstrate clearly that the molecular packing and intermolecular hydrogen bonds are the main features, which make possible the conformational discrimination. The use of conformational mimicry to stabilize the metastable structures of conformational polymorphs now offers a powerful tool for the prediction and development of robust processes for the control of polymorphic systems.

2.7. Characterization of polymorphs using a combination of analytical techniques

The common techniques often fail to differentiate definitively between two structurally similar polymorphs. Hence more advanced techniques or a combination of techniques need to be used to avoid errors of interpretation and in the identification of polymorphs [24]. Combinations of techniques are being employed currently for the characterization of crystalline pharmaceutical solids. For example, conventional single-crystal X-ray diffractometry and polarized microscopy were of no use in distinguishing the two forms I and II of roxifiban, a very promising cardiovascular drug, because of the relatively small crystallite sizes of the polymorphs. Hence, transmission electron microscopy (TEM) and synchrotron X-ray diffraction techniques were employed to characterize the unit cells of the two forms. By coupling the highly resolved synchrotron powder X-ray diffraction data shown in Fig. 8, with in-

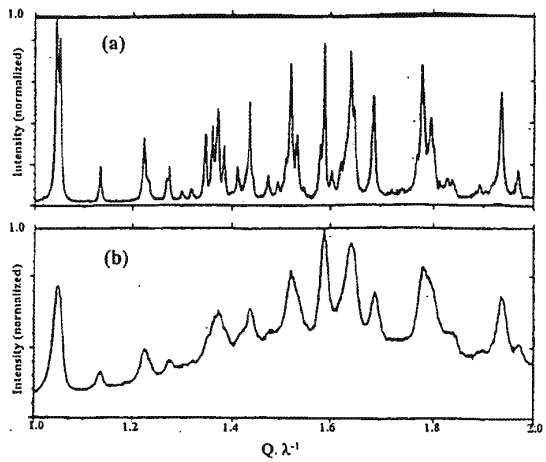


Fig. 8. A partial comparison of (a) a synchrotron pattern of polymorph II of roxifiban, collected using a wavelength of 1.00006 Å with (b) a conventional X-ray diffraction pattern using CuKα radiation in a region where there are many overlapping peaks. The patterns are plotted as a function of $Q = 2\pi/d = 4\pi \sin\theta/\lambda$ to remove the effects of different wavelengths ([61], reproduced with the permission of the American Pharmaceutical Association).

UM00012146
NOVARTIS EXHIBIT 1517
Novartis v. Regents, IPR2023-01347
Page 892 of 4460

formation obtained from TEM diffraction patterns, the unit cell parameters of the two forms of roxifiban were determined [61]. Similarly, the three modifications, I, II and III, of the nonsteroidal antiinflammatory drug, tiaprofenic acid, could not be distinguished by the two traditional spectroscopic methods, FTIR and FT-Raman spectroscopy. The modifications can only be distinguished by a combination of thermoanalytical and powder X-ray diffractometric methods [62].

Another example, to which a combination of techniques has been successfully applied to identify the various conformational polymorphs of a drug, is the characterization of the solid forms of neotame [29]. Neotame, *N*-(3,3-dimethylbutyl)-L-aspartyl-L-phenylalanine methyl ester, a new high-potency sweetener exists in the following phase-pure crystalline forms: monohydrate, the most stable crystalline form of neotame under ambient conditions, a methanol + water solvate [63], a methanol solvate [64], an amorphous anhydrate [29] and a crystalline anhydrate (form A; [65]). The authors conducted a systematic study of the conversion of the monohydrate under vacuum to a mixture of anhydrate forms followed by the reconversion of the anhydrate to the monohydrate upon exposure to moisture under ambient conditions. No significant changes were observed in the powder X-ray diffraction patterns during part of the reconversion process, suggesting that no change in lattice structure had occurred. However, the solid-state ^{13}C-CP-MAS NMR spectra, indicated the presence of several forms of neotame during the reconversion (Fig. 9). This discrepancy in the results between the two techniques was attributed to the conformational change of neotame molecules during reconversion, without significant change in unit cell parameters. This example indicates that both solid-state ^{13}C-CP-MAS NMR spectroscopy and powder X-ray diffractometry are needed to analyze mixtures of solid forms of conformationally flexible molecules, such as neotame.

A combination of solid-state ^{13}C-NMR spectroscopy and single crystal X-ray diffractometry also has been used to examine the solid-state tautomerism of acetohexamide [66,67]. Polymorphism of the antidiabetic drug acetohexamide has been investigated by numerous techniques. On the basis of FTIR data, form A of acetohexamide has been proposed to exist

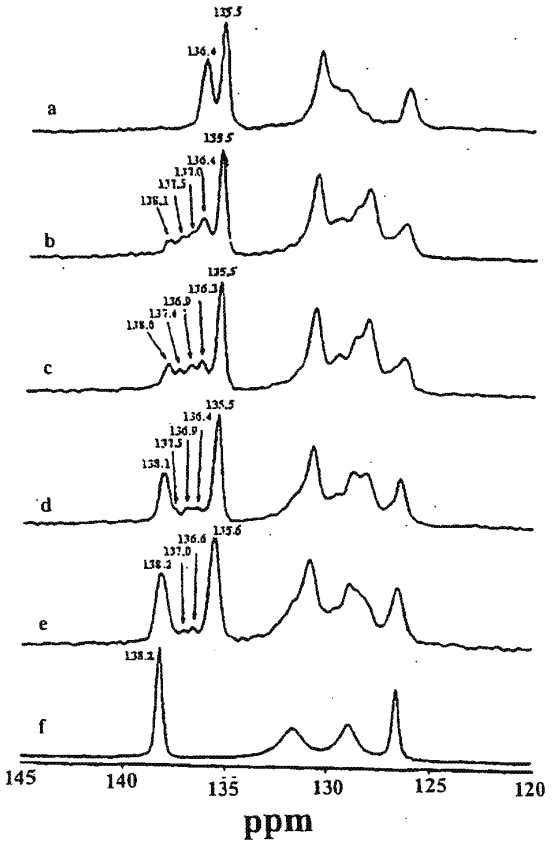


Fig. 9. Resonance signal of the phenyl carbon (C-15) attached to the side chain in the ^{13}C-CP-MAS NMR spectra of neotame anhydrate: (a) sample generated by placing the original monohydrate under vacuum (~1 Torr) for 3 days; (b–e) sample after being sealed in a jar for 2, 4, 6 and 8 days, respectively; (f) sample after being exposed to a relative humidity environment of 84% for 12 days ([29], reproduced with the permission of the American Chemical Society).

in the enol-tautomeric state, whereas form B has been proposed to be in the keto-tautomeric state. Using NMR and crystal structure data it was firmly established that both these acetohexamide polymorphic forms are present in the keto-form. Hence the combination of solid-state NMR spectroscopy and X-ray crystallography provided strong evidence that both forms of acetohexamide exist in the keto-tautomeric state and are truly polymorphic.

UM00012147
NOVARTIS EXHIBIT 1517
Novartis v. Regents, IPR2023-01347
Page 893 of 4460

3. Recent advances in the identification and characterization of hydrates and solvates

3.1. Introduction to solvates and hydrates

It has been estimated that approximately one-third of the pharmaceutically active substances are capable of forming crystalline hydrates [68]. The water molecule, because of its small size, can easily fill structural voids and because of its multidirectional hydrogen bonding capability, is also ideal for linking a majority of drug molecules into stable crystal structures [2]. The mere presence of water in a system is not a sufficient reason to expect hydrate formation, because some compounds, though they are soluble in water, do not form hydrates. It is the activity of water in the medium that determines whether a given hydrate structure will form. Solvates may be formed when a pure organic solvent or a mixture of solvents is used as the solvent for crystallizing the compound. Guillory [69] has discussed the various methods of preparation of hydrates and solvates in detail. Because solvates behave similarly to hydrates, common analytical techniques can be used for characterization of solvates and hydrates.

3.2. Structural aspects

Crystalline hydrates, based on their structure may be classified into three categories. The first category (class I) are the isolated site hydrates, where the water molecules are isolated from direct contact with other water molecules by intervening drug molecules, e.g., cephradine dihydrate. The second category (class 2) are channel hydrates where the water molecules included in the lattice lie next to other water molecules of adjoining unit cells along an axis of the lattice, forming channels through the crystal, e.g., ampicillin trihydrate. The channel hydrates can be subclassified into two subcategories. One category comprises the expanded-channel or nonstoichiometric hydrates, which may take up additional moisture in the channels when exposed to high humidity and for which the crystal lattice may expand or contract as the hydration or dehydration proceeds effecting changes in the dimensions of unit cells, e.g. cromolyn sodium. The other subcategory comprises the planar hydrates, which are channel hydrates in which water is localized in a two-dimensional order, or plane, e.g., sodium ibuprofen. The third category (class 3) of crystalline hydrates are the ion-associated hydrates, in which the metal ions are coordinated with water, e.g., calteridol calcium [8,9].

In this section, some examples of nonstoichiometric hydrates and their characterization will be discussed in detail because these forms pose a special challenge in dosage form development due to unpredictability of water content in the crystals. Following the work of Cox et al. [70] the unusual water uptake and formation of nonstoichiometric hydrates of cromolyn sodium was reinvestigated using single crystal X-ray diffractometry, PXRD, as well as by molecular modeling [71]. Cromolyn sodium, an antiasthmatic drug, exists as two liquid crystalline phases and a crystalline hydrate phase that sorbs and liberates water continuously and reversibly to give a continuous range of nonstoichiometric hydrates [70]. The changes in the PXRD patterns of the crystalline hydrate phase of cromolyn sodium in response to the surrounding relative humidity (RH) were explained in the light of the molecular and crystal structure of cromolyn sodium. Single crystal X-ray diffractometry indicated the space group for cromolyn sodium as $P1$, a chiral space group, even though the molecule itself is achiral. The crystal structure of cromolyn sodium with five or six water molecules per cromolyn sodium molecule, solved at room temperature by Hamodrakas et al. [72], revealed the positions of only one sodium ion and two water molecules and showed that the second sodium ion and the other water molecules are disordered. Recently, the single crystal structure of cromolyn sodium at 76% RH, with 6.44 molecules of water was solved at 173 K by Chen et al. [71]. This work showed that the second undetermined sodium ion is disordered over three sites and that four of the eight water positions are partially occupied. Comparison of the crystal structures determined by Hamodrakas et al. [72] and Chen et al. [71] indicated that the cromolyn anion is flexible. In particular, the bond and torsional angles of the 2-hydroxypropane linking the two cyclic moieties, changed to accommodate lattice expansion or contraction resulting from water sorption and desorption by the crystals. As water is taken up, the relative occupancies of the sites of the

UM00012148
NOVARTIS EXHIBIT 1517
Novartis v. Regents, IPR2023-01347
Page 894 of 4460

second sodium ion and that of water molecules change. As a result, the triclinic structure with $\alpha > 90°$ approaches the monoclinic form with $\alpha \approx 90°$. To summarize, the presence of large water channels, the flexibility of the 2-hydroxypropane link, the disorder of the second sodium ion (Fig. 10) and the disorder of the surrounding water molecules in the crystal lattice explain the reversible and nonstoichiometric water sorption and desorption by cromolyn sodium. This study emphasizes the importance of the detailed single crystal structure in explaining many unusual physico–chemical properties of drug hydrates.

The muscarinic agonist, LY297802 tartarate {i.e., (+)-3-[3-(butylthio)-1,2,5-thiadiazol-4-yl]-1-azabicyclo[2.2.2]octane monohydrogentartrate}, was also found to exhibit an unusual tendency to form nonstoichiometric hydrates of variable, but specific composition, ranging from 0 to 0.5 mol of water [73]. Solid-state ^{13}C-NMR spectroscopy, in conjunction with moisture sorption analysis and X-ray crystallography was used to provide unique insights into nonstoichiometric moisture sorption behavior. The PXRD patterns of the drug exposed to different RH values (0 to 75%), indicated neither a peak shift nor the presence of any new peaks, suggesting that the anhydrous and the hydrated forms of the drug are isomorphic. Fig. 11 shows the significant changes in the SSNMR peaks on exposure to different relative humidities and temperature, indicating that water incorporated into the crystal lattice changes the local chemical environment and causes the observed NMR changes. The incorporation of water into the crystal lattice of the drug was also confirmed by X-ray crystallography. The considerable hygroscopicity of the drug was rationalized in terms of the similar crystal structures of the hydrated and nonhydrated forms, and hence no significant structural modifications are needed for the reabsorption of water into the solids. The rates of dehydration and rehydration are largely determined by the size of the water channels and the strength of the hydrogen-bonding interactions that bind the water molecules in the channels.

Another interesting study with different solvated forms of L-lysine monohydrochloride (LH) was conducted by Bandyopadhyay et al. [74]. LH was found to form: a pure methanol solvate at water activity, $a_w < 0.34$, with methanol activity, $a_m > 0.7$; a dihydrate at $a_w > \sim 0.65$ with $a_m < 0.45$; and mixed solvates at intermediate values of a_w and a_m. It was found that the dihydrate and the mono-

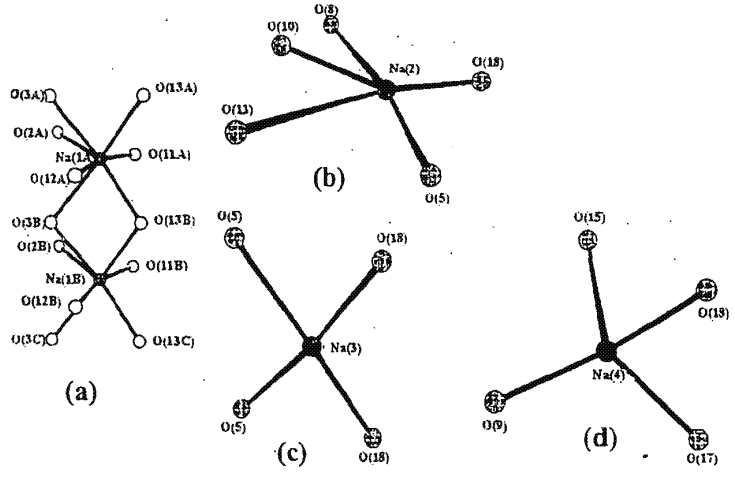


Fig. 10. In hydrated cromolyn sodium, coordination environment of: (a) the first (ordered) sodium ion, Na(1), shown in two neighboring unit cells (A and B); and the second (disordered) sodium ion at the three partially occupied sites, (b) Na(2), (c) Na(3), and (d) Na(4). The striped circles represent the sodium sites. The open circles represent the oxygen atoms coordinated to Na(1). The dotted (gray) circles represent the oxygen atoms coordinated to Na(2), Na(3), or Na(4) ([71], reproduced with the permission of the American Pharmaceutical Association).

UM00012149
NOVARTIS EXHIBIT 1517
Novartis v. Regents, IPR2023-01347
Page 895 of 4460

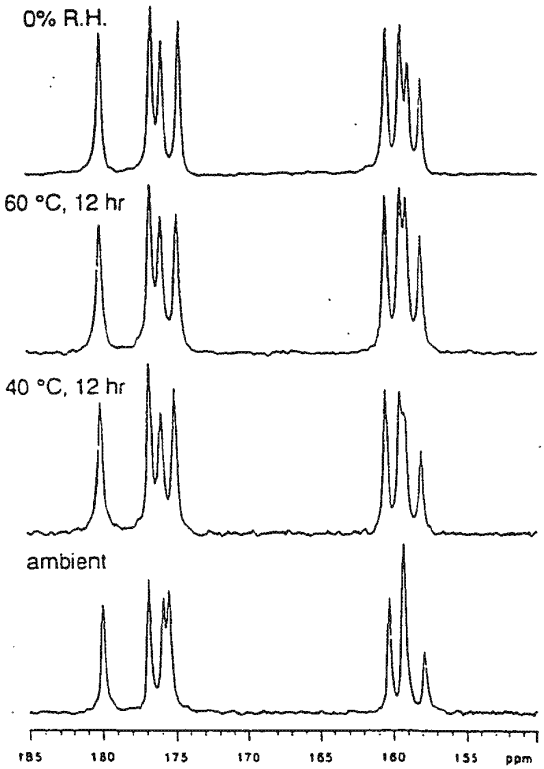


Fig. 11. Solid-state ^{13}C-NMR spectra of LY297802 tartrate {(+)-3-[3-(butylthio)-1,2,5-thiadiazol-4-yl]-1-azabicyclo[2.2.2]octane monohydrogentartrate} after storage at 0% humidity and before and after drying at elevated temperatures ([73], reproduced with the permission of the American Pharmaceutical Association).

methanol solvated forms of LH possessed similar crystal structures, similar PXRD patterns, but differed in the crystal habit. The crystal structures of LH hydrate and methanol solvate indicate that one molecule of methanol in the methanol solvate occupies approximately the same volume as the two water molecules in the dihydrate. During dehydration in the presence of methanol in the crystallization medium, the loss of one or more water molecules from the crystal lattice was compensated by the gradual uptake of methanol into the crystal structure to satisfy the hydrogen bonding pattern within the lattice with minor rearrangements, giving rise to mixed solvates. The similarities of the crystal lattices of the dihydrate and monomethanol solvate explain the similarity of the PXRD patterns.

3.3. Phase transformation of hydrates and solvates

Phase changes due to hydration/dehydration and solvation/desolvation of pharmaceutical compounds during processing or in the final product may result in an unstable system that would effect the bioavailability of drug from solid dosage forms. Various types of phase changes are possible in solid-state hydrated or solvated systems in response to changes in environmental conditions, such as relative humidity, temperature and pressure. For example, some hydrated compounds may convert to an amorphous phase upon dehydration and some may convert from a lower to a higher state of hydration yielding forms with lower solubility. Alternatively, a kinetically favored but thermodynamically unstable form may be converted during pharmaceutical processing to a more stable and less soluble form [8]. The phase transitions in hydrates and solvates can occur at various stages of dosage form development. Morris [9] has discussed the behavior of hydrates during processing, handling and storage of formulations in detail.

The phase transformations associated with exposure to water, such as during solubility measurements, wet granulation processes, dissolution studies and accelerated stability tests are likely to occur via solution mediation. Solution mediated phase transformations depend upon the solution phase to provide the mobility necessary to rearrange in the most stable form and hence are much faster than solid-state transformations. The rate of a solution-mediated transformation is proportional to the solubility of the species involved. Temperature, pressure and relative humidity may increase the rate of phase transformation of hydrates by inducing mobility in the system.

Solution-mediated phase transformations have been reported for many hydrate systems, such as theophylline crystals [17], eprosartan mesylate [75] and nedocromil sodium [76]. Ghosh and Grant [77] have addressed a common problem associated with the characterization of solvates which centers around the determination of solubilities of solvates and of nonsolvates that undergo phase transformation in the presence of an interacting solvent, such as solvation of nonsolvates in the solvent of crystallization or the desolvation of solvates in water. A thermodynamic cycle analogous to Hess's law but based on free

UM00012150
NOVARTIS EXHIBIT 1517
Novartis v. Regents, IPR2023-01347
Page 896 of 4460

energies has been developed to predict the theoretical solubilities of 1,2-dialkyl-3-hydroxy-4-pyridones, which form 1:1 formic acid solvates in the presence of formic acid, and of the 1:1 formic acid solvates which produce the corresponding unsolvated compounds in the presence of water. A good correlation was obtained between the solubility values measured by the standard extrapolation method and that calculated by means of the thermodynamic cycle.

Apart from identifying and characterizing the phases during various stages of drug development, it is very important to gain an understanding of the dehydration/hydration mechanisms and kinetics. Many models have been developed to account for the dehydration kinetics of the crystalline hydrates [78]. Nucleation is the most significant phenomenon in determining the transformation kinetics, that is, the rate of formation of a new phase [8]. The dehydration kinetics to some extent will also depend upon the class of the hydrate system to which the drug belongs, particle size and morphology. The practical applications of understanding the dehydration kinetics, as indicated by Morris [9], are mainly the determination of the conditions for allowable exposure of bulk drug substances during development and processing, proper packaging, allowable temperature ranges for shipping, storage, and labeling of the final product, and the initial selection of a form for development.

3.4. Prediction of the formation of hydrates and solvates

Predicting the formation of solvates or hydrates of a compound and the number of molecules of water or solvent incorporated into the crystal lattice of a compound is complex and difficult. Each solid compound responds uniquely to the possible formation of solvates or hydrates and hence generalizations cannot be made for a series of related compounds. Certain molecular shapes and features favor the formation of crystals without solvent; these compounds tend to be stabilized by efficient packing of molecules in the crystal lattice, whereas other crystal forms are more stable in the presence of water and/or solvents. There may be too many possibilities so that no computer programs are currently available for predicting the crystal structures of hydrates and solvates.

3.5. Characterization of hydrates and solvates

The common methods for the characterization of hydrates and solvates are polarized light microscopy and hot stage microscopy, DSC, TGA, Karl Fischer titrimetry, single-crystal X-ray diffractometry, powder X-ray diffractometry, and infrared spectroscopy. These methods have been reviewed in detail [21] and will also be discussed in detail in later chapters.

Pressure DSC is gaining increasing popularity in the study of solvates and hydrates where dehydration reactions occur above or near the boiling point of water. Using conventional DSC, it is very difficult to measure the heats of dehydration and heat of vaporization separately, but if one conducts DSC experiments at elevated pressures, the two processes may be completely separated. The advantage of using pressure DSC is that the pressure can be precisely controlled and the solids can be subjected to a controlled temperature program while under substantially elevated temperatures. The influence of elevated pressures on the solid-state behavior of carbamazepine dihydrate was studied by Han and Suryanarayanan [79]. In Fig. 12 it is shown that pressure DSC can separate the dehydration and vaporization endotherms of carbamazepine dihydrate during its conversion to the anhydrate form. Also the technique permitted the water liberated on dehydration to remain in intimate contact with the anhydrous phase formed which could significantly influence its solid-state properties.

The combined physical analytical techniques of thermogravimetry and infrared spectroscopy (TG/IR) can permit identification of the solvent incorporated into the crystal lattice. This combined technique has been used to study formulated products, such as capsules and tablets [80].

4. Current challenges and future directions

4.1. Origins of the challenges

A series of flow charts and decision trees have been presented and discussed [11,22] that can be

UM00012151
NOVARTIS EXHIBIT 1517
Novartis v. Regents, IPR2023-01347
Page 897 of 4460

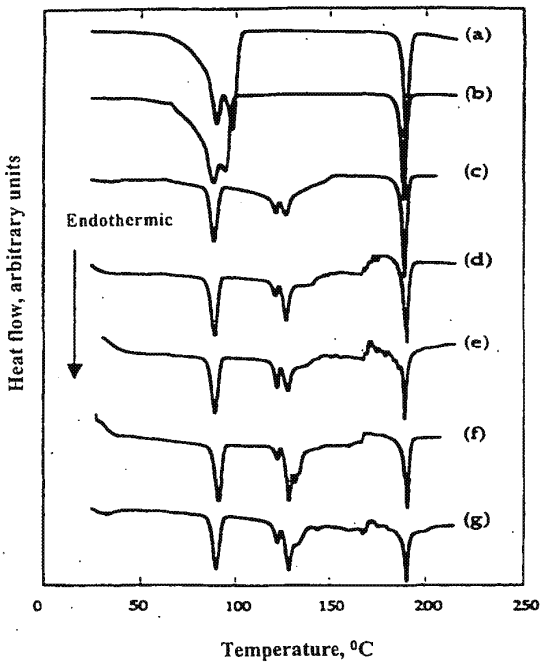


Fig. 12. Differential scanning calorimetry (DSC) curves of carbamazepine dihydrate at different pressures: (a) at atmospheric pressure in a conventional DSC cell, (b) at atmospheric pressure in a pressure DSC (PDSC) cell, (c) 100 p.s.i., (d) 200 p.s.i., (e) 300 p.s.i., (f) 400 p.s.i., and (g) 600 p.s.i. (1 p.s.i. = 6.9 kPa) ([79], reproduced with the permission of Elsevier Science).

used by investigators to characterize the polymorphs and solvates of compounds under development or for registration with regulatory authorities. Due to the complex and nonconventional behavior of various organic drug molecules, there are many opportunities for research and development in the area of characterization of polymorphs and solvates. Some of the problems which are commonly encountered during characterization of crystalline solids and which need to be addressed are: disorder in the crystal lattice due to pharmaceutical processing leading to conversion of a crystalline phase to an amorphous material or phase conversion from one form to the other; quantitating the amount of single polymorph in a mixture of polymorphs; identifying the solid form of the active ingredient in the formulated product, particularly when the drug is a minor component in the presence of numerous other materials (excipients); and the issues of disappearing polymorphs and the appearance of new polymorphs. In the following sections we will address some of these issues and some of the studies that have addressed these problems.

4.2. Phase transformations during processing

The effects of pharmaceutical processing on the crystalline state of drug polymorphs and solvates have been discussed recently by Brittain and Fiese [16]. Exposure to changes in temperature, pressure, relative humidity and comminution are encountered during processes such as drying, granulation, milling and compression. The stresses applied to crystals during pharmaceutical processing can cause defects in their crystal lattices, and contribute to lattice disorder, thus affecting the physical properties of the resulting powder. [81]. This problem has been discussed in detail by Byrn et al. [10]. Arising from different degrees of crystalline disorder, the difficulty in reproducing materials with the same properties is a major concern in the pharmaceutical industry.

Milling, the last processing step in the production of bulk drug substance to reduce particle size, is often accompanied by a decrease in crystallinity due to the creation of lattice defects, beginning at the surface. The defects created by mechanical activation of the solid on the surface can migrate, transform, and change their number and nature. If the defects in the mechanically activated crystal heal to produce a crystal lattice different from the initial lattice, then a polymorphic transformation has taken place. Milling-induced polymorphic changes have been observed for many small drug molecules, such as fostedil, chloramphenicol palmitate, indomethacin and phenylbutazone [16]. Polymorphic transformation of the dipeptide sweetener, aspartame hemihydrate, can occur during milling [82]. Polymorph II of aspartame hemihydrate was found to transform to form I during ball-milling or on heating for 30 min at 160°C in the presence of steam as shown in the X-ray diffraction pattern (Fig. 13). The susceptibility of form II of aspartame hemihydrate to transform to form I has been attributed to the less symmetric crystal structure of form II compared to that of form I as studied by spectroscopic methods.

Some authors, such as Hüttenrauch [81] have

UM00012152
NOVARTIS EXHIBIT 1517
Novartis v. Regents, IPR2023-01347
Page 898 of 4460

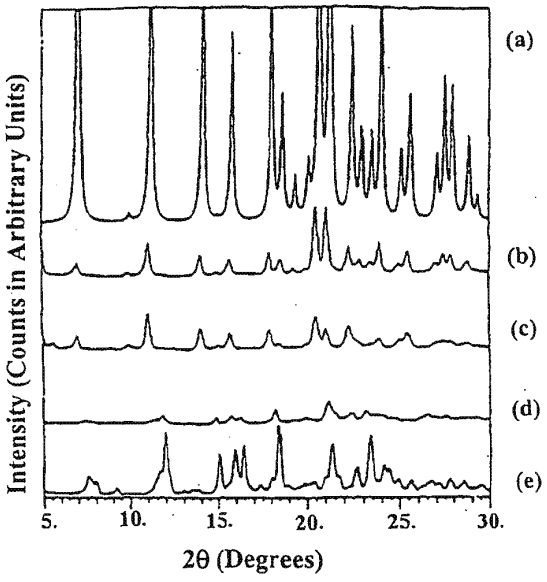


Fig. 13. Powder X-ray diffraction patterns of aspartame hemihydrate: (a) theoretical powder pattern calculated from the crystal structure of aspartame hemihydrate (form I) determined by Hatada et al., (1985) [99], (b) experimental powder pattern of the ball-milled aspartame hemihydrate (form I), (c) experimental powder pattern of aspartame hemihydrate that had been heated for 30 min at 160°C in the presence of steam (form I), (d) experimental powder pattern of aspartame hemihydrate after compression at 250 MPa for 1 min (form II), and (e) aspartame hemihydrate as received (form II) ([82], reproduced with the permission of the American Pharmaceutical Association).

suggested that the trauma to crystals during grinding may lead to a decrease in crystallinity, which should improve the compression capacity and dissolution rate of the drug molecules. This hypothesis was tested by studying the morphology, crystalline state, compression capacity and dissolution properties of native and ground crystals of aspirin and lactose monohydrate [83]. No significant increase in compression capacity was observed when native and ground crystals were compared. Only a slight increase in the dissolution rate was observed for ground aspirin crystals which was attributed to surface defects due to grinding resulting in improved crystal wetting.

The effect of roller compaction on lattice defects and phase change has been examined for aspirin [84]. The water vapor sorption isotherm obtained for aspirin on roller compaction indicated much more water uptake than had been reported previously for other crystalline samples of aspirin under similar conditions. Various possibilities were suggested for the unusual water uptake of aspirin on roller compaction, such as formation of a polymorphic form of aspirin with a much greater affinity for water, formation of a crystalline hydrate in the aspirin sample, or significant reduction in particle size of the aspirin particles thereby providing an increased specific surface area for water vapor adsorption. It is also possible that roller compaction disrupted the crystalline order of some part of the aspirin crystals forming amorphous regions, which then take up relatively large quantities of water into their bulk structure. This example clearly indicates that processes, such as roller compaction, can introduce considerable disorder in the surface of crystals leading to a marked increase in the tendency to sorb water vapor.

Thermal activation, like mechanical activation during processing, also results in a high-energy state of crystals that may reorganize into a different lattice arrangement resulting in a phase change. The thermal stability of drug substances is important, because formulations are often dried at elevated temperatures after wet granulations so that the tablets may contain small regions of high temperature (hot spots) during compression. Various examples have shown that a change of temperature may influence the stability of drug molecules [16]. The effect of low temperatures, such as during freeze–drying, on the crystalline form of the drug has also been studied. The formation of a new mannitol hydrate during freeze–drying has been reported [85]. The formation of a crystalline hydrate by an excipient during freeze–drying may have several practical consequences, such that the difficulty of removing bound water from the crystal lattice can significantly limit the drying rate, while the residual water that is not removed by freeze–drying may be a potential threat to product stability if it is released during storage. The mannitol hydrate formed during freeze–drying survived the typical drying cycle and converted to the anhydrous polymorph of mannitol upon heating.

Spray drying has also been shown to lead to loss of crystallinity in materials, by a combination of processes involving rapid solidification of dissolved material and solid-state transitions due to milling effects in the atomiser. Spray drying leads to conver-

UM00012153
NOVARTIS EXHIBIT 1517
Novartis v. Regents, IPR2023-01347
Page 899 of 4460

sion of a crystalline phase to an amorphous state and, because the amorphous state is metastable with respect to the crystalline form, phase transformations are likely to occur within the shelf life of the pharmaceutical product, resulting in loss of quality and potency in the product [86].

In view of the significant effects that the state of disorder in crystalline solids caused by pharmaceutical processing can have on the properties of pharmaceutical solids, it is important to be able to assess the extent of disorder in a solid quantitatively down to very low levels. Various methods have been used to measure the percent disorder, such as using predetermined mixtures, measurements of X-ray powder diffraction, density and heats of crystallization which revealed limits of detectability down to about 10%. Using water vapor sorption measurements under very carefully controlled conditions, it was possible to detect disorder as low as 1% in milled samples of sucrose [87]. A comparison of the four methods mentioned above for estimating the percent disorder of milled samples of sucrose gave very consistent results, once the underlying factors that make these techniques sensitive to the concentration of amorphous content were recognized and taken into account.

4.3. Degree of crystallinity

The previous section has emphasized that many pharmaceutical processes lead to a decrease in crystallinity of drug phases. Various studies have concluded that the formation of amorphous material during processing is highly undesirable. The amorphous material, being in a thermodynamically metastable state, is susceptible to reconversion to the crystalline state, affecting many physico–chemical characteristics of the drug. A later chapter provides detailed coverage of amorphous materials. An estimation of the degree of crystallinity of a sample before and after processing poses one of the larger challenges facing the pharmaceutical field. Powder X-ray diffractometry is still the commonly used method for determining the degree of crystallinity, though this method suffers from some limitations due to peak broadening, amorphous halo, and preferred orientation which make interpretation and quantitation difficult. DSC may not be a sensitive method for measuring crystallinity due to crystallization of the amorphous content at elevated temperatures and the effects of differences in heat capacity. Solution calorimetry has been proposed as an accurate method for analysis of percent crystallinity [11,88,89]. A decrease in the endothermic enthalpy of solution indicates a decrease in the crystallinity of the sample. However, differences in surface area produced by grinding or by other processing techniques can also result in changes in the heat of wetting of a sample. Judicious choice of solvent can be employed to reduce such surface effects, which themselves contribute to the observed crystallinity of the sample.

Near infrared (NIR) spectroscopy is another technique being used to measure the degree of crystallinity, and has also proved useful in studies of the polymorphism and water content of sugars. The NIR spectrum of a sample contains both physical and chemical information. Being noninvasive, nondestructive and operable at room temperature, the method is a valuable tool with which to assess changes in the amorphous and crystalline state of lactose [90]. NIR has been used to follow the changes in the amorphous state, the onset of crystallization, and the changes between α- and β-lactose, which accompany the onset of crystallization. In another study, the nucleation and crystallization kinetics of amorphous lactose was investigated by gravimetry in an automated vacuum moisture balance. The combination of isothermal and nonisothermal activation energies allowed the investigation of both crystal growth and nucleation mechanisms and led to the separation of activation energies for nucleation and growth [91].

4.4. Characterization of mixtures of polymorphs

Another common problem encountered during drug development is quantitative control of the proportion of polymorphic forms present in a mixture. According to the US FDA regulations, the method of analysis for the proportion of forms must be validated, and also the proportion of forms must remain within stated limits through the retest date of the drug substance and potentially throughout the shelf life of the product. This is a very onerous requirement, especially if the forms have a tendency to interconvert. Byrn et al. [11] suggested that the best way to deal with this problem is probably by

UM00012154
NOVARTIS EXHIBIT 1517
Novartis v. Regents, IPR2023-01347
Page 900 of 4460

developing methods to prepare only one crystal form and maintaining this form throughout processing. Powder X-ray diffractometry is often a useful method to determine the percentages of polymorphs in a mixture. However, the detection limit is variable from case to case, and is sometimes as high as 15%. It is therefore important to develop sensitive analytical methods with a lower limit of detection.

Attenuated total reflectance (ATR) FTIR spectroscopy has been shown to be valuable for the quantitative analysis of the polymorphic content of bulk pharmaceutical materials. The feasibility of using ATR-FTIR for the qualitative and quantitative analysis of mixtures of pharmaceutical polymorphs has been studied using three known polymorphs of ganciclovir as a model compound [92]. Definitive identification and quantitation of all three polymorphs could be achieved using ATR-FTIR spectroscopy in conjunction with partial least-squares modeling. This technique has many advantages, such as speed, nondestructiveness, relative ease of use, and most important, no sample pretreatment before measurement.

Raman spectroscopy is another technique that is being widely used to quantitatively estimate the percentage of one polymorph in a mixture of polymorphs. FT-Raman spectrometry offers many advantages, the most prominent being, minimal sample preparation, sensitivity to polymorphism, and noninterference from water. Two polymorphs of fluconazole were characterized using FT-Raman spectroscopy and principal components regression using cross validation provided quantitative analysis of the percentage of one polymorphic form in the mixture of other forms [93]. A novel sample holder was developed whereby the sample is held in an NMR tube which is rotated around its axis and at the same time moved up and down. This method of sample presentation leads to a large increase in the volume studied and is important for inhomogeneous samples for which sub-sampling is a problem. Possible degradation of the sample through heating by the laser can also be avoided [94].

X-Ray powder diffractometry is still the common method for the quantitative estimation of polymorphs in a mixture of polymorphs. This method requires that at least one high-intensity peak unique to each form is available for intensity measurements and that the plot of the peak intensity ratio as a function of the weight ratio of the components should result in a straight line. Modern computer controlled X-ray powder diffractometers now permit quantitative analysis of multicomponent mixtures using the complete powder diffraction profile rather than a limited amount of low-angle integrated intensity data. Artificial neural networks (ANNs) in quantitative X-ray powder diffractometry were used successfully to identify and quantify the two known modifications of ranitidine hydrochloride even when the weight fraction of one polymorph in the mixture was as low as 0.01 [95]. ANNs have been used mostly in problems of pattern recognition and modeling, and is therefore useful in deciphering the pattern in diffraction data from polymorphic mixtures. The ANNs model predicted concentration precisely, accurately, and with minimal bias through a wide range of ratios of the two known ranitidine hydrochloride polymorphic forms in a mixture (Fig. 14). This method minimizes the problems associated with preferred orientation and overlapping X-ray lines. The same group of researchers has shown the potential of ANNs in combination with DRIFT spectroscopy to analyze the polymorphic purity of crystalline ranitidine hydrochloride as a bulk drug and as an active ingredient of

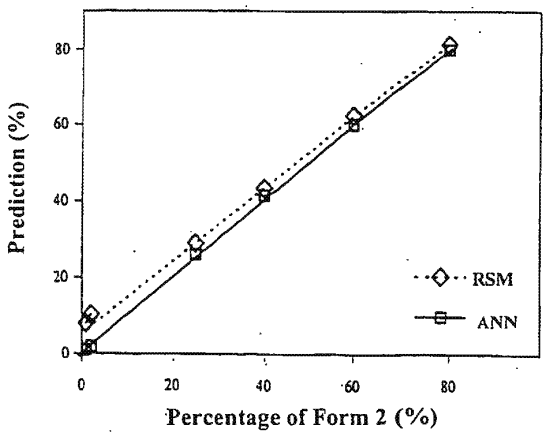


Fig. 14. Predicted concentrations of the two polymorphic forms (form 1 and 2) of ranitidine hydrochloride by the response surface methodology (RSM), a statistical modeling method, and by the artificial neural networks (ANNs) method, plotted against measured percentage of form 2 ([95], reproduced with the permission of Elsevier Science).

UM00012155
NOVARTIS EXHIBIT 1517
Novartis v. Regents, IPR2023-01347
Page 901 of 4460

a tablet formulation. Simultaneous identification and quantification of all the ingredients in the tablet formulation was possible. This study has shown that the complex problem of quantifying a drug in mixtures containing two or more components with overlapping spectra can be solved by the DRIFT-ANNs technique [96].

Another technique, which is gaining popularity in the quantitative analysis of mixtures of polymorphs, is solid-state ^{13}C-CP-MAS NMR spectroscopy. This method was preferred for quantitative analysis of polymorphic mixtures of the herbicide, pendimethalin, which exists as two polymorphs with different colors and crystal habits [27]. ^{13}C-NMR provided the most sensitive and definitive evidence of the transition from the yellow to the orange form. This method enabled as little as 2% of orange pendimethalin to be determined in a sample consisting mostly of the yellow polymorph. It is the least invasive of the instrumental methods and can be used to detect the ratio of the two polymorphs in solid formulations.

A related challenge faced by the pharmaceutical industry is the determination of the polymorphic nature of the drug in the presence of excipients in a dosage form especially when the active drug is present as a low percentage of the overall formulation [97]. This problem can be addressed by developing sensitive techniques with lower limits of detection or by using a combination of techniques.

5. Conclusions

In order to save time and cost it is very important to choose the most suitable form of the crystalline drug in the initial stages of drug development. In recent years a good deal of research has been directed towards achieving this goal. Systematic isolation and early characterization of the largest number of possible forms of a drug reduces the chances of surprises at the late production stage due to identification of a new crystalline form or phase change. With the development of more sophisticated computational tools, the main focus of many investigators is to be able to predict all the possible forms of a drug from its molecular structure. Understanding the origins of the multiple solid forms of a drug molecule, either due to differences in packing arrangement or conformation of the molecules, becomes the first step in prediction. Single crystal X-ray diffractometry and solid-state NMR spectroscopy are two techniques that are gaining increased application in determining the various crystal structures and the origins of polymorphism and pseudo-polymorphism of a particular drug. When crystal structures can be calculated with certainty, it will be possible to predict the various polymorphs of a compound and this information could be used to guide experimental studies. This goal may be difficult to achieve owing to the complex molecular structures of new organic molecules and the presence of several molecules in each asymmetric unit, but the future development of improved force fields and increased computational speeds, may make it achievable.

Improved experimental methods leading to more accurate and detailed phase diagrams are also finding increased use in determining the stability of various polymorphs. It is important to make every effort to prepare and to identify the most stable polymorph in order to guide the selection of the optimal form for development. The emergence of sensitive methods and the use of combination techniques, facilitate the identification and the more accurate characterization of the various polymorphs of a drug molecule. One of the main analytical challenges faced by the pharmaceutical analyst is the development of better quantitative methods for identifying a single polymorph in a mixture of polymorphs and for determining the percentages of amorphous or crystalline content of the drug. More and more sensitive methods are being developed to address this problem.

An increased understanding of the phenomenon of polymorphism should enable pharmaceutical scientists to gain control over the crystallization process in order to selectively obtain the desired polymorph or suppress the growth of an undesired one. Phase changes during processing and scale-up are a problem, which may be avoided by carefully designed initial small-scale studies. The availability of detailed structural data, combined with strategic design of substrates and additives, has led to significant advances in the control over the polymorphs obtained in a particular crystallization [98]. With all the information available from these initial studies, it

UM00012156
NOVARTIS EXHIBIT 1517
Novartis v. Regents, IPR2023-01347
Page 902 of 4460

should be possible to design and to select processing conditions which would give a desired polymorph and maintain the desired form throughout the various stages of drug processing and manufacture.

References

[1] H.G. Brittain, S.R. Byrn, Structural aspects of polymorphism, in: H.G. Brittain (Ed.), Polymorphism in Pharmaceutical Solids, Vol. 95, Marcel Dekker, New York, 1999, pp. 73–124.

[2] S.R. Byrn, R.R. Pfeiffer, J.G. Stowell, Solid-State Chemistry of Drugs, SSCI, West Lafayette, IN, 1999.

[3] T. Hahn (Ed.), International Tables for Crystallography, International Union of Crystallography, Boston, MA, 1987.

[4] M. Kuhnert-Brandstätter, Thermomicroscopy in the Analysis of Pharmaceuticals, Pergamon, Oxford, 1971.

[5] L. Borka, J.K. Haleblian, Crystal polymorphism of pharmaceuticals, Acta Pharm. Jugosl. 40 (1990) 71–94.

[6] L. Borka, Review on crystal polymorphism of substances in the European Pharmacopoeia, Pharm. Acta Helv. 66 (1991) 16–22.

[7] D. Giron, Thermal analysis and calorimetric methods in the characterization of polymorphs and solvates, Thermochim. Acta 248 (1995) 1–59.

[8] K.R. Morris, N. Rodriguez-Hornedo, Hydrates, in: J. Swarbrick, J.C. Boylan (Eds.), Encyclopedia of Pharmaceutical Technology, Vol. 7, Marcel Dekker, New York, 1993, pp. 393–441.

[9] K.R. Morris, Structural aspects of hydrates and solvates, in: H.G. Brittain (Ed.), Polymorphism in Pharmaceutical Solids, Vol. 95, Marcel Dekker, New York, 1999, pp. 125–181.

[10] S.R. Byrn, R.R. Pfeiffer, G. Stephenson, D.J.W. Grant, W.B. Gleason, Solid-state pharmaceutical chemistry, Chem. Mater. 6 (1994) 1148–1158.

[11] S. Byrn, R. Pfeiffer, M. Ganey, C. Hoiberg, G. Poochikian, Pharmaceutical solids: a strategic approach to regulatory considerations, Pharm. Res. 12 (1995) 945–954.

[12] D.J.W. Grant, Theory and origin of polymorphism, in: H.G. Brittain (Ed.), Polymorphism in Pharmaceutical Solids, Vol. 95, Marcel Dekker, New York, 1999, pp. 1–33.

[13] J.K. Haleblian, W.C. McCrone, Pharmaceutical applications of polymorphism, J. Pharm. Sci. 58 (1969) 911–929.

[14] W.I. Higuchi, P.K. Lau, T. Higuchi, J.W. Shell, Polymorphism and drug availability. Solubility relations in the methylprednisolone system, J. Pharm. Sci. 52 (1963) 150–153.

[15] M.J. Nerurkar, S. Duddu, D.J.W. Grant, J.H. Rytting, Properties of solids that affect transport, in: G.L. Amidon, P.I. Lee, E.M. Topp (Eds.), Transport Processes in Pharmaceutical Systems, Vol. 102, Marcel Dekker, New York, 2000, pp. 575–611.

[16] H.G. Brittain, E.F. Fiese, Effects of pharmaceutical processing on drug polymorphs and solvates, in: H.G. Brittain (Ed.), Polymorphism in Pharmaceutical Solids, Vol. 95, Marcel Dekker, New York, 1999, pp. 331–361.

[17] N. Rodríguez-Hornedo, D. Lechuga-Ballesteros, H.J. Wu, Phase transition and heterogeneous/epitaxial nucleation of hydrated and anhydrous theophylline crystals, Int. J. Pharm. 85 (1992) 149–162.

[18] N. Rodríguez-Hornedo, D. Murphy, Significance of controlling crystallization mechanisms and kinetics in pharmaceutical systems, J. Pharm. Sci. 88 (1999) 651–660.

[19] J.W. Mullin, Crystallization, Butterworth–Heinemann, Oxford, 1993.

[20] M.C. Etter, Encoding and decoding hydrogen-bond patterns of organic compounds, Acc. Chem. Res. 23 (1990) 120–126.

[21] H.G. Brittain, Methods for the characterization of polymorphs and solvates, in: H.G. Brittain (Ed.), Polymorphism in Pharmaceutical Solids, Vol. 95, Marcel Dekker, New York, 1999, pp. 227–278.

[22] L. Yu, S.M. Reutzel, G.A. Stephenson, Physical characterization of polymorphic drugs: an integrated characterization strategy, Sci. Pharm. 1 (1998) 118–127.

[23] H.G. Brittain, Spectral methods for the characterization of polymorphs and solvates, J. Pharm. Sci. 86 (1997) 405–412.

[24] D. Giron, Thermal analysis, microcalorimetry and combined techniques for the study of pharmaceuticals, J. Therm. Anal. Cal. 56 (1999) 1285–1304.

[25] H.G. Brittain (Ed.), Physical Characterization of Pharmaceutical Solids, Vol. 70, Marcel Dekker, New York, 1995.

[26] R. Bottom, The role of modulated temperature differential scanning calorimetry in the characterization of a drug molecule exhibiting polymorphic and glass forming tendencies, Int. J. Pharm. 192 (1999) 47–53.

[27] G.W. Stockton, R. Godfrey, P. Hitchcock, R. Mendelsohn, P.C. Mowery, S. Rajan, A.F. Walker, Crystal polymorphism in pendimethalin herbicide is driven by electronic delocalization and changes in intramolecular hydrogen bonding. A crystallographic, spectroscopic and computational study, J. Chem. Soc., Perkin Trans. 2 (1998) 2061–2071.

[28] D.C. Apperley, R.A. Fletton, R.K. Harris, R.W. Lancaster, S. Tavener, T.L. Threlfall, Sulfathiazole polymorphism studied by magic-angle spinning NMR, J. Pharm. Sci. 88 (1999) 1275–1280.

[29] B.E. Padden, M.T. Zell, Z. Dong, S.A. Schroeder, D.J.W. Grant, E.J. Munson, Comparison of solid-state ^{13}C-NMR spectroscopy and powder X-ray diffraction for analyzing mixtures of polymorphs of neotame, Anal. Chem. 71 (1999) 3325–3331.

[30] J. Smith, E. MacNamara, D. Raftery, T. Borchardt, S. Byrn, Application of two-dimensional ^{13}C-solid-state NMR to the study of conformational polymorphism, J. Am. Chem. Soc. 120 (1998) 11710–11713.

[31] M.L. Bray, H. Jahansouz, M.J. Kaufman, Selection of optimal hydrate/solvate forms of a fibrinogen receptor antagonist for solid dosage development, Pharm. Dev. Technol. 4 (1999) 81–87.

[32] A. Burger, R. Ramberger, On the polymorphism of pharmaceuticals and other molecular crystals. I. Theory of thermodynamic rules, Mikrochim. Acta [Wein] II (1979) 259–271.

[33] A. Burger, R. Ramberger, On the polymorphism of pharmaceuticals and other molecular crystals. II. Applicability of thermodynamic rules, Mikrochim. Acta [Wein] II (1979) 273–316.

UM00012157
NOVARTIS EXHIBIT 1517
Novartis v. Regents, IPR2023-01347
Page 903 of 4460

[34] J. Henck, M. Kuhnert-Brandstätter, Demonstration of the terms enantiotropy and monotropy in polymorphism research exemplified by flurbiprofen, J. Pharm. Sci. 88 (1999) 103–108.

[35] L. Yu, Inferring thermodynamic stability relationship of polymorphs from melting data, J. Pharm. Sci. 84 (1995) 966–974.

[36] S. Toscani, An up-to-date approach to drug polymorphism, Thermochim. Acta 321 (1998) 73–79.

[37] G.U. Kulkarni, P. Kumardhas, C.N.R. Rao, Charge density study of the polymorphs of *p*-nitrophenol, Chem. Mater. 10 (1998) 3498–3505.

[38] D. Singh, P.V. Marshall, L. Shields, P. York, Solid-state characterization of chlordiazepoxide polymorphs, J. Pharm. Sci. 87 (1998) 655–662.

[39] N. Blagden, R.J. Davey, H.F. Lieberman, L. Williams, R. Payne, R. Roberts, R. Rowe, R. Docherty, Crystal chemistry and solvent effects in polymorphic systems–sulfathiazole, J. Chem. Soc., Faraday Trans. 94 (1998) 1035–1044.

[40] M.R. Caira, M. Zanol, T. Peveri, A. Gazzaniga, F. Giordano, Structural characterization of two polymorphic forms of piroxicam pivalate, J. Pharm. Sci. 87 (1998) 1608–1614.

[41] M. Yokota, H. Uekusa, Y. Ohashi, Structural analysis of two crystal forms of paroxetine hydrochloride, Bull. Chem. Soc. Jpn. 72 (1999) 1731–1736.

[42] L. Yu, G.A. Stephenson, C.A. Mitchell, C.A. Bunnell, S.V. Snorek, J.J. Bowyer, T.B. Borchardt, J.G. Stowell, S.R. Byrn, Thermochemistry and conformational polymorphism of a hexamorphic crystal system, J. Am. Chem. Soc. 122 (2000) 585–591.

[43] G.A. Stephenson, T.B. Borchardt, S.R. Byrn, J. Bowyer, C.A. Bunnell, S.V. Snorek, L. Yu, Conformational and color polymorphism of 5-methyl-2-[(2-nitrophenyl)amino]-3-thiophenecarbonitrile, J. Pharm. Sci. 84 (1995) 1385–1386.

[44] R.D. Skwierczynski, Disorder, molecular mobility, and solid-state kinetics: the two-environment model, J. Pharm. Sci. 88 (1999) 1234–1236.

[45] S.S. Leung, B.E. Padden, E.J. Munson, D.J.W. Grant, Solid-state stability studies of model dipeptides: aspartame and aspartylphenylalanine, J. Pharm. Sci. 86 (1997) 64–71.

[46] M. Yoshino, K. Takahashi, Y. Ohuda, T. Yoshizawa, N. Fukushima, M. Naoki, Contribution of hydrogen bonds to equilibrium αβ transition of resorcinol, J. Phys. Chem. A 103 (1999) 2775–2783.

[47] A. Schmidt, S. Kabaya, M. Appel, S. Khatib, M. Botoshansky, Y. Eichen, Measuring the temperature width of a first-order single crystal to single crystal phase transition using solid-state NMR: Application to the polymorphism of 2-(2,4-dinitrobenzyl)-3-methylpyridine, J. Am. Chem. Soc. 121 (1999) 11291–11299.

[48] G. McGeorge, R.K. Harris, A.S. Batsanov, A.V. Churakov, J.F. Chippendale, J.F. Bullock, Z. Gan, Analysis of a solid-state conformational rearrangement using ^{15}N-NMR and X-ray crystallography, J. Phys. Chem. A 103 (1999) 3505–3513.

[49] H. Takeshita, Y. Suzuki, Y. Nibu, H. Shimada, R. Shimada, Pressure effect on phase transitions in hexamethylbenzene crystals, Bull. Chem. Soc. Jpn. 72 (1999) 381–387.

[50] A. Ikuta, Y. Suzuki, Y. Nibu, H. Shimada, R. Shimada, Temperature and pressure induced phase transition in tetrafluoro-1,4-benzoquinone crystal, Bull. Chem. Soc. Jpn. 72 (1999) 963–969.

[51] K. Knapman, Polymorphic predictions, Modern Drug Discovery 3 (2000) 53–57.

[52] R.J. Gdanitz, H.R. Karfunkel, F.J.J. Leusen, The prediction of yet-unknown molecular crystal structures by solving the packing problem, J. Mol. Graph. 11 (1993) 275–276.

[53] H.R. Karfunkel, R.J. Gdanitz, Ab initio prediction of possible crystal structures for general organic molecules, J. Comp. Chem. 13 (1992) 1171–1183.

[54] H.R. Karfunkel, F.J.J. Leusen, Practical aspects of predicting possible crystal structures on the basis of molecular information only, Speedup 6 (1992) 43–50.

[55] R.S. Payne, R.J. Roberts, R.C. Rowe, R. Docherty, Examples of successful crystal structure prediction: polymorphs of primidone and progesterone, Int. J. Pharm. 177 (1999) 231–245.

[56] H.R. Karfunkel, Crystal packing calculations and Rietveld refinement in elucidating the crystal structures of two modifications of 4-amidinoindanone guanylhydrazone, Acta Crystallogr. B52 (1996) 555–561.

[57] R.S. Payne, R.C. Rowe, R.J. Roberts, M.H. Charlton, R. Docherty, Potential polymorphs of aspirin, J. Comp. Chem. 20 (1999) 262–273.

[58] P. Verwer, F.J.J. Leusen, Computer simulation to predict possible crystal polymorphs, in: K.B. Lipkowitz, D.B. Boyd (Eds.), Reviews in Computational Chemistry, Vol. 12, Wiley–VCH, New York, 1998, pp. 327–365.

[59] N. Blagden, R.J. Davey, R. Rowe, R. Roberts, Disappearing polymorphs and the role of reaction by-products: the case of sulfathiazole, Int. J. Pharm. 172 (1998) 169–177.

[60] R.J. Davey, N. Blagden, G.D. Potts, R. Docherty, Polymorphism in molecular crystals: stabilization of a metastable form by conformational mimicry, J. Am. Chem. Soc. 119 (1997) 1767–1772.

[61] Z.G. Li, R.L. Harlow, C.M. Foris, H. Li, P. Ma, R.D. Vickery, M.B. Maurin, B.H. Toby, Polymorph determination for the GP IIb/IIIa antagonist, roxifiban, using a combination of electron diffraction and synchrotron X-ray powder diffraction techniques, J. Pharm. Sci. 88 (1999) 297–301.

[62] A. Burger, K.T. Koller, Polymorphism without IR- and Raman-spectroscopic differences: tiaprofenic acid, three modifications, Pharmazie 54 (1999) 365–368.

[63] M. Goodman, R.H. Mattern, P.G.A. Santini, R. Iacovino, M. Saviano, E. Benedetti, X-Ray structures of new dipeptide taste ligands, J. Peptide Sci. 4 (1998) 229.

[64] Z. Dong, Young Jr., V.G., Padden, B.E, Schroeder, S.A., Prakash, I., Munson, E.J., Grant, D.J.W., Crystal structure and physical characterization of neotame methanol solvate, J. Chem. Crystallogr. 29 (2000) 967–975.

[65] Z. Dong, B.E. Padden, S.A. Schroeder, E.J. Munson, D.J.W. Grant, Preparation and characterization of polymorphs of neotame anhydrate, AAPS PharmSci. Suppl. 1 (1999) S-182, 2351.

[66] P. Gao, Determination of the composition of delavirdine mesylate polymorph and pseudopolymorph mixtures using ^{13}C-CP-MAS NMR, Pharm. Res. 13 (1996) 1095–1104.

UM00012158
NOVARTIS EXHIBIT 1517
Novartis v. Regents, IPR2023-01347
Page 904 of 4460

[67] G.A. Stephenson, R.R. Pfeiffer R.P, S.R. Byrn, Solid-state investigation of the tautomerism of acetohexamide, Int. J. Pharm. 146 (1997) 93–99.
[68] H.P. Stahl, The problems of drug interactions with excipients, in: D.D. Braimar (Ed.), Towards Better Safety of Drugs and Pharmaceutical Products, Elsevier/North-Holland Biomedical Press, 1980, pp. 265–280.
[69] K.J. Guillory, Generation of polymorphs, hydrates, solvates, and amorphous solids, in: H.G. Brittain (Ed.), Polymorphism in Pharmaceutical Solids, Vol. 95, Marcel Dekker, New York, 1999, pp. 183–226.
[70] J.S.G. Cox, G.D. Woodard, W.C. McCrone, Solid-state chemistry of cromolyn sodium (disodium cromoglycate), J. Pharm. Sci. 60 (1971) 1458–1465.
[71] L.R. Chen, V.G. Young Jr., D. Lechuga-Ballesteros, D.J.W. Grant, Solid-state behavior of cromolyn sodium hydrates, J. Pharm. Sci. 88 (1999) 1191–1200.
[72] S. Hamodrakas, A.J. Geddes, B. Sheldrick, X-Ray analysis of disodium cromoglycate, J. Pharm. Pharmacol. 26 (1973) 54–56.
[73] S.M. Reutzel, V.A. Russell, Origins of the unusual hygroscopicity observed in LY297802 tartarate, J. Pharm. Sci. 87 (1998) 1568–1571.
[74] R. Bandyopadhyay, K. Erixon, V.G. Young Jr., D.J.W. Grant, Effects of water activity on recrystallized L-lysine monohydrochloride, in: Proceedings of the World Congress on Particle Technology, The Brighton Center, Brighton, 7–9 1998.
[75] J. Sheng, G.M. Venkatesh, S.P. Duddu, D.J.W. Grant, Dehydration behavior of eprosartan mesylate dihydrate, J. Pharm. Sci. 88 (1999) 1021–1029.
[76] R. Khankari, L. Chen, D.J.W. Grant, Physical characterization of nedocromil sodium hydrates, J. Pharm. Sci. 87 (1998) 1052–1061.
[77] S. Ghosh, D.J.W. Grant, Determination of the solubilities of crystalline solids in solvent media that induce phase changes: Solubilities of 1,2-dialkyl-3-hydroxy-4-pyridones and their formic acid solvates in formic acid and water, Int. J. Pharm. 114 (1995) 185–196.
[78] S.R. Byrn, Solid-State Chemistry of Drugs, Academic Press, New York, 1982.
[79] J. Han, R. Suryanarayanan, Applications of pressure differential scanning calorimetry in the study of pharmaceutical hydrates I. Carbamazepine dihydrate, Int. J. Pharm. 157 (1997) 209–218.
[80] C. Rodriguez, D.E. Bugay, Characterization of pharmaceutical solvates by combined thermogravimetric and infrared analysis, J. Pharm. Sci. 86 (1997) 263–266.
[81] R. Hüttenrauch, Molecular pharmaceutics as the basis of modern drug formulation, Acta Pharm. Technol., APV Informationsdienst Suppl. 6 (1978) 55–127.
[82] S.S. Leung, B.E. Padden, E.J. Munson, D.J.W. Grant, Solid-state characterization of two polymorphs of aspartame hemihydrate, J. Pharm. Sci. 87 (1998) 501–507.
[83] P. Longuemard, M. Jbilou, A.M. Guyot-Hermann, J.C. Guyot, Ground and native crystals: comparison of compression capacity and dissolution rate, Int. J. Pharm. 170 (1998) 51–61.
[84] B.C. Hancock, G. Zografi, Effects of solid-state processing on water vapor sorption by aspirin, J. Pharm. Sci. 85 (1996) 246–248.
[85] L. Yu, N. Milton, E.G. Groleau, D.S. Mishra, R.E. Vansickle, Existence of a mannitol hydrate during freeze–drying and practical implications, J. Pharm. Sci. 88 (1999) 196–198.
[86] K.G. Van Scoik, J.T. Carstensen, Nucleation phenomena in amorphous sucrose systems, Int. J. Pharm. 58 (1990) 185–196.
[87] A. Saleki-Gerhardt, C. Ahlneck, G. Zografi, Assessment of disorder in crystalline solids, Int. J. Pharm. 101 (1994) 237–247.
[88] M.J. Pikal, A.L. Lukes, J.E. Lang, K. Gaines, Quantitative crystallinity determinations for beta-lactam antibiotics by solution calorimetry: correlations with stability, J. Pharm. Sci. 67 (1978) 767–769.
[89] H.G. Brittain, D.J.W. Grant, Effects of polymorphism and solid-state solvation on solubility and dissolution rate, in: H.G. Brittain (Ed.), Polymorphism in Pharmaceutical Solids, Vol. 95, Marcel Dekker, New York, 1999, pp. 279–330.
[90] G. Buckton, E. Yonemochi, J. Hammond, A. Moffat, The use of near infra-red spectroscopy to detect changes in the form of amorphous and crystalline lactose, Int. J. Pharm. 168 (1998) 231–241.
[91] E.A. Schmitt, D. Law, G.G.Z. Zhang, Nucleation and crystallization kinetics of hydrated amorphous lactose above the glass transition temperature, J. Pharm. Sci. 88 (1999) 291–296.
[92] A. Salari, R.E. Young, Application of attenuated total reflectance FTIR spectroscopy to the analysis of mixtures of pharmaceutical polymorphs, Int. J. Pharm. 163 (1998) 157–166.
[93] X.J. Gu, W. Jiang, Characterization of polymorphic forms of flucanazole using Fourier transform Raman spectroscopy, J. Pharm. Sci. 84 (1995) 1438–1441.
[94] F.W. Langkilde, J. Sjoblom, L. Tekenbergs-Hjelte, J. Mrak, Quantitative FT-Raman analysis of two crystal forms of a pharmaceutical compound, J. Pharm. Biomed. Anal. 15 (1997) 687–696.
[95] S. Agatonovic-Kustrin, V. Wu, T. Rades, D. Saville, I.G. Tucker, Powder diffractometric assay of two polymorphic forms of ranitidine hydrochloride, Int. J. Pharm. 184 (1999) 107–114.
[96] S. Agatonovic-Kustrin, I.G. Tucker, D. Schmierer, Solid state assay of ranitidine HCl as a bulk drug and as active ingredient in tablets using DRIFT spectroscopy with artificial neural networks, Pharm. Res. 16 (1999) 1477–1482.
[97] H.G. Brittain, Perspective on polymorphism, Pharm, Technol. 18 (1994) 50–52.
[98] J. Bernstein, R.J. Davey, J. Henck, Concomitant polymorphs, Angew. Chem. Int. Ed. 38 (1999) 3440–3461.
[99] M. Hatada, J. Jancarik, B. Graves, S.H. Kim, Crystal structure of aspartame, a peptide sweetener, J. Am. Chem. Soc. 107 (1985) 4279–4282.

UM00012159
NOVARTIS EXHIBIT 1517
Novartis v. Regents, IPR2023-01347
Page 905 of 4460

8

Polymorphism

by Walter C. McCrone, McCrone Associates, Inc., Chicago, Illinois

Contents

I. Introduction 726
II. Mechanisms of Polymorphic Transformations 728
1. Transformations of Secondary Coordination 729
A. Displacive Transformation 729
B. Reconstructive Transformation 729
2. Transformations of Disorder 729
A. Rotational Disorder Transformation 729
B. Substitutional Disorder Transformation 729
3. Transformations of First Coordination 730
A. Dilational Transformation 730
B. Reconstructive Transformation 731
4. Transformations of the Bond Type 731
5. First- and Second-Order Transitions 731
III. Nucleation 732
IV. Phase Diagrams 733
1. Enantiotropic and Monotropic Systems 734
2. Conventions for Naming Polymorphs 736
3. Determining the Melting Points of Metastable Polymorphs . . . 737
4. Binary Systems Involving Polymorphism 737
V. Determination of Transition Temperature 740
1. Solution Phase Transformations 742
2. Solid-Solid Transformations 744
VI. Preparation of Metastable Polymorphs 747
1. Methods Based on Thermodynamic Equilibrium 747
2. Methods Based on Prevention of Thermodynamic Equilibrium . . 747
A. Solution Phase Preparations of Metastable Phases 748
B. Preparation of Metastable Phases from the Melt 749

UM00012160
NOVARTIS EXHIBIT 1517
Novartis v. Regents, IPR2023-01347
Page 906 of 4460

C. Preparation of Metastable Phases from the Vapor 751
3. Stability, Metastability, and Instability 751
VII. Solution Phase Transformation Rates 753
VIII. Pseudopolymorphism 753
1. Desolvation 754
2. Second-Order Transitions 754
3. Dynamic Isomerism 754
4. Mesomorphism 756
5. Polymerism 758
6. Grain Growth (Boundary Migration and Recrystallization) . . . 759
7. Lattice Strain 760
IX. Study of a Compound to Determine whether Polymorphism Exists . . 762
X. Are Two Given Samples Polymorphic Forms of the Same Compound? . 764
XI. Conclusion 765
XII. References 766

I. Introduction

The polymorphism of any element or compound is its ability to crystallize as more than one distinct crystal species (e.g., carbon as cubic diamond or hexagonal graphite). In spite of the fact that different polymorphs of a given compound are, in general, as different in structure and properties as the crystals of two different compounds, most chemists are almost completely unaware of the nature of polymorphism and the potential usefulness of knowledge of this phenomenon in research. As one example of the latter might be mentioned the fact that the efficacy of a drug depends on its solubility in the blood or in the gastric fluids, and the solubility may vary as much as an order of magnitude from one crystal form of a given compound to another. Density, hardness, crystal shape, optical and electrical properties, vapor pressure, etc., all vary with the polymorphic form. In many systems it is possible to obtain different crystal forms and thus obtain the best performance properties for that compound. To do so requires a knowledge of the phenomenon and of the behavior of polymorphs.

Mitscherlich is generally given credit for first using the term *polymorphism* during his work on the isomorphous sulfates of iron (ferrous), cobalt, nickel, magnesium, copper, zinc, and manganese. It is, however, obvious that the idea was not new at that time, since Humphrey Davy in 1809 pointed out that diamond and graphite are both carbon and that the two differ only in their arrangement of carbon atoms in the solid phase. Indeed, Klaproth may have been the first to be aware of polymorphism when he observed (1788) that calcium carbonate crystallizes both as calcite and as aragonite.

Since that time a very large number of compounds, organic and inorganic, as well as the elements themselves, have been shown to crystallize in two or

UM00012161
NOVARTIS EXHIBIT 1517
Novartis v. Regents, IPR2023-01347
Page 907 of 4460

ɔm the Vapor 751
. 751
. 753
. 753
. 754
. 754
. 754
. 756
. 758
l Recrystallization) . . . 759
. 760
er Polymorphism Exists . . 762
ns of the Same Compound? . 764
. 765
. 766

ion

mpound is its ability to crystallize
e.g., carbon as cubic diamond or
at different polymorphs of a given
ı structure and properties as the
t chemists are almost completely
and the potential usefulness of
h. As one example of the latter
cy of a drug depends on its solu-
d the solubility may vary as much
ıl form of a given compound to
optical and electrical properties,
morphic form. In many systems
ıs and thus obtain the best per-
o do so requires a knowledge of
lymorphs.
ırst using the term *polymorphism*
ɜ of iron (ferrous), cobalt, nickel,
It is, however, obvious that the
ey Davy in 1809 pointed out that
that the two differ only in their
ase. Indeed, Klaproth may have
ı when he observed (1788) that
e and as aragonite.
npounds, organic and inorganic,
n shown to crystallize in two or

more different crystalline arrangements—chemically identical, physically different. Besides graphite and diamond there are, to name a few in the mineral field, wurtzite and sphalerite (ZnS); calcite, aragonite, and vaterite ($CaCO_3$); rutile, brookite, and anatase (TiO_2). Most compounds, especially organic ones, do not have special names for the polymorphic forms and instead have been referred to as α, β, γ, etc., or I, II, III, etc., depending on the worker's whim. Many compounds are not content with two or three different crystal forms but have five, six, or seven, and even ten, eleven, or more. Ammonium nitrate has five forms, progesterone also has five, water has eight or nine, tripalmitin has seven, and some drugs have been found to have ten or more different crystal forms.

It is at least this author's opinion that every compound has different polymorphic forms and that, in general, the number of forms known for a given compound is proportional to the time and money spent in research on that compound. A corollary of this Parkinsonian digression is that all the common and important compounds (and elements) show polymorphism—silica, iron, calcium silicate, soap, sulfur, paraffin waxes, etc. It is now apparent that most, if not all, compounds and elements show a variety of different crystal forms. Deffet (*1*) has summarized the properties of a number of organic systems exhibiting polymorphism.

A polymorph is a solid crystalline phase of a given compound resulting from the possibility of at least two different arrangements of the molecules of that compound in the solid state. The molecule itself may be of different shape in the two polymorphs, but that is not necessary and, indeed, certain changes in shape (involving dynamic isomerism or tautomerism) involve formation of different molecules and hence do not constitute polymorphism. Geometrical isomers or tautomers, even though interconvertible and reversibly so, cannot be called polymorphs although they may behave in a confusingly similar manner (see Section VIII-3). Shape changes, permissible in the molecule crystallizing in two or more polymorphic forms, include resonance structures, rotation of parts of the molecule about certain bonds, and minor distortions of bond distances and angles. These distortions of molecular shape result from polarizability effects of one molecule on another due to the change in relative positions of adjacent molecules in the two different crystalline arrangements.

A safe criterion for classification of a system as polymorphic is the following. Two polymorphs will be different in crystal structure but identical in the liquid and vapor states. Dynamic isomers will melt at different temperatures, as do polymorphs, but will give melts of different composition. In time each of these melts changes to an equilibrium mixture of the two isomers with temperature-dependent composition. Some reported cases of polymorphism

UM00012162
NOVARTIS EXHIBIT 1517
Novartis v. Regents, IPR2023-01347
Page 908 of 4460

are undoubtedly dynamic isomerism, since the two behave quite similarly, especially if the equilibrium between the two isomers is very rapidly established.

Polymorphism of the elements is often referred to as *allotropy*, although the same term is also applied to elements such as sulfur and phosphorus, for which different molecular species exist. Sulfur, for example, exists in the melt as a ternary mixture of S_λ, S_μ, S_π molecules, a dynamic equilibrium varying in composition with temperature and pressure. S_λ is the normal form and crystallizes as either of the two common polymorphs, orthorhombic or monoclinic. There seems to be little justification for use of the special word *allotropy* for the elements, since it includes two phenomena identical in character and behavior with true polymorphism and true dynamic isomerism exhibited by compounds in general. Polymorphism must also be carefully differentiated from polymerization. Oxygen (O_2) and ozone (O_3) are different polymers, just as paraldehyde is a polymer of acetaldehyde. Both dynamic isomers (tautomers) and polymers have different liquid as well as different solid phases; polymorphs, again, are different in the solid state but are identical in the liquid phase.

II. Mechanisms of Polymorphic Transformation

Buerger (*2*) has summarized the different types of polymorphic transformations on the basis of the structural changes involved (Table I). He has also included the general range of the rates of transformation for each type. A rough correlation between rate and type of transformation is possible because the energy required to effect a transformation is related to the structural changes involved. However, exceptions to the tabulated rates have

TABLE I

TRANSFORMATION TYPES AND RELATIVE RATES OF TRANSFORMATION

Transformations of secondary coordination (network transformations)	
Displacive	(rapid)
Reconstructive	(sluggish)
Transformations of disorder	
Rotational	(rapid)
Substitutional	(sluggish)
Transformations of first coordination	
Dilational	(rapid)
Reconstructive	(sluggish)
Transformations of bond type	(usually sluggish)

UM00012163

NOVARTIS EXHIBIT 1517
Novartis v. Regents, IPR2023-01347
Page 909 of 4460

the two behave quite similarly,
o isomers is very rapidly estab-

ferred to as *allotropy*, although
h as sulfur and phosphorus, for
lfur, for example, exists in the
lecules, a dynamic equilibrium
nd pressure. S_λ is the normal
mon polymorphs, orthorhombic
ification for use of the special
des two phenomena identical in
sm and true dynamic isomerism
orphism must also be carefully
O_2) and ozone (O_3) are different
f acetaldehyde. Both dynamic
rent liquid as well as different
t in the solid state but are iden-

: Transformation

types of polymorphic trans-
anges involved (Table I). He
tes of transformation for each
pe of transformation is possible
nsformation is related to the
ons to the tabulated rates have

ATES OF TRANSFORMATION

(network transformations)
(rapid)
(sluggish)
(rapid)
(sluggish)
(rapid)
(sluggish)
(usually sluggish)

been observed, and it is usually best to expect unexpected behavior. The red and yellow forms of HgI_2, for example, are related through a reconstructive transformation, and, although this transition is difficult to initiate in single crystals, it progresses rapidly once started. There is the further unusual observation that, when this transformation is repeated in the same crystals by recycling the temperature, the rates of both transformation and initiation are considerably increased.

1. Transformations of Secondary Coordination

A. Displacive Transformation

A displacive transformation of secondary coordination involves bending but no breaking of the lattice network; consequently the rate of transformation can be very rapid and the energy involved is low. The high-temperature form has the higher symmetry and the lower density.

B. Reconstructive Transformation

Here the lattice network is broken and re-formed into a new arrangement. Since first coordination bonds are broken and re-formed, such transformations are usually very sluggish. The high-temperature form usually has the lower density but not necessarily the higher symmetry.

A good example of these two types of transformation is furnished by SiO_2, silica, which has seven crystal forms as shown in Table II.

2. Transformations of Disorder

A. Rotational Disorder Transformation

A rotational disorder transformation is characteristic of a structure in which some weaker bonds are broken while the stronger bonds remain. Parts of the molecule may then rotate about the fixed structure. This transformation resembles the displacive transformation in that the high-temperature form has the higher symmetry and lower density.

B. Substitutional Disorder Transformation

A substitutional disorder transformation takes place in systems in which two different atoms present in the lattice can, from a valence and ionic radius point of view, occupy the same lattice points. In this case, diffusion of one

UM00012164
NOVARTIS EXHIBIT 1517
Novartis v. Regents, IPR2023-01347
Page 910 of 4460

atom species among the other atom species may cause the system to pass from a system of high order to one of disorder. Metals and silicate minerals show this type of transformation. In a feldspar having the formula $Na(Si_3, Al)O_8$ or $Ca(Si_2, Al_2)O_8$, the Si and Al may be ordered with respect to the overall lattice at low temperatures but disordered at high temperatures. Again the high temperature forms have the higher symmetry and the lower density.

TABLE II

TRANSFORMATIONS OF SILICA

Reconstructive	Displacive
Cristobalite	High cristobalite
	↕ 200–270°C
↓ 1470°C	Low cristobalite
	High tridymite
	↕ 160°C
Tridymite	Middle tridymite
	↕ 105°C
↑ 867°C	Low tridymite
	High quartz
Quartz	↕ 573°C
	Low quartz

3. *Transformations of First Coordination*

A. Dilational Transformation

A dilational transformation resembles in some respects a displacive transformation in that it involves small shifts in position, but it also involves a change in coordination number resulting from differential dilation. CsCl, NH_4Cl, and NH_4Br are characterized in the low-temperature form by a cubic lattice having 8-fold coordination. Above the transition temperature the structure expands along a body diagonal and contracts normal to this direction. The net result is a breaking of the contact between the body center atom and the terminal atoms on the body diagonal; this results in closer

UM00012165
NOVARTIS EXHIBIT 1517
Novartis v. Regents, IPR2023-01347
Page 911 of 4460

ıay cause the system to pass from
fetals and silicate minerals show
ıaving the formula $Na(Si_3, Al)O_8$
dered with respect to the overall
t high temperatures. Again the
ımetry and the lower density.

: SILICA

'isplacive

cristobalite

)–270°C

cristobalite

tridymite

°C

le tridymite

°C

tridymite

quartz

°C

ıuartz

Coordination

)me respects a displacive trans-
position, but it also involves
om differential dilation. CsCl,
w-temperature form by a cubic
ıe transition temperature the
nd contracts normal to this
)ntact between the body center
iagonal; this results in closer

coordination with the other six atoms. The CsCl structure with 8-fold symmetry changes thereby to an NaCl structure with 6-fold symmetry.

B. Reconstructive Transformation

When the change from one type of first coordination to another involves a reconstruction similar to the reconstructive transformations involving secondary coordination, the change is said to be a reconstructive transformation involving first coordination. The very sluggish transformation between aragonite and calcite is of this type.

4. Transformations of the Bond Type

These transformations involve a basic change in bond structure from metallic to nonmetallic, as in diamond ⇌ graphite and white tin ⇌ gray tin or from hydrogen bonding to van der Waals bonding in some organic compounds.

5. First- and Second-Order Transitions

There is another convenient way to classify transformations in general: first-order and second-order transitions. The former are the usual type. They occur at precise transition temperatures; or, rather, the free energies of the two forms become equal at a definite transition temperature, although the transformation itself may or may not occur. There is also a sudden change during first-order transformation in all physical properties of the solid (crystal symmetry, refractive indices, cell dimensions, density, specific heat, entropy, conductivity, hardness, melting point, etc.). A second-order transition, on the other hand, involves no abrupt change in entropy at the transition temperature, although the gradual change becomes more rapid at that temperature. The specific heat, however, rises to a high and sharp maximum at the second-order transition point (often called a lambda point).

A second-order transition may or may not involve a change in crystal structure. In any case, the change in lattice is not great and the properties of the two "forms" will be very similar. The ammonium halides show several second-order transitions. Ammonium bromide, for example, is tetragonal, though pseudo-cubic, at low temperatures; but at −39°C the lattice changes to body-centered cubic, and at about 41°C the lattice again changes to face-centered cubic. Both are second-order transitions.

Order-disorder and rotational transformations are often the basis for

UM00012166
NOVARTIS EXHIBIT 1517
Novartis v. Regents, IPR2023-01347
Page 912 of 4460

second-order transitions in solids. In addition, the demagnetization of iron and cobalt on heating falls in this category. Stavely (*3*) has written an excellent discussion of second-order transitions.

III. Nucleation

Attempts to categorize phase transformations have been very successful, especially through the efforts of Buerger (*2*); however, as an increasing number of systems become better understood, it becomes more obvious that there is a continuous spectrum of behavior. Although Buerger's classification gives unequivocal categories for perhaps 90% of all transformations, there will be an increasing number of systems that appear to involve at least two different mechanisms of transformation. This is not meant, in any sense, as a criticism of Buerger's classification but more as a tribute to the versatility of the changes in crystal lattices. More work should, however, be carried out on rate of transformation, and, in particular, the rate of nucleation should be differentiated from the rate of transformation. A transformation may be sluggish either with respect to nucleation alone or to both nucleation and growth. Many metastable systems, once the stable form has nucleated, will transform very rapidly. Systems of polymorphs vary considerably in these respects, and the rates of nucleation and transformation are usually dependent as much on temperature, particle size, purity, and physical agitation as on the nature of the structural change involved.

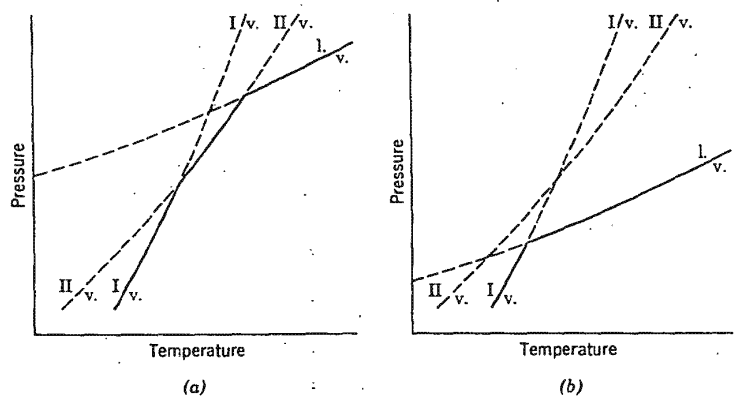


Figure 1. Sublimation and boiling point curves for (*a*) enantiotropic system and (*b*) monotropic system.

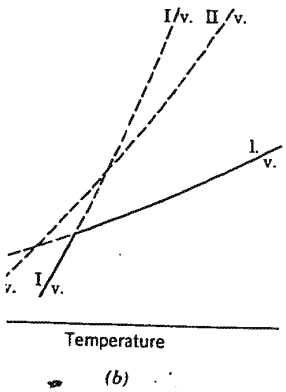
UM00012167

NOVARTIS EXHIBIT 1517
Novartis v. Regents, IPR2023-01347
Page 913 of 4460

on, the demagnetization of iron
Stavely (*3*) has written an excel-

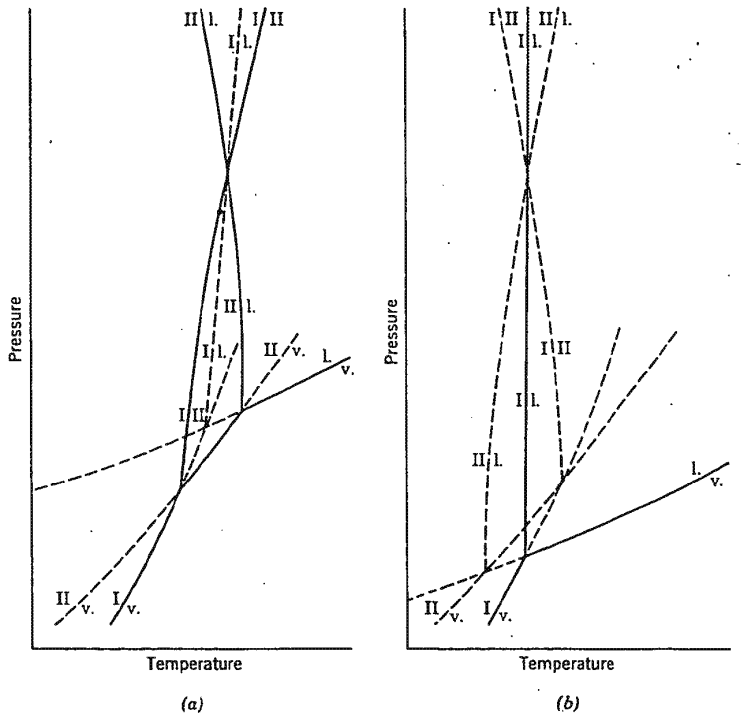
n

ions have been very successful,
2); however, as an increasing
l, it becomes more obvious that
Although Buerger's classification
% of all transformations, there
appear to involve at least two
s is not meant, in any sense, as
re as a tribute to the versatility
should, however, be carried out
the rate of nucleation should
ion. A transformation may be
one or to both nucleation and
stable form has nucleated, will
phs vary considerably in these
sformation are usually depend-
urity, and physical agitation as
d.



(*b*)

(*a*) enantiotropic system and (*b*)



(*a*) (*b*)

Figure 2. Melting point and transition temperature curves added to the curves in Figure 1; (*a*) enantiotropic and (*b*) monotropic.

IV. Phase Diagrams

Before suggesting ways of answering some of the practical questions regarding polymorphism, it is worthwhile to review the types of phase diagrams shown by systems involving polymorphs. This will be done first for a simple example of a system of two forms only.

There will be only one liquid-vapor (boiling point) curve in the pressure-temperature diagram, since both polymorphs give identical liquid phases on melting. Each polymorph, moreover, has its own solid-vapor (sublimation or vapor pressure) curve (Fig. 1) and its own solid-melt (melting point) curve. The complete diagram, of course, contains the melt-vapor, the solid-vapor, and the solid-melt curves (Fig. 2), and these can intersect to give either of two

UM00012168
NOVARTIS EXHIBIT 1517
Novartis v. Regents, IPR2023-01347
Page 914 of 4460

possibilities: the melt-vapor curve may, in general, intersect the two solid-vapor curves above or below their intersection. It is not unknown for the three curves to intersect at the same point. When this occurs, the melting points of the two polymorphic forms and the transition temperature coincide (e.g., for β-naphthol and very nearly for γ-hexachlorocyclohexane, two of whose forms melt only 0.1°C apart).

1. Enantiotropic and Monotropic Systems

It is not necessarily true that the melting point and transition curves intersect at high pressures, but the possibility exists. It is interesting to note that in this case the enantiotropic system becomes a monotropic system at high pressures and vice versa. Considering this situation and the general fact that most systems do not show an easily determined transition temperature, it becomes obvious that these two terms, *enantiotropic* and *monotropic*, are dangerous words indeed. In the first place, the term *enantiotropic* can be used only when the transition temperature has been found to be below the melting point. The converse, no transition temperature below the melting point, cannot usually be interpreted to mean that the system is monotropic, because the transition temperature may be below room temperature (or below the lowest temperature studied), or it may have been unobserved because of slow transition.

There is no absolutely safe generalization relating enantiotropy and monotropy to the properties of the polymorphs, except location of the transition temperature. This is best done by direct observation, but it may be done indirectly by measuring vapor pressure or solubility curves on the two forms since both sets of curves cross at the transition temperature. The form stable

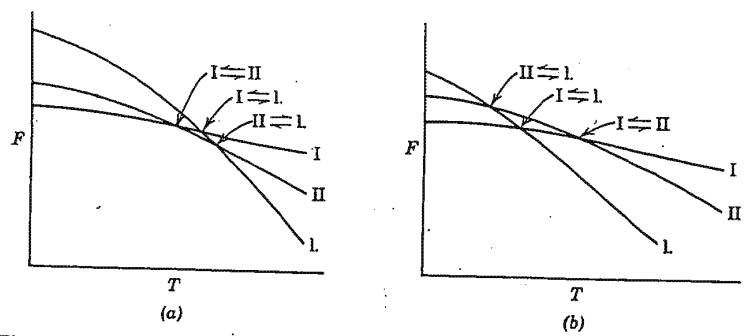


Figure 3. Free energy-temperature curves for (*a*) enantiotropic and (*b*) monotropic systems.

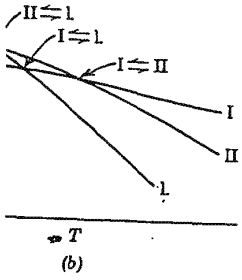
UM00012169
NOVARTIS EXHIBIT 1517
Novartis v. Regents, IPR2023-01347
Page 915 of 4460

neral, intersect the two solid-
. It is not unknown for the
'hen this occurs, the melting
ansition temperature coincide
:xachlorocyclohexane, two of

pic Systems

it and transition curves inter-
It is interesting to note that
monotropic system at high
tion and the general fact that
ed transition temperature, it
otropic and *monotropic*, are
e term *enantiotropic* can be
been found to be below the
perature below the melting
at the system is monotropic,
low room temperature (or
may have been unobserved

ing enantiotropy and mono-
pt location of the transition
vation, but it may be done
lity curves on the two forms
mperature. The form stable



(b)

pic and (*b*) monotropic systems.

at lower temperatures often has the higher density, and the form stable at the melting point always melts higher and has a lower solubility and a lower vapor pressure at that temperature.

The free energy-temperature diagrams at constant pressure are another, and perhaps clearer, way of showing phase diagrams, since the phase having the lowest free energy at a given temperature is always the stable phase at

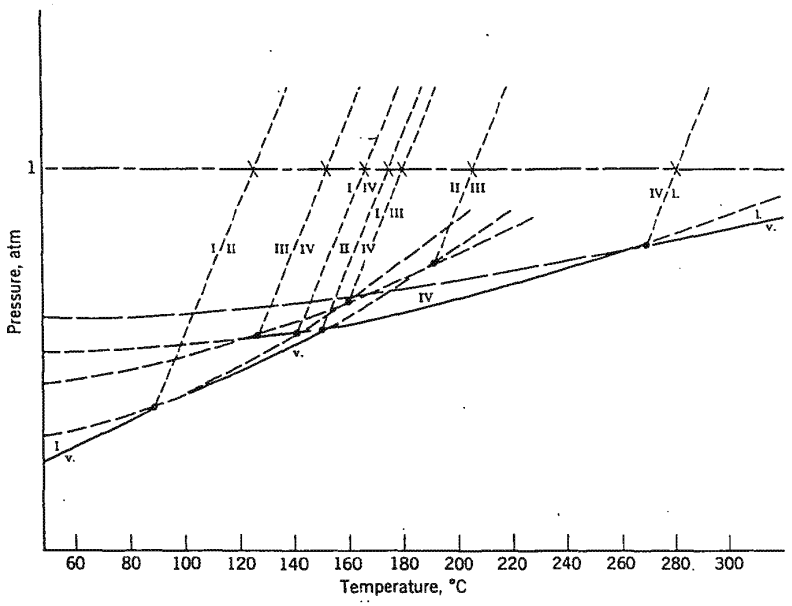


Figure 4. Pressure-temperature diagram for HMX. The diagram is only qualitatively correct except for the intersections on the 1 atm pressure line, which are measured.

that temperature. The diagrams are based on the thermodynamic relationship $(dF/dT)_P = -S$. The free energy F plotted against the temperature T at constant pressure P gives a curve for each phase, the slope of which at any temperature will be the entropy S. Figure 3 shows hypothetical phase diagrams for enantiotropic and monotropic systems.

The diagrams for systems having three or more polymorphic forms can be plotted in the same way. Figures 4 and 5 show schematic P-T and F-T diagrams for HMX (cyclotetramethylene tetranitramine). Both curves are based on measured transition temperatures at atmospheric pressure. Except for these points the curves are schematic and only qualitatively correct.

UM00012170
NOVARTIS EXHIBIT 1517
Novartis v. Regents, IPR2023-01347
Page 916 of 4460

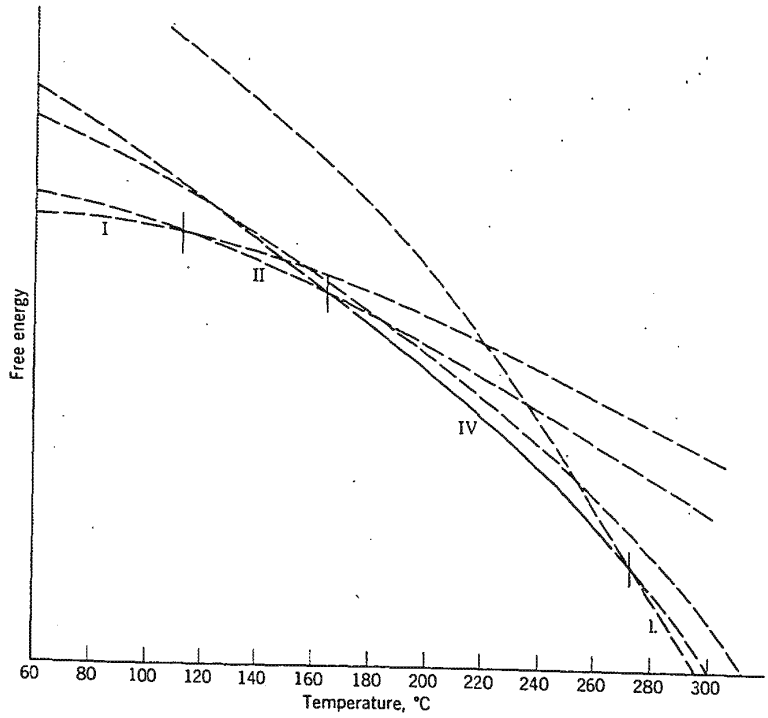


Figure 5. Free energy-temperature diagram for HMX. The intersection temperatures are measured points, but the actual slopes are unknown.

2. *Conventions for Naming Polymorphs*

On the matter of convention, the various polymorphic forms are best designated by Roman numerals: I, II, III, IV, etc. Form I should be the form most stable at room temperature. No rigid convention can be laid down for use of the higher numerals, since further work is always attended by the possibility of discovering an intermediate form *2.5* difficult to designate by Roman numerals and impossible to insert without disrupting the previous assignments of numerals. A system, as logical as it is simple, is to number the forms in the order of their discovery, which should, in general, follow their order of stability. Basing the assignment on melting points is not generally satisfactory, since these data are not always available and, in many systems,

UM00012171
NOVARTIS EXHIBIT 1517
Novartis v. Regents, IPR2023-01347
Page 917 of 4460

cannot be determined. The Kofler suggestion that the Roman numeral be succeeded by the melting point in parentheses is a logical move subject to the preceding limitation.

3. Determining the Melting Points of Metastable Polymorphs

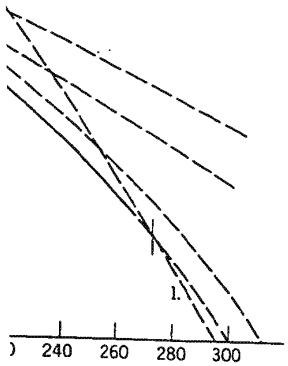
One of the obvious problems in studying polymorphism is the determination of the melting point for a metastable polymorph. This is not only necessary to characterize the system but may also be necessary to tell which form is stable (higher melting); the difference between the melting points is a measure of relative stability. If two polymorphs melt less than 1°C apart, then neither is significantly more nor less stable and either may be easily obtained on crystallization. If the two melt 25 to 50°C apart, the lower-melting form will be very difficult to crystallize and, once crystallized, will easily transform to the stable phase.

The closer the two melting points, the more easily the unstable form can be obtained, and its melting point can usually be obtained easily before a solid-solid transformation occurs. The chance of a solid-solid transformation can be considerably reduced, however, by using very small samples. Individual small crystals of even highly unstable forms can often be melted. Such preparations can often be produced by sublimation with a cold condensing surface.

When all else fails, and the melting point cannot be determined directly, it may be possible to calculate it by using the Le Chatelier equation as suggested by Verstraete (*4*).

4. Binary Systems Involving Polymorphism

Polymorphs often show up in binary systems, and systems involving polymorphs are often more easily studied as part of a binary mixture even if this involves a solvent as a second component. Again, the microscope is an excellent way to study polymorphism in binary systems because, on a small scale, many highly unstable polymorphs are sufficiently metastable to permit measurement of melting points, transition temperatures, and concentrations. The standard macroscopic physical chemical procedures are good for composition diagrams in which thermodynamic equilibrium is established, but the study of polymorphism often depends on purposely avoiding thermodynamic equilibrium or, at least, studying the rate at which equilibrium is established. With the microscope it is possible in most systems to determine a complete composition diagram not only between the stable phases but also



The intersection temperatures

olymorphs

olymorphic forms are best
etc. Form I should be the
convention can be laid down
k is always attended by the
?.5 difficult to designate by
out disrupting the previous
it is simple, is to number the
ıld, in general, follow their
ting points is not generally
able and, in many systems,

UM00012172
NOVARTIS EXHIBIT 1517
Novartis v. Regents, IPR2023-01347
Page 918 of 4460

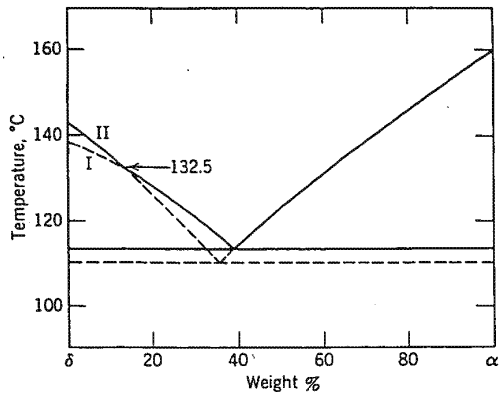


Figure 6. Composition diagram for α- and δ-hexachlorocyclohexane showing the relationship between the two polymorphs of the δ isomer and α.

between all possible pairs of stable and metastable polymorphic forms. Figure 6 shows the composition diagram for two isomers of hexachlorocyclohexane (5), the α and the δ isomers. The δ isomer has two easily obtained polymorphs, and the two melting points of the polymorphs are easily obtained on the pure compound. The transition temperature and the two eutectic temperatures are easily determined on any mixture of α and δ ranging from 5 to 30% α. The system is therefore a simple eutectic diagram of α with each

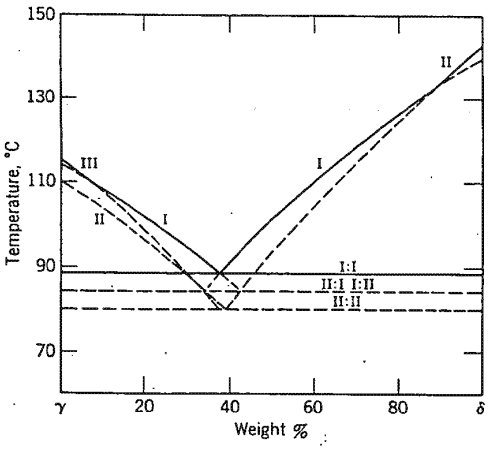
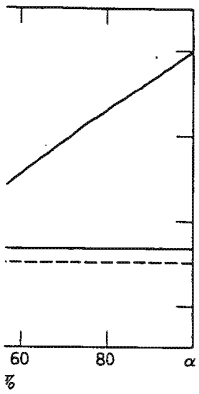


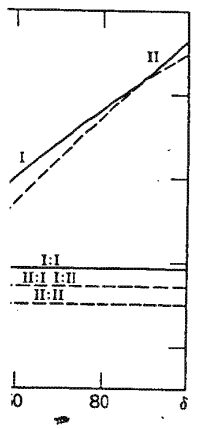
Figure 7. Composition diagram for the three polymorphs of γ- and the two polymorphs of δ-hexachlorocyclohexane.

UM00012173
NOVARTIS EXHIBIT 1517
Novartis v. Regents, IPR2023-01347
Page 919 of 4460



l δ-hexachlorocyclohexane showing the δ isomer and α.

d metastable polymorphic forms. or two isomers of hexachlorocyclo- e δ isomer has two easily obtained the polymorphs are easily obtained temperature and the two eutectic ıy mixture of α and δ ranging from ıple eutectic diagram of α with each



lymorphs of γ- and the two polymorphs

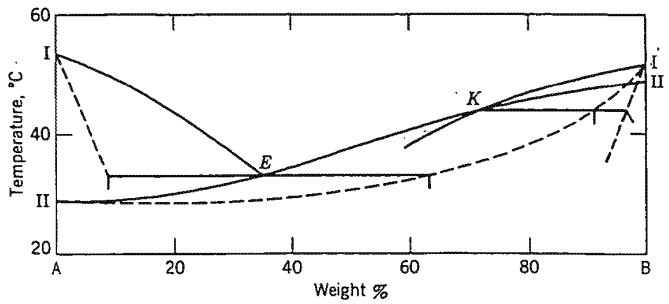


Figure 8. Composition diagram between benzalaniline (A) and dibenzyl (B) showing stabilization of a metastable lattice by solid solution formation in the range from E to K.

polymorph of δ, and the δ isomer has two polymorphs enantiotropic with respect to each other.

Not all binary systems are so simple. Figure 7, for example, shows the relationship between the three forms of γ-hexachlorocyclohexane and the two forms of the δ isomer. The different polymorphs in a given system may form isomorphous solid solutions, eutectics, or molecular addition compounds. In fact, different pairs of polymorphs may show different types of composition diagrams. For example, 1,3,5-trinitrobenzene (I) forms a eutectic with picric acid (I), but forms a continuous series of isomorphous

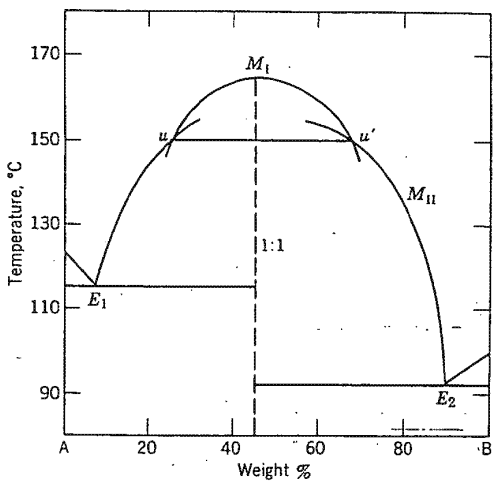


Figure 9. Composition diagram for 1,3,5-trinitrobenzene (A) and phenanthrene (B) showing polymorphism of the addition compound.

UM00012174
NOVARTIS EXHIBIT 1517
Novartis v. Regents, IPR2023-01347
Page 920 of 4460

solid solutions with picric acid (II). Composition diagrams in organic systems can be as complex as the familiar diagrams for metals and inorganic silicates. Benzalaniline and dibenzyl (*6*) form an unusual diagram in which the two metastable polymorphs of each compound form a continuous series of solid solutions, yet, over a range of composition from about 35 to 65% dibenzyl, the solid solutions are the stable phase (Fig. 8).

When the binary system shows an addition compound, it is extremely unlikely that any pair of polymorphs in that system will show any other type of diagram. An addition compound can itself show polymorphs as in the system, 1,3,5-trinitrobenzene and phenanthrene (*7*) (Fig. 9).

V. Determination of Transition Temperature

One of the most important problems in studying polymorphism in a given system is to determine the transition temperature. This not only helps to characterize the system but it also tells which form is stable at low temperatures and when the system is enantiotropic. The transition temperature is

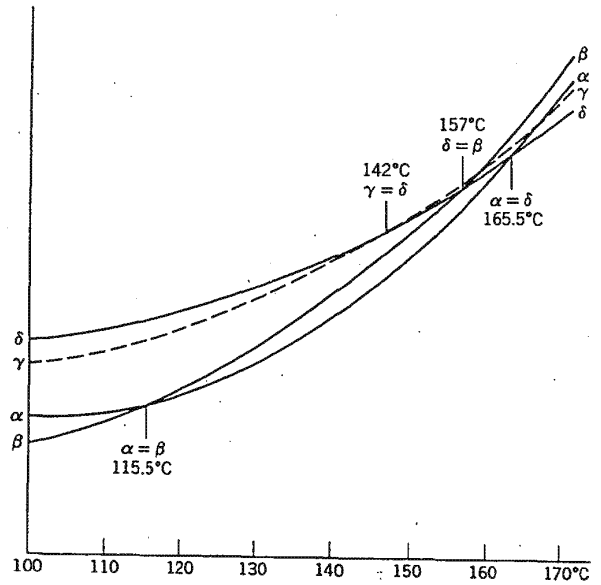


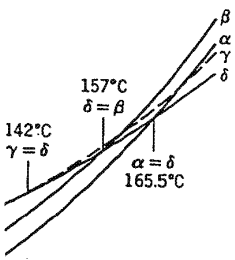
Figure 10. Solubility curves for the four polymorphic forms of HMX. Again the curves are qualitative, although the intersections are based on the measured transition temperatures.

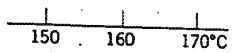
UM00012175
NOVARTIS EXHIBIT 1517
Novartis v. Regents, IPR2023-01347
Page 921 of 4460

Composition diagrams in organic
diagrams for metals and inorganic
form an unusual diagram in which
ompound form a continuous series
mposition from about 35 to 65%
phase (Fig. 8).
dition compound, it is extremely
at system will show any other type
itself show polymorphs as in the
hrene (7) (Fig. 9).

sition Temperature

in studying polymorphism in a
temperature. This not only helps
which form is stable at low tem-
pic. The transition temperature is





hic forms of HMX. Again the curves
on the measured transition tempera-

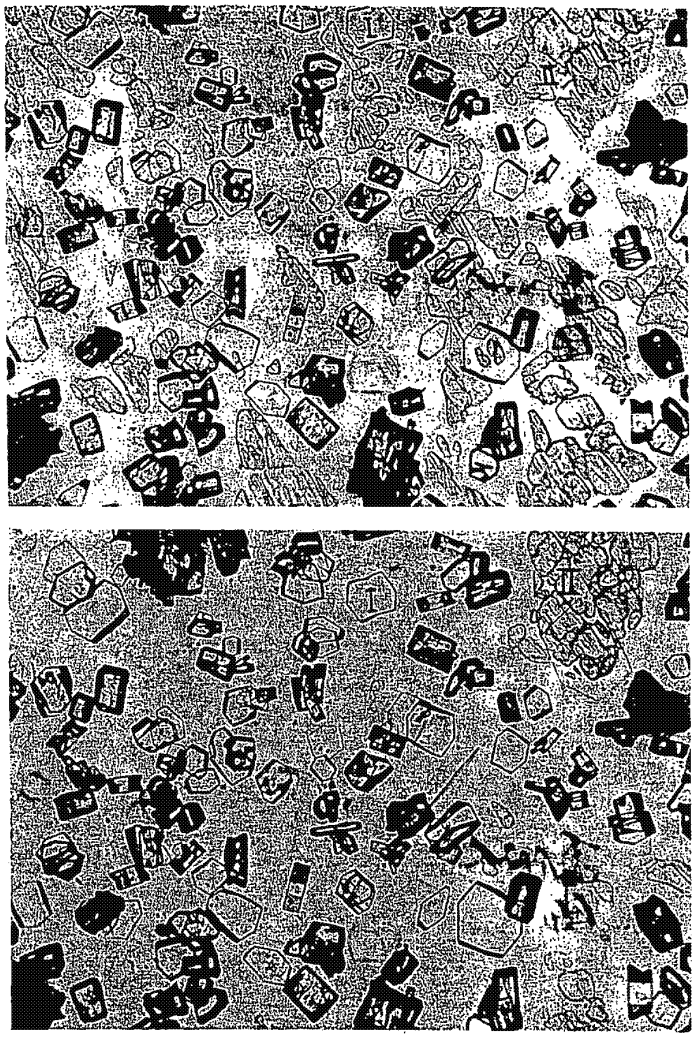


Figure 11. Photomicrographs of the same field of 1,8-dinitronaphthalene during a solution phase transformation in thymol on a microscope slide. The lower picture was taken about 20 minutes after the upper picture.

UM00012176
NOVARTIS EXHIBIT 1517
Novartis v. Regents, IPR2023-01347
Page 922 of 4460

the temperature at which the two polymorphs have identical free energies, and hence, at that temperature, both forms have identical solubilities in any solvent as well as identical vapor pressures. The latter are indicated by the *P-T* diagram in Figure 2. A corresponding diagram can also be drawn, based on the solubility curves (Fig. 10).

1. Solution Phase Transformations

The easy way to determine which of two forms is stable at a given temperature is to observe the relative solubility of the two in a solvent. This is best and most rapidly done by observing crystals of both together in a drop of

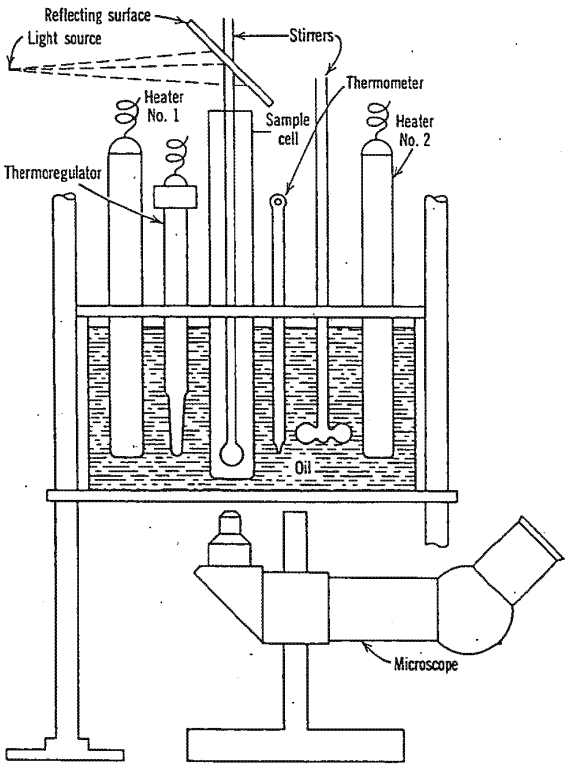


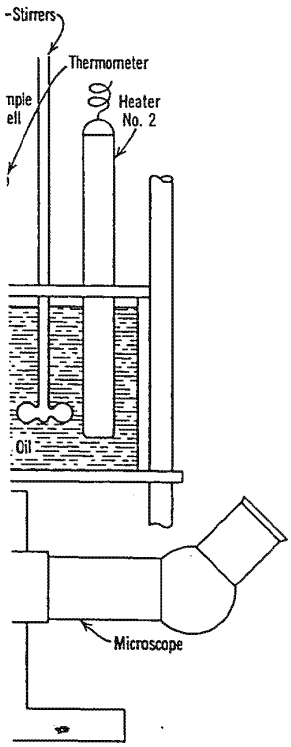
Figure 12. Experimental arrangement for observing solution phase transformations without disrupting experiment or cooling the sample before examination.

UM00012177
NOVARTIS EXHIBIT 1517
Novartis v. Regents, IPR2023-01347
Page 923 of 4460

ymorphs have identical free energies, orms have identical solubilities in any sures. The latter are indicated by the ling diagram can also be drawn, based

Transformations

f two forms is stable at a given tem- bility of the two in a solvent. This is crystals of both together in a drop of



bserving solution phase transformations mple before examination.

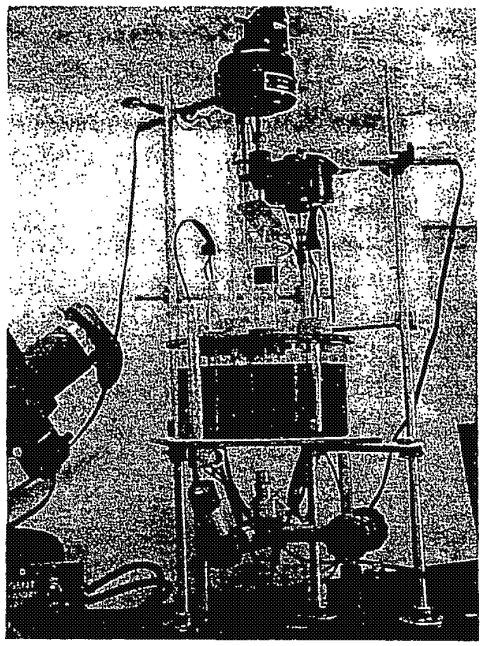


Figure 13. Photograph of apparatus shown in Figure 12.

saturated solution under the microscope. The less soluble form will grow and the more soluble will dissolve (Fig. 11). This is called a solution phase transformation, and it progresses the more rapidly the higher the solubility and the greater the difference in solubility of the two forms. The transition temperature is then the temperature at which the solubilities are equal and at which the transformation rate in either direction is zero. Above the transition temperature one form grows at the expense of the other, and below that temperature the reverse is true. By approaching the transition from both sides, the exact temperature can usually be determined to within a few tenths of a degree. This can often be done using a hot stage microscope if equilibrium is established rapidly. In some systems it is more convenient to use an apparatus which was designed and used to determine the transition temperatures for the polymorphic forms of HMX (*8*). A saturated solution containing excess solid is agitated in a narrow flat-bottomed tube, itself immersed in a carefully controlled constant-temperature bath (Figs. 12 and 13). The stable crystal phase existing at a given temperature can be quickly

UM00012178
NOVARTIS EXHIBIT 1517
Novartis v. Regents, IPR2023-01347
Page 924 of 4460

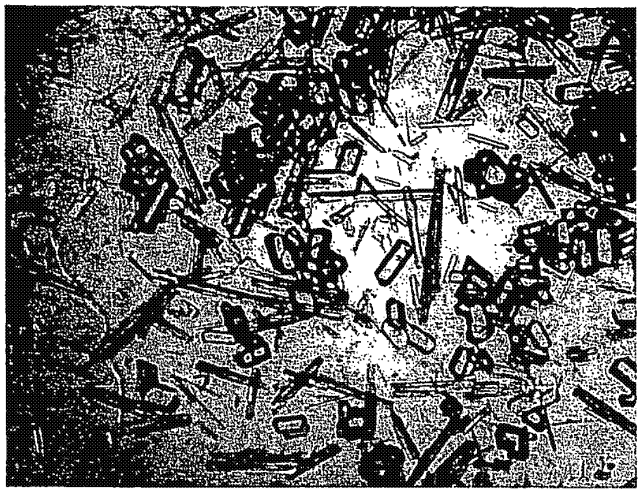


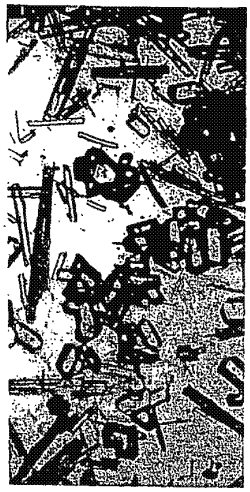
Figure 14. Photomicrograph of needles of HMX (II) transforming in butyrolactone at 110°C to HMX (I). Photomicrograph taken with polaroid camera through the inverted microscope shown in Figures 12 and 13.

checked by stopping the agitator in the long flat-bottomed tube, allowing the crystals to settle to the bottom and observing them microscopically with the inverted microscope. Figure 14 shows a photomicrograph taken through the inverted microscope during an experimental run in which a mixture of HMX (I) and HMX (II) had been agitated for several hours at 110°C. The needles of HMX (II) are gradually dissolving, showing that HMX (I) (which is growing) is the stable phase at that temperature.

2. Solid-Solid Transformations

It is sometimes possible to determine the transition temperature by observing only the solid phase during heating and cooling in the microscope hot stage. It is necessary, however, in this case to repeat the determination several times, and during both heating and cooling, since the transition usually superheats and supercools at least 1°C and often many degrees. The solid-solid transformation of HMX (I) → HMX (IV) always occurs in the range 175 to 190°C on heating and does not usually reverse at all on cooling. (The transition temperature, measured easily by observing the solution phase

UM00012179
NOVARTIS EXHIBIT 1517
Novartis v. Regents, IPR2023-01347
Page 925 of 4460



) transforming in butyrolactone at
aroid camera through the inverted

t-bottomed tube, allowing the
them microscopically with the
tomicrograph taken through
al run in which a mixture of
several hours at 110°C. The
showing that HMX (I) (which
re.

nations

sition temperature by observ-
ooling in the microscope hot
to repeat the determination
cooling, since the transition
and often many degrees. The
X (IV) always occurs in the
ally reverse at all on cooling.
observing the solution phase

transformation, is 165.5°C.) Occasionally, superheating and supercooling of the solid-solid transformation may be avoided by holding a preparation containing both polymorphs in physical contact with each other at a series of temperatures on both sides of the transition temperature and observing the direction of movement of the interface between the two forms. This is best done in a thin crystalline film prepared by crystallization from the melt (Fig. 15). The transition temperature of mercuric iodide (126°C) can be measured in this way. In passing, it is interesting to note that the transformation rate

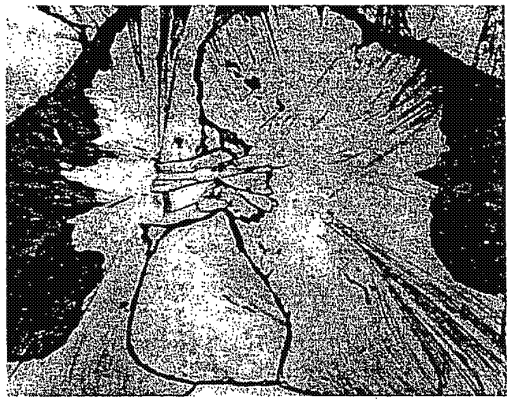


Figure 15. A solid-solid polymorphic transformation taking place in a thin crystalline film of vanillin. The darker area (pseudomorph) is an area originally unstable and now converted to the stable form.

for HgI_2 and for most other systems (referring only to the solid-solid and not to the solution phase transformation) is much more rapid the second time than the first. In other words, a given crystalline film may both nucleate and transform slowly, but, once a given area has undergone a solid-solid transformation, that region can be transformed more readily back and forth. This is presumably true for displacive rather than reconstructive transformations, since the latter are always quite sluggish and the transition temperatures for such systems must usually be measured by solution phase transformation.

The solid-solid transformation as carried out above can be converted to the always more rapid solution phase transformation by the simple expedient of touching a tiny drop of a low-boiling solvent to the edge of the preparation. Capillarity will draw the solvent into the interstices between the crystals and

UM00012180
NOVARTIS EXHIBIT 1517
Novartis v. Regents, IPR2023-01347
Page 926 of 4460

particularly along the interface between the two forms. The rate of the transformation can be considerably increased in this way if the solvent is a good one for the crystals and if the solution thus formed is not too viscous. (This is the real reason for use of a low-boiling solvent.)

A transition temperature lying below room temperature is more difficult to measure, although with the new thermoelectric cold stages for the microscope the same techniques can be used down to about −100°C. Below −100°C it is best to use macro procedures A dry mixture of the two polymorphs, if available, and in as large crystal sizes as possible, is placed in a sealed vial and left for several days in liquid nitrogen. On removal, the crystals are examined microscopically for evidence of pseudomorphs. A pseudomorph is a transformed crystal: the external shape of the original crystal may be discernible even though the internal structure is that of the new form. The pseudomorph may be more or less broken up by the transition if the density difference between the two forms is very great. Occasionally the pseudomorph may crumble to a dust, even with gentle handling. This phenomenon can sometimes be turned to advantage as a substitute for grinding a substance to achieve small particle size; for example, calcium silicate can be effectively reduced to very fine particles by passing it through the transition temperature.

Although the microscopic procedures for determination of the transition temperature work best between −100°C and about 2400°C, there are admittedly other ways of detecting transitions. For example, dilatometry may be used to detect the density change on transformation, x-ray diffraction will detect phase changes due to transformation, and, of course, the solubility or vapor pressure curves can be measured for the two forms in order to find the cross-over temperature (the transition temperature). Special methods may be used in certain cases; for example, with the metals. If an electrolytic cell can be set up with the two different forms acting as the two electrodes, there will be a measurable emf at all temperatures except the transition temperature.

In monotropic systems the transition temperature lies above the melting point of both polymorphs. Hence it cannot be located directly; although Schenk (*9*) has used the following relationship to calculate it:

$$T_t = (F_1K_2 - F_2K_1)/(K_1 - K_2)$$

where F_1 and F_2 are the two melting points and K_1 and K_2 are the molar freezing point depression constants for the two forms. It may also be possible to locate the transition temperature in a monotropic system by measuring the solubility curves or the vapor pressure curves over a range just below the melting points, and extrapolating the curves to their intersection.

UM00012181

NOVARTIS EXHIBIT 1517
Novartis v. Regents, IPR2023-01347
Page 927 of 4460

the two forms. The rate of the trans-
:d in this way if the solvent is a good
ius formed is not too viscous. (This is
solvent.)
v room temperature is more difficult
rmoelectric cold stages for the micro-
ed down to about −100°C. Below
ures A dry mixture of the two poly-
ystal sizes as possible, is placed in a
quid nitrogen. On removal, the crys-
idence of pseudomorphs. A pseudo-
ernal shape of the original crystal may
l structure is that of the new form.
s broken up by the transition if the
rms is very great. Occasionally the
t, even with gentle handling. This
d to advantage as a substitute for
particle size; for example, calcium
ry fine particles by passing it through

s for determination of the transition
0°C and about 2400°C, there are
nsitions. For example, dilatometry
: on transformation, x-ray diffraction
mation, and, of course, the solubility
:d for the two forms in order to find
ion temperature). Special methods
le, with the metals. If an electrolytic
forms acting as the two electrodes,
temperatures except the transition

temperature lies above the melting
annot be located directly, although
nship to calculate it:

$\zeta_1)/(K_1 - K_2)$

oints and K_1 and K_2 are the molar
e two forms. It may also be possible
nonotropic system by measuring the
curves over a range just below the
ves to their intersection.

VI. Preparation of Metastable Polymorphs

1. Methods Based on Thermodynamic Equilibrium

There are two general methods for the crystallization of metastable polymorphs. The first, based on thermodynamic equilibrium, involves holding crystals of one form in the temperature stability range of the desired polymorph until transformation occurs. If the crystals are wetted with a solvent so that a solution phase transformation can occur, the change will be much faster; if seeds of the desired polymorph can be present, the transformation will be even more rapid. The procedure and apparatus for this are not very different from those described above for the determination of the transition temperature (Figs. 12 and 13). It is a help to know the transition temperature, so that the solution phase transformation can be carried out as far as possible from the transition temperature but still in the stability range of the desired polymorph. For example, one can convert HMX (I) to HMX (II) more rapidly at temperatures from 160 to 165°C, whereas HMX (II) would best be prepared from HMX (IV) at about 120°C and from HMX (I) at about 160°C [HMX (I) $\rightleftharpoons$ HMX (II) = 115.5°C; HMX (II) $\rightleftharpoons$ HMX (IV) = 165.5°C]; see Figures 3, 4, and 5. This method of preparing a high-temperature polymorph works, of course, only in enantiotropic systems in which the desired form has a definite temperature stability range.

2. Methods Based on Prevention of Thermodynamic Equilibrium

In monotropic systems it is usually relatively easy to prepare the metastable forms, but it is necessary in so doing to prevent thermodynamic equilibrium by working fast and with small quantities. In general, a metastable polymorph (in enantiotropic systems as well as monotropic systems) can be prepared either by achieving a high degree of supersaturation in the vapor or solution state, or by supercooling in the melt state. The general objective is to find conditions under which the metastable form can crystallize before crystals of the stable form appear. Since the metastable form will always be more soluble and more volatile and will have the lower melting point, it follows that supercooling is necessary in order to crystallize the metastable form from the vapor, melt, or solution. The system must then be supercooled below the melting point of the metastable form, and at the same time one must prevent crystallization of the more stable form or forms. With HMX, for example, it is possible to prepare any one of the four crystal

UM00012182
NOVARTIS EXHIBIT 1517
Novartis v. Regents, IPR2023-01347
Page 928 of 4460

forms from the same solvent and at temperatures all well within the thermodynamic stability range of HMX (I). This is done by supercooling the solution rapidly; the more rapidly, the more unstable will the polymorph be. The rate of cooling is most readily controlled by varying the volume of the solution, since a small volume can be cooled very rapidly.

A. Solution Phase Preparations of Metastable Phases

The various polymorphic forms of HMX are usually obtained by starting with an acetone solution saturated with HMX (I) at 63°C and with no excess solid present. To obtain HMX (I), 200 ml. of this hot solution is cooled spontaneously to room temperature. This gives very slow cooling, low supersaturation, and crystallization of pure HMX (I). To obtain HMX (II), 50 ml. of the same hot solution is cooled to room temperature with gentle agitation (swirling, to improve heat transfer). HMX (III) results if 30 ml. of the same hot solution is cooled with agitation in an ice-water bath. HMX (IV) is formed when 5 ml. of the solution is cooled in a test tube by immersion (with shaking) in a dry-ice cooling bath or by pouring 5 ml. of the hot solution over cracked ice. In every case, the crystals must be filtered off rapidly to avoid solution phase transformation to HMX (I) which is stable up to 115.5°C. Other solvents may also be used; however, the cooling rates must be changed in accordance with the solubility of HMX in that solvent. If HMX is more soluble than in acetone, the rates of cooling must be increased; if less soluble, the rates must be decreased.

There are three reasons for this relationship between solubility and cooling rates, though all are based on the fact that the concentration of the compound is less in the poorer solvent. First, in such a solution it is more difficult to nucleate any solid phase because nucleation is a 2-, 3-, or 4-body collision process and there is less probability of nucleation in a dilute solution. The necessary degree of supercooling can, therefore, be achieved. Second, the high-temperature (low-density, more symmetrical, and more open) structures nucleate most readily when they can (sufficient supercooling). This is the basis for Ostwald's law of successive states, which says that a phase change will occur step by step by the way of successively more stable phases. Third, and finally, in a poor solvent the rate of transformation of a metastable to a more stable polymorph is slower. Hence a metastable form once crystallized can be isolated and dried before it is converted by solution phase transformation to a more stable phase.

In some systems the metastable form is extremely unstable and may be prepared only with more extreme supercooling. This is usually done on a very small scale (even a single drop of solution) with high-boiling liquids, so that a

UM00012183

NOVARTIS EXHIBIT 1517
Novartis v. Regents, IPR2023-01347
Page 929 of 4460

ratures all well within the thermo-
is done by supercooling the solu-
: unstable will the polymorph be.
lled by varying the volume of the
ed very rapidly.

'able Phases

(are usually obtained by starting
4X (I) at 63°C and with no excess
nl. of this hot solution is cooled
is gives very slow cooling, low
HMX (I). To obtain HMX (II),
to room temperature with gentle
). HMX (III) results if 30 ml. of
ion in an ice-water bath. HMX
:ooled in a test tube by immersion
or by pouring 5 ml. of the hot
the crystals must be filtered off
tion to HMX (I) which is stable
used; however, the cooling rates
lubility of HMX in that solvent.
the rates of cooling must be in-
:creased.
ip between solubility and cooling
e concentration of the compound
a solution it is more difficult to
n is a 2-, 3-, or 4-body collision
eation in a dilute solution. The
:fore, be achieved. Second, the
trical, and more open) structures
:ient supercooling). This is the
which says that a phase change
ively more stable phases. Third,
isformation of a metastable to a
ietastable form once crystallized
:ted by solution phase transfor-

:emely unstable and may be pre-
This is usually done on a very
th high-boiling liquids, so that a

saturated solution at a high temperature suddenly cooled to room temperature will achieve a high degree of supersaturation. If, for example, a saturated solution of RDX (cyclotrimethylene trinitramine), HND (hexanitrodiphenylamine), or ammonium picrate in a drop of thymol on a microscope slide at 150 to 200°C is cooled rapidly by placing it on a cold surface, crystals of the corresponding unstable polymorphs will appear. In each case, some crystals of the stable form may also appear, and a slow solution phase transformation may occur. The rate of this transformation will increase with increasing temperature.

B. Preparation of Metastable Phases from the Melt

An analogous behavior results when a melt rather than a solution is supercooled. One of the most interesting systems studied thus far (*10*) is DINA [bis(β-nitroxyethyl)nitramine]. This compound shows four crystalline polymorphs, each of which can be prepared easily from the melt and each of which has a measurable melting point. The melting points are: DINA (I), 52°C; (II), 52°C; (III), 38°C; and (IV), 30°C. DINA (I) melts about 0.05°C higher than DINA (II). A completely melted sample of DINA supercools to room temperature and remains indefinitely without crystallizing. If, at any temperature below 52°C, the glass cover slip is pressed hard into contact with the microscope slide, using the side of a teasing needle or even a pencil eraser, nucleation usually occurs at the point of contact. The temperature of the preparation at the time of crystallization determines the degree of supercooling and therefore the polymorphic form. Below 30°C, DINA (IV) results; at 30 to 35°C, DINA (III); at 40 to 45°C, DINA (II) is the usual product, although DINA (I) or a mixture of I and II may appear. Each of these forms is reasonably stable on a microscope slide, although (IV), as would be expected, is least stable. DINA (III) usually spontaneously nucleates in form (IV) within a few minutes.

Some compounds show an unstable short-lived polymorph when the melt is highly supercooled. Good examples are acetanilide and TNT. Both should be melted completely and allowed to cool quietly and undisturbed. Within a few minutes for acetanilide, or a few hours for TNT, crystallization will occur, but the unstable form will immediately and very rapidly transform to the stable form, leaving an obvious pseudomorph (Fig. 16). As these few examples show, it is not difficult to form a sound idea of the relative stability of the unstable forms of different compounds. The TNT polymorph is probably as unstable as will ever be observed, since it always transforms to the stable form, probably in a few hundredths of a second after it forms. It is necessary to supercool a number of tiny droplets less than 1 to 2 mm in

UM00012184
NOVARTIS EXHIBIT 1517
Novartis v. Regents, IPR2023-01347
Page 930 of 4460

diameter to observe the TNT pseudomorphs, and even then the percentage of crystallizations showing the phenomenon is less than 1%. Acetanilide (II) is somewhat more stable, forming a fair percentage of the time from 2 to 3 mg of melt and with an average life of perhaps a second. Again, it is obvious as a pseudomorph. The DINA polymorphs are much more stable than those of either TNT or acetanilide. There is, of course, no possibility of obtaining TNT (II), acetanilide (II), DINA (III) or (IV), RDX (II), HND (II), ammonium picrate (II), or HMX (IV) on a macro scale.

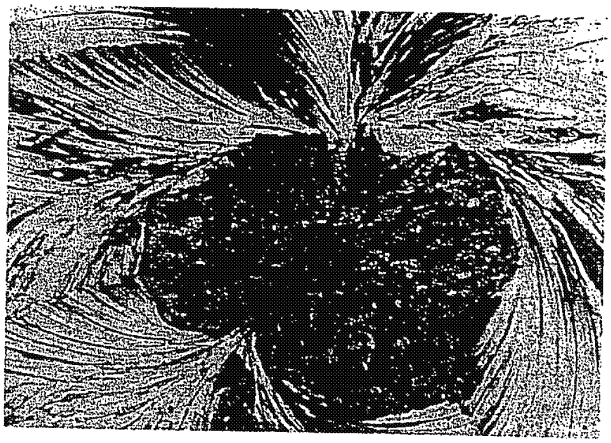
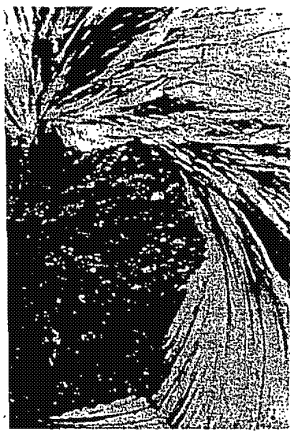


Figure 16. TNT preparation in which the very unstable form II started to crystallize but was almost immediately transformed to form I which nucleated almost simultaneously on the advancing crystal front of II. The remaining melt then crystallized rapidly as form I.

Another interesting example of a highly unstable polymorph is picric acid. Form I melts at 121°C, and form II melts at 75°C. It is understandably difficult to supercool picric acid 46°C without getting crystals of form I, but it can be done in very small preparations (0.1 mg) between a slide and cover slip. It is then necessary to cause form II to crystallize; this has been done by seeding with trinitrobenzene (I), with which picric acid (II) is isomorphous. This is obviously best done in a fusion preparation by recrystallizing TNB as the stable form I, then melting a very tiny amount of picric acid at the edge of the cover slip near the TNB so that it is absorbed (so to speak) by the TNB melt and forms a small pocket of picric acid surrounded on three sides by TNB. On rewarming, the picric acid and a portion of the TNB are melted, and, on cooling, the unmelted TNB (I) seeds the melt including the

UM00012185
NOVARTIS EXHIBIT 1517
Novartis v. Regents, IPR2023-01347
Page 931 of 4460

ıorphs, and even then the percentage
:non is less than 1%. Acetanilide (II)
ıir percentage of the time from 2 to
ɔerhaps a second. Again, it is obvious
rphs are much more stable than those
of course, no possibility of obtaining
or (IV), RDX (II), HND (II), ammo-
acro scale.



ry unstable form II started to crystallize but
I which nucleated almost simultaneously
ıing melt then crystallized rapidly as form I.

ly unstable polymorph is picric acid.
nelts at 75°C. It is understandably
ithout getting crystals of form I, but
s (0.1 mg) between a slide and cover
II to crystallize; this has been done
which picric acid (II) is isomorphous.
preparation by recrystallizing TNB
y tiny amount of picric acid at the
ıat it is absorbed (so to speak) by the
ɔicric acid surrounded on three sides
:id and a portion of the TNB are
'NB (I) seeds the melt including the
picric acid. The rate of crystallization is very rapid through the TNB (I) but slows considerably in the zone of mixing, then speeds up slightly in the picric acid (II). The latter may remain for a few minutes or a few seconds, but it always transforms very soon into picric acid (I) pseudomorphs of (II).

In general, it becomes more difficult to obtain the room temperature stable form as the transition temperature decreases to within 10 to 20°C of room temperature. The compound 1,2,5-trinitronaphthalene melts at 112 to 113°C (II) but has a transition temperature at about 30°C. As a result the stable form I cannot be obtained without experiments below room temperature (or 20°C). If the transition temperature falls below room temperature, the low-temperature form will not usually be observed unless experiments are carried out at lower temperatures within the required temperature range.

It is significant that a given polymorphic form can often be crystallized well below its temperature stability range, but seldom, if ever, above it. Presumably this is due to the fact that a supercooled system will lack the lattice mobility to transform; hence an unstable polymorph well below the transition temperature may be very stable once it is formed. This is useful in telling us that in those cases of great instability of one polymorph, e.g., acetanilide, RDX, HND, the system is probably monotropic.

C. Preparation of Metastable Phases from the Vapor

Preparation of metastable forms by sublimation is a useful procedure, especially because the individual small crystals of the metastable forms are quite stable and can be used directly for melting point determinations. The general procedure utilizes a Kofler sublimation block and a temperature at which the compound sublimes readily. The temperature of the cover slip then determines the crystal form and size of the sublimate. A very small temperature difference between the source and the condensing surface will result in condensation of the stable form at that temperature. Cooling of the cover slip by placing drops of various low-boiling solvents on the top surface will cause condensation of the more unstable forms, the lower temperatures leading to the most unstable forms. A vapor phase transformation may, of course, occur if two different crystal forms condense, since each has a different vapor pressure (Fig. 17).

3. Stability, Metastability, and Instability

The idea that unstable crystal forms can be readily prepared at temperatures far below their normal temperature stability ranges is one of the unappreciated ideas in the study and handling of polymorphs. It is not

UM00012186
NOVARTIS EXHIBIT 1517
Novartis v. Regents, IPR2023-01347
Page 932 of 4460

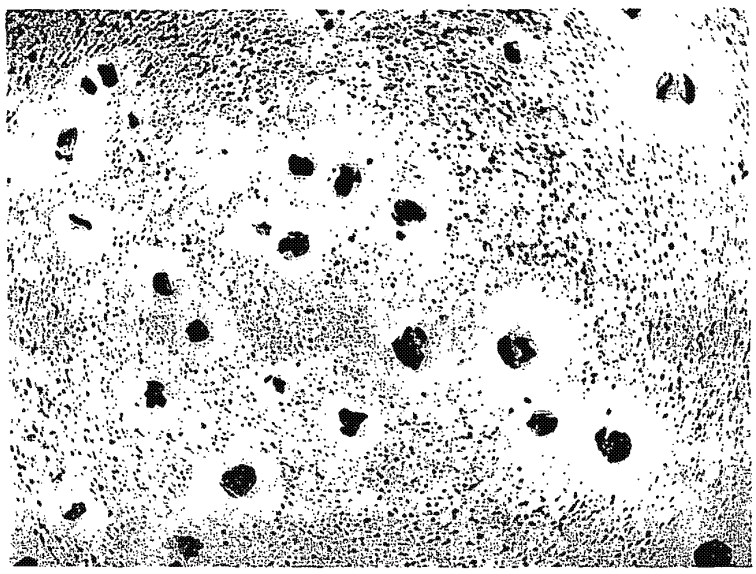


Figure 17. Sublimate of two polymorphic forms of *p*-dimethylaminocinnamaldehyde. The unstable form has vaporized in the neighborhood of (and onto) the stable form.

inconceivable that diamonds, now being produced by attaining thermodynamic stability, i.e., high temperatures and pressures, might some day be made at ordinary pressures and quite low temperatures. The requirement, and for carbon a tough one, is a liquid solvent at temperatures below the range at which diamond changes to graphite by a solid-solid transformation.

Diamond, of course, is unstable thermodynamically at ordinary temperatures and pressures. It is said to be metastable, and many such materials are known. Many minerals (aragonite, anatase, brookite, etc.), many drugs (*11*) (atophane, progesterone, estrone, marfanil, sulfathiazole, veronal, etc.), and even some important metals (copper, silver, zinc, tin, bismuth, and cadmium) are used daily in the metastable form. The degree of stability of a metastable polymorph varies considerably. Diamond is one extreme, although even diamonds often transform, on heating, to graphite. At the other extreme is TNT, which possesses a metastable form so short-lived that no one has even seen it. Only the pseudomorph remains to tell us that a transformation has occurred (Fig. 16). The degree of metastability in a given system can be changed to some extent. For example, crystal size is a definite factor, and

UM00012187

NOVARTIS EXHIBIT 1517
Novartis v. Regents, IPR2023-01347
Page 933 of 4460



limethylaminocinnamaldehyde.
and onto) the stable form.

ced by attaining thermo-
sures, might some day be
atures. The requirement,
it temperatures below the
solid-solid transformation.
cally at ordinary tempera-
d many such materials are
ite, etc.), many drugs (*11*)
iazole, veronal, etc.), and
n, bismuth, and cadmium)
f stability of a metastable
extreme, although even
. At the other extreme is
ived that no one has even
that a transformation has
n a given system can be
is a definite factor, and

large crystals of a metastable form are usually much less stable than small crystals. Large crystals of HMX (IV), 1 mm or more in large dimension, seldom last longer than a few hours before they transform to HMX (I). On the other hand, very small crystals of HMX (IV) less than 50 μ long and 10 μ thick, prepared in 1942, are still unchanged more than twenty years later.

Physical shock, especially grinding, is usually an effective way to convert a metastable crystal form to the stable form. Presumably this conversion occurs most readily for displacive-type transformations, since there are many metastable systems, such as diamond, that can be pounded to angstrom dimensions without transformation. Grinding diamond at elevated temperatures would undoubtedly increase the rate of solid-solid transformation to graphite.

VII. Solution Phase Transformation Rates

The rate of the solution phase transformation in a given system depends on the solubility of each polymorph at that temperature, the rates of solution, and the diffusion rate of the molecules in solution. The rate is higher the higher the solubility and the greater the difference in solubilities. The overall rate, of course, is zero at the transition temperature where the solubilities of the two forms are equal, but the rate increases both as the temperature rises and as it falls. However, as the temperature falls further, two factors cause the rate of transformation to decrease again: first, the solubilities of both forms decrease, thus lowering the concentration in solution; and second, the viscosity of the solution increases. Both factors decrease the diffusion rate of the molecules in solution and lower the rate of transformation. The diffusion rate and therefore the transformation rate can also be increased by agitation of the suspension, by using finely divided crystals, and by having seed crystals of the stable form present.

VIII. Pseudopolymorphism

By this term, which is convenient to use here but which should never be allowed to come into general use, is meant a variety of phenomena sometimes confused with polymorphism. They include desolvation, second-order transitions (some of which are polymorphism), dynamic isomerism, mesomorphism, polymerism, grain growth, boundary migration, recrystallization in the solid state, and lattice strain effects.

UM00012188
NOVARTIS EXHIBIT 1517
Novartis v. Regents, IPR2023-01347
Page 934 of 4460

1. Desolvation

During heating of a crystalline solid in the microscope hot stage, one evidence of polymorphism is a solid-solid transformation. This results in darkening of the crystal, observed by transmitted light. It is due to the breaking up of the crystal (the density change is often 1% or more) and light scattering by the many new air-crystal interfaces. This change is, in visual detail, duplicated when a crystalline solvate gives off solvent of crystallization on heating. There is, however, a simple microscopic procedure to differentiate polymorphism from desolvation. The heating experiment is repeated with the crystals completely immersed under a cover slip in a liquid immiscible with the possible solvent of crystallization. If, then, desolvation is involved, heat will produce the desolvated solid plus a liquid droplet of the solvent. If polymorphism is involved, the change will occur as before but no liquid phase will appear until the final melting point.

2. Second-Order Transitions

Second-order transitions will usually be missed completely on heating under the microscope because of their subtlety. However, there are some that can be observed, and usually the observation is best made by using crossed polars, since small changes in birefringence are easily detected and often occur. One such change with pentaerythritol tetranitrate is visible as a birefringence change as it cools on the microscope slide after crystallizing from the melt. Many high polymers show second-order transitions near their melting points. The ammonium halides also show a variety of such transitions.

3. Dynamic Isomerism

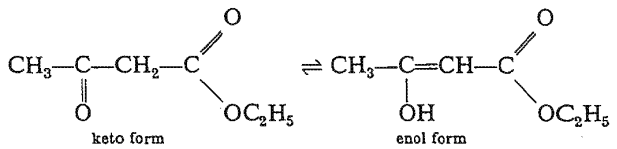
Great care must also be taken to avoid confusing dynamic isomerism with polymorphism. Dynamic isomers (which include geometrical isomers and tautomers) are chemically different, though more or less readily interconvertible in the melt state. The basic difference between dynamic isomers and polymorphs is that equilibrium between two polymorphs can occur in the solid state, and the difference between any two polymorphs disappears in the melt state. Dynamic isomers, on the other hand, exist in both the solid and the melt state. Only one polymorphic form of a given compound is stable at a given temperature (except at the transition temperature, at which two

UM00012189

NOVARTIS EXHIBIT 1517
Novartis v. Regents, IPR2023-01347
Page 935 of 4460

forms are in equilibrium). On the other hand, dynamic isomers are in equilibrium over a wide range of temperature with both isomers stable, though in relative percentages varying with temperature and solvent. Because dynamic isomers are different compounds, a binary phase diagram is necessary to explain their behavior.

A classic example of dynamic isomerism is acetoacetic ester, which exists in a ketonic and an enolic form. At ordinary temperatures liquid acetoacetic ester exists as an equilibrium mixture of the two isomers (93% keto and 7% enol form).



keto form enol form

The rate at which equilibrium is established in a system of dynamic isomers can vary considerably, and it is affected by solvent and by impurities. If the rate is very fast and if the equilibrium changes pure A to pure B over a very narrow temperature range, then the system approaches polymorphism and would be indistinguishable from it except by chemical structure characterization of the two forms. There are many possible gradations in behavior between polymorphism and dynamic isomerism.

Even though a system of dynamic isomers exists as an equilibrium mixture of the two isomers in the melt or solution phase, this equilibrium can be displaced by removal of one isomer by crystallization or by chemical reaction forming a derivative of one isomer. If equilibration proceeds rapidly enough, all the mixture may crystallize as the more insoluble of the two isomers. In solution, the two isomers will have different solubilities, just as two polymorphs will. Not only may the solubility curves cross in either case, but, since with dynamic isomerism both isomers are present, the solution may also become saturated with either form on cooling, no matter where the equilibrium composition lies.

Summarizing, then, polymorphs exist only in the solid state but can convert, in at least one direction, without going through the solution or melt phase (i.e., a solid-solid transformation). Tautomers exist both in the melt (or solution) and the solid state. Each tautomer can also, and probably does, exist in polymorphic forms, further complicating an already complicated situation.

To differentiate between polymorphism and dynamic isomerism the microscope again is a useful tool. Let us assume that two solid phases are known to be related either by polymorphism or by dynamic isomerism. The first step

UM00012190
NOVARTIS EXHIBIT 1517
Novartis v. Regents, IPR2023-01347
Page 936 of 4460

is to melt the two side by side between a microscope slide and cover slip. As crystallization of the two phases progresses, the following possibilities exist:

a. The two crystal fronts could grow at a steady velocity until they come into contact, and one solid phase could then grow through the other to give a solid-solid transformation. This is polymorphism.

b. The two crystal fronts could grow toward each other but slow down as they approach the zone of mixing, and subsequently a eutectic could appear. This is dynamic isomerism.

A second procedure would be to melt each sample by the equilibrium melting procedure (*12*) and observe the melting point as a function of time. If the two are polymorphs, the melting point will not change unless a solid-solid transformation occurs, and even then the change will be sudden and the melting point will remain thereafter unchanged. If both are isomers, the melting point of each will decrease gradually as equilibrium is established. The final melting point will be the same for each, since each form will change in the melt to the same equilibrium composition. One of the isomers will show an apparent solution phase transformation as the melting point is followed through the eutectic composition.

A nonmicroscopic method for differentiating between polymorphism and dynamic isomerism requires spectroscopic evidence of the chemical change involved. If ultraviolet or infrared absorptions show different or changing spectra when crystals of the two forms are dissolved or melted, dynamic isomerism is involved. Spectroscopic differences in the solid state are not an adequate criterion, since different crystalline polymorphs have different spectra. Finally, complete crystal structure determinations, if practical, would answer the question with absolute certainty.

4. Mesomorphism

Many substances show a mesomorphic phase (liquid crystal) on melting (*13,14*). Such phases have some of the properties of a crystalline solid but flow like a liquid. They are usually birefringent (Fig. 18) but do not show an x-ray pattern characteristic of well-crystallized phases. They apparently have some molecular order because of the birefringence and some broad x-ray lines. They have been classified as nematic (molecules arranged parallel but in layers), smectic (arranged parallel and in layers with long axes perpendicular to the layers), and cholesteric (probably a twisted nematic structure with the axis of the twist perpendicular to the long axis of the molecules).

UM00012191
NOVARTIS EXHIBIT 1517
Novartis v. Regents, IPR2023-01347
Page 937 of 4460

oscope slide and cover slip. As
he following possibilities exist:

steady velocity until they come
row through the other to give a
hism.
d each other but slow down as
uently a eutectic could appear.

ch sample by the equilibrium
ıg point as a function of time.
will not change unless a solid-
he change will be sudden and
nged. If both are isomers, the
as equilibrium is established.
h, since each form will change
ion. One of the isomers will
ıtion as the melting point is

g between polymorphism and
lence of the chemical change
ıs show different or changing
issolved or melted, dynamic
ces in the solid state are not
ne polymorphs have different
rminations, if practical, would

e (liquid crystal) on melting
ties of a crystalline solid but
(Fig. 18) but do not show an
hases. They apparently have
ence and some broad x-ray
lecules arranged parallel but
with long axes perpendicular
d nematic structure with the
of the molecules).

A given compound may show one or more mesomorphic phases with the smectic phase stable between the crystalline and the nematic (or cholesteric). There may, in fact, be several nematic or smectic phases in a given system. They usually behave like enantiotropic polymorphs with reproducible transition temperatures, although some systems may be monotropic, and hence the mesomorph will appear only in the supercooled melt and will melt, on heating, lower than the crystalline form. An interesting mesomorphic system is ethyl anisal-*p*-aminocinnamate, which shows two polymorphs, one melting at 83°C and the other at 108°C. On heating, "melting" of the stable

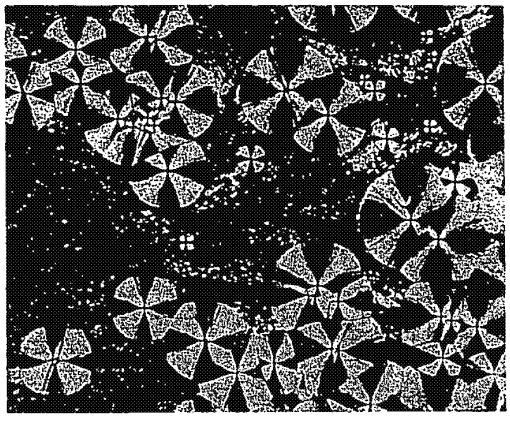


Figure 18. Spherulites of cholesteryl acetate crystallizing from the mesomorphic phase.

phase occurs at 108°C to a smectic phase, which in turn "melts" at 118°C to give a nematic phase, melting finally at 139°C to a true liquid. On cooling, these changes can be observed in reverse, but the stable crystalline phase melting at 108°C may not occur, and further cooling may then show a second smectic phase at 91°C and crystallization of a metastable crystalline solid at 83°C. On reheating, barring appearance of the stable crystalline phase, the metastable phase melts at 83°C to a smectic phase, which changes to a second smectic phase at 91°C, and to a nematic phase at 118°C which then melts at 139°C. Figure 19 shows a schematic free energy-temperature diagram for this system. It is accurate with respect to the observed "transition" temperatures and melting points, but the slopes are, of course, not known and the positions of the unmeasured "transitions" are fortuitous. Such a diagram does explain the observed behavior of the polymorphs and mesomorphs in this system.

UM00012192
NOVARTIS EXHIBIT 1517
Novartis v. Regents, IPR2023-01347
Page 938 of 4460

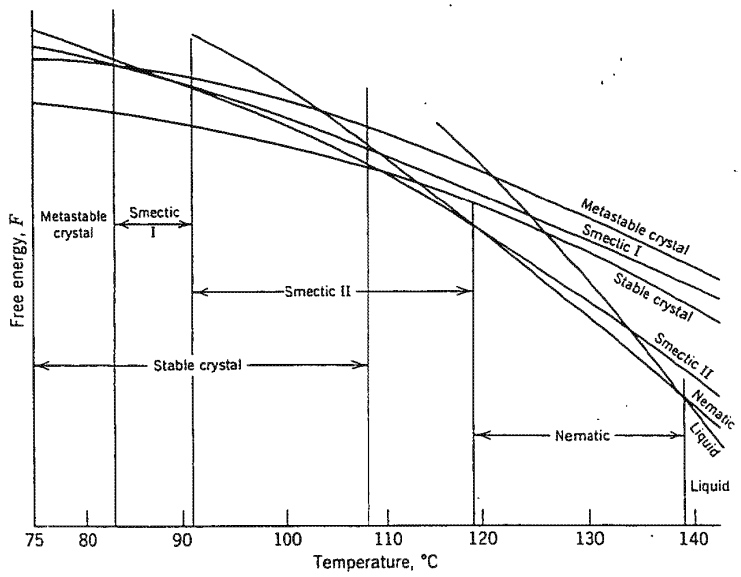


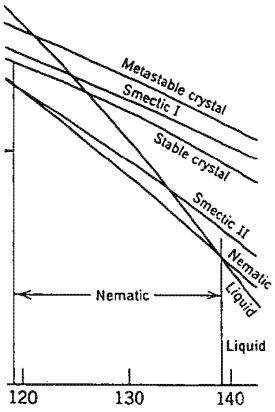
Figure 19. Schematic free energy-temperature diagram for ethyl anisal-*p*-aminocinnamate. The slopes for the curves are not known, but the "transition temperatures" are correctly located.

One significant way in which mesomorphs differ from crystals and resemble liquids lies in the fact that, whereas a solid-solid transformation may be superheated, the "transition" from a crystalline phase to a mesomorph behaves like a melting point in that superheating does not occur. Here again, then, we have a type of physical behavior resembling true polymorphism but with some differences. The present tendency is to refer to liquid crystals as *mesomorphs* and to the phenomenon as *mesomorphism*, and to consider the situation as closely related to, but not identical with, polymorphism.

5. Polymerism

Polymerism includes such systems as acetaldehyde:paraldehyde and oxygen:ozone. These systems often act in the same manner as described above for tautomers. The equilibrium between acetaldehyde and paraldehyde is very slow under ordinary conditions, although addition of a trace of sulfuric acid greatly increases the interconversion rate.

UM00012193
NOVARTIS EXHIBIT 1517
Novartis v. Regents, IPR2023-01347
Page 939 of 4460



for ethyl anisal-*p*-aminocinnamate.
ısition temperatures" are correctly

differ from crystals and re-
ılid-solid transformation may
ılline phase to a mesomorph
ş does not occur. Here again,
ıbling true polymorphism but
: to refer to liquid crystals as
orphism, and to consider the
| with, polymorphism.

:taldehyde:paraldehyde and
: same manner as described
ı acetaldehyde and paralde-
:hough addition of a trace of
:on rate.

6. Grain Growth (Boundary Migration and Recrystallization)

Another type of solid-state behavior easily confused with polymorphism is grain growth (boundary migration or recrystallization), as shown by certain anisotropic solids (Figs. 20 and 21). This behavior looks, at first, precisely like a polymorphic transformation, but it differs in that the two phases showing a solid-solid "transformation" are indistinguishable from each other by

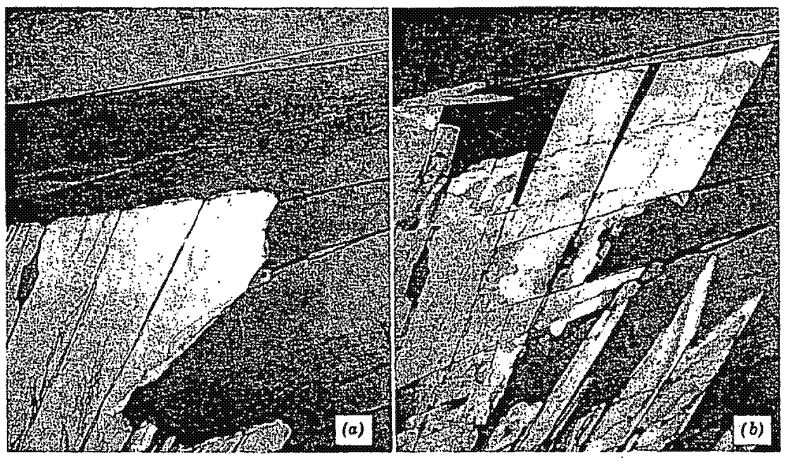


Figure 20. Photomicrographs of the same field of TNT crystals grown from the melt (*a*) before and (*b*) after annealing for 1 hour at 75°C.

crystal optics or x-ray diffraction. Furthermore, the "transformation" proceeds *simultaneously* in *both* directions. This unusual behavior is shown by TNT, DDT, DINA, vitamin K_3 (menadione), and, to a lesser extent, by many other organic compounds. Such compounds must apparently possess sufficient anisotropy of elasticity so that strain also can be present in the lattice distributed directionally (anisotropically). In addition, such compounds must also possess just the right degree of brittleness and plasticity so that the strain induced is not lost through cracking of the crystal or through plastic flow.

To differentiate this behavior from polymorphism, it is necessary only to observe carefully the solid-state recrystallization to see that the "phases" are identical and that both grow into each other. Details on this type of behavior have been published (*15*).

UM00012194
NOVARTIS EXHIBIT 1517
Novartis v. Regents, IPR2023-01347
Page 940 of 4460

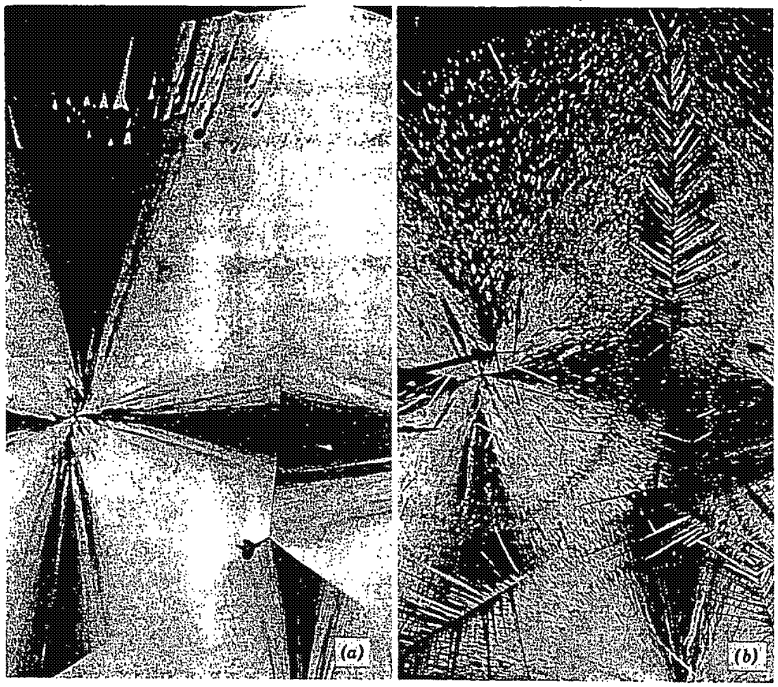
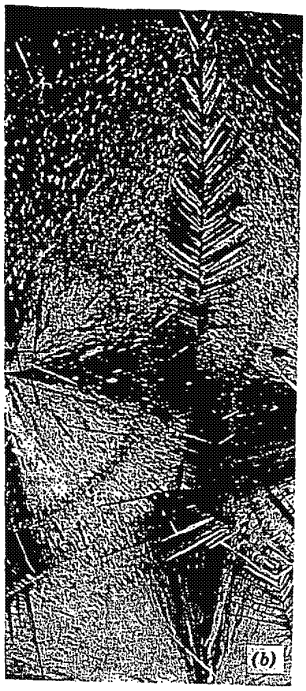


Figure 21. Photomicrographs of the same field of a thin crystalline preparation of DDT (*a*) before and (*b*) after annealing at 100°C.

7. Lattice Strain

Recently additional information has become available which shows that lattice strain may cause energy changes in a lattice, equivalent to the energy changes involved in polymorphism and giving rise to observations of behavior similar to that shown by true polymorphs. Lattice strain can be induced by thermal shock mechanically or by crystallization itself. Strained crystals (Fig. 22) show lower melting points, higher solubilities, and higher vapor pressures than the corresponding unstrained crystals. Melting point lowering of up to 10°C has been observed with vitamin K_3, and "transformations" in the vapor, solution, and solid phases have been observed between strained and unstrained crystals otherwise apparently identical (*16*). Typical systems showing these effects are the same as those listed above as

UM00012195
NOVARTIS EXHIBIT 1517
Novartis v. Regents, IPR2023-01347
Page 941 of 4460



n crystalline preparation of DDT

available which shows that
ce, equivalent to the energy
ıg rise to observations of
rphs. Lattice strain can be
ystallization itself. Strained
ıher solubilities, and higher
ıed crystals. Melting point
h vitamin K_3, and "trans-
ɔhases have been observed
ɜe apparently identical (*16*).
ne as those listed above as

showing grain growth and boundary migration, although other compounds such as HMX have been observed to show some of these effects. Although the effects of strain are not generally important, probably because few lattices can maintain a high degree of strain, strain is important in some compounds because it can cause changes in physical properties (melting point, solubility, and vapor pressure) and performance properties (chemical reactivity, stability, rates of solution, etc.). Strain can reverse the stabilities of two

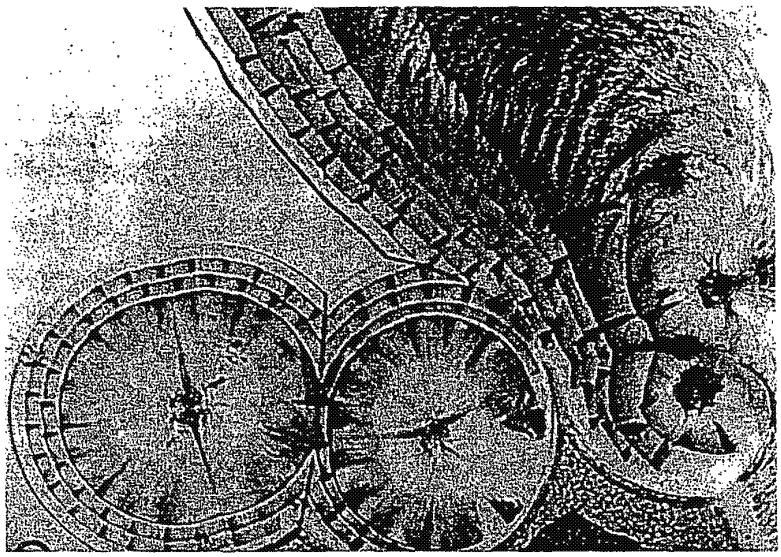


Figure 22. Crystals of DDT growing from thymol solution in the zone of mixing of a mixed fusion. The crystals grow as a clear, highly strained band at the crystal front. Periodically a sudden breaking up (cracking) of the crystals occurs in the band, partially alleviating the strain, and a new strained band begins to form.

polymorphs at a given temperature because the relative solubilities, melting points, or vapor pressures can be reversed if the normally stable form becomes highly strained. Usually the strained lattice is indistinguishable from the corresponding unstrained lattice by x-ray diffraction or by crystal optics. The observation of an apparent polymorphic "transformation" between apparently identical crystalline phases is a characteristic of this situation. This phenomenon needs considerably more study before it can be completely understood; at present it is a type of behavior which can be, and has been, confused with polymorphism.

UM00012196
NOVARTIS EXHIBIT 1517
Novartis v. Regents, IPR2023-01347
Page 942 of 4460

IX. Study of a Compound to Determine whether Polymorphism Exists

It is comparatively easy to determine by microscopic procedures whether a given compound can crystallize in two or more different crystalline polymorphs. The following are standard procedures designed to cause crystallization of the metastable form.

a. Melt completely a small amount of the compound between a slide and cover slip and observe the solidification between crossed polars. If, after spontaneous freezing, a solid-solid transformation occurs spontaneously or can be induced by seeding or scratching, the compound exists in at least two polymorphic forms. The problem, in this case, is to prevent crystallization of the stable form by inducing supercooling. Three steps can be taken to help induce supercooling: First, the sample size should be very small; in fact, a number of separate droplets under the cover glass, ranging in diameter from a few tenths of a millimeter to 1 to 2 mm, will provide the most satisfactory size. Second, the crystals should be melted completely by holding the melt for 30 sec or so about 10 to 20°C above the melting point. Third, the melted preparation should be carefully set aside for several minutes without physical shock before examination. Only under these conditions can the very unstable form of TNT be obtained. To a slightly lesser extent, formation of the metastable form of acetanilide requires the same care. Even in spite of these precautions, the metastable polymorphs of these two compounds are seldom observed; only the pseudomorph remains as evidence of the formation of the metastable form.

This method is satisfactory for a number of compounds; for example, pentaerythritoltetranitrate (PETN), carbon tetrabromide, mercuric iodide, ammonium nitrate, and 1,3,5-trinitrobenzene (TNB). These compounds always crystallize on cooling to give the high-temperature form if they are completely fused. Of this group, PETN, HgI_2, CBr_4, and ammonium nitrate show spontaneous transformations on cooling, but trinitrobenzene must usually be scratched or seeded to induce a transformation.

It is often of value to carry out a meltback (partial remelting) and seed the melt with some of the compound from the stock bottle (presumably, though not always, the stable form). As freezing proceeds, the junction of the two crystal fronts is observed for evidence of polymorphism. In general, if the two crystal fronts are made up of different crystalline modifications, one of them will grow into and through the other on contact.

b. Heat a sample of the compound in a hot stage and observe whether a solid-solid transformation occurs during heating. A transformation will occur with most compounds which show enantiotropic transformations, e.g.,

UM00012197

NOVARTIS EXHIBIT 1517
Novartis v. Regents, IPR2023-01347
Page 943 of 4460

ammonium nitrate, carbon tetrabromide, and ammonium picrate. Many other systems, even though enantiotropic, do not readily transform under these conditions. The chances are greater the larger the preparation; hence 10 to 20 mg should be used.

c. Sublime a small quantity of the compound and attempt to induce a solution phase transformation between the sublimate and the original sample by mixing the two in a drop of saturated solution of one of them. If the two are polymorphs, the more stable will be more insoluble and will grow at the expense of the more soluble metastable form. This process will continue at a rate which depends on the difference in solubility and the absolute solubility until the metastable form is completely transformed to the stable form. If the two samples are not polymorphs but are different compounds, one may dissolve but the other will not grow (except perhaps as the solution evaporates). If the two are identical forms of the same compound, no change will occur on standing in solution. (Remember that the solution in use is, at the beginning, a saturated solution of either one of the two samples.) This method works only for systems in which the compound condenses on sublimation as a polymorph different from the original. To increase this possibility, different condensing surface temperatures should be tried. A low condensing surface temperature favors the formation of a metastable form.

d. Maintain an excess of the solid compound in a small amount of solvent held at a temperature as near the melting point of the compound as possible. Hold for several hours, then isolate the suspended solid by decantation followed by drying at the refluxing temperature. Any method of quickly isolating these crystals or, at least, keeping the temperature from dropping during the entire operation is satisfactory. Test the product with a sample of the original compound for solution phase transformation as outlined above under *c*. This procedure works for any enantiotropic system, e.g., styphnic acid, HMX, Hg_2I_2, in which the material can be maintained in the temperature range of the high-temperature form for a sufficiently long time for the solution phase transformation to occur. Using a solvent boiling in the desired temperature range solves the problems of temperature control and of agitation.

e. Recrystallize the compound from a small amount of solution by cooling very rapidly (pour onto ice, or drop dropwise on a chilled microscope slide, etc.), and observe a portion of the precipitate suspended in a drop of the mother liquor. The drop may then be seeded with the original compound to check for solution phase transformation. If the precipitate is a different polymorph, a solution phase transformation should take place. This method of obtaining polymorphs has been used successfully for hydroquinone and for HMX.

UM00012198
NOVARTIS EXHIBIT 1517
Novartis v. Regents, IPR2023-01347
Page 944 of 4460

A very useful modification of this test involves the use of high-boiling solvents, such as butyrolactone, thymol, benzyl alcohol, and nitrobenzene. If these compounds are used, it is possible to carry out the recrystallization in a drop on a microscope slide. Under these conditions cooling will be very rapid, and it is possible to obtain high-temperature polymorphic forms that have not been prepared by any other method. For example, RDX and HND were found to exist in at least two polymorphic forms by recrystallizing from thymol after all other methods of detecting the presence of polymorphs had failed.

X. Are Two Given Samples Polymorphic Forms of the Same Compound?

Another general problem is the recognition of polymorphism as the relationship between two different crystalline solids. Some general procedures for achieving this are given below. Because many of the phenomena listed in Section VIII (tautomerism, polymerism, strain, etc.) can cause a system to behave as though it is polymorphic, it is necessary to eliminate these possibilities before concluding in any given case that polymorphism is present. In general, if the two phases are different crystallographically (as determined by x-ray diffraction or petrographically), then crystal strain can be eliminated. If the two crystal forms give identical melts or solutions at the instant of melting or dissolving, then tautomerism and polymerism are eliminated. If the two crystal forms are solid (i.e., do not flow with pressure on the cover slip), then mesomorphism is eliminated. In the entire list of procedures to be given below it is assumed that grain growth due to strain has been eliminated.

a. If two samples have different crystal properties, i.e., axial ratios, refractive indices, densities, and x-ray powder patterns, and can be converted into each other through a solid phase or a solution phase transformation, they are polymorphic forms of the same compound.

b. If the two compounds are different in all crystal properties, as in *a*, yet melt to give a liquid having the same refractive index of the melt and the same temperature coefficient of refractive index, the two samples are likely to be polymorphs of the same compound. If the two solids are mixed and heated to the first melting point and held there, a pair of polymorphs will either crystallize completely as the high-melting stable form or will melt completely (if both forms melt very close together). If the system remains as a mixture of solid and melt at that temperature, then the two solids are different compounds.

UM00012199
NOVARTIS EXHIBIT 1517
Novartis v. Regents, IPR2023-01347
Page 945 of 4460

olves the use of high-boiling
alcohol, and nitrobenzene. If
ry out the recrystallization in
nditions cooling will be very
ture polymorphic forms that
or example, RDX and HND
forms by recrystallizing from
presence of polymorphs had

phic Forms of the

n of polymorphism as the
solids. Some general pro-
use many of the phenomena
m, strain, etc.) can cause a
s necessary to eliminate these
hat polymorphism is present.
lographically (as determined
stal strain can be eliminated.
utions at the instant of melt-
rism are eliminated. If the
with pressure on the cover
ntire list of procedures to be
o strain has been eliminated.

erties, i.e., axial ratios, re-
erns, and can be converted
tion phase transformation,
nd.
ystal properties, as in *a*, yet
lex of the melt and the same
vo samples are likely to be
olids are mixed and heated
of polymorphs will either
rm or will melt completely
/stem remains as a mixture
e two solids are different

c. If a mixed fusion between the two samples shows identity, yet the crystal properties are different, as in *a*, then the two samples are polymorphs of the same compound.

d. If one of the samples is fused and allowed to supercool slightly below the melting point, the melt can be seeded at different points with each of the solid samples. If the resulting solidification is observed using a low-power microscope having crossed polars, observation at the junction of the two solids will indicate the presence or absence of polymorphism. If, at the junction, one of the two forms continues to grow through the other solid, the two forms are polymorphs. If the two solids grow together with no subsequent change, even on rewarming and long standing, then the two samples are identical and are not polymorphs (assuming that one of the seed crystals did not transform during the seeding operation). Seeding alone is not, however, proof that the crystal form of the seed material and the growing crystals are the same phase or even, necessarily, the same compound. Seeding with any material involves some physical shock which is often sufficient, by itself, to cause nucleation.

e. If the two samples are mixed dry on a microscope slide beneath a cover slip, they can be wetted by allowing a liquid to run in under the edge of the cover slip. If they are wetted with a saturated solution of either component in a suitable solvent, the occurrence of a solution phase transformation means that the two samples are polymorphic forms of the same compound.

f. If several crystals of each sample are heated close together in a hot stage, a solid-solid transformation of one component followed by melting of both at the same temperature will strongly indicate (but not prove) that the two are polymorphs. If, on heating, one form melts first, then resolidifies completely owing to seeding by the other form, followed by uniform melting on further heating, the two forms are polymorphs.

g. There might also be a vapor phase transformation during heating of the two samples in intimate mixture. This too is characteristic of polymorphism.

XI. Conclusion

An understanding of polymorphism is essential to the analyst interested in the use of crystal properties as a means of identifying compounds since a given compound may crystallize in any one of several lattices. HMX, for example, shows four different crystalline polymorphs (Table III) and the lattices are as dissimilar as the two lattices of, say, calcite and diamond.

The chemist interested in the relationship between chemical structure and performance (e.g., color of dyes and pigments, gloss of a wax or polymer

UM00012200
NOVARTIS EXHIBIT 1517
Novartis v. Regents, IPR2023-01347
Page 946 of 4460

coating, strength of a synthetic fiber, sensitivity of an explosive, blood levels for an orally administered drug, rate of burning of a solid propellant) cannot ignore polymorphism because the crystal properties of solubility, density, crystal shape and size, etc., all have an effect on the performance properties. An extreme case is carbon, with the polymorphs graphite (black, soft, a lubricant) and diamond (white, hard, an abrasive).

TABLE III
CRYSTAL PROPERTIES OF THE HMX POLYMORPHS

	Polymorph			
	I	II	III	IV
Crystal system	Monoclinic	Orthorhombic	Monoclinic	Hexagonal
Density	1.92	1.87	1.82	1.78
Beta angle	102.8°	90°	120°	—
Refractive indices				
α (or ω)	1.589	1.561–1.565	1.537	1.607
β	1.594	1.562–1.566	1.585	—
γ (or ϵ)	1.773	1.72 –1.74	1.666	1.566

Polymorphism is a fertile field of research for the physicist or chemist interested in the solid state. In particular, ferromagnetic materials, semiconductors, and piezoelectric materials are very structure-dependent. Wurtzite, for example, is a good semiconductor, whereas sphalerite is not, even though both are ZnS. Only compounds crystallizing in noncentrosymmetric crystal lattices can be piezoelectric; hence quartz, for example, is piezoelectric, but tridymite, a high-temperature form of silica, is not. In ferromagnetism, MnO has two forms; one, stable below 120°C, is strongly antiferromagnetic, whereas the form stable above 120°C is not. Examples of this sort are endless, and anyone interested in the solid state must consider at all times the crystal lattice involved as much as he considers the chemistry of the compound.

XII. References

1. Deffet, L., *Repertoire des Composés Organiques Polymorphes*, DeSoer, Liège, 1942.
2. Buerger, M. J., Chap. 6 in *Phase Transformations in Solids*, John Wiley and Sons, New York, 1951.
3. Stavely, L. A. K., *Quart. Rev.* (*London*), 3, 65 (1949).
4. Verstraete, K., *Bull. Soc. Chim. Belges*, 43, 513 (1934).
5. Baranski, D., and W. McCrone, unpublished data.

UM00012201

NOVARTIS EXHIBIT 1517
Novartis v. Regents, IPR2023-01347
Page 947 of 4460

ity of an explosive, blood levels
ng of a solid propellant) cannot
operties of solubility, density,
on the performance properties.
orphs graphite (black, soft, a
asive).

IX POLYMORPHS

	III	IV
bic	Monoclinic	Hexagonal
	1.82	1.78
	120°	—
5	1.537	1.607
6	1.585	—
	1.666	1.566

for the physicist or chemist
erromagnetic materials, semi-
e very structure-dependent.
or, whereas sphalerite is not,
ls crystallizing in noncentro-
hence quartz, for example, is
re form of silica, is not. In
able below 120°C, is strongly
ve 120°C is not. Examples of
the solid state must consider
as he considers the chemistry

morphes, DeSoer, Liège, 1942.
in Solids, John Wiley and Sons,

).
4).

6. Brandstatter, M., *Z. Physik. Chem.* (*Leipzig*), **192**, 76 (1943).
7. Kofler, A., *Z. Elektrochem.*, 50, 200 (1944).
8. Slawinska, A., McCrone Associates, unpublished data.
9. Schenk, R., *Z. Physik. Chem.* (*Leipzig*), 33, 445 (1900).
10. McCrone, W. C., in *Microchemical Techniques*, N. D. Cheronis, ed., Interscience Division, John Wiley and Sons, New York, 1962.
11. Brandstatter-Kuhnert, *Oesterr. Apotheker Ztg.*, **13**, 19, 297 (1959).
12. McCrone, W. C., *Fusion Methods in Chemical Microscopy*, Interscience Division, John Wiley and Sons, New York, 1957, pp. 41, 53.
13. Hartshorne, N. H., and A. Stuart, *Crystals and the Polarizing Microscope*, Arnold, London, 1960, Chap. 9.
14. Gray, G. W., *Molecular Structure and Properties of Liquid Crystals*, Academic Press, London, New York, 1962.
15. Ref. 12, p. 192.
16. McCrone, W. C., unpublished data.

UM00012202
NOVARTIS EXHIBIT 1517
Novartis v. Regents, IPR2023-01347
Page 948 of 4460

Physics and chemistry of the organic solid state

Volume II

Editors: *David Fox*
State University of New York at Stony Brook
Stony Brook, New York

Mortimer M. Labes
The Franklin Institute Laboratories
Philadelphia, Pennsylvania

Arnold Weissberger
Eastman Kodak Company
Rochester, New York

Interscience Publishers
a division of John Wiley & Sons, Inc., New York · London · Sydney

1965

UM00012203
NOVARTIS EXHIBIT 1517
Novartis v. Regents, IPR2023-01347
Page 949 of 4460

This Page is Inserted by IFW Indexing and Scanning Operations and is not part of the Official Record

BEST AVAILABLE IMAGES

Defective images within this document are accurate representations of the original documents submitted by the applicant.

Defects in the images include but are not limited to the items checked:

- ☐ BLACK BORDERS
- ☐ IMAGE CUT OFF AT TOP, BOTTOM OR SIDES
- ☐ FADED TEXT OR DRAWING
- ☐ BLURRED OR ILLEGIBLE TEXT OR DRAWING
- ☐ SKEWED/SLANTED IMAGES
- ☐ COLOR OR BLACK AND WHITE PHOTOGRAPHS
- ☐ GRAY SCALE DOCUMENTS
- ☐ LINES OR MARKS ON ORIGINAL DOCUMENT
- ☐ REFERENCE(S) OR EXHIBIT(S) SUBMITTED ARE POOR QUALITY
- ☐ OTHER: _____

IMAGES ARE BEST AVAILABLE COPY.
As rescanning these documents will not correct the image problems checked, please do not report these problems to the IFW Image Problem Mailbox.

[*Acta Cryst.*, (1977), B33, 1455-1459]

Crystal Structure of the 1:1 Sulfacetamide-Caffeine Complex

Authors: --Jean Michel Leger:
Analytical Chemistry Laboratory, School of Pharmacy, *ERA* Number 26, *CNRS,* University of Bordeaux II, 91 rue Leyteire, 33000, Bordeaux, France

--Serge Alberola:
General and Inorganic Chemistry Laboratory, Department of Pharmaceutical and Biological Sciences, Montpellier I, France

--and Alain Carpy:
Crystallography Laboratory Affiliated with the *CNRS,* University of Bordeaux I, cours de la Liberation, 33405, Talence, France.

(Received on October 27, 1976. Accepted on October 28, 1976.)

The crystal structure of the 1:1 complex of sulphacetamide with caffeine has been solved by X-ray diffraction methods. The crystals are monoclinic, space group $P2_1/c$, with a = 7:30 (8), b = 30.76 (7), c = 8.89 (7) Å, β = 108.1 (5)°, and four sulfacetamide and four caffeine molecules in the cell. The full-matrix least-squares refinement of 332 atomic positional and thermal parameters, based on 3365 X-ray intensity data, gave a final R of 0.05. The structure consists of ribbons of sulfacetamide molecules linked by NH...O hydrogen bonds. Caffeine molecules bridge two different sulfacetamide ribbons by NH...N and NH...O hydrogen bonds. A strong van der Walls force is also involved in the complex formation.

Introduction

Within the context of research conducted in relation to combinations of chemical substances of a medicinal nature, Alberola, Rambaud, and Sabon (1976) identified a 1:1 molecular compound consisting of sulfanilamide and caffeine by differential enthalpic analysis.

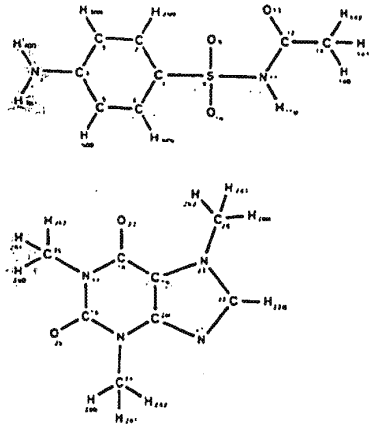


Figure 1: Atomic Numbering.

For defining and comparing the nature of bonds in the solid form and in solutions, determination of the crystal structure of this complex (Figure 1) was initially attempted.

Experimental Phase

Crystals were obtained by gradual evaporation from an ethyl alcohol solution (Alberola *et al.*, 1976). Crystallographic data is as follows: monoclinic system: spatial group-- *P2, 1c*; lattice parameters: $a = 7.30$ (8), $b = 30.76(7)$, $c = 8.89$ (7) A, $\beta = 108.1(5)°$; $V = 1{,}900$ A, $d_m = 1.46$, $d_c = 1.43$ g cm^{-3}, $Z = 4$. Number of reflections: 3,385, with 2,614 having been observed.

Diffracted intensities were measured with a *Siemens* automatic diffractometer which had been equipped with a scintillation counter, by θ - 2θ scanning and with use of Cu $K\alpha$ radiation.

Determination of the Structure

Coordinates for the sulfur atom were determined by deconvolution of Patterson's three-dimensional function for E^2. Fourier sections which were completed with signs for sulfur allowed all of the other atoms to be located. Refinement by the least squares method took place in the manner described within Table 1.*

Table 1: Refining the Structure

Refinement with weighting method: $w = 1$ if $|F_o| < P$ and $w = P^2/F_o$ if $|F_o| > P$, with $P = \sqrt{|F^2_o \text{ (max.)}/10|}$

	R
Refinement with isotropic thermal excitation for S, O, N, C atoms; after five cycles	0.12
Refinement with anisotropic thermal excitation for the same atoms; after three cycles	0.07
Location of hydrogen atoms by Cochran's differential function	
Refinement with isotropic thermal excitation for hydrogen atoms and anisotropic excitation for other atoms; after three cycles	0.05

Results

Table 2 contains parameters for positions and thermal excitation of atoms. Interatomic distances and angles for bonds appear within Tables 3 and 4.

The figures which were obtained are highly consistent with those which were proposed for sulfanilamides by Alleaume (1967) and by Sutor (1958) for hydrated caffeine (Table 5).

Use of a program developed by Schomaker, Waser, Marsh, and Bergman (1959) allowed determination of the following average planes (Table 6): Plane 1, consisting of C(1) to C(6) atoms; Plane 2 consisting of C(16), N(17), C(19), and C(20) atoms; and Plane 3 consisting of S (8), N (11), and C(12) atoms.

---

*Lists of structural factors have been filed with the British Library Lending Division's Records Division (Supplementary Publication Number SUP 32277: 35 pages). It is possible to obtain copies by contacting: The Executive Secretary, International Union of Crystallography, 13 White Friars, Chester CH1 1NZ, England.

UM00012206
NOVARTIS EXHIBIT 1517
Novartis v. Regents, IPR2023-01347
Page 952 of 4460

Table 2: Atomic Coordinates (x10⁴) and Thermal Excitation Factors, β_{ij} (x 10⁴)

	x	y	z	β_{11}	β_{22}	β_{33}	β_{12}	β_{13}	β_{23}
C(1)	1449 (4)	1594 (1)	−533 (3)	172 (7)	9 (0)	101 (4)	0 (2)	57 (8)	2 (2)
C(2)	1198 (4)	1850 (1)	−1860 (4)	199 (7)	10 (0)	118 (4)	9 (2)	63 (8)	10 (2)
C(3)	1104 (5)	1661 (1)	−3290 (3)	224 (8)	10 (0)	107 (4)	5 (3)	60 (9)	9 (2)
C(4)	1300 (4)	1209 (1)	−3397 (4)	194 (7)	11 (0)	120 (4)	−12 (3)	72 (9)	−5 (2)
C(5)	1564 (5)	954 (1)	−2041 (4)	243 (8)	10 (0)	140 (5)	−13 (3)	96 (10)	−1 (2)
C(6)	1625 (5)	1142 (1)	−628 (4)	221 (8)	10 (0)	123 (4)	−9 (3)	82 (9)	5 (2)
N(7)	1198 (5)	1014 (1)	−4808 (3)	360 (9)	14 (0)	127 (4)	−14 (3)	155 (10)	−20 (2)
S(8)	1578 (1)	1826 (0)	1277 (1)	189 (2)	11 (0)	100 (1)	−2 (1)	68 (2)	−2 (0)
O(9)	1007 (4)	1508 (1)	2221 (3)	269 (6)	18 (0)	122 (3)	−35 (2)	135 (7)	5 (2)
O(10)	628 (4)	2235 (1)	1006 (3)	266 (6)	14 (0)	161 (4)	36 (2)	90 (8)	−13 (2)
N(11)	3892 (4)	1897 (1)	2227 (3)	192 (6)	11 (0)	109 (4)	−12 (2)	15 (7)	4 (2)
C(12)	5057 (5)	2196 (1)	1819 (4)	248 (8)	10 (0)	125 (5)	−14 (3)	74 (10)	−4 (2)
O(13)	4486 (4)	2422 (1)	664 (3)	331 (7)	14 (0)	169 (4)	−35 (3)	55 (9)	15 (2)
C(14)	7093 (6)	2211 (1)	2950 (5)	218 (9)	18 (1)	197 (7)	−25 (4)	58 (12)	−4 (3)
N(15)	3415 (4)	−605 (1)	−4509 (3)	235 (7)	13 (0)	127 (4)	7 (2)	71 (8)	6 (2)
C(16)	2732 (5)	−218 (1)	−5238 (4)	226 (8)	12 (0)	157 (6)	1 (3)	53 (11)	−1 (2)
N(17)	2408 (4)	−192 (1)	−6850 (3)	246 (7)	10 (0)	156 (5)	10 (2)	29 (9)	13 (2)
C(18)	2726 (5)	−524 (1)	−7833 (4)	200 (8)	12 (0)	155 (5)	4 (3)	62 (10)	14 (2)
C(19)	3393 (5)	−907 (1)	−6994 (4)	179 (7)	11 (0)	144 (5)	4 (3)	57 (9)	4 (2)
C(20)	3704 (5)	−950 (1)	−5400 (4)	186 (7)	11 (0)	151 (5)	4 (3)	50 (9)	5 (2)
N(21)	4287 (5)	−1351 (1)	−4883 (4)	269 (8)	12 (0)	183 (5)	12 (3)	58 (10)	21 (2)
C(22)	4331 (6)	−1567 (1)	−6210 (5)	274 (10)	13 (0)	199 (7)	16 (3)	105 (12)	12 (3)
N(23)	3781 (4)	−1308 (1)	−7520 (3)	212 (7)	14 (0)	145 (4)	0 (2)	94 (8)	−8 (2)
C(24)	3596 (7)	−667 (2)	−2835 (4)	370 (13)	19 (1)	130 (6)	9 (4)	96 (13)	8 (3)
O(25)	2435 (5)	92 (1)	−4475 (3)	410 (9)	13 (0)	213 (5)	24 (3)	99 (11)	−20 (2)
C(26)	1550 (7)	218 (1)	−7612 (6)	421 (14)	11 (0)	226 (8)	42 (4)	21 (16)	28 (3)
O(27)	2401 (4)	−468 (1)	−9268 (3)	358 (8)	19 (0)	139 (4)	18 (3)	91 (9)	21 (2)
C(28)	3667 (6)	−1448 (2)	−9106 (5)	257 (10)	21 (1)	176 (7)	6 (4)	131 (13)	−23 (3)

	x	y	z	B		x	y	z	B
H(140)	7904 (57)	2356 (12)	2421 (49)	7,0	H(262)	210 (59)	279 (13)	−7474 (49)	7,5
H(141)	7552 (55)	1938 (13)	3366 (45)	6,8	H(280)	4638 (55)	−1282 (13)	−9399 (45)	6,5
H(142)	7088 (58)	2387 (14)	3880 (48)	7,7	H(281)	4336 (63)	−1729 (13)	−8910 (52)	7,9
H(200)	1139 (50)	2168 (10)	−1765 (40)	4,6	H(282)	2420 (62)	−1439 (13)	−9854 (52)	7,9
H(220)	4751 (56)	−1884 (12)	−6217 (47)	6,4	H(300)	933 (53)	1852 (11)	−4250 (45)	5,6
H(240)	2604 (56)	−821 (12)	−2619 (48)	6,9	H(500)	1765 (54)	616 (12)	−2095 (43)	5,6
H(241)	3695 (56)	−403 (12)	−2386 (46)	6,6	H(110)	4450 (54)	1716 (12)	3109 (44)	5,8
H(242)	4791 (60)	−828 (13)	−2331 (50)	7,7	H(600)	1747 (49)	949 (11)	291 (42)	4,9
H(260)	2181 (56)	506 (12)	−7249 (48)	6,7	H(700)	1667 (55)	741 (12)	−4865 (45)	6,3
H(261)	1656 (55)	221 (12)	−8580 (45)	6,5	H(701)	1293 (54)	1180 (13)	−5603 (45)	6,3

Table 3: Interatomic Distances (Å)

C(1)	C(2)	1,383 (4)	N(17)	C(26)	1,476 (5)
C(2)	C(3)	1,380 (4)	C(18)	O(27)	1,236 (4)
C(3)	C(4)	1,404 (4)	N(23)	C(28)	1,453 (5)
C(4)	C(5)	1,403 (5)	N(15)	C(20)	1,380 (5)
C(5)	C(6)	1,372 (5)	C(2)	H(200)	0,984 (32)
C(6)	C(1)	1,401 (4)	C(3)	H(300)	1,012 (37)
C(1)	S(8)	1,737 (3)	C(5)	H(500)	1,053 (36)
S(8)	O(9)	1,434 (3)	C(6)	H(600)	0,993 (35)
S(8)	O(10)	1,422 (3)	N(7)	H(700)	0,914 (37)
S(8)	N(11)	1,652 (3)	N(7)	H(701)	0,894 (39)
N(11)	C(12)	1,376 (4)	N(11)	H(110)	0,945 (37)
C(12)	O(13)	1,203 (4)	C(14)	H(140)	0,973 (42)
C(12)	C(14)	1,515 (6)	C(14)	H(141)	0,937 (40)
C(4)	N(7)	1,372 (4)	C(14)	H(142)	0,988 (41)
N(15)	C(16)	1,374 (5)	C(22)	H(220)	1,023 (39)
C(16)	N(17)	1,382 (5)	C(28)	H(280)	0,973 (41)
N(17)	C(18)	1,411 (5)	C(28)	H(281)	0,981 (42)
C(18)	C(19)	1,398 (5)	C(28)	H(282)	0,947 (46)
C(19)	C(20)	1,371 (5)	C(26)	H(260)	1,005 (39)
C(20)	N(21)	1,339 (4)	C(26)	H(261)	0,888 (39)
N(21)	C(22)	1,363 (5)	C(26)	H(262)	1,042 (46)
C(22)	N(23)	1,365 (5)	C(24)	H(240)	0,935 (42)
N(23)	C(19)	1,380 (4)	C(24)	H(241)	0,898 (39)
N(15)	C(24)	1,466 (5)	C(24)	H(242)	0,982 (44)
C(16)	O(25)	1,227 (5)			

Table 4: Angles for Bonds (°)

C(1)–C(2)–C(3)	120,18 (03)	H(110)–N(11)–C(12)	118,02 (24)	H(280)–C(28)–H(281)	98,37 (37)
C(2)–C(3)–C(4)	120,15 (03)	N(11)–C(12)–O(13)	122,22 (03)	H(280)–C(28)–H(282)	114,74 (37)
C(3)–C(4)–C(5)	119,11 (03)	N(11)–C(12)–C(14)	113,94 (03)	H(281)–C(28)–H(282)	117,86 (40)
C(4)–C(5)–C(6)	120,47 (03)	O(13)–C(12)–C(14)	123,84 (03)	C(28)–N(23)–C(19)	129,71 (03)
C(5)–C(6)–C(1)	119,82 (03)	C(12)–C(14)–H(140)	108,24 (26)	N(23)–C(19)–C(18)	130,29 (03)
S(8)–C(1)–C(2)	120,78 (02)	C(12)–C(14)–H(141)	113,03 (25)	C(19)–C(18)–O(27)	126,29 (03)
C(1)–C(2)–H(200)	119,38 (22)	C(12)–C(14)–H(142)	108,31 (25)	O(27)–C(18)–N(17)	121,51 (03)
H(200)–C(2)–C(3)	120,40 (22)	H(140)–C(14)–H(141)	113,83 (36)	C(18)–N(17)–C(26)	117,61 (03)
C(2)–C(3)–H(300)	119,47 (23)	H(140)–C(14)–H(142)	108,47 (36)	N(17)–C(26)–H(260)	121,28 (25)
H(300)–C(3)–C(4)	120,36 (23)	H(141)–C(14)–H(142)	104,70 (36)	N(17)–C(26)–H(261)	107,47 (27)
C(3)–C(4)–N(7)	121,26 (03)	N(15)–C(16)–N(17)	117,40 (03)	N(17)–C(26)–H(262)	112,32 (25)
C(4)–N(7)–H(700)	122,65 (26)	C(16)–N(17)–C(18)	126,34 (03)	H(260)–C(26)–H(261)	97,71 (36)
H(700)–N(7)–H(701)	111,06 (37)	N(17)–C(18)–C(19)	112,19 (03)	H(260)–C(26)–H(262)	99,07 (35)
C(4)–N(7)–H(701)	118,48 (26)	C(18)–C(19)–C(20)	123,51 (03)	H(261)–C(26)–H(262)	118,83 (36)
N(7)–C(4)–C(5)	119,61 (03)	C(19)–C(20)–N(15)	120,87 (03)	N(17)–C(16)–O(25)	121,76 (03)
C(4)–C(5)–H(500)	119,88 (22)	C(20)–N(15)–C(16)	119,65 (03)	O(25)–C(16)–N(15)	120,84 (03)
H(500)–C(5)–C(6)	119,62 (22)	N(21)–C(20)–C(19)	112,17 (03)	C(16)–N(15)–C(24)	119,82 (03)
C(5)–C(6)–H(600)	117,99 (22)	C(20)–C(19)–N(23)	106,14 (03)	N(15)–C(24)–H(240)	116,41 (26)
H(600)–C(6)–C(1)	122,14 (22)	C(19)–N(23)–C(22)	105,67 (03)	N(15)–C(24)–H(241)	107,68 (27)
C(6)–C(1)–S(8)	118,97 (02)	N(23)–C(22)–N(21)	111,99 (03)	N(15)–C(24)–H(242)	108,42 (27)
C(1)–S(8)–O(9)	108,69 (01)	C(22)–N(21)–C(20)	104,02 (03)	H(240)–C(24)–H(241)	109,04 (38)
C(1)–S(8)–O(10)	108,93 (01)	N(21)–C(20)–C(19)	112,17 (03)	H(240)–C(24)–H(242)	106,71 (37)
O(10)–S(8)–O(9)	119,18 (01)	N(21)–C(22)–H(220)	123,87 (24)	H(241)–C(24)–H(242)	108,35 (38)
C(1)–S(8)–N(11)	106,26 (01)	H(220)–C(22)–N(23)	124,14 (24)	C(24)–N(15)–C(20)	120,07 (03)
O(9)–S(8)–N(11)	103,23 (01)	C(22)–N(23)–C(28)	124,62 (03)	N(15)–C(20)–N(21)	126,96 (03)
O(10)–S(8)–N(11)	109,76 (01)	N(23)–C(28)–H(280)	106,18 (24)	C(6)–C(1)–C(2)	120,25 (03)
S(8)–N(11)–H(110)	117,11 (24)	N(23)–C(28)–H(281)	102,39 (28)	C(26)–N(17)–C(16)	115,95 (03)
S(8)–N(11)–C(12)	124,87 (02)	N(23)–C(28)–H(282)	115,18 (28)		

The results which were obtained provide a basis for the following observations:
--the benzene ring within sulfacetamide is perfectly flat;
--the two caffeine rings are practically flat (Atom C(22), which offers the most significant deviation from the plane, is separated from it by a distance of 0.07 Å).

The dihedral angle formed by ring ϕ (plane 1) and the beginning of the sulfacetamide chain (plane 3) is equal to $\phi = 102.86°$

In terms of the dihedral angle formed by the intermediate planes 1 and 2, it is equal to $\phi = 12.56°$, thereby demonstrating that sulfacetamide's ϕ ring and the two caffeine rings are practically parallel.

Table 5: Interatomic Distances (A) *and Angles* (°) *for Certain Sulfanilamides and for Hydrated Caffeine*

Typical Configuration for Sulfanilamides (Alleaume, 1967)

C(1)–C(2)	1,381	C(1)–C(2)–C(3)	120,7
C(2)–C(3)	1,382	C(2)–C(3)–C(4)	120,2
C(3)–C(4)	1,399	C(3)–C(4)–C(5)	118,0
C(4)–N(7)	1,380	C(4)–C(5)–C(6)	120,0
C(4)–C(5)	1,399	C(5)–C(6)–C(1)	120,7
C(5)–C(6)	1,382	C(6)–C(1)–C(2)	120,0
C(6)–C(1)	1,381	C(2)–C(1)–S(8)	119,8
C(1)–S(8)	1,751	C(6)–C(1)–S(8)	119,8
S(8)–O(9)	1,442	C(1)–S(8)–O(9)	107,3
S(8)–O(10)	1,442	C(1)–S(8)–O(10)	107,3
S(8)–N(11)	1,635	C(1)–S(8)–N(11)	109,8
		O(9)–S(8)–N(11)	106,8
		O(10)–S(8)–N(11)	106,8
		O(9)–S(8)–O(10)	118,3
		C(3)–C(4)–N(7)	120,9
		C(5)–C(4)–N(7)	120,9

NOVARTIS EXHIBIT 1517
Novartis v. Regents, IPR2023-01347
Page 954 of 4460

Configuration for Hydrated Caffeine (Sutor, 1958)

N(15)–C(16)	1.35	C(20)–N(15)–C(16)	122.8
C(16)–N(17)	1.42	N(15)–C(16)–N(17)	112.9
N(17)–C(18)	1.36	C(16)–N(17)–C(18)	127.6
C(18)–C(19)	1.44	N(17)–C(18)–C(19)	115.8
C(19)–C(20)	1.32	C(18)–C(19)–C(20)	119.9
C(20)–N(21)	1.31	C(19)–C(20)–N(15)	121.4
N(21)–C(22)	1.34	C(19)–C(20)–N(21)	110.9
C(22)–N(23)	1.32	C(20)–N(21)–C(22)	105.7
N(23)–C(19)	1.41	N(21)–C(22)–N(23)	112.3
N(15)–C(20)	1.42	C(22)–N(23)–C(19)	103.4
N(15)–C(24)	1.50	N(23)–C(19)–C(20)	107.2
C(16)–O(25)	1.19	C(20)–N(15)–C(24)	119.2
N(17)–C(26)	1.48	C(24)–N(15)–C(16)	117.9
C(18)–O(27)	1.26	N(15)–C(16)–O(25)	124.1
N(23)–C(28)	1.47	C(16)–N(17)–C(26)	112.0
		C(26)–N(17)–C(18)	120.3
		N(17)–C(18)–O(27)	118.4
		C(19)–C(18)–O(27)	126.4
		C(19)–N(23)–C(28)	128.7
		C(22)–N(23)–C(28)	127.5

Cohesion of Crystals

The crystal structure of the complex is characterized by chains consisting of sulfacetamide molecules which are interconnected by N(7^{iii})-H(701^{iii})...O(9^{i}) hydrogen bonds which are parallel to the (100) plane (Figures 2 and 3). The angle for N (7^{iii})-H(701^{iii})...O(9^{i}) is equal to 168.33° (Table 7).

Caffeine molecules are situated between two sulfacetamide periodic chains, and they connect these chains according to the directions identified as (010) and (001) by means of O(25^{i})... H(700^{i})-N(7^{i}) and N(21^{iv})-H(110^{i})...N(11^{i}) bonds respectively. The measurements of the O(25^{i})... H(700^{i})-N(7^{i}) and N (11^{i})-H(110^{i})...N(21^{iv}) angles are 164.06° and 176.99° (Table 7).

The principal van der Waals bonds are indicated within Table 7. One form of contact which is more significant than other forms of contact, namely O(13^{i})-C(22^{vi}) = 3.225 A, should be taken into account.

Table 6: Average Planes for Atoms

Plane 1: $-(0.9694)X - (0.0993)Y + (0.2246)Z = 1.5554$

Atoms which define the plane:

C(1)	0.001 Å	C(3)	−0.007 Å	C(5)	0.005 Å
C(2)	0.006	C(4)	0.002	C(6)	−0.006

Other atoms:

N(7)	−0.011 Å	O(10)	−0.509 Å	O(13)	2.311 Å
S(8)	0.020	N(11)	1.604	C(14)	3.919
O(9)	−0.559	C(12)	2.554		

Plane 2: $(0.9353)X + (0.3090)Y + (0.1724)Z = 2.2453$

Atoms which define the plane:

C(16)	0.006 Å	C(19)	0.005 Å
N(17)	−0.004	C(20)	−0.005

Other atoms:

C(18)	0.008 Å	N(23)	−0.055 Å	C(26)	−0.113 Å
N(15)	0.024	C(24)	−0.105	O(27)	0.001
N(21)	−0.043	O(25)	0.015	C(28)	−0.077
C(22)	−0.074				

Plane 3: $(-0.4361)X + (0.6786)Y + (0.5910)Z = 4.1020$

Atoms which define the plane:

S(1)	N(11)	C(12)

Table 7: Hydrogen Bonds and van der Waals Bonds

Symmetry Code:

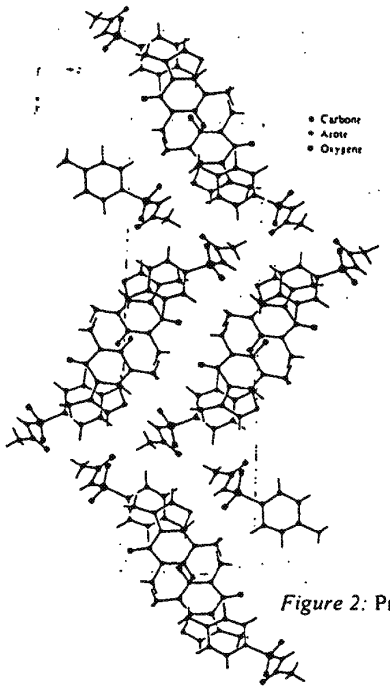
(i)	x	y	z	(v)	$\bar{x}$	$\bar{y}$	$\bar{z}-2$
(ii)	$\bar{x}$	$\bar{y}$	$\bar{z}-1$	(vi)	x	$y+\frac{1}{2}$	$z+\frac{1}{2}$
(iii)	x	y	$z+1$	(vii)	$\bar{x}+1$	$y+\frac{1}{2}$	$\bar{z}-\frac{1}{2}$
(iv)	$\bar{x}+1$	$\bar{y}$	$\bar{z}$	(viii)	$\bar{x}+1$	$\bar{y}$	$\bar{z}-1$

Hydrogen Bonds

$O(25^{i})\cdots N(7^{i})$	2,965 Å		
$O(25^{i})\cdots H(700^{i})$	2,075	$O(25^{i})\cdots H(700^{i})-N(7^{i})$	164,06°
$O(9^{i})\cdots N(7^{iii})$	3,015		
$O(9^{i})\cdots H(701^{iii})$	2,135	$O(9^{i})\cdots H(701^{iii})-N(7^{i})$	168,33
$N(11^{i})\cdots N(21^{iv})$	2,867		
$H(110^{i})\cdots N(21^{iv})$	1,922	$N(11^{i})-H(110^{i})\cdots N(21^{iv})$	176,99

van der Waals Bonds

$C(5^{i})-C(19^{ii})$	3,456 Å	$C(14^{i})-N(21^{iv})$	3,472 Å
$N(15^{i})-N(7^{vi})$	3,470	$C(26^{i})-O(27^{v})$	3,412
$C(4^{i})-N(23^{viii})$	3,443	$O(10^{i})-C(2^{vi})$	3,348
$C(4^{i})-C(22^{viii})$	3,496	$O(13^{i})-C(22^{vii})$	3,225
$C(16^{i})-C(16^{viii})$	3,476		



• Carbon

✶ Nitrogen

■Oxygen

Figure 2: Projection of Structure onto Plane (100)

Discussion and Conclusion

The results which were obtained demonstrate that formation of the complex in a solid phase is provided by two hydrogen bonds. Moreover, for both caffeine, *C*, and sulfacetamide, *S*, combinations are of the *S* ... *C* ... *S* and *C* ... *S* ... *C* type.

These combinations are comparable to those which Craven and Gartland (1970) had identified for the 2:1 barbital-caffeine complex. In that instance, however, caffeine was only connected to the barbital chains by a sole hydrogen bond and by two 3.16 A and 3.35 Å van der Waals bonds.

With the 1:1 sulfacetamide-caffeine contact remaining in solution (Alberola, 1976), infrared spectroscopic analysis was undertaken in order to attempt to determine whether the remaining hydrogen bond is of the NH ... O type or the NH... N type.

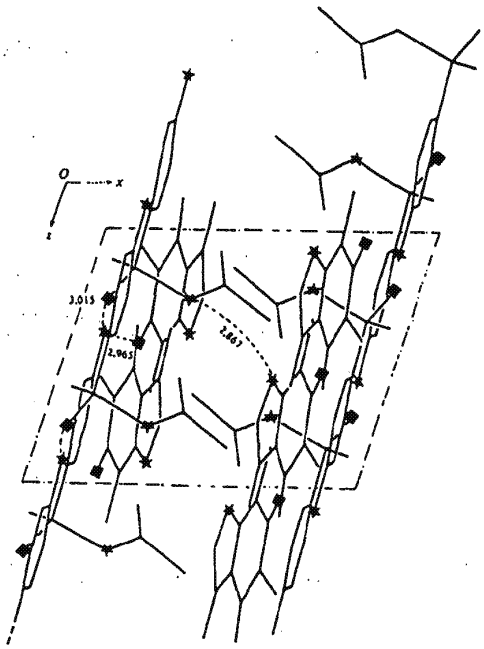


Figure 3: Projection of Structure onto Plane (010)

References

S. Alberola (1976), private correspondence.
S. Alberola, J. Rambaud, & F. Sabon (1976), Bull. Soc. Chim. Fr. Pp. 362-364
M. Alleaume (1967), Doctoral Thesis in Physical Sciences, University of Bordeaux I.
B. M. Craven & G. L. Gartland, J. Pharm. Sci. 59, 1666-1670
V. Schomaker, J. Waser, R. E. Marsh & G. Bergman (1959), Acta Cryst. 12, 600-604
J. D. Sutor (1958), Acta Cryst. 11, 453-458

TG057

Acta Cryst. (1977). B33, 1455–1459

Structure Cristalline du Complexe 1 : 1 Sulfacétamide–Caféine

PAR JEAN MICHEL LEGER

Laboratoire de Chimie Analytique, Faculté de Pharmacie ERA n° 626 CNRS, Université de Bordeaux II, 91 *rue Leyteire*, 33000 *Bordeaux, France*

SERGE ALBEROLA

Laboratoire de Chimie générale et minérale, UER des Sciences Pharmaceutiques et Biologiques, Montpellier I, *France*

ET ALAIN CARPY

Laboratoire de Cristallographie associé au CNRS, Université de Bordeaux I, 351 *cours de la Libération*, 33405 *Talence, France*

(*Reçu le* 27 *octobre* 1976, *accepté le* 28 *octobre* 1976)

The crystal structure of the 1 : 1 complex of sulphacetamide with caffeine has been solved by X-ray diffraction methods. The crystals are monoclinic, space group $P2_1/c$, with $a = 7{\cdot}30\ (8)$, $b = 30{\cdot}76\ (7)$, $c = 8{\cdot}89\ (7)$ Å, $\beta = 108{\cdot}1\ (5)°$, and four sulphacetamide and four caffeine molecules in the cell. The full-matrix least-squares refinement of 332 atomic positional and thermal parameters, based on 3365 X-ray intensity data, gave a final R of 0·05. The structure consists of ribbons of sulphacetamide molecules linked by NH···O hydrogen bonds. Caffeine molecules bridge two different sulphacetamide ribbons by NH···N and NH···O hydrogen bonds. A strong van der Waals force is also involved in the complex formation.

Introduction

Dans le cadre des recherches poursuivies sur les associations de substances chimiques à caractère médicamenteux, Alberola, Rambaud & Sabon (1976) ont mis en évidence un composé moléculaire 1 : 1 entre la sulfacétamide et la caféine, par analyse enthalpique différentielle.

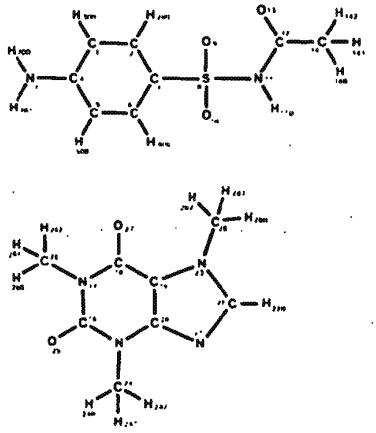


Fig. 1. Numération atomique.

Afin de préciser et de comparer la nature des liaisons dans le solide et en solution, la détermination de la structure cristalline de ce complexe (Fig. 1) a été entreprise dans un premier temps.

Partie expérimentale

Les cristaux ont été obtenus par évaporation lente à partir d'une solution dans l'alcool éthylique (Alberola *et al.*, 1976). Les données cristallographiques sont: système monoclinique; groupe spatial $P2_1/c$; paramètres de la maille: $a = 7{,}30\ (8)$, $b = 30{,}76\ (7)$, $c = 8{,}89\ (7)$ Å, $\beta = 108{,}1\ (5)°$; $V = 1900$ Å^3, $d_m = 1{,}46$, $d_c = 1{,}43$ g cm^{-3}, $Z = 4$. Nombre de réflexions: 3385, dont 2614 observées.

Les intensitées diffractées ont été mesurées sur diffractomètre automatique Siemens équipé d'un compteur à scintillations, en balayage θ–2θ et en utilisant le rayonnement Cu $K\alpha$.

Détermination de la structure

Les coordonnées de l'atome de soufre ont été déterminées par déconvolution de la fonction de Patterson tridimensionnelle en E^2. Des sections de Fourier effectuées avec les signes du soufre ont permis de localiser l'ensemble des autres atomes. L'affinement par la

UM00012212

NOVARTIS EXHIBIT 1517
Novartis v. Regents, IPR2023-01347
Page 958 of 4460

méthode des moindres carrés a été conduit de la façon décrite dans le Tableau 1.*

Résultats

Le Tableau 2 rassemble les paramètres de position et d'agitation thermique des atomes. Dans les Tableaux 3 et 4 sont regroupés les distances interatomiques et les angles de liaisons.

Les valeurs trouvées sont en bon accord avec celles avancées pour les sulfanilamides par Alléaume (1967) et pour la caféine hydratée par Sutor (1958) (Tableau 5).

* La liste des facteurs de structure a été déposée au dépôt d'archives de la British Library Lending Division (Supplementary Publication No. SUP 32277: 35 pp.). On peut en obtenir des copies en s'adressant à: The Executive Secretary, International Union of Crystallography, 13 White Friars, Chester CH1 1NZ, Angleterre.

L'utilisation du programme de Schomaker, Waser, Marsh & Bergman (1959) a permis de déterminer les plans moyens suivants (Tableau 6): plan 1, constitué par les atomes C(1) à C(6); plan 2, constitué par les atomes C(16), N(17), C(19), C(20); et plan 3, constitué par les atomes S(8), N(11), C(12).

Tableau 1. *Affinement de la structure*

Affinement avec le schéma de pondération: $w = 1$ si $|F_o| < P$, et $w = P^2/F_o$ si $|F_o| > P$, avec $P = \sqrt{|F_o^2(\text{max.})/10|}$.

	R
Affinement avec agitation thermique isotrope sur les atomes S, O, N, C; après cinq cycles	0.12
Affinement avec agitation thermique anisotrope sur ces mêmes atomes; après trois cycles	0.07
Localisation des atomes d'hydrogène par fonction différence de Cochran	
Affinement avec agitation thermique isotrope sur les atomes d'hydrogène et anisotrope sur les autres atomes; après trois cycles	0.05

Tableau 2. *Les coordonnées atomiques* ($\times 10^4$) *et les facteurs d'agitation thermique* β_{ij} ($\times 10^4$)

	x	y	z	β_{11}	β_{22}	β_{33}	β_{12}	β_{13}	β_{23}
C(1)	1449 (4)	1594 (1)	−533 (3)	172 (7)	9 (0)	101 (4)	0 (2)	57 (8)	2 (2)
C(2)	1198 (4)	1850 (1)	−1860 (4)	199 (7)	10 (0)	118 (4)	9 (2)	63 (8)	10 (2)
C(3)	1104 (5)	1661 (1)	−3290 (3)	224 (8)	10 (0)	107 (4)	5 (3)	60 (9)	9 (2)
C(4)	1300 (4)	1209 (1)	−3397 (4)	194 (7)	11 (0)	120 (4)	−12 (3)	72 (9)	−5 (2)
C(5)	1564 (5)	954 (1)	−2041 (4)	243 (8)	10 (0)	140 (5)	−13 (3)	96 (10)	−1 (2)
C(6)	1625 (5)	1142 (1)	−628 (4)	221 (8)	10 (0)	123 (4)	−9 (3)	82 (9)	5 (2)
N(7)	1198 (5)	1014 (1)	−4808 (3)	360 (9)	14 (0)	127 (4)	−14 (3)	155 (10)	−20 (2)
S(8)	1578 (1)	1826 (0)	1277 (1)	189 (2)	11 (0)	100 (1)	−2 (1)	68 (2)	−2 (0)
O(9)	1007 (4)	1508 (1)	2221 (3)	269 (6)	18 (0)	122 (3)	−35 (2)	135 (7)	5 (2)
O(10)	628 (4)	2235 (1)	1006 (3)	266 (6)	14 (0)	161 (4)	36 (2)	90 (8)	−13 (2)
N(11)	3892 (4)	1897 (1)	2227 (3)	192 (6)	11 (0)	109 (4)	−12 (2)	15 (7)	4 (2)
C(12)	5057 (5)	2196 (1)	1819 (4)	248 (8)	10 (0)	125 (5)	−14 (3)	74 (10)	−4 (2)
O(13)	4486 (4)	2422 (1)	664 (3)	331 (7)	14 (0)	169 (4)	−35 (3)	55 (9)	15 (2)
C(14)	7093 (6)	2211 (1)	2950 (5)	218 (9)	18 (1)	197 (7)	−25 (4)	58 (12)	−4 (3)
N(15)	3415 (4)	−605 (1)	−4509 (3)	235 (7)	13 (0)	127 (4)	7 (2)	71 (8)	6 (2)
C(16)	2732 (5)	−218 (1)	−5238 (4)	226 (8)	12 (0)	157 (6)	1 (3)	53 (11)	−1 (2)
N(17)	2408 (4)	−192 (1)	−6850 (3)	246 (7)	10 (0)	156 (5)	10 (2)	29 (9)	13 (2)
C(18)	2726 (5)	−524 (1)	−7833 (4)	200 (8)	12 (0)	155 (5)	4 (3)	62 (10)	14 (2)
C(19)	3393 (5)	−907 (1)	−6994 (4)	179 (7)	11 (0)	144 (5)	4 (3)	57 (9)	4 (2)
C(20)	3704 (5)	−950 (1)	−5400 (4)	186 (7)	11 (0)	151 (5)	4 (3)	50 (9)	5 (2)
N(21)	4287 (5)	−1351 (1)	−4883 (4)	269 (8)	12 (0)	183 (5)	12 (3)	58 (10)	21 (2)
C(22)	4331 (6)	−1567 (1)	−6210 (5)	274 (10)	13 (0)	199 (7)	16 (3)	105 (12)	12 (3)
N(23)	3781 (4)	−1308 (1)	−7520 (3)	212 (7)	14 (0)	145 (4)	0 (2)	94 (8)	−8 (2)
C(24)	3596 (7)	−667 (2)	−2835 (4)	370 (13)	19 (1)	130 (6)	9 (4)	96 (13)	8 (3)
O(25)	2435 (5)	92 (1)	−4475 (3)	410 (9)	13 (0)	213 (5)	24 (3)	99 (11)	−20 (2)
C(26)	1550 (7)	218 (1)	−7612 (6)	421 (14)	11 (0)	226 (8)	42 (4)	21 (16)	28 (3)
O(27)	2401 (4)	−468 (1)	−9268 (3)	358 (8)	19 (0)	139 (4)	18 (3)	91 (9)	21 (2)
C(28)	3667 (6)	−1448 (2)	−9106 (5)	257 (10)	21 (1)	176 (7)	6 (4)	131 (13)	−23 (3)

	x	y	z	B		x	y	z	B
H(140)	7904 (57)	2356 (12)	2421 (49)	7,0	H(262)	210 (59)	279 (13)	−7474 (49)	7,5
H(141)	7552 (55)	1938 (13)	3366 (45)	6,8	H(280)	4638 (55)	−1282 (13)	−9399 (45)	6,5
H(142)	7088 (58)	2387 (14)	3880 (48)	7,7	H(281)	4336 (63)	−1729 (13)	−8910 (52)	7,9
H(200)	1139 (50)	2168 (10)	−1765 (40)	4,6	H(282)	2420 (62)	−1439 (13)	−9854 (52)	7,9
H(220)	4751 (56)	−1884 (12)	−6217 (47)	6,4	H(300)	933 (53)	1852 (11)	−4250 (45)	5,6
H(240)	2604 (56)	−821 (12)	−2619 (48)	6,9	H(500)	1765 (54)	616 (12)	−2095 (43)	5,6
H(241)	3695 (56)	−403 (12)	−2386 (46)	6,6	H(110)	4450 (54)	1716 (12)	3109 (44)	5,8
H(242)	4791 (60)	−828 (13)	−2331 (50)	7,7	H(600)	1747 (49)	949 (11)	291 (42)	4,9
H(260)	2181 (56)	506 (12)	−7249 (48)	6,7	H(700)	1667 (55)	741 (12)	−4865 (45)	6,3
H(261)	1656 (55)	221 (12)	−8580 (45)	6,5	H(701)	1293 (54)	1180 (13)	−5603 (45)	6,3

UM00012213
NOVARTIS EXHIBIT 1517
Novartis v. Regents, IPR2023-01347
Page 959 of 4460

Les résultats obtenus conduisent aux remarques suivantes:

– le cycle benzénique de la sulfacétamide est parfaitement plan;

– les deux cycles de la caféine sont pratiquement plans [l'atome C(22) présentant le plus grand écart avec le plan est distant de 0,07 Å].

L'angle dièdre formé par le cycle φ (plan 1) et le départ de la chaîne de la sulfacétamide (plan 3) est égal à $\varphi_1 = 102,86°$.

Quant à l'angle dièdre formé par les plans moyens 1 et 2, il est égal à $\varphi_2 = 12,56°$, ce qui montre que le cycle φ de la sulfacétamide et les deux cycles de la caféine sont pratiquement parallèles.

Tableau 3. *Distances interatomiques* (Å)

C(1)	C(2)	1,383 (4)	N(17)	C(26)	1,476 (5)
C(2)	C(3)	1,380 (4)	C(18)	O(27)	1,236 (4)
C(3)	C(4)	1,404 (4)	N(23)	C(28)	1,453 (5)
C(4)	C(5)	1,403 (5)	N(15)	C(20)	1,380 (5)
C(5)	C(6)	1,372 (5)	C(2)	H(200)	0,984 (32)
C(6)	C(1)	1,401 (4)	C(3)	H(300)	1,012 (37)
C(1)	S(8)	1,737 (3)	C(5)	H(500)	1,053 (36)
S(8)	O(9)	1,434 (3)	C(6)	H(600)	0,993 (35)
S(8)	O(10)	1,422 (3)	N(7)	H(700)	0,914 (37)
S(8)	N(11)	1,652 (3)	N(7)	H(701)	0,894 (39)
N(11)	C(12)	1,376 (4)	N(11)	H(110)	0,945 (37)
C(12)	O(13)	1,203 (4)	C(14)	H(140)	0,973 (42)
C(12)	C(14)	1,515 (6)	C(14)	H(141)	0,937 (40)
C(4)	N(7)	1,372 (4)	C(14)	H(142)	0,988 (41)
N(15)	C(16)	1,374 (5)	C(22)	H(220)	1,023 (39)
C(16)	N(17)	1,382 (5)	C(28)	H(280)	0,973 (41)
N(17)	C(18)	1,411 (5)	C(28)	H(281)	0,981 (42)
C(18)	C(19)	1,398 (5)	C(28)	H(282)	0,947 (46)
C(19)	C(20)	1,371 (5)	C(26)	H(260)	1,005 (39)
C(20)	N(21)	1,339 (4)	C(26)	H(261)	0,888 (39)
N(21)	C(22)	1,363 (5)	C(26)	H(262)	1,042 (46)
C(22)	N(23)	1,365 (5)	C(24)	H(240)	0,935 (42)
N(23)	C(19)	1,380 (4)	C(24)	H(241)	0,898 (39)
N(15)	C(24)	1,466 (5)	C(24)	H(242)	0,982 (44)
C(16)	O(25)	1,227 (5)			

Cohésion cristalline

La structure cristalline du complexe est caractérisée par des chaînes formées de molécules de sulfacétamide liées entre elles par liaison hydrogène $N(7^{iii})$–$H(701^{iii})\cdots O(9^{i})$, parallèles au plan (100) (Figs. 2 et 3). L'angle $N(7^{iii})$–$H(701^{iii})\cdots O(9^{i})$ est égal à 168,33° (Tableau 7).

Les molécules de caféine s'insèrent entre deux chaînes périodiques de sulfacétamide et les relient dans les directions (010) et (001) par l'intermédiaire des liaisons hydrogène $O(25^{i})\cdots H(700^{i})$–$N(7^{i})$ et $N(21^{iv})\cdots H(110^{i})$–$N(11^{i})$ respectivement. Les angles $O(25^{i})$–$H(700^{i})$–$N(7^{i})$ et $N(11^{i})$–$H(110^{i})\cdots N(21^{iv})$ ont pour valeur 164,06 et 176,99° (Tableau 7).

Les principales liaisons de van der Waals sont rassemblées dans le Tableau 7. Il est à noter un contact plus important que les autres, $O(13^{i})$–$C(22^{vi})$ = 3,225 Å.

Tableau 4. *Angles de liaisons* (°)

C(1)–C(2)–C(3)	120,18 (03)	H(110)–N(11)–C(12)	118,02 (24)	H(280)–C(28)–H(281)	98,37 (37)
C(2)–C(3)–C(4)	120,15 (03)	N(11)–C(12)–O(13)	122,22 (03)	H(280)–C(28)–H(282)	114,74 (37)
C(3)–C(4)–C(5)	119,11 (03)	N(11)–C(12)–C(14)	113,94 (03)	H(281)–C(28)–H(282)	117,86 (40)
C(4)–C(5)–C(6)	120,47 (03)	O(13)–C(12)–C(14)	123,84 (03)	C(28)–N(23)–C(19)	129,71 (03)
C(5)–C(6)–C(1)	119,82 (03)	C(12)–C(14)–H(140)	108,24 (26)	N(23)–C(19)–C(18)	130,29 (03)
S(8)–C(1)–C(2)	120,78 (02)	C(12)–C(14)–H(141)	113,03 (25)	C(19)–C(18)–O(27)	126,29 (03)
C(1)–C(2)–H(200)	119,38 (22)	C(12)–C(14)–H(142)	108,31 (25)	O(27)–C(18)–N(17)	121,51 (03)
H(200)–C(2)–C(3)	120,40 (22)	H(140)–C(14)–H(141)	113,83 (36)	C(18)–N(17)–C(26)	117,61 (03)
C(2)–C(3)–H(300)	119,47 (23)	H(140)–C(14)–H(142)	108,47 (36)	N(17)–C(26)–H(260)	121,28 (25)
H(300)–C(3)–C(4)	120,36 (23)	H(141)–C(14)–H(142)	104,70 (36)	N(17)–C(26)–H(261)	107,47 (27)
C(3)–C(4)–N(7)	121,26 (03)	N(15)–C(16)–N(17)	117,40 (03)	N(17)–C(26)–H(262)	112,32 (25)
C(4)–N(7)–H(700)	122,65 (26)	C(16)–N(17)–C(18)	126,34 (03)	H(260)–C(26)–H(261)	97,71 (36)
H(700)–N(7)–H(701)	111,06 (37)	N(17)–C(18)–C(19)	112,19 (03)	H(260)–C(26)–H(262)	99,07 (35)
C(4)–N(7)–H(701)	118,48 (26)	C(18)–C(19)–C(20)	123,51 (03)	H(261)–C(26)–H(262)	118,83 (36)
N(7)–C(4)–C(5)	119,61 (03)	C(19)–C(20)–N(15)	120,87 (03)	N(17)–C(16)–O(25)	121,76 (03)
C(4)–C(5)–H(500)	119,88 (22)	C(20)–N(15)–C(16)	119,65 (03)	O(25)–C(16)–N(15)	120,84 (03)
H(500)–C(5)–C(6)	119,62 (22)	N(21)–C(20)–C(19)	112,17 (03)	C(16)–N(15)–C(24)	119,82 (03)
C(5)–C(6)–H(600)	117,99 (22)	C(20)–C(19)–N(23)	106,14 (03)	N(15)–C(24)–H(240)	116,41 (26)
H(600)–C(6)–C(1)	122,14 (22)	C(19)–N(23)–C(22)	105,67 (03)	N(15)–C(24)–H(241)	107,68 (27)
C(6)–C(1)–S(8)	118,97 (02)	N(23)–C(22)–N(21)	111,99 (03)	N(15)–C(24)–H(242)	108,42 (27)
C(1)–S(8)–O(9)	108,69 (01)	C(22)–N(21)–C(20)	104,02 (03)	H(240)–C(24)–H(241)	109,04 (38)
C(1)–S(8)–O(10)	108,93 (01)	N(21)–C(20)–C(19)	112,17 (03)	H(240)–C(24)–H(242)	106,71 (37)
O(10)–S(8)–O(9)	119,18 (01)	N(21)–C(22)–H(220)	123,87 (24)	H(241)–C(24)–H(242)	108,35 (38)
C(1)–S(8)–N(11)	106,26 (01)	H(220)–C(22)–N(23)	124,14 (24)	C(24)–N(15)–C(20)	120,07 (03)
O(9)–S(8)–N(11)	103,23 (01)	C(22)–N(23)–C(28)	124,62 (03)	N(15)–C(20)–N(21)	126,96 (03)
O(10)–S(8)–N(11)	109,76 (01)	N(23)–C(28)–H(280)	106,18 (24)	C(6)–C(1)–C(2)	120,25 (03)
S(8)–N(11)–H(110)	117,11 (24)	N(23)–C(28)–H(281)	102,39 (28)	C(26)–N(17)–C(16)	115,95 (03)
S(8)–N(11)–C(12)	124,87 (02)	N(23)–C(28)–H(282)	115,18 (28)		

UM00012214
NOVARTIS EXHIBIT 1517
Novartis v. Regents, IPR2023-01347
Page 960 of 4460

Tableau 5. *Distances* (Å) *et angles* (°) *interatomiques pour quelques sulfanilamides et pour la caféine hydratée*

Configuration moyenne de sulfanilamides (Allèaume, 1967)

C(1)–C(2)	1,381	C(1)–C(2)–C(3)	120,7
C(2)–C(3)	1,382	C(2)–C(3)–C(4)	120,2
C(3)–C(4)	1,399	C(3)–C(4)–C(5)	118,0
C(4)–N(7)	1,380	C(4)–C(5)–C(6)	120,0
C(4)–C(5)	1,399	C(5)–C(6)–C(1)	120,7
C(5)–C(6)	1,382	C(6)–C(1)–C(2)	120,0
C(6)–C(1)	1,381	C(2)–C(1)–S(8)	119,8
C(1)–S(8)	1,751	C(6)–C(1)–S(8)	119,8
S(8)–O(9)	1,442	C(1)–S(8)–O(9)	107,3
S(8)–O(10)	1,442	C(1)–S(8)–O(10)	107,3
S(8)–N(11)	1,635	C(1)–S(8)–N(11)	109,8
		O(9)–S(8)–N(11)	106,8
		O(10)–S(8)–N(11)	106,8
		O(9)–S(8)–O(10)	118,3
		C(3)–C(4)–N(7)	120,9
		C(5)–C(4)–N(7)	120,9

Configuration de la caféine hydratée (Sutor, 1958)

N(15)–C(16)	1,35	C(20)–N(15)–C(16)	122,8
C(16)–N(17)	1,42	N(15)–C(16)–N(17)	112,9
N(17)–C(18)	1,36	C(16)–N(17)–C(18)	127,6
C(18)–C(19)	1,44	N(17)–C(18)–C(19)	115,8
C(19)–C(20)	1,32	C(18)–C(19)–C(20)	119,9
C(20)–N(21)	1,31	C(19)–C(20)–N(15)	121,4
N(21)–C(22)	1,34	C(19)–C(20)–N(21)	110,9
C(22)–N(23)	1,32	C(20)–N(21)–C(22)	105,7
N(23)–C(19)	1,41	N(21)–C(22)–N(23)	112,3
N(15)–C(20)	1,42	C(22)–N(23)–C(19)	103,4
N(15)–C(24)	1,50	N(23)–C(19)–C(20)	107,2
C(16)–O(25)	1,19	C(20)–N(15)–C(24)	119,2
N(17)–C(26)	1,48	C(24)–N(15)–C(16)	117,9
C(18)–O(27)	1,26	N(15)–C(16)–O(25)	124,1
N(23)–C(28)	1,47	C(16)–N(17)–C(26)	112,0
		C(26)–N(17)–C(18)	120,3
		N(17)–C(18)–O(27)	118,4
		C(19)–C(18)–O(27)	126,4
		C(19)–N(23)–C(28)	128,7
		C(22)–N(23)–C(28)	127,5

Discussion et conclusion

Les résultats obtenus montrent que la formation du complexe en phase solide est assurée par deux liaisons hydrogène. D'autre part, soit *C* la caféine et *S* la sulfacétamide, les associations dans le cristal sont du type $S\cdots C\cdots S'$ et $C\cdots S\cdots C'$.

Ces associations sont comparables à celles trouvées par Craven & Gartland (1970) pour le complexe 2:1 barbital–caféine. Dans ce cas cependant, la caféine n'est liée aux chaînes de barbital que par une seule liaison hydrogène et par deux contacts de van der Waals à 3,16 et 3,35 Å.

Le complexe 1:1 sulfacétamide–caféine subsistant en solution (Alberola, 1976), une étude par spectroscopie IR a été entreprise pour tenter de préciser si la liaison hydrogène qui demeure est du type NH···O ou du type NH···N.

Tableau 6. *Plans moyens d'atomes*

Plan 1: $(0,9694)X + (0,0993)Y + (0,2246)Z = 1,5554$

Atomes définissant le plan

C(1)	0,001 Å	C(3)	−0,007 Å	C(5)	0,005 Å
C(2)	0,006	C(4)	0,002	C(6)	−0,006

Autres atomes

N(7)	−0,011 Å	O(10)	−0,509 Å	O(13)	2,311 Å
S(8)	0,020	N(11)	1,604	C(14)	3,919
O(9)	−0,559	C(12)	2,554		

Plan 2: $(0,9353)X + (0,3090)Y + (0,1724)Z = 2,2453$

Atomes définissant le plan

C(16)	0,006 Å	C(19)	0,005 Å
N(17)	−0,004	C(20)	−0,005

Autres atomes

C(18)	0,008 Å	N(23)	−0,055 Å	C(26)	−0,113 Å
N(15)	0,024	C(24)	−0,105	O(27)	0,001
N(21)	−0,043	O(25)	0,015	C(28)	−0,077
C(22)	−0,074				

Plan 3: $(-0,4361)X + (0,6786)Y + (0,5910)Z = 4,1020$

Atomes définissant le plan

S(1)	N(11)	C(12)

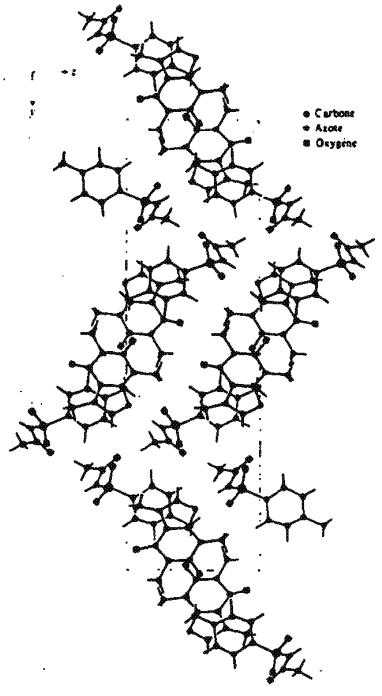


Fig. 2. Projection de la structure sur le plan (100).

UM00012215

NOVARTIS EXHIBIT 1517
Novartis v. Regents, IPR2023-01347
Page 961 of 4460

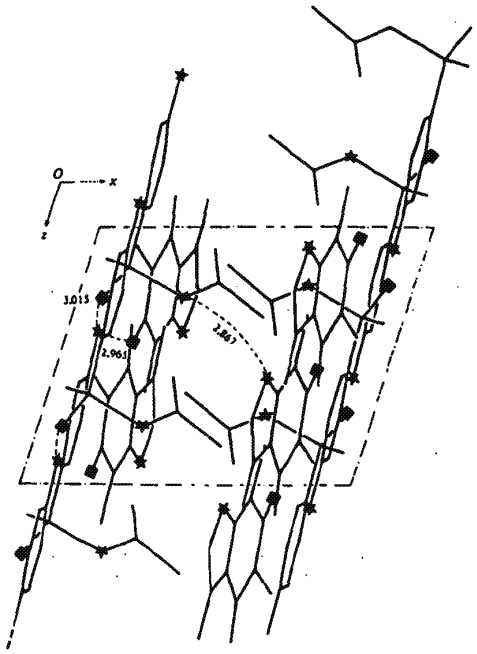


Fig. 3. Projection de la structure sur le plan (010).

Tableau 7. *Liaisons hydrogène et de van der Waals*

Code de symétrie

(i)	x	y	z	(v)	$\bar{x}$	$\bar{y}$	$\bar{z}-2$
(ii)	$\bar{x}$	y	$\bar{z}-1$	(vi)	x	$y+\frac{1}{2}$	$\bar{z}+\frac{1}{2}$
(iii)	x	y	$z+1$	(vii)	$\bar{x}+1$	$y+\frac{1}{2}$	$\bar{z}-\frac{1}{2}$
(iv)	$\bar{x}+1$	$\bar{y}$	$\bar{z}$	(viii)	$\bar{x}+1$	$\bar{y}$	$\bar{z}-1$

Liaisons hydrogène

$O(25^{i})\cdots N(7^{i})$	2,965 Å	$O(25^{i})\cdots H(700^{i})-N(7^{i})$	164,06°
$O(25^{i})\cdots H(700^{i})$	2,075		
$O(9^{i})\cdots N(7^{iii})$	3,015	$O(9^{i})\cdots H(701^{iii})-N(7^{i})$	168,33
$O(9^{i})\cdots H(701^{iii})$	2,135		
$N(11^{i})\cdots N(21^{iv})$	2,867	$N(11^{i})-H(110^{i})\cdots N(21^{iv})$	176,99
$H(110^{i})\cdots N(21^{iv})$	1,922		

Liaisons de van der Waals

$C(5^{i})-C(19^{ii})$	3,456 Å	$C(14^{i})-N(21^{iv})$	3,472 Å
$N(15^{i})-N(7^{ii})$	3,470	$C(26^{i})-O(27^{v})$	3,412
$C(4^{i})-N(23^{viii})$	3,443	$O(10^{i})-C(2^{vi})$	3,348
$C(4^{i})-C(22^{viii})$	3,496	$O(13^{i})-C(22^{viii})$	3,225
$C(16^{i})-C(16^{viii})$	3,476		

Références

ALBEROLA, S. (1976). Communication privée.

ALBEROLA, S., RAMBAUD, J. & SABON, F. (1976). *Bull. Soc. Chim. Fr.* pp. 362–364.

ALLÉAUME, M. (1967). Thèse Doctorat ès Sciences Physiques, Bordeaux I.

CRAVEN, B. M. & GARTLAND, G. L. (1970). *J. Pharm. Sci.* **59**, 1666–1670.

SCHOMAKER, V., WASER, J., MARSH, R. E. & BERGMAN, G. (1959). *Acta Cryst.* **12**, 600–604.

SUTOR, J. D. (1958). *Acta Cryst.* **11**, 453–458.

UM00012216

NOVARTIS EXHIBIT 1517
Novartis v. Regents, IPR2023-01347
Page 962 of 4460

(19) JAPANESE PATENT OFFICE

(11) Japanese Unexamined Patent Application
No. 54-16494

Official Gazette for Unexamined Patent Applications

(51) Int.Cl.[2]	Ident. Symbols	(52) Japanese Classification	Internal Office Nos.
C 07 D 323/00		**16 E 581**	6670-4C
C 07 C 143/80		16 C 712	6742-4H
C 07 D 237/20		16 E 341	7431-4C
C 07 D 239/44 //		16 E 461	6670-4C
A 61 K 31/63	ADZ	16 E 463	6617-4C
A 61 K 31/635	ADZ	30 C 2	6617-4C
		30 G 144	
		30 H 612	

(43) Disclosure Date: 7 February 1979

Number of Inventions: 1
Request for Examination: Not yet requested

(Total of 6 pages)

(54) Complexes of Crown Ethers and Sulfonamides

(21) Application No.: 52-81572

(22) Application Date: 8 July 1977
Presented at the 97th Annual Symposium of the Japanese Chemical Society on 10 March 1977 in conformance to Paragraph 1, Article 30, of the Patent Act

(72) Inventor: Kozo Takayama
6-24-18 Arajuku-machi, Kawagoe-shi

(71) Applicant: Yamanouchi Pharmaceutical Company, Ltd.

(72) Inventor: Tsuneji Nagai
12-205 Tamagawa Residence (to), 3-1-180 Somechi, Chofu-shi
5-1 Hon-machi 2-chome, Nihonbashi, Chuo-ku, Tokyo-to

(74) Agent: Koichi Sasaki, Patent Attorney

Continued on last page

SPECIFICATION

1. Title of the Invention
Complexes of Crown Ethers and Sulfonamides

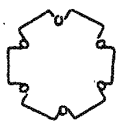
2. Claims
(1) Complexes of 18-crown-6 and sulfonamides.

(2) Complexes as described in Claim (1) in which the sulfonamide is sulfamonomethoxine or sulfamethoxazole.

3. Detailed Description of the Invention
Crown ethers, and 18-crown-6 in particular have a large cyclic structure and have the property of forming stable complexes with various types of metal salts and ammonium salts as guest molecules. it is knows that crown ethers form complexes with some organic compounds. In this case, the organic compounds are limited exclusively to aliphatic amines and hydrochlorides thereof [Journal of American Chemical Society, **89**, 7017 (1967)].

The inventors conducted research on complexes of organic medicinal drug products and crown ethers and perfected this invention by discovering that a series of sulfonamides forms stable complexes with 18-crown-6.

Specifically, the present invention relates to complexes of 18-crown-6 and sulfonamides. Here, 18-crown-6 signifies a,1,4,7,10,13,16-hexaoxacyclooctadecane, which is indicated by the following formula.



Further, the sulfonamides are p-aminobenzenesulfonic acid amides or a series of their derivatives, and, in the present invention, include, for example, the following compounds, which are useful as medicinal drugs: Sulfamethoxine, sulfamonomethoxine, sulfadimethoxine, sulfamethoxazole, sulfamethizole, sulfamine, acetosulfamine, sulfaguanidine, sulfathiazole, sulfadiazine, sulfamerazine, sulfamethazine, sulfaisomidine, sulfaisoxazole, sulfamethoxypyridazine, sulfaphenazole.

The following tables show comparisons of changes over time in plasma concentrations of sulfamonomethoxine when a complex of the present invention (sulfamonomethxine/18-crown-6 complex) and when sulfamonomethoxine hydrate were administered orally to Beagle dogs (see the test method described subsequently).

Table I. Changes Over Time in Plasma Concentrations of Unchanged Sulfamonomethoxine

Test material	Changes over time in plasma concentrations (μg/ml)						
	1 hr	2 hr	4 hr	6 hr	8 hr	12 hr	24 hr
Sulfamonomethoxine /18-crown-6 complex	26.0 ±7.6	31.8 ±7.3	33.9 ±5.6	39.6 ±5.5	45.1 ±9.8	46.8 ±13	27.9 ±9.2
Sulfamonomethoxine hydrate	0.153 ±0.12	18.8 ±7.1	31.9 ±10	33.6 ±10	35.2 ±12	34.5 ±10	20.3 ±6.6

Table II. Changes Over Time in Plasma Concentrations of Total Sulfamonomethoxine

Test material	Changes over time in plasma concentrations (μg/ml)						
	1 hr	2 hr	4 hr	6 hr	8 hr	12 hr	24 hr
Sulfamonomethoxine/18-crown-6 complex	28.0 ±7.5	33.7 ±7.1	37.6 ±5.7	40.6 ±4.2	44.9 ±9.7	49.4 ±13	29.5 ±9.2
Sulfamonomethoxine hydrate	0.540 ±0.36	19.3 ±7.0	33.9 ±10	34.3 ±10	35.0 ±9.9	35.6 ±10	20.9 ±6.8

The physical stability of the complex is also good. The stability of complexes of the present invention in benzene and chloroform obtained in the working examples to be described subsequently or by methods based on them are shown in the following table.

Table III

Sulfonamide	Stability constant (M^{-1})	
	In benzene	In chloroform
Sulfamethoxine	34.30	20.52
Sulfamonomethoxine	165.97	14.11
Sulfamethoxazole	-	10.00
Sulfaphenazole	41.95	6.68
Sulfamethoxypyridazine	29.71	10.60
Sulfadimethoxine	50.38	10.52
Sulfamethizole	-	11.21
Sulfaisoxazole	80.37	13.35
Sulfaisomidine	-	5.44
Sulfamerazine	-	22.38
Sulfathiazole	-	21.08
Sulfanilamide	-	48.54

The complexes of the present invention are stable not only in benzene and chloroform as described above but also in other inorganic solvents such as, for example, carbon tetrachloride and cyclohexane, and, as required, can be isolated from these solvents as solids.

Complexes of the present invention that have been isolated as solids can be administered in unaltered form or can be prepared as suitable solid preparations or semi-solid preparations. Tablets, powders and capsule preparations are suitable as solid preparations. Preparation of these solid preparations can be performed as necessary by standard methods in which lubricants, excipients, binders and disintegrating agents such as magnesium stearate, talc, silicon oxide, starch, lactose, calcium hydrogenphosphate, crystalline cellulose, gum arabic, methyl cellulose, polyvinyl pyrrolidone, gelatin, and carboxymethyl cellulose calcium. Preparation of semi-solid preparations, as necessary, can be performed by standard methods by adding cellulose derivatives such as, for example, Metrose SM (brand name), carboxymethyl cellulose sodium, for example, Celogen F-SB (brand name), hydroxypropyl cellulose, hydroxypropylmethyl cellulose, polyvinyl pyrrolidone, and polyvinyl alcohol; oils and fats such as peanut butter oil, coconut oil, Olive oil, soybean oil, rapeseed oil, cottonseed oil, sesame oil, corn oil, rice-bran oil, camellia oil, cacao oil, lard, wool fat and beef tallow, substances obtained by modifying them by hydrogenation, acetylation and cleavage extraction, and aqueous or oleaginous preparations of esters of fatty aids of 6 to 30 carbon atoms and alcohols of 2 to 8 carbons atoms, for example isopropyl myristate (for example, IPM®(EX) manufactured by Nikko Chemicals).

By means of this invention, complexes of various types of sulfonamides and 18-crown-6 can be manufactured as follows.

They can be manufactured by stirring equimolar or excess quantities of 18-crown-6 relative to the sulfonamide in a nonpolar solvent and at room temperatures or lower. The nonpolar solvents that can be used include, for example, benzene, chloroform, carbon tetrachloride and cyclohexane. In executing this method, the sulfonamide is dissolved in the nonpolar solvent, after which 18-crown-6 is added and the mixture is stirred or both the sulfonamide and the 18-crown-6 are stirred in the nonpolar solvent.

The quantity of 18-crown-6 used relative to the sulfonamide is usually an equimolar quantity or a suitable amount greater than that. When 18-crown-6 is used in an excess quantity, for example, more than 20 times the number of moles, a decrease in yield is brought about and complexes of high purity can be obtained.

In order to gather the complex that is produced, the solid substance that is precipitated may be filled, suitably washed and desiccated.

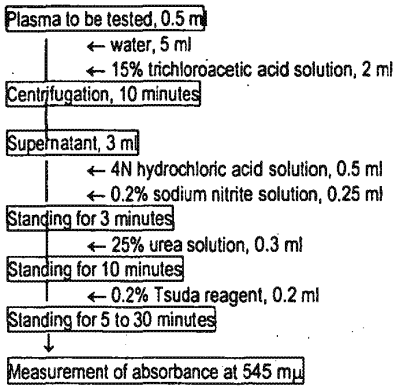
Test Method

Six beagle dogs (male; body weights, approximately, 10 Kg) were divided at random in two groups and administration experiments were performed by cross-over tests. Sulfamonomexine/18-crown-6 complex or sulfamonomethoxine hydrate were administered to 3 animals in each group, and, after 1 week, the test materials were switched and the same test was performed. The test materials, which were powders, were packaged using two wafers and were administered orally. The doses of the test materials were 319.3 mg of sulfamonomethoxine hydrate and 499.2 mg of complex. The beagle dogs were fasted for 24 hours before execution and for 12 hours after execution.

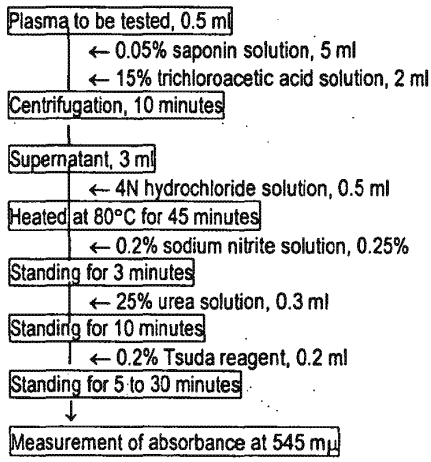
3 ml of blood was collected from the forepaw at 1, 2, 4, 6, 8, 12 and 24 hours after administration. It was centrifuged immediately, the plasma was collected and the blood was frozen and stored at -10°C.

The concentrations of unchanged sulfamonomethoxine and total sulfamonomethoxine in the plasma were measured quantitatively by the modified Bratton-Marshall method. The details of these quantitative determination methods are shown in the figures below.

Quantitative Measurement Method of Unchanged Sulfamonomethoxine in Plasma



Quantitative Measurement Method of Total Sulfamonomethoxine in Plasma



Next, we shall further describe the method of manufacture of the complexes of this invention by presenting working examples.

Working Example 1

Complex of sulfamonomethoxine and 18-crown-6

600 ml of benzene was added to 40 mg of sulfamonomethoxine and 632 mg of 18-crown-6 and the mixture was stirred vigorously for 24 hours at 10°C. The solution was filtered, 888 mg of 18-crown-6 was added to the filtrate and the mixture was shaken for 72 hours at 10°C. The fine crystals that precipitated were washed thoroughly using benzene, after which they were dried under decreased pressure.

Working Example 2

Complex of sulfamonomethoxine and 18-crown-6

100 ml of benzene was added to 4 mg of sulfamonomethoxine and 66 g of 18-crown-6 and the mixture was shaken for 10 days at 10°C. During this period, it was stirred vigorously for approximately 1 hour each day. After 10 days, the complex that was formed was filtered and washed with benzene, after which it was dried under reduced pressure.

Working Example 3

Complex of sulfamethoxazole and 18-crown-6

200 ml of benzene was added to 20 mg of sulfamethoxazole and the mixture was stirred for 24 hours at 10°C. The solution was filtered, 65.27 mg of 1.-8-crown-6 was added to the filtrate and the mixture was shaken for 72 hours at 10°C. The fine crystals that precipitated were filtered and thoroughly washed using benzene, after which they were dried under decreased pressure.

Working Example 4

Complex of sulfamethoxazole and 18-crown-6

100 ml of benzene was added to 5 g of sulfamethoxazole and 6.52 g of 18-crown-6 and the mixture was shaken for 10 days at 10°C. During this period, it was stirred vigorously 1 hour each day. After 10 days, the complex that formed was washed using benzene, after which it was dried under decreased pressure.

Working Example 5

Complex of sulfamethoxypyridazine and 18-crown-6

28.0 mg of sulfamethoxypyridazine and 652.7 mg of 18-crown-6 were used and 28.0 mg of sulfamethoxypyridazine and 105.3 mg of 18-crown-6 were used and were dissolved, respectively, in chloroform and heavy chloroform to make precisely 10 ml.

4. Brief Explanation of the Figures

Figure 1 and Figure 2, respectively, show comparisons of the infrared absorption spectrum of sulfamonomethoxine—18-crown-6 complex (indicated in the figure as (a)) and that of a physical mixture of sulfamonomethoxine and 18-crown-6 (indicated in the figure as (b)), which is a differential scanning thermogram.

Figure 3 through Figure 5, respectively, show the infrared absorption curves of sulfamonomethoxine—18-crown-6 complex (Figure 3), sulfamethoxazole (Figure 4) and –18-crown-6 (Figure 5).

Figure 6 and Figure 7, respectively, show comparisons of the infrared absorption spectrum of sulfamethoxazole—18-crown-6 complex (indicated in the figure as (a)) and that of a physical mixture of sulfamethoxazole and 18-crown-6 (indicated in the figure as (b)), which is a differential scanning thermogram

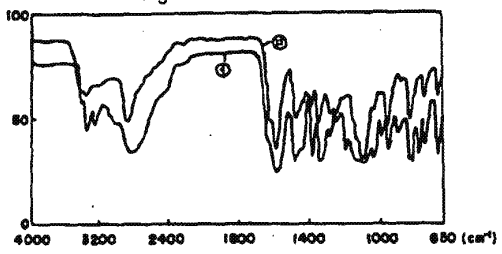
(temperature elevation rate, 8°/minute and an X-ray diffraction pattern).
[NOTE: The final close parenthesis is missing and is assumed by the translator.]

Figure 8 shows comparisons of partial infrared absorption spectra of complexes of sulfamethoxypyridazine—18-crown-6 (in the figure, (a)-1 indicating a mixture ratio of 0.01 mol : 0.01 mol and (a)-2 indicating a mixture ratio of 0.01 mol : 0.02 mol) in the vicinity of 3400 cm-1 and in the vicinity of 1100 cm-1, with that sulfamethoxypyridazine alone (in the figure, indicated by (c))and that of 18-crown-6 alone (in the figure indicated by (b)).

Figure 9 through Figure 12 show the nuclear magnetic resonance spectra of two types of sulfamethoxpyridazine—18-crown-6 complexes (two types of compounding ratios of sulfamethoxpyridazine and 18-crown-6 of 0.01 mol to 0.04 mol (Figure 9) and 0.01 mol to 0.02 mol (Figure 10)), of 18-crown-6 alone (Figure 11) and of sulfamethoxypyridazine (Figure 12).

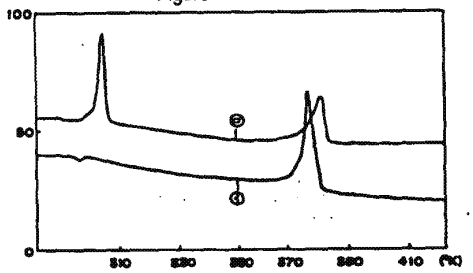
Agent Koichi Sasaki

Figure 1



(b)
(a)

Figure 2



(b)
(a)

Figure 3

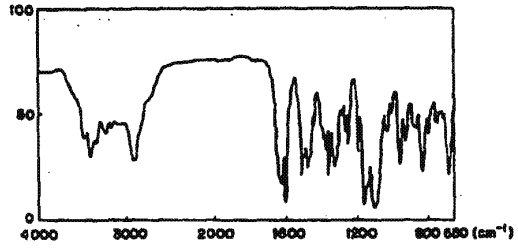


Figure 4

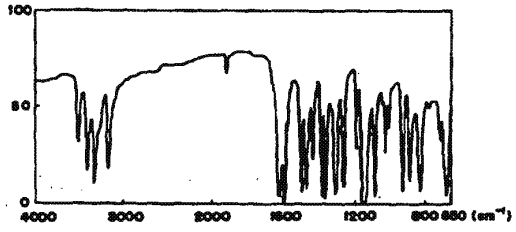


Figure 5

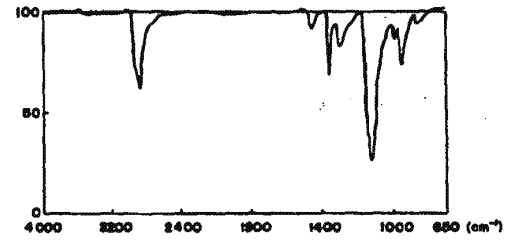
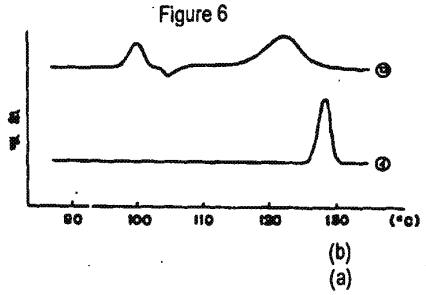


Figure 6

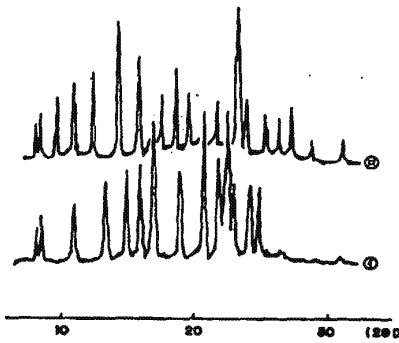


(b)
(a)

(vertical axis) Heat absorption

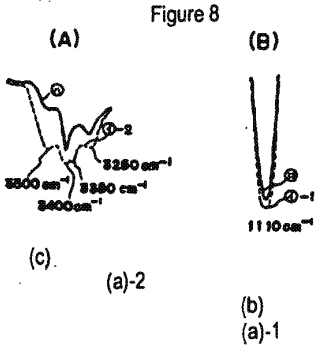
Figure 9

Figure 7



(b)
(a)

Figure 8



(c)
(a)-2
(b)
(a)-1

Figure 11

NOVARTIS EXHIBIT 1517
Novartis v. Regents, IPR2023-01347
Page 967 of 4460

Figure 9

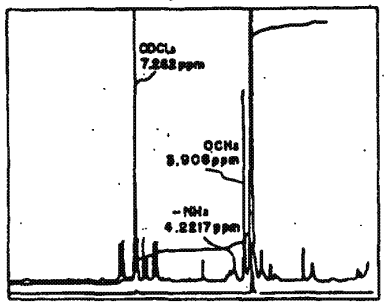


Figure 11

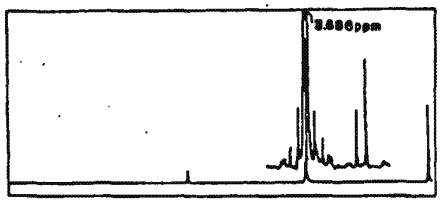


Figure 10

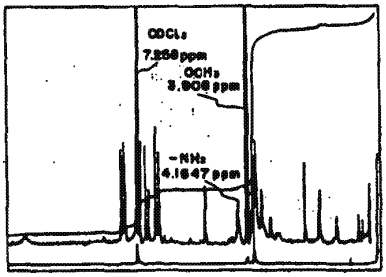
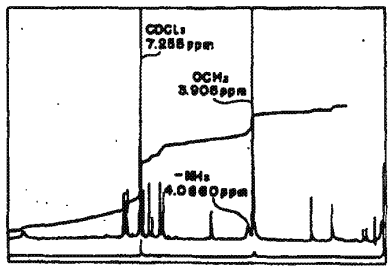


Figure 12



Continued from page 1

(72) Inventor: Naoki Nanbu
4-23-32-101 Nishi Tsujigaoka, Chofu-shi

T9059

⑲日本国特許庁　　⑪特許出願公開

公開特許公報　　昭54—16494

⑤Int. Cl.²	識別記号	⑤日本分類	庁内整理番号
C 07 D 323/00		16 E 581	6670—4C
C 07 C 143/80		16 C 712	6742—4H
C 07 D 237/20		16 E 341	7431—4C
C 07 D 239/44 //		16 E 461	6670—4C
A 61 K 31/63	ADZ	16 E 463	6617—4C
A 61 K 31/635	ADZ	30 C 2	6617—4C
		30 G 144	
		30 H 612	

⑬公開　昭和54年(1979)2月7日

発明の数　1

審査請求　未請求

（全 6 頁）

⑭クラウンエーテルとスルフォンアミド類との複合体

⑳特　　願　昭52—81572

㉒出　　願　昭52(1977)7月8日

特許法第30条第1項適用　昭和52年3月10日

日本薬学会第97年会講演会において発表

⑫発　明　者　永井恒司

調布市染地3—1—180　多摩川住宅（ト）12—205

⑫発　明　者　髙山幸三

川越市新宿町6—24—18

⑪出　願　人　山之内製薬株式会社

東京都中央区日本橋本町2丁目5番地1

⑭代　理　人　佐々木晃一

最終頁に続く

明　細　書

1. 発明の名称

クラウンエーテルとスルフォンアミド類との複合体。

2. 特許請求の範囲

(1) 18－クラウン－6とスルフォンアミド類との複合体。

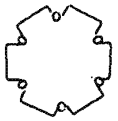
(2) スルフォンアミド類がスルファモノメトキシンまたはスルファメトキサゾールである特許請求の範囲第(1)項記載の複合体。

3. 発明の詳細な説明

クラウンエーテル類，殊に18－クラウン－6は大環状構造を有し，その特性として各種金属の塩やアンモニウム塩などをゲスト分子とした安定な複合体を形成することが知られている。クラウンエーテル類は一部有機化合物と複合体を形成することも知られているが，この場合の有機化合物は専ら脂肪族アミンで且つその塩酸塩に限られていた〔ジャーナル，オブ，アメリカン，ケミカル，ソサエティー，89，7017(1967)〕。

本発明者等は，有機医薬品とクラウンエーテル類との複合体についての研究を進めてきたが，一連のスルフォンアミド類が18－クラウン－6と安定な複合体を形成することを見出し，本発明を完成した。

すなわち本発明は，18－クラウン－6とスルフォンアミド類との複合体に関する。茲に18－クラウン－6とは次式で示される1，4，7，10，13，16－ヘキサオキサシクロオクタデカンを意味している。



また，スルフォンアミド類とはパラアミノベンゼンスルフォン酸アミドまたはその一連の誘導体であって，本発明ではこのうち医薬として有用な，たとえば下記の化合物を包含する。

UM00012223

NOVARTIS EXHIBIT 1517
Novartis v. Regents, IPR2023-01347
Page 969 of 4460

スルファメトミジン，スルファモノメトキシン，スルファジメトキシン，スルファメトキサゾール，スルファメチゾール，スルファミン，アセトスルファミン，スルファグアニジン，スルファチアゾール，スルファジアジン，スルファメラジン，スルファサジン，スルフイソミジン，スルフイソキサゾール，スルフイソメゾール，スルファメトキシピリダジン，スルファフェナゾール。

本発明の複合体は単なる物理的混合物とは明確に異り，高い溶解性とバイオアベラビリティが期待されている。

次表は本発明の複合体（スルファモノメトキシン／18－クラウン－6複合体）をビーグル犬に経口投与した場合におけるスルファモノメトキシンの血漿中濃度の経時変化をスルファモノメトキシン水和物を同様に投与した場合のそれと対比して示したものである（後記実験方法参照）。

表Ⅰ　血漿中未変化スルファモノメトキシンの濃度の経時変化

試料	血漿中濃度（$\mu g/ml$）の経時変化						
	1 hr	2hr	4hr	6hr	8hr	12hr	24hr
スルファモノメトキシン／18－クラウン－6複合体	26.0 ± 7.6	51.8 ± 7.3	55.9 ± 5.6	59.6 ± 5.5	45.1 ± 9.8	46.8 ± 1.5	27.9 ± 9.2
スルファモノメトキシン水和物	0.153 ±0.12	16.8 ± 7.1	51.9 ± 1.0	55.6 ± 1.0	55.2 ± 1.2	54.5 ± 1.0	20.3 ± 4.6

表Ⅱ　血漿中総スルファモノメトキシンの濃度の経時変化

試料	血漿中濃度（$\mu g/ml$）の経時変化						
	1 hr	2 hr	4 hr	6 hr	8 hr	12hr	24hr
スルファモノメトキシン／18－クラウン－6複合体	28.0 ± 7.5	55.7 ± 7.1	57.6 ± 5.7	60.6 ± 4.2	44.9 ± 9.7	49.4 ± 1.5	29.5 ± 9.2
スルファモノメトキシン水和物	0.540 ±0.56	19.5 ± 7.0	55.9 ± 1.0	54.5 ± 1.0	55.0 ± 9.9	55.6 ± 1.0	20.9 ± 4.8

また，複合体の物理的安定性も良好である。今，後記実施例あるいはこれに準ずる方法で得られた本発明の複合体のベンゼンおよびクロロホルム中における安定性を表示するとつぎの通りである。

表Ⅲ

スルフォンアミド類	安定度定数　（M^{-1}）	
	ベンゼン中	クロロホルム中
スルファメトミジン	34.30	20.52
スルファモノメトキシン	165.97	14.11
スルファメトキサゾール	－	10.00
スルファフェナゾール	41.95	6.68
スルファメトキシピリダジン	29.71	10.60
スルファジメトキシン	50.38	10.52
スルファメチゾール	－	11.21
スルフイソキサゾール	80.71	13.35
スルフイソミジン	－	5.44
スルファメラジン	－	22.38
スルファチアゾール	－	21.08
スルファニルアミド	－	48.54

本発明の複合体は，上記ベンゼンあるいはクロロホルム中に限らず，その他の無極性溶媒たとえば四塩化炭素，シクロヘキサンなどの中でも安定であり，必要によりこれらの溶媒中から固体として単離することもできる。

固体として単離した本発明の複合体は，そのままあるいは適宜の固体製剤あるいは半固体製剤に調製して投与される。固形剤形としては錠剤，散剤，カプセル剤等が適当である。これらの固形剤形の調製は，必要によりステアリン酸マグネシウム，タルク，酸化ケイ素，デンプン，乳糖，リン酸水素カルシウム，結晶セルロース，アラビアゴム，メチルセルロース，ポリビニルピロリドン，ゼラチン，カルボキシメチルセルロースカルシウムなどの滑沢剤，賦形剤，結合剤，崩壊剤などを添加し，常法により行ないうる。また，半固体製剤の調製は，必要によりセルロース誘導体たとえばメトローズSM（商品名），カルボキシメチルセルロースナトリウムたとえばセロゲンF－SB（商品名），ハイドロキシプロピルセルロース，ハイドロキシプロピルメチルセルロース，ポリビニルピロリドン，ポリビニルアルコール；ラッカセイ油，ヤシ油，オリーブ油，大豆油，ナタネ油，メンジツ油，ゴマ油，トウモロコシ油，ヌカ油，ツバキ油，カカオ脂，豚脂，羊毛脂，牛脂等の油脂，これ等を水素添加，アセチル化，分別抽出等により改質したもの，

UM00012224
NOVARTIS EXHIBIT 1517
Novartis v. Regents, IPR2023-01347
Page 970 of 4460

炭素数6～30の脂肪酸と炭素2～8のアルコールとのエステル例えばイソプロピルミリステート（例えば日光ケミカルズ社製IPM®(EX)）等の水溶性あるいは油性基剤を加え，常法により行ないうる。

本発明によれば，各種スルフォンアミド類と18－クラウン－6との複合体はつぎのようにして製造できる。

スルフォンアミド類とこれに対し等モル乃至過剰量の18－クラウン－6とを無極性溶媒中室温乃至それ以下の温度でかきまぜることによって製造できる。無極性溶媒としてはたとえばベンゼン，クロロホルム，四塩化炭素，シクロヘキサン等が使用される。この方法を行なうにはスルフォンアミド類を無極性溶媒中に溶解させたのち，18－クラウン－6を添加し，かきまぜるか，あるいはスルフォンアミド類と18－クラウン－6の両者を無極性溶媒中でかきまぜる。

スルフォンアミド類に対する18－クラウン－6の使用量は通常等モル量乃至それ以上が適当である。18－クラウン－6を大過剰量たとえば20倍モル以上使用するときは，収率の低下を来たすが高純度の複合体を得ることができる。

生成した複合体を採取するには析出する固形物を沪取し，適宜洗浄，乾燥すればよい。

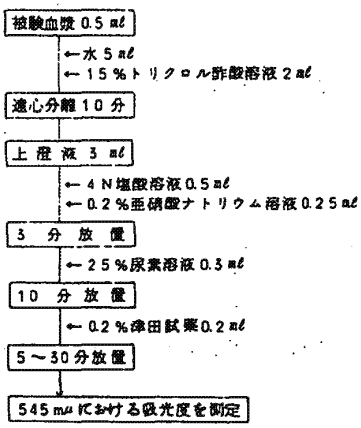
実験方法

6匹のビーグル犬（雄性，体重約10Kg）を無作為に2群に分け交叉（cross-over）試験により投与実験を実施した。各群3匹ずつに対しスルファモノメキシン／18－クラウン－6複合体，あるいはスルファモノメキシン(ナトリウム塩)を投与し1週間後，試料(ナトリウム塩)を交換し同様の試験を行なった。投与は，粉末とした各試料をオブラート2枚を用いてほゞ同様の大きさに包み，経口にて投与した。また各試料の投与量はスルファモノメキシン(ナトリウム塩)319.3mgおよびスルファモノメキシン複合体499.2mgである。ビーグル犬は実施前24時間および実施後12時間絶食させた。

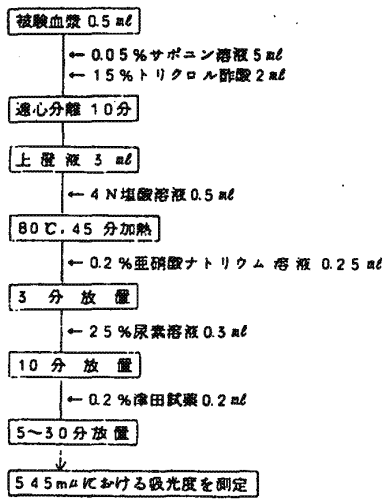
投与後1，2，4，6，8，12および24時間後に前肢より血液3mlを採取し，直ちに遠心分離して血漿を分取し－10℃にて凍血保存した。

血漿中の未変化スルファモノメトキシンおよび総スルファモノメトキシンの濃度は改良Bratton-marshall法により定量した。それらの定量法の詳細を図式で示すとつぎのとおりである。

血漿中未変化スルファモノメトキシンの定量法



血漿中総スルファモノメトキシンの定量法



つぎに実施例を挙げて本発明の複合体の製造方法をさらに説明する。

UM00012225
NOVARTIS EXHIBIT 1517
Novartis v. Regents, IPR2023-01347
Page 971 of 4460

実施例 1

スルファモノメトキシンと18－クラウン－6との複合体

スルファモノメトキシン40mgおよび18－クラウン－6 632mgにベンゼン600mlを加え10℃で24時間激しくかきまぜる。この溶液を戸過し，戸液に18－クラウン－6 888mgを加えて10℃で72時間振盪する。析出した微結晶をベンゼンを用いてよく洗浄した後，減圧乾燥する。

実施例 2

スルファモノメトキシンと18－クラウン－6との複合体

スルファモノメトキシン4gおよび18－クラウン－6 6gにベンゼン100mlを加え，10℃で10日間振盪する。この間，毎日約1時間は激しくかきまぜる。10日後，形成した複合体を戸取し，ベンゼン用いて洗浄したのち減圧乾燥する。

実施例 3

スルファメトキサゾールと18－クラウン－6との複合体

スルファメトキサゾール20mgにベンゼン200mlを加え，10℃で24時間激しくかきまぜる。この溶液を戸過し，戸液に18－クラウン－6 5.27mgを加え，10℃で72時間振盪する。析出した微結晶を戸取し，ベンゼンを用いて良く洗った後減圧乾燥する。

実施例 4

スルファメトキサゾールと18－クラウン－6との複合体

スルファメトキサゾール5gおよび18－クラウン－6 5.2gにベンゼン100mlを加え，10℃で10日間振盪する。この間毎日1時間激しくかきまぜる。10日後に形成した複合体を戸取し，ベンゼンを用いて洗浄したのち減圧乾燥する。

実施例 5

スルファメトキシピリダジンと18－クラウン－6との複合体

スルファメトキシピリダジン28.0mgおよび18－クラウン－6 52.7mgを用いた場合並びにスルファメトキシピリダジン28.0mgおよび18－クラウン－6 105.3mgを用いた場合について夫々クロロホルム並びに重クロロホルムに溶解し，正確に10mlとする。

4. 図面の簡単な説明

第1図及び第2図は夫々スルファモノメトキシン－18－クラウン－6複合体（図中②で示されている）の赤外線吸収スペクトル及び差動走査熱量曲線であってスルファモノメトキシン及び18－クラウン－6の物理的混合物（図中⑤で示されている）のそれらと対比して示したものである。

第3図～第5図は夫々スルファメトキサゾール－18－クラウン－6複合体（第3図），スルファメトキサゾール（第4図）および18－クラウン－6（第5図）の赤外線吸収スペクトルを示す。

第6図及び第7図は夫々スルファメトキサゾール－18－クラウン－6複合体（図中②で示されている）の差動走査熱量曲線（昇温速度8℃／分及びX－線回折曲線であって，スルファメトキサゾールと18－クラウン－6の物理的混合物（図中⑤で示されている）のそれと対比して示したものである。

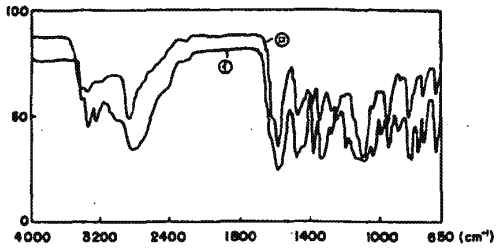
第8図はスルファメトキシピリダジン－18－クラウン－6複合体（図中②－1は混合比0.01モル：0.01モル，②－2は混合比0.01モル：0.02モルのものを示している）の3400 cm^{-1}付近及び1100 cm^{-1}付近の部分赤外線吸収スペクトルをスルファメトキシピリダジン単独（図中①で示されている）及び18－クラウン－6単独（図中⑤で示されている）と対比して示したものである。

第9～12図はスルファメトキシピリダジン－18－クラウン－6複合体2種類（スルファメトキシピリダジンと18－クラウン－6との配合比率0.01モル対0.02モル（第9図）および0.01モル対0.04モル（第10図）の2種類），18－クラウン－6単独（第11図）およびスルファメトキシピリダジン（第12図）の核磁気共鳴スペクトルを示したものである。

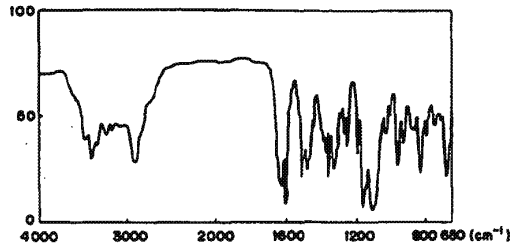
代理人 佐々木 晃 一

UM00012226
NOVARTIS EXHIBIT 1517
Novartis v. Regents, IPR2023-01347
Page 972 of 4460

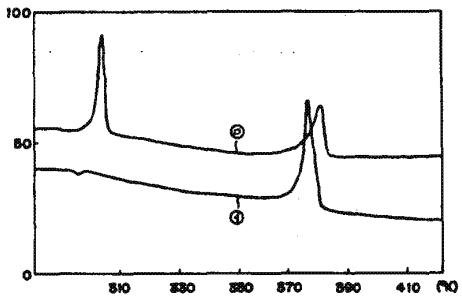
第 1 図



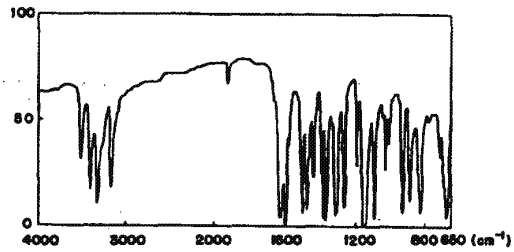
第 3 図



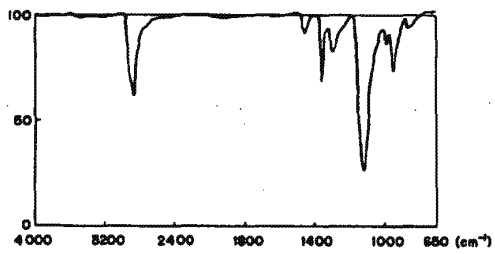
第 2 図



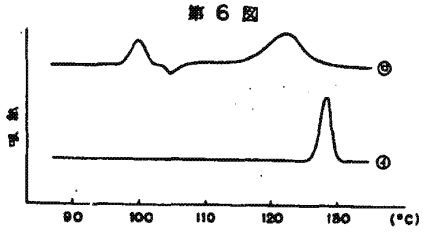
第 4 図



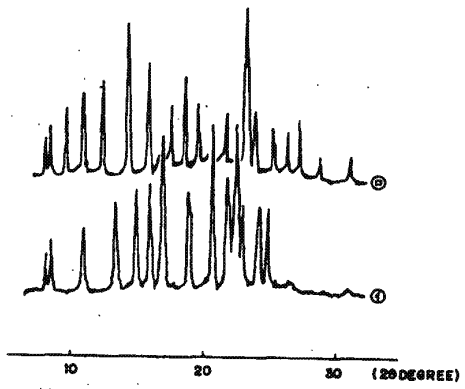
第 5 図



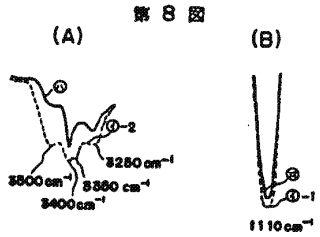
第 6 図



第 7 図

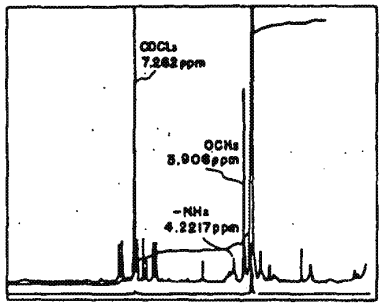


第 8 図

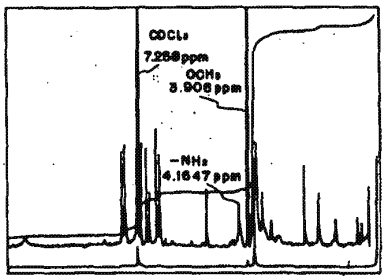


UM00012227
NOVARTIS EXHIBIT 1517
Novartis v. Regents, IPR2023-01347
Page 973 of 4460

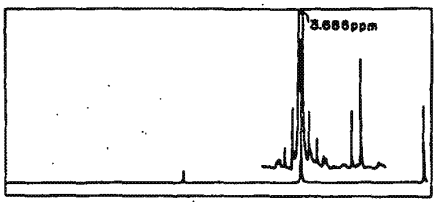
第９図



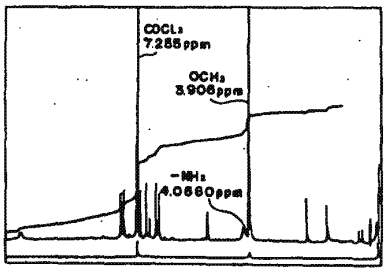
第10図



第11図



第12図



第１頁の続き

⑫発　明　者　南部直樹
調布市西つつじケ丘4－23－32
－101

UM00012228
NOVARTIS EXHIBIT 1517
Novartis v. Regents, IPR2023-01347
Page 974 of 4460

MINISTRY OF INDUSTRY, COMMERCE, AND CRAFTS
OFFICE FOR DEVELOPMENT OF PRODUCTION
AND COMPETITIVE CAPABILITY

ITALIAN PATENT AND TRADEMARK BUREAU

MANUFACTURING PATENT NO. 01303251

The present patent is being issued for the invention to which the subsequently indicated application pertains

Application Number	*Year*	*Provincial Office –Industry, Commerce, and Crafts*	*Date for Submission of Application*	*Classification*
002290	1998	Milan	October 26, 1998	C07H019

REGISTRANT: INDUSTRIALE CHIMICA, S.R.L., in Milan

REPRESENTED BY: GEMMA GERVASI

ADDRESS: NOTARBARTOLO & GERVASI, S.P.A.
Corso di Porta Vittoria 9
20122, Milan

TITLE: INDUSTRIAL PROCESS FOR PURIFYING 2', 3'-DIDEHYDRO-3'-DEOXYTHYMIDINE

INVENTORS: MARIACRISTINA FOCHI
ALBERTO SALA

Rome, November 6, 2000

Director of Division XIX:
Giovanna Morelli

1666PTIT

[Duty stamp with illegible Seal superimposed]

To: THE MINISTRY OF INDUSTRY, COMMERCE, AND CRAFTS **FORM A**
ITALIAN PATENT AND TRADEMARK BUREAU, Rome
APPLICATION FOR MANUFACTURING PATENT, FILING OF OBSERVATIONS, ADVANCE ACCESSIBILITY FOR THE PUBLIC

A. THE APPLICANT (1):
1) Name: INDUSTRIA CHIMICA, S.r.l. SR
Address: MILAN Code: 07462480158
2) Name:
Address: Code:

B. APPLICANT'S REPRESENTATIVE FOR PATENT AND TRADEMARK OFFICE
Surname, Name: Dr. Gemma Gervasi et al. Fiscal Code:
Name of Firm: Notarbartolo & Gervasi, S.p.A.
Address: Corso di Porta Vittoria 9 City: Milan Postal Code: 20122 Province: Milan

C. DESIGNATED LEGAL ADDRESS FOR ADDRESSEE:
Street: No. City: Postal Code: Province:

D. TITLE Proposed Category (Section/Category/Division C07H Group/Subgroup:
Industrial Process for Purifying 2', 3'-didehydro-3'-deoxythymidine

ADVANCE ACCESSIBILITY FOR THE PUBLIC: Yes ☐ No ☐ PETITION: DATE: / / Protocol Number:

E. DESIGNATED INVENTORS:

	Surnames Names		Surnames Names
(1)	FOCHI, MARIACRISTINA	(3)	
(2)	SALA, ALBERTO	(4)	

F. PRIORITY:

	Nation or Organization	Type of Priority	Application Date	Filing S/R	Issuing of Observations: Date	Protocol No.
(1)	NONE					
(2)						

G. APPROVED SITE FOR COLLECTING CULTURES OF MICROORGANISMS (Name):

H. SPECIAL ANNOTATIONS:
NONE

ACCOMPANYING DOCUMENTATION

	No. of Copies			Issuing of Observations: Date	Protocol No.
Doc. 1	2	Submitted	No. of Pages [14] Summary with Principal Drawings, Description, and Claims) (1 copy is obligatory)...		
Doc. 2	2	Submitted	Item No. [01] Drawings (Obligatory if cited within description -1 copy).....		
Doc. 3	1	RIS	Letter of Appointment, Power of Attorney, or Reference to General Power of Attorney.....		
Doc. 4	0	RIS	Designation of Inventor		
Doc. 5	0	RIS	Documents concerning Priority, with Italian Translation Comparison Individual Priority.....	[Bob..missing text? C.]	
Doc. 6	0	RIS	Authorization or Transfer Agreement.....		
Doc. 7	0	RIS	Applicant's Full Name.....		

8) Attestations concerning Payments, Total Amount: Three Hundred and Sixty-Five Thousand *Lire* Obligatory

PREPARED ON October 26, 1998 APPLICANT'S SIGNATURE: GEMMA GERVASI

CONTINUATION YES / NO [NO] [Signature]

IS A CERTIFIED COPY OF THE PRESENT DOCUMENT BEING REQUESTED? YES / NO [Yes]

PROVINCIAL OFFICE--INDUSTRY, COMMERCE, AND CRAFTS: Milan Code: 15

FILING REPORT: APPLICATION NUMBER: MI 98/AQ02290 Record A

Year: Nineteen hundred and ninety-eight Date: Twenty-sixth Month: October

The previously cited Applicant has submitted the present application to me, accompanied by [00] supplementary pages, for issuing of the previously cited patent.

I. MISCELLANEOUS ANNOTATIONS BY OFFICIAL WHO HAS DRAFTED THIS DOCUMENT:

FILED BY [Signature] **OFFICE SEAL** **OFFICIAL WHO HAS DRAFTED DOCUMENT** [Signature] MAURIZIO CORTONESI

1665PTIT
SUMMARY OF INVENTION WITH PRINCIPAL DRAWINGS, DESCRIPTION, AND CLAIMS

APPLICATION NUMBER: [M198A002290] Record A Filing Date: [1/26/1998]
PATENT NUMBER: [ ] Issuing Date: [ ]

B. TITLE:

[Industrial Process for Purifying 2', 3'-Didehydro-3'-Deoxythymidine]
[ ]
[ ]
[ ]

[Stamped inscription]:

Amended Description
(Article 49, Presidential Decree No. 338/1979)
Petition Filed on

November 11, 1998

L. SUMMARY

This invention describes a new industrial process for purifying 2', 3'-didehydro-3'-deoxythymidine (d4T; stavudine). This process is characterized by formation of solvates with N, N-dimethylacetamide and by a subsequent desolvation reaction whereby pure stavudine is obtained.

M. DRAWING

UM00012231
NOVARTIS EXHIBIT 1517
Novartis v. Regents, IPR2023-01347
Page 977 of 4460

Application for a manufacturing patent entitled:

"Industrial Process for Purifying 2', 3'-Didehydro-3'-Deoxythymidine"

on behalf of: **INDUSTRIALE CHIMICA, S.r.l.,**

whose main office is located in: **MILAN** [stamp] **MI 9 8 A 0 0 2 2 9 0**

Designated inventors: MARIACRISTINA FOCHI, ALBERTO SALA

Filed on as Number

* * * * *

[Stamped inscription]: **OCTOBER 26, 1998**

FIELD OF THE INVENTION

The present invention pertains to the field of synthesizing antiviral products and especially didehydro-dideoxynucleoside derivatives. The invention describes a process for purifying 2', 3'-didehydro-3'-deoxythymidine (stavudine), which is an antiviral compound which is useful for treating infections caused by the HIV virus.

PRIOR ART

Stavudine (2', 3'-didehydro-3'-deoxythymidine) is a thymidine derivative with antiviral action. This product was recently approved for treating acquired immunodeficiency syndrome (AIDS), especially among patients who are intolerant or refractory to other antiviral therapies (Drugs Future, 1994, 19(10), 925-932; New Products Intros., Drug Persp., 1994, 7(7), 402).

In consideration of the substantial pharmaceutical significance of this molecule, there are many studies whose purpose is to identify an efficient method of preparing it.

Various methods of synthesis have been identified with thymidine as a point of departure, for example:

- Opening the ring within a 3'5'-anhydrous intermediate substance [J.P. Horwitz *et al., J. Org. Chem.*, **32,** 817 (1967)];

UM00012232
NOVARTIS EXHIBIT 1517
Novartis v. Regents, IPR2023-01347
Page 978 of 4460

- β-elimination of a 3'-selenoxide molecule [J. Vial *et al.*, *Nucleosides & Nucleotides*, **9**, 245 (1990)];

- Reductive β-elimination of an O^2, 3'-cyclic nucleoside [B.V. Joshi *et al.*, *J. Chem. Soc.*, Perkin Trans. 1, 2537 (1992);

- Basic β-elimination by means of a 3'-mesylate [Horwitz *et al.*, *J. AM. Chem. Soc.*, **86**, 1896 (1964)].

A critical point in preparing stavudine consists of purification of the product, which is normally obtained in a crude form upon completion of existing synthesis processes. The purification processes which are ordinarily used, such as chromatography, crystallization, resin treatments, etc., are not highly satisfactory in terms of yields or applicability on an industrial scale. Isolating the product by means of DMSO under intensively basic conditions and at high temperatures results in decomposition of the product (Horwitz *et al., op. cit.*).

In consideration of the previously cited limitations of existing technology, the need for a stavudine purification process which is easily and efficiently applicable on an industrial scale has been recognized.

SUMMARY

The present invention describes a new industrial process for purifying 2', 3'-didehydro-3'-deoxythymidine (d4T; stavudine). The process is characterized by formation of solvates with N,N-dimethylacetamide and by a subsequent desolvation reaction, whereby pure stavudine shall be obtained.

DESCRIPTION OF DRAWINGS:

A) Figure 1: Synthesizing stavudine

1) *β-thymidine*

2) *5'-O-Benzoilthymidine*

3) *5'-0-Benzoil-3'-O-methanesulfonylthymidine*

4) *2',3'-Didehydro-3'-deoxythymidine*

UM00012233
NOVARTIS EXHIBIT 1517
Novartis v. Regents, IPR2023-01347
Page 979 of 4460

DETAILED DESCRIPTION OF THE INVENTION

The present invention describes a new industrial process for purifying crude 2', 3'-didehydro-3'-deoxythymidine (d4T; stavudine).

The process according to the present invention can be used in any situation where obtaining pure stavudine from the respective crude product may be necessary. In particular, it can be applied to any synthesis process resulting in formation of crude stavudine. It can also be used as an alternative for previously described existing procedures for purifying this product. Certain examples of these processes have been cited heretofore during the analysis of prior art.

According to a preferred version, the present process is applicable to synthesis of stavudine as described within the accompanying application which was filed on October 26, 1998 on behalf of the Applicant. This application is included herein for reference. Synthesis of this kind includes treatment of a 5'-O-benzoyl-3'-alkylsulfonyl-thimidine or a 5'-O-benzoyl-3'-O-arylsulfonyl-thymidine, with formation of stavudine in a single stage.

The preferred derivatives for the synthesis in this form are 5'-O-benzoyl-3'-O-mesyl-thymidine or 5'-O-benzoyl-3'-O-tosyl-thymidine.

The base used for this type of synthesis can be a single compound, or it can advantageously consist of a pair of derivatives of a basic nature, preferably (i) sodium or potassium t-butylate, and (ii) sodium methylate.

The diagram for this synthesis reaction appears within Figure 1.

The purification process to which the present invention pertains is characterized by formation of a solvate with N, N-dimethylacetamide (DMA) and by the subsequent purification-desolvation reaction.

For the purpose of forming a solvate, stavudine is placed within an excessive portion of DMA (from 2 to 10 volumetric units of DMA per gram of stavudine). The solution must undergo stirring at ambient temperature for a period varying between 30 minutes and two hours, and it must then

UM00012234
NOVARTIS EXHIBIT 1517
Novartis v. Regents, IPR2023-01347
Page 980 of 4460

undergo dilution with a suitable amount of solvent at ambient temperature. Solvents which are suitable for precipitating a solvate from stavudine especially include ethers, ketones, and hydrocarbons. Favorable results have been obtained with use of ethyl ether and isopropyl ether. In order to complete precipitation of the solvate, it may be necessary to allow cooling to 0° C.

The solvate which is obtained in this manner contains from 0.5 to 1 moles of DMA per mole of stavudine, and it unexpectedly offers optimal stability. Indeed, the stability of the solvate is sufficient to allow easy isolation and eventual purification. Moreover, its stability is not excessively high, so that obtaining of pure stavudine by desolvation within appropriate solvents is therefore possible, without being obliged to introduce drastic conditions (high temperatures, long periods of time, etc.) which may be detrimental to stavudine's own purity and stability.

DMA offers the additional advantage of being characterized by low costs and of ensuring high yields of the purified product.

The solvate obtained in this manner can be easily desolvated by treatment with appropriate solvents, so that purified free stavudine can be obtained. It is possible for ketone solvents (acetone, for example), esters (isopropyl acetate, butyl acetate, etc.), and alcohols (for example, isopropanol) to be used, with heating to a temperature between 20° C. and 50° C.

Another form of purification of the solvate consists of dissolving it, which may possibly be facilitated by heating it slightly within DMA, with subsequent reprecipitation by means of suitable solvents such as the previously cited solvents.

When necessary, the previously described purification cycle can be repeated for a second time.

At this point, the present invention shall be described in terms of the following nonrestrictive examples.

UM00012235
NOVARTIS EXHIBIT 1517
Novartis v. Regents, IPR2023-01347
Page 981 of 4460

Experimental Section

Example 1:

5'-O-Benzoylthymidine

A solution of thymidine (180 g) in pyridine (1,800 ml) must be cooled to 0° C. - 5° C., and it must be gradually treated with benzoyl chloride (121.3 g). Upon completion of addition of the latter substance, the solution is warmed to ambient temperature, and stirring must occur for three days. Most of the pyridine undergoes evaporation under vacuum conditions, and the resulting solution is then poured into water and ice, while vigorous stirring occurs. The suspension must be stirred for two hours, and the solid portion must be filtered and suitably rinsed with water, before being dried under vacuum conditions. The solid which is obtained then undergoes purification in toluene (2,500 ml). The toluene suspension must undergo stirring at 100° C. for 30 minutes, with cooling to 60° C. before being filtered and rinsed inside the filter with heated toluene. If necessary, the purification phase should be repeated another time. 5'-O-benzoyl-thymidine can be recovered with an 84% yield.

Example 2:

5'-O-benzoyl-3'-methanesulfonyl-thymidine

A solution of 5'-O-benzoyl-thymidine (210 g) in pyridine (1,000 ml), which must be cooled to a temperature of less than 10° C., and it must be treated drop by drop with mesyl chloride (83.2 g). Upon completion of addition of the latter substance, the solution is heated to 20° C., and it must undergo stirring for four hours. Evaporation of pyridine is performed under vacuum conditions, and it is dissolved again with water (900 ml) and methylene chloride (1,800 ml). The organic phase then undergoes filtration and cooling at 0° C. - 5° C. Formation of a precipitate occurs, and this precipitate must be filtered and rinsed with cold methylene chloride. After drying, 5'-O-benzoyl-3'-O-methanesulfonyl-thymidine is obtained with a 93% yield.

UM00012236
NOVARTIS EXHIBIT 1517
Novartis v. Regents, IPR2023-01347
Page 982 of 4460

Example 3:

2', 3'-didehydro-3'-deoxythymidine (Synthesis)

A solution of 5'-O-benzoyl-3'-O-methanesulfonyl-thymidine (255 g) in N, N-dimethylformamide (1,200 ml) must be treated at a temperature of 20° C. with portions of potassium t-butylate (202 g). Upon completion of addition of the latter substance, stirring is performed at ambient temperature for four hours. The suspension which is obtained is then poured into cold toluene (5,500 ml). Stirring at room temperature is performed for 30 minutes, and the gummy solid which is obtained is redissolved until complete dissolution in water (700 ml) occurs. The toluene phase must then be separated. The aqueous solution is then cooled to a temperature of less than 15° C., and it must be neutralized with concentrated hydrochloric acid before undergoing evaporation under vacuum conditions at approximately 30° C. - 35° C. Traces of water can be removed by treating the remaining product with butanol and by evaporation under vacuum conditions until drying occurs. The remaining product is then extracted with portions of acetone (total of 2,000 ml). The solution must then be treated with carbon, filtered, and evaporated under vacuum conditions, with crude 2', 3'-didehydro-3'-deoxythymidine being obtained.

Example 4:

2', 3'-didehydro-3'-deoxythymidine (synthesis with a pair of bases)

A solution of 5'-O-benzoyl-3'-O-methanesulfonyl-thymidine (255 g) in N,N-dimethylformamide (900 ml) and tetrahydrofurane (900 ml) is treated at a temperature of 20° C. with portions of potassium t-butylate (169 g). Upon completion of addition of the latter substance, stirring is performed at ambient temperature for one hour, and subsequently, the solution is treated by portions of sodium methylate (25 g). Stirring is continued at ambient temperature for one hour. The suspension which is obtained must then be poured into cold toluene (5,500 ml). Stirring is performed at ambient temperature for 30 minutes, and the gummy solid which is obtained is filtered. It is then added to water (700 ml) until complete dissolution occurs. The toluene phase must be separated. The aqueous solution must be cooled to a temperature of less than 15° C.,

UM00012237
NOVARTIS EXHIBIT 1517
Novartis v. Regents, IPR2023-01347
Page 983 of 4460

and it must be neutralized with concentrated hydrochloric acid before undergoing vacuum evaporation at approximately 30° C. - 35 ° C. Traces of water are removed by treating the remaining product with butanol and by performing evaporation under vacuum conditions until drying occurs. The remaining product is extracted with acetone according to portions (total of 2,000 ml). The solution is then treated with carbon, filtered, and evaporated under vacuum conditions, until crude 2', 3'-didehydro-3'-deoxythymidine is obtained.

Example 5:

2', 3'-didehydro-3'-deoxythymidine (purification)

Crude 2', 3'-didehydro-3'-deoxythymidine (obtained according to Example 3) is treated at ambient temperature with N, N-dimethylacetamide (DMA, 500 ml) (For obtaining complete dissolution, it is necessary to apply heat for several minutes at 40° C.). The solution is stirred at ambient temperature for 30 minutes, and it is then treated with isopropyl ether (1,100 ml). The solid substance which is obtained must be stirred for two hours while it is cool, and it must be filtered.

'H-NMIR analysis of a sample after drying reveals formation of a solvate by 2', 3'-didehydro-3'-deoxythymidine and DMA with a molar ratio of 1/0.75:

'H-NMR (DMSO, ppm): 11.27 (s, 1H), 7.62 (s, 1H), 6.37 (d, 1H), 5.89 (d, 1H), 4.97 (m, 1H), 4.76 (m, 1H), 3.59 (m, 2H), 2.93 (s,2.3H), 2.76 (s, 2.3H), 1.94 (s, 2.3H), 1.71 (s, 3H).

The solid substance is then suspended in DMA (170 ml) and is treated with isopropyl ether (250 ml) at ambient temperature, with stirring for one hour. After filtration, it must be dissolved in isopropanol (700 ml) under heat, and it must be treated with carbon and filtered. Isopropanol must then be concentrated under vacuum conditions (removal of approximately 400 ml of the solvent), and the solution must be cooled. After filtration and drying, 2',3'-didehydro-3'-deoxythymidine can be isolated with a yield of more than 40% (computed by means of crude 5'-O-benzoyl-3'-O-methanesulfonyl-thymidine) and with an HPLC purity of 99.1%.

UM00012238
NOVARTIS EXHIBIT 1517
Novartis v. Regents, IPR2023-01347
Page 984 of 4460

The structure of this substance can be confirmed by means of 'H-NMR analyses (DMSO, ppm): 11.27 (s, 1H), 7.62 (s, 1H), 6.80 (m, 1H), 6.37 (d, 1H), 5.89 (d, 1H), 4.97 (m, 1H), 4.76 (m, 1H), 3.59 (m, 2H), 1.71 (s, 3H).

Example 6:

2', 3'-didehydro-3'-deoxythymidine (purification)

Crude 2', 3'-didehydro-3'-deoxythymidine (50% of the amount obtained within Example 4) is treated at ambient temperature with N,N-dimethylacetamide (DMA, 250 ml) (For obtaining complete dissolution, it is necessary to apply heat for several minutes at 40° C.). The solution is stirred at ambient temperature for 30 minutes, and it is then treated with isopropyl ether (550 ml). The solid substance which is obtained must be stirred for two hours while it is cool, and it must be filtered.

Analysis of a sample with 'H-NMR after drying reveals formation of a solvate by 2', 3'-didehydro-3'-deoxythymidine and DMA with a molar ratio of 1/0.75 (Data consistent with the data provided within Example 5).

The solid substance is then dissolved in DMA (85 ml) and is heated to 40° C., and it is treated with isopropyl ether (125 ml) at ambient temperature, while being stirred for one hour. Isopropanol must then be concentrated under vacuum conditions (removal of approximately 200 ml of the solvent), and the solution must be cooled. After filtration and drying, 2',3'-didehydro-3'-deoxythymidine can be isolated with a yield of more than 50% (computed by means of crude 5'-O-benzoyl-3'-O-methanesulfonyl-thymidine) and with an HPLC purity of 99.0%.

'H-NMR analysis has confirmed the structure of stavudine (data consistent with that which was provided in Example 5).

UM00012239
NOVARTIS EXHIBIT 1517
Novartis v. Regents, IPR2023-01347
Page 985 of 4460

Example 7

2', 3'-didehydro-3'-deoxythymidine (stavudine); purification with:

(a) N,N-diethylformamide

Crude 2', 3'-didehydro-3'-deoxythymidine (1 g) is treated at ambient temperature with N, N-diethylformamide (2ml) (In order to obtain complete dissolution, heating for several minutes at approximately 50° C. is necessary). The solution must then be stirred at ambient temperature for 30 minutes, and it must subsequently be treated with isopropyl ether (5 ml). An oil which is gradually transformed into a gummy solid is gradually separated at ambient temperature. After filtration and drying, 0.45 g of partially purified stavudine (yellow solid) (TLC eluent: methylene chloride- methanol-9-1) is obtained. Analysis with 'H-NMR demonstrates the presence of mere traces of N, N-diethylformamide, and isolation of a solvate form can therefore be excluded.

(b) N, N-diethylacetamide

Crude 2', 3'-didehydro-3'-deoxythymidine (1 g) is treated at ambient temperature with N, N-diethylformamide (2ml) (In order to obtain complete dissolution, heating for several minutes at approximately 50° C. is necessary). The solution must then be stirred at ambient temperature for 30 minutes, and it must subsequently be treated with isopropyl ether (5 ml). An oil which is gradually transformed into a gummy solid is gradually separated at ambient temperature. After filtration and drying, 0.60 g of partially purified stavudine (yellow solid) (TLC eluent: methylene chloride- methanol-9-1) is obtained. Analysis with 'H-NMR demonstrates the presence of mere traces of N, N-diethylformamide, and isolation of a solvate form can therefore be excluded.

c) N-methylpropionamide:

Crude 2', 3'-didehydro-3'-deoxythymidine (1 g) is treated at ambient temperature with N, N-methylpropionamide (2ml) (In order to obtain complete dissolution, heating for several minutes at approximately 50° C. is necessary). The solution must then be stirred at ambient temperature for 30 minutes, and it must subsequently be treated with isopropyl ether (5 ml). A dense oil which is

UM00012240
NOVARTIS EXHIBIT 1517
Novartis v. Regents, IPR2023-01347
Page 986 of 4460

gradually transformed into a gummy solid is gradually separated at ambient temperature. After filtration and drying, 0.65 g of partially purified stavudine (whitish solid) (TLC eluent: methylene chloride- methanol-9-1) is obtained. Analysis with 'H-NMR demonstrates the presence of mere traces of N, N-methylpropionamide and isolation of a solvate form can therefore be excluded.

Example 7 demonstrates that oils or gummy solids which are obtained by the reaction between stavudine and primary or secondary amines other than DMA only contain modest proportions of the solvent, thereby confirming the fact that a solvate does not form or is at least unstable.

The stavudine which was obtained in Example 7 with amides other than DMA possessed unacceptable quality in terms of purity and crystalline properties.

UM00012241
NOVARTIS EXHIBIT 1517
Novartis v. Regents, IPR2023-01347
Page 987 of 4460

CLAIMS

1. A process for purifying 2', 3'-didehydro-3'-deoxythymidine (stavudine) characterized by the fact that said process includes solvation of stavudine by a reaction with N, N-dimethylacetamide (DMA) and subsequent desolvation of the solvate which is obtained.
2. A process according to Claim Number 1, where the solvate which is obtained contains (DMA) and stavudine in molar ratios situated between 0.5: 1 and 1:1.
3. A process according to Claim Number 1, where desolvation is accomplished by treating solvates at temperatures situated between 20° C. and 50° C. within solvents selected among amides, ethers, ketones, esters, and alcohols.
4. A process according to Claim Number 3, where the solvent used for desolvation is selected among butyl acetate, isopropanol, and acetone.
5. A process according to Claim Number 1, where the stavudine which is to be purified has been obtained by means of a process which includes treatment of 5'-O-benzoyl-3'-O-alkylsulfonylthymidine or 5'-O-benzoyl-3'-O-alkylsulfonylthymidine in the presence of a base, with stavudine being formed during a single stage.
6. An N, N-dimethylacetamide (DMA)/stavudine solvate with molar ratios situated between 0.5:1 and 1:1.
7. A solvate according to Claim Number 6, where the molar ratio between N,N-dimethylacetamide (DMA) and stavudine is equivalent to 0.75:1.

(GER/pd)

[initials]

Milan, October 26, 1998

On behalf of *INDUSTRIALE CHIMICA, S.r.l.*

Agent:

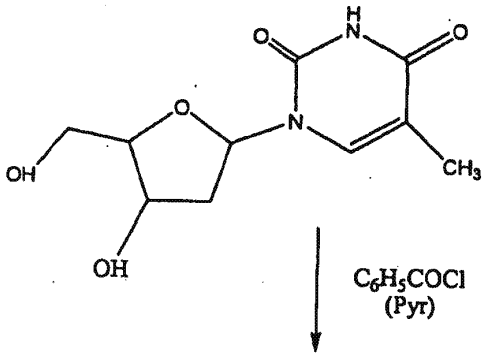
[Signature]
Dr. Gemma Gervasi

NOTARBARTOLO & GERVASI, S.p.A.

[Signature] [Illegible seal] [Illegible signature]

UM00012242
NOVARTIS EXHIBIT 1517
Novartis v. Regents, IPR2023-01347
Page 988 of 4460

[Illegible signature]

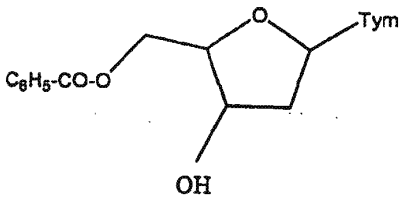


(1)

C_6H_5COCl
(Pyr)

Key:
{ (Pyridine)

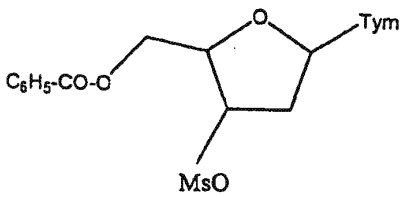
MI98A002290



(2)

CH_3ClO_2S
(Pyr)

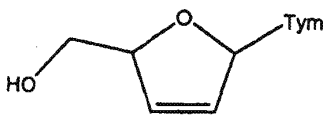
Key:
{ (Pyridine)



(3)

MeONa/ButOK
(DMF-THF)

[illegible signature]
[illegible Seal]



(4)

[initials]

PETITION

NOVARTIS EXHIBIT 1517
Novartis v. Regents, IPR2023-01347
Page 990 of 4460

1665PTIT

Protocol No.:

[Seal]

MINISTRY OF INDUSTRY, COMMERCE, AND CRAFTS

Office for Development of Production and Competitive Capability [Stamped inscription]:

ITALIAN PATENT AND TRADEMARK BUREAU Patent MI. V.

COPY OF STATEMENT CONCERNING FILING OF PETITIONS AND DOCUMENTS 002640

In the year **1998**, on the **eleventh** day of the month of **November**,

the company known as **INDUSTRIA CHIMICA, s.r.l.**,

whose main office is located in **Milan**,

whose agents are: **Dr. Diego Pallini (Registration Number 484)**,

and whose designated address for legal purposes is **Corso di Porta Vittoria 9**,

at the offices of **Notarbartolo & Gervasi, S.p.A.** in Milan,

- subsequent to an application for a **PATENT**, which was filed in **Milan**, on **October 26, 1998**, according to

Protocol Number **MI98A002290**,

filed the subsequently indicated documents with this Office:

1. **PETITION FOR CORRECTION AND INCLUSION**
2. **PAGE 4, ANNOTATION**
3. **PAGE 4, EX NOVO**
4.
5.

[Seal]: Ministry of Industry, Commerce, and Crafts
Province of Milan Office for Industry, Commerce, and Crafts, Patent Bureau

APPLICANT: ISSUING OFFICIAL:

[Signature] [Signature]
Giuseppe Rescali

For copy identical to the original.
"It is specified that, for an application of this kind and for accompanying duties for stamps shall be waived in accordance with Bulletin Number 163/83 issued by the Patent Bureau, and subsequent amendments thereto, subject to possible additional duties which may be requested by said Bureau within the context of approval."

On behalf of the Director:
(Pier Daniele Melegari)
[Illegible signature]
Dr. M. Colosimo

MINISTRY OF INDUSTRY, COMMERCE, AND CRAFTS

Italian Patent and Trademark Bureau — Rome

[Duty stamp with seal superimposed]

Application for a Manufacturing Patent whose title is:

"Industrial Process for Purifying 2', 3'-Didehydro-3'-Deoxythymidine"

on behalf of: **INDUSTRIALE CHIMICA, S.r.l.**

whose main office is located in **MILAN.**

Filed on **OCTOBER 26, 1998**, with the number **MI98A002290**.

[Stamped inscription]:
PATENT MI-V.
002640

* * * * *

PETITION FOR CORRECTION AND INCLUSION

On the basis of Article 49 of Presidential Decree Number 338, which was issued on June 22, 1979, the undersigned company, INDUSTRIALE CHIMICA, S.r.l., whose main office is located in Milan, is requesting through its Agent, Dr. Diego Pallini (Registration Number 484), who is affiliated with NOTARBARTOLO & GERVASI, S.p.A., of Corso di Porta Vittoria 9, in Milan, which has been designated as a legal address for all legal purposes, that permission should be granted for providing the following correction, as indicated hereinafter.

NOTE 1, Page 4, Line 21, after the expression "likewise pending," insertion of "Number MI98A002289."

Milan, November 11, 1998.

[stamped inscription]

Commerce, and Crafts.
November 11, 1998
Milan

On behalf of INDUSTRIALE CHIMICA, S.r.l
Provincial Office for Industry,
Agent:
[Signature]
Dr. Diego Pallini

[Seal] Ministry of Industry, Commerce, and Crafts
Province of Milan Office for Industry, Commerce, and Crafts, Patent Bureau

NOTARBARTOLO & GERVASI, S.p.A.

... obtaining pure stavudine.

DESCRIPTION OF DRAWINGS

A) Figure 1: Synthesizing stavudine

1) *β-thymidine*
2) *5'-O-Benzoylthymidine*
3) *5'-O-Benzoyl-3'-O-methanesulfonylthymidine*
4) *2', 3'-Didehydro-3'-deoxythymidine*

[Stamped inscription]:

PATENT MI-V.
002640

DETAILED DESCRIPTION OF THE INVENTION

The present invention describes a new industrial process for purifying crude 2', 3'-didehydro-3'-deoxythymidine (d4T; stavudine).

The process to which the present invention pertains is usable under any circumstances where obtaining pure stavudine from the respective crude product is intended. In particular, this method may be applied to any synthesis process which may result in formation of crude stavudine; it can also be used as an alternative to existing purification processes which have been described for this product. Some examples of these processes have been cited heretofore in analyzing prior art.

According to a preferred version, the present process is applicable to synthesis of stavudine, as described within concurrently pending Application Number MI98A002289, which was filed on behalf of the Applicant on October 26, 1998, and is included herein for reference. This form of synthesis includes treatment of 5'-O-benzoyl-3'-O-alkylsulfonylthymidine, or 5'-O-benzoyl-3'-O-arylsulfonylthymidine in the presence of a base, with formation of stavudine occurring in a single stage.

[Stamped inscription]: November 11, 1998. Milan.

[Seal]: Ministry of Industry, Commerce, and Crafts
Province of Milan Office for Industry, Commerce,
and Crafts, Patent Bureau

MINISTERO DELL'INDUSTRIA DEL COMMERCIO E DELL'ARTIGIANATO

DIREZIONE GENERALE PER LO SVILUPPO PRODUTTIVO E LA COMPETITIVITA'

UFFICIO ITALIANO BREVETTI E MARCHI

BREVETTO PER INVENZIONE INDUSTRIALE

N. 01303251

Il presente brevetto viene concesso per l'invenzione oggetto della domanda sotto specificata:

num. domanda	anno	U.P.I.C.A.	data pres. domanda	classifica
002290	1998	MILANO	26/10/1998	C07H019

TITOLARE INDUSTRIALE CHIMICA S.R.L. A MILANO

RAPPR.TE GERVASI GEMMA

INDIRIZZO NOTARBARTOLO & GERVASI S. P. A.
C.SO DI PORTA VITTORIA, 9
20122 MILANO

TITOLO PROCESSO INDUSTRIALE PER LA PURIFICAZIONE DI 2', 3'- DIDEIDRO-3'- DEOSSITIMIDINA.

INVENTORE FOCHI MARIACRISTINA
SALA ALBERTO

Roma, 6 NOVEMBRE 2000

IL DIRETTORE DELLA DIV. XIX
GIOVANNA MORELLI

1665PTIT

AL MINISTERO DELL'INDUSTRIA DEL COMMERCIO E DELL'ARTIGIANATO
UFFICIO ITALIANO BREVETTI E MARCHI - ROMA
DOMANDA DI BREVETTO PER INVENZIONE INDUSTRIALE, DEPOSITO RISERVE, ANTICIPATA ACCESSIBILITÀ AL PUBBLICO

MODULO A

A. RICHIEDENTE (I)
1) Denominazione: INDUSTRIALE CHIMICA S.r.l.
Residenza: MILANO codice 07462480158
2) Denominazione:
Residenza: codice

B. RAPPRESENTANTE DEL RICHIEDENTE PRESSO L'U.I.B.M.
cognome nome: Dr.ssa Gemma Gervasi ed altri cod. fiscale:
denominazione studio di appartenenza: Notarbartolo & Gervasi S.p.A.
via: C.so di Porta Vittoria n. 9 città: Milano cap: 20122 (prov) MI

C. DOMICILIO ELETTIVO destinatario:
via: n. città: cap: (prov)

D. TITOLO classe proposta (sez/cl/scl) C07H gruppo/sottogruppo /
Processo industriale per la purificazione di 2',3'-dideidro-3'-deossitimidina.

ANTICIPATA ACCESSIBILITÀ AL PUBBLICO: SI NO SE ISTANZA: DATA / / N° PROTOCOLLO

E. INVENTORI DESIGNATI (cognome nome)
1) FOCHI MARIACRISTINA
2) SALA ALBERTO
3)
4)

F. PRIORITÀ

	nazione o organizzazione	tipo di priorità	numero di domanda	data di deposito	allegato S/R
1)	NESSUNA			/ /	
2)				/ /	

SCIOGLIMENTO RISERVE (Data / N° Protocollo)
1) / / / 2) / / /

G. CENTRO ABILITATO DI RACCOLTA COLTURE DI MICRORGANISMI, denominazione:

H. ANNOTAZIONI SPECIALI
NESSUNA

DOCUMENTAZIONE ALLEGATA

	N. es.			
Doc. 1)	2	PROV	n. pag. 14	riassunto con disegno principale, descrizione e rivendicazioni (obbligatorio 1 esemplare)
Doc. 2)	2	PROV	n. tav. 01	disegno (obbligatorio se citato in descrizione, 1 esemplare)
Doc. 3)	1	RIS		lettera d'incarico, procura o riferimento procura generale
Doc. 4)	0	RIS		designazione inventore
Doc. 5)	0	RIS		documenti di priorità con traduzione in italiano
Doc. 6)	0	RIS		autorizzazione o atto di cessione
Doc. 7)	0			nominativo completo del richiedente

SCIOGLIMENTO RISERVE (Data / N° Protocollo)
/ / / / / / / / / / / / confronta singole priorità / / /

8) attestati di versamento, totale lire Trecentosessantacinquemila.= obbligatorio

COMPILATO IL 26/10/1998 FIRMA DEL(I) RICHIEDENTE(I) Gemma Gervasi

CONTINUA SI/NO NO

DEL PRESENTE ATTO SI RICHIEDE COPIA AUTENTICA SI/NO SI

=£(15

UFFICIO PROVINCIALE IND. COMM. ART. DI Milano codice

VERBALE DI DEPOSITO NUMERO DI DOMANDA MI 98/A002290 Reg. A.

L'anno millenovecento NOVANTOTTO, il giorno VENTISEI, del mese di OTTOBRE

8(i) richiedente(i) sopraindicato(i) ha(hanno) presentato a me sottoscritto la presente domanda, corredata di n. 00 fogli aggiuntivi per la concessione del brevetto sopraripportato.

I. ANNOTAZIONI VARIE DELL'UFFICIALE ROGANTE

IL DEPOSITANTE

timbro dell'Ufficio

L'UFFICIALE ROGANTE
CORTONESI MAURIZIO

1665PTIT

PROSPETTO A

RIASSUNTO INVENZIONE CON DISEGNO PRINCIPALE, DESCRIZIONE E RIVENDICAZIONE

NUMERO DOMANDA MI98A002290 REG. A DATA DI DEPOSITO 26/10/1998

NUMERO BREVETTO DATA DI RILASCIO

D. TITOLO

Processo industriale per la purificazione di 2',3'-dideidro-3'-deossitimidina.

Descrizione modificata
(art. 49 D.P.R. n. 338/1979)
istanza dep. il
11/11/98

L. RIASSUNTO

Questa invenzione descrive un nuovo processo industriale per la purificazione della 2',3'-dideidro-3'-deossitimidina (d4T; stavudina). Il processo è caratterizzato dalla formazione di solvati con N,N-dimetilacetammide e dalla successiva reazione di desolvatazione, con l'ottenimento di stavudina pura.

M. DISEGNO

UM00012250
NOVARTIS EXHIBIT 1517
Novartis v. Regents, IPR2023-01347
Page 996 of 4460

Domanda di brevetto per invenzione industriale dal titolo:

"Processo industriale per la purificazione di 2',3'-dideidro-3'-deossitimidina"

a nome di INDUSTRIALE CHIMICA S.r.l.

con sede in MILANO MI 9 8 A 0 0 2 2 9 0

Inventori designati: FOCHI MARIACRISTINA, SALA ALBERTO

depositata il con n.

*****

26 OTT. 1998

CAMPO DELL'INVENZIONE

La presente invenzione riguarda il campo della sintesi dei prodotti antivirali, ed in particolare dei derivati dideidro-dideossinucleosidici. L'invenzione descrive un processo per la purificazione della 2',3'-dideidro-3'-deossitimidina (stavudina), un composto antivirale utile per il trattamento delle infezioni da virus HIV.

TECNICA ANTERIORE

La stavudina (2',3'-dideidro-3'-deossitimidina) è un derivato della timidina ad azione antivirale. Questo prodotto è stato recentemente approvato per il trattamento della sindrome da immunodeficienza acquisita (AIDS), in particolare in quei pazienti che sono intolleranti o refrattari ad altre terapie antivirali (Drugs Future, 1994, 19(10), 925-932; New Products Intros., Drug Persp., 1994, 7(7), 402).

Considerato l'elevato interesse farmaceutico di questa molecola, molti sono gli studi diretti a trovare un metodo efficiente per la sua preparazione.

Partendo dalla timidina sono state individuate varie vie sintetiche, quali

UM00012251
NOVARTIS EXHIBIT 1517
Novartis v. Regents, IPR2023-01347
Page 997 of 4460

ad esempio:

- apertura di anello di un intermedio 3',5'-anidro [J.P. Horwitz et al., J. Org. Chem., **32**, 817 (1967)];

- β-eliminazione di un 3'-selenossido [J. Vial et al., Nucleosides & Nucleotides, **9**, 245 (1990)];

- β-eliminazione riduttiva di un nucleoside O^2,3'-ciclico [B.V. Joshi et al., J. Chem. Soc. Perkin Trans.1, 2537 (1992)];

- β-eliminazione base assistita di un 3'-mesilato è [Horwitz et al., J. Am. Chem. Soc., **86**, 1896 (1964).

Un punto critico nella preparazione della stavudina è costituito dalla purificazione del prodotto, che normalmente viene ottenuto in forma grezza al termine dei processi di sintesi noti. I processi di purificazione comunemente usati quali cromatografia, cristallizzazione, trattamento con resine, ecc. risultano poco soddisfacenti sul piano delle rese e della applicabilità su scala industriale. L'isolamento del prodotto da DMSO in condizioni fortemente basiche e ad elevate temperature porta alla decomposizione del prodotto (Horwitz et al., op.cit.).

In vista delle suddette limitazioni della tecnica nota, risulta sentita la necessità di un processo di purificazione della stavudina che sia effettuabile facilmente ed efficientemente su scala industriale.

SOMMARIO

Questa invenzione descrive un nuovo processo industriale per la purificazione della 2',3'-dideidro-3'-deossitimidina (d4T; stavudina). Il processo è caratterizzato dalla formazione di solvati con N,N-dimetilacetammide e dalla successiva reazione di desolvatazione, con

UM00012252
NOVARTIS EXHIBIT 1517
Novartis v. Regents, IPR2023-01347
Page 998 of 4460

l'ottenimento di stavudina pura.

DESCRIZIONE DELLE FIGURE

(A) Figura 1: Sintesi di stavudina

(1) *β-timidina*

(2) *5'-O-Benzoiltimidina*

(3) *5'-O-Benzoil-3'-O-metansolfoniltimidina*

(4) *2',3'-Dideidro-3'-deossitimidina*

DESCRIZIONE DETTAGLIATA DELL'INVENZIONE

La presente invenzione descrive un nuovo processo industriale per la purificazione della 2',3'-dideidro-3'-deossitimidina grezza (d4T; stavudina).

Il processo secondo la presente invenzione è utilizzabile in ogni circostanza si voglia ottenere stavudina pura a partire dal corrispondente prodotto grezzo. Può essere in particolare applicato a qualsiasi processo di sintesi che porti alla formazione di stavudina grezza; può inoltre essere impiegato in alternativa ai procedimenti noti di purificazione descritti per tale prodotto. Alcuni esempi di tali processi sono stati citati precedentemente nell'analisi della tecnica anteriore.

Secondo una realizzazione preferita, il presente processo è applicabile alla sintesi della stavudina descritta nella domanda co-pendente depositata il 26 ottobre 1998 a nome della Richiedente, qui incorporata per riferimento. Tale sintesi comprende il trattamento, in presenza di una base, di una 5'-O-benzoil-3'-O-alchilsolfonil-timidina o di una 5'-O-benzoil-3'-O-arilsolfonil-timidina, con formazione, in un solo stadio, di stavudina.

UM00012253
NOVARTIS EXHIBIT 1517
Novartis v. Regents, IPR2023-01347
Page 999 of 4460

I derivati preferiti per questa sintesi sono la 5'-O-benzoil-3'-O-mesil-timidina o la 5'-O-benzoil-3'-O-tosil-timidina.

La base utilizzata in detta sintesi può essere un unico composto o può vantaggiosamente essere costituita da una coppia di derivati di natura basica, preferibilmente (i) sodio o potassio t-butilato e (ii) sodio metilato.

Lo schema di questa reazione di sintesi è riportato nella figura 1.

Il processo di purificazione oggetto della presente invenzione è caratterizzato dalla formazione di un solvato con N,N-dimetilacetammide (DMA) e nella sua successiva reazione di purificazione-desolvatazione.

Allo scopo di formare il solvato, la stavudina viene sciolta ad una temperatura compresa tra 20 e 40°C in un eccesso di DMA (da 2 a 10 volumi di DMA per grammo di stavudina); la soluzione è agitata a temperatura ambiente per un tempo variabile tra 30 minuti e 2 ore e diluita a temperatura ambiente con una opportuna quantità di solvente. Solventi adatti a precipitare il solvato della stavudina sono soprattutto eteri, chetoni e idrocarburi. Buoni risultati sono stati ottenuti con l'uso di etere etilico e etere isopropilico. Per completare la precipitazione del solvato può essere necessario raffreddare a 0°C.

Il solvato così ottenuto contiene da 0,5 ad 1 mole di DMA per mole di stavudina e presenta, inaspettatamente, una stabilità ottimale. La sua stabilità è infatti tale da permetterne facilmente l'isolamento e l'eventuale purificazione; d'altra parte la stessa stabilità non è troppo elevata, permettendo così l'ottenimento della stavudina pura mediante desolvatazione in opportuni solventi, senza dover ricorrere a condizioni

UM00012254
NOVARTIS EXHIBIT 1517
Novartis v. Regents, IPR2023-01347
Page 1000 of 4460

drastiche (temperature elevate, tempi lunghi, etc.) nocive alla purezza e alla stabilità della stavudina stessa.

La DMA presenta l'ulteriore vantaggio di avere un basso costo e di garantire rese elevate di prodotto purificato.

Il solvato così ottenuto viene facilmente desolvatato per trattamento con opportuni solventi, ottenendo la stavudina libera purificata. Si utilizzano solventi chetonici (ad esempio acetone), esterei (isopropilacetato, butilacetato, etc.), alcolici (ad esempio isopropanolo), riscaldando ad una temperatura compresa tra 20 e 50°C.

Un altro modo di purificazione del solvato è la sua dissoluzione, eventualmente facilitata da un leggero riscaldamento, nella stessa DMA e successiva riprecipitazione con gli opportuni solventi sopra citati.

Quando necessario, il ciclo di purificazione sopra descritto può venire ripetuto una seconda volta.

La presente invenzione viene ora descritta mediante i seguenti esempi non limitativi.

Parte sperimentale

Esempio 1

5'-O-Benzoil-timidina

Una soluzione di timidina (180 g) in piridina (1800 ml) è raffreddata a 0-5°C e trattata lentamente con benzoil cloruro (121,3 g). Terminata l'aggiunta si porta a temperatura ambiente e si agita per 3 giorni. La maggior parte della piridina è evaporata sotto vuoto e la soluzione risultante è versata in acqua e ghiaccio sotto vigorosa agitazione. La sospensione è agitata per 2 ore e il solido è filtrato, lavato bene con

UM00012255
NOVARTIS EXHIBIT 1517
Novartis v. Regents, IPR2023-01347
Page 1001 of 4460

acqua e seccato sotto vuoto. Il solido ottenuto è purificato in toluene (2500 ml). La sospensione toluenica è agitata a 100°C per 30 minuti, raffreddata a 60°C e filtrata lavando sul filtro con toluene caldo. Se necessario, la fase di purificazione viene ripetuta una seconda volta. La 5'-O-benzoil-timidina è recuperata con resa dell'84%.

Esempio 2

5'-O-Benzoil-3'-O-metansolfonil-timidina

Una soluzione di 5'-O-benzoil-timidina (210 g) in piridina (1000 ml) raffreddata ad una temperatura inferiore a 10°C e trattata goccia a goccia con mesil cloruro (83,2 g). Terminata l'aggiunta si porta a 20°C e si agita per 4 ore. Si evapora sotto vuoto la piridina, si riprende con acqua (900 ml) e metilene cloruro (1800 ml). La fase organica è filtrata e raffreddata a 0-5°C. Si ha formazione di precipitato che è filtrato e lavato con metilene cloruro freddo. Dopo essiccamento si ottiene 5'-O-benzoil-3'-O-metansolfonil-timidina con resa del 93%.

Esempio 3

2',3'-Dideidro-3'-deossitimidina (sintesi)

Una soluzione di 5'-O-benzoil-3'-O-metansolfonil-timidina (255 g) in N,N-dimetilformammide (1200 ml) è trattata ad una temperatura di 20°C a porzioni con potassio t.butilato (202 g). Terminata l'aggiunta si agita a temperatura ambiente per 4 ore. La sospensione ottenuta è versata in toluene freddo (5500 ml). Si agita a temperatura ambiente per 30 minuti e si filtra il solido gommoso ottenuto che è ripreso fino a completa dissoluzione in acqua (700 ml). La fase toluenica è separata. La soluzione acquosa raffreddata ad una temperatura inferiore a 15°C, è

UM00012256
NOVARTIS EXHIBIT 1517
Novartis v. Regents, IPR2023-01347
Page 1002 of 4460

neutralizzata con acido cloridrico concentrato e quindi evaporata sotto vuoto a circa 30-35°C. Le tracce di acqua vengono eliminate riprendendo il residuo con butanolo ed evaporando a secco sotto vuoto. Il residuo è estratto con acetone a porzioni (in totale 2000 ml). La soluzione è trattata con carbone, filtrata ed evaporata sotto vuoto ottenendo la 2',3'-dideidro-3'-deossitimidina grezza.

Esempio 4

2',3'-Dideidro-3'-deossitimidina (sintesi con coppia di basi)

Una soluzione di 5'-O-benzoil-3'-O-metansolfonil-timidina (255 g) in N,N-dimetilformammide (900 ml) e tetraidrofurano (900 ml) è trattata ad una temperatura di 20°C a porzioni con potassio t.butilato (169 g). Terminata l'aggiunta si agita a temperatura ambiente per 1 ora e, successivamente, si tratta a porzioni con metilato di sodio (25 g). Si agita sempre a temperatura ambiente, per 1 ora. La sospensione ottenuta è versata in toluene freddo (5500 ml). Si agita a temperatura ambiente per 30 minuti e si filtra il solido gommoso ottenuto che è ripreso fino a completa dissoluzione in acqua (700 ml). La fase toluenica è separata. La soluzione acquosa raffreddata ad una temperatura inferiore a 15°C, è neutralizzata con acido cloridrico concentrato e quindi evaporata sotto vuoto a circa 30-35°C. Le tracce di acqua vengono eliminate riprendendo il residuo con butanolo ed evaporando a secco sotto vuoto. Il residuo è estratto con acetone a porzioni (in totale 2000 ml). La soluzione è trattata con carbone, filtrata ed evaporata sotto vuoto ottenendo la 2',3'-dideidro-3'-deossitimidina grezza.

UM00012257
NOVARTIS EXHIBIT 1517
Novartis v. Regents, IPR2023-01347
Page 1003 of 4460

Esempio 5

2',3'-Dideidro-3'-deossitimidina (purificazione)

La 2',3'-dideidro-3'-deossitimidina grezza (ottenuta dall'esempio 3) è trattata a temperatura ambiente con N,N-dimetilacetammide (DMA, 500 ml) (per ottenere completa dissoluzione è necessario scaldare alcuni minuti a 40°C). La soluzione è agitata a temperatura ambiente per 30 minuti e quindi trattata con etere isopropilico (1100 ml). Il solido ottenuto è agitato a freddo per 2 ore e filtrato.

L'analisi mediante ^{1}H-NMR di un campione dopo essiccamento mostra la formazione di un solvato tra 2',3'-dideidro-3'-deossitimidina e DMA in rapporto molare 1/0,75.

^{1}H-NMR (DMSO, ppm): 11,27 (s, 1H), 7,62 (s, 1H), 6,80 (m, 1H), 6,37 (d, 1H), 5,89 (d, 1H), 4,97 (m, 1H), 4,76 (m, 1H), 3,59 (m, 2H), 2,93 (s, 2,3H), 2,76 (s, 2,3H), 1,94 (s, 2,3H), 1,71 (s, 3H).

Il solido è quindi sospeso in DMA (170 ml), trattato a temperatura ambiente con etere isopropilico (250 ml) e agitato per 1 ora. Dopo filtrazione il solido è sciolto a caldo in isopropanolo (700 ml), trattato con carbone e filtrato. L'isopropanolo è concentrato sotto vuoto (solvente eliminato circa 400 ml) e la soluzione è raffreddata. Dopo filtrazione e essiccamento si isola la 2',3'-dideidro-3'-deossitimidina con resa superiore al 40% (calcolata da 5'-O-benzoil-3'-O-metansolfonil-timidina grezza) e con purezza HPLC del 99,1%.

La struttura è stata confermata mediante analisi ^{1}H-NMR (DMSO, ppm): 11,27 (s, 1H), 7,62 (s, 1H), 6,80 (m, 1H), 6,37 (d, 1H), 5,89 (d, 1H), 4,97 (m, 1H), 4,76 (m, 1H), 3,59 (m, 2H), 1,71 (s, 3H).

UM00012258
NOVARTIS EXHIBIT 1517
Novartis v. Regents, IPR2023-01347
Page 1004 of 4460

Esempio 6

2',3'-Dideidro-3'-deossitimidina (purificazione)

La 2',3'-dideidro-3'-deossitimidina grezza (50% di quanto ottenuto nell'esempio 4) è trattata a temperatura ambiente con N,N-dimetilacetammide (DMA, 250 ml) (per ottenere completa dissoluzione è necessario scaldare alcuni minuti a 40°C). La soluzione è agitata a temperatura ambiente per 30 minuti e quindi trattata con etere isopropilico (550 ml). Il solido ottenuto è agitato a freddo per 2 ore e filtrato.

L'analisi mediante ^{1}H-NMR di un campione dopo essiccamento mostra la formazione di un solvato tra 2',3'-dideidro-3'-deossitimidina e DMA in rapporto molare 1/0,75 (dati corrispondenti a quelli riportati nell'esempio 5).

Il solido è quindi sciolto in DMA (85 ml) riscaldando a 40°C, trattato a temperatura ambiente con etere isopropilico (125 ml) e agitato per 1 ora. Dopo filtrazione il solido è sciolto a caldo in isopropanolo (350 ml), trattato con carbone e filtrato. L'isopropanolo è concentrato sotto vuoto (solvente eliminato circa 200 ml) e la soluzione è raffreddata. Dopo filtrazione e essiccamento si isola la 2',3'-dideidro-3'-deossitimidina con resa superiore al 50% (calcolata da 5'-O-benzoil-3'-O-metansolfonil-timidina grezza) e con purezza HPLC del 99,0%.

L'analisi ^{1}H-NMR ha confermato la struttura della stavudina (dati corrispondenti a quelli riportati nell'esempio 5).

Esempio 7

2', 3'-Dideidro-3'-deossitimidina (stavudina): purificazione con:

UM00012259
NOVARTIS EXHIBIT 1517
Novartis v. Regents, IPR2023-01347
Page 1005 of 4460

a) N,N-dietilformammide

La 2',3'-dideidro-3'-deossitimidina grezza (1 g) è trattata a temperatura ambiente con N,N-dietilformammide (2 ml) (per ottenere completa dissoluzione è necessario scaldare alcuni minuti a circa 50°c). La soluzione è agitata a temperatura ambiente per 30 minuti e quindi trattata con etere isopropilico (5 ml). Si separa un olio che lentamente a temperatura ambiente si trasforma in un solido gommoso. Dopo filtrazione e essiccamento si ottengono 0,45 g di stavudina (solido giallo) solo parzialmente purificata (TLC eluente metilene cloruro-metanolo 9-1). L'analisi mediante ^{1}H-NMR mostra la presenza solo di tracce di N.N-dietilformammide escludendo di conseguenza l'isolamento di una forma solvata.

b) N,N-dietilacetammide

La 2',3'-dideidro-3'-deossitimidina grezza (1 g) è trattata a temperatura ambiente con N,N-Dietilacetammide (2 ml) (per ottenere completa dissoluzione è necessario scaldare alcuni minuti a circa 50°C). La soluzione è agitata a temperatura ambiente per 30 minuti e quindi trattata con etere isopropilico (5 ml). Si separa un olio che lentamente a temperatura ambiente si trasforma in un solido gommoso. Dopo filtrazione e essiccamento si ottengono 0,6 g di stavudina (solido giallo) solo parzialmente purificata (TLC eluente metilene cloruro- metanolo 9-1). L'analisi mediante ^{1}H-NMR mostra la presenza solo di tracce di N,N-dietilacetammide escludendo di conseguenza l'isolamento di una forma solvata.

c) N-metilpropionammide

UM00012260
NOVARTIS EXHIBIT 1517
Novartis v. Regents, IPR2023-01347
Page 1006 of 4460

La 2',3'-dideidro-3'-deossitimidina grezza (1 g) è trattata a temperatura ambiente con N-metilpropionammide (2 ml) (per ottenere completa dissoluzione è necessario scaldare alcuni minuti a circa 50°C). La soluzione è agitata a temperatura ambiente per 30 minuti e quindi trattata con etere isopropilico (5ml). Si separa un olio denso che lentamente a temperatura ambiente si trasforma in un solido gommoso. Dopo filtrazione e essiccamente si ottengono 0,65 g di stavudina (solido biancastro) solo parzialmente purificata (TLC eluente metilene cloruro-metanolo 9-1). L'analisi mediante ^{1}H-NMR mostra la presenza solo di tracce di N-metilpropionammide escludendo di conseguenza l'isolamento di una forma solvata.

L'esempio 7 mostra che gli oli o solidi gommosi ottenuti per reazione della stavudina con ammidi primarie o secondarie diverse dalla DMA contengono solo modeste proporzioni di solvente, a conferma del fatto che il solvato non si forma o è comunque instabile.

La stavudina ottenuta nell'esempio 7 con ammidi diverse dalla DMA ha presentato una qualità non accettabile per purezza e cristallinità.

UM00012261
NOVARTIS EXHIBIT 1517
Novartis v. Regents, IPR2023-01347
Page 1007 of 4460

RIVENDICAZIONI

1. Processo per la purificazione della 2',3'-dideidro-3'-deossitimidina (stavudina) caratterizzato dal comprendere la solvatazione della stavudina per reazione con N,N-dimetilacetammide (DMA), e la successiva desolvatazione del solvato ottenuto.
2. Il processo secondo la rivendicazione 1, dove il solvato ottenuto contiene (DMA) e stavudina in rapporti molari compresi tra 0,5:1 e 1:1.
3. Il processo secondo la rivendicazione 1, dove la desolvatazione viene ottenuta per trattamento dei solvati a temperature comprese tra 20°C e 50°C in solventi scelti tra ammidi, eteri, chetoni, esteri, alcoli.
4. Il processo secondo la rivendicazione 3, dove il solvente utilizzato per la desolvatazione è scelto tra butilacetato, isopropanolo, ed acetone.
5. Il processo secondo la rivendicazione 1, dove la stavudina da purificare è stata ottenuta mediante un processo che comprende il trattamento, in presenza di una base, di una 5'-O-benzoil-3'-O-alchilsolfonil-timidina o di una 5'-O-benzoil-3'-O-arilsolfonil-timidina, con formazione, in un solo stadio, di stavudina.
6. Solvato di N,N-dimetilacetammide (DMA) / stavudina in rapporti molari compresi tra 0,5:1 e 1:1
7. Solvato secondo la rivendicazione 6, dove il rapporto molare N,N-dimetilacetammide (DMA) / stavudina è pari a 0.75:1

(GER/pd)

UM00012262
NOVARTIS EXHIBIT 1517
Novartis v. Regents, IPR2023-01347
Page 1008 of 4460

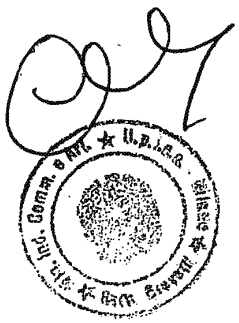
Milano, li 26 Ottobre 1998

p. INDUSTRIALE CHIMICA S.r.l.

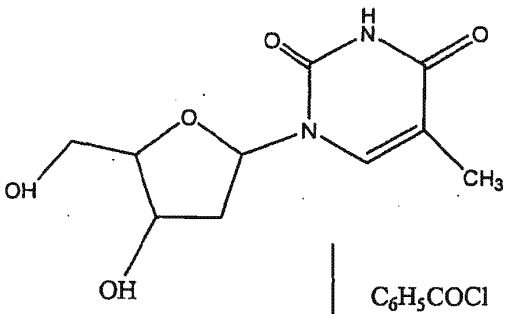
Il Mandatario

Dr.ssa Gemma Gervasi

NOTARBARTOLO & GERVASI S.p.A.



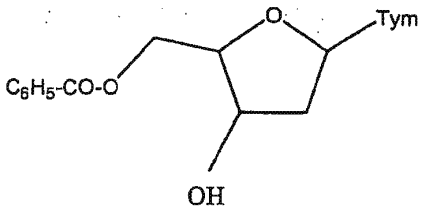
UM00012263
NOVARTIS EXHIBIT 1517
Novartis v. Regents, IPR2023-01347
Page 1009 of 4460



(1)

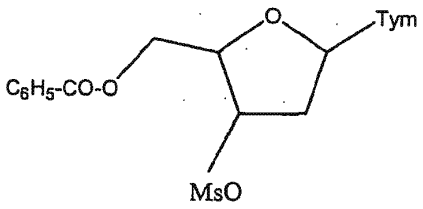
C_6H_5COCl
(Pyr)

MI 98 A 002290



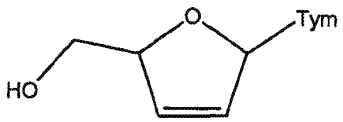
(2)

CH_3ClO_2S
(Pyr)



(3)

MeONa/ButOK
(DMF-THF)



(4)

ISTANZA

NOVARTIS EXHIBIT 1517
Novartis v. Regents, IPR2023-01347
Page 1011 of 4460

1665PTIT ATTI

Protocollo n°..................................

BREV. MI V

002640

MINISTERO DELL'INDUSTRIA DEL COMMERCIO E DELL'ARTIGIANATO

Ufficio Provinciale Industria Commercio e Artigianato di Milano

SERVIZIO DEI BREVETTI PER INVENZIONI, MODELLI E MARCHI

COPIA DEL VERBALE DI DEPOSITO DI ISTANZE E DOCUMENTI

L'anno 1998 il giorno undici del mese di novembre

la Ditta ~~Signor~~ INDUSTRIALE CHIMICA S.r.l.

con sede ~~residente~~ in MILANO

a mezzo mandatari : Dr. Diego Pallini (albo n. 484)

ed elettivamente domiciliato agli effetti di legge a Milano - ~~via~~ C.so di Porta Vittoria 9

presso Notarbartolo & Gervasi S.p.A.

- a seguito di domanda per INVENZIONE ~~MODELLO~~ ~~MARCHIO~~ depos. a Milano il 26.10.1998 con.

Protocollo n. MI98A002290

~~[illegible]~~

ha depositato presso questo Ufficio i sottoelencati documenti :

1 - ISTANZA DI CORREZIONE ED INTEGRAZIONE

2 - PAG. 4 POSTILLATA

3 - PAG. 4 EX NOVO

4 -

5 -

Serv. Brevetti * Min. Ind. Comm. e Art. * U.p.i.c.a. - Milano

IL DEPOSITANTE

L'UFFICIALE ROGANTE

Giuseppe Rescali

Per copia conforme all'originale

«Si precisa che per tale domanda e allegati l'imposta di bollo è stata assolta conformemente alla circolare n° 163/83 dell'U.C.B. e succ. modif., con riserva di eventuali integrazioni che saranno dallo stesso richieste in sede di concessione.»

p. Il Direttore (Dott. Daniele Melegari)

Dott. M. Colosimo

MINISTERO DELL' INDUSTRIA, COMMERCIO E ARTIGIANATO

Ufficio Italiano Brevetti e Marchi ROMA

Domanda di Brevetto per Invenzione Industriale dal titolo:

"Processo industriale per la purificazione di 2',3'-dideidro-3'-deossitimidina"

a nome: INDUSTRIALE CHIMICA S.r.l.

con sede in MILANO

depositata il 26.10.1998 con il n. MI98A002290

BREV. MI-V 002640

*****

ISTANZA DI CORREZIONE ED INTEGRAZIONE

In base all'art. 49 del D.P.R. 22 Giugno 1979, N. 338, la sottoscritta INDUSTRIALE CHIMICA S.r.l., di nazionalità italiana, con sede in MILANO, a mezzo Mandatario Dr. Diego Pallini (albo N. 484) della NOTARBARTOLO & GERVASI S.p.A., C.so di Porta Vittoria, 9 Milano, presso cui ha eletto domicilio a tutti gli effetti di legge, chiede che le venga concesso di apportare la seguente correzione qui di seguito specificata.

POSTILLA 1 - Pagina 4 - riga 21, dopo la parola "co-pendente" inserire "No. MI98A002289"

Milano, li 11 Novembre 1998

p. INDUSTRIALE CHIMICA S.r.l.

Il Mandatario

Dr. Diego Pallini

NOTARBARTOLO & GERVASI S.p.A.

U.P.I.C.A. BREVETTI 11 NOV. 1998 MILANO

U.p.i.c.a. - Milano ★ Min. Ind. Comm. e Art. ★ Serv. Brevetti

l'ottenimento di stavudina pura.

DESCRIZIONE DELLE FIGURE

(A) Figura 1: Sintesi di stavudina

(1) *β-timidina*

(2) *5'-O-Benzoiltimidina*

(3) *5'-O-Benzoil-3'-O-metansolfoniltimidina*

(4) *2',3'-Dideidro-3'-deossitimidina*

BREV MI-V
002640

DESCRIZIONE DETTAGLIATA DELL'INVENZIONE

La presente invenzione descrive un nuovo processo industriale per la purificazione della 2',3'-dideidro-3'-deossitimidina grezza (d4T; stavudina).

Il processo secondo la presente invenzione è utilizzabile in ogni circostanza si voglia ottenere stavudina pura a partire dal corrispondente prodotto grezzo. Può essere in particolare applicato a qualsiasi processo di sintesi che porti alla formazione di stavudina grezza; può inoltre essere impiegato in alternativa ai procedimenti noti di purificazione descritti per tale prodotto. Alcuni esempi di tali processi sono stati citati precedentemente nell'analisi della tecnica anteriore.

Secondo una realizzazione preferita, il presente processo è applicabile alla sintesi della stavudina descritta nella domanda co-pendente No. MI98A002289 depositata il 26 ottobre 1998 a nome della Richiedente, qui incorporata per riferimento. Tale sintesi comprende il trattamento, in presenza di una base, di una 5'-O-benzoil-3'-O-alchilsolfonil-timidina o di una 5'-O-benzoil-3'-O-arilsolfonil-timidina, con formazione, in un solo stadio, di stavudina.

11 NOV. 1998
MILANO

Min. Ind. Comm. e Art. * U.p.i.c.a. - Milano * Serv. Brevetti *

UM00012268
NOVARTIS EXHIBIT 1517
Novartis v. Regents, IPR2023-01347
Page 1014 of 4460

THE FRENCH REPUBLIC

MINISTRY OF COMMERCE AND INDUSTRY

PATENT AND TRADEMARK OFFICE

PATENT

Group 14, Category 1 Number 769,586

Method of Preparing Derivatives of Oxypyridine and Aminopyridine Combinations

The company known as: *CHEMISCHE FABRIK VON HEYDEN Aktiengesellschaft,* which is registered in Germany.

Application filed on March 5, 1934, at 1:05 P.M., in Paris.
Issued on June 11, 1934. Published on August 28, 1934.

(Patent application filed in Germany on March 31, 1933. Applicant's statement.)

It has been observed that oxypyridine and aminopyridine combinations tend to combine as molecular combinations with substituted barbituric acids. Derivatives obtained in this manner form specific crystalline combinations whose physical properties essentially distinguish them from the raw materials which are used in each instance.

Derivatives of this kind are obtained from oxypyridine and aminopyridine combinations when the latter combinations are blended, for example, in order to yield an amount corresponding to 2 molecules for 1 or 2 molecules of a substituted barbituric acid. It is also possible, however, to cause the aforementioned components to act upon one another within solvents and to obtain molecular combinations by crystallization or evaporation, or to produce reactions between salts of barbituric acids and salts of the previously cited pyridine combinations.

Example 1: 2, 3 parts 4-oxy-5-nitropyridine and 3 parts diethylbarbituric acid are dissolved in 60 parts of water according to volume, while being heated. As a result of cooling, a combination which melts at 245° is separated by crystallization, and, for 1 mole of $C_8H_{12}O_3N_2$, it contains 1 mole of $C_5H_4O_3N_2$.

Example 2: 1 part diethylbarbituric acid and 2 parts 2-ethoxy-5-acetaminopyridine are melted at 140°. After solidification of the clear melted mass, crystallization is obtained in water or benzene. The combination obtained in this manner melts at 112°-115°, and it contains 2 moles of $C_9H_{12}O_2N_2$ for 1 mole of $C_8H_{12}O_3N_2$,

Example 3: 12 parts N-methyl-α-pyridone are added to a suspension consisting of 16 parts diethylbarbituric acid in 90 parts of heated benzene according to volume. As a result of stirring, a solution is promptly obtained. The combination, which is separated by crystallization during cooling, melts at approximately 120°, and it consists of the respective raw materials in a 1:1 ratio.

Example 4: 17 parts phenylethylbarbituric acid are intensively mixed

with 8 parts N-methyl-α-pyridone, and solidification occurs extremely quickly, with heat being released. After cooling, the product is powdered, and it is mixed with ether. Then it is filtered with a tube and is allowed to dry. In this way, it is possible to obtain a combination which melts at approximately 122° and contains 1 mole C_6H_7ON for 1 mole of $C_{12}H_{12}O_3N_2$.

Example 5: 20 parts diethylbarbituric acid and 25 parts α-aminopyridine are dissolved in 100 parts of 20% alcohol by volume while being heated. After cooling, the crystals which are separated are filtered with a tube. Then rinsing with 20% alcohol and drying take place. It is possible to clean these crystals by dissolving them in ether and by precipitation with petroleum ether. The crystals then melt at 82°-85°. This combination contains 2 moles of $C_5H_6N_2$ for 1 mole of $C_8H_{12}O_3N_2$.

SUMMARY

The present invention pertains to:

1. A method of preparing derivatives of oxypyridine and aminopyridine combinations, characterized by the fact that said oxypyridine and aminopyridine combinations are caused to act upon substituted barbituric acids.
2. Methods of applying the process identified within 1, whereby:
   a) The components are melted at an increased temperature.
   b) The components are caused to act upon one another within a solution or a suspension.
   c) A double reaction is produced between salts of the aforementioned components.

The company known as: *CHEMISCHE FABRIK VON HEYDEN Aktiengesellschaft*, which is registered in Germany.

By power of attorney:
Societe DONY et ARMENGAUD aine.

NOVARTIS EXHIBIT 1517
Novartis v. Regents, IPR2023-01347
Page 1016 of 4460

T9055

RÉPUBLIQUE FRANÇAISE.

MINISTÈRE DU COMMERCE ET DE L'INDUSTRIE.

DIRECTION DE LA PROPRIÉTÉ INDUSTRIELLE.

BREVET D'INVENTION.

Gr. 14. — Cl. 1. **N° 769.586**

Procédé de préparation de dérivés de combinaisons oxy- et aminopyridiques.

Société dite : CHEMISCHE FABRIK VON HEYDEN Aktiengesellschaft résidant en Allemagne.

Demandé le 5 mars 1934, à 13h 5m, à Paris.
Délivré le 11 juin 1934. — Publié le 28 août 1934.
(Demande de brevet déposée en Allemagne le 31 mars 1933. — Déclaration du déposant.)

Il a été constaté que des combinaisons oxy- et aminopyridiques ont tendance à se réunir en combinaisons moléculaires avec des acides barbituriques substitués. Les dérivés ainsi obtenus constituent des combinaisons cristallisées déterminées, qui se distinguent esentiellement, dans leurs propriétés physiques, des matières premières employées dans chaque cas.

On obtient des dérivés de ce genre de combinaisons oxy- et aminopyridiques, en fondant par exemple ces dernières dans une quantité correspondant à 2 molécules pour 1 ou 2 molécules d'un acide barbiturique substitué. Mais on peut également faire agir les composants l'un sur l'autre dans des solvants et obtenir les combinaisons moléculaires par cristallisation ou évaporation, ou faire réagir des sels d'acides barbituriques avec des sels des combinaisons mentionnées de la pyridine.

Exemple 1. — On dissout à chaud 2,3 parties de 4-oxy-5-nitropyridine et 3 parties d'acide diéthylbarbiturique dans 60 parties en volume d'eau. Par refroidissement, il se sépare par cristallisation une combinaison, fondant à 245°, qui pour 1 mol. de $C^8H^{12}O^3Az^2$, contient 1 mol. de $C^5H^4O^3Az^2$.

Exemple 2. — On fond à 140° 1 partie d'acide diéthylbarbiturique et 2 parties de 2-éthoxy-5-acétaminopyridine. Après solidification de la masse fondue claire, on fait cristalliser dans de l'eau ou du benzène. La combinaison ainsi obtenue fond à 112°-115° et contient, pour 1 mol. de $C^8H^{12}O^3Az^2$, 2 mol. de $C^9H^{12}O^2Az^2$.

Exemple 3. — A une suspension de 16 parties d'acide diéthylbarbiturique dans 90 parties en volume de benzène chaud, on ajoute 12 parties de N-méthyl-α-pyridone. Par agitation, il se produit bientôt une solution. La combinaison, se séparant par cristallisation lors du refroidissement, fond à environ 120° et se compose des matières première dans le rapport 1 : 1.

Exemple 4. — On mélange intimement 17 parties d'acide phényléthylbarbiturique avec 8 parties de N-méthyl-α-pyridone; il se produit très rapidement une solidification avec dégagement de chaleur. Après le refroidissement, on pulvérise le produit, on malaxe avec de l'éther, on filtre à la trompe et on sèche. On obtient ainsi une combinaison, fondant à 122° environ, qui contient, pour 1 mol. de $C^{12}H^{12}O^3Az^2$, 1 mol. de C^6H^7OAz.

Exemple 5. — On dissout à chaud 20 parties d'acide diéthylbarbiturique et 25 parties de α-aminopyridine dans 100 parties en volume d'alcool à 20 0/0. Après refroidisse-

Prix du fascicule : 5 francs.

UM00012271
NOVARTIS EXHIBIT 1517
Novartis v. Regents, IPR2023-01347
Page 1017 of 4460

ment, on filtre à la trompe les cristaux qui se sont séparés, on lave avec de l'alcool à 20 0/0 et on sèche. On peut les nettoyer par dissolution dans de l'éther et par précipitation avec de l'éther de pétrole; ils fondent alors à 82°-85°. Cette combinaisou contient, pour 1 mol de $C^8H^{12}O^3Az^2$, 2 mol. de $C^5H^6Az^2$.

RÉSUMÉ.

L'invention concerne :

1° Un procédé de préparation de dérivés de combinaisons oxy- et aminopyridiques, caractérisé en ce qu'on fait agir des combinaisons oxy- et aminopyridiques sur des acides barbituriques substitués;

2° Des modes d'exécution du procédé suivant 1°, dans lesquels :

a. On fond les constituants à température accrue;

b. On fait agir les constituants l'un sur l'autre en solution ou en suspension;

c. On produit une double réaction entre les sels des constituants.

Société dite : CHEMISCHE FABRIK VON HEYDEN AKTIENGESELLSCHAFT.

Par procuration :

Société Dony et Armengaud aîné.

Pour la vente des fascicules, s'adresser à l'Imprimerie Nationale, 27, rue de la Convention, Paris (15e)

UM00012272

NOVARTIS EXHIBIT 1517
Novartis v. Regents, IPR2023-01347
Page 1018 of 4460

[Page 438]

Substitution Products of Hexanes, Hexenes, etc.

[Translator's Note: The first part of page 438 is the concluding part of the preceding section that has not been translated. The pertinent bibliographic references in the following sections, which have been translated, are to be found at the end of this translation.]

d-glucose - sodium chloride - monohydrate (glucose-sodium chloride) =
$2C_6H_{12}O_6.NaCl.H_2O$

Specific gravity 1.55-1.59 in accordance with older determinations.
Trigonal trapezohedral.

$\alpha = 74° 10.5'$ ($a:c = 1:1.7854$ Traube[36]))

Kobell[37]) observed the combination of the two correlate rhombohedra $r\{100\}$ and $\rho\{22\bar{1}\}$, with $d\{411\}$, $a\{10\bar{1}\}$ and $\alpha\{1\bar{1}0\}$; Schabus[15]) (loc. cit. 21), who erroneously designated the compound "glucose", was apparently describing hexagonal bipyramids (combination of r and ρ of the same magnitude) with the subordinate forms $m\{2\bar{1}\bar{1}\}$, $a\{10\bar{1}\}$ and $\alpha\{1\bar{1}0\}$ and also crystals at which $r\{100\}$ predominated, and $\delta\{110\}$ and $c\{111\}$ occurred in addition to ρ, a, and α. Heintze[38]), like Kobell, observed $r\{100\}$ usually dominating over $\rho\{22\bar{1}\}$ but also on occasions r alone. Traube found that the crystals that form from aqueous or diluted alcoholic solution initially exhibited r and ρ in equilibrium and then ρ receded more and more and m, a, α, d (often rather large) and δ developed of which $d\{411\}$ and $\delta\{110\}$ seldom occurred on a [sic; one?] crystal; $c\{111\}$ also appeared on crystals from solution in nitric acid.

	Calculated:	Observed:			
		Traube:	Heintze:	Schabus:	Kobell:
$r:r = (100):(010) =$	$102°22\frac{1}{2}'$	$102°24'$	—	$102°18'$	—
$r:c = (100):(111) =$	64 6	64 31	63°42′	63 45	63°15′
$r:\varrho = (100):(22\bar{1}) =$	53 28	53 16	53 14	53 20	53 2
$d:d = (411):(141) =$	—	*76 52	—	—	—

The ability to be cleaved was not observed. Etch patterns on $r\{100\}$ and $\rho\{22\underline{1}\}$ differed; asymmetrical quadrilaterals in both cases.

Birefringence positive, optical rotation capacity not measurable. Optical anomalies are frequent, especially on the crystals that separated from diabetics' urine, with a distinct composition comprising biaxial sectors; hence Pasteur[39]) and Des Cloizeaux[40]) regarded the crystals as being rhombic [twin] crystals comprising three single crystals in accordance with a pseudo-hexagonal prism.

***d*-glucose - sodium bromide - monohydrate** (glucose-sodium bromide) = $2C_6H_{12}O_6.NaBr.H_2O$

Trigonal trapezohedral.

$\alpha = 72° 18'$ ($a:c = 1:1.8614$ Traube[36]))

When recrystallized from hot [ethyl] alcohol in accordance with the work of Miller[41]), this substance, which was first synthesized by Stenhouse[41]), exhibits the combination $r\{100\}$ with a rounded base $c\{111\}$. As in the case of the preceding compound, Traube (loc. cit. 517) first observed the formation of rhombohedra $r\{100\}$; the following also occurred upon prolonged growth: $\rho\{22\bar{1}\}$, $m\{2\bar{1}\bar{1}\}$, $a\{10\bar{1}\}$, $\alpha\{1\bar{1}0\}$, $s\{210\}$, $\sigma\{201\}$.

	Calculated:	Observed:	
		Traube:	Miller:
$r:r = (100):(0\bar{1}0) =$	$103° 29\frac{1}{2}'$	$103° 19'$	$103° 20'$
$r:c = (100):(\bar{1}11) =$	—	*65 3	64 46
$r:\varrho = (100):(2\bar{2}\bar{1}) =$	53 55	54 4	—
$s:\sigma = (210):(20\bar{1}) =$	45 $49\frac{1}{2}$	46 1	—
$s:\varrho = (210):(2\bar{2}\bar{1}) =$	28 50	28 46	—
$s:r = (210):(100) =$	74 $39\frac{1}{2}$	74 38	—

No distinct ability to be cleaved.
Birefringence positive, intense. Optical anomalies as in the case of the preceding substance.

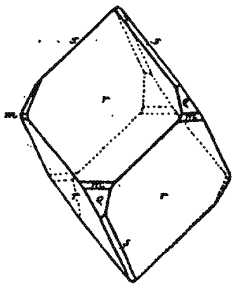
***d*-glucose - sodium iodide - monohydrate** (glucose-sodium iodide) = $2C_6H_{12}O_6.NaI.H_2O$

Trigonal trapezohedral.

$\alpha = 72° 50'$ ($a:c = 1:1.8388$ Traube[36]))

Fig. 1252

In accordance with the work of Traube (loc cit. 515), this compound crystallizes from a solution of the components in the ratio of the formula in combinations of $r\{101\}$ with subordinate $\rho\{22\bar{1}\}$, $m\{2\bar{1}\bar{1}\}$ and $s\{210\}$ (Fig. 1252); very narrow surfaces comprising sigma$\{201\}$ and $a\{10\bar{1}\}$ or $\alpha\{1\bar{1}0\}$ also form in the case of prolonged continuing growth in the mother liquor.



	Calculated:	Observed:
$r:r = (100):(010) =$	—	*104° 4′
$r:c = (100):(111) =$	64° 44′	64 56
$r:\varrho = (100):(22\bar{1}) =$	53 46	53 32
$s:\sigma = (210):(201) =$	45 32	45 46
$s:\varrho = (210):(22\bar{1}) =$	28 47	28 52
$s:r = (210):(100) =$	74 43	74 29

Cohesion relationships and etch patterns identical to those [before]Birefringence positive; optical anomalies similar to those of the chloro compound. No measurable optical rotation capacity.

Foreign language references:

[36]) H. Traube, N. Jahrb. f. Min. usw. 1893; Beil.-Bd. [Volume] 8, 518. Extract from Zeitschr. f. Krystal. **24**, 182.

[38]) Heintze, Kryst. Unters. org. Verb. ["Crystallographic investigation of organic compounds"] Dissertation. Göttingen 1884, 22. Extract Zeitschr. Krystall. **11**, 87.

[39]) Pasteur, Ann. Chim. Phys. 1851 93), **31**, 92.

[40]) Des Cloizeaux, Ann. d. mines 1857, (5) **11**, 322 and 1858, (5) **14**, 369.

[41]) Stenhouse (Crystal determination by Miller), Journ. Chem. Soc. London 1863, (2) **1**, Ann. d. Chemie 1864, **129**, 286.

P. Groth Chemische Krystallographie (1910)

T9054

	Berechnet:	Beobachtet: Becke:	Beobachtet: Březina:
$m : {}'m = (1\bar{1}0) : (\bar{1}\bar{1}0)$	$= 60°24'$	$60°24'$	$60°26'$
$l : c = (101) : (001)$	$= 44\ 23$	$44\ 31$	$43\ 49$
$d' : c' = (\bar{1}01) : (00\bar{1})$	$= 52\ 7$	$52\ 7$	$52\ 7$
$m : c = (1\bar{1}0) : (001)$	$= 86\ 0$	$85\ 59$	$85\ 38$
$'m : d' = (\bar{1}\bar{1}0) : (\bar{1}01)$	$= 69\ 30$	$69\ 27$	$69\ 15$
$m : l = (1\bar{1}0) : (101)$	$= 66\ 31$	$66\ 27$	$68\ 32$

Die Krystalle lösen sich von der nicht ausgebildeten (rechten) Seite her in Wasser viel schneller, als von der linken Seite, und dementsprechend zeigen auch die Ätzfiguren auf $c\{001\}$ und $l\{101\}$ links gerundete, rechts scharfe Flächen.

Ebene der optischen Axen senkrecht zu $b\{010\}$, 1. Mittellinie ungefähr senkrecht zu $l\{101\}$, Axenwinkel groß; $\gamma - \alpha = 0{,}019$.

d-Glykose-Natriumchlorid-Monohydrat (Traubenzucker-Chlornatrium) = $2C_6H_{12}O_6 . NaCl . H_2O$.

Spec. Gew. 1,55—1,59 nach älteren Bestimmungen.

Trigonal trapezoëdrisch.

$$a = 74°10\tfrac{1}{2}' \ (a : c = 1 : 1{,}7854 \text{ Traube}^{36})).$$

Kobell[37]) beobachtete die Combination der beiden correlaten Rhomboëder $r\{100\}$ und $\varrho\{22\bar{1}\}$, mit $d\{\bar{4}11\}$, $a\{10\bar{1}\}$ und $\alpha\{1\bar{1}0\}$; Schabus[15]) (l. c. 21), welcher die Verbindung irrtümlich als »Traubenzucker« bezeichnete, beschrieb scheinbar hexagonale Bipyramiden (Combination von r und ϱ in gleicher Größe) mit den untergeordneten Formen $m\{2\bar{1}\bar{1}\}$, $a\{10\bar{1}\}$ und $\alpha\{1\bar{1}0\}$, ferner Krystalle, an denen $r\{100\}$ vorherrschte und außer ϱ, a und α noch $\delta\{110\}$ und $c\{111\}$ auftraten. Heintze[38]) beobachtete, wie Kobell, $r\{100\}$ meist über $\varrho\{22\bar{1}\}$ herrschend, zuweilen aber auch r allein. Traube fand, daß die aus wässeriger oder verdünnter alkoholischer Lösung sich bildenden Krystalle anfangs r und ϱ im Gleichgewichte zeigten, dann trat ϱ immer mehr zurück, und es entwickelten sich m, $'a$, α, d (oft ziemlich groß) und δ, von denen $d\{\bar{4}11\}$ und $\delta\{110\}$ selten an einem Krystall auftraten; an Krystallen aus salpetersaurer Lösung erschien auch $c\{111\}$.

	Berechnet:	Beobachtet: Traube:	Heintze:	Schabus:	Kobell:
$r : r = (100) : (010)$	$= 102°22\tfrac{1}{2}'$	$102°24'$	—	$102°18'$	—
$r : c = (100) : (111)$	$= 64\ 6$	$64\ 31$	$63°42'$	$63\ 45$	$63°15'$
$r : \varrho = (100) : (22\bar{1})$	$= 53\ 28$	$53\ 16$	$53\ 14$	$53\ 20$	$53\ 2$
$d : d = (\bar{4}11) : (1\bar{4}1)$	$=$ —	$*76\ 52$	—	—	—

Spaltbarkeit nicht beobachtet. Ätzfiguren auf $r\{100\}$ und $\varrho\{22\bar{1}\}$ verschieden; in beiden Fällen unsymmetrische Vierecke.

Doppelbrechung positiv, Drehungsvermögen nicht meßbar. Häufig sind optische Anomalien, besonders an den aus Diabetesharn abgeschiedenen Krystallen, mit deutlicher Zusammensetzung aus zweiaxigen Sectoren, daher Pasteur[39])

36) H. Traube, N. Jahrb. f. Min. usw. 1893, Beil.-Bd. 8, 548. Ausz. Zeitschr. f. Krystall 24, 482.

37) F. v. Kobell, Journ. f. prakt. Chemie 1843, 28, 489.

38) Heintze, Kryst. Unters. org. Verb. Dissert. Göttingen 1884, 22. Ausz. Zeitschr. Krystall. 11, 87.

39) Pasteur, Ann. chim. phys. 1851 (3) 31, 92.

UM00012276
NOVARTIS EXHIBIT 1517
Novartis v. Regents, IPR2023-01347
Page 1022 of 4460

und Des Cloizeaux[40]) die Krystalle als rhombische Drillinge nach einem pseudohexagonalen Prisma auffaßten.

d-Glykose-Natriumbromid-Monohydrat (Traubenzucker-Bromnatrium) = $2C_6H_{12}O_6 . NaBr . H_2O$.

Trigonal trapezoëdrisch.

$$\alpha = 72^\circ 18' \quad (a : c = 1 : 1{,}8614 \text{ Traube}^{36})).$$

Die zuerst von Stenhouse[41]) dargestellte Substanz zeigt, aus heißem Alkohol umkrystallisiert, nach Miller[41]) die Combination $r\{100\}$ mit gerundeter Basis $c\{111\}$. Traube (l. c. 517) beobachtete, wie bei der vorigen Verbindung, zuerst die Bildung von Rhomboëdern $r\{100\}$, bei längerem Wachstum traten außerdem auf: $o\{22\bar{1}\}$, $m\{2\bar{1}\bar{1}\}$, $a\{10\bar{1}\}$, $\alpha\{1\bar{1}0\}$, $s\{210\}$, $\sigma\{201\}$.

	Berechnet:	Beobachtet: Traube:	Miller:
$r : r = (100) : (010) =$	$103^\circ 29\frac{1}{2}'$	$103^\circ 19'$	$103^\circ 20'$
$r : c = (100) : (111) =$	—	*65 3	64 46
$r : \varrho = (100) : (2\bar{2}\bar{1}) =$	53 55	54 4	—
$s : \sigma = (210) : (201) =$	45 $49\frac{1}{2}$	46 1	—
$s : \varrho = (210) : (2\bar{2}\bar{1}) =$	28 50	28 46	—
$s : r = (210) : (100) =$	74 $39\frac{1}{2}$	74 38	—

Keine deutliche Spaltbarkeit.
Doppelbrechung positiv, stark. Optische Anomalien wie beim vor. Körper.

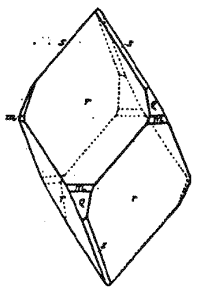
d-Glykose-Natriumjodid-Monohydrat (Traubenzucker-Jodnatrium) = $2C_6H_{12}O_6 . NaJ . H_2O$.

Trigonal trapezoëdrisch.

$$\alpha = 72^\circ 50' \quad (a : c = 1 : 1{,}8388 \text{ Traube}^{36})).$$

Die Verbindung krystallisiert nach Traube (l. c. 515) aus einer Lösung der Bestandteile im Verhältnisse der Formel in Combinationen von $r\{100\}$ mit untergeordnetem $\varrho\{22\bar{1}\}$, $m\{2\bar{1}\bar{1}\}$ und $s\{210\}$ (Fig. 1252); bei längerem Fortwachsen in der Mutterlauge bilden sich noch sehr schmale Flächen von $\sigma\{201\}$ und $a\{10\bar{1}\}$ bzw. $\alpha\{1\bar{1}0\}$.

Fig. 1252.



	Berechnet:	Beobachtet:
$r : r = (100) : (010) =$	—	*104° 4'
$r : c = (100) : (111) =$	64° 44'	64 56
$r : \varrho = (100) : (22\bar{1}) =$	53 46	53 32
$s : \sigma = (210) : (201) =$	45 32	45 46
$s : \varrho = (210) : (22\bar{1}) =$	28 47	28 52
$s : r = (210) : (100) =$	74 43	74 29

Cohäsionsverhältnisse und Ätzfiguren gleich dem vor Doppelbrechung positiv; optische Anomalien ähnlich denen der Chlorverbindung. Kein meßbares Drehungsvermögen.

[40]) Des Cloizeaux, Ann. d. mines 1857, (5) **11**, 322 und 1858, (5) **14**, 369.
[41]) Stenhouse (Krystallbest. v. Miller), Journ. Chem. Soc. London 1863, (2) **1**, Ann. d. Chemie 1864, **129**, 286.

UM00012277
NOVARTIS EXHIBIT 1517
Novartis v. Regents, IPR2023-01347
Page 1023 of 4460

This Page is Inserted by IFW Indexing and Scanning Operations and is not part of the Official Record

BEST AVAILABLE IMAGES

Defective images within this document are accurate representations of the original documents submitted by the applicant.

Defects in the images include but are not limited to the items checked:

- ☐ BLACK BORDERS
- ☐ IMAGE CUT OFF AT TOP, BOTTOM OR SIDES
- ☐ FADED TEXT OR DRAWING
- ☐ BLURRED OR ILLEGIBLE TEXT OR DRAWING
- ☐ SKEWED/SLANTED IMAGES
- ☐ COLOR OR BLACK AND WHITE PHOTOGRAPHS
- ☐ GRAY SCALE DOCUMENTS
- ☐ LINES OR MARKS ON ORIGINAL DOCUMENT
- ☐ REFERENCE(S) OR EXHIBIT(S) SUBMITTED ARE POOR QUALITY
- ☐ OTHER: _____

IMAGES ARE BEST AVAILABLE COPY.
As rescanning these documents will not correct the image problems checked, please do not report these problems to the IFW Image Problem Mailbox.

Zeitschrift für Kristallographie

International Journal for Structural, Physical, Chemical Aspects of Crystalline Materials

Vol. 162 No. 1-4 1983

Reviews of the 23rd Discussion Meeting of the Crystallography Work Group of the German Mineralogical Society, the German Physical Society and the Society of German Chemists: Annual Meeting of the Swiss Society for Crystallography and the Section for Crystal Growth, March 7 through 10, 1983 in Tübingen

Corrections to the reviews **238**

C.F. Woensdregt
Structural Morphology of high sanidine ($KAlSi_3O_8$) [in English] **239**

M.P. Gupta, K. Banerjee
The crystal structure of calcium maleate dihydrate **257**

A. Kutoglu
Crystal structure of the calcium/vanadium bronzes $Ca_xV^{4+}_{2x}V^{5+}_{2-2x}O_5$ **263**

G.F. Schäfer, K.F. Fischer
Determination of the dependence on wavelength and on scattering angle of the imaginary part of the atomic shape factor of barium.
II. Diffraction experiments [in German] **273**

K. Rohwer, W. Gunsser
Blot program for Laue patterns of single crystals in arbitrary orientation **283**

K.-H. Breuer, W. Eysel
Crystal chemistry of compounds $M_3O[TO_4]$. I. The system Pb_3GeO_5-Pb_3SiO_5-Cd_3SiO_5-"Cd_3GeO_5" [in English] **289**

(Continuation: see cover p. 4)

//Bilingual footer//

[Translator's Note: 1- The header on the odd numbered pages reads: Reviews;
2- The header on the even numbered page reads: 23rd Discussion Meeting of the Crystallography Work Group.
3- The first part of page 213 constitutes the end of a separate paper.]

UM00012279
NOVARTIS EXHIBIT 1517
Novartis v. Regents, IPR2023-01347
Page 1025 of 4460

J.J. Stezowski and R.-D Stigler (Institute for Organic Chemistry, Biochemistry and Isotope Research, University of Stuttgart), N. Karl and K. Schuller (Physical Institute 3, University of Stuttgart).
Characterization of a 1:1 complex of an unusual structure in the phenothiazine/phenazine binary phase diagram

A black-red adduct was obtained from phenothiazine $C_{12}H_9NS$ and phenazine $C_{12}H_8N_2$, which both form pale yellow crystals, whereby this adduct was obtained by means of co-sublimation and also from communal melts; the strong red shift in the absorption suggested that one can infer the formation of a π-electron donor/acceptor complex. The phase diagram was recorded with a Perkin Elmer DSC-2 differential calorimeter. This does in fact exhibit a maximum at a stoichiometry of 1:1.

A complete x-ray structural analysis (at 300 K) generated a uniform phase of space group $P2_1/c$ with a = 9.072 (2), b = 8.872 (2), c = 25.934 (5) Å, β = 112.65 (2) ° and Z = 4. Interactions between the components can be seen from the crystal structure, whereby these interactions deviate markedly from those of conventional (weak) π-electron donor/acceptor complexes: the planes of the phenothiazine and phenazine molecules do not lie alternatingly one above the other (as, for example, in the phenothiazine/PMDA donor/acceptor complex [1] but, rather, they lie more or less perpendicularly relative to one another. A closely adjacent phenazine pair occurs in the structure with a separation of 3.714 Å between the planes of the two phenazine molecules. Two phenothiazine molecules, which are each linked via their >NH group by means of a hydrogen bond to a nitrogen atom in the one or the other phenazine molecule in each case, are arranged on opposite sides approximately perpendicularly to it [translator: the aforementioned pair of phenazine molecules]. This $(C_{12}H_9NS)_2/(C_{12}H_8N_2)_2$ dimer has to be regarded as the crystallographic packing unit: see Fig. 1. The strong bathochromic shift that is found in the absorption spectrum would, to some extent, be compatible with the small ionization energy of phenothiazine [2] and the large electron affinity of phenazine [3] within the context of an electron charge transfer transition from phenothiazine to phenazine, but the angular bending of the phenothiazine molecule (159.7 °) and the possibility of hydrogen bond interaction evidently prohibit the formation of the continuously alternating donor/acceptor stack that is usual for weak donor/acceptor complexes. The aspect of whether the hydrogen bonds mediate a charge transfer interaction of the essentially orthogonal molecules remains to be examined.

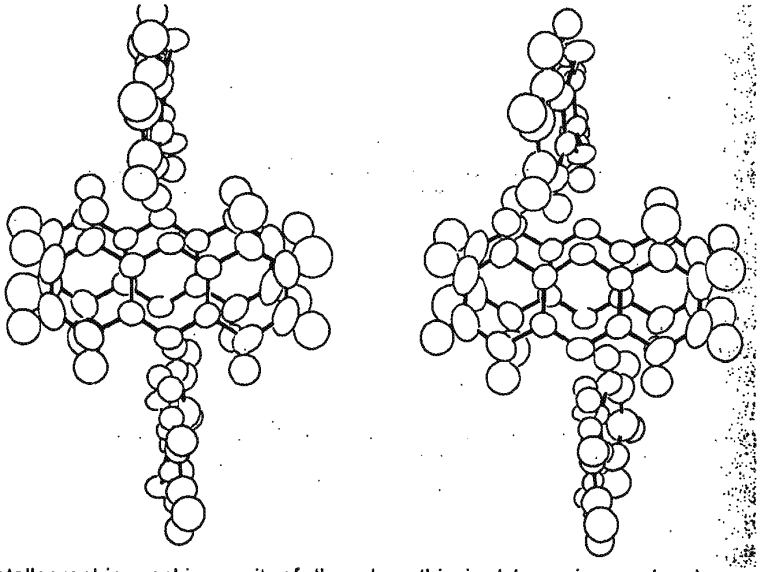


Fig.1. The crystallographic packing unit of the phenothiazine/phenazine molecular complex, stereoscopic projection onto the plane of the phenazine molecule. An inversion center lies between the phenazine molecules.

This study was carried out within the framework of a project that was sponsored by the Volkswagen Company Foundation, reference I 35 974.

UM00012280
NOVARTIS EXHIBIT 1517
Novartis v. Regents, IPR2023-01347
Page 1026 of 4460

Bibliography

1. Anthonj, R., Karl, N., Robertson, B.E., Stezowski, J.J.: J. Chem. Phys. **72**, 1244 (1980)
2. Karl, N., Sato, N., Seki, K., Inokuchi, H.: J. Chem. Phys. **77**, 4870 (1982)
3. Probst, K.H., Karl, N.: Phys. Status Solidi (a) **27**, 499 (1975), erratum: (a) **31**, 793 (1975)

[Translator's Note: The information and diagram on page 4 relates to a new subject matter.]

NOVARTIS EXHIBIT 1517
Novartis v. Regents, IPR2023-01347
Page 1027 of 4460

T9060

itschrift für ristallographie

ational Journal for Structural, Physical, Chemical Aspects of Crystalline Materials

11338301 (2)

Vol. 162 No. 1–4 1983

UNIVERSITY OF CALIFORNIA SCIENCE LIBRARY

Referate der 23. Diskussionstagung der Arbeitsgemeinschaft Kristallographie der Deutschen Mineralogischen Gesellschaft, der Deutschen Physikalischen Gesellschaft und der Gesellschaft Deutscher Chemiker, Jahrestagung der Schweizerischen Gesellschaft für Kristallographie und der Sektion für Kristallwachstum, 7. bis 10. März 1983 in Tübingen

Berichtigungen zu den Referaten **238**

C. F. Woensdregt
Structural morphology of high sanidine ($KAlSi_3O_8$) **239**

M. P. Gupta, K. Banerjee
The crystal structure of calcium maleate dihydrate **257**

A. Kutoglu
Kristallstruktur der Calcium-Vanadium-Bronze $Ca_xV^{4+}_{2x}V^{5+}_{2-2x}O_5$ **263**

G. F. Schäfer, K. F. Fischer
Bestimmung der Wellenlängen- und Streuwinkelabhängigkeit des Imaginärteils des Atomformfaktors von Barium.
I. Beugungsexperimente **273**

K. Bohmer, W. Gunsser
Plot program for Laue patterns of single crystals in arbitrary orientation **283**

K.-H. Breuer, W. Eysel
Crystal chemistry of compounds $M_3O[TO_4]$. I. The system Pb_3GeO_5–Pb_3SiO_5–Cd_3SiO_5–"Cd_3GeO_5" **289**

(Continuation see cover p. 4)

Akademische Verlagsgesellschaft · Wiesbaden

Z. Kristallogr. 162, 1–324 (1983) Indexed in Current Contents ISSN 0044-2968

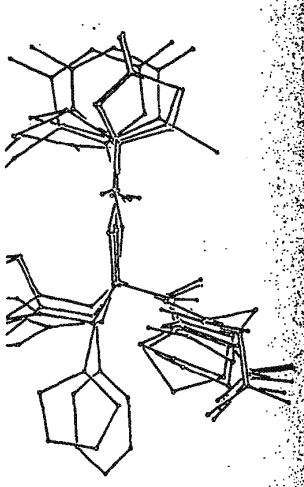
UM00012282

NOVARTIS EXHIBIT 1517
Novartis v. Regents, IPR2023-01347
Page 1028 of 4460

...mie, Biochemie und Isotope... **nationelle Eigenschaften vo... gsuntersuchungen.**

...llstrukturanalysen von TRH... ...tionellen Eigenschaften und... ...is heute haben wir folgende... ...ruktur Nr. 11); [3S, 6R]-6... ...-Pro-NH_2 (Nr. 1, 2); [3S, 6S]... ...s-L-Pro-NH_2, (Nr. 3); 5-Ethy... ...orotyl-L-His-L-Pro-NH_2, (Nr... ...3) und 2-Oxo-thiazolidinyl-4...

...istallstrukturanalysen berich... ...2-TRH $P2_1$-Modifikation, [3]... ..., (Nr. 14, 15).
...metrischer Einheit vorhanden... ...ibhängige Beobachtungen für... ...on TRH und Analogen.
...ese Strukturuntersuchungen... ...konformationeller Integrität... ...leste, die für die Strukturen... Eine begrenzte konformatio...



...ierend auf einem least-squares-fit...

nelle Freiheit ergibt sich für den Prolinamid-Rest, für den Imidazol-Rest und für den p-Glu-Rest bzw. den ihn ersetzenden Heterozyklus. Das Bild, das sich aus diesen Untersuchungen für die TRH-Konformation ergibt, ist mindestens zum Teil im Einklang mit Strukturuntersuchungen in Lösung. Es unterstützt die daraus abgebildete Folgerung, daß ein in Lösung maßgeblich vorhandenes TRH-Konformer eine „extended backbone"-Konformation besitzt, die keine intramolekularen Wasserstoffbrücken benötigt und, daß wahrscheinlich die β- und γ-Kohlenstoffatome des Prolinrings erhöhte Beweglichkeit zeigen.

Wir danken W. Voelter, Universität Tübingen, und L. Flohé, Chemie Grünenthal GmbH, für die freundliche Überlassung von Proben.

Literatur

1. Stezowski, J. J., Bürvenich, C., Voelter, W.: Angew. Chem. Int. Ed. Engl. **18**, 225 (1979)
2. Kamiya, K., Takamoto, M., Eada, Y., Fujino, M., Nishikawa, M.: J. Chem. Soc. Chem. Commun. **1980**, 438
3. Stensland, B., Castensson, S.: zur Veröffentlichung in J. Mol. Biol. eingereicht (1982)

J. J. Stezowski und R.-D. Stigler (Inst. für Org. Chemie, Biochemie und Isotopenforschung, Universität Stuttgart), N. Karl und K. Schuller (Physikalisches Inst. 3, Universität Stuttgart). **Charakterisierung eines 1:1 Komplexes von ungewöhnlicher Struktur im binären Phasendiagramm Phenothiazin-Phenazin.**

Aus Phenothiazin, $C_{12}H_9NS$, und Phenazin, $C_{12}H_8N_2$, die beide blaß gelbe Kristalle bilden, wurde durch Kosublimation sowie aus der gemeinsamen Schmelze ein schwarzrotes Addukt erhalten; die starke Rotverschiebung der Absorption legte nahe, auf die Bildung eines π-Elektronen-Donator:Akzeptor-Komplexes zu schließen. Mit einem Perkin Elmer DSC-2 Differentialkalorimeter wurde das Phasendiagramm aufgenommen. Dieses weist in der Tat ein Maximum bei einer 1:1-Stöchiometrie auf.

Eine vollständige Röntgenstrukturanalyse (bei 300 K) lieferte eine einheitliche Phase der Raumgruppe $P2_1/c$ mit $a = 9{,}072\ (2)$, $b = 8{,}872\ (2)$, $c = 25{,}934\ (5)$ Å, $\beta = 112{,}65\ (2)°$ und $Z = 4$. Aus der Kristallstruktur werden Wechselwirkungen zwischen den Komponenten ersichtlich, die merklich von denen üblicher (schwacher) π-Elektronen-Donator:Akzeptor-Komplexe abweichen: Die Phenothiazin- und Phenazin-Molekülebenen liegen nicht alternierend übereinander (wie etwa in dem Donator:Akzeptor-Komplex Phenothiazin: PMDA [1]), sondern mehr oder weniger senkrecht zueinander. In der Struktur tritt ein eng benachbartes Phenazin-Paar auf mit einem Abstand der beiden Phenazin-Molekülebenen von 3,714 Å. Auf gegenüberliegenden Sei-

UM00012283
NOVARTIS EXHIBIT 1517
Novartis v. Regents, IPR2023-01347
Page 1029 of 4460

ten sind etwa senkrecht dazu zwei Phenothiazin-Moleküle angeordnet, die
durch eine Wasserstoffbrücke mit ihrer > NH Gruppe an je ein Stickstoffato
des einen bzw. des anderen Phenazinmoleküls gebunden sind. Diese
$(C_{12}H_9NS)_2$:$(C_{12}H_8N_2)_2$-Dimer muß als die kristallographische Packungsein
heit angesehen werden, s. Abb. 1. Die gefundene starke bathochrome Ver
schiebung des Absorptionsspektrums wäre zwar mit der kleinen Ionisierung
energie des Phenothiazins [2] und der großen Elektronenaffinität des Phena
zins [3] im Sinne eines Elektronen-Charge-Transfer-Übergangs von Pheno
thiazin zu Phenazin einigermaßen verträglich, die Abwinkelung des Pheno
thiazin-Moleküls (159,7°) und die Möglichkeit einer Wasserstoffbrücken
Wechselwirkung verbieten aber offensichtlich die Ausbildung der für schwa
che Donator:Akzeptor-Komplexe üblichen durchgehenden alternierenden
Donator-Akzeptor-Stapel. Es bleibt zu prüfen, ob die Wasserstoffbrücken
eine Charge-Transfer-Wechselwirkung der nahezu orthogonalen Moleküle
vermitteln.

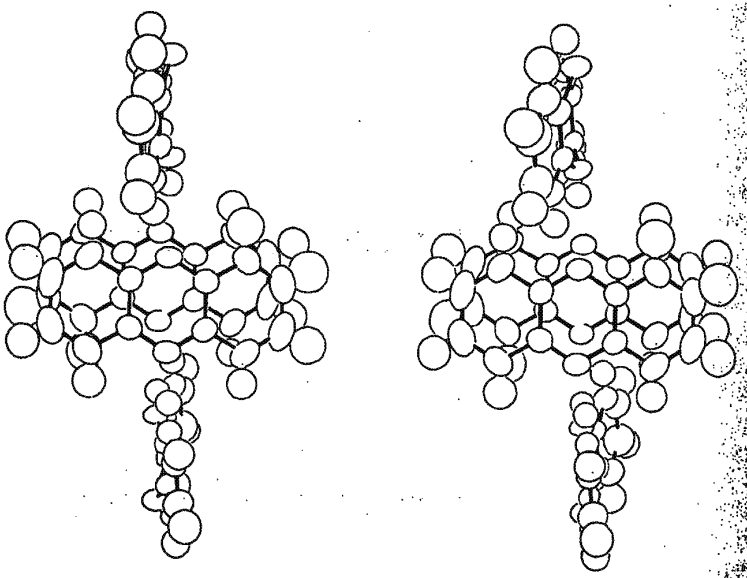


Abb. 1. Die kristallographische Packungseinheit des Phenothiazin-Phenazin-Molekülkom
plexes, stereoskopische Projektion auf die Phenazin-Molekülebene. Zwischen den Phena
zin-Molekülen liegt ein Inversionszentrum

Diese Arbeit wurde im Rahmen eines von der Stiftung Volkswagenwerk unter I 35 91
geförderten Projekts durchgeführt.

Literatur

1. Anthonj, F
2. Karl, N., S
3. Probst, K.

F. Stollmaie
Stuttgart). N

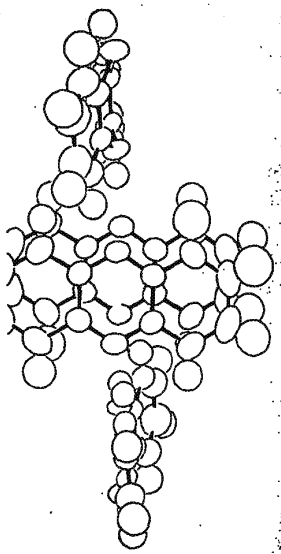
Nb_6I_{11} ist au
verknüpft s
Aufspaltung
gespannte I
war die Ann
bleibt und n

Abb. 1. Perspel
Ellipsoide)

UM00012284
NOVARTIS EXHIBIT 1517
Novartis v. Regents, IPR2023-01347
Page 1030 of 4460

einschaft Kristallograph

leküle angeordnet, die je
ppe an je ein Stickstoffatom
üls gebunden sind. Diese
tallographische Packungsein-
ne starke bathochrome Ver-
mit der kleinen Ionisierungs-
lektronenaffinität des Phena-
nsfer-Übergangs von Pheno-
die Abwinkelung des Pheno-
it einer Wasserstoffbrücken-
ie Ausbildung der für schwa-
rchgehenden alternierenden
, ob die Wasserstoffbrücken
ıezu orthogonalen Moleküle



nothiazin-Phenazin-Molekülkom-
ekülebene. Zwischen den Phena-

3 Volkswagenwerk unter I 35 974

Literatur

1. Anthonj, R., Karl, N., Robertson, B. E., Stezowski, J. J.: J. Chem. Phys. **72**, 1244 (1980)
2. Karl, N., Sato, N., Seki, K., Inokuchi, H.: J. Chem. Phys. **77**, 4870 (1982)
3. Probst, K. H., Karl, N.: Phys. Status Solidi (a) **27**, 499 (1975), erratum: (a) **31**, 793 (1975)

F. Stollmaier, A. Simon, J. Geyer Lippmann (MPI für Festkörperforschung, Stuttgart). **Nb_6I_{11}-Reaktionen mit Aminen unter Erhalt der Nb_6I_8-Baueinheit.**

Nb_6I_{11} ist aus $[Nb_6I_8^i]$-Einheiten aufgebaut, die allseitig durch 6 $I_{1/2}^{a-a}$ weiter verknüpft sind. In Ammoniak reagiert diese Verbindung spontan unter Aufspaltung parallel (011). Diese Richtung zeichnet sich in der Struktur durch gespannte Iod-Brücken aus [1]. Unser Ausgangspunkt der Untersuchungen war die Annahme, daß bei dieser Reaktion die Clustereinheit Nb_6I_8 erhalten bleibt und nur die Iod-Brücken aufgebrochen werden.

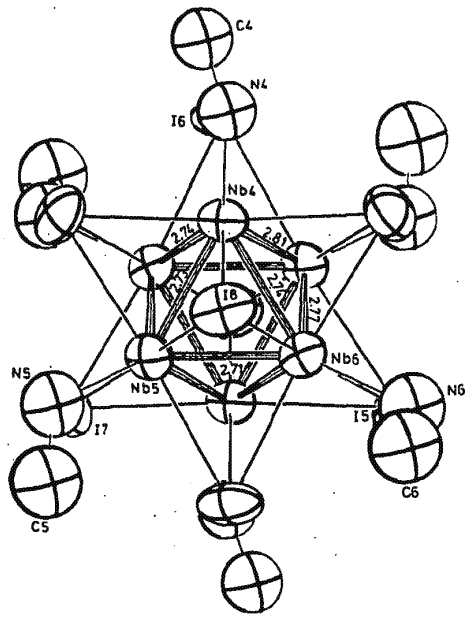


Abb. 1. Perspektivische Projektion eines $Nb_6I_8(NH_2CH_3)_6$-Moleküls (ORTEP-Plot 50% Ellipsoide)

UM00012285
NOVARTIS EXHIBIT 1517
Novartis v. Regents, IPR2023-01347
Page 1031 of 4460

This Page is Inserted by IFW Indexing and Scanning Operations and is not part of the Official Record

BEST AVAILABLE IMAGES

Defective images within this document are accurate representations of the original documents submitted by the applicant.

Defects in the images include but are not limited to the items checked:

- ☐ BLACK BORDERS
- ☐ IMAGE CUT OFF AT TOP, BOTTOM OR SIDES
- ☐ FADED TEXT OR DRAWING
- ☐ BLURRED OR ILLEGIBLE TEXT OR DRAWING
- ☐ SKEWED/SLANTED IMAGES
- ☐ COLOR OR BLACK AND WHITE PHOTOGRAPHS
- ☐ GRAY SCALE DOCUMENTS
- ☐ LINES OR MARKS ON ORIGINAL DOCUMENT
- ☐ REFERENCE(S) OR EXHIBIT(S) SUBMITTED ARE POOR QUALITY
- ☐ OTHER: _____

IMAGES ARE BEST AVAILABLE COPY.
As rescanning these documents will not correct the image problems checked, please do not report these problems to the IFW Image Problem Mailbox.

[*Acta Cryst.*, (1977), B33, 3337-3341]

Crystalline and Molecular Structure of Sulfanilimide-Antipyrine

Authors:

--Serge Alberola and Fernand Sabon:

General and Inorganic Chemistry Laboratory, Department of Pharmaceutical and Biological Sciences
Montpellier 1, France

and Joel Jaud and Jean Galy:
Crystallography Department, *CNRS* Coordinating Chemistry Laboratory, B.P. 4142,
31030, Toulouse, CEDEX, France

(Received on March 17, 1977. Accepted on April 19, 1977)

The 1:1 sulphanilamide–antipyrine molecular compound crystallizes in the orthorhombic system, space group $P2_12_12_1$, with $a = 12{\cdot}500$, $b = 14{\cdot}677$, $c = 9{\cdot}799$ Å. The crystal structure (refined to an R of 0·046) contains four units per cell. The conformation of the molecules and their association by hydrogen bonds have been determined.

Introduction

Within the context of research conducted in relation to combinations of chemical substances of a medicinal nature, Alberola, Rambaud, and Sabon (1976) identified a 1:1 molecular compound consisting of sulfanilamide and antipyrine. Infrared spectroscopic analysis of this new phase revealed a characteristic decrease, $\Delta\nu$(NH), in ν(NH) frequencies for the amide and sulfonamide radicals. This shift appears to be attributable to hydrogen bonds if prior research concerning sulfanilimides (Novak, Lascombe, and Josien, 1966) is consulted.

It was not possible for this particular hypothesis to be confirmed by analysis with a dilute solution on account of the fact that this compound is insoluble in nonpolar solvents (Alberola, 1976). Determination of the crystal structure of this complex, $C_6H_8N_2O_2S.C_{11}H_{12}N_2O$ (Figure 1), was therefore undertaken for the purpose of defining the nature of bonds on one hand, and, moreover, of defining the role which each bond occupies in relation to formation of this particular complex.

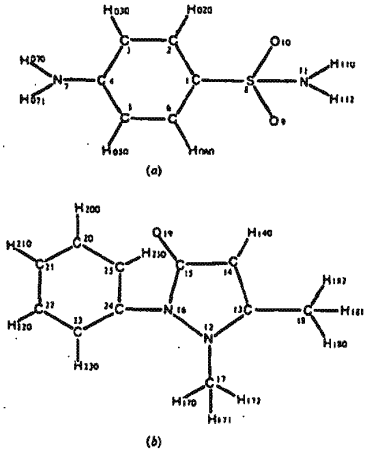


Figure 1: Atomic numbering. (a) Sulfanilamide. (b) Antipyrine.

UM00012287
NOVARTIS EXHIBIT 1517
Novartis v. Regents, IPR2023-01347
Page 1033 of 4460

Table 1: Measuring Conditions and Experimental Results

Physical and crystallographic data:

Formula: $C_{17}O_3N_4SH_{30}$. Molecular weight: 360.25.
Crystal system: Orthorhombic
Space group: $P2_12_12_1$
a = 12.500(3)A. V = 1,798 A^3
b = 14.677 (3) Z = 4
c = 9.799 (2) $F(000)$ = 190
P_{exp} = 1.357 (4), p_x = 1.333 g cm^3
Absorption coefficient: μ = 17.65 cm^{-1}
Morphology: Prism-- 0.8 x 0.7 x 1.2 mm

Recording Conditions:

Temperature: 25° C.
Radiation: Cu $K\alpha$ (λ 1.5418 A)
Monochromatization: Graphite monochromator
Crystal-detector distance: 208 mm
Detector opening: height = 4 mm, length = (3 + 0.75 tg θ) mm
"Take-off" angle: 3.25°
Scanning mode: θ - 2θ
Maximum Bragg angle: 78°
Scanning amplitude: (0.60 + 0.147 tg θ)
Values which determine scanning speed:
$\sigma_{pri?}$ = 0.4, σ = 0.018. V_{pre} Minimum of 1° in θ, T_{max} = 70 sec.

	Intensity Verification	Orientation Verification
Reflections Selected	306, 036, 326	14.0, 0.800, 0.0, 10
Periodicity	Per hour of Irradiation	Every 100 spots

Refinement Conditions:
Number of reflections for refining reticular parameters: 25
Number of reflections recorded: 2,202
Number of independent reflections: 2,202
Number of reflections used: 1,658 $|I > 2\sigma(I)|$
Reliability factors:

$$R = \sum(k|F_o| - |F_c|)/\sum k|F_o| = 4{,}6\%$$

$$R = [\sum w^2(k|F_o| - |F_c|)^2/\sum w^2 k^2 F_o^2]^{1/2} = 6{,}1\%$$

*These values were defined by Mosset, Bonnet, and Galy (1977).

Crystals were prepared by recrystallization of a physical mixture of the compound in acetone, with sulfanilamide representing 48.08%. The crystals, which possessed a prismatic shape, were translucent, and they were stable when exposed to air.

Radiocrystallographic Analysis-- Determination of the Structure

A prior analysis where a precession camera was used had allowed determination of [lattice] parameters and the space group for the sulfanilamide-antipyrine complex (Alberola *et al.*, 1976). A new monocrystal whose quality was verified by means of an optical goniometer and a polarizing microscope and whose shape was that of an 0.8 x 0.7 x 1.2 mm prism was selected.

Measurement of *hkl* reflections was performed by means of a Nonius automatic diffractometer of the CAD-4 type for copper $K\alpha$ radiation.

All of the measuring conditions and experimental results are summarized within Table 1. Methods which were adopted for selecting measurement requirements are described within a prior publication (Mosset, Bonnet, and Galy, 1977).

Structural aspects were determined by deconvolution of the Patterson function and the Fourier series. Refinement was accomplished in the following manner:

--Refinement by the least squares method with isotropic temperature factors for all of the atoms (except for hydrogen): R = 0.125.

--Refinement with anisotropic temperature factors for these atoms: R = 0.066.

--Locating hydrogen atoms according to differential methods.

--A refinement cycle involving coordinates and an average isotropic temperature factor for hydrogen atoms.

--Lastly, refinement with anisotropic temperature factors for all of the atoms except for hydrogen atoms, which were simply introduced into computations: R = 0.046.*

Description of the Structure and Discussion

Table 2 defines atomic coordinates for sulfur, oxygen, nitrogen, and carbon atoms, while Table 3 indicates atomic coordinates and isotropic temperature factors for hydrogen atoms. Within this table, standard deviation figures are not indicated, because final refining did not take place with respect to these atoms.

UM00012288
NOVARTIS EXHIBIT 1517
Novartis v. Regents, IPR2023-01347
Page 1034 of 4460

Interatomic distances and bond angles for both molecules within the complex, along with standard deviations, are summarized within Tables 4 and 5.

Average planes for the different rings which are present within this complex were determined, and they are indicated within Figure 6.

*Lists of structure factors and anisotropic temperature factors have been filed with the British Library Lending Division's Records Division (Supplementary Publication Number SUP 32668: 7 pages). It is possible to obtain copies by contacting: The Executive Secretary, International Union of Crystallography, 13 White Friars, Chester CH1 1NZ, England.

Table 2: Atomic Coordinates (x10^4) *for Heavy Atoms*

The numbering method which has been adopted is that which is described within Figure 1.

	x	y	z
C(1)	3667 (3)	−744 (3)	1018 (5)
C(2)	3572 (4)	−1351 (3)	50 (5)
C(3)	4204 (4)	−2131 (3)	−88 (4)
C(4)	4927 (4)	−2313 (3)	−959 (4)
C(5)	5017 (4)	−1682 (3)	−2033 (4)
C(6)	4387 (4)	−905 (3)	2057 (4)
N(7)	5544 (3)	3083 (3)	910 (4)
S(8)	2850 (1)	226 (1)	1071 (1)
O(9)	2538 (3)	456 (2)	−306 (3)
O(10)	3406 (3)	896 (2)	1855 (4)
N(11)	1771 (3)	−8 (3)	1856 (4)
N(12)	1583 (4)	6040 (3)	2067 (5)
C(13)	1158 (5)	6626 (3)	2979 (6)
C(14)	624 (4)	6163 (3)	3979 (6)
C(15)	738 (4)	5226 (3)	3722 (5)
N(16)	1396 (3)	5159 (3)	2574 (4)
C(17)	2471 (6)	6176 (5)	1195 (7)
C(18)	1319 (6)	7634 (4)	2973 (7)
O(19)	327 (3)	4536 (2)	4251 (4)
C(20)	913 (6)	3681 (6)	−386 (7)
C(21)	1433 (6)	2896 (5)	16 (8)
C(22)	1964 (5)	2871 (4)	1223 (7)
C(23)	1972 (5)	3642 (4)	2063 (6)
C(24)	1422 (4)	4400 (3)	1680 (6)
C(25)	891 (5)	4421 (4)	436 (7)

Table 3: Atomic Coordinates (x 10^3) *and Isotropic Temperature Factors for Hydrogen Atoms*

	x	y	z	B (Å²)
H(020)	305	−123	−83	4,7
H(030)	411	−257	−93	4,7
H(050)	555	−182	284	3,7
H(060)	447	−42	291	4,3
H(070)	586	−322	175	5,2
H(071)	523	−358	30	5,0
H(110)	192	−12	276	5,0
H(111)	110	−30	150	4,9
H(140)	9	647	463	4,9
H(170)	299	655	143	4,2
H(171)	248	563	36	5,4
H(172)	261	667	35	5,4
H(180)	90	784	361	4,9
H(181)	98	779	195	4,9
H(182)	219	783	289	4,9
H(200)	40	366	−129	5,9
H(210)	156	236	−54	4,4
H(220)	228	225	151	5,0
H(230)	237	362	301	5,3
H(250)	46	498	24	5,1

Table 4: Bond Lengths (Å)

C(1)–C(2)	1,379 (6)	N(16)–N(12)	1,405 (5)
C(2)–C(3)	1,390 (6)	N(12)–C(17)	1,415 (7)
C(3)–C(4)	1,394 (6)	C(13)–C(18)	1,504 (7)
C(4)–C(5)	1,406 (6)	C(15)–O(19)	1,248 (5)
C(5)–C(6)	1,386 (6)	N(16)–C(24)	1,417 (6)
C(6)–C(1)	1,379 (6)	C(20)–C(21)	1,380 (9)
C(4)–N(7)	1,369 (5)	C(21)–C(22)	1,356 (9)
C(1)–S(8)	1,754 (4)	C(22)–C(23)	1,400 (8)
S(8)–O(9)	1,445 (3)	C(23)–C(24)	1,360 (7)
S(8)–O(10)	1,429 (3)	C(24)–C(25)	1,387 (8)
S(8)–N(11)	1,591 (4)	C(25)–C(20)	1,353 (9)
C(2)–H(020)	1,02	C(14)–H(140)	1,02
C(3)–H(030)	1,06	C(17)–H(170)	0,87
C(5)–H(050)	1,05	C(17)–H(171)	1,13
C(6)–H(060)	1,10	C(17)–H(172)	1,11
N(7)–H(070)	0,94	C(18)–H(180)	1,00
N(7)–H(071)	1,02	C(18)–H(181)	0,95
N(21)–H(110)	0,93	C(18)–H(182)	1,13
N(11)–H(111)	1,00	C(20)–H(200)	1,09
N(12)–C(13)	1,349 (6)	C(21)–H(210)	0,97
C(13)–C(14)	1,366 (7)	C(22)–H(220)	1,03
C(14)–C(15)	1,406 (8)	C(23)–H(230)	1,05
C(15)–N(16)	1,396 (6)	C(25)–H(250)	0,99

UM00012289
NOVARTIS EXHIBIT 1517
Novartis v. Regents, IPR2023-01347
Page 1035 of 4460

Table 5: Interratomic Bond Angles (°)

C(6)–C(1)–C(2)	120,4 (8)	O(9)–S(8)–N(11)	105,8 (5)	H(171)–C(17)–N(12)	109
C(6)–C(1)–S(8)	119,3 (8)	O(9)–S(8)–C(1)	108,6 (4)	H(181)–C(18)–C(13)	106
C(2)–C(1)–S(8)	119,7 (7)	N(11)–S(8)–C(1)	109,4 (4)	H(180)–C(18)–C(13)	97
H(020)–C(2)–C(1)	121	H(110)–N(11)–S(8)	109	H(182)–C(18)–C(13)	111
H(020)–C(2)–C(3)	118	H(111)–N(11)–S(8)	126	H(200)–C(20)–C(25)	119
C(1)–C(2)–C(3)	120,1 (8)	C(13)–N(12)–N(16)	106,6 (7)	H(200)–C(20)–C(21)	118
H(030)–C(3)–C(2)	118	C(13)–N(12)–C(17)	128,2 (8)	C(25)–C(20)–C(21)	120,5 (8)
H(030)–C(3)–C(4)	121	N(16)–N(12)–C(17)	118,3 (9)	H(210)–C(21)–C(22)	112
C(2)–C(3)–C(4)	120,4 (8)	N(12)–C(13)–C(14)	110,5 (6)	H(210)–C(21)–C(20)	126
N(7)–C(4)–C(3)	119,8 (8)	N(12)–C(13)–C(18)	119,5 (8)	C(22)–C(21)–C(20)	120,1 (9)
N(7)–C(4)–C(5)	121,7 (7)	C(14)–C(13)–C(18)	129,9 (9)	H(220)–C(22)–C(21)	117
C(3)–C(4)–C(5)	118,4 (8)	H(140)–C(14)–C(13)	123	H(220)–C(22)–C(23)	123
H(050)–C(5)–C(6)	120	H(140)–C(14)–C(15)	127	C(21)–C(22)–C(23)	119,6 (9)
H(050)–C(5)–C(4)	119	C(13)–C(14)–C(15)	108,0 (9)	H(230)–C(23)–C(24)	120
C(6)–C(5)–C(4)	120,6 (8)	O(19)–C(15)–N(16)	121,3 (8)	H(230)–C(23)–C(22)	119
H(060)–C(6)–C(11)	121	O(19)–C(15)–C(14)	132,6 (7)	C(24)–C(23)–C(22)	119,6 (8)
H(060)–C(6)–C(5)	119	N(16)–C(15)–C(14)	105,7 (9)	C(23)–C(24)–C(25)	120,1 (9)
C(1)–C(6)–C(5)	119,9 (8)	C(15)–N(16)–N(12)	108,5 (9)	C(23)–C(24)–N(16)	118,9 (7)
H(070)–N(7)–C(4)	112	C(15)–N(16)–C(24)	124,5 (8)	C(25)–C(24)–N(16)	120,9 (8)
H(071)–N(7)–C(4)	113	C(15)–N(16)–C(24)	120,0 (5)	H(250)–C(25)–C(20)	123
O(10)–S(8)–O(9)	118,2 (4)	H(170)–C(17)–N(12)	120	H(250)–C(25)–C(24)	116
O(10)–S(8)–N(11)	107,5 (4)	H(172)–C(17)–N(12)	131	C(20)–C(25)–C(24)	119,7 (9)
O(10)–S(8)–C(1)	106,9 (4)				

Table 6: Average Planes for Atoms

Plane 1: -(0.70636)x -(0.49633)y + (0.50410)z + 2.19525 - 0

Atoms which define the plane:

C(1)	0,002 Å	C(4)	0,006 Å
C(2)	0,001	C(5)	−0,003
C(3)	−0,005	C(6)	−0,007

Other atoms:

N(7)	−0,001 Å	O(9)	−0,529 Å
S(8)	0,043	O(10)	−0,550

Plane 2: -(0.82855)x - (0.33637)y + (0.44762)z +2.92083-0

Atoms which define the plane:

C(20)	−0,011 Å	C(23)	−0,017 Å
C(21)	0,005	C(24)	0,012
C(22)	0,009	C(25)	0,002

Plane 3: -(0.83248)x - (0.00822)y - (0.55400)z + 2.87883 = 0

Atoms which define the plane:

N(12)	0,036 Å	C(13)	−0,023 Å
C(14)	−0,006	C(15)	0,028
N(16)	−0,033		

Other atoms:

C(17)	−0,409 Å	O(19)	0,176 Å
C(18)	−0,102		

Table 7: Hydrogen Bonds

O(9)^{I}···H(110)^{II}	2,074 Å
O(9)^{I}···N(11)^{II}	2,985
N(11)^{II}–H(110)^{II}···O(9)^{I}	171,9°
O(10)^{IV}···H(070)^{I}	2,090 Å
O(10)^{IV}···N(7)^{I}	2,964
N(7)^{I}–H(070)^{I}···O(10)^{IV}	152,8°
O(19)^{IV}···H(111)^{I}	1,944 Å
O(19)^{IV}···N(11)^{I}	2,915
N(11)^{I}–H(111)^{I}···O(19)^{IV}	161,8°

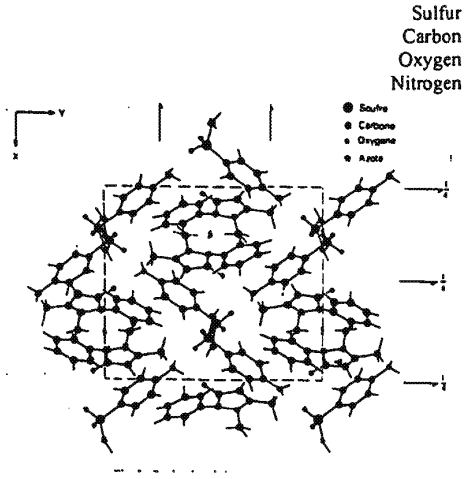


Figure 2: Projection of Structure onto Plane (001).

The general pattern for positioning of the two molecules within the crystal network is indicated according to a projection onto plane (001) within Figure 2.

From the standpoint of the two molecules' structure, bond lengths and bond angles are analogous to those which are described within pertinent literature, insofar as both sulfanilamide (Alleaume and Decap, 1965) and antipyrine (Singh and Vijayan, 1974) may be concerned.

As these authors had previously observed, the sulfanilamide ring is flat, as is likewise true for each antipyrine ring. The dihedral angle formed between planes 2 and 3 is 63.6°, whereas it is only 12° between planes 1 and 2, which indicates that the two benzene rings were substantially parallel.

The only noteworthy difference in relation to the previously cited results pertains to the angle between benzene and the pyrrole rings and antipyrine, which appears to vary from one compound to another, insofar as it may represent possible rotation around the N(16)-C(24) bond which connects these two rings.

From the standpoint of the molecular arrangement, it is possible to observe that cohesion of the crystal lattice is ensured by three types of hydrogen bonds, with two of these bonds connecting sulfanilamide molecules, while the third bond ensures sharing of an antipyrine molecule and the sulfanilamide molecule (Table 7 and Figure 3).

Consultation of Figure 2 reveals that the sulfanilamide molecules are organized according to a spiral whose axis converges with the crystallographic axis identified as *z*, thereby demarcating a type of tunnel into which the antipyrine molecules fit.

The authors' research confirms the existence of hydrogen bonds, on one hand, so that the hypothesis expressed by Alberola (1976) on the basis of infrared spectroscopy analysis is confirmed, and, on the other hand, it confirms the preponderant role of nitrogen, N(11), within the sulfonamide radical in relation to forming the 1:1 sulfanilamide-antipyrine molecular compound. This result is comparable to results obtained by Shefter and Sackman (1971) for the sulfanilamide-sulfathiazole complex and by Leger, Alberola, and Carpy (1977) in relation to a sulfacetamide-caffeine combination.

The *CNRS*, the *DGRST*, and the *DESR* provided material support for completion of this research.

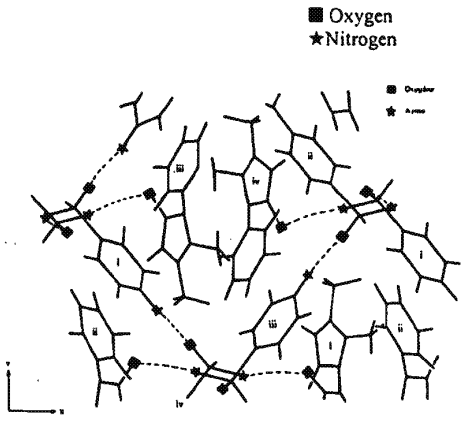


Figure 3: Projection of Structure onto Plane (001); Hydrogen Bonds.

[Translated Reference]:

S. Alberola (1976). Private correspondence.

References

ALBEROLA, S. (1976). Communication privée.
ALBEROLA, S., RAMBAUD, J. & SABON, F. (1976). *Trav. Soc. Pharm. Montpellier*, 36(1), 59–64.

ALLÉAUME, M. & DECAP, J. (1965). *Acta Cryst.* 19, 934–938.
LEGER, J. M., ALBEROLA, S. & CARPY, A. (1977). *Acta Cryst.* B33, 1455–1459.
MOSSET, A., BONNET, J.-J. & GALY, J. (1977). *Acta Cryst.* B33, 2639–2644.
NOVAK, A., LASCOMBE, J. & JOSIEN, M. L. (1966). *J. Phys. Radium*, 27, C2.
SHEFTER, E. & SACKMAN, P. (1971). *J. Pharm. Sci.* 60, 282–286.
SINGH, T. P. & VIJAYAN, M. (1974). *Acta Cryst.* B30, 557–562.

UM00012292
NOVARTIS EXHIBIT 1517
Novartis v. Regents, IPR2023-01347
Page 1038 of 4460

T9058

Acta Cryst. (1977). B33, 3337–3341

Structure Cristalline et Moléculaire de la Sulfanilamide–Antipyrine

PAR SERGE ALBEROLA ET FERNAND SABON

Laboratoire de Chimie Générale et Minérale, UER des Sciences Pharmaceutiques et Biologiques, Montpellier 1, *France*

ET JOËL JAUD ET JEAN GALY

Service de Cristallographie, Laboratoire de Chimie de Coordination du CNRS, BP 4142, 31030 *Toulouse CEDEX, France*

(*Reçu le* 17 *mars* 1977, *accepté le* 19 *avril* 1977)

The 1:1 sulphanilamide–antipyrine molecular compound crystallizes in the orthorhombic system, space group $P2_12_12_1$, with $a = 12{\cdot}500$, $b = 14{\cdot}677$, $c = 9{\cdot}799$ Å. The crystal structure (refined to an R of 0·046) contains four units per cell. The conformation of the molecules and their association by hydrogen bonds have been determined.

Introduction

Dans le cadre des recherches poursuivies sur les associations de substances chimiques à caractère médicamenteux Alberola, Rambaud & Sabon (1976) ont caractérisé un composé moléculaire 1:1 entre la sulfanilamide et l'antipyrine. L'étude par spectroscopie infra-rouge de cette phase nouvelle met en évidence un abaissement caractéristique $\Delta\nu$(NH) pour les fréquences ν(NH) des fonctions amine et sulfonamide. Ce déplacement semble attribuable si l'on se réfère aux précédents travaux sur les sulfanilamides (Novak, Lascombe & Josien, 1966) à des liaisons hydrogène.

Cette hypothèse n'a pu être confirmée par une étude en solution diluée du fait de l'insolubilité de ce composé dans les solvants non-polaires (Alberola, 1976). La détermination de la structure cristalline de ce complexe $C_6H_8N_2O_2S.C_{11}H_{12}N_2O$ (Fig. 1) a donc été entreprise afin de préciser d'une part la nature des liaisons, d'autre part le rôle joué par chacune d'elle dans la formation de ce complexe.

Les cristaux ont été préparés par recristallisation dans l'acétone d'un mélange physique de composition correspondant à 48,08% en sulfanilamide. Ils sont translucides, stables à l'air et de forme prismatique.

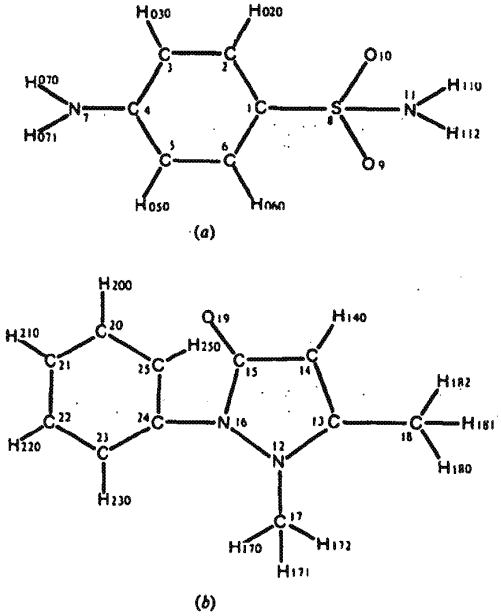


Fig. 1. Numérotation atomique. (*a*) Sulfanilamide. (*b*) Antipyrine.

Analyse radiocristallographique – détermination de la structure

Une étude antérieure sur chambre de précession avait permis de déterminer les paramètres et le groupe spatial du complexe sulfanilamide–antipyrine (Alberola *et al.*, 1976). Un nouveau monocristal de qualité contrôlée au goniomètre optique et au microscope polarisant se présentant sous la forme d'un prisme de 0,8 × 0,7 × 1,2 mm a été sélectionné.

La mesure des réflexions hkl a été effectuée à l'aide d'un diffractomètre automatique Nonius de type CAD-4 pour la radiation K_α du cuivre.

L'ensemble des conditions de mesure et les résultats expérimentaux sont résumés dans le Tableau 1. Les méthodes présidant au choix des conditions de mesure

UM00012293

NOVARTIS EXHIBIT 1517
Novartis v. Regents, IPR2023-01347
Page 1039 of 4460

Tableau 1. *Conditions de mesure et résultats expérimentaux*

Données physiques et cristallographiques

Formule: $C_{11}O_3N_4SH_{20}$, masse moléculaire: 360,25
Système cristallin: orthorhombique
Groupe spatial $P2_12_12_1$
a = 12,500 (3) Å — V = 1798 Å^3
b = 14,677 (3) — Z = 4
c = 9,799 (2) — $F(000)$ = 190
ρ_{exp} = 1,357 (4), ρ_x = 1,333 g cm^{-3}
Coefficient d'absorption: μ = 17,65 cm^{-1}
Morphologie: prisme, 0,8 × 0,7 × 1,2 mm

Conditions d'enregistrement

Température: 25 °C
Radiation: Cu $K\alpha$ (λ = 1,5418 Å)
Monochromatisation: monochromateur graphite
Distance cristal–détecteur: 208 mm
Fenêtre du détecteur: hauteur = 4 mm, largeur = (3 + 0,75 tg θ) mm
Angle de 'take-off': 3,25°
Mode de balayage: θ–2θ
Angle de Bragg maximum: 78°
Amplitude de balayage: (0,60 + 0,147 tg θ)°
Valeurs déterminant la vitesse de balayage:
σ_{rel}^* = 0,4, σ^* = 0,018, V_{rel}^* = 1° min^{-1} en θ, T_{max}^* = 70s

	Contrôles d'intensité	Contrôles d'orientation
Réflexions choisies	306, 036, 326	14,0,0, 800, 0,0,10
Périodicité	Par heure d'irradiation	Toutes les 100 taches

Conditions d'affinement

Nombre de réflexions pour affinement des paramètres réticulaires: 25
Nombre de réflexions enregistrées: 2202
Nombre de réflexions indépendantes: 2202
Nombre de réflexions utilisées: 1658 [$I > 2\sigma(I)$]
Nombre de variables affinées: 227
Facteurs de reliabilité
$R = \sum(k\|F_o\| - \|F_c\|)/\sum k\|F_o\| = 4,6\%$
$R = [\sum w^2(k\|F_o\| - \|F_c\|)^2/\sum w^2k^2F_o^2]^{1/2} = 6,1\%$

* Ces valeurs ont été définies par Mosset, Bonnet & Galy (1977).

figurent dans une précédente publication (Mosset, Bonnet & Galy, 1977).

La structure a été déterminée par déconvolution de la fonction de Patterson et séries de Fourier. L'affinement a été conduit de la manière suivante:

– affinement par moindre carrés avec agitation thermique isotrope sur tous les atomes (hydrogènes exceptés): R = 0,125.

– affinement avec agitation thermique anisotrope sur ces atomes: R = 0,066.

– localisation des atomes hydrogène par fonction différence.

– un cycle d'affinement portant sur les coordonnées et un facteur d'agitation thermique isotrope moyen pour les atomes d'hydrogène.

– affinement enfin, avec agitation thermique anisotrope sur tous les atomes sauf les hydrogènes, ceux-ci étant simplement introduit dans le calcul: R = 0,046.*

Description de la structure et discussion

Le Tableau 2 rassemble les coordonnées atomiques des atomes de soufre, d'oxygène, d'azote et de carbone, tandis qu'au Tableau 3 figurent les coordonnées atomiques et les coefficients d'agitation thermique isotrope des hydrogènes; dans ce tableau les écarts-standard ne sont pas indiqués puisqu'il n'y a pas eu d'affinement final sur ces atomes.

Les distances et angles interatomiques des deux molécules du complexe, avec leurs écarts-type, sont résumés dans les Tableaux 4 et 5.

Les plans moyens des différents cycles présents dans le complexe ont été déterminés et figurent dans le Tableau 6.

* Les listes des facteurs de structure et des facteurs d'agitation thermique anisotrope ont été déposées au dépôt d'archives de la British Library Lending Division (Supplementary Publication No. SUP 32668: 7 pp.). On peut en obtenir des copies en s'adressant à: The Executive Secretary, International Union of Crystallography, 13 White Friars, Chester CH1 1NZ, Angleterre.

Tableau 2. *Coordonnées atomiques* (×10^4) *des atomes lourds*

La numérotation adoptée est celle décrite dans Fig. 1.

	x	y	z
C(1)	3667 (3)	−744 (3)	1018 (5)
C(2)	3572 (4)	−1351 (3)	50 (5)
C(3)	4204 (4)	−2131 (3)	−88 (4)
C(4)	4927 (4)	−2313 (3)	−959 (4)
C(5)	5017 (4)	−1682 (3)	−2033 (4)
C(6)	4387 (4)	−905 (3)	2057 (4)
N(7)	5544 (3)	3083 (3)	910 (4)
S(8)	2850 (1)	226 (1)	1071 (1)
O(9)	2538 (3)	456 (2)	−306 (3)
O(10)	3406 (3)	896 (2)	1855 (4)
N(11)	1771 (3)	−8 (3)	1856 (4)
N(12)	1583 (4)	6040 (3)	2067 (5)
C(13)	1158 (5)	6626 (3)	2979 (6)
C(14)	624 (4)	6163 (3)	3979 (6)
C(15)	738 (4)	5226 (3)	3722 (5)
N(16)	1396 (3)	5159 (3)	2574 (4)
C(17)	2471 (6)	6176 (5)	1195 (7)
C(18)	1319 (6)	7634 (4)	2973 (7)
O(19)	327 (3)	4536 (2)	4251 (4)
C(20)	913 (6)	3681 (6)	−386 (7)
C(21)	1433 (6)	2896 (5)	16 (8)
C(22)	1964 (5)	2871 (4)	1223 (7)
C(23)	1972 (5)	3642 (4)	2063 (6)
C(24)	1422 (4)	4400 (3)	1680 (6)
C(25)	891 (5)	4421 (4)	436 (7)

UM00012294
NOVARTIS EXHIBIT 1517
Novartis v. Regents, IPR2023-01347
Page 1040 of 4460

Le schéma général de la disposition des deux molécules dans le réseau cristallin est donné en projection sur le plan (001) à la Fig. 2.

Du point de vue de la conformation des deux molécules, les longueurs et angles de liaisons sont analogues à ceux rencontrés dans la littérature, aussi bien en ce qui concerne la sulfanilamide (Allèaume & Decap, 1965) que l'antipyrine (Singh & Vijayan, 1974).

Comme l'avaient déjà observé ces auteurs, le cycle de la sulfanilamide est plan, ainsi que chacun des cycles de l'antipyrine. L'angle dièdre formé entre les plans 2 et 3 est de 63,6°, alors qu'il n'est que de 12° entre les plans 1 et 2 indiquant que les deux cycles benzéniques sont sensiblement parallèles.

La seule différence notable avec les résultats antérieurs concerne l'angle entre les cycles benzénique et pyrrolique et l'antipyrine, celui ci semble varier d'un composé à l'autre traduisant une rotation possible

Tableau 3. *Coordonnées atomiques* ($\times 10^3$) *et facteurs d'agitation thermique isotrope des atomes d'hydrogène*

	x	y	z	B (Å^2)
H(020)	305	−123	−83	4,7
H(030)	411	−257	−93	4,7
H(050)	555	−182	284	3,7
H(060)	447	−42	291	4,3
H(070)	586	−322	175	5,2
H(071)	523	−358	30	5,0
H(110)	192	−12	276	5,0
H(111)	110	−30	150	4,9
H(140)	9	647	463	4,9
H(170)	299	655	143	4,2
H(171)	248	563	36	5,4
H(172)	261	667	35	5,4
H(180)	90	784	361	4,9
H(181)	98	779	195	4,9
H(182)	219	783	289	4,9
H(200)	40	366	−129	5,9
H(210)	156	236	−54	4,4
H(220)	228	225	151	5,0
H(230)	237	362	301	5,3
H(250)	46	498	24	5,1

Tableau 4. *Distances interatomiques* (Å)

C(1)–C(2)	1,379 (6)	N(16)–N(12)	1,405 (5)
C(2)–C(3)	1,390 (6)	N(12)–C(17)	1,415 (7)
C(3)–C(4)	1,394 (6)	C(13)–C(18)	1,504 (7)
C(4)–C(5)	1,406 (6)	C(15)–O(19)	1,248 (5)
C(5)–C(6)	1,386 (6)	N(16)–C(24)	1,417 (6)
C(6)–C(1)	1,379 (6)	C(20)–C(21)	1,380 (9)
C(4)–N(7)	1,369 (5)	C(21)–C(22)	1,356 (9)
C(1)–S(8)	1,754 (4)	C(22)–C(23)	1,400 (8)
S(8)–O(9)	1,445 (3)	C(23)–C(24)	1,360 (7)
S(8)–O(10)	1,429 (3)	C(24)–C(25)	1,387 (8)
S(8)–N(11)	1,591 (4)	C(25)–C(20)	1,353 (9)
C(2)–H(020)	1,02	C(14)–H(140)	1,02
C(3)–H(030)	1,06	C(17)–H(170)	0,87
C(5)–H(050)	1,05	C(17)–H(171)	1,13
C(6)–H(060)	1,10	C(17)–H(172)	1,11
N(7)–H(070)	0,94	C(18)–H(180)	1,00
N(7)–H(071)	1,02	C(18)–H(181)	0,95
N(21)–H(110)	0,93	C(18)–H(182)	1,13
N(11)–H(111)	1,00	C(20)–H(200)	1,09
N(12)–C(13)	1,349 (6)	C(21)–H(210)	0,97
C(13)–C(14)	1,366 (7)	C(22)–H(220)	1,03
C(14)–C(15)	1,406 (8)	C(23)–H(230)	1,05
C(15)–N(16)	1,396 (6)	C(25)–H(250)	0,99

Tableau 5. *Angles interatomiques* (°)

C(6)–C(1)–C(2)	120,4 (8)	O(9)–S(8)–N(11)	105,8 (5)	H(171)–C(17)–N(12)	109
C(6)–C(1)–S(8)	119,3 (8)	O(9)–S(8)–C(1)	108,6 (4)	H(181)–C(18)–C(13)	106
C(2)–C(1)–S(8)	119,7 (7)	N(11)–S(8)–C(1)	109,4 (4)	H(180)–C(18)–C(13)	97
H(020)–C(2)–C(1)	121	H(110)–N(11)–S(8)	109	H(182)–C(18)–C(13)	111
H(020)–C(2)–C(3)	118	H(111)–N(11)–S(8)	126	H(200)–C(20)–C(25)	119
C(1)–C(2)–C(3)	120,1 (8)	C(13)–N(12)–N(16)	106,6 (7)	H(200)–C(20)–C(21)	118
H(030)–C(3)–C(2)	118	C(13)–N(12)–C(17)	128,2 (8)	C(25)–C(20)–C(21)	120,5 (8)
H(030)–C(3)–C(4)	121	N(16)–N(12)–C(17)	118,3 (9)	H(210)–C(21)–C(22)	112
C(2)–C(3)–C(4)	120,4 (8)	N(12)–C(13)–C(14)	110,5 (6)	H(210)–C(21)–C(20)	126
N(7)–C(4)–C(3)	119,8 (8)	N(12)–C(13)–C(18)	119,5 (8)	C(22)–C(21)–C(20)	120,1 (9)
N(7)–C(4)–C(5)	121,7 (7)	C(14)–C(13)–C(18)	129,9 (9)	H(220)–C(22)–C(21)	117
C(3)–C(4)–C(5)	118,4 (8)	H(140)–C(14)–C(13)	123	H(220)–C(22)–C(23)	123
H(050)–C(5)–C(6)	120	H(140)–C(14)–C(15)	127	C(21)–C(22)–C(23)	119,6 (9)
H(050)–C(5)–C(4)	119	C(13)–C(14)–C(15)	108,0 (9)	H(230)–C(23)–C(24)	120
C(6)–C(5)–C(4)	120,6 (8)	O(19)–C(15)–N(16)	121,3 (8)	H(230)–C(23)–C(22)	119
H(060)–C(6)–C(11)	121	O(19)–C(15)–C(14)	132,6 (7)	C(24)–C(23)–C(22)	119,6 (8)
H(060)–C(6)–C(5)	119	N(16)–C(15)–C(14)	105,7 (9)	C(23)–C(24)–C(25)	120,1 (9)
C(1)–C(6)–C(5)	119,9 (8)	C(15)–N(16)–N(12)	108,5 (9)	C(23)–C(24)–N(16)	118,9 (7)
H(070)–N(7)–C(4)	112	C(15)–N(16)–C(24)	124,5 (8)	C(25)–C(24)–N(16)	120,9 (8)
H(071)–N(7)–C(4)	113	C(15)–N(16)–C(24)	120,0 (5)	H(250)–C(25)–C(20)	123
O(10)–S(8)–O(9)	118,2 (4)	H(170)–C(17)–N(12)	120	H(250)–C(25)–C(24)	116
O(10)–S(8)–N(11)	107,5 (4)	H(172)–C(17)–N(12)	131	C(20)–C(25)–C(24)	119,7 (9)
O(10)–S(8)–C(1)	106,9 (4)				

UM00012295
NOVARTIS EXHIBIT 1517
Novartis v. Regents, IPR2023-01347
Page 1041 of 4460

autour de la liaison N(16)–C(24) reliant ces deux cycles.

Du point de vue de l'arrangement moléculaire, nous pouvons observer que la cohésion du réseau cristallin est assurée par trois types de liaisons hydrogène, deux d'entre elles liant les molécules de sulfanilamide tandis que la troisième assure le partage d'une molécule d'antipyrine à celle de sulfanilamide (Tableau 7 et Fig. 3).

L'examen de la Fig. 2 montre que les molécules de sulfanilamide s'organisent suivant une hélice dont l'axe est confondu avec l'axe cristallographique z délimitant une sorte de tunnel dans lequel s'insèrent les molécules d'antipyrine.

Ces travaux confirment d'une part l'existence de liaisons hydrogène vérifiant ainsi l'hypothèse émise par Alberola (1976) fondée sur une étude par spectroscopie infra-rouge, d'autre part le rôle prépondérant de l'azote N(11) de la fonction sulfonamide, dans la formation du composé moléculaire 1 : 1 sulfanilamide–antipyrine. Ce résultat est comparable à ceux obtenus par Shefter &

Tableau 6. *Plans moyens d'atomes*

Plan 1: $-(0.70636)x - (0.49633)y + (0.50410)z + 2.19525 = 0$

Atomes définissant le plan

C(1)	0,002 Å	C(4)	0,006 Å
C(2)	0,001	C(5)	−0,003
C(3)	−0,005	C(6)	−0,007

Autres atomes

N(7)	−0,001 Å	O(9)	−0,529 Å
S(8)	0,043	O(10)	−0,550

Plan 2: $-(0.82855)x - (0.33637)y + (0.44762)z + 2.92083 = 0$

Atomes définissant le plan

C(20)	−0,011 Å	C(23)	−0,017 Å
C(21)	0,005	C(24)	0,012
C(22)	0,009	C(25)	0,002

Plan 3: $-(0.83248)x - (0.00822)y - (0.55400)z + 2.87883 = 0$

Atomes définissant le plan

N(12)	0,036 Å	C(13)	−0,023 Å
C(14)	−0,006	C(15)	0,028
N(16)	−0,033		

Autres atomes

C(17)	−0,409 Å	O(19)	0,176 Å
C(18)	−0,102		

Tableau 7. *Liaisons hydrogène*

O(9)^{i}···H(110)^{ii}	2,074 Å
O(9)^{i}···N(11)^{ii}	2,985
N(11)^{ii}–H(110)^{ii}···O(9)^{i}	171,9°
O(10)^{iv}···H(070)^{i}	2,090 Å
O(10)^{iv}···N(7)^{i}	2,964
N(7)^{i}–H(070)^{i}···O(10)^{iv}	152,8°
O(19)^{iv}···H(111)^{i}	1,944 Å
O(19)^{iv}···N(11)^{i}	2,915
N(11)^{i}–H(111)^{i}···O(19)^{iv}	161,8°

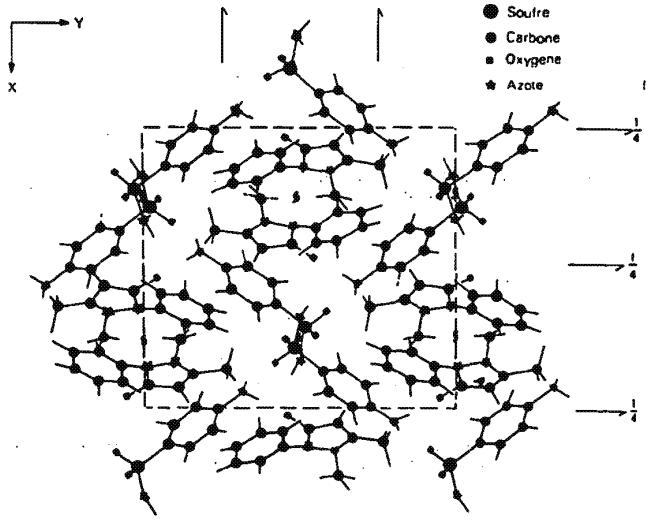


Fig. 2. Projection de la structure sur le plan (001).

UM00012296
NOVARTIS EXHIBIT 1517
Novartis v. Regents, IPR2023-01347
Page 1042 of 4460

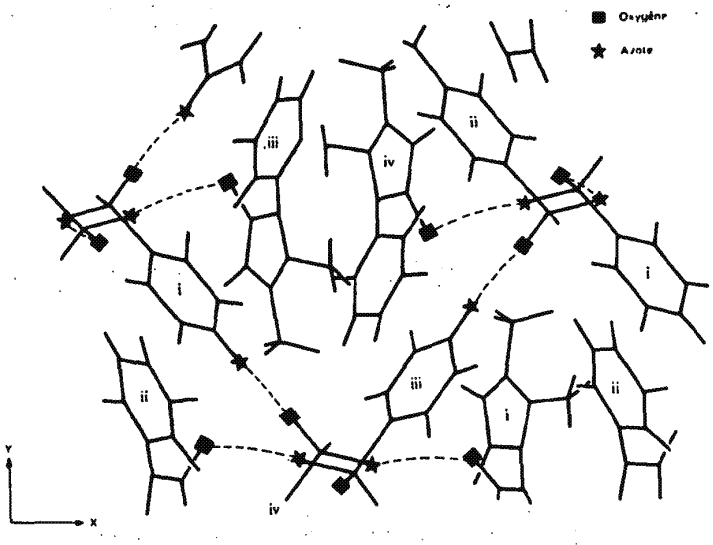


Fig. 3. Projection de la structure sur le plan (001): liaisons hydrogène.

Sackman (1971) pour le complexe sulfanilamide–sulfathiazole et par Leger, Alberola & Carpy (1977) pour l'association sulfacétamide–caféine.

Le CNRS, la DGRST, et la DESR ont apporté leur aide matérielle à la réalisation de ce travail.

Références

ALBEROLA, S. (1976). Communication privée.

ALBEROLA, S., RAMBAUD, J. & SABON, F. (1976). *Trav. Soc. Pharm. Montpellier*, **36**(1), 59–64.

ALLÉAUME, M. & DECAP, J. (1965). *Acta Cryst.* **19**, 934–938.

LEGER, J. M., ALBEROLA, S. & CARPY, A. (1977). *Acta Cryst.* B**33**, 1455–1459.

MOSSET, A., BONNET, J.-J. & GALY, J. (1977). *Acta Cryst.* B**33**, 2639–2644.

NOVAK, A., LASCOMBE, J. & JOSIEN, M. L. (1966). *J. Phys. Radium*, **27**, C2.

SHEFTER, E. & SACKMAN, P. (1971). *J. Pharm. Sci.* **60**, 282–286.

SINGH, T. P. & VIJAYAN, M. (1974). *Acta Cryst.* B**30**, 557–562.

UM00012297

NOVARTIS EXHIBIT 1517
Novartis v. Regents, IPR2023-01347
Page 1043 of 4460

The Allen Translation Service
T9049 Translated from Russian 6 Pages

JOURNAL OF PHYSICAL CHEMISTRY

Vol. 34 *(1960)* *pp. 2742 – 2747*

INVESTIGATION OF EUTECTIC MELTING IN SYSTEMS COMPOSED OF ORGANIC SALTS AND ACIDS

M. Kh. Gluzman and V. P. Rubtsova

In the process of studying melting points of eutectics of binary systems in which one of the components was a high melting point, nonmelting, or heat-decomposable organic salt or molecular compound, an observation was made that low melting point eutectics were the easiest to form when the second component [of the system] was an organic acid. When the components in the amount of 2 - 5 grams were mixed in a tube, a quite noticeable decrease in temperature was observed. For example, in the calcium lactate – chloroacetic acid system the temperature decreased from 29 °C to 21 °C, while in the calcium levulinate – chloroacetic acid system it decreased from 21 °C to 16 °C; during this process, a quite noticeable melting occurred. This phenomenon can be used to identify high melting point or nonmelting salts by means of selecting acids that, together with these salts, form eutectics that melt in the temperature range convenient for observation.

Using our contact method of eutectic temperature measurement [1 – 4], we selected as tests a number of acids that, combined with the salts to be identified, formed eutectics with melting points in the range of 10 °C – 120 °C (see Table 1). The purity of the salts was checked by titration of a sample in the amount of approximately 0.04 – 0.05 g in 20 ml of glacial acetic acid using 0.1 N perchloric acid in the presence of crystal violet indicator. This salt titration method was developed earlier by N. A. Izmailov and N. P. Dziuba [5] ([for the salts] Nos. 1 – 5, 7, 10 – 13 [in the Table]) , and we were the first to analyze the remaining salts [in the Table] using this method. However, the purity of ammonium oxalate and of sodium trioxyglutarate was determined by other methods since they dissolve poorly in glacial acetic acid. The salts under Nos. 17 – 24 were pure substances of pharmaceutical grade. The eutectic temperature measurement was performed using oven-dried salts containing water of crystallization. The numbers under the horizontal lines[1] in the table cells refer to crystal hydrates of the salts.

For eutectics with melting temperatures below room temperature, the measurements were performed on a specially designed small table described in the paper by one of the authors [6].

It is evident from this Table that the results of parallel measurements agreed rather closely, and the differences did not exceed 1 – 2 °C. When identifying salts by this method, it is possible to use crystal hydrates, eliminating the need for the salt to be dried.

[Translator's Note: There are no lines in the cells of Table 1 of the Russian Original. However, note the alignment of numbers in the cells.]

NOVARTIS EXHIBIT 1517
Novartis v. Regents, IPR2023-01347
Page 1044 of 4460

Table 1

Identification of Salts and Molecular Compounds by Eutectic Temperature Measurement

No.	Salt	Percentage	Eutectic melting point when contacting with acids				
			Mandelic acid (melting point 118 °C)	Maleic acid (melting point 131°C)	Crotonic acid (melting point 70 °C)	Phenylacetic acid (melting point 75 °C)	Chloroacetic acid (melting point 61 – 62°C)
1	Sodium salicylate	100.10	115.3 114.8 113.3 114.3	115.1 114.9 115.4 115.9	26.0 25.0 18.0 17.7	22.0 23.0 18.3	23.0 23.0
2	Sodium benzoate	100.20	117.4 118.0 114.5 114.5	116.9 117.9 115.9 116.9	56.2 56.7 50.3 50.3	10.0 11.0	Lower than 23
3	Calcium lactate	99.50	118	111.3 111.8 112.3 113.3	-	65.7 66.4 66.4 66.4	17.5 19.0 15
4	Trisodium citrate	99.80	115.9 114.9 111.3 110.3	101.6 101.6 101.0 99.0	14.5 15.0	75.0 68.5 70.5	17.5 19.0
5	Sodium formate	100.40	115.8 115.8 112.3 113.5	116.4 116.4	-	63.3 62.9 64.1 62.9	25.0
6	Sodium mandelate	99.96	118.0 118.0 116.9 115.9	96.6 96.6 91.6 92.6	68.5 67.5 65.3 66.8	65.2 65.0	20.0
7	Lithium salicylate	99.68	118.0	120.4 120.4	33.5 34.0 35.0 34.0	24.0 23.0	-
8	Sodium trioxyglutarate		112.8 112.3	91.5 93.5 93.5	-	-	10.0 9.0 10.0
9	Ammonium oxalate		102.0 102.0 98.3 97.6	99.6 98.6 94.5 92.5	-	61.9	33.4
10	2-amino-benzene-sulfamido-thiazole sodium (norsulfasol sodium)	99.30	106.0 104.0 100.0 100.0	93.5 94.5 91.7	-	54.0 56.0	30.5 30.0
11	1-Phenyl-2,3-dimethyl-5-pyrazolone-4-methylaminomethylene-sulfonate sodium[2] (analgin)	100.50	80.5 81.0	77.0 77.0 76.5 76.5	-	43.2 45.5	-

[Translator's Note: All relevant analgin aliases at http://www.chemindustry.com/apps/chemicals contain "methane" instead of "methylene".]

			Eutectic melting point when contacting with acids				
12	Double salt of 3,7-dimethylxanthine sodium and sodium salicylate (diuretin)	100.50	114.9 113.5 100.2 109.7	119.4 119.0 111.3 112.3	-	51.3 51.3 41.0 42.0	6.0
13	Sodium sulfanylacetamide	99, 92	107.7 102.0	97.6 98.6	-	45.2	-
14	Calcium levulinate	100, 04	118.0	-	22.0 22.0 18.0 18.5	24.5 23.5 17.0 18.0	-
15	Sodium phenylacetate	99.54	116.3	116.3 116.3	36.0	15.0 10.0	
16	Calcium phenylacetate	99.89	118.0	128.4 128.4	14.0 14.5	32.0 32.0	-
17	1,3-dimethylxanthine [3] sodium (theophylline sodium)	-	-	99.6 99.6	-	-	-
18	Double salt of 1,3-dimethylxanthine and ethylenediamine (euphylline)	-		112.2 112.7	-	-	-
19	Sodium diethylbarbiturate (medinal)	-	102.0 101.5	-	-	69.0 69.5	
20	Bismuth subsalicylate		--	-	-	49.2 49.7	
21	Sodium ethylisoamylbarbiturate (barbamyl)	-	104.0 104.0	117.4 117.4	-	-	-
22	2-Ethoxy-6, 9-diaminoacridinium lactate (rivanol)	-	-	-	-	45.1 46.1	
23	Caffeine sodium bensoate	-	-	91.6 92.1	45.0 46.0		
24	Sodium benzenesulfonchloramide + $3H_2O$ (chloramine B)		96.6 98.6	99.6 99.6	-	-	-

Since there exists a possibility of chemical reactions between salts and acids, we set ourselves the task of finding out whether the eutectics we had studied were of binary systems consisting of components under investigation or [of systems] consisting of products of possible interaction between these components. In order to do that, let us consider the melting temperatures of eutectics of the systems under investigation in the presence or absence of such a chemical interaction.

Let us denote the reactants (the salt and the acid) by the subscript 1, and the reaction products (the salt and the acid) – by the subscript 2. Three following alternatives are possible:

1. The salt and the acid form an eutectic without a chemical interaction:

$$\underset{\text{eutectic}_1}{\text{salt}_1 + \text{acid}_1} \xrightarrow[\text{interaction}]{\text{no}} (\text{salt}_2 + \text{acid}_2 \text{ were not produced})\ \underset{\text{eutectic}_2}{}$$

The melting point of the eutectic$_1$ ≠ the melting point of the eutectic$_2$.

2. The salt and the acid in the solid phase enter into an exchange reaction, and the observed eutectic melting

[Translator's Note: In the Russian Original: the "d" in " dimethylxanthine" was missing.]

NOVARTIS EXHIBIT 1517
Novartis v. Regents, IPR2023-01347
Page 1046 of 4460

point value is that of the resulting salt + acid system:

$$\begin{array}{lcl} \text{salt}_1 + \text{acid}_1 & \xrightarrow{\text{interact}} & \text{salt}_2 + \text{acid}_2 \\ \text{no eutectic}_1 & \text{in the solid phase} & \text{eutectic}_2 \end{array}$$

3. The salt and the acid that cannot interact in the solid phase form an eutectic and interact in the molten state. In this case, the eutectic melting point of the newly formed system should differ from the observed one:

$$\begin{array}{lcl} \text{salt}_1 + \text{acid}_1 & \xrightarrow{\text{form an eutectic melt}} & \text{salt}_2 + \text{acid}_2 \\ \text{eutectic}_1 & \text{in which they interact} & \text{eutectic}_2 \end{array}$$

The melting point of the eutectic$_1$ ≠ the melting point of the eutectic$_2$.

In addition, when an interaction takes place, it is feasible that the following eutectics can be formed: four binary system eutectics

$\text{salt}_1 + \text{salt}_2$; $\text{salt}_1 + \text{acid}_2$; $\text{acid}_1 + \text{salt}_2$; $\text{acid}_1 + \text{acid}_2$

as well as four eutectics of three component systems and one eutectic of a four component system,

We studied three acid + salt systems and determined the eutectic melting points of all possible binary systems that could be formed as a result of such combination. The results are presented in Table 2.

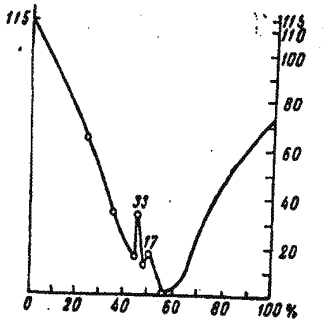
Table 2

No.	Components		Eutectic melting point (degrees)
	System 1		
1	Sodium benzoate	Phenylacetic acid	11.0; 10.0
2	Sodium phenylacetate	Benzoic acid	122
3	Sodium benzoate	Sodium phenylacetate	115 did not melt
4	Phenylacetic acid	Benzoic acid	51.5; 52.5
5	Sodium benzoate	Benzoic acid	122
6	Sodium phenylacetate	Phenylacetic acid	15.0; 16.0
	System 2		
1	Sodium salicylate	Phenylacetic acid	22.0; 23.0
2	Sodium phenylacetate	Salicylic acid	155
3	Sodium salicylate	Sodium phenylacetate	150 did not melt
4	Phenylacetic acid	Salicylic acid	66.5; 67.5
5	Sodium salicylate	Salicylic acid	154
6	Sodium phenylacetate	Phenylacetic acid	15.0; 16.0
	System 3		
1	Calcium levulinate	Phenylacetic acid	23.5; 24.5
2	Calcium levulinate	Levulinic acid	19.5; 16 – 18.0
3	Calcium levulinate	Calcium phenylacetate	56 softened
4	Phenylacetic acid	Levulinic acid	14; 12 -- 13
5	Calcium phenylacetate	Levulinic acid	7.8; 6.7
6	Calcium phenylacetate	Phenylacetic acid	32.0; 32.0

NOVARTIS EXHIBIT 1517
Novartis v. Regents, IPR2023-01347
Page 1047 of 4460

It is apparent from the table that there were no interchange reactions because in the systems containing phenylacetic acid and sodium benzoate or sodium salicylate, the melting points of the mixtures of sodium phenylacetate and benzoic or salicylic acids that may form as the result of chemical interaction (Systems 1 and 2 in Table 2), were the same as the melting points of pure acids. Therefore, the observed eutectic melting points of the system sodium benzoate + phenylacetic acid (11 – 12 °C) and of the system sodium salicylate + phenylacetic acid (22 – 23 °C) pertain to systems without chemical interaction in the solid phase. Also, there was no reaction in the eutectic melt because, when the solidified melt of the phenylacetic acid + sodium benzoate or sodium salicylate mixtures was heated, we had observed only the melting point of phenylacetic acid (75 °C) rather than the eutectic melting point of the sodium phenylacetate + phenylacetic acid system (15 – 16 °C) or that of the phenylacetic acid and benzoic acid system (51.5 – 52.5 °C).

It was somewhat difficult to assess the presence of chemical interaction in the phenylacetic acid + calcium levulinate system (with eutectic melting point of 23 – 24 °C) because the melting point of the eutectic that could form as the result of the interchange reaction in the calcium phenylacetate + levulinic acid system (7 – 8 °C) is below the eutectic melting point of the reactant system. Therefore we had constructed a state diagram of the calcium levulinate + phenylacetic acid system using the thermal method (see the Figure). The system turned out to be convenient for the study since calcium levulinate is one of the few salts that melt at relatively low temperatures (110 – 114 °C). While frequent supercoolings and glass formation hindered the construction of a precise state diagram, nevertheless, it is possible to locate in the diagram a few points indicative of the existence of chemical interaction in the melt of the components.



Both the singular point corresponding to the melting point of 33 °C for levulinic acid, and the point corresponding to the eutectic of the calcium levulinate + levulinic acid system (18 – 19 °C), are clearly visible in the diagram. The formation of levulinic acid and of its eutectic with calcium levulinate was possible only as the result of a double exchange reaction between phenylacetic acid and calcium levulinate. Such a displacement of levulinic acid is natural because the dissociation constant of phenylacetic acid is equal to 5.2×10^{-5}, while that of levulinic acid is equal to 2.55×10^{-5}. However, it should be taken into account that the dissociation constants of these acids were determined for water solutions, while here chemical interactions in the component melt were involved.

At the same time, we detected the formation of an acid salt having a melting point of 17 °C, with the following chemical composition:

$$(CH_3COCH_2CH_2COO)_2Ca \cdot C_6H_5CH_2COOH$$

and with composition 1:1.

In the diagram of the calcium levulinate + levulinic acid system, no eutectic having a melting point of 23° was found since this is a system with chemical interaction. The method of contact melting offers advantages over the thermal method because the formation of an eutectic occurs when the components are in contact with each other in the solid state rather than in the melt. Therefore this method makes it possible to detect the eutectic of the initial components [7].

Conclusions

1. We discovered that organic salts in combination with many organic acids were capable of forming binary systems characterized by low melting point eutectics.
2. We proposed a method for identification of salts and molecular compounds by measuring melting points of eutectics of binary systems composed of the salt to be identified and acids used for testing.

3. We constructed a state diagram of the calcium levulinate + levulinic acid system and established the presence of chemical interaction.

Received on March 18, 1959

References

1. M. Kh. Gluzman, A. L. Gershuns, Ya. E. Geguzin. Journal of Applied Chemistry (Russian), 26, 1223, 1953.
2. M. Kh. Gluzman, V. P. Rubtsova. Journal of Analytic Chemistry (Russian), 11, 640, 1956.
3. M. Kh. Gluzman, V. P. Rubtsova. Journal of General Chemistry (Russian), 27, 704, 1957.
4. M. Kh. Gluzman, V. P. Rubtsova. Journal of Pharmacetics (Russian: "Aptechnoe Delo"), 1, 10, 1957.
5. 5. N.A. Izmailov, N. P. Dziuba. Proceedings of the Kharkov Chemical Physics Research Institute, 2, 1957.
6. M. Kh. Gluzman. Proceedings of the Chemistry Research Institute of the Kharkov State University, 18, 254, 1957.
7. M. Kh. Gluzman, A. L. Gershuns, L. S. Palatnik, D. E. Plotkina, R. S. Milner. ENPhKh[4] (Russian), 27, Issue 10, 1304, 1953.

4 The Russian acronym is unknown. — Translator's Note.

ЖУРНАЛ ФИЗИЧЕСКОЙ ХИМИИ
Т. XXXIV 1960 № 12

T9049

ИССЛЕДОВАНИЕ ЭВТЕКТИЧЕСКОГО ПЛАВЛЕНИЯ СИСТЕМ, СОСТОЯЩИХ ИЗ ОРГАНИЧЕСКИХ СОЛЕЙ И КИСЛОТ

М. Х. Глузман и В. П. Рубцова

В процессе изучения температур плавления эвтектик бинарных систем, в состав которых входят в качестве одного компонента тугоплавкие, неплавящиеся или разлагающиеся при нагревании органические соли или молекулярные соединения, было сделано наблюдение, что легче всего образуются низкоплавкие эвтектики, когда вторым компонентом является органическая кислота. При смешении в пробирке 2—5 *г* компонентов наблюдается весьма заметное понижение температуры. Так, например, в системе молочнокислый кальций — хлоруксусная кислота температура понизилась с 29 до 21°С, а в системе ленулиновокислый кальций — хлоруксусная кислота с 21 до 16°С; при этом идет весьма заметное плавление. Это явление можно использовать для идентификации высокоплавких и неплавящихся солей путем подбора кислот, дающих с солями эвтектики, плавящиеся в удобном для наблюдения интервале температур.

Пользуясь ранее разработанным нами контактным методом определения температур плавления эвтектик [1—4], мы подобрали в качестве тестов ряд кислот, дающих с идентифицируемыми солями эвтектики, плавящиеся в пределах 10—120° (табл. 1). Чистота солей проверялась титрованием навески, порядка 0,04—0,05 *г* в 20 *мл* безводной уксусной кислоты 0,1 *N* хлорной кислотой в присутствии индикатора кристаллвиолета. Такой метод титрования солей (№ 1—5, 7, 10—13) ранее разработан Н. А. Измайловым и Н. П. Дзюбой [5], остальные соли таким методом анализировались нами впервые. Исключение составляют щавелевокислый аммоний и триоксиглутаровокислый натрий, чистота которых определялась другими способами, так как они плохо растворяются в ледяной уксусной кислоте. Соли, отмеченные № 17—24, представляют собой чистые вещества фармакопейного достоинства. Определение температур плавления эвтектик проводилось с солями, высушенными до постоянного веса и содержащими кристаллизационную воду. Цифры, помещенные под чертой, относятся к кристаллогидратам солей.

В тех случаях, когда эвтектики плавились при температурах ниже комнатной, определение проводилось на специальном столике, описание которого дано в статье одного из нас [6].

Из таблицы видно, что совпадаемость параллельных определений не превышает 1—2°С. Для идентификации солей этим способом можно пользоваться кристаллогидратами, не прибегая к обезвоживанию.

Так как между кислотами и солями возможно химическое взаимодействие, мы поставили задачу выяснить, принадлежат ли наблюдаемые эвтектики бинарным системам взятых для исследования компонентов или возможным продуктам их взаимодействия. Для этой цели рассмотрим, при каких температурах должны плавиться эвтектики исследованных систем при наличии или отсутствии химического взаимодействия.

Обозначим исходные соль и кислоту индексом 1, а полученные в результате взаимодействия новые соль и кислоту—индексом 2. Мыслимы три возможности.

Исследование э

Идентификация солей и молекул

№	Наименование солей	%-ное содер-жание
1	Натрий салицилово-кислый	100,10
2	Натрий бензойно-кислый	100,20
3	Кальций молочно-кислый	99,50
4	Натрий лимонно-кислый трехза-мещенный	99,80
5	Натрий муравьи-новокислый	100,40
6	Натрий миндаль-нокислый	99,96
7	Литий салицилово-кислый	99,68
8	Натрий триокси-глутаровокис-лый	
9	Аммоний щавеле-вокислый	
10	2-амино-бензол-сульфамидо-натрий-тиазол (нор-сульфазол-натрий)	99,30
11	1-фенил-2,3-диме-тил-5-пираво-лон-4-метилами-нометилен-сер-нистокислый натрий (аналь-гин)	100,50
12	Двойная соль 3,7-диметил-ксан-тинната-трия с са-лицилово-кислым натрием (диуретин)	100,50

Zhurnal Fizicheskoi Khimii Vol. 34 pg. 2742-2747 (1960)

UM00012304
NOVARTIS EXHIBIT 1517
Novartis v. Regents, IPR2023-01347
Page 1050 of 4460

ПЛАВЛЕНИЯ СИСТЕМ, Х СОЛЕЙ И КИСЛОТ

І. Рубцова

ия эвтектик бинарных систем, компонента тугоплавкие, нении органические соли или мо- юдение, что легче всего обра- орым компонентом является бирке 2—5 *г* компонентов наб- ературы. Так, например, в сис- ная кислота температура по- овокислый кальций — хлорук- т весьма заметное плавление. тификации высокоплавких и дающих с солями эвтектики, ервале температур.
онтактным методом определе- мы подобрали в качестве тес- ми солями эвтектики, плавя- а солей проверялась титрова- безводной уксусной кислоты икатора кристаллвиолета. Та- —13) ранее разработан Н. А. соли таким методом анализи- ляют щавелевокислый амино- истота которых определялась воряются в ледяной уксусной ставляют собой чистые веще- ние температур плавления эв- до постоянного веса и содер- помещенные под чертой, от-

при температурах ниже комн- льном столике, описание ко-

араллельных определений ис й этим способом можно поль- обезвоживанию.
ожно химическое взаимодей- адлежат ли наблюдаемые эв- следования компонентов пли ля этой цели рассмотрим, при ектики исследованных систем заимодействия.
сом 1, а полученные в резуль- —индексом 2. Мыслимы три

Таблица 1

Идентификация солей и молекулярных соединений методом определения температур плавления эвтектик

№	Наименование солей	%-ное содержание	Температура плавления эвтектик при контактировании с кислотами: миндальная кислота, т. пл. 118°	малеиновая кислота, т. пл. 131°	протоковая кислота, т. пл. 70°	фенилуксусная кислота, т. пл. 75°	монохлоруксусная кислота, т. пл. 61—62°
1	Натрий салицилово-кислый	100,10	115,3 114,8 113,3 114,3	115,1 114,9 115,4 115,9	26,0 25,0 18,0 17,7	22,0 23,0 18,3	23,0 23,0
2	Натрий бензойно-кислый	100,20	117,4 118,0 114,5 114,5	116,9 117,9 115,9 116,9	56,2 56,7 50,3 50,3	10,0 11,0	Ниже 23
3	Кальций молочно-кислый	99,50	118	111,3 111,8 112,3 113,3	—	65,7 66,4 66,4 66,4	17,5 19,0 15
4	Натрий лимонно-кислый трехзамощенный	99,80	115,9 114,9 111,3 110,3	101,6 101,6 101,0 99,0	14,5 15,0	75,0 68,5 70,5 63,3	17,5 19,0
5	Натрий муравьиновокислый	100,40	115,8 115,8 112,3 113,5	116,4 116,4	—	62,9 64,1 62,9	25,0
6	Натрий миндальнокислый	99,96	118,0 118,0 116,9 115,9	96,6 96,6 91,6 92,6	68,5 67,5 65,3 66,8	65,2 65,0	20,0
7	Литий салицилово-кислый	99,68	118,0	120,4 120,4	33,5 34,0 35,0 34,0	24,0 23,0	—
8	Натрий триокси-глутаровокис-лый		112,8 112,3	91,5 93,5 93,5	—	—	10,0 9,0 10,0
9	Аммоний щавелево-кислый		102,0 102,0 98,3 97,6	99,6 98,6 94,5 92,5	—	61,9	33,4
10	2-амино-бензол-сульфамидо-натрий-тиазол (нор-сульфазол-натрий)	99,30	106,0 104,0 100,0 100,0	93,5 94,5 91,7	—	54,0 56,0	30,5 30,0
11	1-фенил-2,3-диме-тил-5-пираво-лон-4-метилами-нометилсп-сер-нистокислый патрий (анальгин)	100,50	80,5 81,0	77,0 77,0 76,5 76,5	—	43,2 45,5	—
12	Двойная соль 3,7-диметил-ксан-тинпатрия с са-лицилловокис-лым натрием (диуретин)	100,50	114,9 113,5 109,2 109,7	119,4 119,0 111,3 112,3	—	51,3 51,3 41,0 42,0	6,0

UM00012305
NOVARTIS EXHIBIT 1517
Novartis v. Regents, IPR2023-01347
Page 1051 of 4460

Таблица 1 (*продолжение*)

№	Наименование солей	%-ное содержание	Температура плавления эвтектик при контактировании с кислотами				
			миндальная кислота, т. пл. 118°	малеиновая кислота, т. пл. 131°	кротоновая кислота, т. пл. 70°	фенилуксусная кислота, т. пл. 75°	монохлоруксусная кислота, т. пл. 61—62°
13	Сульфанил-ацетамид-натрия	99,92	107,7 102,0	97,6 98,6	—	45,2	—
14	Кальций левулиновокислый	100,04	118,0	—	22,0 22,0 18,0 18,5	24,5 23,5 17,0 18,0	—
15	Натрий фенилуксуснокислый	99,54	116,3	116,3 116,3	36,0	15,0 16,0	
16	Кальций фенилуксуснокислый	99,89	118,0	128,4 128,4	14,0 14,5	32,0 32,0	—
17	1,3-диметилксантин-натрий (теофиллин-натрий)	—	—	99,6 99,6	—	—	—
18	Двойная соль 1,3-диметил-ксантина с этилендиамином (эуфиллин)	—		112,2 112,7	—	—	—
19	Диэтилбарбитурат-натрий (мединал)	—	102,0 101,5	—	—	69,0 69,5	
20	Висмут салициловокислый основной		—	—	—	49,2 49,7	
21	Натриевая соль этилизоамил барбитуровой кислоты (барбамил)	—	104,0 104,0	117,4 117,4	—	—	—
22	Лактат 2-этокси-6,9-диаминоакридин (риванол)	—	—	—	—	45,1 46,1	
23	Кофеин-бензойнокислый натрий	—	—	91,6 92,1	45,0 46,0		
24	Бензолсульфохлорамид-натрий + $3H_2O$ (хлорамин Б)		96,6 98,6	99,6 99,6	—	—	—

1. Соль и кислота дают эвтектику без химического взаимодействия:

$$\underset{\text{эвтектики}_1}{\text{соль}_1 + \text{кислота}_1} \xrightarrow[\text{нет}]{\text{взаимодействия}} (\text{соль}_2 + \underset{\text{эвтектика}_2}{\text{кислота}_2}\ \text{не образовались})$$

$$\text{Т. пл. эвтектики}_1 \neq \text{т. пл. эвтектики}_2$$

2. Соль и кислота вступают в твердой фазе в реакцию обмена, и наблюдаемая т. пл. эвтектики принадлежит уже образовавшейся в результате

Исследование

взаимодействия новой систе

$$\text{соль}_1 + \text{кислота}_1$$

эвтектики$_1$ —

3. Соль и кислота, несп
образуют эвтектику и реагир
ления эвтектики вновь обра
блюдаемой:

$$\text{соль}_1 + \text{кислота}_1 \xrightarrow{\text{образ}}$$

эвтектика$_1$

Т. пл. э

Помимо этого, в случае
рех эвтектик бинарных сис

$$\text{соль}_1 + \text{соль}_2; \quad \text{соль}_1 + \text{кисл}$$

и четырех эвтектик трехко
систем.

Мы изучили три системы
плавления эвтектик всех би
зультате сочетания. В табл.

№	
1	Натрий бензойнокислый
2	Натрий фенилуксуснокислый
3	Натрий бензойнокислый
4	Фенилуксусная кислота
5	Натрий бензойнокислый
6	Натрий фенилуксуснокислый
1	Натрий салициловокислый
2	Натрий фенилуксуснокислый
3	Натрий салициловокислый
4	Фенилуксусная кислота
5	Натрий салициловокислый
6	Натрий фенилуксуснокислый
1	Кальций левулиновокислый
2	Кальций левулиновокислый
3	Кальций левулиновокислый
4	Фенилуксусная кислота
5	Кальций фенилуксуснокисла
6	Кальций фенилуксусно кисл

Из таблицы видно, что р
как в системах, содержащих
кислый или салициловокисл
те химического взаимодейст
ной или салициловой кислот
чистых кислот. Следователь
тектик систем натрий бенз

UM00012306
NOVARTIS EXHIBIT 1517
Novartis v. Regents, IPR2023-01347
Page 1052 of 4460

Таблица 1 (*продолжение*)

ления эвтектик при контактировании с кислотами			
новая ота, 131°	кротоновая кислота, т. пл. 70°	фенилуксусная кислота, т. пл. 75°	монохлоруксусная кислота, т. пл. 61—62°
,6		45,2	
,6	—		—
–	22,0	24,5	
	22,0	23,5	—
	18,0	17,0	
	18,5	18,0	
		15,0	
,3	36,0	16,0	
,4	14,0	32,0	—
,4	14,5	32,0	
			—
,6	—	—	—
,6			
,2			
,7	—	—	—
	—	69,0	
		69,5	
	—	49,2	
		49,7	
4			
4	—	—	—
	—	45,1	
		46,1	
6	45,0		
1	46,0		
6			
6	—	—	—

химического взаимодействия:

ита$_2$ не образовались)
гектика$_2$

эвтектики$_2$

в реакцию обмена, и наблю-
образовавшейся в результате

взаимодействия новой системе соль + кислота:

$$\underset{\text{эвтектики}_1 \text{ — нет}}{\text{соль}_1 + \text{кислота}_1} \xrightarrow{\text{реагируют в твердой фазе}} \underset{\text{эвтектика}_2}{\text{соль}_2 + \text{кислота}_2}$$

3. Соль и кислота, неспособные к взаимодействию в твердой фазе, образуют эвтектику и реагируют в плаве. В этом случае температура плавления эвтектики вновь образующейся системы должна отличаться от наблюдаемой:

$$\underset{\text{эвтектика}_1}{\text{соль}_1 + \text{кислота}_1} \xrightarrow[\text{в котором реагируют:}]{\text{образуют эвтектический плав,}} \underset{\text{эвтектика}_2}{\text{соль}_2 + \text{кислота}_2}$$

$$\text{Т. пл. эвтектики}_1 \neq \text{т. пл. эвтектики}_2.$$

Помимо этого, в случае взаимодействия возможно образование четырех эвтектик бинарных систем:

$$\text{соль}_1 + \text{соль}_2; \quad \text{соль}_1 + \text{кислота}_2; \quad \text{кислота}_1 + \text{соль}_2; \quad \text{кислота}_1 + \text{кислота}_2,$$

и четырех эвтектик трехкомпонентных и одной — четырехкомпонентной систем.

Мы изучили три системы кислота + соль и определили температуры плавления эвтектик всех бинарных систем, могущих образоваться в результате сочетания. В табл. 2 сведены полученные результаты.

Таблица 2

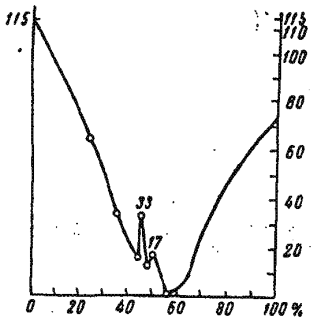
№	Компоненты		Т. пл. эвтектик (в градусах)
	Система I		
1	Натрий бензойнокислый	Фенилуксусная кислота	11,0; 10,0
2	Натрий фенилуксуснокислый	Бензойная кислота	122
3	Натрий бензойнокислый	Натрий фенилуксуснокислый	115 не пл.
4	Фенилуксусная кислота	Бензойная кислота	51,5; 52,5
5	Натрий бензойнокислый	Бензойная кислота	122
6	Натрий фенилуксуснокислый	Фенилуксусная кислота	15,0; 16,0
	Система II		
1	Натрий салициловокислый	Фенилуксусная кислота	22,0; 23,0
2	Натрий фенилуксуснокислый	Салициловая кислота	155
3	Натрий салициловокислый	Натрий фенилуксуснокислый	150 не пл.
4	Фенилуксусная кислота	Салициловая кислота	68,5; 67,5
5	Натрий салициловокислый	Салициловая кислота	154
6	Натрий фенилуксуснокислый	Фенилуксусная кислота	15,0; 16,0
	Система III		
1	Кальций левулиновокислый	Фенилуксусная кислота	23,5; 24,5
2	Кальций левулиновокислый	Левулиновая кислота	19,5; 16—18,0
3	Кальций левулиновокислый	Кальций фенилуксуснокислый	56 размягч.
4	Фенилуксусная кислота	Левулиновая кислота	14; 12—13
5	Кальций фенилуксуснокислый	Левулиновая кислота	7,8; 6,7
6	Кальций фенилуксусно кислый	Фенилуксусная кислота	32,0; 32,0

Из таблицы видно, что реакции взаимного обмена не имели места, так как в системах, содержащих фенилуксусную кислоту и натрий бензойнокислый или салициловокислый, смеси могущих образоваться в результате химического взаимодействия фенилуксуснокислого натрия и бензойной или салициловой кислот (системы I и II, табл. 2) плавятся при т. пл. чистых кислот. Следовательно, наблюдаемые температуры плавления эвтектик систем натрий бензойнокислый + фенилуксусная кислота (11—

UM00012307
NOVARTIS EXHIBIT 1517
Novartis v. Regents, IPR2023-01347
Page 1053 of 4460

12°) и натрий салициловокислый + фенилуксусная кислота (22—23°) относятся к системам без химического взаимодействия в твердой фазе. Реакция в эвтектическом плаве также не имела места, так как при нагревании застывшего плава смесей фенилуксусной кислоты + натрий бензоат или салицилат наблюдается лишь т. пл. фенилуксусной кислоты (75°), а не т. пл. эвтектик систем фенилуксусновокислый натрий + фенилуксусная кислота (15—16°) или фенилуксусная и бензойная кислоты (51,5—52,5°).

Несколько сложнее судить о наличии химического взаимодействия в системе фенилуксусная кислота + левулиновокислый кальций (т. пл. эвтектики 23—24°), так как т. пл. эвтектики, могущей образоваться в результате реакции обмена системы кальций фенилацетат + левулиновая кислота (7—8°), лежит ниже температуры плавления эвтектики исходной системы. В связи с этим мы построили диаграмму состояния системы левулиновокислый кальций + фенилуксусная кислота, пользуясь термическим методом (рисунок). Система оказалась удобной для изучения в том смысле, что левулинат кальция, одна из немногих солей, плавится при относительно низкой температуре, 110—114°. Правда, составлению точной диаграммы состояния мешают частые переохлаждения и стеклообразование, все же на диаграмме можно обнаружить несколько точек, указывающих на наличие химического взаимодействия в плаве компонентов.



Отчетливо видна сингулярная точка с температурой плавления 33°, отвечающая левулиновой кислоте, и эвтектика системы левулиновокислый кальций + левулиновая кислота (18—19°). Появление левулиновой кислоты в эвтектики ее с левулинатом кальция возможно лишь в результате реакции двойного обмена между фенилуксусной кислотой и левулиновокислым кальцием. Такое вытеснение левулиновой кислоты закономерно, так как константа диссоциации фенилуксусной кислоты равна $5{,}2 \cdot 10^{-5}$, а левулиновой — $2{,}55 \cdot 10^{-5}$. При этом следует, однако, учесть, что константы диссоциации этих кислот определены для водных растворов, а здесь идет речь о химическом взаимодействии в плаве компонентов.

Одновременно было обнаружено образование кислой соли состава:

$$(CH_3COCH_2CH_2COO)_2Ca \cdot C_6H_5CH_2COOH,$$

плавящейся при 17° и имеющей состав 1 : 1.

На диаграмме системы кальций левулиновокислый + фенилуксусная кислота эвтектика с температурой плавления 23° не обнаружена, так как эта система с химическим взаимодействием. Метод же контактного плавления имеет то преимущество перед термическим, что появление эвтектики наблюдается при соприкосновении компонентов в твердом состоянии, а не в плаве. Поэтому он позволяет обнаружить эвтектику и самих исходных компонентов [7].

Выводы

1. Обнаружена способность органических солей к образованию со многими органическими кислотами бинарных систем, характеризующихся низкоплавкими эвтектиками.

2. Предложен метод идентификации солей и молекулярных соединений путем определения температур плавления эвтектики бинарных систем, состоящих из идентифицируемой соли и кислотных тестов.

3. Построена диаграмма
ций + фенилуксусная кисл
имодействия.

1. М. Х. Глузман, А. Л. Г
1223, 1953.
2. М. Х. Глузман, В. П. Р
3. М. Х. Глузман, В. П. Р
4. М. Х. Глузман, В. П. Р
5. Н. А. Измайлов, Н. П.
6. М. Х. Глузман, Труды
254, 1957.
7. М. Х. Глузман, А. Л. Г
Р. С. Мильнер, ЭНФХ

EUTECTIC MELTING OF

M. Kh. Gluzm

Organic salts have been foun
systems characterized by low me
fying salts and molecular compo
of binary systems consisting of t
calcium levulinate + phenylacet
interaction has been established

UM00012308
NOVARTIS EXHIBIT 1517
Novartis v. Regents, IPR2023-01347
Page 1054 of 4460

3. Построена диаграмма состояния системы левулиновокислый кальций + фенилуксусная кислота и установлено наличие химического взаимодействия.

Поступила
18. III. 1959

ЛИТЕРАТУРА

1. М. Х. Глузман, А. Л. Гершунс, Я. Е. Гегузин, Ж. прикл. химии, 26, 1223, 1953.
2. М. Х. Глузман, В. П. Рубцова, Ж. аналит. химии, 11, 640, 1956.
3. М. Х. Глузман, В. П. Рубцова, Ж. общей химии, 27, 704, 1957.
4. М. Х. Глузман, В. П. Рубцова, Аптечное дело, № 1, 10, 1957.
5. Н. А. Измайлов, И. П. Дзюба, Тр. ХНИХФИ, 2, 1957.
6. М. Х. Глузман, Труды научно-исследовательского института химии ХГУ, 18, 254, 1957.
7. М. Х. Глузман, А. Л. Гершунс, Л. С. Палатник, Д. Е. Плоткина, Р. С. Мильнер, ЭНФХ, 27, вып. 10, 1304, 1953.

EUTECTIC MELTING OF SYSTEMS OF ORGANIC SALTS AND ACIDS

M. Kh. Gluzman and *V. P. Rubtsova (Kharkov)*

Summary

Organic salts have been found capable of forming with many organic acids binary systems characterized by low melting eutectics. A method has been proposed for identifying salts and molecular compounds by determining the melting points of the eutectics of binary systems consisting of the unknown salt and of acid tests. A diagram of state of calcium levulinate + phenylacetic acid has been plotted and the presence of chemical interaction has been established.

UM00012309
NOVARTIS EXHIBIT 1517
Novartis v. Regents, IPR2023-01347
Page 1055 of 4460